

Potential Impacts of Climate Change on Ecological Resources and Biodiversity in the San Pedro Riparian National Conservation Area, Arizona.



A report to U.S. EPA

From the American Bird Conservancy
November, 2005

Jeff Price, California State University, Chico

Hector Galbraith, Galbraith Environmental Services

Mark Dixon, Arizona State University

Julie Stromberg, Arizona State University

Terry Root, Stanford University

Dena MacMykowski, Stanford University

Tom Maddock, University of Arizona

Kate Baird, University of Arizona

TABLE OF CONTENTS

SECTION 1. INTRODUCTION AND PROJECT BACKGROUND	9
1.2 Ecosystem Services Provided by the SPRNCA.....	12
1.3 Stakeholders and their Involvement.....	17
1.4 Overview of Studies.....	18
1.5 Report structure.....	19
SECTION 2. HYDROLOGY, STRESSORS, HISTORICAL CHANGE AND BIODIVERSITY IN THE SAN PEDRO RIPARIAN ECOSYSTEM.....	20
2.1 Climate.....	20
2.2 Hydrology	21
2.3 Human Population Growth	23
2.4 Geomorphological and Ecological Changes along the San Pedro River.....	23
SECTION 3. PROJECTING THE EFFECTS OF ENVIRONMENTAL CHANGE ON RIPARIAN VEGETATION IN THE SPRNCA.....	26
3.1 Introduction.....	26
3.2 Ecology of southwestern riparian vegetation and drivers of change	32
3.3 Historic and recent changes along the San Pedro River	45
3.4 Simulation of vegetation response to climate change.....	51
3.5 Discussion.....	75
SECTION 4 CHANGES IN BIODIVERSITY	83
4.1 Environmental Protection Agency Vulnerability Framework	83
4.1.1 The EPA framework and its modifications.....	83
4.1.2 Application of the modified EPA Framework to SPRNCA birds.	98
4.1.3 Summary	108
4.2 SPRNCA Vulnerability Framework	109
4.3 Vegetation modeling and Habitat Suitability Index Models.....	122
4.3.1 The qualitative analysis.....	123
4.3.2 The quantitative analysis.....	127
4.4 Avian Bioenergetics as a Potentially Limiting Factor	136
4.4.1 Migratory Bird Use of the SPRNCA	137
4.4.2 Determining Avian Energetic Needs	153
4.4.3 Determining habitat requirements based on bioenergetics	155
4.5 Bioclimatic Modeling of Avian Range Changes	160
SECTION 5 CHANGES IN ECOSYSTEM SERVICES.....	178
5.1 Ecosystem Services - General.....	178
5.2 Ecosystem Services in the SPRNCA	179
SECTION 6 REFERENCES	182
ATTACHMENT 1 - SIMULATED VEGETATION TRANSITIONS.....	203
ATTACHMENT 2 – Modified EPA Framework	223
ATTACHMENT 3 – HSI Models.....	241
ATTACHMENT 4 – Publications on the HSI model.....	326
ATTACHMENT 5 – Hydrologic Modeling	347
ATTACHMENT 6 – Evapotranspiration/Hydrology Publications	373
6.1 – Simulation riparian evapotranspiration: a new methodology and application for groundwater models.....	373
6.2 Linking riparian dynamics and groundwater: an ecohydrological approach to modeling groundwater and riparian vegetation	389
6.3 Rip-ET Evapotranspiration Users Manual.....	404
6.4 RIP-ET Preprocessor Users Manual.....	472

EXECUTIVE SUMMARY

In the arid southwestern United States, riparian ecosystems are critical for sustaining regional biodiversity and supporting species that are rare or restricted in their distributions within the U.S. due to the widespread destruction of riparian habitats. They also typically support numbers of organisms that are disproportionate to their relatively limited spatial areas. The Upper San Pedro River riparian ecosystem in southeastern Arizona and northern Sonora contains one of the richest assemblages of species and is one of the most important migratory bird habitats in western North America.

The biodiversity of the San Pedro riparian ecosystem matches or exceeds that found almost anywhere else in the United States: more than twenty different biotic communities occur in the basin, and the river sustains three biotic types considered threatened - Fremont cottonwood/Goodding willow forests, cienegas and big sacaton grasslands. Vascular plant diversity is very high, with 608 species from 92 families identified within the San Pedro Riparian National Conservation Area (SPRNCA) alone (Makings in press). Among these is the Huachuca water umbel (*Lilaeopsis schaffneriana* spp. *recurva*), a federally endangered species. The area is of critical importance in maintaining regional biodiversity at the ecotones between the Sonoran and Chihuahuan deserts and the Plains grassland.

The area also has one of the highest vertebrate diversities found anywhere in the United States. The SPRNCA has one of the highest bird diversities of any area of its size in the United States, with more than 350 recorded species, 250 of which are Neotropical migrants. Between one million and four million migrating songbirds use the riparian habitat annually as they move between their wintering grounds in Mexico and Central America and their breeding grounds in the United States and Canada. Twelve bird species found annually on the SPRNCA have previously been classified by the State of Arizona as Wildlife of Special Concern, representing 41% of the bird species on that list. Of the 107 species on the 1988 Partners in Flight 'WatchList', 52 have occurred in the San Pedro Basin at least once and 19 of them either breed or winter in the area. Of the top scoring 45 species on Arizona Partners in Flight species of concern, 42 have occurred at least once in the basin and 25 occur annually (9 breed, 5 winter and 11 migrate through). The SPRNCA has been designated as critical habitat for the endangered Southwestern Willow Flycatcher. Additionally, a globally significant number of Western Yellow-billed Cuckoos, a species that groups have petitioned the USFWS to consider listing as a threatened or endangered species, breed along the San Pedro.

The SPRNCA also currently contains, or contained within the last 150 years, more than 80 species of mammals – for its area, one of the richest assemblages of land mammal species in the world. More than 40 species of reptiles and amphibians have also been found within the boundaries of the SPRNCA.

The Nature Conservancy has recognized the high ecological value of the area through the designation of the upper San Pedro as one of the "Last Great Places". Approximately 58,000 ha are protected along a 50-km reach of the river within the SPRNCA, administered by the U.S. Department of the Interior Bureau of Land Management.

The regionally, nationally, and internationally important ecological resources of SPRNCA also provide valued ecosystem services. The main service addressed in this report is the support of important plant and wildlife habitat and the resulting biodiversity. Human residents and visitors to the area obviously regard this habitat-diversity relationship as being an outstanding service: the SPRNCA is nationally and internationally recognized for its birdwatching opportunities, one of the fastest growing recreational activities in the U.S. Most birdwatching in Arizona occurs in the southeastern portion of the state and the San Pedro basin is one of the three major areas visited. Total tourism revenues within Cochise County were estimated at \$180 million annually. In the period 1991-1992, 11,700 tourists visited the San Pedro and 26,300 visited Ramsey Canyon, elsewhere in the watershed. This visitation was estimated to have led to direct expenditures in the area of \$1.2 million for a total economic impact of \$2 million. By 1997, the annual number of visitors to the SPRNCA had grown to an estimated 100,000 visitors.

Of equal or greater importance is the enhancement to the quality of life of local residents attributable to the river, its riparian vegetation and the bird life it supports. These values depend on the quality of the aquatic ecosystem. Marginal deterioration of a natural resource such as the SPRNCA imposes losses both to economic activity as well as to public values.

In addition to the non-market value of the river (quality of life, riparian habitat, etc.) to local residents, an ecosystem such as the San Pedro services an area larger than it runs through. The birds migrating through the area to their breeding areas further north or their wintering areas further south provide ecosystem services (including recreation and pest control) to a much larger part of the U.S., Canada, and Central and South America.

The ecological resources of the San Pedro riparian ecosystem are currently under considerable threat from anthropogenic stress. Particularly, groundwater withdrawals for human consumption jeopardize the riparian habitat by lowering the water table in the basin. More recently a new potential threat has been recognized: global climate change, through the effect that a changing climate may directly exert on temperature and precipitation patterns, and indirectly on water tables and evapotranspiration rates, may also have the potential of changing the valued riparian ecosystem of the San Pedro.

In this research project we evaluated the potential effect that global climate change, in concurrence with existing stressors, may have on the ecological resources and biodiversity of the SPRNCA. Our results show that:

- Changes in the representation of the main vegetation communities (riparian and mesic and xeric) were projected through 2102 under four main future climate change scenarios: no change from present, warmer with similar precipitation, warmer and drier, and warmer and wetter. Modeled future vegetation conditions were greatly affected by the scenario selected.
- Changes in river baseflow, soil water content, channel migration, and the incidence and intensity of wildfires were also modeled under the climate change scenarios.
- Model results suggest that even with no change in climate a decrease in coverage by pioneer woody vegetation across the floodplain of the upper San Pedro will occur over the next 100 years. In particular, coverage of cottonwood/willow patches may decline as

old patches established during the channel narrowing process will senesce. The extensive cottonwood and willow patches found currently along portions of the river are largely the legacy of channel widening and subsequent channel narrowing and floodplain reconstruction over the last century. Long-term coverage by cottonwood/willow in particular, and pioneer patch types in general, will depend heavily on how much opportunity there is for new recruitment of these species in the future.

- Recruitment of cottonwood/willow depends heavily on the formation of moist, mineral seedbeds by channel migration and on the timing of floods. Hence, the influence of climate change on pioneer riparian communities will depend largely on how precipitation regimes change. The warmer and drier climate change scenario incurs the greatest reductions in the representation of cottonwood/willow dominated communities.
- Projections from the scenario with increased winter precipitation result in larger and more frequent winter floods, higher channel migration rates, and higher recruitment rates by cottonwood and willow. If increases in precipitation are high enough, then it is possible that pioneer patch types could be maintained at high levels in the floodplain of the San Pedro.
- Warmer and drier conditions will favor the replacement of the cottonwood/willow riparian forest by local vegetation communities that are better adapted to mesic or xeric conditions. These include grasslands and mesquite scrubland.
- Warmer and drier conditions will favor an increase in the representation of the invasive shrub saltcedar in the basin. Thus, the upper San Pedro may come to more closely resemble areas further downstream where saltcedar has, in many areas, replaced native vegetation.
- Model results suggest somewhat higher fire frequencies under all warming scenarios, with particularly higher frequencies under a warmer, drier climate. This would favor the expansion of mesquite and other mesic or xeric communities, to the detriment of cottonwood/willow.
- Other factors could also have important effects on cover of different vegetation communities in the floodplain. Direct and interactive effects of increases in CO₂ and temperature on plant physiology (e.g., water use efficiency, rates of photosynthesis and respiration) may strongly influence plant growth rates and competitive interactions among species, particularly between woody shrubs and grasses
- Perhaps the dominant factor influencing vegetation patterns along the San Pedro today is its geomorphic history. The channel incision and widening events of the late 19th through early 20th century set the template that influenced subsequent development of the new floodplain and riparian ecosystem. Reoccurrence of a catastrophic channel incision/widening event in the near future seems unlikely, given improvements in upland land use. However, channel cutting and filling have been cyclical events in the region across geologic history and projected effects of global warming include increases in climatic extremes. In addition, recent and ongoing changes in land cover (expansion of urban areas and mesquite patches) in the San Pedro watershed may be increasing the

flashiness of watershed response. Against this setting, large increases in the size or variability of precipitation events could also increase the vulnerability of the system to channel entrenchment from a catastrophic flood event. Unfortunately, the climatic and geomorphic thresholds for such catastrophic events are not well known. Occurrence of a major incision and widening event could reset the system to conditions that prevailed in the first half of the 20th century, before channel recovery processes led to channel narrowing and formation of the vegetated riparian corridor we see today.

- The avian community of the SPRNCA includes species that are highly dependent on riparian cottonwood/willow forest. This is also the habitat that supports most of the migratory birds moving through the area in the spring and fall. A different suite of species is typical of the more arid grasslands and mesquite shrublands that abut the riparian ecosystem. The high overall avian diversity of the area is largely due to the juxtaposition of these two very different habitat types.
- Many of the bird species that are dependent on the riparian habitat in the SPRNCA is rare or restricted in their North American distributions. However, the species that occur in the mesic or xeric habitats abutting the SPRNCA are typically widely distributed and relatively common the desert southwest and in northern Mexico.
- The “no change” and “warmer and drier” climate scenarios, acting through their projected adverse impacts on the SRPNCA riparian cottonwood and willow habitats are likely to adversely affect the ability of the area to continue supporting the bird species dependent on this habitat type.
- Specifically, rare and restricted distribution species such as grey hawk, yellow-billed cuckoo, and green kingfisher are likely to suffer under the no change and the warmer and drier climate scenarios.
- Some species will likely benefit under the no change and warmer and drier scenarios (e.g., Abert’s towhee, Botteri’s sparrow, Bewick’s wren, and verdin). However, unlike the riparian habitat-dependent species, these are all organisms that are widely distributed and relatively common in the desert southwest.
- We project that the net result of the no change and warmer and drier scenarios will be a reduction of about 25% in the overall avian biodiversity of the SPRNCA. Furthermore, this 25% is comprised largely of the rarer species that attract most of the visitors to the area. Without these species the San Pedro ecosystem becomes less outstanding as a target for ecotourism.
- The warm and wet, and the warm and very wet climate change scenarios that were modeled did not have such adverse effects on the structure and representation of the riparian communities. Under these scenarios, increased or maintained river flows were projected to ensure the existence of seeding and sapling habitats for cottonwood and willow, thereby supporting the continued existence of the riparian forest.
- Recent anthropogenic changes in the riparian system have introduced factors that have not been included in this modeling exercise. Specifically, beaver have been re-introduced

to the system, and are apparently flourishing. It is too early to tell what effects these animals may have on the vegetation and geomorphology of the system. Nor is it possible at this stage to predict how beaver activity may interact with others stressors, such as climate change. However, it is possible that the activity of the beaver may help shift the riparian community back to a pre-20th century conditon where gallery forest was not so widespread and cienaga marshlands and ponds dominated the landscape.

SECTION 1. INTRODUCTION AND PROJECT BACKGROUND

This study examines the effects of climate change, land-use (population growth and groundwater pumping) and the combination of the two on the ability of the Upper San Pedro River to continue to support a healthy riparian ecosystem with its important ecological resources and supply valued ecosystem services. Our focus is on the riparian habitat for its biodiversity, especially that located within the San Pedro Riparian National Conservation Area (SPRNCA). The goal of the project is to assess how global change-related alterations in surface hydrology, subsurface hydrology, water quantity, water quality and seasonality may affect these systems. Through this project, an investigative, methodological framework will be developed that can be applied to similar basins elsewhere.

In the arid southwestern United States, riparian ecosystems are critical for sustaining regional biodiversity and supporting the existence of species that are now otherwise rare or restricted in their distributions within the U.S. (Naiman *et al.*, 1993; Noss *et al.*, 1995). They also typically support numbers of organisms that are disproportionate to their relatively limited spatial areas. For example, although riparian habitats comprise less than 1% of the western landscape, 82% of breeding bird species in northern Colorado occur in this habitat (Knopf, *et al.*, 1998); in Montana 89% of bird species exploit riparian habitats during their breeding seasons, while 36% are limited to these habitats (Mosconi and Hutto, 1981).

Historically, most rivers and riparian habitats in the U.S. have been severely degraded through flow diversion and dams, groundwater depletion, land use change, urbanization, overgrazing by livestock, contaminants, and other anthropogenic stressors (Stromberg *et al.*, 1996; Galbraith *et al.*, 1996; Knopf *et al.*, 1998; Mooney and Hobbs, 2000;). These stressors have also been responsible for highly fragmented distribution of riparian and riverine habitat. Climatic change may present a new challenge to conserving riparian habitats. Climate change may directly affect ecological resources, or it may interact with existing stressors in complex ways, potentially exacerbating or ameliorating their effects.

This report compiles and presents the results of research projects that focus on the potential effects of climate change, together with existing stressors, on the riparian ecosystems of the San Pedro River in southern Arizona. These studies examine important drivers of change in this system, which, because of its relatively unaltered condition and high levels of biodiversity, is a reference system for riparian areas of the Southwest, and projects potential ecosystem changes due to future climate change. This research was funded by U.S. EPA's Office of Research and Development.

This project employs a risk assessment approach as the process for achieving results (see the EPA's *Guidelines for Ecological Risk Assessment*, US EPA 1998) and will use the concept of "ecosystem services" to articulate specific objectives and project endpoints. The term "ecosystem services" describes both the conditions and the processes through which ecosystems sustain and fulfill human life (Daily 1997). Ecosystem services maintain biodiversity, produce goods, and perform life-support functions. Along the Upper San Pedro, ecosystem services include flood and drought alleviation, waste assimilation and purification capacity, and recreational opportunities – all revolving around the exceptional biodiversity in the Basin. In the Upper San Pedro riparian ecosystem the ecosystem services are not restricted to the immediate area but extend south into Mexico and Central America and north into Canada and Alaska.

These are the ecosystem services, including recreation, pollination, seed dispersal and pest control, provided by the migratory songbirds using the Upper San Pedro riparian ecosystem (SPRE) to refuel during their migratory journeys. The reason for employing the concept of ecosystem services in this project is that it enables individuals from a cross section of society (e.g., ecologists, economists, the general public) to express the values they hold for ecological processes or functions using a common language. Common expressions of value help frame analyses to produce information relevant to decision making. Translating changes in ecological functioning and processes into changes in ecosystem services also enables clearer communication of the effects of global change on ecosystems as a whole. Both social and ecological consequences may be captured and expressed using this concept.

1.1 The San Pedro Riparian Ecosystem and its Biodiversity Importance

The Upper San Pedro River riparian ecosystem (SPRE) in southeastern Arizona and northern Sonora (figure 1-1) contains one of the richest assemblages of species and supports one of the most important migratory bird habitats in western North America (Arias Rojo *et al.*, 1999). The biodiversity of the SPRE matches or exceeds that found almost anywhere else in the United States: more than twenty different biotic communities occur in the basin, and the river sustains three biotic types considered threatened - Fremont cottonwood/Goodding willow forests, cienegas and big sacaton grasslands (Figures 1-2 through 1-4). Vascular plant diversity is very high, with 608 species from 92 families identified within the SPRNCA alone (Makings in press). Among these is the Huachuca water umbel (*Lilaeopsis schaffneriana* spp. *recurva*), a federally endangered species. The SPRE is of critical importance in maintaining regional biodiversity at the ecotones between the Sonoran and Chihuahuan deserts and the Plains grassland.

The Nature Conservancy has recognized the high ecological value of the area through the designation of the upper San Pedro as one of the “Last Great Places”. Approximately 58,000 ha are protected along a 50-km reach of the river within the San Pedro Riparian Conservation Area (SPRNCA), administered by the U.S. Department of the Interior Bureau of Land Management (BLM).

The San Pedro River begins near the town of Cananea in the state of Sonora, Mexico and flows 240 km north through Arizona, to its confluence with the Gila River near Winkelman, Arizona (Arias Rojo *et al.*, 1999). Total drainage area is about 1900 km² at the border and about 12,000 km² at its confluence with the Gila River (Stromberg, 1998a). For most of its course, the San Pedro is a low elevation, low gradient (0.002-0.005 m/m) alluvial stream (Stromberg, 1998), with elevation ranging from 1300 m at the Mexican border to 586 m at the confluence of the Gila River, a distance of 198 km (Huckleberry, 1996). The river is typically divided into upper and lower reaches, with varying definitions. Typically, the upper San Pedro is considered the reach extending from the headwaters in Sonora, Mexico to a bedrock constriction near Benson known as the Narrows (Wood, 1997). Geomorphically, the upper San Pedro carries a mixed sediment load (suspended sediments and bedload) and has a relatively narrow, braided low flow channel, but a sinuous flood channel (floodplain) between arroyo walls. The sediment in the channel bed is coarser than in the arroyo walls. The lower San Pedro (downstream from the Narrows) is wider and less sinuous entrenched channel and is more of a bedload system (Huckleberry, 1996). Upland vegetation of the lower valley (north of Cascabel) is characterized by Sonoran desertscrub, while the upper valley is characterized by Chihuahuan desertscrub, with semi-desert grassland and Madrean evergreen woodland at higher elevations (Brown, 1994).

For its size, the area has one of the highest vertebrate diversities found anywhere in the United States. The SPRNCA has one of the highest bird diversities of any area of its size in the United States, with more than 350 recorded species (Kreuper, 1997), 250 of which are Neotropical migrants. Between one million and four million migrating songbirds use the riparian habitat annually as they move between their wintering grounds in Mexico and Central America and their breeding grounds in the United States and Canada (Arias Rojo *et al.*, 1999). Twelve bird species found annually on the SPRNCA have previously been classified by the State of Arizona as Wildlife of Special Concern, representing 41% of the bird species on that list. Of the 107 species on the 1988 Partners in Flight 'WatchList', 52 have occurred in the San Pedro Basin at least once and 19 of them either breed or winter in the area. Of the top scoring 45 species on Arizona Partners in Flight species of concern, 42 have occurred at least once in the basin and 25 occur annually (9 breed, 5 winter and 11 migrate through). The SPRNCA has been designated as critical habitat for the endangered Southwestern Willow Flycatcher. Additionally, a globally significant number of Western Yellow-billed Cuckoos, a species that groups have petitioned the USFWS to consider listing as a threatened or endangered species, breed along the San Pedro (Arias Rojo *et al.*, 1999).

The SPRNCA currently contains, or contained within the last 150 years, more than 80 species of mammals – for its area, one of the richest assemblages of land mammal species in the world. More than 40 species of reptiles and amphibians have also been found within the boundaries of the SPRNCA (Arias Rojo *et al.*, 1999). However, the fish population of the San Pedro River in the U.S. is impoverished with only 2 of 13 native species persisting. Many of the native fish species were eradicated during a spill of toxic pollutants from the Cananea mine in the Mexican reach of the river. Now that the quality of water has improved the USFWS considers the San Pedro River to be potential habitat for reintroduction of several endangered fish species (in Arias Rojo *et al.*, 1999).

The San Pedro watershed in Mexico is also considered 'regionally outstanding' for its biological values. Four major biotic communities have been identified in the watershed, supporting some 260 species of vertebrates of which 64 are considered threatened, endangered or rare. More than 117 species of birds have been identified in the area, with 16 listed under some protection status. Since 1970, there has been a notable decline in natural riparian habitat, particularly along reaches near the U.S. border (Arias Rojo *et al.*, 1999)

In the arid southwestern United States, riparian ecosystems are critical for sustaining regional biodiversity and supporting the existence of species that are now otherwise rare or restricted in their distributions within the U.S. (Naiman *et al.*, 1993; Noss *et al.*, 1995). They also typically support numbers of organisms that are disproportionate to their relatively limited spatial areas. For example, although riparian habitats comprise less than 1% of the western landscape, 82% of breeding bird species in northern Colorado occur in this habitat (Knopf, *et al.*, 1998); in Montana 89% of bird species exploit riparian habitats during their breeding seasons, while 36% are limited to these habitats (Mosconi and Hutto, 1981).

Historically, most rivers and riparian habitats in the U.S. have been severely degraded through flow diversion and dams, groundwater depletion, land use change, urbanization, overgrazing by livestock, contaminants, and other anthropogenic stressors (Stromberg *et al.*, 1996; Galbraith *et al.*, 1996; Knopf *et al.*, 1998; Mooney and Hobbs, 2000;). These stressors have also been responsible for highly fragmented distribution of riparian and riverine habitat. Climatic change may present a new challenge to conserving riparian habitats. Climate change may directly affect

ecological resources, or it may interact with existing stressors in complex ways, potentially exacerbating or ameliorating their effects.

This report compiles and presents the results of research projects that focus on the potential effects of climate change, together with existing stressors, on the riparian ecosystems of the San Pedro River in southern Arizona. These studies examine important drivers of change in this system, which, because of its relatively unaltered condition and high levels of biodiversity, is a reference system for riparian areas of the Southwest, and projects potential ecosystem changes due to future climate change. This research was funded by U.S. EPA's Office of Research and Development.

1.2 Ecosystem Services Provided by the SPRNCA

In this project, the concept of "ecosystem services" is used to articulate specific objectives and project endpoints. The term "ecosystem services" describes both the conditions and the processes through which ecosystems sustain and fulfill human life (Daily 1997). Ecosystem services maintain biodiversity, produce goods, and perform life-support functions.

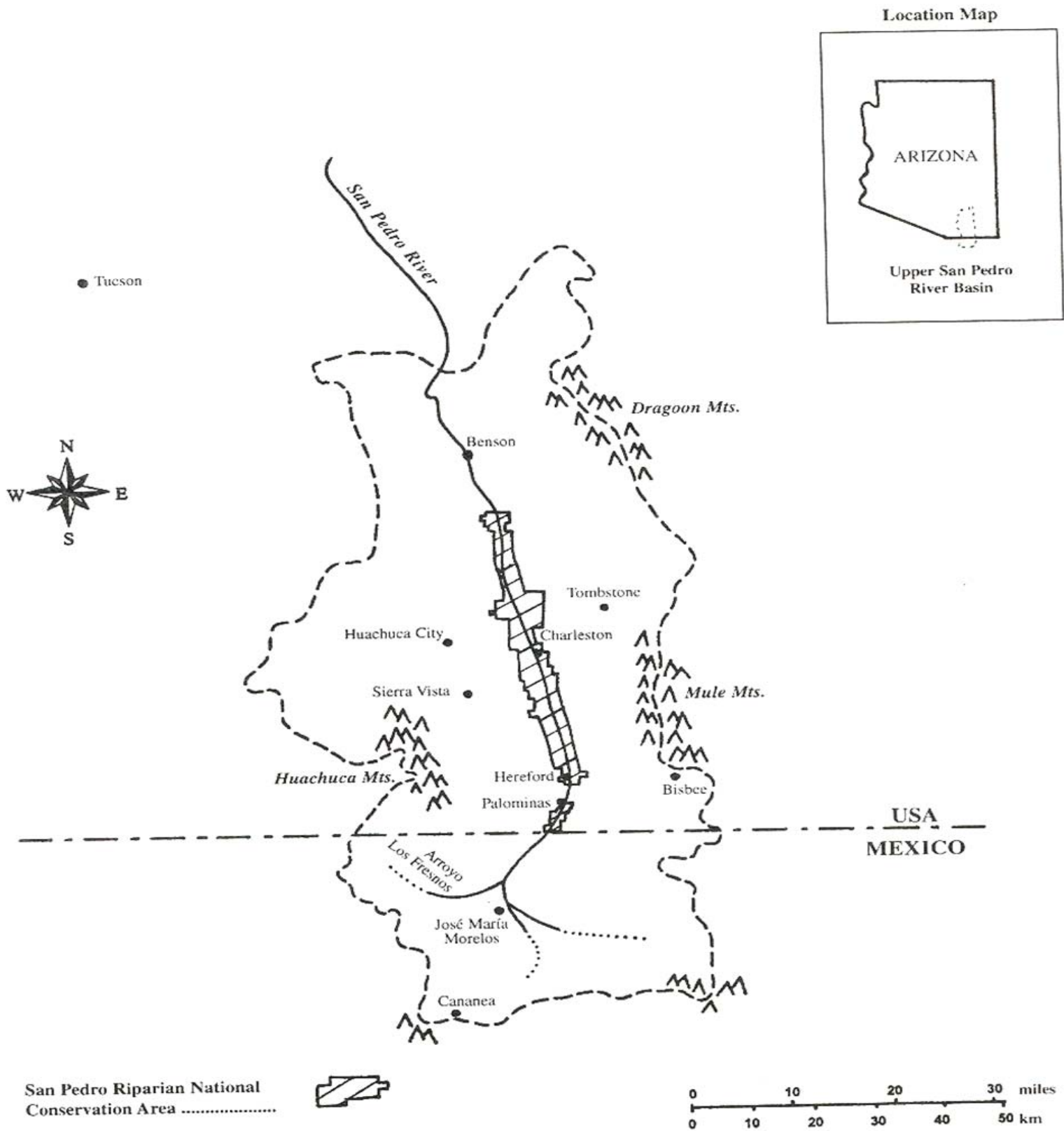


Figure 1-1. Map showing the location of the San Pedro River, the SPRNCA, and nearby cities



Figure 1-2. A general view of the SPRNCA looking south to Mexico.



Figure 1-3. The San Pedro River flowing through the SPRNCA and showing the cottonwood/willow gallery forest that adjoins the river.



Figure 1-4. Showing the ecotone in the SPRNCA between the riparian ecosystem and the sacaton grassland and mesquite scrub.

The principal service provided by the SPRNCA and addressed in this report is the support of important plant and wildlife habitat and the resulting biodiversity. Human residents and visitors to the area obviously regard this habitat-diversity relationship as being an outstanding service: the SPRNCA is nationally and internationally recognized for its birdwatching opportunities, one of the fastest growing recreational activities in the U.S. The watershed as a whole contains an additional 2-3 major and numerous minor birdwatching locations. In 1991, birdwatching was estimated to generate more than \$128 million in retail sales and supported more than 3800 jobs. Most birdwatching in Arizona occurs in the southeastern portion of the state and the San Pedro basin is one of the three major areas visited. Total tourism revenues within Cochise County were estimated at \$180 million annually. In the period 1991-1992, 11,700 tourists visited the San Pedro and 26,300 visited Ramsey Canyon, elsewhere in the watershed. This visitation was estimated to have led to direct expenditures in the area of \$1.2 million for a total economic impact of \$2 million. By 1997, the annual number of visitors to the SPRNCA had grown to an estimated 100,000 visitors. However, no new economic impact studies have been done. A site receiving similar visitation rates for similar purposes is Laguna Atascosa NWR in Texas. Total non-consumptive visitor-related expenditures at Laguna Atascosa in 1995 were approx. \$3.5

million for a local economic impact of \$6 million (Arias Rojo *et al.*, 1999). There is also a limited amount of consumptive uses of the SPRE for recreational fishing and some hunting.

Of equal or greater importance is the enhancement to the quality of life of local residents attributable to the river, its riparian vegetation and the bird life it supports. These values depend on the quality of the aquatic ecosystem. Marginal deterioration of a natural resource such as the SPRNCA imposes losses both to economic activity as well as to public values. Many individuals mentioned the river as an attribute contributing to their choice of living in the area.

In addition to the non-market value of the river (quality of life, riparian habitat, etc.) to local residents, an ecosystem such as the San Pedro services an area larger than it runs through. The birds migrating through the area to their breeding areas further north or their wintering areas further south provide ecosystem services (including recreation and pest control) to a much larger part of the U.S., Canada, and Central and South America. Application of wetland function valuation approach or a contingent valuation method could perhaps be used to estimate the non-market or willingness to pay value for the Upper San Pedro. Additionally consideration needs to be given to the function of the riparian ecosystem in carbon sequestration, of marsh vegetation in purifying the water and to regional cooling effects afforded by the transpiration of the vegetation (modified from Arias Rojo *et al.*, 1999).

1.3 Stakeholders and their Involvement

A fundamental component of this project was to engage the variety of stakeholders who have an interest and a role in helping to preserve the biodiversity of the Upper San Pedro riparian ecosystem, so they could aid in the analytic design, analysis, evaluation and interpretation of information. Stakeholders guided the selection and prioritization of analytic activities, helped establish project goals, shared expertise, and provided information in a variety of areas including public values, equity considerations, and relevant decision processes. Their continuous input about their information needs enhanced the relevance and credibility of results.

The San Pedro Climate Change Project was designed to be an adaptive project, able to make some changes in response to feedback from other researchers, landowners and conservation groups in the surrounding area. Unlike the Upper Chesapeake and San Francisco Bay watershed projects currently being studied under the auspices of EPA, the San Pedro is mostly important for its biodiversity and recreational values. The river provides no direct drinking water for surrounding communities, has no current livestock grazing in the primary area of the study, and only provides a limited amount of direct irrigation for agriculture just outside of the primary area of the study. Therefore, the main goal of the study is to investigate the impacts of climate change and land-use change on the biodiversity service of the riparian ecosystem and on potential 'downstream' ecological effects (e.g., reduction of bird populations breeding in the U.S. and Canada) relating to the biodiversity of the riparian ecosystem.

The limited number of primary ecosystem services being provided by the San Pedro riparian ecosystem also restricts, somewhat, the composition of the key stakeholder groups interested in the project. The initial analysis of stakeholder groups included -

Federal Agencies - Bureau of Land Management, National Park Service, Department of Defense, U.S. Forest Service, U.S. Fish and Wildlife Service

State Agencies - Arizona Game and Fish Department

Non-profit Organizations - Southeast Arizona Bird Observatory, The Nature Conservancy, Huachuca Audubon Society, American Bird Conservancy and Friends of the San Pedro.

In addition, The San Pedro Partnership, a group composed of representatives of various state, federal and municipal governments, and non-profit organizations, has been informally briefed on the study and kept informed of all major findings.

A meeting was held in year one of the study, attended by representatives of most of these groups. Stakeholder groups that did not attend the original meeting were contacted and briefed on the project. At this meeting and during subsequent conversations discussions were held concerning the overall endpoints of the study. These conversations helped to focus and narrow the scope of some the study as well as to identify the key species of interest to the stakeholder groups (see preliminary results).

1.4 Overview of Studies -

The primary goal of this suite of studies was to model the likely effects of climate change, coupled with existing stressors (agriculture, ranching, urbanization), on selected ecological services of the SPRNCA. Specifically, we evaluated the future ability of the SPRNCA to remain a high quality, self-sustaining riparian ecosystem able to continue to provide those ecological services that it currently provides.

Subsumed within the above overall objective are three connected “sub-objectives.” These were to evaluate how:

- Existing stressors and changes in the climate in the SPRNCA will likely affect the hydrologic conditions that determine the structure and composition of vegetation communities
- Existing stressors and climate change may affect the structure, composition, and representation of vegetation communities in the SPRNCA
- Changes in the SPRNCA vegetation communities under climate change will affect their ability to continue to support important ecological resources (riparian vegetation communities, aquatic biota, amphibians and reptiles, mammals and birds).

Modeling approaches, coupled with field data, were used to address each of these research objectives. These approaches and their results are described in the main body of this report.

1.5 Report structure

The remainder of this report comprises 6 main sections. In Section 2, the main ecological drivers and stressors of the SPRE are identified and discussed. In Section 3 the methods used, and the results of, the vegetation modeling are presented. In Section 4, the approaches to analyzing the effects of climate change on biodiversity, including translating projected vegetation changes into effects on selected bird species and avian communities and biodiversity, are described. Section 5 briefly discusses the implications of the projected vegetation and wildlife changes on the main ecosystem service provided by the SPRNCA – support of wildlife habitat and biodiversity.

SECTION 2. HYDROLOGY, STRESSORS, HISTORICAL CHANGE AND BIODIVERSITY IN THE SAN PEDRO RIPARIAN ECOSYSTEM

This section of the American Bird Conservancy report identifies the main climatic and geophysical drivers of the condition and quality of the San Pedro riparian ecosystem, particularly in the SPRNCA, and discusses how these have changed, and the ecological changes that they have set in train, over the last century. It is intended to set the context for the specific studies that are described in the remainder of the report. It also describes past and recent changes in the main anthropogenic stressors on the system – agriculture and local population growth and their demands on the hydrology of the system.

2.1 Climate

The current climate in the SPRNCA is generally considered semiarid, with temperatures exceeding 100° F in the summer to occasional lows below freezing in the winter. Precipitation in the basin averages from between 9” and 25” per year and falls in a bimodal pattern. Winter precipitation, accounting for approximately 30% of the total, usually falls in the form of steady rains brought in by storms from the Pacific Ocean. The bulk of the precipitation, 70%, falls in summer from convective thunderstorms, known as monsoons. Summer precipitation is highly variable with some areas receiving a great deal of rain while nearby areas may receive none. Fall and spring are both usually dry. Overall the amount of precipitation increases and the average temperature decreases at the higher elevations in the watershed.

Year-to-year and multi-decadal variability in winter precipitation related to the El Niño Southern Oscillation (ENSO) and the Pacific Decadal Oscillation (PDO) has a strong influence on ecological dynamics in the region. Periods of high winter rains in El Niño years also have a strong influence on the occurrence of winter floods.

Spatial and temporal variability in water availability affect the dynamics of ecosystems in the region. Recent changes in climate have had a strong influence on riparian ecosystems, with wetter conditions since about 1960 resulting in an increase in the frequency of winter floods and recruitment opportunities by pioneer riparian trees. This period roughly corresponds to the positive (warm) phase of the Pacific Decadal Oscillation that occurred from 1976-1998, during which El Niño events were more frequent than previously. In the last 5 years, however, the climate system may have transitioned to a drier phase with the juxtaposition of a negative (cool) Pacific Decadal Oscillation (PDO) and a positive (warm) Atlantic Multidecadal Oscillation (AMO), a configuration that last occurred during the mega-drought of the mid-1950s.

2.1.1 Future Climate Change

Climate change projections for the Southwest Region of the United States suggest an increase in mean seasonal temperatures of 2-7 ° C over the next 100 years. All climate change models agree in this regard. However, climate models used in the Southwest Region Assessment differ in their projections for precipitation, with the Canadian Climate Centre model and the Hadley 2 model projecting strong increases in winter precipitation, and the Regional Model by the National Center for Atmospheric Research (NCAR) suggesting a decrease in winter precipitation. Thus, the general consensus about future climate conditions in the study area is that it will be significantly hotter, but that it may be wetter, drier or similar to current conditions. This

precipitation change uncertainty is important in projecting future ecological change. Therefore, the climate change scenarios on which our vegetation modeling is based are designed to capture and reflect this range of potential precipitation outcomes (Section 3).

2.2 Hydrology

A hydrological system can be thought of in terms of its inputs and outputs, while a pristine system can best be thought of as being in a state of dynamic equilibrium: over time the amount of water leaving the system is offset by water entering the system. In many systems this in-stream flow is primarily caused by run-off. While there is some seasonal run-off in the San Pedro River, the majority of the flow in the river actually comes from the groundwater aquifer. The primary regional aquifer for the San Pedro River is made up of upper and lower alluvial units in direct hydraulic connection with each other. The floodplain aquifer beneath the San Pedro is long, narrow, and shallow, with a thickness ranging from more than 150' to non-existent in areas where bedrock is close to the surface. Fed by this aquifer, the San Pedro River is generally perennial between Hereford and Charleston. From Charleston to Redington, streamflow conditions are largely governed by the surrounding geology. In general, flow in the San Pedro is intermittent from the 'Narrows' downstream to Redington. Much of the base flow in the San Pedro River comes from the floodplain aquifer – the perennial flow being largely due to the groundwater discharging to the stream (Goode and Maddock, 2000).

The primary sources of recharge for this aquifer are mountain front recharge and excess irrigation water trickling down to the groundwater. Mountain front recharge includes all of the waters draining down off of the mountains surrounding the watershed. This includes both direct flows from tributaries, but is mainly from water percolating down into the alluvial layers (Goode and Maddock, 2000). There may also be some recharge from wetlands built at the Sierra Vista sewage ponds but this recharge has not been quantified (Arias Rojo *et al.*, 1999). In general the amount of recharge is calculated as the amount of precipitation minus the evapotranspiration of the plants.

Evapotranspiration from the riparian vegetation is one of the natural water users of system and needs to be factored in to any hydrologic balance. Evapotranspiration is important not only from the riparian vegetation that supports the ecosystem services in the SPRNCA, but also from vegetation in the watershed and on the uplands along the river that capture some of the mountain front recharge.

Pumping disrupts the natural balance in the system as an additional discharge and should be considered the primary stressor in the San Pedro River Ecosystem. The amount of water pumped from the aquifer supporting the San Pedro riparian ecosystem has increased dramatically in the last 50-60 years. From small amounts of pumping (<25,000 m³/day) in 1940, the amount of water pumped from the aquifer has increased to >200,000 m³/day over the period 1976-1985, a level of intensity that continued into 1997 (Goode and Maddock, 2000). Much of this water is pumped for agricultural use. While there is some return of water to the aquifer via percolation, on average 70% of the water used for agriculture is lost. Basin wide, the amount of land in irrigation has remained fairly constant since the creation of the SPRNCA in 1988. While some wells near the river have been retired, others have been put into service. The amount of water used for irrigation has increased from <20,000 m³/day in 1940-41 to between 100,000-120,000

m³/day for the period of 1985-1997. Agriculture is the largest user of water on the U.S. side of the border.

Other users of water on the U.S. side of the river are municipal water supply wells (500 m³/day in 1940-41 increasing to 29597 m³/day in 1997); other domestic water wells (<500 m³/day in 1940-41 to >3500 m³/day in 1997); stock wells (<1000 m³/day in 1940-1941 to >10,000 m³/day in 1997; declining since 1989) and some military and industrial use (Goode and Maddock, 2000). On the Mexico side of the basin, pumping estimates are harder to come by. Pumping for domestic use has been estimated at only around 90 m³/day. The largest user of water in the Mexico portion of the watershed is the mine at Cananea. Groundwater pumping at the mine peaked at 50,000 m³/day in 1990 falling off to a little over 30,000 m³/day in 1997. There has also been some agricultural pumping along the river but it does not seem to be a regular occurrence at this time (Arias Rojo *et al.*, 1999).

Results projected by hydrological models for the years 1940- 1997 show that the levels of anthropogenic water use described above have resulted in: 1) a reduction in streamflow in the San Pedro River; 2) a reduction in evapotranspiration by riparian vegetation along the floodplain of the San Pedro River; and 3) the formation of significant cones of depression near many communities with accompanying large losses of groundwater storage. Depletion in base flows of the San Pedro River is most noticed around Benson (Figure 1-1) where many reaches are now dry. Overall, nearly 20% of the water pumped in the San Pedro basin was taken from the river. Since 1940 the perennial flow in the river near Charleston (Figure 1-1) has been reduced by more than 30%. Another 15% of the water pumped in 1997 was taken from evapotranspiration thus affecting the riparian vegetation in the SPRE (Goode and Maddock, 2000).

2.2.1 Hydrology and Vegetation

The biodiversity and health of the San Pedro riparian ecosystem is strongly influenced by the hydrologic regime of the river – both its timing and overall flow as determined by surface and groundwater flows. Critical components of surface flows for riparian biota include low flows (base flows) and high flows (flood flows). Base flows are the major source of water for the ecosystem during the driest part of the years. Declining base flows are usually indicative of declining groundwater levels. Flood flows are also important for establishment of new vegetation and act to recharge the shallow alluvial aquifer (Arias Rojo *et al.*, 1999).

The lowest stream flows in the San Pedro River occur from April to June. During this time, the base flows come primarily from groundwater and are essential for the survival of riparian species. While some species can tolerate the intermittent loss of stream flow, many require perennial flow. This period of low flows also occurs when birds are migrating through and when they are establishing breeding territories. Thus, flows in the river during the driest times of the year are vital.

As water availability changes, the composition and abundance of riparian and aquatic communities also change. The composition of the riparian plant community changes as the depth to groundwater changes, because of differences between species in rooting depth, drought tolerance and saturation tolerance (Stromberg *et al.*, 1996). Perennial flows are also necessary to support aquatic plants, fish and some aquatic invertebrates, while floodplain soils underlain by shallow groundwater (mean depths of less than 0.25 m below the surface) are necessary to support obligate wetland herbaceous marsh plants. Groundwater becomes inaccessible to most

herbaceous species at depths approaching five meters. Of the trees in the riparian ecosystem, Goodding willow, *Salix goodingii*, and Fremont cottonwood, *Populus fremontii*, require the shallowest groundwater level (Stromberg, 1998). Seedlings require the groundwater table to be within 0.5 and 1.5 meters of the surface. High quality stands of these species grow primarily in areas where the depth to groundwater is less than three meters, although some will grow in areas with a depth to groundwater of 5 m (in Arias Rojo *et al.*, 1999).

Permanent declines of groundwater of more than one meter have been observed to lead to a loss of vigor and eventual death of Fremont cottonwoods (Stromberg *et al.*, 1996). However, the introduced species salt cedar flourishes in these conditions, often replacing cottonwoods as the soil becomes drier. In the perennial reaches of SPRNCA, cottonwoods are healthy and depth to groundwater typically fluctuates by less than 0.5 m. At the north and south ends of SPRNCA the ecosystems are less healthy; signs of drought stress have been noted in the vegetation and groundwater levels have fluctuated by 0.5-1 meter and occasionally by two meters (Stromberg *et al.*, 1996).

2.3 Human Population Growth

The human population of the land adjacent to the San Pedro River has grown dramatically in recent decades. The population of Sierra Vista, the largest city near the Upper San Pedro grew from 24,937 in 1980 to 41,325 in 1999. Since 1990, the population in the area has grown by 23.3% and the current average is a growth rate of 2.4% a year. The University of Arizona, in strategic planning for a campus in the area, estimates a continued growth of 2% a year for the foreseeable future. Much of the growth and water-use affecting the river comes not from Sierra Vista but from the unincorporated areas of the county around the SPRNCA. Between 1960 and 2000 the population in Cochise County grew from 55,039 to 117,755 (U.S. Census data). Projected growth for the county as a whole is for a population of 160,049 by 2030 and 174,556 by 2050 (Pima Association of Governments). Not all of this growth will be in areas potentially impacting the SPRNCA, as it also includes the cities of Benson, Willcox and Bisbee. While agricultural water use in the area is expected to decrease over the next few decades, the amount of urbanized land and concomitant water use will grow rapidly.

Historically, the principal user of water in the U.S. side of the basin has been agriculture. However, this use has a relatively low return per unit of water as the water is typically used for low value crops such as pasture and alfalfa. The loss of economic activity from retiring agricultural pumping is estimated to be less than \$1 million while the economic benefit of ecotourism in the same area is estimated to be more than \$6 million per year (Arias Rojo *et al.*, 1999).

2.4 Geomorphological and Ecological Changes along the San Pedro River

The SPRE has changed over time, in responses to changes in climate, land use, fire and flood regimes, species introductions and losses, and other human influences. The journals of early explorers describe the watershed as being composed of grasses tall enough to hide a man on horseback and the river bottom as a broad marsh full of beaver and fish (Arias Rojo *et al.*, 1999).

Sometime between the 1850s and the turn of the 20th century a major episode of arroyo cutting occurred lowering the channel several meters below the floodplain surface (Hastings, 1959). This was likely due to several factors including extreme climatic events (including several large floods), deforestation, water diversions and overgrazing by livestock (Bahre, 1991, Tellman *et al.*, 1997). This led to changes in the biotic character of the river with the loss of much of the marshland vegetation (Hendrickson and Minckley 1984). Mesquite brushlands also became more common in the surrounding watershed.

The widespread channel incision and entrenchment of the late 19th and early 20th centuries may exert a strong influence on current geomorphology and riparian vegetation on the San Pedro and other rivers in the region. The pre-entrenchment (pre-1850) San Pedro appears to have been shallow and marshy, with longer reaches of perennial flow, and the vegetation a mosaic of riverine marshlands (cienegas), sacaton grasslands, and more scattered riparian woodlands of cottonwood, willow, and ash (Arias Rojo *et al.*, 1999). Degraded range conditions, coupled with large floods, led first to episodes of severe channel down-cutting (incision), followed by entrenchment and formation of a wide, braided river channel. In the upper San Pedro, channels incised 1-10 m (1-5 m upstream from Lewis Springs and 5-10 m downstream). Near Hereford, entrenched channel widths increased from 25-40 m in the early 1900s to around 80-100 m or more in the late 1930s. Enlargement of the entrenched channel (floodplain) slowed beginning in the 1950s, with total floodplain area relatively stable since the 1970s, suggesting that channel processes may have reached a dynamic steady state. Since the 1950s, flood magnitude has declined and rates of fluvial disturbance have slowed, allowing vegetation colonization, channel narrowing, and formation cottonwood-willow gallery forest on a new, inset floodplain within the entrenched channel banks. Most of the present cottonwood and willow forests originated in the 1960s and 1970s, with narrower bands of recruitment since then. This suggests that rates of channel migration and pioneer tree recruitment may have declined in recent years as the channel has narrowed and the banks have become stabilized with riparian vegetation.

A few pockets of Fremont cottonwood dating back at least 1900 have persisted on the old floodplain (Stromberg 1998). Some of the current cottonwood-willow forest lining the channel banks throughout much of the area expanded in the new floodplain between 1900-1950. However, most cottonwoods seen today were established in the 1960s and 1970s. Some cottonwoods have become established in the 1980s and 1990s but these cover a much smaller area. Riparian vegetation along the San Pedro approximately doubled in acreage from the 1930s to the 1960s (Arias Rojo *et al.* 1999). There has been very little increase in overall riparian area since 1966 and current estimates are that it probably will not increase much more. In Mexico, loss of riparian vegetation has been severe between 1970 and 1992. Increase in brush, especially mesquite, is pronounced. Introduction of invasive exotic plant species has also influenced portions of the SPRNCA. Salt cedar, *Tamarix chinensis*, native to Eurasia, was introduced in the 1800s and has become abundant on parts of the river since about the 1960s, especially in those areas that can no longer support cottonwood-willow forests (Stromberg 1998).

Since the 1850s, riparian vegetation has changed considerably along the upper San Pedro River. Riverine marsh/cienega, once a dominant cover type, has declined considerably, likely due to reductions in stream flow permanence, drops in alluvial groundwater that accompanied channel incision, and the extirpation of beaver. Riparian forests and shrublands dominated by cottonwood, willow, or tamarisk have increased in area, with present-day forest vegetation occupying the inset floodplain formed from narrowing of the previous wide, entrenched channel. Coverage and productivity by sacaton (*Sporobolus wrightii*) grasslands have declined throughout

the region. Coverage by mesquite coverage may have increased, particularly in upland areas. Fire appears to have increased in importance along the San Pedro over the last decade, perhaps linked to increases in fine fuel since the removal of grazing in 1988 and increased plant productivity from wet winters associated with El Niño events. These fires may be reducing coverage by woody species and increasing grassland area. Finally, increases in groundwater pumping in the basin since the 1940s have reduced alluvial groundwater levels and decreased baseflow along portions of the upper San Pedro.

SECTION 3. PROJECTING THE EFFECTS OF ENVIRONMENTAL CHANGE ON RIPARIAN VEGETATION IN THE SPRNCA

3.1 Introduction

Riparian areas function as keystone elements of the landscape, having a functional importance that far exceeds their proportional area. Ecosystem services provided by riparian areas include their roles as buffers controlling lateral movements of pollutants or sediments between aquatic and terrestrial environments, corridors for facilitating longitudinal movement of organisms or materials across the landscape, and highly productive habitats that are often hotspots for biodiversity (Naiman *et al.*, 1993, Naiman and Decamps, 1997). In the southwestern United States, riparian habitats are particularly important for sustaining regional biodiversity, with a large proportion of species dependent on riparian systems (Patten, 1998). Southwestern riparian systems may have an important influence on continental diversity of Neotropical migrant birds, providing critical migratory corridors and stopover habitats through an otherwise arid region (Skagen *et al.*, 1998). Finally, as ecotones between terrestrial and aquatic ecosystems, riparian zones may be highly sensitive indicators (but see Grimm *et al.*, 1997) or integrators of environmental change in the watersheds within which they occur (Decamps, 1993). Because of their position at the land-water interface, riparian zones are potentially impacted by environmental changes that occur anywhere within the watershed. Watershed level changes in hydrologic processes (e.g., runoff, groundwater recharge, evapotranspiration) hence may inflict a particularly strong imprint on the structure and function of riparian zones.

Watersheds and riparian systems of semi-arid to arid regions, such as the southwestern United States, should be particularly sensitive to environmental changes that influence hydrologic processes. Water is a limiting resource in the Southwest, both for natural ecosystems and for humans, presenting an important challenge for balancing economic development and the conservation of native ecosystems. The majority of riparian and river systems in the desert Southwest have been strongly degraded through a variety of anthropogenic stressors, including flow diversion and dams, groundwater depletion, land use change, urbanization, and overgrazing by livestock (Tellman *et al.*, 1997, Patten, 1998).

New challenges exist with the increasingly recognized effects of anthropogenically-induced climatic change. General Circulation Models of the climate system project large changes in temperature and precipitation patterns over the next 50-100 years as a result of accelerated accumulation of greenhouse gases in the atmosphere, largely from the burning of fossil fuels (SRAG, 2000, Houghton *et al.*, 2001). There is increasing evidence that global and regional climate has changed over the last 100 years, particularly since the 1950s. Climatic change may interact with other stressors in complex ways, potentially exacerbating the effects of some stressors or ameliorating the effects of others. However, the diversity of stressors impacting southwestern riparian systems, climatic change, and the inherent variability in historic climatic conditions make the effects of individual stressors, or even “naturally” versus “anthropogenically” induced changes, difficult to separate (Grimm *et al.*, 1997).

This report reviews some of the important drivers of change in southwestern riparian systems and projects how riparian vegetation community structure and function might be affected by changes in climate, land use, and water consumption within the basin of the San Pedro River. In addition to reviewing the literature on southwestern riparian systems, this report also examines the implications of several plausible climate change scenarios for riparian vegetation dynamics,

using a simulation model developed and parameterized for the upper San Pedro. The San Pedro is presented as a case study because of the availability of data on the factors influencing ecological structure and function for the system, the high species richness and biological value of the area, the high ecological integrity of the system compared to other southwestern watersheds, and the array of factors that challenge the long-term sustainability of the system.

3.1.1 Study site: San Pedro River and SPRNCA

The San Pedro is one of the few low-elevation rivers of its size in the desert Southwest that contains significant reaches of perennial flow and is not regulated by dams. These characteristics support a lush riparian corridor with gallery forests of cottonwood and willow on perennial reaches. The presence of this riparian corridor within this arid landscape provides critical migratory and breeding habitat for many bird species, as well as habitat for a high diversity of mammals, reptiles and amphibians, butterflies, and other animals (Arias Rojo *et al.*, 1999). The Nature Conservancy has recognized this high ecological value through the designation of the upper San Pedro as one of the “Last Great Places”. Approximately 58,000 ha (Steinitz *et al.*, 2003) are protected along a 50-km reach of the river within the San Pedro Riparian Conservation Area (SPRNCA), administered by the U.S. Department of the Interior Bureau of Land Management (BLM). Protection began in 1988 (Yunceovich, 1993) in recognition of the significant biological resources that exist in the river corridor.

The San Pedro River begins near the town of Cananea in the state of Sonora, Mexico and flows 240 km north through Arizona, to its confluence with the Gila River near Winkelman, Arizona (Arias Rojo *et al.*, 1999). Total drainage area is about 1900 km² at the border and about 12,000 km² at its confluence with the Gila River (Stromberg, 1998a). For most of its course, the San Pedro is a low elevation, low gradient (0.002-0.005 m/m) alluvial stream (Stromberg, 1998a), with elevation ranging from 1300 m at the Mexican border to 586 m at the confluence of the Gila River, a distance of 198 km (Huckleberry, 1996). The river is typically divided into upper and lower reaches, with varying definitions. Typically, the upper San Pedro is considered the reach extending from the headwaters in Sonora, Mexico to a bedrock constriction near Benson known as the Narrows (Wood, 1997). Geomorphically, the upper San Pedro carries a mixed sediment load (suspended sediments and bedload) and has a relatively narrow, braided low flow channel, but a sinuous flood channel (floodplain) between arroyo walls. The sediment in the channel bed is coarser than in the arroyo walls. The lower San Pedro (downstream from the Narrows) is wider and less sinuous entrenched channel and is more of a bedload system (Huckleberry, 1996). Upland vegetation of the lower valley (north of Cascabel) is characterized by Sonoran desertscrub, while the upper valley is characterized by Chihuahuan desertscrub, with semi-desert grassland and Madrean evergreen woodland at higher elevations (Brown, 1994).

Although perennial flow likely occurred over most of the river in the past (Arias Rojo *et al.*, 1999), it is now spatially discontinuous. Perennial reaches occur where baseflow is sustained by regional groundwater inputs to the alluvial aquifer (Arias Rojo *et al.*, 1999; Pool and Coes, 1999; Goode and Maddock, 2000). Most perennial reaches occur on the upper San Pedro, north of the Mexican border and south of Benson, Arizona. Flow is intermittent in Mexico and near the Mexican border in the U.S., is perennial between Hereford and Charleston, and is intermittent again downstream from Charleston. Downstream of Benson, there are several reaches with perennial flow but most of the river is intermittent, owing to the underlying geology, two flow

diversions (Pomerene canal and St. David's Ditch) near St. David, and to groundwater pumping for agriculture, domestic use, and mining.

The perennial flow and shallow groundwater along much of the upper San Pedro supports thriving riparian vegetation communities, including regionally threatened vegetation types like Sonoran cottonwood-willow (*Populus fremontii* – *Salix gooddingii*) gallery forest, riverine marsh or cienega, mesquite (*Prosopis velutina*) woodland or bosque, and sacaton (*Sporobolus wrightii*) grassland. Maintenance of the cottonwood-willow forests, in particular, is viewed as critical for sustaining the high biodiversity of the riparian corridor. Several endangered plant and animal species, a high diversity of mammal, reptile and butterfly species, and around 390 bird species have been found along the upper San Pedro (Arias Rojo *et al.*, 1999; Kreuper *et al.*, 2003).

Groundwater pumping for agricultural, industrial, and domestic use has formed cones of depression in the regional aquifer around the growing communities of Sierra Vista – Huachuca City and Benson. Hydrologic studies suggest that this local depletion of the regional aquifer may threaten alluvial aquifer levels (Arias Rojo *et al.*, 1999; Goode and Maddock, 2000; Steinitz *et al.*, 2003) by reducing the gradient in hydraulic head from the recharge zone (west side) across the valley toward the river. Modeling studies suggest an annual overdraft (pumping minus recharge) of approximately 7000 acre-feet in the Sierra Vista sub-basin and declines in river baseflow have occurred since 1940 at Palominas and Charleston (Arias Rojo *et al.*, 1999; Goode and Maddock, 2000; Pool and Coes, 1999). Declines in the alluvial aquifer of the San Pedro could reduce surface flow frequencies and lead to “terrestrialization” of riparian communities, such as complete loss of riverine marsh habitat and conversion of cottonwood-willow forests to exotic saltcedar (*Tamarix chinensis*) shrublands, or even xeric native shrublands (*Hymenoclea*, *Ericameria*, *Acacia*, *Prosopis*) (Stromberg *et al.*, 1996).

3.1.2 Climate of the Southwest

Any discussion of the effects of climate change must begin with an understanding of the current climate of the Southwest and recognition of its inherent variability (Sheppard *et al.*, 2002). As a semi-arid to arid region, the energy available to evaporate water (potential evapotranspiration) greatly exceeds the inputs of water via precipitation, on an annual basis (Patten, 1998). However, there are critical periods of time when delivery of water temporally exceeds evapotranspiration, and when water can be stored in less labile reservoirs. Hence, the magnitude and seasonality of precipitation events strongly influences the temporal availability of water. Ecologically (and hydrologically) important variation in temporal availability of water occurs over daily, seasonal, annual, and multi-decadal time scales (Sheppard *et al.*, 2002). In addition, there is spatial variability across the region in the seasonality and magnitude of precipitation seasonality and in potential evapotranspiration. The combination of spatial and temporal variability in water availability, along with other physical controls and biogeographical legacies, and human land use patterns strongly affects the broad and fine scale patterning of ecosystems in the region (Brown, 1994). For example, the four major desert biomes in the region (Great Basin, Mojave, Sonoran, and Chihuahuan) are characterized by differences in the relative frequency and magnitude of winter rains and summer rains.

Ecological dynamics in the Southwest correspond to precipitation-defined and temperature-defined seasons. In Arizona, the period of April – June (pre-monsoon season) constitutes the beginning of the growing season for most perennial plant species, but is typically very dry. During July-September (monsoon season), locally heavy convective precipitation may occur, derived from moisture from the Gulf of California, eastern Pacific, and Gulf of Mexico

(Sheppard *et al.*, 2002). The months of October and November typically comprise a relatively dry, and cooler, post-monsoon season. However, large precipitation events associated with dissipating tropical storms from the eastern Pacific occasionally occur during late summer and fall. Finally, the winter and early spring form a cool rainy season, with more widespread, longer duration frontal rains derived from moisture in the eastern Pacific (Graf, 1985; Webb and Betancourt, 1992; Huckleberry, 1994).

The relative importance of summer (monsoon) and fall/winter precipitation varies temporally according to variations in atmosphere-ocean circulation patterns and spatially along a geographic gradient from west to east. During positive phases (El Niño) of the El Niño Southern Oscillation Index (ENSO) associated with warmer sea surface temperatures (SSTs) in the equatorial Pacific, moisture-laden winter frontal systems from the Pacific are steered eastward over the Southwest, leading to higher winter precipitation and cooler winter temperatures. In contrast, during the negative phase of ENSO (La Niña), drier and warmer winter conditions occur in the Southwest, while wetter conditions occur in the Pacific Northwest (Andrade and Sellers, 1988; Webb and Betancourt, 1992; Hamlet and Lettenmaier, 1999; SRAG, 2000; Sheppard *et al.*, 2002). Further, the relative frequency and strength of El Niño and La Niña events appears to be modulated by conditions associated with the Pacific Decadal Oscillation (PDO), a lower frequency climatic cycle connected with sea surface temperatures in the upper Pacific (Mantua *et al.*, 1997). Under positive (warmer) values of the PDO index, El Niño conditions are more frequent, while under negative conditions, La Niña conditions predominate (Sheppard *et al.*, 2002). Phases of the PDO appear to last about 20-30 years. From approximately 1976 to 1998, positive PDO conditions occurred and the Southwest experienced a time of enhanced winter precipitation and winter floods. Since about 1998, negative values of the PDO index have predominated, perhaps signally a shift to drier conditions in the region. There is also evidence that interdecadal cycles in the north Atlantic (Atlantic Multidecadal Oscillation, AMO) may have an important influence on the timing of severe droughts in the Southwest and other parts of the country, with periods of particularly severe drought coinciding with the joint occurrence of a negative PDO and a positive AMO (McCabe *et al.*, 2004). This climatic configuration (-PDO and +AMO) occurred during the prolonged drought of the 1950s and is occurring at the beginning of the 21st century (from 1998-present).

As with precipitation regimes, flood regimes in the region may be best understood as a mixed population of floods of different seasonality and of different types of climatic drivers, whose absolute and relative frequency changes under different sets of large-scale climatic regimes. On the Santa Cruz River near Tucson, the proportion of annual floods occurring in fall or winter has increased since 1960, while fewer annual floods have occurred in the summer (Webb and Betancourt, 1992). Strong differences emerge if the flood series is partitioned by ENSO conditions, with 100-year floods during El Niño years twice the magnitude of the 100-year flood in other years. During 1960-1986, floods on the Santa Cruz of 10-year return interval or greater were dominated by dissipating tropical cyclones, with an estimated 100-year return flood of 1660 cms and 6 of the 7 largest floods in the historic record for the basin. In contrast, 1930-59 was dominated by monsoonal (summer) floods and had an estimated 100-year return flood of 323 cms. The annual peak flow occurred in winter or fall in just 3% of the years between 1930 and 1959, 39% of the years 1960-86, and 53% of the years before 1930. A higher proportion of floods are generated by frontal cutoff low-pressure systems and tropical cyclones during meridional circulation patterns, such as those that occurred between 1960 and 1986 (Webb and Betancourt, 1992; Huckleberry, 1994). Although changes in precipitation regimes have not been as clear-cut on the nearby San Pedro (Hereford, 1993), there has been a similar increase in the

frequency and magnitude of winter floods since the 1960s, along with a possible decline in the magnitude of summer monsoonal floods and annual flood peaks (Hereford, 1993; Arias Rojo *et al.*, 1999).

The upper San Pedro occurs at the ecotone between Chihuahuan and Sonoran climatic conditions and plant communities, with summer rains making up a larger proportion of the annual precipitation and floods in most years, but with winter rains producing ecologically and geomorphically significant floods in El Niño years. Climatic conditions along the San Pedro also vary spatially, with a more “Sonoran” climate (35% summer, 65% winter precipitation), characterized by a higher proportion of winter rainfall, at the north (lower) end of the basin and a more “Chihuahuan” climate (60% summer, 40% winter precipitation), characterized by a higher proportion of summer rainfall, at the southern (upper) end of the basin (Skirvin *et al.*, 2000). Upland vegetation patterns follow climatic patterns, with Sonoran desertscrub dominating the lower basin (below Cascabel) and Chihuahuan desertscrub in the upper basin (Brown, 1994).

Recent Climatic Change

The high temporal variation in precipitation from year to year and decade to decade makes characterization of a typical climatic regime difficult, if not impossible. Based on tree ring records, the last 100 years may have included both the 3rd worst period of drought (1950s drought, especially 1956) and the 3rd wettest period (1976-1995) in the last 1000 years (J.L. Betancourt, seminar at Arizona State University, 2003). The period from 1976 to the late 1990s was characterized in particular by warm, wet winters and variable summer precipitation, with unprecedented high rates of tree-ring growth at higher elevations (Swetnam and Betancourt, 1998). Severe drought appears to be cyclical, with a return time of approximately 80 years (SRAG, 2000). The most prolonged drought of the last 300 years may have ended at the beginning of the 20th century (1840-1905). As suggested above, the late 1990s may have ushered in another dry period, with the same climatic configuration associated with the 1950s megadrought, but with higher temperatures (McCabe *et al.*, 2004).

Overall, there appears to have been an increase in annual mean temperature of 1.1-1.7° C across the region (as defined by the Southwest Regional Assessment) over the last century (SRAG, 2000). Significant changes in precipitation also occurred, but varied by region, with increases in southern Nevada, Utah, New Mexico, and central Arizona, and decreases in southeastern California, southern Arizona, and the central Rockies.

Projecting Future Climatic Change

Projections from three climate models were presented by the Southwest Regional Assessment of the U.S. Global Change Program (SRAG, 2000) for the region encompassing Colorado, Utah, Nevada, New Mexico, Arizona, and southeastern California (Table 3-1). These were the Hadley 2 Model (Hadley Centre for Climate Prediction and Research, United Kingdom Meteorological Office), the model from the Canadian Centre for Climate Modeling and Analysis, and NCAR (National Center for Atmospheric Research) Regional Model (Giorgi *et al.*, 1998; Doherty and Mearns, 1999; Mearns *et al.*, 1999). The Hadley and Canadian models utilize a coarse grid cell size (about 350 km on a side) and project a 1% annual increase in atmospheric CO₂ concentrations, with a doubling of pre-industrial CO₂ levels by about 2060. The NCAR model was designed for finer scale, regional projections. Projections of the NCAR Regional Model are

made for the climate under a doubling of pre-industrial CO₂ levels and hence should be comparable to the Hadley and Canadian projections for 2060.

Projections from the Hadley and Canadian Climate Centre models suggest that the Southwest region will experience significant warming, and along with it, increases in precipitation over the next 60-90 years (SRAG, 2000). Seasonal mean temperature increases across the region are projected at 1.5-4° C by 2060, and up to 7° C for winter temperature by 2090 under the Canadian model. These increases suggest the likelihood of extreme temperature events that are unprecedented in the historic record (SRAG, 2000). The strongest increases in both temperature and precipitation are projected to be in the winter, with possibly a doubling in winter precipitation. Both models project warmer, wetter winters. Empirical relationships between ENSO occurrence and climate warming further suggest that El Niño conditions are likely to be increased in frequency by warmer temperatures, bringing greater winter/spring precipitation (Hunt, 1999; Timmerman *et al.*, 1999; SRAG, 2000).

Projections from a regional model developed at NCAR also suggest significant temperature increases in all seasons, but suggest a decrease in winter precipitation (SRAG, 2000). Consistent with the possibility for decreased winter precipitation is the likelihood that the climate has transitioned into the negative phase of the Pacific Decadal Oscillation, signaling a possible 20-30 year period of reduced El Niño conditions (Hamlet and Lettenmaier, 1999; Mantua *et al.*, 1997; McCabe *et al.*, 2004), reduced winter precipitation, and possibly reduced precipitation in general. Co-occurrence of negative (cool) PDO conditions and a positive (warm) AMO index, along with global warming, could signal the occurrence of severe drought for the Southwest at the beginning of this century (McCabe *et al.*, 2004).

Several characteristics of the existing models, however, limit their ability to adequately represent and forecast climatic changes for the region. First of all, the two General Circulation Models (GCMs, Hadley 2 and Canadian) were not developed to represent local and regional changes in climate and hence utilize a coarse grid cell size (350 km on a side) that averages over local variation. In addition, existing GCMs do not adequately simulate convective precipitation, effects of local topography on climate, nor ENSO dynamics, all of which are important components of climate in the Southwest (SRAG 2000). The NCAR Regional model provides projections at a finer resolution, but otherwise suffers from the same limitations. Overall, climate projections for temperature increases have relatively high confidence, with precipitation projections highly uncertain.

Projections for the three models, averaged across the Southwest region, are given below (Table 3-1). Estimates in Table 3-1 do not take into account the range of uncertainty in model projections for the region nor spatial variation in projections within the region. Problems arise in particular for projecting the regional changes under the NCAR model to southern Arizona, with decreases in precipitation per day for the winter exceeding current mean winter rainfall levels.

Table 3-1. Means of temperature and precipitation projections for the Southwest Region from the Hadley 2, Canadian, and NCAR High Resolution Climate Model (from SRAG, 2000).

Year	2030		2060			2090	
Model	Hadley Centre Model 2	Canadian Climate Centre Model	Hadley Centre Model 2	Canadian Climate Centre Model	NCAR Regional Climate Model	Hadley Centre Model 2	Canadian Climate Centre Model
Mean Temperature Change (° C)							
Winter	+2.5	+3.0	+2.0	+4.0	+4.0	+4.0	+7.0
Spring	+1.5	+2.0	+1.5	+3.0	+4.0	+2.0	+6.0
Summer	+1.5	+2.0	+2.5	+3.0	+5.0	+3.0	+5.0
Fall	+1.5	+1.5	+3.0	+4.0	+4.0	+3.0	+5.0
Mean Precipitation Change (mm/day)							
Winter	+1.0	+1.5	+1.5	+1.5	-1.0	+5.0	+4.5
Spring	+0.5	+0.3	+0.3	+0.5	+0.3	+2.0	+1.0
Summer	+0.3	0.0	0.0	-0.3	-0.3	0.0	0.0
Fall	0.0	+0.5	-0.3	+1.0	0.0	+3.0	+1.0

3.2 Ecology of southwestern riparian vegetation and drivers of change

Vegetation patch types

A review of the ecology of all southwestern riparian vegetation types is beyond the scope of this report. The focus of this report will be on lowland riparian biotic communities (<1750 m elevation; Brown, 1994) that occur along the San Pedro and some upland vegetation types that occur in the basin. For the purposes of this report, these vegetation associations are summarized into several riparian patch types. These include cottonwood-willow forests and woodlands, riverine marsh, mesquite woodland or bosque, saltcedar shrublands, hydromesic shrublands, xeric riparian scrublands, and sacaton grasslands. Besides Fremont cottonwood and Goodding’s willow, the cottonwood-willow patch type also includes mesic broadleaf tree species of temperate affiliation (e.g., *Juglans major*, *Fraxinus velutina*, *Platanus wrightii*, *Celtis reticulata*). Hydromesic shrub species, such as seepwillow (*Baccharis salicifolia*), also are associated with cottonwood-willow patch types. Xeric riparian scrublands occur on coarse sediment deposits and are characterized by species such as burrobrush (*Hymenoclea monogyra*) and rabbitbrush (*Ericameria nauseosa*), and may also include desert scrub species. Riverine marsh communities include perennial species from wetland genera such as *Scirpus*, *Typha*, *Juncus*, *Eleocharis*, and other emergent species. True “ciénega” communities, which were a variety of riverine or spring-fed wetlands, were once dominant along many rivers in the region, but have now become very rare (Hendrickson and Minckley, 1984). Finally, sacaton grasslands are another important

riparian patch type along portions of the San Pedro. Sacaton grasslands once covered large areas along river valleys in the region, but now too have been greatly decreased in extent or degraded in quality (Cox *et al.*, 1983).

Upland vegetation in the San Pedro basin is dominated by Chihuahuan Desertscrub in the upper part of the basin (south of Cascabel) and Sonoran Desertscrub in the lower basin. Vegetation in higher elevations in the upper basin includes areas of Plains and Great Basin Grassland, Semidesert Grassland, Madrean Evergreen Woodland (evergreen oaks, juniper, pinyon pine), and Rocky Mountain and Madrean Montane Conifer Forests (ponderosa pine, Douglas-fir, aspen, etc.) at the highest elevations in the Huachuca Mountains (Brown, 1994; Steinitz *et al.*, 2003).

Drivers of riparian vegetation dynamics

a. Flooding – erosion and sedimentation, dispersal

Flooding is an important driver of riparian vegetation dynamics. Reproduction of the dominant pioneer woody species in the system, Fremont cottonwood, Goodding's willow, and saltcedar, depends on the formation of moist, mineral seedbeds for germination and survival of seedlings (Fenner *et al.*, 1985; Stromberg *et al.*, 1991). Floods prepare such seedbeds by scouring vegetation off of bars, depositing sediment, and by inducing channel change through point bar migration (meandering) or channel avulsion (Scott *et al.*, 1996). Floods also cause mortality of established plants and can trigger major channel realignment. Sedimentation from floods also leads to progressive terrestrialization as sediment deposition increases the elevation of the surface, thus increasing the depth to groundwater and reducing the frequency of inundation (Stromberg *et al.*, 1996; Patten, 1998). Average sediment texture tends to change with progressive aggradation of the plot and successional age, with finer textured sediments (suspended sediments, those carried in the water column) deposited on higher surfaces or those with dense vegetation (Stromberg *et al.*, 1991; Stromberg unpublished; Patten, 1998). In addition to creating open mineral substrates by deposition, floodwaters may also be important for scouring away leaf litter and woody debris. Build up of litter in the floodplain limits recruitment by some riparian plants (Xiong *et al.*, 2001) and may also increase the risk of fire, as seen along some leveed portions of the Rio Grande (Ellis, 2001). Floodwaters and the sediments they deliver may be an important source of soil nutrients.

Frequent flooding may also be important for reducing salinization of soils, with increased salinity in the absence of flooding potentially favoring saltcedar and other salt-tolerant species (Shafroth *et al.*, 1995; Busch and Smith, 1995). The presence of frequent flooding on the San Pedro may be one factor that constrains saltcedar dominance and reduces some of the negative effects often attributed to saltcedar (Stromberg, 1998b). Moisture inputs from floods are important for recharging water levels in alluvial aquifers and floodplain soils (Arias Rojo *et al.*, 1999). Finally, floods may be important for dispersing seeds or vegetative propagules of cottonwood, willow, saltcedar or other riparian species (Fenner *et al.*, 1985; Shafroth *et al.*, 1998). The relative contributions of these different flood effects are difficult to separate, but occur as a suite of factors that contribute to the often-observed lateral and longitudinal gradients in vegetation communities along riverbanks (Auble *et al.*, 1994; Bendix, 1994; Dixon and Johnson, 1999).

The timing and magnitude of flooding are both important for vegetation dynamics. Recruitment of pioneer tree species that colonize river alluvium, such as Fremont cottonwood, Goodding

willow and saltcedar, appears to be closely related to ENSO and perhaps PDO cycles on the San Pedro and other rivers in the region (Stromberg *et al.*, 1991, 1993a; Stromberg, 1997, 1998). Successful establishment of all three species is closely linked with large non-growing season floods that occur in El Niño years. Recent recruitment success on the middle San Pedro may be related to wetter climatic conditions associated with the positive (warm) phase of the Pacific Decadal Oscillation from the mid-1970s to late 1990s, although some years of strong recruitment also occurred during the previous dry (negative) phase of the PDO (Stromberg 1998a). Floods in the fall, winter or spring rework sediment, cause channel movement, scour channel bar vegetation, or may produce overbank sediment deposits, creating bare alluvial surfaces that can be colonized by seedlings of spring-dispersing pioneer riparian species (Scott *et al.*, 1996). Subsequent floods or moist conditions into the pre-monsoon and monsoon season further favor survival of seedlings, if the floods are small and do not scour out the young seedlings (Stromberg *et al.*, 1991; Stromberg, 1998a). Dry conditions following winter/spring floods may cause mortality of the seedlings, or may shift composition of the cohort towards the deeper-rooted and more drought-tolerant saltcedar (Stromberg, 1997).

Rainfall (in areas with abundant summer rains) and large summer floods generated from monsoonal rains favor continuous to episodic recruitment of mesquite seedlings (Stromberg *et al.*, 1991). The effect of monsoon-season floods on saltcedar recruitment is not clear, although the long dispersal period of saltcedar suggests that this species may be able to establish after some summer floods (Shafroth *et al.*, 1998; Horton, 1977). However, these floods are typically of shorter duration than the occasional large winter floods and may not have as strong of an effect on formation of alluvial surfaces (Huckleberry, 1994; Arias Rojo *et al.*, 1999). In addition, competition by herbaceous species may be high following growing season floods, lowering survival of pioneer tree seedlings (Stromberg, 1998a). Overall, there is little evidence of salt cedar establishing after monsoonal floods. Instead, at least on the San Pedro, recruitment by both saltcedar and cottonwood/willow has been associated more strongly with fall-winter floods (Stromberg, 1998a), although saltcedar may show greater amplitude of conditions and mechanisms under which it establishes (Cooper *et al.*, 2003).

Floods of any season, but particularly large floods of longer duration (generally in the fall or winter), appear to be important for removal of vegetation by scour and sometimes channel widening, shifting (avulsion), meandering, or incision (Stromberg *et al.*, 1991, 1993a; Huckleberry, 1994). Such large floods are important for patch turnover and may be important for renewal of particular vegetation types. Stromberg *et al.* (1997) observed the formation of riverine marsh on the Hassayampa River following a large winter flood in 1993 that eroded floodplain terraces, widened the channel from 3 to 50 m, and recharged the floodplain aquifer, leading to much of the floodplain occurring very close to the water table. Conversely, another flood in 1995 scoured most of the channel vegetation and aggraded the floodplain, leading to a floodplain that was generally too high to support marsh vegetation. Minckley and Clark (1984) report that large floods were partially responsible for both formation and destruction of a mesquite bosque on the Gila River, with an earlier flood providing coarse sediments for establishment and a later flood widening the channel and removing much of the bosque. Large floods associated with very dry climatic conditions followed by periods of high intensity precipitation, along with overgrazing in the watersheds, contributed to region-wide channel incision and widening during the latter part of the 19th and early part of the 20th century (Hastings, 1959; Hereford 1993). Legacies of these events still strongly influence the geomorphology, hydrology, and vegetation of streams and rivers throughout the region.

Given the influence of floods on riparian structure and function, climatic changes that influence flood magnitude and seasonality may have strong effects on riparian systems in the Southwest. For instance, increases in winter precipitation would likely increase the frequency of large winter floods, channel realignment (migration), and recruitment of pioneer riparian tree species. Small changes in precipitation can lead to large changes in surface flow, with flooding and annual flow particularly sensitive to changes in cool season precipitation (Dahm and Molles, 1992 in Grimm *et al.*, 1997).

Besides climate, other environmental drivers that could influence the frequency, timing, and magnitude of flooding include land-use in the watershed and management of tributaries. Construction of check dams on ephemeral tributaries to the San Pedro has been suggested as one means to increase recharge of the regional aquifer (Arias Rojo *et al.*, 1999; Steinitz *et al.*, 2003). The influence of such check dams on mainstem dynamics on the San Pedro is unknown. Tributaries may be important sources of propagules, sediment, and flood discharge. Reductions in sediment inputs from tributaries could increase channel incision and reduce rates of floodplain aggradation. Reduced rates of flooding by tributaries could reduce the frequency and magnitude of channel migration, especially in the vicinity of tributary junctions. Together, these changes would likely reduce opportunities for recruitment by pioneer riparian trees, particularly cottonwood and willow (Arias Rojo *et al.*, 1999). The potential effects of proposed tributary dams on San Pedro vegetation, flow, and sediment supply deserve further examination through studies of ecological dynamics at tributary junctions and hydrologic modeling of runoff and sediment movement in the basin.

Other management practices in the watershed may also have strong influences on the delivery of flow and sediment to the river channel. Past overgrazing in desert grasslands and deforestation in the mountains have been suggested as contributing factors to the high runoff events and large floods that were associated with region-wide, severe channel incision during the late 1800s and early 1900s (Hastings, 1959; Bahre and Shelton, 1993). On the San Pedro, improved range condition through better land management and increased precipitation may be related to changes in rainfall-runoff relationships and reduced frequency of large floods since around 1960 (Hereford, 1993). Others, however, have suggested that recent and ongoing changes in the watershed, including increases in impervious surfaces from urbanization and expansion of mesquite and other shrublands at the expense of desert grassland, may lead to increased “flashiness” of watershed response to precipitation (Hernandez *et al.*, 2000; Kepner *et al.*, 2002, 2004; Miller *et al.*, 2002).

b. Groundwater and Baseflow

The availability of groundwater strongly influences the distribution, composition, and function of riparian vegetation in the Desert Southwest. On the upper San Pedro, depth to groundwater is an important factor influencing the spatial distribution of species and plant communities (Stromberg *et al.*, 1996). Species differ in their rooting depths and in their relative reliance on groundwater versus soil moisture or stream flow. Fremont cottonwood and Goodding’s willow are considered obligate phreatophytes, meaning that they cannot survive without continual access to water from saturated (phreatic) soil zones (Smith *et al.*, 1998). Facultative phreatophytes, such as saltcedar and velvet mesquite, make use of phreatic water when available, but also take up moisture from unsaturated soil layers. In actuality, the dichotomy between obligate and facultative is somewhat arbitrary, in that different species occur along a gradient of dependence on phreatic water and may vary in their dependence depending on climatic conditions or location. In a study on the

San Pedro River, Snyder and Williams (2000) examined the relative use of shallow soil water and groundwater during the growing season in one facultative (velvet mesquite) and two obligate phreatophytes (Fremont cottonwood and Goodding's willow) across sites that differed in depth to groundwater. Goodding's willow appeared to be a true obligate phreatophyte, using groundwater exclusively, regardless of groundwater depth and summer rainfall. The relative proportion of water used for transpiration by cottonwood and mesquite depended on depth to the water table and on rainfall. Cottonwood used mostly groundwater, but also made some use of shallow soil water (estimated 26-33% of its transpiration) on an ephemeral tributary where groundwater was deep (>4m) and when summer precipitation occurred. Mesquite use of shallow moisture increased as depth to groundwater increased (>50% when groundwater was >4 m deep on the ephemeral site), but derived essentially all moisture from groundwater when shallow soil moisture was unavailable. Work by Scott *et al.*, (2000, 2003) showed that mesquite stands at different sites along the San Pedro differed in their relative use of groundwater and soil water derived from seasonal precipitation.

Since rooting depths change with plant age, so too suitable groundwater depths vary according to plant age or life stage, with some phreatophytic species requiring shallow groundwater for recruitment and seedling survival, but able to tap into groundwater at greater depths as adults. Successful cottonwood or willow recruitment requires that the phreatic zone be near the surface and that rates of decline not exceed the ability of the growing seedlings to track the declining water table via root growth. This is an important component of the "recruitment box" model devised by Mahoney and Rood (1998) for prescribing flow management to favor cottonwood/willow establishment. Work by Segelquist *et al.*, (1993) showed that plains cottonwood (*Populus deltoides* subsp. *monilifera*) seedlings were able to survive water table declines of 2.9 cm per day in coarse alluvial sands (47% of germinated seedlings) and final water table depths of 80 cm, although highest survival occurred at slower rates of decline. This maximum rate of decline is close to the 2.5 cm/day rule-of-thumb used by Mahoney and Rood (1998) in their recruitment box model. *Populus* seedlings have been reported to survive groundwater declines at rates of 2-4 cm/day, to have root growth rates of 0.6-1.3 cm/day, and total first season root depths of 72-162 cm (Mahoney and Rood, 1998; Horton and Clark, 2001). Cottonwood response to water table decline is highly dependent on soil texture, with finer textures resulting in a thicker capillary fringe of available moisture above the alluvial water table. Thus, the recruitment box concept, with consideration of the capillary fringe, leads to the prediction of successful cottonwood recruitment up to 0.6-2 m above the summer low flow levels, depending on the cottonwood/willow species, the sediment texture, and climate or geographic location (Mahoney and Rood, 1998; Kalischuk *et al.*, 2001; Amlin and Rood, 2002).

Goodding's willow seedlings appear to be less tolerant of water table decline than cottonwood and saltcedar. In an experiment comparing growth and survival of Goodding's willow and saltcedar seedlings under simulated water table declines in coarse sediment, willow grew best under no water table decline (continually saturated soils) and had decreasing survival and growth with progressively greater rates of water table decline (Horton and Clark, 2001). Saltcedar had higher survival across all groundwater treatments and greater root elongation, with optimal rates of root growth at the 1-cm/day rate of decline (Horton and Clark, 2001). Amlin and Rood (2001, 2002) found higher tolerance of inundation in some species of *Salix* than in *Populus* and also found evidence of greater vulnerability to water table decline in some species of *Salix*.

Continued survival of cottonwood and willow saplings also depends on consistent access to saturated moisture. In general, mature cottonwood/willow stands grow on sites within 3 m of the

water table, but may occur up to 5 m above the permanent water table. Because fine roots are concentrated in the capillary fringe, just above the water table, these species may be sensitive to large seasonal fluctuation in water table or to permanent declines, particularly on coarser soils with a narrower capillary fringe (Shafroth *et al.*, 2000). Species from both genera have low thresholds of plant water potential at which xylem embolism/cavitation may occur and a narrow “safety margin” between water potentials at which stomatal conductance declines and levels at which significant cavitation of the water column occurs (Pockman and Sperry, 2000). Research by Scott and colleagues (Scott *et al.*, 1999, 2000) suggests that adult cottonwood trees may experience high mortality from abrupt, permanent drops in water table of 1.0 m or more. On a site in Colorado with medium alluvial sands, a permanent water table decline of >1 m (due to sand mining) produced canopy die back and declines in growth within weeks, followed by mortality of 88% of the trees within a three year period (Scott *et al.*, 1999). More modest water table declines (around 0.5 m) did not appear to influence mortality or most growth parameters, but did produce a significant decline in annual branch growth. Similar results were found on a site along the Mojave River, where a large flood was believed to have caused locally significant channel incision (up to 3.6 m decline in local channel elevation). Stand mortality ranged from 58-93% on sites with water table declines of 1.5 m or greater, but only 7-13% on sites with declines of less than 1 m. Under more moderate or temporary cases of water stress, cavitation in peripheral branches and subsequent branch “sacrifice” or canopy die-back may actually be a survival mechanism to improve water status of the rest of the plant (Rood *et al.*, 2000).

Facultative phreatophytic species such as saltcedar and mesquite have a greater tolerance for groundwater decline, but still may be adversely affected if groundwater declines consistently below the rooting zone. Saltcedar often increases on reaches in which groundwater declines have made conditions unsuitable for cottonwood and willow, but may be eliminated when groundwater levels decline to 10 m or more below the ground surface (Graf, 1985). Permanent groundwater decline was identified as the likely cause of death of velvet mesquite trees on the Casa Grande National Monument (Judd *et al.*, 1971). Work by Stromberg *et al.*, (1992, 1993b) suggests that individual tree morphology and physiology (canopy dieback, leaf morphology, leaf water potential) and mesquite stand characteristics vary as a function of groundwater depth. Although mesquite roots may reach as far as 15 m below the surface or even more (Phillips, 1963; Stromberg, 1993), development and maintenance of healthy mesquite bosque, with tree-sized mesquite, appears limited to sites with shallow to moderate groundwater depths (2-10 m) (Stromberg *et al.*, 1993b; Stromberg, 1993; pers. obs.). On sites with deeper groundwater, plant height, canopy cover, and leaf area all decline, with mesquites not exceeding shrub size on xeric riparian sites with groundwater deeper than 15 m (Stromberg *et al.*, 1992, 1993b). Canopy dieback by trees in response to groundwater decline, and the ability of mesquite to resprout suggest the possibility that individual mesquites may be able to readjust their morphology and leaf area in response to permanent groundwater declines. Shrub-sized mesquites growing in upland situations may also have very different root morphology than riparian mesquites, with shallower and more extensive lateral distribution of roots. Work by Martinez and Lopez-Portillo (2003) suggests that stand characteristics of mesquite in upland environments may also differ considerably according to landform and soil characteristics.

Productivity of sacaton grasslands may also be influenced by groundwater depth. On floodplains and terraces along the Santa Cruz and San Pedro Rivers, Tiller *et al.*, (in prep.) found that stem water content, percent live green stems, and percent live biomass of sacaton was significantly related to groundwater depth during the dry, pre-monsoon season (June), with live biomass highest for sites with groundwater less than 4 m below the surface. Post-monsoon measurements

(August and September) showed a weaker relationship with groundwater depth and a stronger relationship to soil moisture at 60 cm. Productivity was lowest, however, at two San Pedro terrace sites with groundwater depths greater than 8 m below the surface. These results suggest that sacaton uses groundwater at least seasonally, with plants with access to shallow groundwater (< 4 m) exhibiting higher productivity during the pre-monsoon dry season, but with productivity more related to soil moisture after the summer monsoon. Work by Scott *et al.* (2000, 2003, unpub. data) at two sites along the San Pedro similarly suggests that sacaton primarily uses rain-derived soil water, but uses some groundwater at sites where the groundwater is shallow (< ca. 3 m).

Besides the direct effects of groundwater depth, the frequency of river surface flow also may have an important influence on the composition and function of riparian vegetation. Baseflow and groundwater dynamics are inextricably intertwined. Baseflow is the flow in the river that is solely supplied by groundwater, hence it is the flow minus any inputs from storm runoff. Gaining stream reaches are those in which the hydraulic gradient points toward the stream, such that groundwater discharges into the stream and creates baseflow. Losing reaches are those in which the hydraulic gradient is flat or points away from the stream, so that water flows from the stream to the groundwater. Losing reaches effectively do not have baseflow, or have it only during times of the year that the hydraulic gradient points toward the stream, perhaps as a result of bank storage from earlier floods. Hence, streams with groundwater levels consistently higher than the deepest part of the channel (thalweg) tend to have perennial flow, those with groundwater consistently below the channel tend to be ephemeral (flow only following storms), and those with a shallow hydraulic gradient or seasonal reversals in hydraulic gradient tend to be intermittent (Arias Rojo *et al.*, 1999; Rood *et al.*, 2003; Figure 3-1).

Consistently shallow groundwater and/or perennial flow may be critical for sustaining some riparian plant communities. Cover of wetland obligate perennial plants drops off rapidly as the frequency of surface flow in a stream declines below perennial (Bagstad, 2003). On the San Pedro, importance of cottonwood and willow relative to saltcedar also declines with reductions in surface flow frequency and corresponding declines in groundwater (Lite, 2003). Annual fluctuation in groundwater levels tends to be lower in perennial, gaining streams than in intermittent or ephemeral losing streams. Cover by wetland perennial herbs and obligate phreatophytic trees tends to be lower on sites where annual fluctuation in groundwater level is high.

Phreatophyte control or clearing has been proposed as a way to reduce groundwater losses due to evapotranspiration and increase baseflow (Arias Rojo *et al.*, 1999, Steinitz *et al.*, 2003). Such experiments in the past have had mixed results, with some early savings of groundwater and boosts in stream flow realized, but typically little effect over the long run. Stream evaporation rates may increase and bank stability decrease with removal of overhanging woody cover. In addition, water savings may require continual clearing of phreatophytes, which (particularly saltcedar) may recolonize after a few years (Graf, 1985). Nevertheless, phreatophytes can have a significant influence on daily and seasonal groundwater fluctuations (Scott *et al.*, 2002), suggesting that reductions in phreatophyte cover through clearing, natural disturbance (e.g., fire) or successional change (e.g., senescence of old cottonwoods) may have a significant impact on floodplain water balance and potentially on groundwater levels and stream baseflow.

Over the long term, climatic change could influence regional groundwater levels in the San Pedro basin through changes in mountain front recharge. Most recharge likely occurs during the

winter, when evapotranspiration rates are lower. Hence, increases in winter precipitation would increase recharge, while increased winter and summer temperatures would increase evapotranspiration and reduce recharge. Over shorter time scales, variation in temperature and humidity can influence rates of transpiration, and hence uptake of groundwater, by phreatophytes. In the San Pedro basin, the strongest effects of climate change on groundwater levels would likely be indirect, through climate-induced changes in land cover (e.g., conversion from grassland to mesquite) and anthropogenic water usage. With or without climate change, changes in development patterns, per capita water use, and human population in the basin are likely to have the greatest short- and long-term impacts on future groundwater levels along the San Pedro River (Arias Rojo *et al.*, 1999; Steinitz *et al.*, 2003).

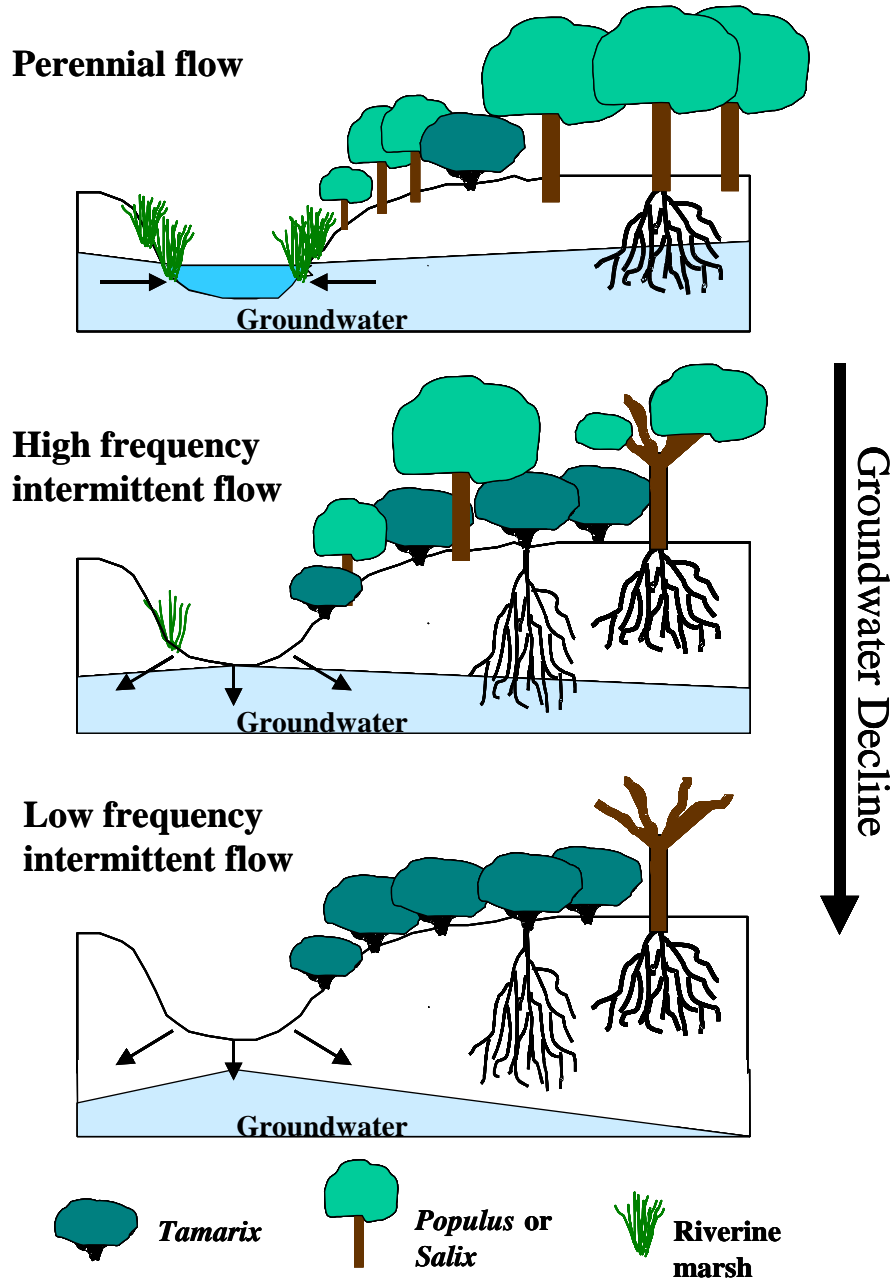


Figure 3-1. Schematic depicting the three major hydrologic reach types and corresponding vegetation patterns along the upper San Pedro River.

c. Precipitation and Soil Water

Precipitation is highly variable from day to day, season to season, and year to year in the Desert Southwest. In Arizona, rainfall tends to have a bimodal pattern, with separate summer and winter rainy season often separated by a short fall dry season and a more severe spring dry season. The relative contribution of cool (winter) vs. warm season (summer) rains may have important implications for dominance by different functional groups of plants.

Water use strategies by plant functional groups in the desert grassland can be divided into intensive and extensive users (Burgess, 1995). Intensive users include most perennial grasses and other herbs, concentrate their roots near the soil surface, and are generally are most active during the summer. In a climate with summer monsoonal rains, these species are most dependent on summer precipitation and shallow soil moisture, and track the water potential of the shallow surface soil. Because summer rains are often of short duration and evapotranspiration rates are high, little of this moisture may get past the surface layers (Sala *et al.*, 1992; Burgess, 1995). Extensive users are often woody plants like mesquite that have far ranging root systems with both shallow and deep roots and can tap into more stable deeper soil water or other local water sources. Because of their greater reliance on deeper soil water, these species may be more influenced by non-growing season precipitation that is able to infiltrate and add water to the deeper soil layers (where turnover is slower) and may be less efficient at exploiting summer precipitation, except when long-duration storms result in deeper percolation of water down the soil profile. Hence, a climate shift towards a greater proportion of precipitation in the summer may benefit the intensive, shallow rooted strategy, while a greater proportion of rainfall in the winter may benefit the extensive water users (Gao and Reynolds, 2003; McAuliffe, 2003).

Along the San Pedro River, herbaceous annual plants are highly responsive to seasonal precipitation, with some species responding to the more dependable summer precipitation, and others to the more variable winter precipitation. High winter precipitation may increase productivity of both annual and perennial herbaceous plants by wetting deeper soil layers through infiltration and by causing large, longer-duration cool-season floods, which recharge both deeper soil layers and the alluvial aquifer (Arias Rojo *et al.*, 1999). Recruitment of some woody species of subtropical origin, such as mesquite, may be keyed in high summer precipitation for initial recruitment (Stromberg *et al.*, 1991), but may subsequently benefit from winter rain or flood events that supply more stable deep soil moisture for the growing seedling (Weltzin and McPherson, 1997).

d. Fire

Although fire is not often considered as an important driver of vegetation dynamics in riparian areas, it may have strong effects on riparian patch dynamics, particularly in the Southwest, where the high productivity of riparian zones occurs in a climate with high temperatures and low relative humidity: factors that combine to increase fire risk.

Riparian species differ in their resilience following fire. Saltcedar, some willow species, velvet ash, and mesquite all resprout from the base vigorously following fire, as long as the fire is of low enough intensity that the tree is only top-killed (basal meristems not killed). Cottonwoods appear to have lower rates of resprouting (Busch, 1995), although this may differ considerably

from species to species and place to place (Ellis, 2001). Hence, one might expect saltcedar, willow, and mesquite to increase in dominance, relative to cottonwood, in burned sites (Busch, 1995; Busch and Smith, 1995). There is also good circumstantial evidence that thickets of saltcedar, especially older patches with high litter build up, may be especially fire prone and may contribute to the demise of cottonwood by increasing fire intensity and frequency in the patches in which they co-occur (Busch, 1995).

As at other grassland-shrubland ecotones throughout the world (Scholes and Archer, 1997), fire may be an important factor influencing the relative cover of herbaceous plants vs. shrubs within the riparian zone and in the uplands. Fire suppression has been suggested as one of the factors leading to expansion by shrubs in the desert grassland and other grasslands worldwide during the 20th century (Bahre and Shelton, 1993; Grover and Musick, 1990; Van Auken, 2000). Although mesquite is a vigorous resprouter following low-moderate intensity fires, high intensity fires may cause high mortality, particularly of younger plants (Glendening and Paulsen, 1955; McPherson, 1995). The seasonality of fires may be particularly important to their effects, with woody plants generally less susceptible to fires during their winter dormant season than during the growing season (Glendening and Paulsen, 1955). Hence, in the Southwest, fires during the warm spring dry season may have a much stronger ecological effect than cool-season fires. However, particularly hot fires may also reduce the vigor and cover of some grass species like sacaton (*Sporobolus wrightii*), leading to creation of more bare ground, and favoring productivity of annual forbs (Bock and Bock, 1978; Cox and Morton, 1986; Cox, 1988). Hence, frequent enough fires could tip the balance toward grass-dominated ecosystems or to savannahs with low densities of larger mesquite. As tree densities increase, however, there may be a threshold (phase change) beyond which the availability of fine fuels is too sparse or their connectivity too low to ignite and carry fires of sufficient intensity to kill the trees or shrubs (Archer *et al.*, 1988; Kepner *et al.*, 2002).

Fire may interact strongly with other ecological (disturbance) drivers, such as flooding and grazing. On some sites along the Rio Grande which have been isolated from river flooding by levees, high woody debris build up has led to increased probabilities of intense fires in the riparian forest (Ellis, 2001). Reductions in flooding along the Colorado River from flow regulation, in combination with characteristics of saltcedar that may increase flammability, may contribute to increased riparian fires and replacement of relict patches of cottonwood with saltcedar thickets (Busch, 1995; Busch and Smith, 1995).

Fire and precipitation have a strong, but complex relationship in the Southwest. On a regional scale, the frequency of fires may be related to the cyclic nature of ENSO events (Swetnam and Betancourt, 1990, 1998) and the patterns of precipitation and drought that accompany them. Area burned in Arizona and New Mexico in 1920-1990 closely tracked variation in the Southern Oscillation Index (SOI), with larger areas burned during dry years associated with the La Niña (positive) phase. Major fire years tend to be associated with the switch from El Niño (wet) to La Niña (dry) conditions (Swetnam and Betancourt, 1998; Kitzberger *et al.*, 2001). Higher winter precipitation in El Niño years tends to increase productivity of cool season herbaceous plants, leading to the buildup of fine fuels. These high fuel loads then contribute to high fire frequency and intensity during the subsequent spring dry season or drought years. The effect of moist conditions in previous years for enhancing fuel buildup and increasing subsequent fire occurrence and area burned is strongest for grassland, shrubland, and open woodland ecosystems, where fine fuels predominate (Westerling *et al.*, 2003). Area burned on public lands in southeastern Arizona between 1980 and 2000 was positively related to prior moisture

conditions (as measured by the Palmer Drought Severity Index), with the strongest relationship with moisture conditions about 2 years prior to the burn season (Westerling *et al.*, 2003).

Climatic warming would likely increase the frequency and intensity of fires in southwestern riparian areas. As suggested above, an increase in the intensity and frequency of El Niño events, and corresponding increases in winter rains, would increase herbaceous productivity and fine fuel loads. Hotter temperatures during intervening drier periods would increase the probability of ignition and the intensity and rate of spread of resulting fires. It is less clear how a warmer, drier climate might influence fire occurrence. Hotter, drier conditions should increase ignition probabilities and fire intensities, but lower winter precipitation might also reduce herbaceous productivity and fine fuel loads (McPherson, 1995). Perhaps a warmer wetter climate would result in a higher frequency of large fires (due to higher accumulation and connectivity of fine fuels), while a warm dry climate might result in more frequent, but smaller and lower intensity fires (Gardner *et al.*, 1996). As with the effects of climate change on groundwater levels, climate-induced changes in land cover (e.g., shrubland vs. grassland) and land management (e.g., grazing) would have a very strong influence on future fire frequencies in southwestern watersheds and their riparian landscapes (McPherson, 1995).

e. Grazing

Grazing, browsing, and trampling by cattle, and in some cases by native ungulates, may have a profound influence on both upland and riparian systems (Kauffman and Krueger, 1984). Impacts of cattle on riparian zones are variable, depending on the duration, seasonality, and stocking rates of cattle and may include effects on both riparian vegetation structure and channel morphology. Presence of cattle in the riparian zone may reduce successful establishment of cottonwood, willow, sycamore, and other riparian pioneers (Glinski, 1977; Auble and Scott, 1998; Samuelson and Rood, 2004) and could contribute to shifting species composition toward less palatable species such as saltcedar, Russian-olive, and *Baccharis*. Removal of cattle from portions of the upper San Pedro in 1988 was associated with dramatic increases of riparian vegetation and with it bird densities (Kreuper *et al.*, 2003). This vegetation recovery could contribute to increased narrowing, deepening, and stability of channels, with consequent reductions in channel migration rates (Arias Rojo *et al.*, 1999).

Overgrazing may have important landscape impacts on vegetation composition and watershed hydrology. Livestock grazing is thought to have been one of the drivers of shrub increases in desert grasslands of the Southwest, which (unlike the Great Plains) did not historically have large populations of native ungulates (Hastings, 1959; Grover and Musick, 1990; Bahre and Shelton, 1993; Van Auken, 2000). Soil compaction and reductions in herbaceous cover from grazing may influence rain-runoff relationships, resulting in a flashier hydrograph. Such changes may have contributed to very large floods on the San Pedro River and other southwestern rivers in the late 19th and early 20th centuries that were associated with sheet and gully erosion and subsequent arroyo formation.

In addition to interacting with watershed hydrology and erosion, grazing also interacts with fire, particularly in upland rangelands. Heavy grazing reduces litter accumulation from grass production and may also reduce the connectivity of fine fuels. These fuel reductions may decrease the frequency, intensity and rates of spread of wildland fire (Bahre and Shelton, 1993). In addition, reductions in grass and litter cover may directly favor recruitment of woody shrubs and reductions in fire frequency associated with grazing may favor persistence and spread of

shrubs. Hence, conversion of grassland to shrubland associated with heavy grazing may in itself reduce fire frequencies. Conversely, some have attributed increases in mesquite and other shrubs in the San Pedro basin to increasing urbanization and removal of grazing, with the rationale that ranchers used prescribed fire and removed shrubs to keep rangelands open (Steinitz *et al.*, 2003).

f. Temperature

The effects of temperature are pervasive and influence other drivers, such as fire and water use by vegetation. High evapotranspiration rates and water stress may be associated with high temperatures and low relative humidity. Along the San Pedro and other rivers and streams in the region, the vegetation is a mixture of species with more northern and mesic lineages (such as *Populus*) and those that have a more subtropical affiliation (such as mesquite) (Brown, 1994). More vernaly-adapted species like cottonwood, which are part of the relictual temperate Tertiary flora (Brown, 1994) appear to be more tolerant of frost and have an earlier leaf-on (and hence longer growing season) than mesquite in the upper basin. Increases in temperatures may increase growth rates of subtropical species due to more frequent occurrence of temperature optima for photosynthesis, longer growing seasons (earlier spring thaw and later fall frost), and reductions in the occurrence of the killing frosts that place important constraints on the distribution of some subtropical species (Turnage and Hinckley, 1938; Glinski and Brown, 1982). This could result in expansion of the latitudinal and elevational ranges for some temperature-limited species.

Using a climate-correlative envelope approach, Skirvin *et al.* (2000) suggested that a modest mean annual temperature increase of 2° C and shifts in mean cool or warm season precipitation of 10% could result in strong shifts in habitable area for some upland species across the entire San Pedro watershed. Suitable habitat for some heat-tolerant Sonoran desert species (*Carnegieia gigantea* and *Cercidium* spp.) would expand uphill under warmer climate scenarios with no change in precipitation patterns or an increase in winter precipitation, while habitat for mid-elevation chaparral species (*Quercus* spp., *Nolina microcarpa*, *Juniperus* spp., *Arctostaphylos* spp.) and tarbush (*Flourensia cernua*), a Chihuahuan desert shrub species, could decline strongly. Mesquite and related leguminous shrub/tree species (*Prosopis velutina*, *Olneya tesota*, *Acacia* spp.) and creosotebush (*Larrea tridentata*) showed only modest changes (slight declines for mesquite) under the warming scenarios.

The distribution, physiognomy, and relative dominance of velvet mesquite may be influenced by frost severity and frequency. In December of 1978, severe cold temperatures were associated with heavy topkill or canopy dieback in velvet mesquite in the San Pedro basin, with higher topkill rates highest close to the Mexican border, and declining northward with decreasing elevation (Glinski and Brown, 1982). Little effect was observed north of Cascabel, which occurs at the boundary between the Chihuahuan and Sonoran desertscrub biotic communities (Brown, 1994). Cooler temperatures with more frequent frosts and shorter growing seasons higher in the basin may limit dominance of mesquite and development of mesquite bosques to elevations below approximately 1200 m, with sparser and more shrub-like mesquites at higher elevations and higher coverage by sacaton grassland (Stromberg *et al.*, 2003). The shrub-like growth form could also predispose upper basin mesquites to higher mortality from fire, further favoring the maintenance of grasslands. If frost limits the current mesquite distribution in the San Pedro basin, then warmer temperatures, and with them, reductions in the severity and frequency of frost events, could favor expansion of mesquite woodlands and shrublands along higher elevation, upstream portions of the San Pedro.

Changes in temperature could also influence competitive relationships between saltcedar and other riparian pioneers. Growth rates and stand development of saltcedar may be lower in cooler climates at the northern end of its naturalized range (Lesica and Miles, 2001) or at higher elevations along the San Pedro River corridor (Stromberg 1998a). In addition, saltcedar appears to have a higher photosynthetic temperature optimum than cottonwood and willow (Horton *et al.*, 2001).

g. Carbon dioxide

Increases in CO₂ could lead to increases in productivity across species and functional types, but may favor species utilizing the C3 photosynthetic pathway (e.g., many shrubs like mesquite) more than those utilizing the C4 pathway (e.g., warm season grasses like sacaton). This explanation has been put forward as a possible contributing mechanism for the spread of shrubs in desert grasslands throughout the Southwest and the increases in shrub cover throughout semi-arid and arid grasslands and savannahs throughout the world (Idso, 1992; Archer *et al.*, 1995). Increases in CO₂ would reduce the relative advantage that C4 species have in productivity and water use efficiency at high temperatures.

3.3 Historic and recent changes along the San Pedro River

The recent history of the San Pedro and other rivers in the region has been dynamic, with a mixture of natural and anthropogenic factors influencing riparian vegetation structure, composition, distribution, and dynamics and upland vegetation and land use.

Geomorphic Change

Current distribution and abundance of pioneer riparian trees may be largely a function of historic geomorphic legacies along the San Pedro (Arias Rojo *et al.*, 1999). Like many other southwestern streams, the San Pedro experienced episodes of severe channel incision, entrenchment, and channel widening during the late 19th century through the middle part of the 20th century. Historic accounts suggest that the pre-1850 river was shallow and narrow, with longer reaches of perennial flow (Hastings, 1959; Hastings and Turner, 1965; Davis, 1982; Arias Rojo *et al.*, 1999). Vegetation may have been a mosaic of riverine marshlands (cienegas), sacaton grasslands, and more scattered riparian woodlands of cottonwood, willow, and ash (Arias Rojo *et al.*, 1999; Davis, 1982). Channel incision and entrenchment began as early as 1850 in some areas and extended into the 1930s (Huckleberry, 1996; Wood, 1997; Hereford, 1993). Degraded range conditions, coupled with large floods, led first to episodes of severe channel down-cutting (incision), followed by entrenchment and formation of a wide, braided river channel. The flood of record in September 28, 1926 (98,000 cfs at Charleston) was probably largely responsible the last major episode of incision, entrenchment and widening of much of the channel in the upper San Pedro. Subsequent declines in floodplain groundwater levels and high fluvial disturbance in the widened channel destroyed most of the existing riparian vegetation and the former river floodplain (Bryan, 1928; Hastings, 1959; Hereford, 1993). The root causes of channel entrenchment are uncertain and controversial, but likely included climatic variability, with periods of severe drought followed by a period of greater rainfall and higher intensity storms, and changes in runoff characteristics in the basin due to the effects of grazing

on soil infiltration and due to increases in shrub cover relative to grasses (Bryan, 1928; Hastings, 1959; Hastings and Turner, 1965; Hereford, 1993; Bahre and Shelton, 1993). Other possible contributing factors include forest cutting in the uplands and the occurrence of a large earthquake in 1887 that may have particularly influenced groundwater hydrology in the basin. In the upper San Pedro, channels incised 1-10 m (1-5 m upstream from Lewis Springs and 5-10 m downstream). Near Hereford, entrenched channel widths increased from 25-40 m in the early 1900s to around 80-100 m (Huckleberry, 1996) or more in the late 1930s. Enlargement of the entrenched channel (floodplain) slowed beginning in the 1950s, with total floodplain area relatively stable since the 1970s, suggesting that channel processes may have reached a dynamic steady state (Hereford, 1993).

Since the 1950s, flood magnitudes have declined and rates of fluvial disturbance have slowed, allowing vegetation colonization, channel narrowing, and formation of a new, inset floodplain within the entrenched channel banks (Hereford, 1993). Part of the decline in flood magnitudes may be due to changes in the rainfall-runoff relationship (lower runoff for a given rainfall event) since around 1960, which may be related to improved range condition in the uplands (Hereford, 1993). Feedbacks between vegetation colonization and sediment deposition have likely been a key part of the channel recovery process and the original channel entrenchment and widening events have likely enabled the establishment of the cottonwood-willow gallery forest that exists along the upper San Pedro River today. Most of the present cottonwood and willow forests in the upper basin originated in the 1960s and 1970s, with narrower bands of recruitment since then (Stromberg, 1998a). This suggests that rates of channel migration and pioneer tree recruitment may have declined in recent years as the channel has narrowed and the banks have become stabilized with riparian vegetation. This pattern of narrowing, with recruitment of cottonwoods and willows during the narrowing phase, matches the pattern observed on other western streams that have undergone cycles of floodplain destruction and reconstruction (Friedman *et al.*, 1996).

Change in vegetation communities

Riparian vegetation - Coverage of cottonwood and willow forests has probably changed considerably over time on the San Pedro. Although these communities were present in the past (1850s or before), they probably occupy a larger extent today (Arias Rojo *et al.*, 1999). Much of the riparian forest present at the beginning of the 20th century was likely destroyed during large flood events associated with channel entrenchment and widening during the first several decades of the century. As of 1928, Bryan (1928) states that most of the former riparian forest and grassland had disappeared, with only a fringe of mesquite remaining. Recovery of riparian forest has occurred since then, with channel narrowing through development of an inset floodplain within the formerly widened, entrenched channel. Recovery of riparian forest likely accompanied and contributed to declines in channel widening between 1955 and 1970 (Hereford, 1993), with the establishment of a new dynamic equilibrium between river discharge and channel dimensions. Most cottonwoods, willows, and saltcedar currently on the San Pedro date to the 1960s and 1970s (Stromberg, 1998a). An assessment of changes in the area of riparian vegetation from aerial photos in the 1930s and 1970s suggests an approximate doubling of the area of dense riparian cover (includes cottonwood-willow forest, tamarisk, and dense mesquite) during that interval (Reichardt *et al.*, 1978). More recent assessments from satellite imagery suggest slight declines in riparian area between 1973 and 1986 and little change since then (Kepner *et al.*, 2002).

Increases in cottonwood/willow and saltcedar recruitment have also been linked with an increase in the size and frequency of winter floods since about 1960, while summer floods during the same period may have decreased in magnitude (Hereford, 1993; Stromberg, 1998a). Recruitment has continued in recent years with winter floods (1991, 1993, 1997) but with progressively narrower patches, as the availability of open substrate for colonization has declined with channel narrowing (Stromberg, 1998a). Another contributing factor to recent recruitment appears to have been the removal of cattle from the SPRNCA in 1988. Following cattle removal there was an increase in riparian vegetation density and cover and with it an increase in densities of many riparian bird species. Removal of cattle may have initially favored tree recruitment, as well as increases in herbaceous and shrub cover (Kreuper *et al.*, 2003). Overall increases, however, in shrubs and herbaceous cover may reduce the space further for tree recruitment and may also reduce formation of open surfaces by channel migration, as higher vegetation cover may be stabilizing the river banks and inducing local channel deepening (Arias Rojo *et al.*, 1999; Stromberg *et al.*, 2003).

Cienega and riverine marsh - Accompanying widespread channel entrenchment throughout the Southwest was the near disappearance of riverine marshlands or cienegas as a major vegetation community. Understanding of cienegas is limited, but they appear to have been a dominant (or the dominant) community type along large portions of the upper San Pedro (Hastings, 1959; Davis, 1982; Hendrickson and Minckley, 1984; Arias Rojo *et al.*, 1999). Cienegas were characterized by high water tables, organic and anoxic soils, and small, low-energy, shallow river channels. Characteristic species in cienegas included wetland obligate species of Cyperaceae (*Scirpus*, *Juncus*, *Eleocharis*) and some grasses (Hendrickson and Minckley, 1984). Loss of cienega vegetation along the San Pedro and other rivers in the region were likely linked to high-energy floods that deepened and widened channels and led to abrupt drops in groundwater levels in the floodplain (Bryan, 1928). In the San Pedro basin, a large earthquake in 1887 may have also contributed to changes in cienega coverage, as changes in groundwater hydrology were observed, with some springs ceasing to flow and some wells becoming artesian (Arias Rojo *et al.*, 1999).

Local extirpation of beavers (*Castor canadensis*) in the 1880s may also have strongly influenced the formation or maintenance of cienega habitats. The San Pedro formerly had a high density of beaver, earning it the unofficial label of “Beaver River” in the 1800s (Bryan, 1928; Davis, 1982; Arias Rojo *et al.*, 1999). Beaver dams create miniature impoundments that slow the flow of water, induce sedimentation and aggradation of the stream bed, and raise water tables. A high density of beavers and a high frequency of dam building could have important landscape-level effects on the San Pedro, as they have had in some landscapes in the Midwest (Naiman *et al.*, 1988; Arias Rojo *et al.*, 1999). Some have even hypothesized that extirpation of beaver may have contributed to arroyo formation, with the removal of dams increasing the flow rate and erosive power of water in the rivers (Parker, 1985, in Arias Rojo *et al.*, 1999). C. H. Bayless, a rancher along the San Pedro in the 19th century, speculated that extermination of beaver, along with overgrazing, had led to incision and widening of channels and drainage of bottomlands (Griffith, 1901 cited in Wood, 1997)

Beaver were reintroduced to the upper San Pedro in 1999-2002 (Mark Fredlake, BLM, personal communication) and appear to be having important local effects on vegetation structure and hydrology. Fifteen individuals were reintroduced originally, and, as of January 2004, approximately 70-80 beaver are thought to be living on the upper San Pedro, with 19 dams

spanning the river. In addition to influencing hydrology and sedimentation, beavers also directly affect vegetation structure and composition, by cutting/felling of trees, particularly favored species like cottonwood and willow. Hence, cutting by beavers could locally reduce densities of cottonwood and willow, or increase the frequency of resprouts. High water tables induced by beaver impoundments may also limit the distribution of some species of plants that are intolerant of anoxic conditions and favor others that require standing water or high water tables.

Changes in upland cover types and land cover - Analysis of satellite imagery (Landsat-TM) from 1973-1997 suggests changes in landscape composition across the upper San Pedro watershed (Kepner *et al.*, 2000, 2002). The dominant changes have been an approximate four-fold increase in coverage by both upland mesquite and urban areas, with corresponding declines in desert scrub and grassland. Nearly all of the increase in mesquite coverage occurred between 1973 and 1986, with increases in both the number of patches and average patch size. Coverage by urban land uses increased two-fold between 1973 and 1986, and had doubled again by 1997. Desert scrub and grassland decreased 22% and 16% respectively since 1973, with strongest declines in 1973-1986. Possible contributing factors to land cover transitions included short-term drought, livestock grazing, urbanization, and fire suppression (Kepner *et al.*, 2002). Modeling of watershed processes suggests that the increase in urban, agricultural, and mesquite land cover from 1973 to 1997 may have implications for watershed hydrology, with higher volumes of runoff and sediment transport resulting (Miller *et al.*, 2002).

Fire - Fire appears to have been an important disturbance factor structuring riparian vegetation along the upper San Pedro River over at least the last 10 years. Fires were historically frequent in the upland forests of the region, but little is known of historic fire frequencies in the riparian corridor. Data on fire occurrence within the SPRNCA since 1986 (BLM, unpublished) suggests an increase in the frequency and size of fires beginning in the mid-1990s (Figure 3-2) with individual fires in 1999 and 2003 exceeding 1000 acres (400 ha.). Area burned since 1994 equals approximately 10% of the area of the entire SPRNCA (about 2400 hectares), with perhaps even a larger proportion of riparian habitats influenced by fire during that time. The majority of fires and the largest area burned have been in the dry pre-monsoon months of March-July (Figure 3-2). Recent increases in the size and frequency of fires along the San Pedro may be linked to increases in fine fuels levels after removal of cattle from the Conservation Area in 1987 (Kreuper *et al.*, 2003). Another contributing factor could be high productivity by herbaceous plants following winter rains in recent El Niño years (1991-95, 1997-98; www.cdc.noaa.gov/ENSO/enso.mei_index.html), providing fine fuel buildup for fires during the spring dry season. Most fires have been attributed to human causes, at least in terms of the initial ignition, with some recent fires being attributed to powerline collapse, ignition near roads, or undocumented border-crossers from Mexico (Stromberg *et al.*, 2003).

Current research on the effects of wildfires on vegetation structure and landscape pattern along the San Pedro suggest high topkill rates of mesquite on terraces and outer floodplains and locally high mortality of cottonwoods and willows. On one recently (2003) burned site, willows and mesquites have shown high rates of resprouting, although some trees were killed. Some resprouting has also been observed in cottonwoods. Other studies of riparian fire in the Southwest suggest lower rates of resprouting for cottonwoods than for many of the other species (mesquite, willow, saltcedar) (Busch, 1995), with mortality rates and resprouting related to the degree of fuel buildup (woody debris) in the floodplain (Ellis, 2001). Ambient air temperature, relative humidity, and burn season also strongly influence fire intensity, tree mortality, and

resprout rates (Glendening and Paulsen, 1955; McPherson, 1995; Ansley *et al.*, 1998; Drewa, 2003) On the San Pedro, a January fire near Palominas in 1994 appeared to have a much smaller influence on tree mortality and patch type dynamics than spring fires (March-June) at other sites in the late 1990s and near Palominas in 2003 (Stromberg and Rychener pers. obs.). There is some evidence for higher proportions of grassland and lower proportions of riparian forest (and woodland) on sites burned in the last 10 years relative to nearby, paired unburned sites along the San Pedro (Rychener and Stromberg, unpublished). Fire not only affected landscape pattern, but its effects were also influenced by landscape pattern. In an analysis of the effects of landscape pattern on the relative area of cottonwood/willow patches burned, the distance of the patch from the channel, the size of the patch, and the fractal dimension (shape complexity) were important factors. Larger patches were more likely to experience at least some burning, as were patches farther from the river channel. A higher percent area per patch was burned for riparian patches that were farther from the river channel and a lower percentage was burned for patches with a complex shape (high fractal dimension). For one individual site where fire occurred in 2003, the proportion of the patch boundary that bordered grass-forb patch types was also associated with a higher proportion burned. Overall, these results suggest that riparian landscapes with more complex patch shapes were more likely to retain riparian forest after a fire, and that riparian fire on balance may narrow the riparian forest corridor by eliminating more distal patches.

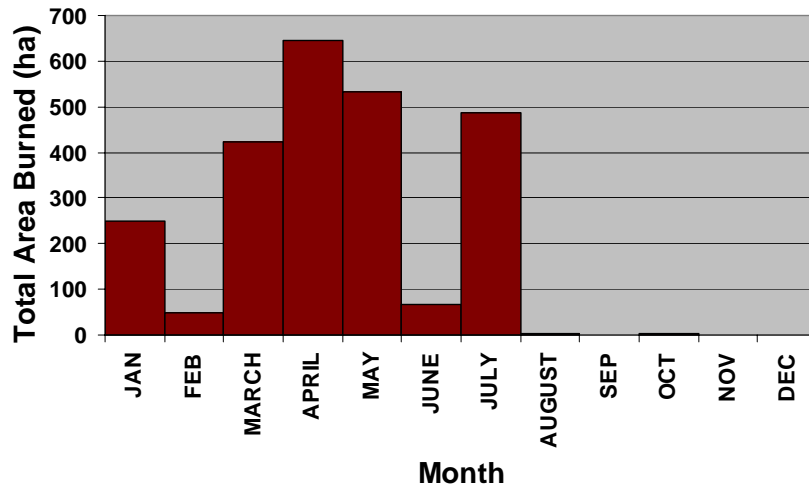
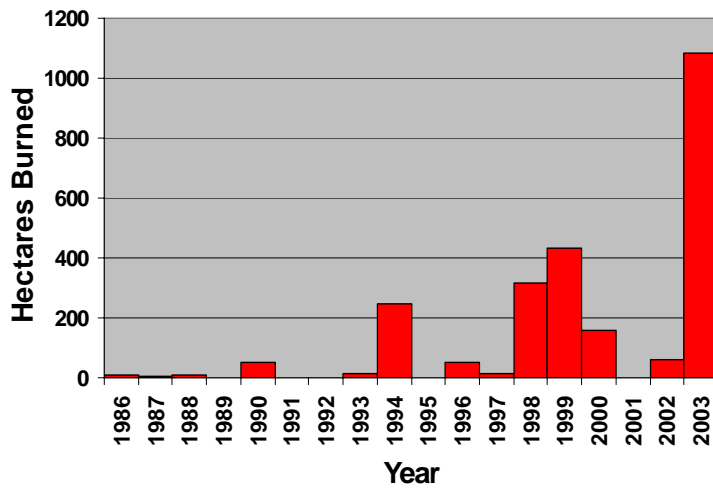
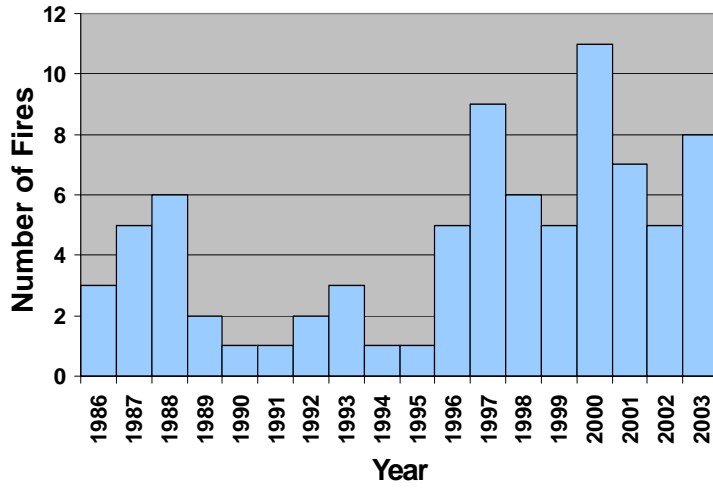


Figure 3-2. Historical frequency, impacts and seasonality of fires in the San Pedro Basin

Changes in groundwater and baseflow - The advent of rural electrification around 1940, and with it, high-powered electronic pumps, made possible much greater rates of groundwater withdrawal in the San Pedro basin (Goode and Maddock, 2000) for agricultural, mining, and domestic uses. Rates of groundwater extraction increased strongly from about 1940 until the designation of the San Pedro Riparian National Conservation Area in 1988 (Arias Rojo et al., 1999; Goode and Maddock, 2000) and have declined somewhat with recent retirement of irrigated agricultural land in the upper basin. Modeling studies suggest declines in river baseflow and groundwater levels from 1940 until present, with significant impacts occurring by the 1960s and 1970s (Arias Rojo et al., 1999; Goode and Maddock, 2000), and estimate that current levels of groundwater discharge may be only 30% of levels prior to 1940 (Arias Rojo et al., 1999). Significant declines in baseflow have also been observed at the Palominas and Charleston stream gages since about 1940 (Pool and Coes, 1999). Vionnet and Maddock (1992) projected that continued pumping at 1988 levels would effectively dry up the river in 20 years, with no baseflow remaining along the upper San Pedro. The annual overdraft (pumping minus recharge) for the Sierra Vista sub-basin is currently estimated at about 7000 acre-feet and could rise to 13,000 acre-feet per year by 2020, assuming a 45% increase in population within the basin (Arias Rojo et al., 1999). Future changes in alluvial groundwater levels and stream baseflow are highly dependent on changes in human population in the basin, spatial patterns of housing development, types of land-use, and the spatial location of pumping (Arias Rojo et al., 1999, Steinitz et al., 2003)

3.4 Simulation of vegetation response to climate change

Methods

1. Vegetation model

A simulation approach was used to evaluate the effects of several plausible climate change scenarios on riparian vegetation structure and dynamics at three sites along the upper San Pedro River. The model was developed using the STELLA II Dynamic Simulation software (ISEE Systems, Lebanon, NH) and simulates the effects of changes in environmental drivers (e.g., groundwater, streamflow, precipitation, temperature, fire) on the composition, structure, and dynamics of riparian vegetation. Specifically, the model simulates the recruitment, growth, and mortality of 10 species or functional groups of southwestern riparian plants - Fremont cottonwood, Goodding's willow, saltcedar, velvet mesquite, velvet ash, a hydromesic shrub group (e.g., *Baccharis salicifolia*), a xeric riparian shrub group (e.g., *Ericameria nauseosa*, *Hymenoclea monogyra*), herbaceous annuals, wetland perennials (e.g., *Typha*, *Scirpus*, *Eleocharis*), and mesic perennial grasses (e.g., *Sporobolus wrightii*) – in relation to their life history characteristics and changes in environmental drivers, at the scale of individual sampling plots (about 10 x 10 m). Details of the model development have been provided in earlier reports (Dixon, 2003a,b). Vegetation change was simulated at three sites that were chosen to represent the range of hydrologic conditions and vegetation composition that occurs along the upper San Pedro River.

Climatic inputs to the vegetation model include incident solar radiation, average minimum and maximum temperature, daily precipitation, relative humidity, and maximum daily wind speed, all averaged (or summed) over the 5-day time step of the model. Incident solar radiation and

mean daily temperature (average of minimum and maximum) are used to calculate potential evapotranspiration using the Jensen-Haise (Wright and Hanson, 1990) and Hargreaves (Wu, 1997) methods. Soil and plant moisture dynamics are modeled as a function of precipitation, plant cover and moisture uptake, and potential evapotranspiration. Plant growth is modeled as a function of light availability (modified by leaf area above the plant), crowding, air temperature, moisture availability (soil water and groundwater), disturbance, and plant life history characteristics. Relative humidity, temperature, wind speed, and precipitation are used for modeling fine fuel moisture, probabilities of fire occurrence, and fire intensity.

2. Climate scenarios

A 52-year daily time series of historic weather data (1951-2002) from the National Weather Service station at Tombstone (station ID 028619, 31.7° latitude, -110.05° longitude) was used to create five transient climate scenarios for the period 2003-2102. The daily 52-year record was cycled through twice to generate the 100-year scenario, with simulation years 2003 and 2054 initialized with the adjusted 1951 daily data. Historic temperature trends from 1951 to 2003 were not removed from the time series. Using data from 1951 to represent climatic conditions starting in 2003 may be appropriate, given the combination of the negative phase of the Pacific Decadal Oscillation and the positive phase of the Atlantic Multidecadal Oscillation in both years. This climatic configuration was associated with the severe drought conditions in the mid-1950s (McCabe *et al.*, 2004).

The station at Tombstone was used because of its proximity to the study area and the length and completeness of its record. The scenarios were chosen to represent a reasonable set of potential climate trajectories, given the range of projections for the region derived from climate models (SRAG, 2000). The scenarios are as follows:

1. No climate change (1951-2002 daily temperature and precipitation repeated)
2. Warm: progressive temperature warming over 100 years, with a 4° C increase in maximum daily temperature and a 6° C increase in minimum daily temperature by 2102
3. Warm dry: progressive temperature warming as in #2 and a progressive decline in winter (nonmonsoonal: October 1 – May 31) daily precipitation of 50% by 2102
4. Warm wet: progressive temperature warming as above, with a progressive increase in winter daily precipitation of 50% by 2102.
5. Warm very wet: progressive temperature warming as above, with a progressive increase in winter daily precipitation of 100% by 2102.

All of the climate scenarios are transient, beginning with the same conditions in 2003 and progressively diverging over the 100-year simulation period. Changes in temperature and precipitation, relative to historic values, were applied linearly over the 100-year period. Hence, for the warming scenarios (scenarios 2-5), daily minimum temperatures were increased 0.06° C per year and daily maximum temperatures 0.04° C per year over 2003-2102. Similarly, for the precipitation increases (scenarios 4 and 5), winter precipitation was increased 0.5% and 1% per year, respectively, from 2003-2102. Changes in precipitation were applied only to days in the historic record that had measurable precipitation. Hence, precipitation totals for individual days were adjusted upward or downward, without changing the frequency of rain events. For the wetter scenarios, this effectively increased the magnitude of extreme events, which is one expectation of climatic change (Easterling *et al.*, 2000, Houghton *et al.*, 2001). For a fixed amount of total rainfall, the ecological and hydrologic effects of changes in the event size versus

changes in the number of events may be very different, particularly in a semi-arid environment (Gao and Reynolds, 2003). The implications of these two approaches, or a gradient of intermediate approaches (i.e., changes in both event size and frequency), could be explored in future simulation exercises.

Changes in temperature were of roughly the magnitude projected for the region by the Canadian Climate Centre (CCC), Hadley 2, and NCAR Regional models (SRAG, 2000). A stronger increase in minimum temperature than maximum was assumed, in agreement with general trends projected by IPCC and observed under recent climatic changes (Houghton *et al.*, 2001). The range of changes in fall-spring precipitation reflected the disagreement among climate models (SRAG, 2000) on the direction and magnitude of winter precipitation changes for the region, with the CCC and Hadley 2 models suggesting strong increases (perhaps a doubling or more) and the NCAR Regional Model suggesting a decrease. None of the models projected a significant change in summer (monsoonal) precipitation, so historic daily values for June 1 – September 30 were retained in the scenarios. Transient scenarios were used, instead of applying a fixed climate change over the entire record, to more realistically represent gradual changes in climate over the next 100 years. Use of daily historic data preserved the important seasonal and year-to-year patterns of climatic variation (e.g., influences of ENSO and PDO) that characterize the climate of the Southwest.

Incident solar radiation and relative humidity were simulated based on daily temperature and precipitation data, using the MTCLIM4.3 software (<http://www.ntsug.umt.edu/bioclimateology/mtclim/>) (Glassy and Running, 1994; Thornton and Running, 1999). This software package uses an improved algorithm for simulating relative humidity for arid environments in which minimum temperature may be much higher than dew point temperatures (Kimball *et al.*, 1997). Daily wind speed data were obtained from the weather station at the Fort Huachuca airport for the years 1991-2003. I used the maximum wind speed for each day, took the average of the maximum values over each 5-day period in the historic record, and then calculated the mean and standard deviation of these values by month. These values were then used to represent wind speed probabilistically for each time step (5 days) in the vegetation model. Because temperature and relative humidity are likely to differ considerably from the streamside sites simulated in the model and the upland location of the Tombstone weather station, I compared daily temperature and relative humidity data from 2001-2003 from ecohydrology study sites (Goodrich *et al.*, 2000; Scott *et al.*, 2000, 2003) at Palominas and Charleston to values on the same days at the Tombstone weather station. Mean differences were applied uniformly by month to adjust the Tombstone data (assumed to represent regional conditions) to local conditions at the study sites (Charleston adjustments used for Contention, Palominas adjustments used for Palominas and Kolbe).

3. Streamflow projections

The Soil Water Assessment Tool (SWAT, Arnold *et al.* 1994, www.brc.tamus.edu/swat/) was used for modeling the effects of different climate scenarios on daily streamflow in the upper San Pedro River. SWAT is a physically-based, quasi-distributed hydrologic model designed to project the effects of land management practices on water and sediment yield in large, complex watersheds over long periods of time (Neitsch *et al.*, 2002). Input data include daily weather, soils, topography, vegetation, and land management practices. SWAT is primarily a runoff model, but includes input parameters for representing streamflow-groundwater interactions as well. I used the Automated Geospatial Watershed Assessment Tool (AGWA) interface

(<http://www.tucson.ars.ag.gov/agwa>, Hernandez *et al.*, 2000, 2003; Kepner *et al.*, 2004) for ArcView 3.2 with a digital elevation model (DEM) of the basin to delineate the watershed and sub-basins for the upper San Pedro, for streamflow at Charleston. Land cover data based on 1997 classified Landsat-TM imagery (North American Landscape Characterization, NALC), basin topography, and STATSGO soil data were used to derive spatially quasi-distributed runoff parameters (sub-basin curve numbers) based on lookup tables supplied for the upper San Pedro from the AGWA website. Additional adjustments to hydrologic parameter settings were applied to the sub-basins based on model calibration to historic annual stream flow values by Mariano Hernandez of the Agricultural Research Service (Hernandez *et al.*, 2000, 2003).

SWAT is designed more for representing long-term water yield than for simulating flood routing in response to individual precipitation events (Neitsch *et al.*, 2002). Other distributed hydrologic models, such as KINEROS (Hernandez *et al.*, 2000, 2003) are better suited to representing flood routing from individual storm events and require much finer temporal scale precipitation data. The temporal resolution of the available input data and desired output data in this assessment was intermediate between that of a single storm event and annual water yield. SWAT was used for this assessment because of the availability of annually calibrated parameter settings for the upper San Pedro (Hernandez *et al.*, 2000, 2003) and the ability of the program to accommodate long-term daily climate inputs and provide daily streamflow outputs over a long time interval (100+ years). The reasonable fit between simulated peak annual flows and simulated flows supports the validity of using SWAT for this assessment (see Results section, Figure 3-4). Better fit between simulated and historic flows may be achievable by further calibration of parameters.

Climatic inputs to the SWAT model were derived for 5 weather stations distributed across the upper San Pedro basin. Temperature data for the basin were represented by historic daily values (1951-2002) at Tombstone. Precipitation data were represented by complete daily time series (1951-2002) at 5 stations (principal stations in Table 3-2), with values from neighboring stations used to fill in missing values. Precipitation inputs were distributed to the sub-basins based on the Thiessen polygon approach used in AGWA. Climate scenarios used in the vegetation model runs were also applied to the temperature and precipitation data used in SWAT model runs (i.e., no change over 1951-2002 data, 4° C daily maximum and 6° C minimum temperature increases, 50% or 100% increase and 50% decrease in winter precipitation). Weather stations used for constructing the precipitation time series are shown below in Table 3-2.

Table 3-2. Weather stations used in SWAT model runs. Principal stations used for precipitation point locations in the model are shown in bold. The other, neighboring stations were used to estimate missing values in the records of the principal stations. Latitude and longitude are in decimal degrees.

Station Name	Station ID	Lat (DD)	Long (DD)	Elev (m)	Period of Record
Apache Powder Company	020309	31.9	-110.25	1124.4	1923-1990
Benson	020680	31.97	-110.3	1118.9	1900-1975
Benson 6 SE	020683	31.88	-110.23	1124.7	1990-2003
Tombstone	028619	31.7	-110.05	1405.1	1897-2003
Fairbank 1 S	022902	31.72	-110.18	1174.1	1909-1973
Sierra Vista	027880	31.55	-110.28	1402.1	1982-2003
Fort Huachuca	023120	31.57	-110.33	1421.9	1900-1920, 1954-1981
Y Lightning Ranch	029562	31.45	-110.23	1399.0	1939-2003
Coronado National Monument	022140	31.35	-110.25	1597.8	1960-2003

4. Channel migration projections

Projected changes in channel location under different climatic scenarios were made by Alex Fremier and Eric Larsen of the University of California, Davis, using the program MEANDER (Larsen and Greco, 2002). MEANDER simulates lateral channel migration as a function of channel hydraulics, annual stream power, and spatial heterogeneity in bank erodibility, calibrated against past changes in channel location and configuration. Model output is in the form of ArcView/ArcGIS shapefiles with associated attribute data on sinuosity, axis of curvature, etc. of channel bends. In addition to simulating lateral point bar migration, MEANDER now includes an algorithm to simulate channel cutoffs, given thresholds for peak flow, sinuosity, and bend length at which avulsion occurs. Channel migration in the model was calibrated against observed channel locations from 1973 and 1996 aerial photographs (Dixon, 2003c), and annual cumulative stream power from historic daily flows at the Charleston (0947100), Palominas (09470500), and Redington (0947200) USGS streamflow gages over 1973-1996. Parameter settings for the cutoff algorithm were determined through an iterative process, with the final parameter settings those that minimized the difference between actual and simulated channel positions during the calibration period (1973 to 1996). Among reaches, the sinuosity thresholds for avulsion ranged from 1.7 to 2.0 (reach 1: 2.0, reach 2: 1.8, reach 3: 1.7) and the threshold bend length varied from 20 to 40 channel widths (reach 1: 25, reach 2: 40, reach 12: 20). The peak flow threshold for avulsion was assumed to be 50 cms (1766 cfs). High river terrace boundaries (pre-entrenchment surface) digitized from maps generated by Hereford (1993) were used to partially constrain lateral migration. Other inputs included estimates of bankfull discharge (assumed 1000 cfs), bankfull channel width and depth, channel slope, median particle size (D50) of streambed sediments.

MEANDER was run using daily streamflow outputs from SWAT under the 5 climate scenarios (no change, warm, warm dry, warm wet, warm very wet) for the reaches including the three study sites (reach 1: Palominas UA, reach 2: Kolbe, reach 12: Contention). Differences in the

projected location of the channel midpoint along each study transect at the end of each 5-year interval were used to represent channel location and patch turnover on each study site cross-section.

5. Study sites

The three sites chosen for simulation runs all occur within the SPRNCA and roughly correspond to the three classes of the Riparian Condition Index developed by Lite (2003). The three reach types and representative sites are (1) perennial (Kolbe site); (2) wet intermittent (Palominas UA site); and (3) dry intermittent flow (Contention site). The perennial flow type can be characterized as a hydrologically “gaining” reaches, in which shallow groundwater supports baseflow throughout the year; while the intermittent flow types represent “losing” reaches in which baseflow may cease during seasons in which the groundwater level falls below the river thalweg (Figure 3-1). Wet intermittent reaches are those that have surface flow during the majority of months during a normal year (but are not perennial), while dry intermittent reaches flow less frequently, typically less than 60% of the time.

Kolbe: Kolbe (lat-long: 31.42°, -110.1°; elevation: 1274 m) is classified as a perennial flow site, based on observations of flow in 100% of the days during the 2002 water year (Stromberg *et al.*, 2003). Groundwater levels exceeded the elevation of the thalweg in the non-growing season and were nearly equal with the thalweg during the growing season in water year 2002 (Figure 3-3, Table 3-3), with a relatively low range of fluctuation in groundwater levels near the channel (about 0.4 m) and with baseflow supported by groundwater inputs (a “gaining” stream reach). Consistent with the riparian assessment model of Lite (2003), overstory vegetation near the channel is dominated by tall-stature, obligate phreatophytic species of riparian trees, Fremont cottonwood and Goodding’s willow with little cover of the more drought-tolerant saltcedar (Table 3-3).

Palominas UA: Palominas UA (lat-long: 31.37°, -110.12°; elevation: 1289 m) is classified as a wet intermittent flow site, based on observations of flow in 70% of the days during the 2002 water year (Stromberg *et al.*, 2003). Groundwater levels exceeded the elevation of the thalweg during the non-growing season, but fell slightly below the thalweg (here about -0.3 m near the channel) during periods of high groundwater demand during the growing season (Table 3-4, Figure 3-3). Consistent with the riparian assessment model, the Palominas UA site contains a mixture of obligate phreatophytic (cottonwood) and facultative phreatophytic (saltcedar) riparian trees (Table 3-4).

Contention: Contention (lat-long: 31.76°, -110.2°; elevation: 1154 m) is classified as a dry intermittent flow site, based on observations of flow in 56% of the days during the 2002 water year (Stromberg *et al.*, 2003). Groundwater levels were slightly lower than the elevation of the thalweg during the non-growing season (-0.14 m at the channel), fell substantially below the thalweg (here about -2.3 m near the channel) during periods of high groundwater demand during the growing season, and hence exhibited a large range of fluctuation (about 2 m) in groundwater levels during water year 2002 (Figure 3-3, Table 3-5). Riparian vegetation at Contention was consistent with projections of the riparian assessment model, with dominance by patch types characterized by facultative phreatophytic species such as saltcedar and mesquite, and the near absence of obligate phreatophytic riparian trees (cottonwood, willows) (Table 3-5).

6. Plot conditions and vegetation model runs

The model was run for vegetation plots along a transect instrumented with piezometers at each site, for which detailed groundwater, topographic, and stage-discharge data were available. Plots on the high terrace (pre-entrenchment surface) were excluded; only plots on the post-entrenchment floodplain/terrace were used. Initial conditions for each model run consisted of the vegetation, elevation above the river thalweg, and seasonal depth to groundwater (growing season and non-growing season) for each plot that was sampled along the transect. Depth and seasonal fluctuation in groundwater levels were based on minimum and maximum groundwater levels in a dry year (2002), measured from nested piezometers on the site (Leenhouts, unpublished data). Transect topography was based on topographic surveys by the USGS in combination with patch widths delineated by the Stromberg group. Initial vegetation conditions were based on field data on vegetation composition and structure collected in 2001 for each plot. Each plot was taken to represent the conditions in the entire patch in which it was found and its contribution to the vegetation of the entire transect was weighted by the width of the patch relative to the width of the entire floodplain.

Initial conditions for vegetation were represented by the stem density (per 100 m² plot) and mean effective diameter (weighted diameter based on total basal area divided by stem density for each species) in study plots, for five of the six most abundant tree species (Freemont cottonwood, Gooding willow, saltcedar, mesquite, and ash) in the riparian corridor. (The other common tree, *Celtis reticulata*, which often occurs as a subdominant in mesquite woodlands, was assumed to be ecologically equivalent to the more abundant mesquite and hence was lumped with that species in the model input and output).. Initial conditions also included density and coverage of a general group designated as xeric riparian shrubs (e.g., *Hymenoclea monogyra*, *Ericameria nauseosa*, *Acacia greggii*) and hydric pioneer shrubs (e.g., seep-willow, *Baccharis salicifolia*), and by cover values for three functional groups of herbaceous plants (wetland perennials, annuals, and mesic perennial grasses such as sacaton. Sacaton has the greatest average cover of all perennial herbs in the Upper San Pedro floodplain, with *Sorghum halapense* and *Cynodon dactylon* also being common). For the purpose of these model runs, I initialized all plots with 20% cover each of annuals and wetland perennial plants. Initial rooting depth of all woody plants present on the plots at the beginning of the simulation were set as the deepest groundwater depth during the course of the year or the maximum rooting depth for the species, whichever was smaller. In cases in which the patch was designated as a forest or woodland of a particular type (e.g., old growth cottonwood woodland), but no trees of that species were present on the sampled plot, I assumed a density of 0.5 trees per 100 m² and an effective diameter corresponding to the age class (young, mature, old growth) of that species. Soil texture on all plots was assumed to be 80% sand, 10% clay, and 10% silt.

The vegetation model was run for plots from each of the three sites under four of the five climate scenarios (no change, warm, warm wet, warm dry), with four replicates of each run, for 2003-2102. Model runs were not made for the wettest climate scenario (doubling of winter precipitation). Flow data were taken from SWAT model runs for stream segments corresponding to each study site and were summarized over 5-day intervals, based on the maximum daily mean flow during each period. Stage-discharge relationships were extrapolated from HEC-RAS model runs for the 2-100 year return floods at each site (Leenhouts, 2003). Shifts in channel position along each transect were derived from MEANDER runs under each climate/flow scenario for each 5-year interval. Shifts in channel position were assumed to erode portions of existing

patches on the outside of the bend and form point bars available for colonization of new vegetation on the inside of the bend, thus creating new patches and eroding old ones during the course of the simulation. New patches were initialized with a plot elevation of 0.5 meters above the river thalweg and were assigned a patch width corresponding to the amount of simulated channel migration that had occurred since the last recruitment event. During each 5-year interval, new vegetation plots were initiated in the year with the highest peak daily discharge exceeding 6000 cfs at Charleston (>5721 at Palominas). This flow threshold was the peak daily flow (maximum mean daily flow for the year) exceeded in approximately 10% of the years during 1951-2002 at the Charleston gage, and reflected the assumption that major vegetation colonization events are associated with the 10-year return flood (Stromberg *et al.*, 1993a, 1998a). The effects of long-term declines in alluvial aquifer levels were not simulated for this report. Studies of groundwater hydrology in the basin, however, suggest that current rates of groundwater extraction could lead to strong future declines in alluvial aquifer levels, reduction of stream baseflow, and degradation of riparian vegetation (Vionnet and Maddock, 1992; Pool and Coes, 1999; Goode and Maddock, 2000; Steinitz *et al.*, 2003). Scenarios of groundwater decline will be incorporated in future runs of this model, as results from a seasonal groundwater model currently under development become available.

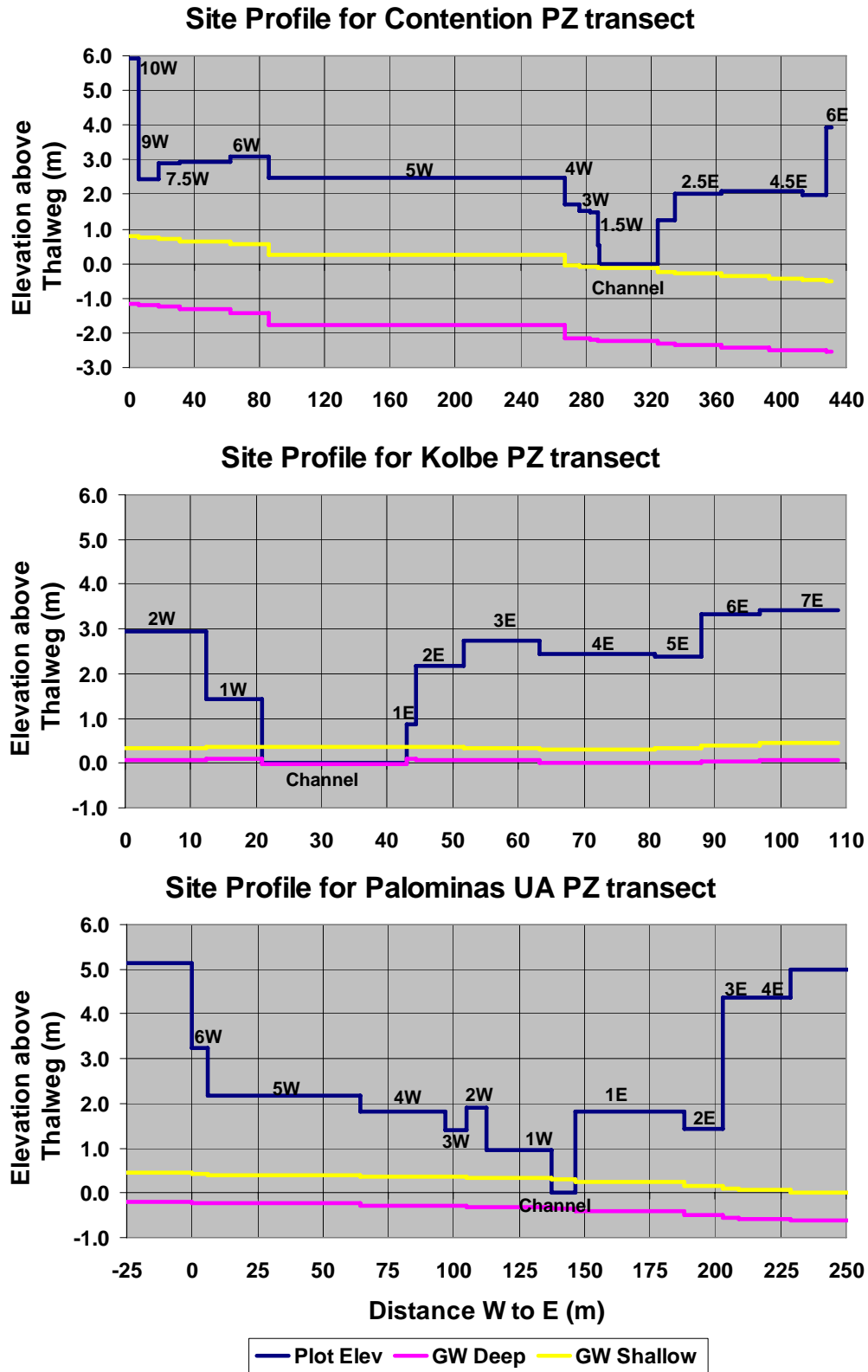


Figure 3-3. Topography, groundwater levels, and plot numbers at the three study transects.

Table 3-3. Starting plot conditions for simulation runs on the vegetation transect at Kolbe. Cases in which plot vegetation (starting vegetation for the model runs) differed substantially from the field-designated patch type are shown in bold. Plot and groundwater elevations are relative to the river thalweg.

Plot ID	Field Patch Type	Simulation Patch Type	Landform	Plot Elev (m)	Groundwater Elevation (m)		Patch Width (m)
					Summer	Winter	
2W	Spiny aster shrubland	Mature1 willow forest	Floodplain	2.94	0.06	0.34	12.3
1W	Mixed grassland	Mixed open	Floodplain	1.42	0.09	0.36	8.5
	Active Channel			0.00	-0.02	0.37	22.1
1E	Mature willow woodland	Young willow forest	Floodplain	0.88	0.09	0.36	1.4
2E	Mature willow forest	Mature1 willow forest	Floodplain	2.17	0.08	0.35	7.3
3E	Mature cottonwood forest	Mature1 cottonwood forest	Floodplain	2.73	0.05	0.33	11.6
4E	Other grassland	Mixed open	Floodplain	2.44	0.01	0.31	17.7
5E	Mature willow forest	Forbland or sacaton grassland	Floodplain	2.38	0.01	0.32	7.0
6E	Mature willow forest	Old cottonwood/ willow forest	Floodplain	3.33	0.04	0.41	9.0
7E	Old cottonwood woodland	Old cottonwood forest	Floodplain	3.42	0.07	0.46	11.8
Total Width = 108.7							

Table 3-4. Starting plot conditions for simulation runs on Palominas UA transect. Cases in which plot vegetation (starting vegetation for the model runs) differed substantially from the field-designated patch type are shown in bold. Plot and groundwater elevations are relative to the river thalweg.

Plot ID	Field Patch Type	Simulation Patch Type	Landform	Plot Elev (m)	Groundwater Elevation (m)		Patch Width (m)
					Summer	Winter	
6W	Mature cottonwood forest	Mature1 cottonwood forest	Floodplain	3.23	-0.22	0.44	6.1
5W	Old cottonwood forest	Mature1 cottonwood woodland	Floodplain	2.17	-0.24	0.41	58.0
4W	Mature cottonwood forest	Mature1 cottonwood forest	Floodplain	1.83	-0.28	0.37	32.7
3W	Mature cottonwood woodland	Mature2 cottonwood forest	Floodplain	1.41	-0.30	0.35	8.0
2W	Open patch	Young cottonwood forest	Floodplain	1.90	-0.30	0.34	7.5
1W	Open patch	Young cottonwood woodland	Floodplain	0.96	-0.32	0.33	25.3
	Active Channel			0.00	-0.34	0.30	8.8
1E	Other grassland	Young cottonwood shrubland	Floodplain	1.81	-0.40	0.25	41.5
2E	Mature saltcedar shrubland	Young saltcedar shrubland	Floodplain	1.43	-0.49	0.16	15.0
3E	Spiny aster shrubland	Mature1 saltcedar woodland	Floodplain	4.36	-0.54	0.11	6.0
4E	Spiny aster shrubland	Xeric shrubland	Floodplain	4.36	-0.59	0.05	20.0
Total Width =							328.9

Table 3-5. Starting plot conditions for simulation runs on Contention transect. Cases in which plot vegetation (starting vegetation for the model runs) differed substantially from the field-designated patch type are shown in bold. Plot and groundwater elevations are relative to the river thalweg.

Plot ID	Field Patch Type	Simulation Patch Type-	Landform	Plot Elev (m)	Groundwater Elevation (m)		Patch Width (m)
					Summer	Winter	
10W	Old mesquite shrubland	Mature mesquite shrubland	Floodplain	5.93	-1.15	0.77	6.0
9W	Old willow woodland	Mature2 willow forest	Floodplain	2.45	-1.20	0.74	12.0
7.5W	Mature mesquite shrubland	Sacaton grassland or mixed open	Floodplain	2.93	-1.28	0.67	44.0
6W	Open patch	Mixed open	Floodplain	3.10	-1.41	0.56	23.4
5W	Mature mesquite shrubland	Mixed open	Floodplain	2.49	-1.79	0.25	182.0
4W	Forbland	Mixed open	Floodplain	1.70	-2.15	-0.06	8.7
3W	Sacaton grassland	Sacaton grassland	Floodplain	1.50	-2.17	-0.08	6.6
1.5W	Grassland	Mixed open	Floodplain	1.36	-2.20	-0.10	5.9
	Active Channel			0	-2.25	-0.14	36.1
1E	Grassland	Mature1 saltcedar shrubland	Floodplain	1.26	-2.32	-0.23	9.8
2.5E	Forbland	Mixed open	Floodplain	2.05	-2.40	-0.33	58.0
4.5E	Mature mesquite shrubland	Sacaton grassland	Floodplain	2.04	-2.50	-0.46	36.1
6E	Atriplex shrubland	Mature mesquite shrubland	Floodplain	3.93	-2.54	-0.51	2.6
Total Width =							430.7

7. Simulation of fire effects

Unlike earlier versions of the vegetation model (Dixon, 2003a,b) the model runs in this report include the simulation of fire occurrence and its effects on vegetation composition and structure. Data on fire occurrence within the SPRNCA for 1991-2003 (BLM, unpublished) was used to develop statistical relationships between occurrence of fires of ≥ 10 acres (4 ha.) in size and 5-day regional (Tombstone) climatic conditions, using logistic regression. The regression equation selected for use in the model is shown below:

$$\text{logit (fire)} = 0.0757 * (\text{mean Tmax}) - 0.981 * (\text{precip over previous 35 days}) + 0.6968 * \text{windspeed} - 9.6907$$

$$\text{fire probability} = 1 / (1 + \text{EXP}(-\text{logit}))$$

where precipitation is in cm, maximum temperature in degrees Celsius, and windspeed in meters per second. Hence, the probability of occurrence (during a given 5-day period) of a fire of ≥ 10 acres in the SPRNCA during a given 5-day period increased significantly with increases in mean daily maximum windspeed and mean maximum temperature and decreased with the total precipitation in the current (5-day) time step plus the previous month (six previous time steps).

Given the occurrence of a fire somewhere within the SPRNCA, the probability of occurrence at a given study site was assumed to be ratio between the size of the fire and the total area of the riparian corridor within the Conservation Area, under the assumption that the majority of large fires occur within the riparian corridor. The area of the riparian corridor was defined as the area of the floodplain (post-entrenchment surface) plus a 100-meter buffer, for the length of the river within the Conservation Area. This comprised approximately 29% of the total area of the SPRNCA, or about 7300 ha. For a given fire event, area burned was simulated probabilistically, randomly drawing fire size from a normal distribution based on the mean and standard deviation of the log-transformed areas of all fires ≥ 10 acres within the Conservation Area during 1991-2003. Finally, the occurrence of a fire in a given plot was also a function of local fuel moisture, with no fires occurring if fuel moisture exceeded the extinction moisture threshold of 25% (Rothermel, 1972). Fuel moisture was expressed as a function of the moisture status of the live herbaceous plants (based on soil moisture availability), estimated moisture content of the herbaceous leaf litter, and the proportion of dead to live herbaceous leaf area. The maximum moisture content (i.e., when soil moisture is not limiting) of live herbaceous plants was assumed to be 233% of stem dry weight (based on stem water content of 70% for sacaton; Tiller *et al.* in prep.). Dead fuel moisture was modeled as a function of maximum temperature and relative humidity (based on the McArthur Grassland Fire Index, meter 5, from Noble *et al.*, 1980).

Local fire intensity was simulated using the Rothermel fire spread equations (Rothermel, 1972), based on local climatic and fine fuel (herbaceous litter) conditions. Scorch height was modeled using the equation of van Wagner (1973), as modified by Miller and Urban (1999). Tree topkill was modeled as a function of scorch height, tree height, and bark thickness, using equations developed by Ryan and Reinhardt (1988), Reinhardt (pers comm.), and Keane *et al.* (1996). Probability of tree or shrub resprouting after fire was determined for each species based on values found in the literature and data from the field.

8. Analysis

Model runs were made for each plot for four climate scenarios (no change, warm, warm wet, warm dry), for a total of approximately 900 separate runs. For each year, across the four replicates of each scenario and plot, model results were summarized by calculating the mean cover for each species or functional group, the leaf area above 5 m, and (for trees) the mean diameter per species on each plot. These values were then used to classify plots according to patch type, using rules similar to those used for defining patch types in the field, using physiognomy (forest, woodland, shrubland, herbaceous, open), dominant species, and age-size structure (stem diameter classes for cottonwood, willow, saltcedar, and mesquite). Rules for physiognomy were as follows:

Forest	=	canopy >5 m tall, with 60-100% canopy cover
Woodland	=	canopy >5 m tall, with 25-59.9% canopy cover
Shrubland	=	<25% canopy cover over 5 m tall, but >25% woody cover in 1-5 m
Herbaceous	=	<25% woody cover, >25% herbaceous cover
Open	=	<25% woody cover and <25% herbaceous cover

Floodplain-wide changes in proportional cover of patch types were summarized on 25-year intervals (2003, 2027, 2052, 2077, 2102) for each site by weighting each plot according to the width of the patch it represented, summing patch widths across patch types, and dividing by the total floodplain width.

9. Simulation Results

Flood Modeling with SWAT

SWAT simulations using historic precipitation and temperature data matched the timing and magnitude of large winter and annual floods reasonably well, but was much poorer at simulating flood events associated with summer monsoonal rains (Figure 3-4) and low flows, and considerably underestimated the size of the fall peak flood in 1977.

SWAT model results showed relatively weak effects of climate warming alone on annual peak flow magnitude, but strong effects of changes in winter precipitation (Figure 3-5). Increases of 4° C for maximum temperature and 6° C for minimum temperature slightly reduced the magnitude of maximum annual mean daily flows by the end of the simulation. Effects of changes in winter precipitation had a much stronger effect, with a 50% decline in the size of winter precipitation events essentially shutting off winter floods. No fall/winter floods exceeded 6000 cfs (the threshold for vegetation recruitment used in the model) under the warm dry scenario, with the only two floods exceeding 6000 cfs occurring in the summer monsoon season (in 2007 and 2059). A progressive 50% increase in the size of winter precipitation events resulted in a large increase in the number of years with fall/winter floods exceeding 6000 cfs, with such floods occurring in 16 different years (2019, 2029, 2035, 2045, 2046, 2052, 2069, 2071, 2081, 2082, 2083, 2087, 2088, 2089, 2097, and 2098) and with peak flood magnitudes about three times larger than those under the no change scenario by the end of the simulation. Predictably, a doubling of winter precipitation resulted in even larger and more frequent winter floods, with flood magnitude around 5-6 times larger than under the no change scenario by 2102 (Figure 3-6).

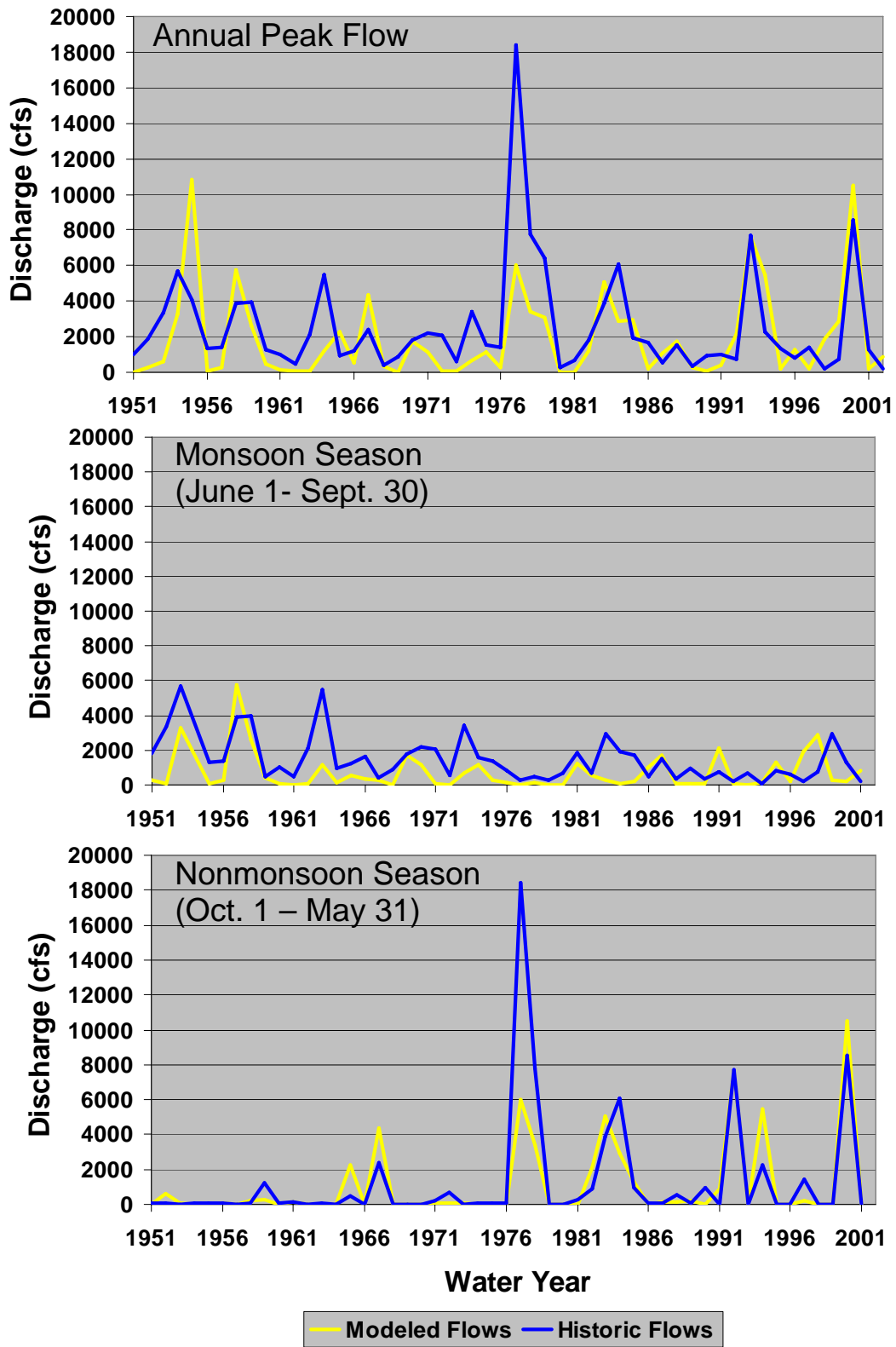


Figure 3-4. Comparison of historic and modeled peak flows (maximum mean daily flows) at Charleston gage. Flows were modeled using SWAT.

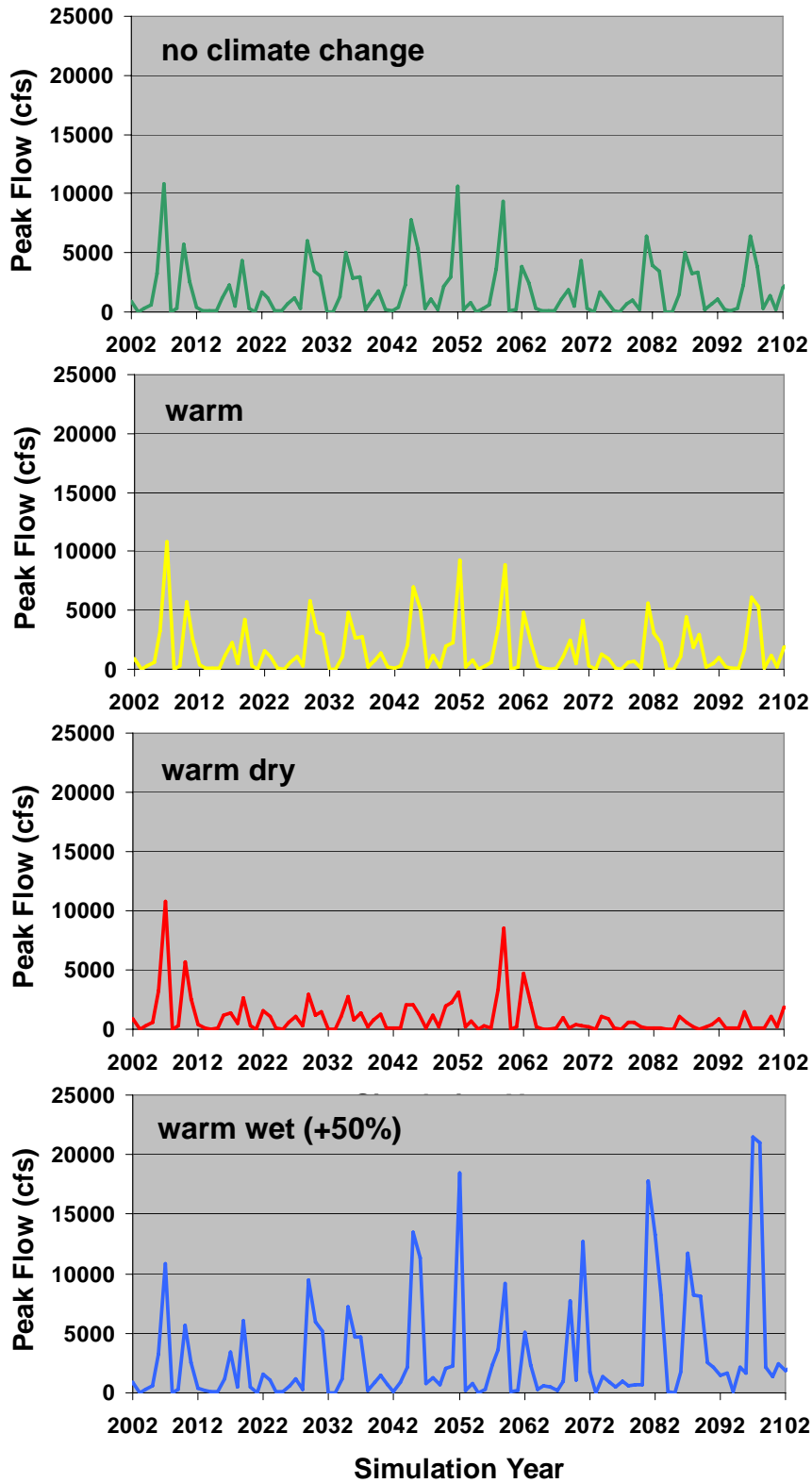


Figure 3-5. Simulated annual peak flows from SWAT under the no change, warm, warm dry, and warm wet climate scenarios.

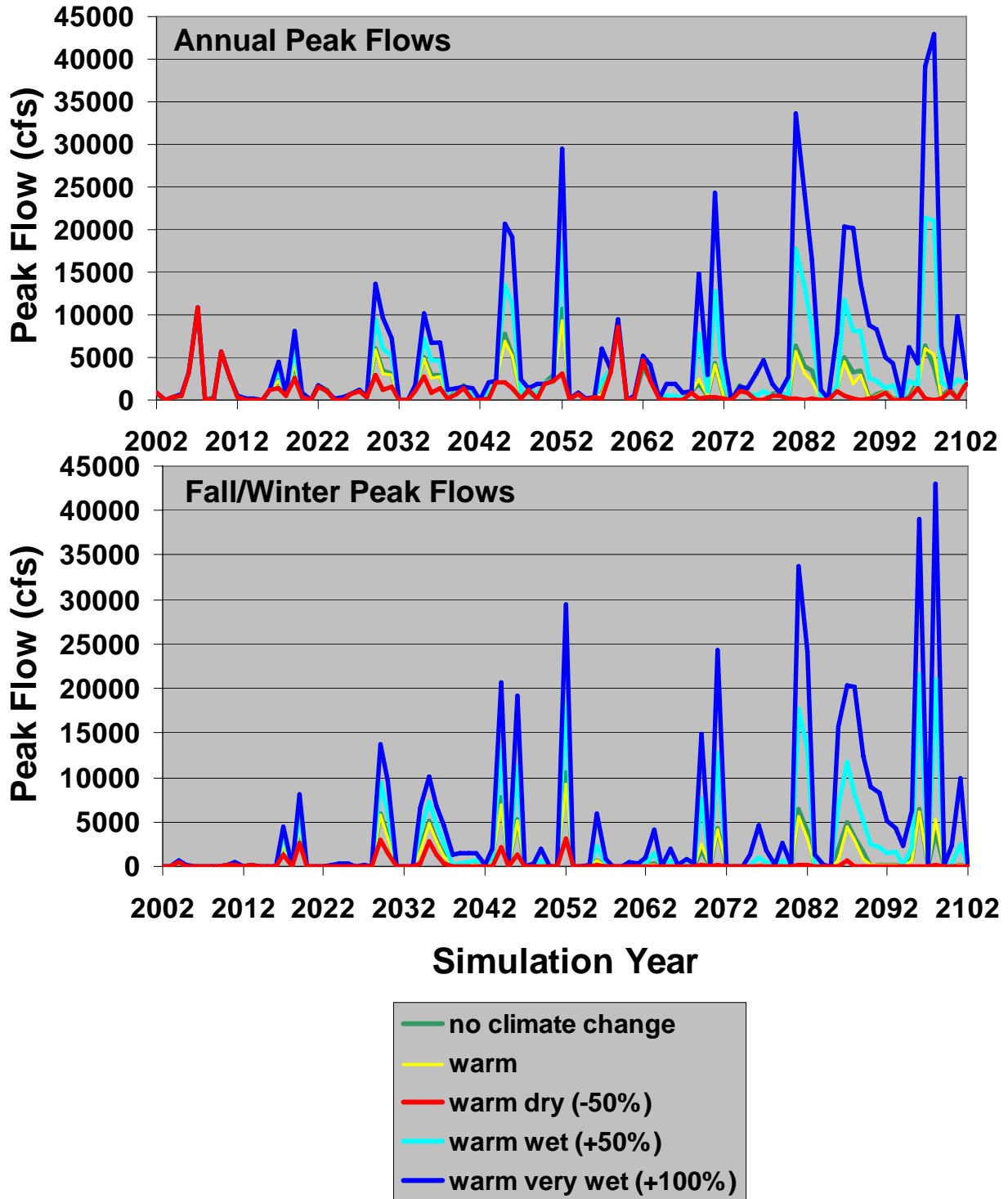


Figure 3-6. Comparison of simulated peak flows from SWAT model runs for the five climate scenarios: (a) annual peak flows, (b) fall/winter peak flows.

a. Channel migration

Channel migration rates varied considerably among scenarios and sites, with much higher migration rates under the two scenarios with increased winter precipitation; much lower rates under the warmer, drier scenario; and slightly lower rates under the climate warming with no change in precipitation than under the no change scenario (Figures 3-7 through 3-9, Table 3-6). Among sites, migration rates were much lower on the Palominas and Kolbe transects than at Contention, under the no change, warm, and warm dry scenarios. Migration rates at all sites increased strongly under the wetter scenarios, with the strongest relative increases at Kolbe and the smallest at Palominas. Total channel movement from 2002 to 2099 also varied considerably within each reach, suggesting that single measurements along the vegetation transects may not adequately represent reach-level channel and vegetation dynamics.

b. Fire

Climate scenario had a significant influence on the frequency of fire occurrence per patch at each study site. Fires were significantly more frequent under the warm dry scenario than under all other scenarios and were significantly more frequent under both the warm and warm dry scenario than under the no change scenario. The mean number of intense fires (fireline intensity >500 kW/m²) per patch per 100 years was 2.2 for the warm dry (45-year return interval), 1.8 for the warm (55-year return interval), 1.7 for the warm wet (60.3-year return interval), and 1.4 for the no climate change scenario (72-year return interval). There were also differences among study sites in fire frequency, with the highest frequency at Palominas and the lowest at Contention, with Kolbe intermediate.

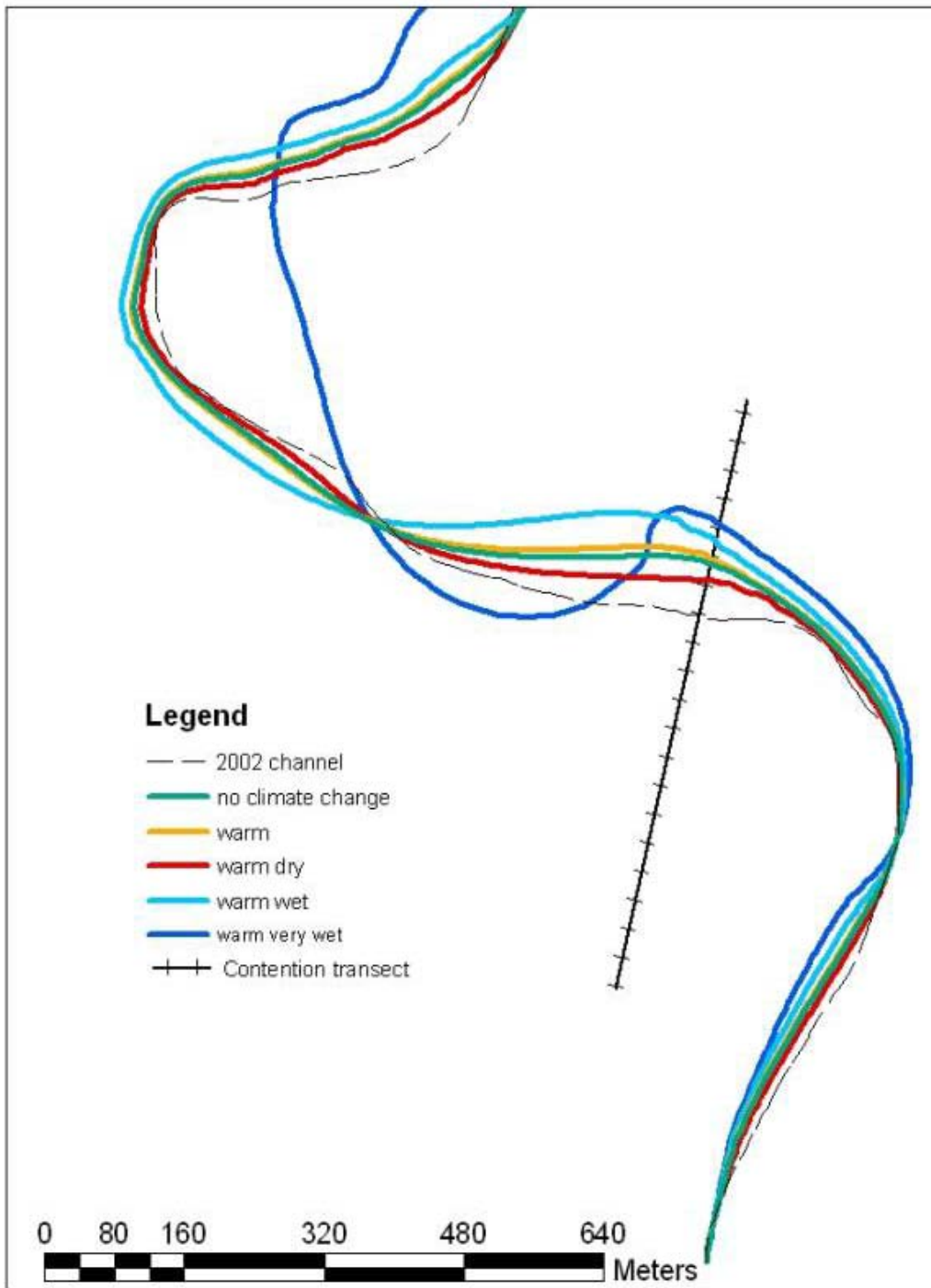


Figure 3-7. Simulated channel position by 2099 at Contention under the five climate scenarios. The starting (2002) channel position is shown as a dashed line. Channel migration was simulated using the program MEANDER (Larsen and Greco, 2002).

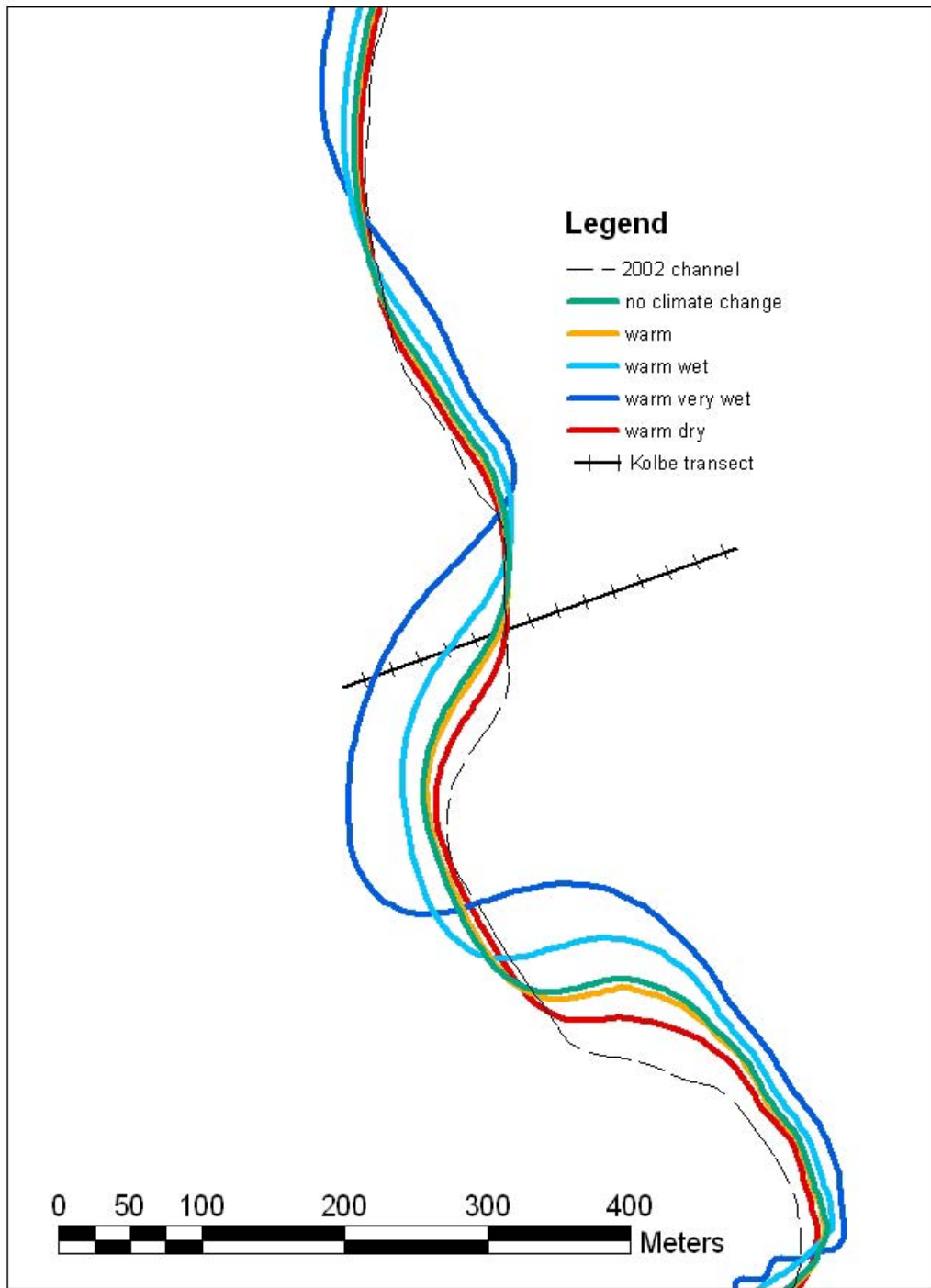


Figure 3-8. Simulated channel position by 2099 at Kolbe under the five climate scenarios. The starting (2002) channel position is shown as a dashed line. Channel migration was simulated using the program MEANDER (Larsen and Greco, 2002).

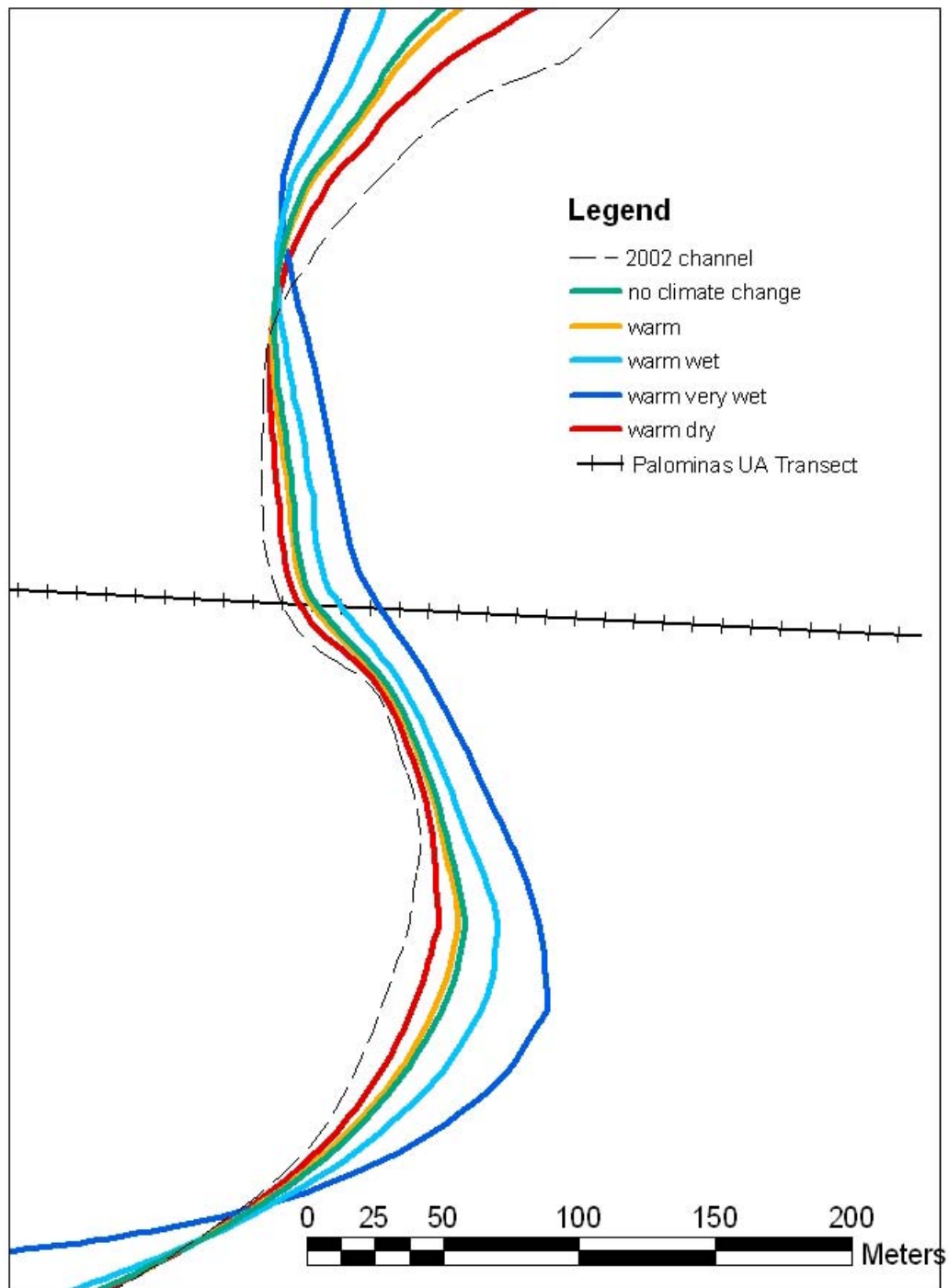


Figure 3-9. Simulated channel position by 2099 at Palominas UA under the five climate scenarios. The starting (2002) channel position is shown as a dashed line. Channel migration was simulated using the program MEANDER (Larsen and Greco, 2002).

Table 3-6. Cumulative horizontal displacement (in meters) in simulated channel position, relative to 2002, along each transect, for five climate scenarios. Channel migration was simulated using the program MEANDER (Larsen and Greco 2002). Positive values indicate eastward movement of the channel, negative values indicate westward movement.

Site	Scenario	Cumulative Displacement (m)			
		2027	2052	2077	2099
Contention	no change	16.9	35.9	49.0	59.3
	warm	16.7	33.7	45.3	54.3
	warm dry	15.7	25.6	34.7	36.6
	warm wet	17.8	43.9	60.5	77.6
	warm very wet	19.4	56.9	75.4	95.0
Kolbe	no change	0.8	0.4	-3.3	-9.8
	warm	0.8	0.6	-2.1	-5.9
	warm dry	0.7	1.0	0.5	0.2
	warm wet	0.9	-1.5	-11.9	-43.4
	warm very wet	0.9	-8.1	-37.0	-96.8
Palominas UA	no change	2.6	6.6	9.8	13.0
	warm	2.5	6.0	9.2	12.8
	warm dry	2.4	4.2	6.2	8.0
	warm wet	2.7	8.8	13.8	24.1
	warm very wet	3.0	12.4	20.5	39.1

c. Simulated vegetation change

Contention - In 2003, the floodplain at Contention was dominated (about 80%) by vegetation classified as “mixed open” in the model (Table 3-5, Figure 3-10), meaning that species composition was mixed (no dominant species) and total cover was insufficient (<25%) to be classified as herbaceous, shrubland, woodland or forest. In the field, however, these patches had been originally classified as mesquite shrubland (72% by patch width), forbland (21%), open (7%), and a tiny amount as grassland (<1%) (Table 3-3). Had these patches been initially classified the same in the model as in the field, then mesquite would have dominated floodplain coverage from 2003 through 2102 for most of the climate scenarios. By 2027, most of the mixed open patches had converted to mesquite, sacaton, or saltcedar-dominated patches (Figure 10). In three of the four scenarios, mesquite remained the dominant patch type through the rest of the simulation. The one exception was the no change scenario, in which sacaton occupied over 60% of the floodplain by 2077 and 2102. Dominance of sacaton under the no change scenario was largely due to conversion of patch 5W (Table 3-5), which covered 47% of the floodplain, from mesquite shrubland to sacaton grassland (Attachment 1). Similarly, the high coverage by sacaton under the warm dry scenario in 2027 was also due to conversion of patch 5W to sacaton. Sacaton coverage subsequently declined in this scenario as the patch converted to mesquite shrubland by 2052. The relative balance of sacaton versus mesquite coverage on an individual date may depend on how recently fire had occurred in an individual model run. This varied among individual model runs, as fire was simulated as a probabilistic event in each run and each patch.

Saltcedar maintained a relatively small, but fairly constant proportion of the floodplain through the simulations (Figure 3-10). Initial increases in patch dominance occurred in all scenarios between 2003 and 2027, with some conversion of open or grassland patches to saltcedar (Attachment 1) and some recruitment on new patches formed by channel migration (Figure 3-14). Thereafter, saltcedar increased slightly in the warm scenario and remained constant or declined slightly in the other scenarios. Cottonwood-willow patch types occupied a small proportion of the floodplain initially, but died out and did not colonize new patches created by channel migration.

Kolbe - The floodplain vegetation at Kolbe shifted from dominance by cottonwood and willow in 2003 to dominance by mesquite, sacaton, and in some cases, ash, in 2102 (Figure 3-11). Across scenarios, cottonwood/willow patch types occupied 60-70% of the total floodplain width from 2003 through 2027. After 2027, coverage declined steadily, with cottonwood/willow patch types declining to a low of 3% under no climate change, 6% under the warm scenario, and less than 1% of the floodplain under the warm dry scenario. Under the warm wet scenario, total coverage by cottonwood/willow patch types declined to 21% by 2077 and then rebounded to 37% by year 2102. In all scenarios, cottonwood/willow coverage by 2102 was almost completely composed of new patches formed by channel migration (Figures 3-11, 3-13), with cottonwood/willow patches present in 2003 occupying less than 1% of the 2102 floodplain. Patch 1E, which was only 1.4 meters wide, was the only original patch that still had significant cottonwood/willow coverage by the end of the simulation, with old-growth cottonwood woodland or forest in 2102 under all scenarios (Table 3-3).

Change in coverage by mesquite patch types was nearly a mirror image of the cottonwood changes (Figure 3-11). No patch types were dominated by mesquite in 2003 (Table 3-3), but the

proportion of the floodplain covered by mesquite increased strongly from 2027 to 2102, with final coverage ranging from about 30% in the no change and warm wet scenarios to nearly 70% in the warm scenario (Figure 3-11). Across scenarios, all patches (with the exception of patch 1E) that began as cottonwood/willow in 2003 had converted to mesquite, sacaton, or mixed open by 2102. Sacaton grassland had a variable response across scenarios, occupying 13-24% of the floodplain by 2102 in three of the four scenarios, but co-dominant with mesquite patch types (each covering about 40% of the floodplain) in the warm dry climate. Across scenarios, ash woodland/forest occupied about 20% of the floodplain in 2027 and 2052, remaining constant in the no change and warm dry scenarios to 2102, but converting to mesquite patch types in the other two scenarios (Figure 3-11). All ash coverage was on one patch (4E) that began as a mixed open patch in 2003 (Table 3-3).

Palominas UA - As at Kolbe, the floodplain at Palominas UA was dominated by cottonwood/willow patch types in 2003 (81%), with coverage by cottonwood/willow declining steadily in all scenarios after 2027 (Figure 3-12). Saltcedar occupied about 10% of the floodplain in 2003, increased to 14-22% by 2052, and then declined sharply to 2102 in all scenarios. By 2102 sacaton and/or mesquite dominated the floodplain, with highest coverage by sacaton patch types under the no change scenario (75%) and highest mesquite coverage under the warm wet scenario (75%). Somewhat surprisingly, coverage by cottonwood/willow patches was highest in 2102 under the warm dry scenario, with old-growth cottonwood forest remaining on two fairly wide patches (1W and 4W). Aside from these two patches under the warm and warm dry scenarios, all patches that began as cottonwood/willow in 2003 had transitioned to other patch types (mostly sacaton or mesquite), by 2102. Rates of channel migration and recruitment of new cottonwood/willow and saltcedar patches were low at the transect location (Figures 3-13, 3-14) and hence were insufficient to counterbalance loss of these patch types from senescence of the original stands. No successful recruitment of cottonwood/willow occurred on patches formed by channel migration under the warm dry scenario (only summer floods) and very low recruitment of saltcedar occurred under the warm wet scenario, despite higher channel migration under this scenario than the others.

An important trend across simulations, scenarios, and study sites was an increase in coverage of mesquite, and sometimes sacaton, patch types from 2003-2102 (Figures 3-10 – 3-12). On Kolbe and Palominas UA, coverage of cottonwood/willow patch types declined strongly during the simulations, showing the inverse pattern to changes in mesquite coverage. Overall, most patches occupied by pioneer patch types in 2003 transitioned to other patch types (often mesquite or sacaton) by 2102, as pioneer stands senesced. Hence, long-term coverage by pioneer patch types was closely linked to rates of channel migration, with species composition (i.e., cottonwood/willow or saltcedar) influenced by flood season and groundwater hydrology. Only for Contention did migration rates appear sufficient to maintain stable coverage of pioneer woody patch types (saltcedar) in the floodplain, with highest coverage under the warm wet scenario (Figures 3-10, 3-14). At Palominas, migration rates under even the warm wet scenario were insufficient to maintain the initially high cottonwood/willow coverage in the floodplain (Figure 3-12). At Kolbe, recruitment of new cottonwood/willow patches was four-fold greater under the warm wet scenario than under the no climate change scenario (Figure 3-13). Migration rates under this scenario may be sufficient to maintain high coverage of pioneer patch types, if precipitation levels reached by the end of the transient scenario (50% increase in fall/winter precipitation) continue into the next century. The substantially higher migration rates observed in the MEANDER runs with a doubling of winter precipitation by 2102 may be sufficient to

maintain high coverage of pioneer patch types at all sites, but vegetation model runs were not conducted for this scenario (Figures 3-7 through 3-9, Table 3-6).

3.5 Discussion

Discrepancies in patch type designations

In several cases, starting (2003) patch type definitions based on plot-level vegetation and the equations used in the model differed from their designation in the field (e.g., Palominas UA, plots 1W and 2W; Kolbe, plots 2W and 5E; Contention, plots 1E, 4.5E, 5W, 7.5W; Tables 3-3 through 3-5). These differences arose for several possible reasons. First of all, field patch-type designations were made based on the entire patch, with the individual sampling plot intended to represent patch-level vegetation patterns. However, the small (100-200 m²) individual plots may not adequately characterize the vegetation of the entire patch (e.g., a mesquite tree may, by chance, occur within a plot in a patch otherwise dominated by grassland). Hence, in some cases, applying the patch delineation rules to an individual plot may result in a different designation for the plot than for the patch as a whole. Second, in the vegetation model it is implicitly assumed that the cover of any plant in the plot is entirely contained within the plot. In the field, however, individual trees may occur at the edge of the plot, and hence have a lower canopy cover in the plot than projected by the model, or the canopies of trees outside the plot may extend into the plot, producing a higher canopy cover in the plot than is projected by the model. Discrepancies between model and field patch designations can be attributed mostly to these two causes. Discrepancies could also arise, however, if model equations for particular species consistently over- or underestimate canopy cover. In the model exercises reported here, model equations may have underestimated mesquite canopy cover in plots 5W, 7.5W, and 4.5E at Contention (Table 3-5) and may have overestimated cover for mature cottonwoods and willows for some plots at Kolbe and Palominas UA (Tables 3-3 and 3-4). Unfortunately, such discrepancies are difficult to evaluate, because individual plots are not large enough to contain the full canopies of all trees rooted within the plots.

For consistency, this report uses patch-type designations derived from plot vegetation data (the actual inputs to the model) and model equations, rather than the field-delineated patch types. Other approaches (e.g., using average vegetation patterns to represent generalized patch types, rather than plot-specific vegetation) could be considered for future model runs.

Projected vegetation changes

Generally, model results suggest a decrease in coverage by pioneer woody vegetation across the floodplain of the upper San Pedro over the next 100 years. In particular, coverage of cottonwood/willow patches may decline as old patches established during the channel narrowing process will senesce. The extensive cottonwood and willow patches found currently along portions of the river are largely the legacy of channel widening and subsequent channel narrowing and floodplain reconstruction over the last century. Long-term coverage by cottonwood/willow in particular, and pioneer patch types in general, will depend heavily on how much opportunity there is for new recruitment of these species in the future. Recruitment of these species depends heavily on the formation of moist, mineral seedbeds by channel migration and on the timing of floods, with cottonwoods and willows particularly dependent on the occurrence of fall, winter or spring floods (Stromberg *et al.*, 1991; 1993a; Stromberg, 1998a).

Hence, the influence of climate change on pioneer riparian communities will depend largely on how precipitation regimes change. Decreases in winter precipitation will likely result in less frequent winter floods, lower rates of channel migration, and much lower rates of recruitment by cottonwood and willow. Increases in winter precipitation should result in larger and more frequent winter floods, higher channel migration rates, and higher recruitment rates by cottonwood and willow. If increases in precipitation are high enough, then it is possible that pioneer patch types could be maintained at high levels in the floodplain of the San Pedro. Relative coverage by cottonwood/willow versus saltcedar patch types may be influenced by changes in the seasonality of precipitation and flooding, with increases in winter flooding favoring cottonwood/willow. Although saltcedar also recruits after winter floods, its longer dispersal interval may also enable it to recruit after floods later in the spring or summer (Horton, 1977, Shafroth *et al.*, 1998). Changes in depth to groundwater, however, are likely to have a stronger influence on the relative importance of these two groups (Lite, 2003), with saltcedar much more tolerant of drought and more variable and deeper groundwater levels. Future rates of groundwater extraction in the basin could have a strong impact on the relative coverage of saltcedar vs. cottonwood and willow patch types.

According to model results, coverage by later successional communities such as mesquite, ash patch types, and perhaps sacaton grassland, should increase over the next 100 years. The relative balance between mesquite forest/woodland and grassland/shrubland coverage may depend heavily on how fire frequency and intensity changes in the future. Model results suggest somewhat higher fire frequencies under all warming scenarios, with particularly higher frequencies under a warmer, drier climate. Model simulation of fire, however, was done probabilistically on a patch-by-patch basis, with no spatially explicit simulation of fire spread among patches. Spatial effects could be very important for both future fire regimes and for population dynamics of mesquite. Fire is likely to be frequent and effective within a landscape dominated by high coverage and connectivity of grassland patches than one in which such patches are small and disconnected. As an animal-dispersed species, recruitment of mesquite may also be strongly influenced by spatial context. Shifts between mesquite and grassland dominated landscapes could represent phase changes between alternative stable states, with either state tending to persist in the absence of changes in disturbance or land use (Archer *et al.*, 1988). These effects of spatial context could not be captured in the plot-based unit model used in these simulations. Conversion to a true landscape model, with spatially interactive processes among cells, could better simulate the effects of spatial context and perhaps yield better projections for landscape change. Future changes in land management, particularly grazing, could also have a strong influence on fire frequency in the system and on relative coverage of grassland and woody shrubland or forest (Dixon, 2003b).

Other factors could also have an important impact on coverage of different patch types in the floodplain. Direct and interactive effects of increases in CO₂ and temperature on plant physiology (e.g., water use efficiency, rates of photosynthesis and respiration) may strongly influence plant growth rates and competitive interactions among species, particularly between woody shrubs and grasses on the more xeric portions of the floodplain, and perhaps between saltcedar and cottonwood. Indeed, some have suggested historic increases in CO₂ as a possible factor favoring the spread of woody shrubs within the semidesert grasslands (Idso, 1992; Archer *et al.*, 1995). Although the vegetation model did include simple empirical functions relating soil water potential and temperature to growth of different species, physiological processes were not simulated explicitly, nor were CO₂ fertilization effects.

Finally, perhaps the dominant factor influencing vegetation patterns along the San Pedro today is its geomorphic history. The channel incision and widening events of the late 19th through early 20th century set the template that influenced subsequent development of the new floodplain and riparian ecosystem. Likely contributing factors to the widespread arroyo cutting that occurred across the desert Southwest were overgrazing and deforestation in the uplands and riparian zone and the transition between very dry and very wet climate regimes (Hastings and Turner, 1965). Reoccurrence of a catastrophic channel incision/widening event in the near future seems unlikely, given improvements in upland land use and a less flashy watershed response to precipitation events (Hereford, 1993). However, channel cutting and filling have been cyclical events in the region across geologic history (Haynes, 1987 in Huckleberry, 1996) and projected effects of global warming include increases in climatic extremes (Easterling *et al.*, 2000; Houghton *et al.*, 2001). In addition, recent and ongoing changes in land cover (expansion of urban areas and mesquite patches) in the San Pedro watershed may be increasing the flashiness of watershed response (Miller *et al.*, 2002; Kepner *et al.*, 2004). Against this setting, large increases in the size or variability of precipitation events could also increase the vulnerability of the system to channel entrenchment from a catastrophic flood event. Unfortunately, the climatic and geomorphic thresholds for such catastrophic events are not well known. Occurrence of a major incision and widening event could reset the system to conditions that prevailed in the first half of the 20th century, before channel recovery processes led to channel narrowing and formation of the vegetated riparian corridor we see today.

Future model exercises

The simulation results presented in this report suggest probable trajectories of vegetation change under several climate scenarios. The conclusions, however, could be improved in several ways. First of all, the number of replicate runs (four) was likely insufficient to average out the influence of run-to-run stochasticity in fire occurrence and seedling recruitment. Hence, a larger number of replicate runs are necessary to generate stable mean projections for vegetation composition and structure for comparing the climate scenarios. Second, given the importance of channel migration rates for maintenance of cottonwood/willow patch types in the landscape, future runs of the vegetation model should also include the warm very wet scenario (+100% for winter precipitation by 2102), which falls within the range of possible precipitation changes under the Hadley 2 and Canadian Centre climate model projections (SRAG, 2000). Third, given the importance of potential groundwater decline for the San Pedro basin, vegetation simulations should include projected changes in groundwater levels under different climatic and development scenarios, as groundwater model results become available. Fourth, because these were transient climate scenarios, the full effects of the climate adjustments were not reached until the end of the simulations (by 2102). The implications of a longer-term, steady state shift in climate on vegetation and channel migration could be explored by extending the model runs until 2202 under the precipitation and temperature changes reached by 2102. Finally, in the climate scenarios used in this report, precipitation changes were represented by changing the magnitude of individual events (increasing or decreasing rainfall on a given day), rather than altering the number of rainfall events. For a given change in total winter precipitation, changes in event size and changes in event frequency may have very different ecological and hydrological effects, and both types of changes could occur under future climates. Hence, it may be useful to explore the sensitivity of ecological and hydrological response to a range of changes in event size and frequency, for a given change in total winter precipitation.

Vegetation Changes at Contention

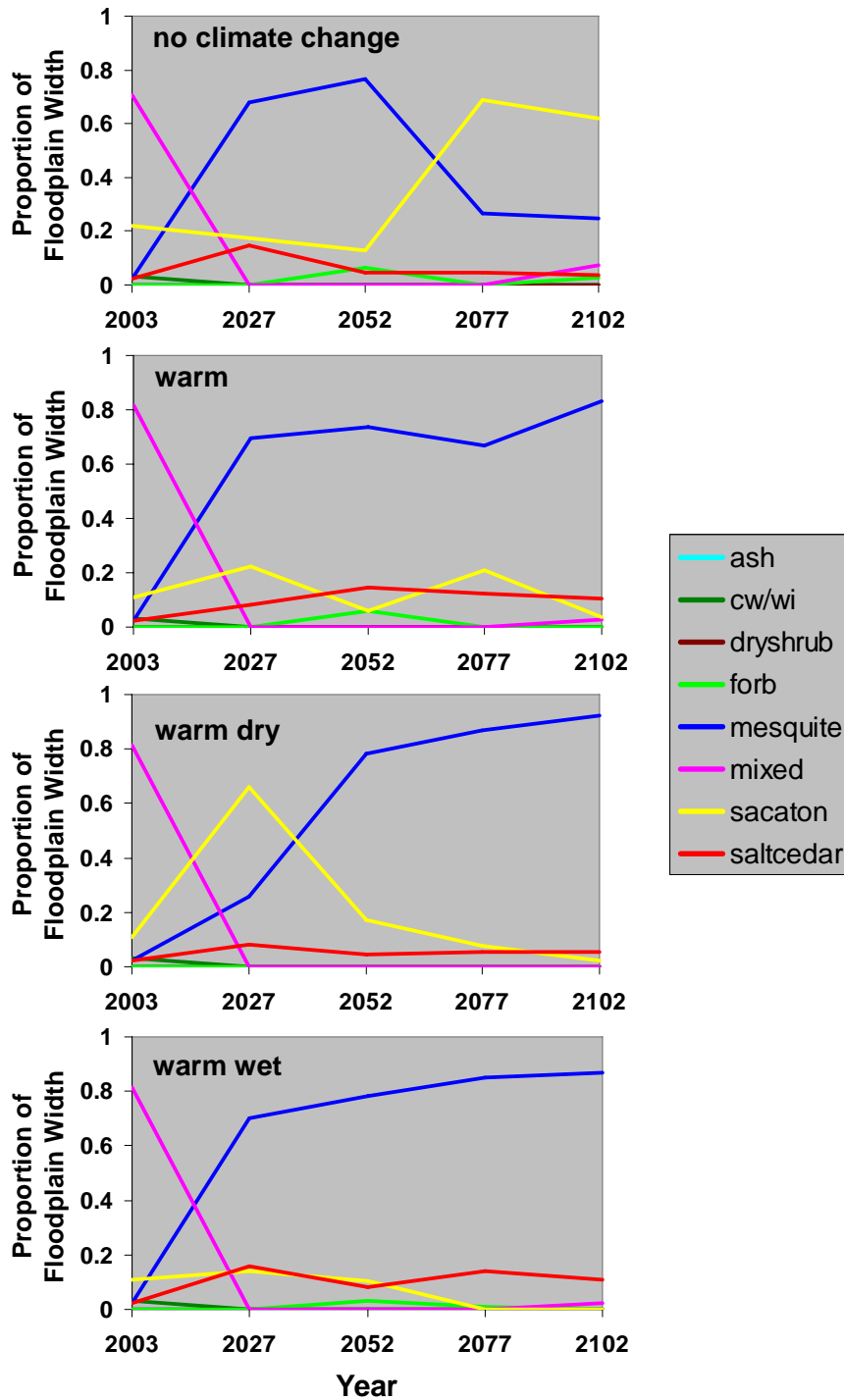


Figure 3-10. Simulated changes in proportional coverage by different patch types (summarized by dominant species) on the vegetation transect at Contention, under four climate scenarios.

Vegetation Changes at Kolbe

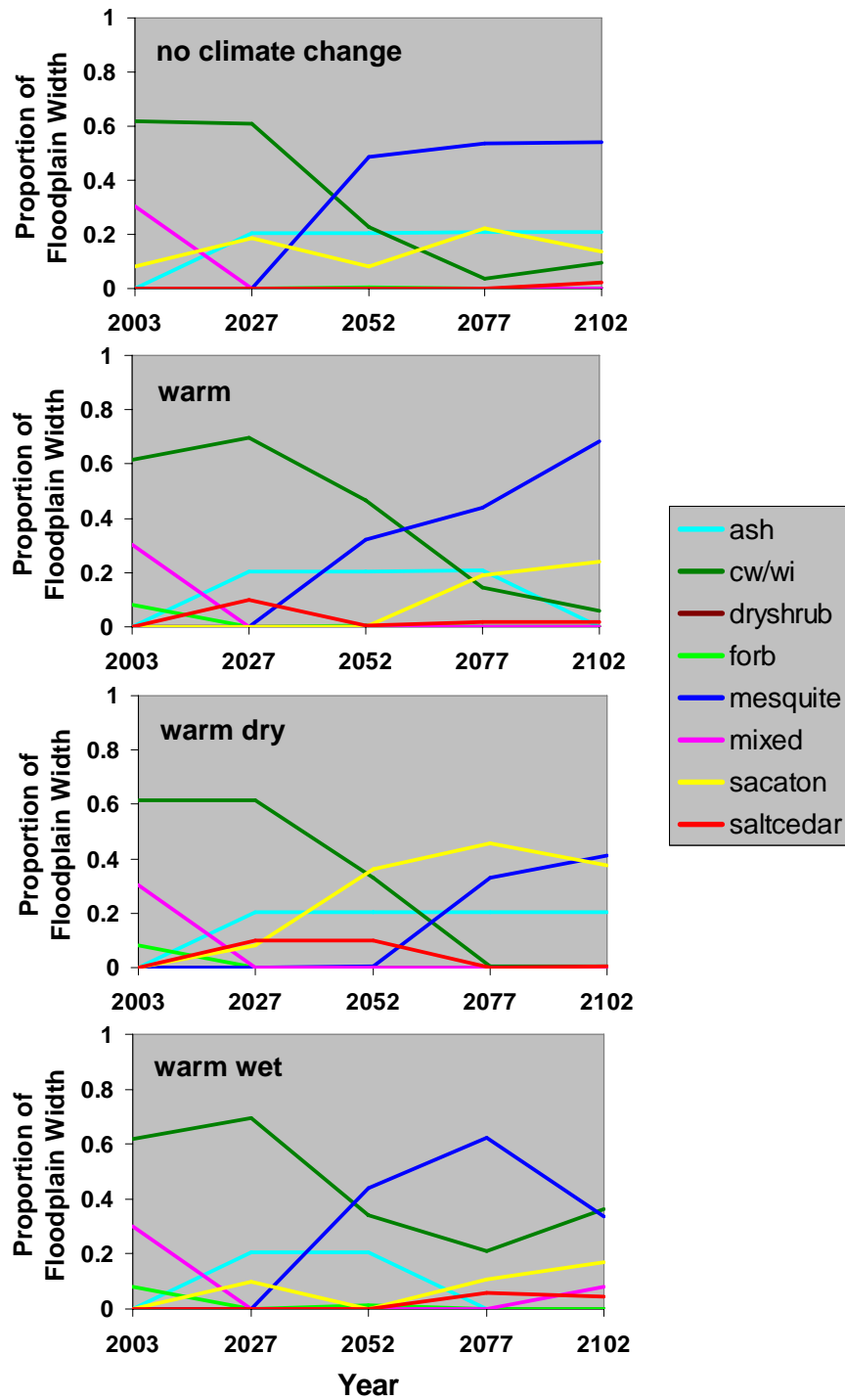


Figure 3-11. Simulated changes in proportional coverage by different patch types (summarized by dominant species) on the vegetation transect at Kolbe, under four climate scenarios.

Vegetation Changes at Palominas UA

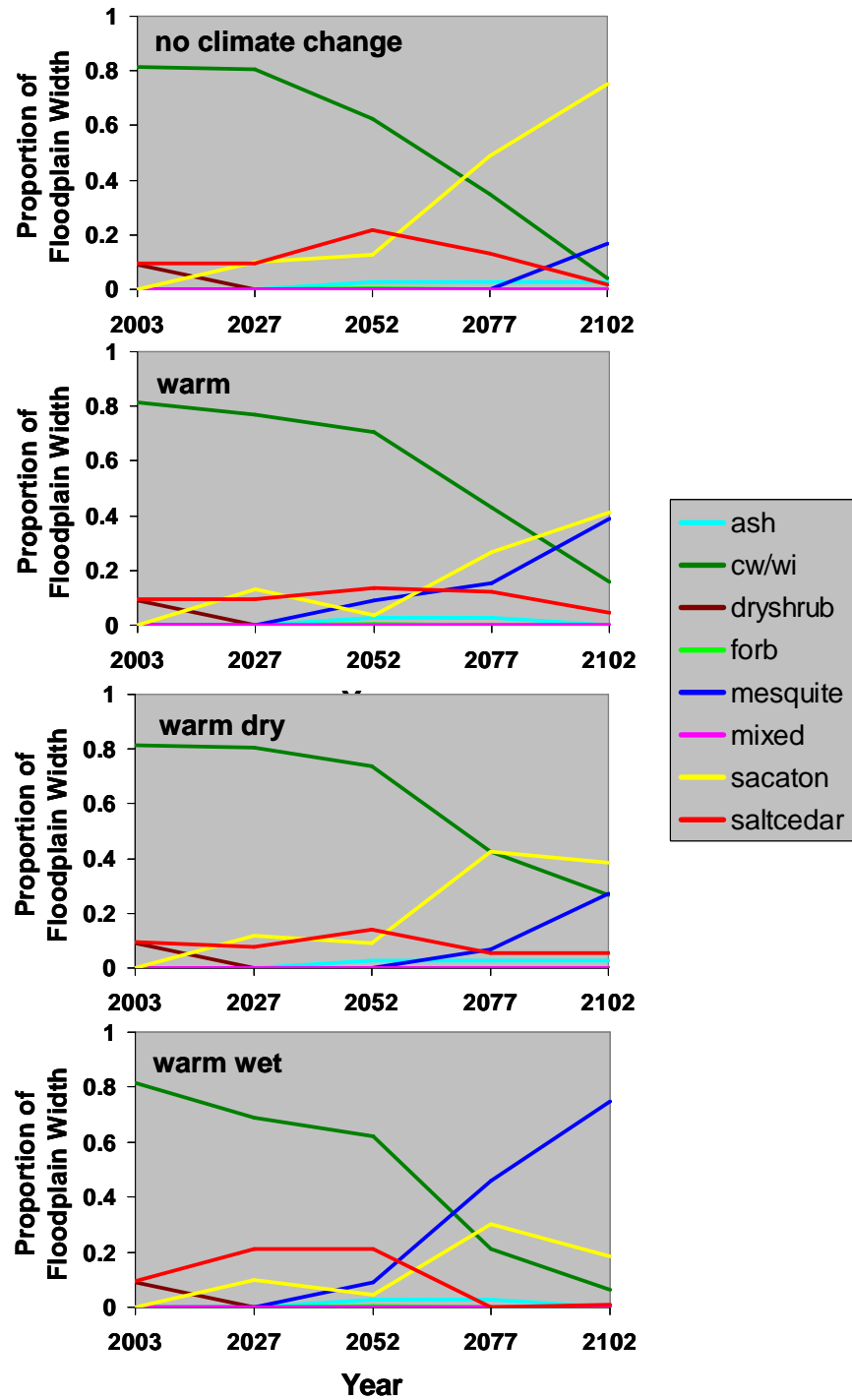


Figure 3-12. Simulated changes in proportional coverage by different patch types (summarized by dominant species) on the vegetation transect at Palominas UA, under four climate scenarios.

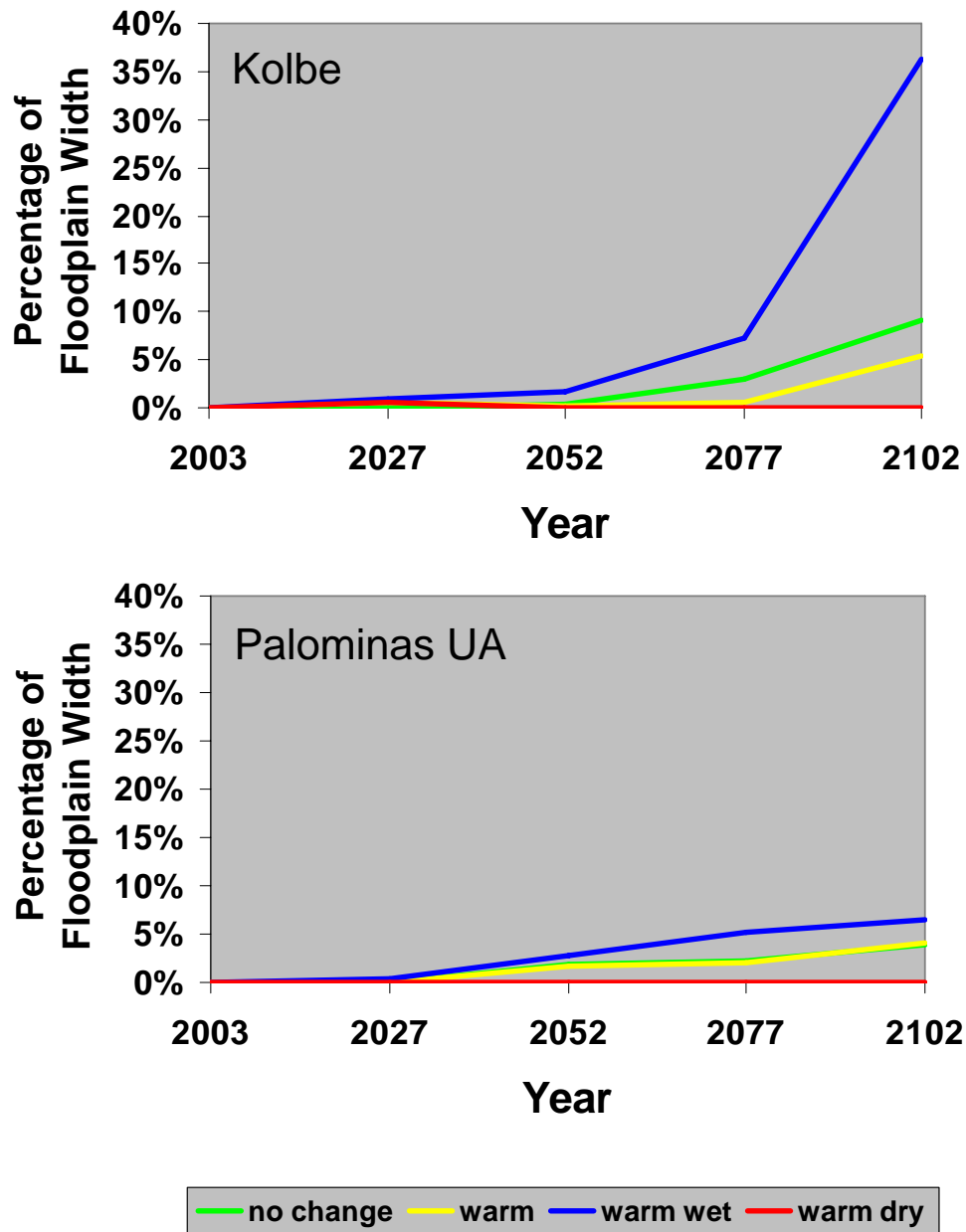


Figure 3-13. Proportion of the floodplain covered by patches of cottonwood/willow that established on new plots created by channel migration under the four climate scenarios. No successful recruitment occurred at Contention under any of the scenarios.

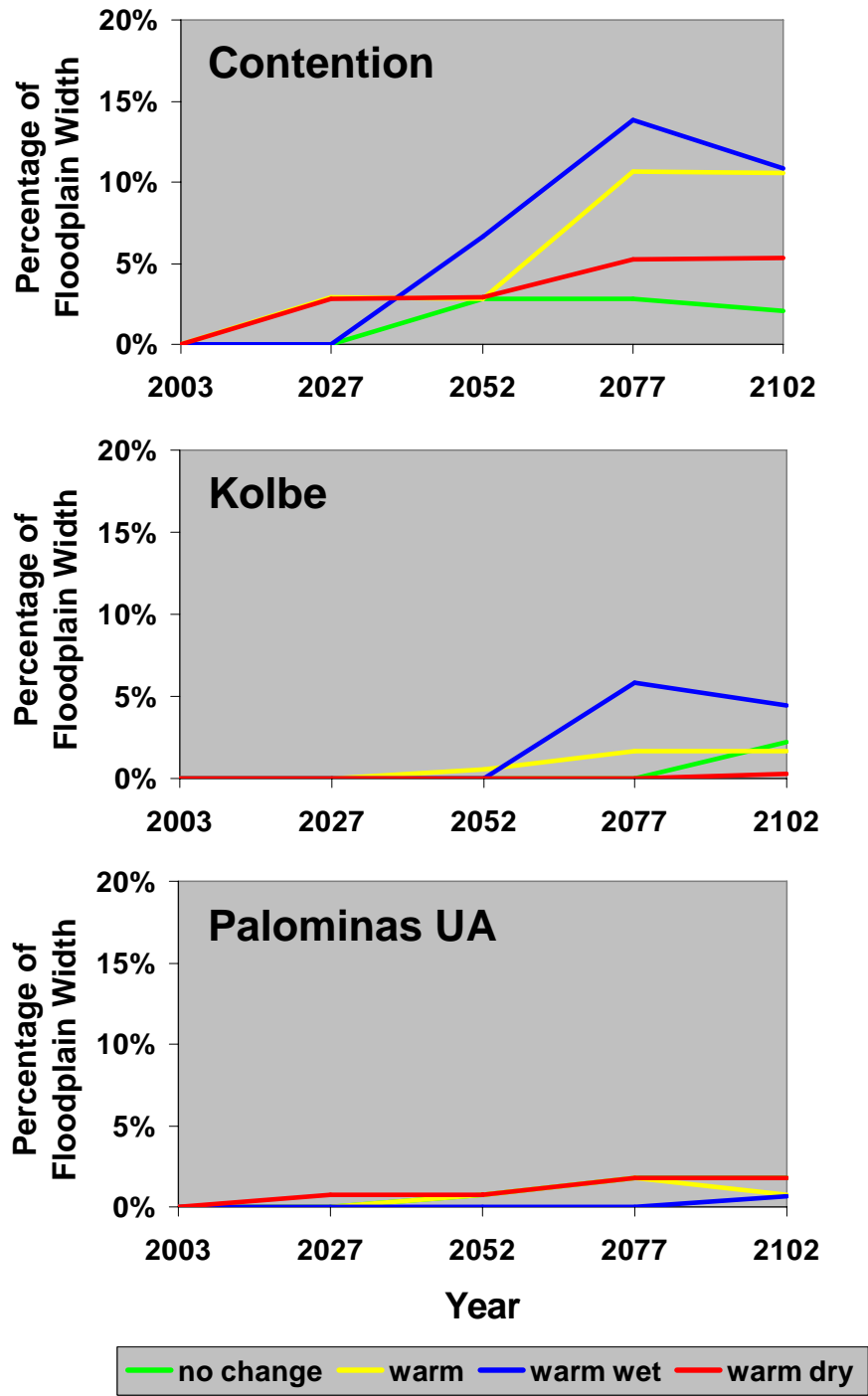


Figure 3-14. Proportion of the floodplain covered by patches of saltcedar that established on new plots created by channel migration under the four climate scenarios.

SECTION 4 CHANGES IN BIODIVERSITY

4.1 Environmental Protection Agency Vulnerability Framework

Galbraith and Price (2005) developed for U.S. EPA's Office of Research and Development a spreadsheet-based predictive framework intended to be used to evaluate the relative vulnerabilities of animal species listed under the Endangered Species Act of 1973 (16 U.S.C. 15631 *et seq.*) to climate change and to other current stressors. Animals listed as Threatened or Endangered (T&E species) under the Endangered Species Act suffer a significant risk of extinction due to the adverse effects of current natural or anthropogenic stressors (e.g., habitat destruction, contaminants, etc.). Climate change, either acting alone or by exacerbating the effects of these current stressors, may constitute an important new threat for many of these species, (Peters, 1992; Tucker and Heath, 1994; Schneider and Root, 2002; Walther *et al.*, 2002).

The Galbraith and Price (2005) framework ("the EPA framework") has been modified for this report to evaluate the comparative vulnerabilities of selected bird species in the SPRNCA. Refocusing the EPA framework required that certain of the variables be changed, or variables added, so that it more adequately addressed site-specific relationships rather than the larger spatial scale and more general issues for which it was developed.

This section of the report briefly describes the EPA framework (further detail can be obtained in Galbraith and Price, 2005), the modifications made to it for these analyses, and applies it to three selected bird species in the SPRNCA: willow flycatcher (*Empidonax traillii*), yellow-billed cuckoo (*Coccyzus erythrophthalmus*), and Botteri's sparrow (*Aimophila bottertii*). These species were chosen for two reasons: first, other analyses described in this report indicate that they cover the range of likely species' reactions to climate change, from adversely affected, through unlikely to be affected, to likely to benefit. This wide range of potential responses will assist in evaluating the validity of the modified framework. Second, the relative vulnerabilities of these species are also assessed in this report by two other methods (HSI models together with vegetation modeling, and the avian community diversity vulnerability framework). Assessing their vulnerabilities by this method provides the ability to cross-reference all of the methods used and evaluate their validities, and potential consistencies and inconsistencies.

4.1.1 The EPA framework and its modifications

4.1.1.1 The original framework

The EPA Framework for evaluating risks to a T&E species due to climate change and other stressors, comprises four connected modules and a narrative (Figure 4-1). Module 1 categorizes the comparative vulnerabilities of T&E species to existing stressors (i.e., not including climate change). This "baseline" vulnerability is subsequently combined with the categorization in Module 2 (evaluating vulnerability to climate change) into an estimate of overall future vulnerability in Module 3. Module 4 combines certainty scores from Modules 1 and 2 into an evaluation of the overall degree of certainty that we can assign to the framework predictions.

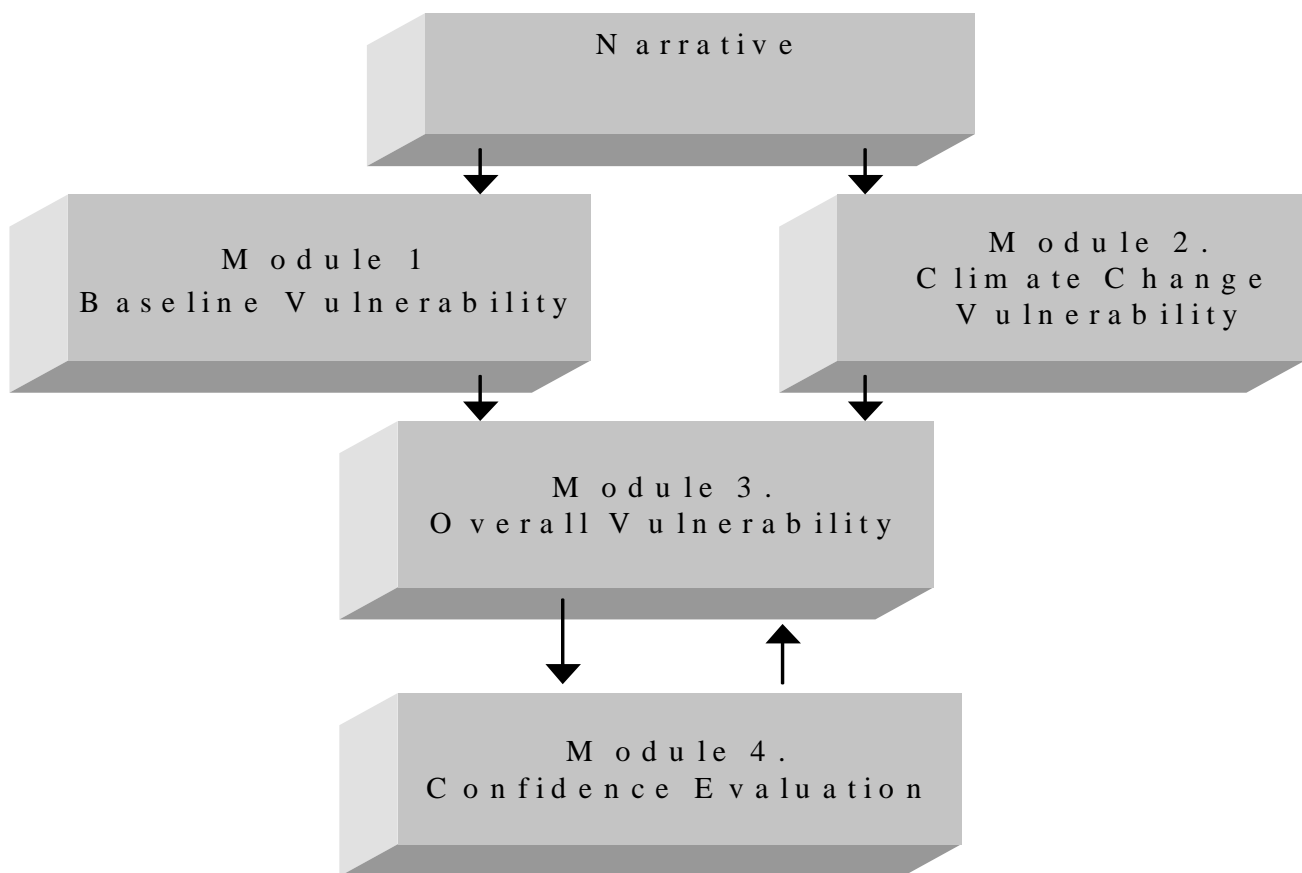


Figure 4-1. EPA Framework for Evaluating Effects of Existing Stressors and Climate Change

The narratives

Most categorizations in Modules 1 through 4 of the EPA framework will be based largely on the results of literature reviews for each species being evaluated, and on expert judgment. The narrative module of the framework reports the relevant results of those reviews and opinions and the justifications for the individual categorization scores in the modules. Thus, the primary aim of the narratives is to make transparent the thought processes and assumptions that result in the scores in Modules 1 through 4.

The narratives have three additional important aims:

- 1) To identify main sources of uncertainty and those areas where additional data might reduce uncertainty.
- 2) To identify and describe the roles of the main stressors (climate and non-climate) in the estimate of vulnerability of the study species.
- 3) To qualitatively describe potential population responses of the study species to the addition of climate change to the already existing stressors, and any resulting change in extinction risk.

Module 1 – evaluating baseline vulnerability

In this module of the EPA Framework, the probable baseline (i.e., current) vulnerability of the study species to extinction or major population reduction are ranked by scoring those elements of their ecologies, demographics, and conservation status that influence the likelihood of survival or extinction (irrespective of the potential effects of future climate change). This is based on determining ordinal rankings for 10 Module 1 variables (Table 4-1). The scoring of these and the treatment of uncertainty is described in greater detail below

Each variable is assigned a “best estimate” certainty score, together with an “alternate” (i.e., possible, but less likely) score(s). This will allow subjective confidence limits to be applied to the overall framework prediction in Module 3. For some species and variables, there may be enough confidence underlying the best estimate certainty score that no other score is considered necessary.

1) Current population size	6) Likely current stressor future trends
2) Population trend in last 50 years	7) Individual replacement time
3) Current population trend	8) Future vulnerability to stochastic events
4) Range trend in last 50 years	9) Future vulnerability to policy/management changes
5) Current range trend	10) Future vulnerability to natural stressors

The component categorizations and the scores used in Module 1 are presented in Table 4-2.

Current population size. The importance of this variable is that, in general, species with small populations are likely to be less resilient and more vulnerable to extinction risk than those with larger populations.

Past and current population trends. The importance of these variables is that, in general, species with reduced and/or currently declining populations are likely to be more vulnerable to extinction risk than those with stable or increasing populations. The greater the past population reduction and the more rapid the current rate of decline, the more vulnerable the species is likely to be. Thus, in assessing a species’ baseline vulnerability to extinction it is important to know to what extent its population has been reduced in the past and its current rate of reduction. Quantitative data on many species’ populations in North America have only begun to be gathered since about 1950. For this reason, the past reduction category focuses on this time period. The current rate of population reduction variable focuses on the current 10-year period. The past trend categorization scheme used is similar to and based on that used in the IUCN Red List scheme (Mace and Stuart, 1993). The current trend categorization scheme assigns one of 4 categories: rapid or slow population decline, or stable or increasing populations.

Past and current range trends. As with population trends, species that have suffered range contractions in the past, or that are currently suffering such contractions, are likely to be more vulnerable to extinction risk than those with stable or increasing ranges. The greater the past range contraction and the more rapid the current contraction rate, the more vulnerable the species is likely to be. Thus, in assessing a species' baseline vulnerability to extinction it is important to know to what extent its distribution has changed in the past and its current rate of change. Similar to the population trend categories, the past range change category focuses on the time period over the last 50 years. The current rate of range change focuses on the current 10-year period.

Future trends in the magnitude and/or extent of non-climate stressors that could affect the species' distribution or population status. Species that are, or that may be, affected by non-climate stressors that are likely to increase in their future intensities, frequencies, or spatial extents (e.g., habitat loss due to urban sprawl), are likely to be more vulnerable than those affected by stressors that are reducing or stable (e.g., environmental DDE concentrations). In this module component the likely future trends in the frequencies and/or intensities of non-climate stressors are categorized as likely to increase, remain stable, or decrease.

Minimum individual replacement time. k-selected species (i.e., those with deferred maturity, slow reproductive rates, post-natal care, etc.) may generally be more at risk of extinction than r-selected species (i.e., fast reproducers). k-selected species are best adapted to stable environments with low stresses, whereas r-selected organisms are best able to exploit unpredictable and stressed environments. A population of a k-selected species that is reduced by a stochastic event has less opportunity than an r-selected species to quickly make good its losses before the next stochastic event. Approximate minimum individual replacement time (the time between the birth of an organism and the earliest date at which it produces independent young) is a useful index for k or r selection status.

Vulnerability to stochastic events. Some species, because of their habitat preferences or distributions, may be more at risk to stochastic events than others. For example, organisms that inhabit areas that are vulnerable to tropical storms, fires, tidal surges, or "red tides" may be more vulnerable than organisms that live in more predictable environments.

Table 4-2. Module 1 components and scores used in categorizing the “baseline” vulnerabilities (Vb) of T&E species

Current population size	Score	Range trend in last 50 years	Score	Minimum individual replacement time	Score
<100	1	>80% reduction	1	>5 years	1
100-500	2	>50% reduction	2	2-5 years	2
500-1,000	3	>20% reduction	3	<2 years	3
1,000 – 10,000	4	Apparently stable	4	<1 year	4
10,000 – 50,000	5	Increasing	5	<i>Certainty:</i>	high (3)
>50,000	6	<i>Certainty:</i>	high (3)		medium (2)
<i>Certainty:</i>	high (3)		medium (2)		low (1)
	medium (2)		low (1)		
	Low (1)			Future vulnerability to stochastic events	Score
		Current range trend	Score	Highly vulnerable	1
Population trend in last 50 yrs	Score	Rapid reduction	1	Vulnerable	2
>80% reduction	1	Slow reduction	2	Not vulnerable	3
>50% reduction	2	Stable	3	Benefiting	4
>20% reduction	3	Increasing	4	<i>Certainty:</i>	high (3)
Apparently stable	4	<i>Certainty:</i>	high (3)		medium (2)
Increasing	5		medium (2)		low (1)
<i>Certainty:</i>	high (3)		Low (1)		
	medium (2)			Vulnerability: policy/management change	Score
	Low (1)			Highly vulnerable	1
				Vulnerable	2
				Not vulnerable	3
Current population trend	Score	Future non-climate stressors	Score	Benefiting	4
Rapid decline	1	Increase	1	<i>Certainty:</i>	high (3)
Slow decline	2	Stable	2		medium (2)
Stable	3	Reduction	3		low (1)
Increasing	4	<i>Certainty:</i>	high (3)		
<i>Certainty:</i>	high (3)		medium (2)		
	medium (2)		Low (1)	Future vulnerability to natural stressors	Score
	Low (1)			Highly vulnerable	1
				Vulnerable	2
				Not vulnerable	3
				<i>Certainty:</i>	high (3)
					medium (2)
					Low (1)

Vulnerability to policy/management changes. Because their fates depend to a great extent on societal values or policy objectives (either of which may change through time), species that are heavily dependent on human intervention or management, or specific policies for their continuing survival are likely to be more vulnerable than those that depend less, or not at all, on such interventions.

Vulnerability to natural stressors. Some species may be more vulnerable to currently-acting natural stressors, such as disease, or invasive species than others are. Seabirds, for example, appear to be particularly susceptible to botulism and to predation by introduced predators, while rodents are vulnerable to outbreaks of sylvatic plague. A species' vulnerability to such events could affect its ability to persist.

Each of these variables is assigned a numerical score, reflecting their ordinal rankings. These individual scores are then combined in Module 1 into one of four baseline vulnerability rankings:

- *Highly vulnerable (Vb1)* - species that are likely to be at imminent risk of extinction.
- *Vulnerable (Vb2)*- species that may be close to such an extinction risk and are likely to be re-categorized as critically vulnerable if their populations or ranges are diminished further.
- *Least vulnerable(Vb3)* - species that are not in imminent danger of extinction but that could be so in the future if their population and range trends continue.
- *Not vulnerable (Vb4)* - species that have comparatively large and stable (or increasing) populations or ranges.

Module 1 - Certainty evaluations

Two methods for evaluating certainty/uncertainty were incorporated into the EPA Framework: First, where necessary, each variable in Table 4-2 is assigned a “best estimate” score and an “alternate” score. The former is a professional judgment of the most likely case, whereas the latter is a less likely, but not an unreasonably unlikely, estimate. In this, an attempt was made to capture legitimate uncertainty about the individual scorings. In cases where there is very little uncertainty only best estimate scores are given. Summing each of these scores provides some indication of the accuracy or reliability of the total best estimate scores and the extent to which they may be in error.

Second, each “best estimate” score in Module 1 is also assigned a numeric certainty evaluation [high (scores 3), medium (scores 2), or low (scores 1)], which is used in Module 4 to evaluate the overall degree of certainty that can be assigned to the framework predictions. These are ordinal rankings, based on expert judgment about the quantity and quality of the available data (or required, but missing, data) that support the “best estimate” variable scores. The three scores should be viewed as approximately equivalent to probabilities of: high – equal to or greater than about 70%; medium – greater than about 30% but less than 70%; or low – less than 30%.

Module 2 – evaluating vulnerability to climate change

In this module of the EPA Framework, the likely vulnerability of a species to future climate change is assessed and categorized by scoring those elements of its physiology, life history, and ecology that will likely be important determinants of its responses. This is based on determining ordinal rankings for 10 Module 2 variables (Table 4-3). The scoring of these is described in greater detail below as is the treatment of certainty/uncertainty.

The scoring system used in Module 2 allows for the possibility that some species may actually benefit from climate change. For example, species that could benefit from an increased frequency of climate change-induced stochastic events.

Each variable is assigned a “best estimate” certainty score, together with an “alternate” (i.e., possible, but less likely) score. This will allow subjective confidence limits to be applied to the overall framework prediction in Module 3. For some species and variables, there may be enough certainty underlying the best estimate certainty score that no other score is considered necessary.

1) Physiological vulnerability to temperature change	6) Likely extent of habitat loss due to climate change
2) Physiological vulnerability to precipitation change	7) Abilities of habitats to shift at same rate as species
3) Vulnerability to climate change-induced extreme weather events	8) Habitat availability within new range of species
4) Dispersive capability	9) Dependence on temporal inter-relationships
5) Degree of habitat specialization	10) Dependence on other species

Scoring Module 2 components (Table 4-4)

The species’ likely physiological or behavioral sensitivity to two main aspects of climate change, temperature and precipitation. Some species are more likely than others to be directly affected by climate change because their physiological tolerances may be narrower, or their behaviors may lack the necessary flexibility to adapt (though some species could benefit). For example, cold-water fish species, such as some salmonids, may be affected more by increased water temperature. These species may more readily avoid affected areas than warm-water fish (e.g., cyprinids or ictalurids) that are physiologically or behaviorally tolerant to increased temperatures and/or lowered oxygen levels. Thus, it will be critical in evaluating a species’ likely sensitivity to climate change to be able to assess its intrinsic limits to physiological adaptation to changing temperature or precipitation regimes. Ideally, such evaluations would be based on experimental evidence for the species being evaluated, or rigorous observational data from the field.

Unfortunately, however, such data are scarce for most species, and the ordinal rankings in Module 2 will likely be based on inferences about closely-related species, or from current limits to the species distribution correlated with climate variables (e.g., Root, 1988), or recent range changes.

The sensitivity categories for this variable of Module 2 are not intended to imply a high degree of accuracy or precision, but to delineate broad “response categories” that reflect varying degrees

of physiological/behavioral sensitivity. Assigning a species to any category would typically be based on expert judgment about the species (or a surrogate).

The species' likely vulnerability to an increased frequency or magnitude of climate change-induced extreme weather events. Some species (e.g., forest-nesting birds, or species confined to small low-lying islands) may be put at greater risk of extinction or population reduction if climate change results in stochastic events, such as lightning-caused fires or hurricanes or storm surges, increasing in frequency or magnitude. In general, species that are dependent on habitat components that are vulnerable to fire, wind storms, or storm surges may be most vulnerable. The vulnerability categories for this variable of Module 2 are not intended to imply a high degree of accuracy or precision, but to identify broad “vulnerability profiles” that reflect varying degrees of potential sensitivity. Assigning a species to any category would typically be based on expert judgment about the species (or a surrogate).

Dispersive characteristics that may ameliorate or exacerbate the effects of climate change. Species with high dispersal capabilities (e.g., birds or flying insects) may be less vulnerable to climate change than sedentary organisms (e.g., amphibians or reptiles). In this component of Module 2, species are ranked according to this characteristic and its likely modifying influence. This allocation is based on the species' *potential* ability to disperse from the localized effects of climate change, where a “low” rank is assigned to species that are unlikely to move more than a few or tens of kilometers from their natal area and, hence, may be most vulnerable to the localized effects of climate change; a “moderate” ranking refers to species that may be able to disperse as much as a few hundreds of kilometers; and a “high” ranking refers to highly mobile animals that could, potentially, disperse as much as many hundreds or some thousands of kilometers.

Table 4-4. Module 2 components and scores used in categorizing the vulnerabilities of T&E species to climate change (Vc)					
Physiological vulnerability to temp. increase	Score	Degree of habitat specialization	Score	Availability of habitat in new range	Score
Likely highly sensitive	1	Highly specialized	1	None	1
Likely moderately sensitive	2	Moderately specialized	2	Limited extent	2
Likely insensitive	3	Generalist	3	Large extent	3
Likely to benefit	4	<i>Certainty:</i>	high (3)	<i>Certainty:</i>	high (3)
<i>Certainty:</i>	high (3)		medium (2)		medium (2)
	medium (2)		low (1)		low (1)
	Low (1)				
		Likely future habitat loss due to climate change	Score	Dependence on temporal inter-relations	Score
Physiological vulnerability to precipitation change	Score	All or most (>50%)	1	Highly dependent	1
Likely highly sensitive	1	Some (20-50%) trend	2	Moderately dependent	2
Likely moderately sensitive	2	No change	3	Independent	3
Likely insensitive	3	Some gain (20-50%)	4	<i>Certainty:</i>	high (3)
Likely to benefit	4	Large gain (>50%)	5		medium (2)
<i>Certainty:</i>	high (3)	<i>Certainty:</i>	high (3)		low (1)
	medium (2)		medium (2)		
	Low (1)		Low (1)	Dependence on other species	Score
				Highly dependent	1
Vulnerability to change in frequency or degree of extreme weather events	Score	Ability of habitats to shift at same rate as species	Score	Moderately dependent	2
Likely highly sensitive	1	Highly unlikely	1	Independent	3
Likely moderately sensitive	2	Unlikely	2	<i>Certainty:</i>	high (3)
Likely insensitive	3	Likely	3		medium (2)
Likely to benefit	4	<i>Certainty:</i>	high (3)		low (1)
<i>Certainty:</i>	high (3)		medium (2)		
	medium (2)		Low (1)	Dispersive capability	Score
	Low (1)			Low	1
				Moderate	2
				High	3
				<i>Certainty:</i>	high (3)
					medium (2)
					Low (1)

The species' degree of habitat specialization. Species that have a high degree of habitat specialization (i.e., that are not flexible in their choice of habitats), may be most vulnerable to climate change because their “fates” are not only a function of their own responses to climate change, but to those of their critical habitat components. In scoring this Module 2 variable, a species is assigned to one of three habitat specialization categories:

- *Highly specialized* - species that are restricted by their behaviors or physiologies to a well-defined habitat (e.g., a vegetation community).
- *Moderately specialized* - species found in a broad category of habitats. Examples might include wetland organisms that can tolerate a wide variety of wetlands from bogs to marshes, to lakes and rivers (e.g., the bald eagle).
- *Generalists* – species that are able to exploit a wide variety of habitats.

The likely extent of habitat loss or gain due to climate change. In this variable, expert opinion is used to judge the likely impact of climate change on the spatial extents of the T&E species' main habitats. These classifications will necessarily be speculative and should not be assumed to imply a high degree of accuracy or precision. They are intended to be reasonable approximations.

The likely ability of critical habitats to shift at same rate as species in response to climate change. Some habitats may be able to shift in response to climate change. For example, the southern boundary of boreal forest in northern New England may shift north into Canada, and the corresponding northern habitat ecotone move further north in Labrador (Neilson and Drapek, 1998). Also, montane plant communities in the European Alps are shifting upslope due to the warming climate (Grabherr et al., 1994). In such cases, animal species dependent on these habitats could, potentially, shift with them. However, the success with which this may occur is dependent on synchronicity (i.e., the habitat being able to shift in approximate synchrony with the species). If a species' physiological tolerances are exceeded and it is forced to shift its range into regions where its optimal habitat does not already exist, its future prospects will be affected by how quickly its habitat can also shift into that new area. For example, if the species being assessed is a songbird that breeds in California coastal redwood forest and it is forced to move north into less optimal conifer habitat, it may take so long for its habitat to catch up that the species' existence may be jeopardized. If, however, the species' habitat was grassland or shrub, the habitat may be able to move in a relatively short time frame. For this variable, expert judgment is used to score the likelihood of the critical habitat being able to shift along with the species.

Availability of habitat within the new range. A species that is forced to track its climatic envelope and shift its range into areas where its critical habitat already exists, may suffer less from climate change than one that is forced to move into areas where no such habitat exists. In the latter case, the persistence of the organisms may depend on whether or not its habitat can shift in synchrony (see above).

The degree of dependence that the species has on other species or the temporal relationships between species. Species that are highly dependent on another for some critical life history requirement (for example the golden-cheeked warbler’s dependence on Ashe juniper, or a species that depends for its food supply during an energetic bottleneck on the emergence of a specific life-stage of another species) may be more vulnerable to the effects of climate change since their likely fates are closely dependent on those of another species.

Each of the above 10 variables is assigned numerical scores. These individual scores are then combined in Module 2 into an overall evaluation of the species’ potential vulnerability to climate change:

- Highly vulnerable (Vc1)
- Vulnerable (Vc2)
- least vulnerable (Vc3)
- Not vulnerable (Vc4), lowest scoring species may be likely to benefit from climate change.

Module 2 - Certainty evaluation

Two methods for evaluating certainty/uncertainty in Module 2 were incorporated into the EPA framework. These are identical to the methods developed for Module 1 (described above).

Module 3 – Evaluating overall vulnerability

In this module of the EPA Framework, the “best estimate” scores from modules 1 and 2 are combined in a matrix to produce an overall best estimate evaluation and score of the species’ vulnerability to climate change and important existing stressors. In doing so, species are categorized as either: highly vulnerable (Vo1), vulnerable (Vo2), least vulnerable (Vo3), or likely to benefit from climate change (Vo4). It is important to note that these are likely approximations of each species’ comparative vulnerability. They are not measures or indices of absolute vulnerability.

The Module 3 evaluation matrix is presented in Table 4-5.

Table 4-5. Module 3 - Overall vulnerability best estimate scoring matrix				
	Baseline (Module 1) vulnerability scores			
Climate change (Module 2) vulnerability scores	Vb1	Vb2	Vb3	Vb4
Vc1	Vo1	Vo1	Vo2	Vo3
Vc2	Vo1	Vo1	Vo2	Vo3
Vc3	Vo1	Vo2	Vo3	Vo4
Vc4	Vo1	Vo2	Vo3	Vo4
Vc5	Vo2	Vo3	Vo4	Vo4

The “alternate” certainty evaluations are also used in Modules 1 and 2 to develop subjective confidence limits on the Module 3 estimate.

Module 4 – Certainty evaluation

The approximate level of certainty with which each “best estimate” score in Modules 1, 2, and 3 is categorized is recorded separately in the modules. These are codified as high (approximate probability of 70% or more); medium (approximate probability of between 30 and 70%); or low (less than approximately 30%). These qualitative scores correspond to numeric scores of 3, 2, and 1, respectively. For the most part, these categorizations will be the product of expert judgment, rather than a strictly quantitative appraisal.

In module 4, the best estimate certainty scores assigned to each of the variables in Modules 1 and 2 are combined into an index of the certainty associated with the overall vulnerability score in Module 3. The levels of certainty are High, Medium, and Low. It is important to note that these categorizations are indices of the certainty associated with the overall “best estimate” score.

4.1.1.2 The Modifications to the EPA Framework for Use in the SPRNCA

The main modifications to Module 1 (Table 4-6) that were necessary for this research are largely a function of differing geographical scales of analysis. The original EPA Framework was intended to be applied to the North American ranges and population sizes of species, whereas the SPRNCA-modified version is intended to be applicable to, at the most, regional ranges and populations. This required that variables 1 through 5 be converted to express regional or SPRNCA-specific relationships (e.g., regional population trends, current population size in the SPRNCA, responses to gains or losses in particular plant communities). While it is true that national characteristics and relationships may ultimately be expressed in regional or local population fates, quantifying those translations between the larger and smaller scales is not possible. Regional or local parameters allow us to better evaluate the fates of species within the SPRNCA.

Four modifications were made to Module 2 to reflect conditions in the SPRNCA (Table 4-7):

- A variable that categorizes the species ability to persist in both wetland and mesic and xeric habitats. This variable was included because the vegetation modeling indicated a change from hydrophytic or mesic vegetation to more xeric communities
- A variable that reflects the likely increase predicted in the vegetation modeling in invasive plant species (e.g., saltcedar) in the SPRNCA under climate change
- A variable that categorizes dependencies of species on riparian gallery forest (one the main vegetation changes predicted in the vegetation modeling)
- A variable that categorizes dependencies of standing or flowing water (another of the main changes likely under climate change).

Modules 3 and 4 remain unchanged.

Table 4-6. Module 1 - Categorizing the "baseline" vulnerability (Vb) of species in the SPRNCA

Current population size in SPRNCA		Score	Likely future non-climate stressor trends		Score
	<50	1		increase	1
	50-100	2		stable	2
	>100	3		reduction	3
Certainty:	high (3) medium (2) Low (1)		Certainty:	high (3) medium (2) low (1)	
Regional population trend in last 50 years		Score	Minimum individual replacement time		Score
	>50% reduction	1		> 5 years	1
	>20% reduction	2		2-5 years	2
	Apparently stable	3		<2 years	3
	Increasing	4		<1 year	4
Certainty:	high (3) medium (2) Low (1)		Certainty:	high (3) medium (2) low (1)	
Current regional population trend		Score	Likely future vulnerability to stochastic events		Score
	rapid decline	1		vulnerable	1
	Slow decline	2		not vulnerable	2
	Stable	3		benefiting	3
	Increasing	4			
Certainty:	high (3) medium (2) Low (1)		Certainty:	high (3) medium (2) low (1)	
Regional range trend in last 50 years		Score	Likely future vulnerability to policy or management changes		Score
	>50% reduction	1		Highly vulnerable	1
	>20%reduction	2		vulnerable	2
	Apparently stable	3		not vulnerable	3
	Increasing	4			
Certainty:	high (3) medium (2) low (1)		Certainty:	high (3) medium (2) low (1)	
Current regional range trend		Score	Likely future vulnerability to natural stressors		Score
	rapid reduction	1		Highly vulnerable	1
	Slow reduction	2		vulnerable	2
	Stable	3		not vulnerable	3
	Increasing	4			
Certainty:	high (3) medium (2) low (1)		Certainty:	high (3) medium (2) low (1)	

Table 4-7. Module 2 - Categorizing the vulnerability of SPRNCA species to climate change (Vc)

Physiological vulnerability to temperature increase		Score	Dependence on temporal inter-relations		
	Likely highly sensitive	1		highly dependent	1
	Likely moderately sensitive	2		moderately dependent	2
	Likely insensitive	3		Independent	3
	likely to benefit	4	Certainty:	high (3)	
Certainty:				medium (2)	
				low (1)	
Physiological vulnerability to precipitation change		Score	Dependence on other species		Score
	Likely highly sensitive	1		highly dependent	1
	Likely moderately sensitive	2		moderately dependent	2
	Likely insensitive	3		independent	3
	Likely to benefit		Certainty:	high (3)	
Certainty:				medium (2)	
				low (1)	
Vulnerability to change in frequency/degree Of extreme weather events		Score	Ability to utilize mesic or xeric habitats		Score
	Likely highly sensitive	1		Not able	1
	Likely moderately sensitive	2		Able	2
	Likely insensitive	3	Certainty:	high (3)	
	likely to benefit			medium (2)	
Certainty:				low (1)	
Recolonization capability		Score	Ability to utilize non-native vegetation		Score
	Low	1		Not able	1
	Moderate	2		Able	2
	High	3	Certainty:	high (3)	
Certainty:				medium (2)	
				low (1)	
Degree of habitat specialization		Score	Dependence on gallery forest		Score
	Highly specialized	1		Highly dependent	1
	Moderately specialized	2		Somewhat dependent	2
	Generalist	3		Independent	3
Certainty:			Certainty:	high (3)	
				medium (2)	
				low (1)	
Likely extent of habitat change due to climate change		Score	Dependence on wetland, or standing or flowing water		
	All or most (>50%)	1		Highly dependent	1
	some (20-50%)	2		Somewhat dependent	2
	No change	3		Independent	3
	some gain (20-50%)	4	Certainty:	high (3)	
	large gain (>50%)	5		medium (2)	
Certainty:		6		low (1)	

4.1.2 Application of the modified EPA Framework to SPRNCA birds.

The modified EPA Framework was applied to three species of birds that inhabit the SPRNCA: the willow flycatcher, yellow-billed cuckoo, and Botteri's sparrow. Other analyses described in this report indicate that these species cover the range of likely species' reactions to climate change, from adversely affected, through unlikely to be affected, to likely to benefit. This wide range of potential responses assists in evaluating the validity of the modified framework. Also, the relative vulnerabilities of these species are further assessed in this report by two other methods (HSI models together with vegetation modeling, and the avian community diversity vulnerability framework). Assessing their vulnerabilities by this method provides the ability to cross-reference all of the methods used and evaluate their validities, and potential consistencies and inconsistencies.

4.1.2.1 Willow Flycatcher

This section of the report documents the application of the modified EPA Vulnerability Framework to the population of the southwestern willow flycatcher, *Empidonax traillii extimus*, that is breeding or that may eventually breed in the SPRNCA. The results are shown in Attachment 2. The rationales for the scores shown in Attachment 2 are described below.

Willow flycatcher – general

This species is a summer visitor to North America and to southern Arizona. It spends the winter in Central and South America, is insectivorous, and first breeding occurs in the first or second summer after leaving the nest (Sedgwick, 2000).

Willow flycatcher - habitat relationships

Throughout most of its North American breeding range the willow flycatcher is confined to brushy thickets associated with standing or slow-moving water (Sedgwick, 2000). The southwestern race of the willow flycatcher (the form that breeds in Californian, Arizona, and Nevada) is largely restricted as a breeding species to riparian shrubby thickets in an otherwise arid or semi-desert landscape (Sogge and Marshall, 2000; U.S. Fish and Wildlife Service, 1997; U.S. Fish and Wildlife Service, 2001; Arizona Game and Fish Department unpublished data;). In Arizona, the species is almost entirely confined as a breeding species to riparian shrub habitats and forests with well-developed shrub understories, particularly those dominated by willows (*Salix* spp.) and by salt cedar (*Tamarix chinensis*) (Sogge and Marshall, 2000; U.S. Fish and Wildlife Service, 1997; U.S. Fish and Wildlife Service, 2001; Sedgwick, 2000). It shows a strong preference throughout its range for denser, lush shrub canopies, particularly at nest site height (typically 3-5 meters), and avoids sparser cover.

The species does not seem to need a tree canopy (i.e., older or mature willows and cottonwoods greater than 10m in height) at its nesting sites. Many nesting sites are shrub-dominated, with few or no trees present. At other sites, birds do nest in riparian forest, but only where there is a lush shrub understory. Thus, it appears that it is the shrub habitat layer that is most important to the

nesting birds. In Arizona, the two breeding sites with the largest populations, Roosevelt Lake and the Gila/San Pedro River confluence, are largely shrub dominated with only scattered tree canopies. Between them, these two sites held over 70% of the total Arizona breeding population in 2000 (Paradzick and Woodward, in press).

While, historically, southwestern willow flycatchers were largely confined to salix-dominated habitats, they, apparently, are able to inhabit and successfully breed in habitats with high proportions, or even dominated by, invasive shrubs (especially saltcedar). At many areas in the two main breeding sites in Arizona (Lake Roosevelt and the Gila/San Pedro River confluence) saltcedar is an important co-dominant (with willow), or is dominant (Paradzick and Woodward, in press). Nesting success does not appear to be impaired by nesting in saltcedar-dominated habitats: in Arizona between 1993 and 1999, percent nest success (the percentage of nests that fledged one or more young) was 54% in saltcedar-dominated habitats and 39% in native spp.-dominated habitats (U.S. Fish and Wildlife Service, 2001).

Being a riparian obligate species, southwestern willow flycatchers are found only in areas close to standing or slowly-moving water. However, within such sites, there is some evidence that flycatchers prefer areas closer to water as nest sites. Marshall (2000) states that territories are seldom more than a “few dozen meters” from water or saturated soil, and often nests are placed over water (Whitfield and Enos, 1996; Sferra *et al.*, 1997). The highest densities of nesting willow flycatchers at the lower San Pedro and Gila study sites have consistently been in areas immediately adjacent (i.e., within 10 m) to the river channel or where the habitat is flooded either by beaver activity or irrigation (Paradzick and Woodward *pers comm*, Galbraith *pers obs.*). During the summer drought of 2002, such areas were among the few in which flycatchers persisted in their breeding attempts and that were successful in raising young. In such areas, the soil moisture content typically ranges from moist to permanently or intermittently saturated.

As a riparian species, southwestern willow flycatchers typically inhabit shaded humid areas in an otherwise arid matrix. However, it is unknown whether this is a direct preference for such conditions or a consequence of requiring riparian shrub habitat (which is generally shaded and humid). The main Arizona breeding sites for southwestern willow flycatcher are at Roosevelt lake and the Gila/San Pedro River confluence, which are 3000 feet lower in elevation than the SPRNCA and where average maximum June/July temperatures are about 10°F higher than on the SPRNCA, and where rainfall is generally 6-10 inches less [data obtained from the Internet (<http://www.wrdc.dri.edu/cgi-bin/cliRECTM.pl?azwink>) from weather stations at Fort Huachuca, Maricopa, Winkelman, Sacaton, and Florence]. Thus, if climate change were to result in hotter and more arid conditions prevailing on the SPRNCA, this might not necessarily adversely affect its suitability as a habitat for flycatchers.

Based on the above general comments and habitat relationships, the following variable scores were assigned in Modules 1 and 2:

Module 1.

Willow flycatcher - population and range trends

The breeding distribution of the southwestern willow flycatcher once included most of the riparian river reaches in the southwestern states (California, Arizona, Utah, New Mexico, Colorado, Nevada, and Texas). However, the status and distribution of the species has been greatly altered during the late 19th and 20th centuries by human land use patterns. Widespread destruction of riparian habitat by agriculture, mining, dams, water withdrawals, and urbanization has led to the eradication of many subpopulations and a radical reduction in range and numbers. Throughout its breeding range there are now likely to be fewer than 850 occupied territories, with about 341 at 91 sites in Arizona, 224 at 65 sites in California, 263 at 32 sites in New Mexico, and 37 at 5 sites in Colorado (the remainder are in Utah and Nevada) (Sogge *et al.*, 2001). In response to these low numbers and to continuing anthropogenic threats to the subspecies' habitats, U.S. Fish and Wildlife Service listed the subspecies under the Endangered Species Act as "endangered" in 1995.

Southwestern willow flycatchers have bred or have been reported occupying territories in the SPRNCA: at Charleston in 1977 and Hereford in 1989 (Krueper, 1997); at Gray Hawk ranch in 1994 and two territories in the "upper San Pedro" in 1996, and one in 1997 (Paradzick and Woodward, in review). They may be considered intermittent and rare breeders in the area.

Based on the above information, category scores of 1 have been assigned to the "Current population size" variable, 2 (with an alternate score of 1) to the "Regional population trend in the last 50 years" variable, 2 (with an alternate of 3) to the "regional range trend in the last 50 years" variable, and 2 (with an alternate of 3) the "Current regional range trend variable".

Minimum individual replacement time – this is most likely to occur in the first summer after the bird has left the nest, but could also occur in the following year.

Likely future non-climate stressor trends – A score of 2 has been applied to this variable (with an alternate of 3) because the most important current and past stressors on the population viability of willow flycatchers in the desert southwest has been agriculture, particularly grazing of riparian areas. Many of the willow flycatcher breeding subpopulations that remain in the southwest are on land protected from grazing. Also the status of Endangered under the Endangered Species Act, confers a degree of protection on the species' habitat that did not exist in the past.

Using the same reasoning, a score of 2 (with an alternate of 1) has been applied to the *Likely future vulnerability to policy/management change* variable. This is because the remaining few breeding populations in the southwest are largely dependent on the regulatory status of the species, the creation of reserves, and federal and state limitations imposed on land-uses.

Likely future vulnerabilities to stochastic events and natural stressors. Since the willow flycatcher inhabits vegetation communities that are to a great extent successional (scrub, rather than forest), it has been assumed that and increased occurrence of stochastic events (the most

prevalent in the desert southwest being fire) that result in the replacement of forest by earlier successional stages would actually benefit the species.

Module 2.

Recolonization capability – because it is a highly mobile species and breeds (albeit in small numbers) throughout the southwest, the recolonization ability of this species is scored as “high”.

Degree of habitat specialization – while being confined to riparian scrub habitat, the willow flycatcher can inhabit a variety of scrub types from willow, to Baccharis scrub, to developing gallery forest, to saltcedar. It can also be found breeding in Arizona along the scrubby margins of riparian canopy forest, and within forests with well developed scrub understories. It is, accordingly, scored only “moderately specialized” in its degree of habitat specialization. For these reasons it also scores low in the *dependence on gallery forest variable*. Also, because most willow Flycatchers breeding in southern Arizona are found close to flowing or standing water or areas of saturated soils, the species is scored “somewhat dependent” for the *Dependence on wetland or standing or flowing water variable*.

Likely extent of habitat change due to climate change – one of the major predictions of the vegetation modeling described in this report is that, because of changing water table, the tendency in the SPRNCA is for gallery forest to be replaced by scrub habitats, including saltcedar. Accordingly it is assumed that the extent of potential breeding habitat for willow flycatchers will increase by 20-50%, and, possibly, even more than that.

Ability to utilize mesic or xeric habitats and non-native species – while the willow flycatcher is confined as a breeding species to scrub associated with riparian areas, it is able to exist in the most mesic of such habitats – salt cedar. For this reason it is scored “able” to utilize mesic (but not xeric) habitats and is scored as “able” to utilize plant communities dominated by the most likely non-native species (saltcedar).

Physiological vulnerability to temperature and precipitation change – since willow flycatchers exist (or previously existed) over such a large geographical extent and within so many differing climatic regimes, it is not expected that changes in temperature or precipitation would have marked direct physiological effects. Thus they are scored as being likely insensitive in these variables.

Vulnerability to extreme weather events – It is unlikely that localized extreme weather events would have any *direct* impact on willow flycatchers. Indeed they may benefit indirectly through the creation of earlier successional stages in vegetation communities (i.e., scrub) in areas where forest has been reduced by (e.g.,) fire, drought, or wind storms.

Dependence on temporal inter-relations or other species – there is no evidence that willow flycatchers are particularly dependent on either of these relationships and it scores “independent” as the best estimate for each.

Willow flycatcher - results

This species is categorized as “Least Vulnerable” in Module 1. It fails to achieve the status of currently “Not Vulnerable” largely because of its vulnerability to policy or management change, and to its rapid rates of historic and current regional population and range trends.

In Module 2, willow flycatcher is categorized as “May Benefit” from the effects of climate change. This is largely due to the species’ nesting habitat being essentially successional, its independence from gallery forest, and its ability to breed successfully in mesic and non-native plant communities (particularly saltcedar).

The scores from Modules 1 and 2 combine in Module 3 into an overall vulnerability score of “Not Vulnerable”. This is the result of the species being likely to benefit from climate change, though currently vulnerable to a limited extent. Because a great deal is known about this relatively well-studied species, its certainty score in Module 4 is High.

4.1.2.2 Yellow-billed Cuckoo

This section of the report documents the application of the modified EPA Vulnerability Framework to the population of the western race of the yellow-billed cuckoo, *Coccyzus americanus*, that breeds in the SPRNCA. The results are shown in Attachment 2. The rationales for the scores shown in Attachment 2 are described below.

Yellow-billed cuckoo - general

The yellow-billed cuckoo is a summer visitor to North America, wintering in Central and South America (Kaufman, 1996; Hughes, 1999). Prior to the beginning of the twentieth century, the breeding range of western yellow-billed cuckoos extended throughout western North America from southern Arizona and New Mexico north to British Columbia. However, widespread destruction of riparian habitat by agriculture, mining, dams, water withdrawals, and urbanization has led, since then, to a radical reduction in its range and numbers. Currently, the species no longer breeds in British Columbia, Washington, Idaho, or Oregon. It has been reduced drastically in numbers in more southern western states; for example in the Central Valley of California where thousands of pairs once bred there now are only a few tens of pairs (Haltermann, 1991). In Arizona, yellow-billed cuckoos were relatively widespread 50 years ago (Phillips et al., 1964). However, they now breed regularly only in isolated populations along the Gila, San Pedro, Bill Williams, and Colorado Rivers. It is likely that, at most, 600 pairs now breed in Arizona, with 50-100 of these in the SPRNCA (Laymon and Haltermann, 1987; Krueper, 1997). The rapid population decreases and range reductions of western yellow-billed cuckoos have recently prompted efforts (thus far unsuccessful) to have the race listed under the Endangered Species Act (e.g., CBD, 1998).

Yellow-billed cuckoo – habitat relationships

In the southwestern states, including Arizona, the yellow-billed cuckoo is confined as a breeding species to riparian forests, particularly those dominated by cottonwoods and willows (Hughes,

1999). Forests with a relatively lush, woody understory (either of willow or cottonwood saplings) are preferred (Gaines and Laymon, 1984). This type of habitat is generally found most extensively in functioning riparian systems where scour of vegetation due to floods and recolonization occurs. In areas where flow is controlled to prevent floods or where grazing has reduced shrub cover, such dense layered habitat is less prevalent. The species also avoids areas dominated by invasive species such as salt cedar. Thus the western yellow-billed cuckoo could be considered an indicator organism for functioning, healthy western riparian systems.

The western yellow-billed cuckoo generally builds its nest in shrubby vegetation, particularly denser patches of willows, between 1 and 6 metres above the ground (Hughes, 1999). While the birds nest in willows, much of the feeding by the adults occurs in the cottonwood canopy (Laymon, 1980). Thus, the species utilizes vertically layered habitats.

The configuration of riparian forest patches is an important factor contributing to their suitability for yellow-billed cuckoos. Gaines and Laymon (1984) and Laymon and Halterman (1989) found that larger and wider patches provided better habitat. Small and narrow patches were either marginal or not used by cuckoos.

Being a riparian species, western yellow-billed cuckoos typically inhabit shaded humid areas in an otherwise arid matrix. However, it is unknown whether this is a direct preference for such conditions or a consequence of requiring riparian forest habitat (which is generally shaded and humid). In addition to nesting on the SPRNCA where the average maximum June/July temperature is 90°F and annual rainfall is 15.6 inches, the species also nests 3000 feet lower in elevation on the Gila River where average maximum June/July temperatures reach 102-107°F and rainfall is generally less than 12 inches [data obtained from the Internet (<http://www.wrdc.dri.edu/cgi-bin/cliRECTM.pl?azwink>) from weather stations at Fort Huachuca, Maricopa, Winkelman, Sacaton, and Florence]. Thus, while yellow-billed cuckoos nest in comparatively cool, moist habitat in the SPRNCA, they also nest in hotter, drier areas further downriver on the Gila. This suggests that the availability of riparian forest is the most important factor, of which the micro-climatic conditions may be a consequence. It should also be noted that at one time the species nested as far north as British Columbia and as far south as Mexico, indicating, a degree of flexibility in its climatic requirements.

Based on the above general comments and habitat relationships, the following variable scores were assigned in Modules 1 and 2:

Module 1.

Yellow-billed cuckoo - population and range trends

The breeding distribution of the yellow-billed cuckoo once included most of the riparian river reaches in the western states (from California and Arizona in the south to Oregon and Washington in the north, to Colorado, New Mexico and Texas in the east. However, the status and distribution of the species has been greatly altered during the late 19th and 20th centuries by human land use patterns. Widespread destruction of riparian habitat by agriculture, mining,

dams, water withdrawals, and urbanization has led to the eradication of many subpopulations and a radical reduction in range and numbers. Only about 600 pairs now breed in Arizona, with about 50-100 in the SPRNCA (Krueper, 1997).

Based on these range and population changes, category scores of 2 (with an alternate score of 1) have been assigned to the “Current population size” variable, 2 (with an alternate score of 1) to the “Regional population trend in the last 50 years” variable, 2 (with an alternate of 1) to the “regional range trend in the last 50 years” variable, and 2 (with an alternate of 3) the “Current regional range trend variable”.

Minimum individual replacement time – this is most likely to occur in the first summer after the bird has left the nest, but could also occur in the following year (Hughes, 1999).

Likely future non-climate stressor trends – A score of 2 has been applied to this variable (with an alternate of 1) because the most important current and past stressors on the population viability of yellow-billed cuckoos in the desert southwest has been agriculture, particularly grazing of riparian areas. Many of the yellow-billed cuckoo breeding subpopulations that remain in the southwest are on land protected from grazing.

A score of 2 (with an alternate of 3) has been applied to the *Likely future vulnerability to policy/management change* variable. This is because the remaining few breeding populations in the southwest are largely dependent on the regulatory status of the species, the creation of reserves, and federal and state limitations imposed on land-uses.

Likely future vulnerabilities to stochastic events and natural stressors. The yellow-billed cuckoo inhabits mature riparian gallery forest. It has been assumed that an increased occurrence of stochastic events (the most prevalent in the desert southwest being fire) would result in the replacement of forest by earlier successional stages and that this would reduce the availability of habitat for the species. Also, insect attack, disease and drought could also reduce the habitat available for this species. Thus the species has been scored vulnerable in both of these variables.

Module 2.

Recolonization capability – because it is a highly mobile species and breeds (albeit in small numbers) throughout the southwest, the recolonization ability of this species is scored as “high”.

Degree of habitat specialization – since it is confined in the southwestern states to mature riparian gallery forest the species has been scored as Highly Specialized. Consequently it also scores high in the *dependence on gallery forest variable*. Also, because most yellow-billed cuckoos breeding in southern Arizona are in riparian areas and, therefore, found close to flowing or standing water or areas of saturated soils, the species is scored “somewhat dependent” for the *Dependence on wetland or standing or flowing water variable*.

Likely extent of habitat change due to climate change – one of the major predictions of the vegetation modeling described in this report is that, because of changing water table, the tendency in the SPRNCA will be for gallery forest to be replaced by scrub habitats, including

saltcedar under climate change. Accordingly it is assumed that the extent of potential breeding habitat for yellow-billed cuckoos will decrease 50% or more, with an alternate of a 20-50% reduction.

Ability to utilize mesic or xeric habitats and non-native species – The yellow-billed cuckoo is confined as a breeding species to riparian gallery forest dominated by cottonwoods or wilows and it does not inhabit scrub habitats whether dominated by native or invasive species. For these reasons it is scored “not able” to utilize mesic or xeric habitats. and “not able” to utilize plant communities dominated by the most likely non-native species (saltcedar).

Physiological vulnerability to temperature and precipitation change – since yellow-billed cuckoos in the southwest inhabit mature, moist and shady gallery forest, it is assumed that there is a possibility that they may be directly sensitive temperature and humidity. Thus, they are scored as being “likely moderately sensitive” to temperature and precipitation change.

Vulnerability to extreme weather events – Since an increase in the frequency of extreme weather events (e.g., gales or droughts) could result in the destruction of gallery forest, yellow-billed cuckoos are scored as “likely moderately sensitive” in this variable.

Dependence on temporal inter-relations or other species – yellow-billed cuckoos are highly adapted to feed on caterpillars and may shift their distributions from year to year to track changing densities of their prey. This high level of dependence is reflected in the score of “highly dependent”. Also since the timing of the emergence and growth of the caterpillars is likely to affect the breeding success of the cuckoo, they also score “highly dependent” in the dependence of temporal inter-relations variable.

Yellow-billed cuckoo - results

This species is categorized as “Vulnerable” in Module 1, with a low alternate score of “Highly Vulnerable”. In Module 2 it scores “Vulnerable” with an alternate score of “Highly Vulnerable”. These scores combine in Module 3 into an overall categorization of “Highly Vulnerable” to the potential effects of climate change, with an alternate categorization of “Vulnerable”. The relatively high vulnerability to climate change for this species, in comparison to willow flycatcher, is a reflection of its specialized habitat requirements and its apparent inability to utilize mesic or xeric vegetation communities

Because this is a comparatively well-studied species, the certainty evaluation in Module 4 is “High”.

4.1.2.3 Botteri’s Sparrow

This section of the report documents the application of the modified EPA Vulnerability Framework to the population of Botteri’s sparrow, *Aimophila botterii*, breeding in the SPRNCA. The results are shown in Attachment 2. The rationales for the scores shown in Attachment 2 are described below.

Botteri's sparrow - general

Currently the Botteri's sparrow is limited as a breeding species in North America to two distinct and non-contiguous areas: southeastern Arizona and southwestern New Mexico, and coastal south Texas. There is evidence that its historical breeding distribution may have been more extensive (though confined to the arid southwest and Texas) but contracted due to habitat fragmentation and loss through overgrazing by livestock (Webb and Bock, 1996). The wintering range of the Arizona subpopulation (*A. b. arizonae*) is not known but is probably in central and southern Mexico.

Within the SPRNCA, the species is a common summer resident and breeder from Charleston south to Palominas (Kreuper, 1997). First arrivals in the spring are in late April and the birds usually leave the area in Sep-Oct (Kreuper, 1997, Webb and Bock, 1996). Its breeding distribution in the SPRNCA and southeastern Arizona, in general, is confined to areas of tall native grasslands, primarily giant sacaton stands in relatively flat outwash areas (Jack Whetstone, BLM, *pers. comm.*). It differs from the closely related Cassin's sparrow (*Aimophila cassinii*) in that the latter prefers less tall and less dense grassland stands and can tolerate greater densities of shrubs such as mesquite (Dunning *et al.*, 1999).

The species' timing of breeding is largely determined by the advent of the summer rains in southeastern Arizona, which typically occurs from July to August. This timing allows the birds to exploit the seasonal flush of invertebrate biomass, particularly Orthopterans (Webb and Bock, 1996).

Botteri's sparrow – habitat relationships

Botteri's sparrow is confined as a breeding bird in southern Arizona to stands of grasslands, particularly to giant sacaton stands. Densities are highest in those sacaton stands that are tall and dense with a high representation of senescent plants (Webb and Bock, 1996). They generally avoid areas of high shrub density or grasslands that are dominated by non-native species. Thus, overgrazing of native grasslands, and their reduced density or replacement by invasive species reduces their attractiveness to Botteri's sparrows. This may have been responsible for the range fragmentation and habitat loss that occurred in the past in the southwest. When overgrazed or disturbed areas have been reseeded with native species of grasses, Botteri's sparrows may recolonize (Webb and Bock, 1996).

The grassland stands most favored by Botteri's sparrows are to a great extent limited by topography, occurring only on relatively flat and poorly drained outwash areas, or on riparian flats. Better drained, steeper grasslands tend to be dominated by less lush growths of other grass species.

Based on the above general comments and habitat relationships, the following variable scores were assigned in Modules 1 and 2:

Module 1.

Botteri's sparrow - population and range trends

The breeding distribution of the Botteri's sparrow in the desert southwest of the U.S. was, in the past less fragmented than it is now. However, it is doubtful if this species suffered the same degree of habitat destruction as willow flycatchers or yellow-billed cuckoos, species that demand habitats most valued and modified by agriculture. Within the SPRNCA Botteri's sparrows are relatively common, occurring wherever there are stands of giant sacaton (*pers obs*). Based on this, category scores of 3 have been assigned to the "Current population size" variable, the "Regional population trend in the last 50 years" variable, the "regional range trend in the last 50 years" variable, and the "Current regional range trend variable".

Minimum individual replacement time – this is most likely to occur in the first summer after the bird has left the nest, but could also occur in the following year. Thus, minimum replacement time has been scored as 4 (within the first year of life), with an alternate score of 3.

Likely future non-climate stressor trends – A score of 3 has been applied to this variable because the most important current and past stressor on Botteri's sparrow in the desert southwest has been agriculture. At present, agriculture primarily threatens riparian forested and scrub habitats. Conversion of such habitats to grass-dominated communities could benefit this species.

Using the same reasoning, a score of 3 has been applied to the *Likely future vulnerability to policy/management change* variable.

Likely future vulnerabilities to stochastic events and natural stressors. Since the Botteri's sparrow inhabits grasslands, it has been assumed that an increased occurrence of stochastic events (the most prevalent in the desert southwest being fire) that result in the replacement of forest by scrub and grassland communities would actually benefit the species. A score of 3 has been applied to this variable.

Module 2.

Recolonization capability – because it is a highly mobile species and breeds in suitable habitat throughout southern Arizona, the recolonization ability of this species is scored as "high".

Degree of habitat specialization – since it is confined to a particular type of grassland (sacaton) and apparently does not tolerate non-native vegetation, the species is scored "highly specialized". Also, since it is an arid land species it is scored "independent" for the *Dependence on wetland or standing or flowing water* variable.

Likely extent of habitat change due to climate change – one of the major predictions of the vegetation modeling described in this report is that, because of changing water table or increased risk of fire, the tendency in the SPRNCA will be for gallery forest to be replaced by scrub habitats and grasslands. Accordingly it is assumed that the extent of potential breeding habitat for Botteri's sparrows will increase by >50%.

Ability to utilize mesic or xeric habitats and non-native species – the Botteri’s sparrow is confined as a breeding species to mesic or xeric grasslands. For this reason it is scored “able” to utilize mesic and xeric habitats, but is scored as “not able” to utilize plant communities dominated by non-native species (see above).

Physiological vulnerability to temperature and precipitation change – Botteri’s sparrows breed in Mexican grasslands far to the south of the SPRNCA, where they are likely to be exposed to higher temperatures than prevail in southern Arizona. For this reason, they are scored as likely “insensitive” to direct temperature change effects. It is also unlikely that they are sensitive to *direct* effects from precipitation change.

Vulnerability to extreme weather events – It is unlikely that localized extreme weather events would have any *direct* impact on Botteri’s sparrows. Indeed they may benefit indirectly through the creation of grass-dominated vegetation communities in areas where forest has been fragmented by fire, drought, or wind storms. Thus, the best estimate score for this variable is 3 (with an alternate of 4).

Dependence on temporal inter-relations or other species – Botteri’s sparrow breeding phenology is determined by the timing of the summer monsoon in southern Arizona. It cannot be predicted how climate change might affect this timing. Thus it is conservatively assumed that the sparrow is “moderately dependent” on temporal inter-relations. However, except for its association with sacaton-dominated grasslands, Botteri’s sparrows are not known to be dependent on other species, and therefore scores “independent”.

Botteri’s sparrow - results

This species is categorized as “Not Vulnerable” in Module 1. This is because of its current population status and its dependence on habitats that are not as vulnerable to current stressors than riparian wooded habitats.

In Module 2, Botteri’s sparrow is categorized as “May Benefit” (Vc4) from the effects of climate change. This is largely due to the species’ nesting habitat being essentially successional, and its independence from gallery forest.

The scores from Modules 1 and 2 combine in Module 3 into an overall vulnerability score of “Not Vulnerable” (Vo4). This is the result of the species being likely to benefit from climate change, and the comparatively healthy state of its local and regional populations. Because the species is relatively well-studied, its certainty score in Module 4 is High.

4.1.3 Summary

This application of the EPA Framework produces results that can be used to compare the relative vulnerabilities of three bird species characteristic of the SPRNCA and riparian areas in the southwest in general. Scoring the 22 variables in Modules 1 and 2 of the EPA Framework results in the following vulnerability ranking (most vulnerable to least vulnerable): yellow-billed

cuckoo>willow flycatcher>Botteri's sparrow. This ranking is a reflection of differences in the habitat demands of the three species, past and current population ranges and trends, and likely effects of future climate change on the availability of their preferred habitats. The yellow-billed cuckoo is scored as the most vulnerable species because it is tied tightly to a specific habitat type (gallery forest), moreover, this is the habitat that vegetation modeling has shown to be most vulnerable to the climate change scenarios. Also, the yellow-billed cuckoo does not, apparently, tolerate invasive forest and/or scrub types. It can, therefore be viewed as a specialist which, unfortunately, specializes in a set of conditions highly vulnerable to climate change.

The willow flycatcher and Botteri's sparrow are scored as less vulnerable than the yellow-billed cuckoo. This is largely because of two factors: their preference for successional (non-forest) habitats, and, in the case of the willow flycatcher, its ability to exploit habitats dominated by non-native vegetation. Given the habitat changes predicted in the SPRNCA from the vegetation modeling described in this report, it is possible that willow flycatchers, and likely that Botteri's sparrows may actually benefit from future climate change.

It should be noted that the results described above are model predictions, and like all model predictions, are surrounded with some degree of uncertainty. Therefore the species-specific results and relative rankings should be considered as incorporating some degree of hesitancy. Only time will tell how accurate they may be.

4.2 SPRNCA Vulnerability Framework

The riparian vegetation communities of the San Pedro River in southern Arizona support highly diverse animal populations. For example, over 100 species of birds breed there and an additional 250 use the area during migration or in winter (Krueper, 1997). This biodiversity has resulted in the riparian corridor of the San Pedro River being designated a National Conservation Area. To varying extents, riparian plants are hydrophytic and depend on root access to surface water flow or to groundwater. In the San Pedro, for example, there is a marked zonation in the species composition of vegetation communities dictated by root length and depth to the alluvial groundwater aquifer (Stromberg *et al.*, 1996). Any stressor that reduces the plants' access to water could make the continued existence of such riparian communities less viable and result in their replacement by drought-tolerant species such as saltcedar or mesquite, *Prosopis* spp.

Within the San Pedro Riparian National Conservation Area (SPRNCA) agricultural and urban water withdrawals from the groundwater aquifers may be resulting in lowered water tables (Goode and Maddock, 2000; Vionnet and Maddock, 1992), with consequent adverse impacts on the riparian gallery forests, and invasion by drought-tolerant species such as saltcedar, *Tamarix* spp., (Stromberg, 1998; Stromberg *et al.*, 1996). These stressors could eventually result in changes to the structure and composition of the San Pedro riparian forests and scrub, with consequent impairments of their ability to support wildlife. Climate change is another potentially important stressor in the SPRNCA. Climate change, through changes in precipitation, drying, and evapotranspiration, could result in the depth to the water table being increased with subsequent adverse impacts to the riparian vegetation communities.

One of the main aims of the research being conducted as part of this EPA-funded project is to evaluate the potential effects of groundwater withdrawals and climate change on the SPRNCA vegetation communities and the wildlife that they support. The main goal of this element of the overall San Pedro research project is to assess, at least qualitatively, the potential impacts of climate change and ground water withdrawals on the biodiversity supported by the SPRNCA. Attempting to evaluate these effects on all of the taxa that comprise this biodiversity would be problematic due to uncertainties regarding the habitat ecologies of some of the less well-studied taxa (e.g., nocturnal mammals, fish, or invertebrates), and limitations in our knowledge about their exact status within the SPRNCA. In contrast, we do have adequate information about one important taxon that uses the SPRNCA – birds. The status and habitat relationships of the 350 or more bird species that occur in the SPRNCA are comparatively well-known.

The main goal of this element of the San Pedro research is to develop and apply a predictive model that will project the effects of changes in the riparian vegetation communities (caused by groundwater withdrawals and climate change) on the avian component of biodiversity in the SPRNCA. The results of this modeling exercise can then be compared with two other modeling procedures developed for evaluating the vulnerabilities of SPRNCA birds, the combined HSI and vegetation models (Section 4-3 of this report), and the modified EPA vulnerability framework (Section 4-1).

4.2.1 Overall Methodological Approach

Vegetation modeling has shown (Section 3 of this report) that some of the most fundamental potential impacts of changing hydrology and climate change on vegetation communities in the SPRNCA include the fragmentation of the existing riparian and wetland communities, and their replacement by more mesic or xeric communities (i.e., communities more typical of the desert matrix within which the SPRNCA is set). The overall approach of this phase of the studies has been to develop a predictive framework, based on the habitat preferences of avian species that inhabit the SPRNCA, that will categorize their relative vulnerabilities to the vegetation changes identified above and project potential impacts to their population status within the study area.

We have chosen to focus on the 87 species of birds that have been classified by Kreuper (1997) as being either “abundant”, “common”, or “fairly common” within the SPRNCA (Table 4-8). “Uncommon”, “rare”, “casual”, or “accidental” species have not been evaluated. Because of their relatively abundant status, the species that we have evaluated will comprise the majority of the birds using the SPRNCA at any particular time, and will provide a more reliable indication of impacts to diversity.

4.2.2 Framework Variables

Based on the predicted changes in vegetation communities and the known habitat relationships of the 87 bird species, four variables that are most likely to predict future population changes were identified. For each of these variables a scoring system was developed. The scores for any species are indices of its likely vulnerability to the projected habitat changes.

Variable 1. Degree of dependence on dominance by riparian species in vegetation community. This variable characterizes the extent to which the species being evaluated is restricted in the SPRNCA to stands of riparian vegetation for one or more of three limiting life-history requirements: foraging habitat, cover, and/or nest sites. The latter includes other reproductive requirements, such as song or display sites, in addition to nest sites, themselves.

In the SPRNCA riparian stands would include vegetation communities dominated by hydrophytic and, to a lesser extent, mesic species. Dominance in this context means that these species are the major determinants of the overall structure and composition of the community. It is not intended to imply that individuals of non-hydrophytic species cannot exist in such communities. Thus, willow scrub (a shrub community largely composed of hydrophytic willow species) is a riparian vegetation community, whereas mesquite scrub (largely composed of the xeric mesquite) is not. In the SPRNCA, riparian vegetation communities are typically dominated by Fremont cottonwood, Gooding's willow, and/or baccharis (Stromberg *et al.*, 1996).

Table 4-8. Bird species evaluated in the analyses. Relative abundance categories: a = abundant, c = common, fc = fairly common. . Seasonal occurrence categories: yr = year-round resident, sr = summer resident, wr = winter resident, m = migrant

SPECIES	ABUNDANCE	SEASONALITY	SPECIES	ABUNDANCE	SEASONALITY
Great blue heron	Fc	Yr	Cactus wren	Fc	yr
Turkey vulture	C	sr, m	Bewick's wren	C	yr
Northern harrier	C	Wr	Ruby-crowned kinglet	C	m
Sharp-shinned hawk	Fc	wr, m	Northern mockingbird	Fc	yr
Cooper's hawk	Fc	Yr	Curve-billed thrasher	C	ty
Gray hawk	C	Sr	Loggerhead shrike	Fc	yr
Red-tailed hawk	C	Yr	European starling	Fc	yr
American kestrel	C	Yr	Bell's vireo	C	sr
Scaled quail	C	Yr	Warbling vireo	C	m
Gambel's quail	C	Yr	Orange-crowned warbler	C	m
Virginia rail	C	Wr	Lucy's warbler	C	sr
Sora rail	Fc	Wr	Yellow warbler	C	m
Spotted sandpiper	Fc	M	Yellow-rumped warbler	C	m
Wilson's snipe	Fc	wr, m	MacGillivray's warbler	Fc	m
White-winged dove	C	Sr	Common yellowthroat	A	sr
Mourning dove	C	Yr	Wilson's warbler	C	m
Common ground dove	Fc	Yr	Yellow-breasted chat	C	sr
Yellow-billed cuckoo	C	Sr	Summer tanager	C	sr
Greater roadrunner	Fc	Yr	Western tanager	C	m
Western screech owl	C	Yr	Black-headed grosbeak	C	m
Great Horned owl	C	Yr	Blue grosbeak	C	sr
Lesser nighthawk	C	Sr	Green-tailed towhee	C	m
Black-chinned hummingbird	C	Sr	Canyon towhee	C	yr
Belted kingfisher	Fc	Wr	Abert's towhee	Fc	yr
Gila woodpecker	Fc	Yr	Botteri's sparrow	C	sr
Ladder-backed woodpecker	C	Yr	Cassin's sparrow	C	sr
Northern flicker	Fc	Yr	Chipping sparrow	C	wr
Western wood pewee	C	Sr	Brewer's sparrow	C	wr, m
Dusky flycatcher	Fc	M	Vesper sparrow	C	wr, m
Gray flycatcher	C	M	Lark sparrow	C	wr
Pacific-slope flycatcher	Fc	M	Black-throated sparrow	C	yr
Black phoebe	C	Sr	Lark bunting	Fc	wr

Table 4-8 continued

Say's phoebe	Fc	Yr	Savannah sparrow	C	wr, m
Vermilion flycatcher	C	Sr	Song sparrow	C	yr
Ash-throated flycatcher	C	Sr	Lincoln's sparrow	C	wr
Cassin's kingbird	C	Sr	White-crowned sparrow	A	wr, m
Western kingbird	C	Sr	Red-winged blackbird	A	wr, m
Tree swallow	C	M	Yellow-headed blackbird	C	wr
Violet-green swallow	Fc	M	Brewer's blackbird	C	wr, m
Northern rough-winged swallow	C	Sr	Brown-headed cowbird	A	yr
Cliff swallow	C	Sr	Hooded oriole	C	sr, m
Chihuahuan raven	C	Yr	Bullock's oriole	C	sr
Verdin	Fc	Yr	Scott's oriole	C	sr
			Lesser goldfinch	C	yr

Five numerical scores of dependency were developed. These are based on the degree to which the species being evaluated are known to be typically restricted to riparian habitat for either or all of the three life-history requirements in the SPRNCA:

Score	Habitat Utilization
5	Typically found only in riparian habitat
4	Typically found mainly in riparian habitat, but may also occur infrequently in more xeric habitats
3	May typically occur in either riparian or more xeric habitats
2	More typical of xeric habitats but may also occur in riparian
1	Largely restricted to xeric habitats

Variable 2. Degree of dependence on extensive and non-fragmented stands of riparian forest

This variable characterizes the extent to which the species being evaluated is restricted by its habitat preferences to extensive and non-fragmented stands of riparian forest vegetation for one or more of three limiting life-history requirements: foraging habitat, cover, and/or nest sites. The latter includes other reproductive requirements, such as song or display sites, in addition to nest sites, themselves.

The categorization of non-fragmented forest applies to individual stands dominated by either Fremont cottonwood or Goodding’s willow that extend over at least several acres, rather than isolated and smaller fragments.

Three numerical scores of dependency were developed. These are based on the degree to which the species being evaluated are known to be typically restricted to extensive and non-fragmented stands of riparian forest for either or all of the three life-history requirements in the SPRNCA:

Score	Habitat Utilization
3	Typically found only in such stands
2	Typically found mainly in such stands, but may also occur infrequently in less extensive habitat
1	May typically occur in either extensive and non-fragmented or restricted and fragmented stands

Variable 3. Degree of dependence on wetland habitat

This variable characterizes the extent to which the species being evaluated is restricted by its habitat preferences to wetland habitats for one or more of three limiting life-history requirements: foraging habitat, cover, and/or nest sites. The latter includes other reproductive requirements, such as song or display sites, in addition to nest sites, themselves.

In the SPRNCA, wetland habitats comprise communities dominated by hydrophytic floating and emergent plant species such as sedges, rushes, grasses, bullrushes, and equisetum species (Stromberg *et al.*, 1996). These communities are typically found surrounding cienagas, at beaver dams, or intermittently flooded channels.

Five numerical scores of dependency were developed. These are based on the degree to which the species being evaluated are known to be typically restricted to wetland habitat for either or all of the three life-history requirements in the SPRNCA:

Score	Habitat Utilization
5	Typically found only in wetland habitat
4	Typically found mainly in wetland habitat, but may also occur infrequently in more xeric habitats
3	May typically occur in either wetland or more xeric habitats
2	More typical of xeric habitats but may also occur in wetlands
1	Largely restricted to xeric habitats

Variable 4. Degree of dependence on running or standing water

This variable characterizes the extent to which the species being evaluated is restricted by its habitat preferences to areas that include permanent or largely permanent areas of running or standing water. Species that are dependent on such habitats are usually so because of their diets (at least partly reliant on fish, aquatic invertebrates, or aquatic vegetation).

Five numerical scores of dependency were developed. These are based on the degree to which the species being evaluated are known to be typically restricted to areas with running or standing water:

Score	Habitat Utilization
5	Typically associated only with aquatic habitats
4	Typically associated mainly with aquatic habitats, but not exclusively so
3	May be associated with either aquatic or non-aquatic habitats

- 2 More typical of xeric, non-aquatic habitats
- 1 Largely restricted to xeric habitats

4.2.3 Results of Framework Analyses

The framework scores for the 87 bird species are shown in Table 4-9. Each of the framework scores were based on information contained in the scientific literature, particularly the individual species accounts in the “Birds of North America series (BNA, various dates) and Kaufman (1996). Table 4-10 groups the results of the total scores in Table 2 into four vulnerability categories: Highly Vulnerable; Vulnerable; Less Vulnerable; and Least Vulnerable. 26% of the 87 species can be categorized as either Highly Vulnerable or Vulnerable. These are the species most likely to be adversely affected by the projected vegetation changes. The 25% of species in the Less Vulnerable categories can be viewed as species that are relatively insensitive to the projected vegetation changes since they are not closely tied to the existence of riparian or wetland vegetation communities, rather than more mesic or xeric community types, and might not be greatly adversely affected under a shift from continuous riparian forests and wetlands to (for example) increased cover of ash or mesquite woodlands. More than half of the 43 species in the category: Least Vulnerable are adapted to the desert or arid grassland environments of southern Arizona. Such species might be expected to benefit from the conversion of riparian forest and wetland habitats within The SPRNCA to more mesic or xeric environments.

4.2.4 Conclusions

This analysis has shown that approximately 26% of the most abundant bird species currently inhabiting the SPRNCA are likely to be vulnerable to and adversely affected by the changes to the vegetation communities projected by the vegetation analyses in Section 3 of this report. An additional 25% may be relatively unaffected and 43% may benefit. Although some species are likely to benefit from the projected changes, in terms of overall biodiversity the results of this analysis do not provide grounds for optimism: the species that are projected to be adversely affected are largely of high conservation value in that they are typical of a declining and reduced habitat (riparian forest and scrub), are already limited in their ranges and distributions, and many of them are identified in state and federal statutes and “watchlists” as being of particular conservation importance (willow flycatcher, yellow-billed cuckoo, grey hawk, etc.). Further losses of these species in the “benchmark” riparian area of the SPRNCA will be a relatively large adverse impact to the overall status and condition of these populations. Also, while it is true that some species that are typical of xeric habitats may spread into the SPRNCA from further south as the climate and vegetation changes, the potential for such additions to redress the losses of biodiversity due to riparian species being lost is limited. Most of the northern Mexican desert or arid grassland species that could inhabit a more desert-like SPRNCA already exist there in the desert matrix on the San Pedro floodplain and would not be new additions to the regional avifauna.

While this analysis cannot be directly extended to other non-avian taxa, it does, nevertheless, raise concerns. Just as continuing aridification of the SPRNCA has been projected to result in losses of avian diversity, it is likely that this pattern will be repeated in other taxa including mammals and invertebrates (many of whom are also likely to depend on riparian or wetland habitats). The result will be a net loss of diversity in this nationally important center of biodiversity.

Table 4-9. Species vulnerability scores.

SPECIES	Dependence on dominance of riparian veg.	Dependence on riparian forest	Dependence on wetland habitat	Dependence on standing water or perennial river flow	Total Score
Great blue heron	2	1	5	5	13
Turkey vulture	1	1	1	1	4
Northern harrier	1	1	1	1	4
Sharp-shinned hawk	3	2	1	1	7
Cooper's hawk	3	2	1	1	7
Gray hawk	5	3	5	2	15
Red-tailed hawk	3	2	1	1	7
American kestrel	2	1	1	1	5
Scaled quail	1	1	1	1	4
Gambel's quail	1	1	1	1	4
Virginia rail	1	1	5	4	11
Sora rail	1	1	5	4	11
Spotted sandpiper	3	1	4	4	12
Wilson's snipe	1	1	5	4	11
White-winged dove	1	1	1	1	4
Mourning dove	1	1	1	1	4
Common ground dove	1	1	1	1	4
Yellow-billed cuckoo	5	3	3	2	13
Greater roadrunner	1	1	1	1	4
Western screech owl	4	1	1	1	7
Great Horned owl	4	3	1	1	9
Lesser nighthawk	1	1	1	1	4
Black-chinned hummingbird	1	1	1	1	4
Belted kingfisher	3	1	5	5	14
Gila woodpecker	2	2	1	1	6
Ladder-backed woodpecker	4	2	1	1	8
Northern flicker	4	2	1	1	8
Western wood pewee	5	3	1	1	10
Dusky flycatcher	3	1	1	1	6
Gray flycatcher	1	1	1	1	4

Table 4-9 continued

Pacific-slope flycatcher	3	2	1	1	7
Black phoebe	4	1	4	4	13
Say's phoebe	1	1	1	1	4
Vermilion flycatcher	1	1	1	1	4
Ash-throated flycatcher	1	1	1	1	4
Cassin's kingbird	1	1	1	1	4
Western kingbird	1	1	1	1	4
Tree swallow	3	1	4	4	12
Violet-green swallow	1	1	1	3	6
Northern rough-winged swallow	1	1	2	3	7
Cliff swallow	1	1	3	4	9
Chihuahuan raven	1	1	1	1	4
Verdin	1	1	1	1	4
Cactus wren	1	1	1	1	4
Bewick's wren	1	1	1	1	4
Ruby-crowned kinglet	2	3	1	1	7
Northern mockingbird	1	1	1	1	4
Curve-billed thrasher	1	1	1	1	4
Loggerhead shrike	1	1	1	1	4
European starling	1	1	1	1	4
Bell's vireo	3	1	2	2	8
Warbling vireo	4	2	3	1	10
Orange-crowned warbler	1	2	1	1	5
Lucy's warbler	1	1	1	1	4
Yellow warbler	5	2	4	3	14
Yellow-rumped warbler	2	2	1	1	6
MacGillivray's warbler	1	1	1	1	4
Common yellowthroat	5	2	4	3	14
Wilson's warbler	5	2	3	3	13
Yellow-breasted chat	3	2	4	2	11
Summer tanager	5	3	1	1	10
Western tanager	1	1	1	1	4
Black-headed grosbeak	3	2	1	1	7
Blue grosbeak	3	2	1	1	7
Green-tailed towhee	1	1	1	1	4

Table 4-9 continued

Canyon towhee	1	1	1	1	4
Abert's towhee	1	1	1	1	4
Botteri's sparrow	1	1	1	1	4
Cassin's sparrow	1	1	1	1	4
Chipping sparrow	1	1	1	1	4
Brewer's sparrow	1	1	1	1	4
Vesper sparrow	1	1	1	1	4
Lark sparrow	1	1	1	1	4
Black-throated sparrow	1	1	1	1	4
Lark bunting	1	1	1	1	4
Savannah sparrow	1	1	1	1	4
Song sparrow	4	1	3	1	9
Lincoln's sparrow	4	1	4	1	10
White-crowned sparrow	3	1	1	1	6
Red-winged blackbird	3	1	3	3	10
Yellow-headed blackbird	3	1	3	3	10
Brewer's blackbird	3	1	3	3	10
Brown-headed cowbird	2	1	2	2	7
Hooded oriole	3	3	3	1	10
Bullock's oriole	3	2	2	1	8
Scott's oriole	1	1	1	1	4
Lesser goldfinch	1	1	1	1	4

Table 4-10. Vulnerability categories. Species in bold are desert or arid grassland species in southern Arizona.

14-18 Highly Vulnerable	10-13 Vulnerable	6-9 Less Vulnerable	<6 Least Vulnerable
Gray hawk	Great blue heron	Sharp-shinned hawk	Turkey vulture
Belted kingfisher	Virginia rail	Cooper's hawk	Northern harrier
Common yellowthroat	Sora rail	Red-tailed hawk	Scaled quail
Yellow warbler	Spotted sandpiper	Western screech owl	Gambel's quail
	Wilson's snipe	Great Horned owl	American kestrel
4 (5%)	Yellow-billed cuckoo	Gila woodpecker	White-winged dove
	Western wood pewee	Ladder-backed woodpecker	Mourning dove
	Black phoebe	Northern flicker	Common ground dove
	Tree swallow	Pacific-slope flycatcher	Greater roadrunner
	Warbling vireo	Dusky flycatcher	Lesser nighthawk
	Wilson's warbler	Violet-green swallow	Black-chinned hummingbird
	Yellow-breasted chat	Northern rough-winged swallow	Gray flycatcher
	Summer tanager	Cliff swallow	Say's phoebe
	Lincoln's sparrow	Ruby-crowned kinglet	Vermilion flycatcher
	Red-headed blackbird	Bell's vireo	Ash-throated flycatcher
	Yellow-headed blackbird	Yellow-rumped warbler	Cassin's kingbird
	Brewer's blackbird	Black-headed grosbeak	Western kingbird
	Hooded oriole	Blue grosbeak	Chihuahuan raven
		Song sparrow	Verdin
	18 (21%)	White-crowned sparrow	Cactus wren
		Brown-headed cowbird	Bewick's wren
		Bullock's oriole	Northern mockingbird
			Curve-billed thrasher
		22 (25%)	Loggerhead shrike
			Lucy's warbler
			MacGillivray's warbler
			Orange-crowned warbler
			Western tanager
			Green-tailed towhee
			Canyon towhee
			Abert's towhee

4.3 Vegetation modeling and Habitat Suitability Index Models

In addition to evaluating avian vulnerability to future climate change using the EPA and Vulnerability frameworks, as described in Sections 4.1 and 4.2, respectively, the potential vulnerabilities of five species (willow flycatcher, yellow-billed cuckoo, Botteri's sparrow, and Wilson's and yellow warblers) were also investigated by combining the vegetation change model described in Section 3 of this report with Habitat Suitability Index (HSI) models specifically developed for this purpose. These models are described in detail in Attachment 3 to this report.

HSI models evaluate the likely impacts of any actual or potential changes in habitat quality on carrying capacity (defined here as the habitat's capacity to support organisms) for either a single species, a guild of species, or biodiversity in general. HSI models achieve this by:

1. Identifying the critical habitat variables that affect the carrying capacity of habitat.
2. Establishing quantitative relationships between the occurrence of these variables and the carrying capacity of habitat. Each variable is assigned a suitability index (SI). This is a score of between 0 and 1, where the former is completely unsuitable habitat (i.e., minimal carrying capacity) and the latter is optimal habitat (i.e., greatest carrying capacity).
3. Developing metrics that can be used in the field to quantify the occurrence of the critical habitat components (and, therefore, the carrying capacity of the habitat)
4. Developing algorithms that combine the variable scores (SIs) into an expression of the overall carrying capacity of the habitat. This final score is the HSI and can be between 0 (unsuitable for species or guild) and 1 (optimal habitat).

Previous applications of HSI models have included the prediction of the possible effects of particular land management alternatives on biota (Brand *et al.*, 1986; Schamberger and Farmer, 1978), the quantification of past injuries to ecosystem wildlife carrying capacities (Galbraith *et al.*, 1996; LeJeune *et al.*, 1996), evaluating the potential effects of climate change and aquifer depletion on biota (Galbraith *et al.*, *in press*), and estimating the exposure to contaminants of wildlife species. If the structures, extents, and/or compositions of post-change vegetation communities can be predicted, it becomes possible to use HSI models to quantify and compare pre- and post-change habitat quality and potential carrying capacities.

U.S. Fish and Wildlife Service has developed approximately 160 HSI models. These include 85 terrestrial species (62 birds, 17 mammals, and 6 reptiles and amphibians). The remainder comprise marine and freshwater organisms. Most of the models have specific geographic, habitat, and seasonal areas of applicability. For example, the model for American woodcock, *Scolopax minor*, applies only to the species' wintering range in the southeastern states (Cade, 1985). In addition to the single-species HSI models, U.S. Fish and Wildlife has also developed a few models that quantify the carrying capacity of habitat for groups of species, for example habitat guild models (Short, 1983), or for wildlife diversity in general (Short, 1984).

No previously developed HSI model existed for any of the five species listed above. Correspondingly, they were developed for the species in their breeding range and migration habitats in southern Arizona and it might not be applicable, without modification, elsewhere in its breeding range.

In the analyses below, we used the HSI models to identify the important habitat variables for each of the five species. We then proceeded in two ways:

1. We used the general conclusions regarding how the vegetation communities in the SPRNCA might change in the future under four climate change scenarios (no change, warmer, warmer and drier, warmer and wetter) to arrive at qualitative assessments of how the individual variables might alter under these vegetation changes for each of the study species. This is referred to hereafter as the Qualitative Analysis.
2. We also used the vegetation model to simulate quantitative changes in each of the HSI variables for each of the study species. This then allowed us to project changes in the overall HSI score for each species under each of the four climate change scenarios. This is referred to hereafter as the Quantitative Analysis.

The results of each of these analytical approaches are reported in Sections 4.3.1 and 4.3.2, respectively.

4.3.1 The qualitative analysis

Table 4-11 summarizes the main changes projected by the Vegetation modeling in Section 3 of this report. The overall conclusion is that for all of the futures scenarios, except one – warmer and wetter, the future vegetation conditions will be characterized by reductions in the representation of cottonwood/willow gallery forest and cienaga wetlands, with increased cover by invasive saltcedar and mesic and/or xeric shrublands, as the desert matrix in which the SPRNCA exists gradually invades the areas currently under riparian forest. The rate and extent to which these changes will take place is dependent on the scenario, with the lowest extents of replacement occurring under the no change and warmer scenarios. The replacement extent is likely to be most rapid and widespread under the warmer and drier scenario since this will have the greatest detrimental effect on surface flow and depth to groundwater (see Section 3).

Table 4-11. Summary of projected changes to main vegetation communities under climate change scenarios				
	Cottonwood/willow forest	Cienaga wetlands	Saltcedar Scrub	Mesic/xeric grass/shrubland
No change	Reduction	reduction	increase	Increase
Warmer	Reduction	reduction	increase	Increase
Warmer and drier	Reduction	reduction	increase	Increase
Warmer and wetter	no change	no change	no change	no change

The warmer and very wet scenario was not included in this analysis because the results projected for the vegetation community approximately mirrored those of the warm and wet scenario and also because the warmer and very wet scenario could be considered an extreme projection, and less likely to occur than the warmer, warmer and drier and warmer and wetter scenarios.

Ranked projections of how we expect the main vegetation change projections to affect the HSI variables for each of the five study species are presented in Tables 4-12 through 4-16. Figure 4-2 presents a comparison of how the vegetation changes projected under the no change, warmer, and warmer and drier scenarios will affect the total HSI score for each species. The warmer and wetter scenario is not included in Figure 4-2 because, as can be seen in Tables 4-12 through 4-16 it did not result in major changes in the habitat quality.

Table 4-12. Qualitative assessment of effects of climate change scenarios on willow flycatcher HSI scores (+2 = markedly increase; +1 = increase; 0 = no change or uncertain; -1 = reduce; -2 = markedly reduce)				
	No change	Warmer	Warmer and drier	Warmer and wetter
Isolation and extent of riparian shrub patches	+1	+1	+1	0
Width of riparian patches	+1	+1	+1	0
% shrub canopy cover	+1	+1	+1	0
Shrub foliage density	+1	+1	+1	0
Shrub canopy height	+1	+1	+1	0
Tree canopy cover	+1	+1	+2	0
Distance to water	0	0/-1	-1	0
Soil waterlogging	0	0/-1	-1	0
Total score change	+6	+6-+4	+5	0

Table 4-13. Qualitative assessment of effects of climate change scenarios on yellow-billed cuckoo HSI scores (+2 = markedly increase; +1 = increase; 0 = no change or uncertain; -1 = reduce; -2 = markedly reduce)

	No change	Warmer	Warmer and drier	Warmer and wetter
Linear continuity of riparian forest	-1	-1	-2	0
Width of riparian forest patches	-1	-1	-2	0
Percent shrub canopy	+1	+1	+1	0
Shrub canopy height	+1	+1	+1	0
Tree canopy height	-1	-1	-2	0
Cottonwood/willow dominance in tree canopy	-1	-1	-2	0
Cottonwood/willow dominance in shrubs	-1	-1	-2	0
Saltcedar dominance	0	-1	-2	0
Total score change	-3	-4	-10	0

Table 4-14. Qualitative assessment of effects of climate change scenarios on Botteri's sparrow HSI scores (+2 = markedly increase; +1 = increase; 0 = no change or uncertain; -1 = reduce; -2 = markedly reduce)

	No change	Warmer	Warmer and drier	Warmer and wetter
% grass cover	+1	+1	+2	0
Sacaton dominance	+1	+1	+2	0
Sacaton height	0	0	0	0
Sacaton density	0	0	0	0
Sacaton senescence	0	0	0	0
% forbs/native grasses	0	0	0	0
Total score change	+2	+2	+4	0

Table 4-15. Qualitative assessment of effects of climate change scenarios on Wilson's warbler sparrow HSI scores (+2 = markedly increase; +1 = increase; 0 = no change or uncertain; -1 = reduce; -2 = markedly reduce)				
	No change	Warmer	Warmer and drier	Warmer and wetter
Riparian forest patch size	-1	-1	-2	0
shrub canopy cover	0	0	-1	0
% cottonwood/willow in shrub canopy	-1	-1	-2	0
Shrub canopy height	0	0	0	0
% saltcedar dominance	-1	-1	-2	0
Total score change	-3	-3	-7	0

Table 4-16. Qualitative assessment of effects of climate change scenarios on yellow warbler sparrow HSI scores (+2 = markedly increase; +1 = increase; 0 = no change or uncertain; -1 = reduce; -2 = markedly reduce)				
	No change	Warmer	Warmer and drier	Warmer and wetter
Riparian forest patch size	-1	-1	-2	0
Tree canopy cover	-1	-1	-2	0
Shrub canopy cover	0	0	-1	0
Cottonwood/willow dominance in tree canopy	-1	-1	-2	0
Cottonwood/willow dominance in shrub canopy	-1	-1	-2	0
Shrub canopy height	0	0	0	0
Mesic or xeric vegetation dominance	-1	-1	-2	0
Total score change	-5	-5	-11	0

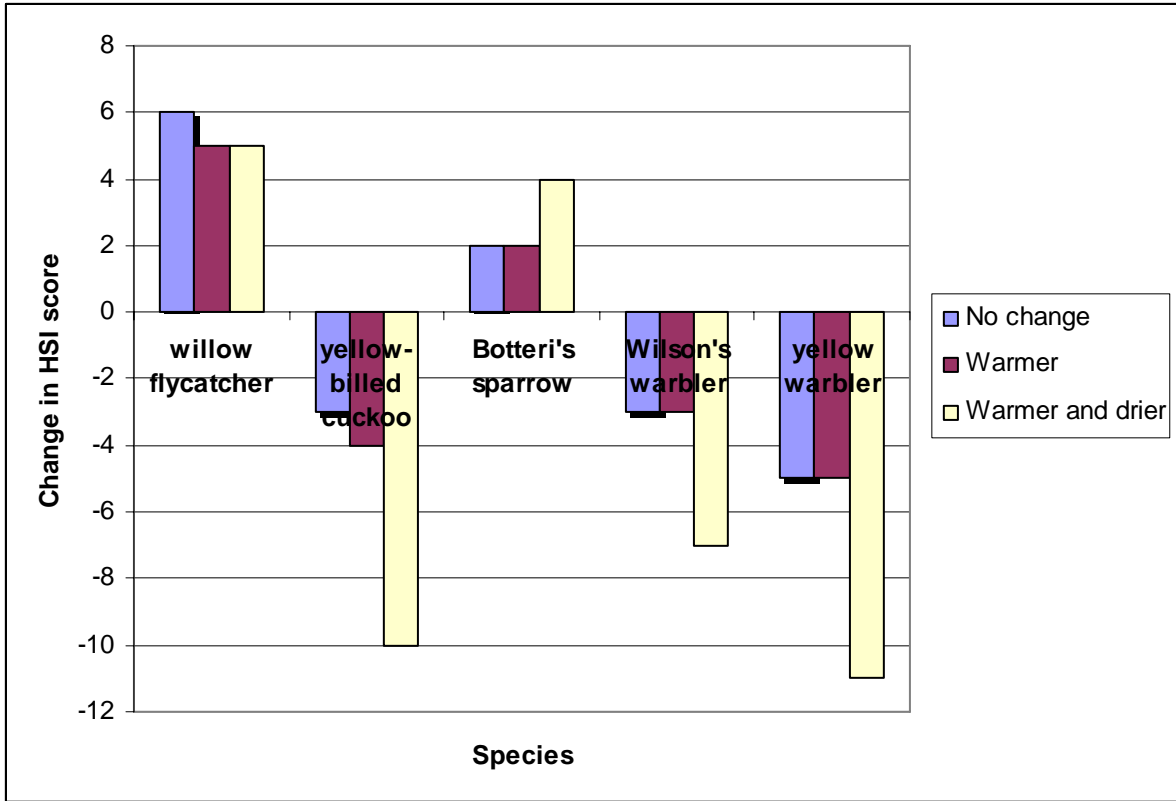


Figure 4-2. Projected relative changes in total HSI scores for five bird species under three future climate scenarios.

The results reported in Tables 4-12 through 4-16 and Figure 4-2 show that different species have different vulnerabilities to climate change. Those species that are most dependent on the continuation of the existing hydric riparian forest and wetland habitats (yellow-billed cuckoo, Wilson’s and yellow warblers) have the greatest vulnerability to climate change-induced effects. This matches the results obtained in the two previous methods of analysis reported in this section of the report. In contrast, Botteri’s sparrow is relatively invulnerable to the climate change scenarios investigated. Given its habitat preferences, it may well benefit as xeric desert-like habitats replace the riparian gallery forest. Willow flycatcher may also benefit from the climate change-induced vegetation shifts as mesic shrubs replace the gallery forest in the SPRNCA.

4.3.2 The quantitative analysis

In this section we use the vegetation model described in Section 3 and the bird HSI models described above and in Attachment 3 to project changes in the HSI values for three species (yellow-billed cuckoo, willow flycatcher, and Botteri’s sparrow) at three sites in the SPRNCA: Kolbe, Palominas, and Contention (see Section 3 for the rationales for selecting these three study sites). Using the vegetation model and the variables from the three HSI models we ran the former to project changes in the latter until 2102 and under three climate change scenarios: no

change, warmer, warmer and drier, and warmer and wetter. It should be noted that this analysis is continuing and the results presented below should be considered interim. Future runs of the model will include two more HSI species (yellow and Wilson's warblers) and additional model simulations. Nevertheless, we believe that the results reported below are important in that they provide at least a strong indication of how the results are emerging. This section of the report will be revised as additional results become available.

Methods – merging the vegetation and HSI models

Some of the variables from the HSI models could not be included in the vegetation model without some modification. These changes are listed below:

Willow Flycatcher

V1 – Area and Degree of Isolation of Riparian Shrub Patch

Since the vegetation model results were expressed as lateral transects at the study sites it was not possible to estimate patch length. Thus we estimated patch area using the patch width output from the model and by assuming that the patch length was a fixed 100 meters.

V4 – Shrub foliage density at 3-5 m

The vegetation model continuous results were converted to the rankings used in the HSI models by assuming the following relationships:

>80% = Very Dense

>60% = Dense

>20% = Moderately Dense

<20% = Sparse

V5 – Average shrub canopy height within 20 m

The vegetation models output was converted by dividing shrub cover up into different height layers (0-1, 1-2, ..., 6-9.9 meters), the midpoint of the layer that had the greatest cover was assigned as the average shrub canopy height.

V8 – Degree of soil waterlogging

The depth to groundwater output of the vegetation model was converted to variables compatible with the HSI model by assuming the following relationships:

<0.25 m – saturated

0.25-0.5 m – wet

0.5-1.0 m – generally damp

>1 m – completely dry

Yellow-billed Cuckoo

V1 – Linear Continuity of Habitat

This variable could not be estimated using the vegetation model. It was, therefore, excluded from the analysis.

V4 – Average shrub canopy height within 50 m

The vegetation models output was converted by dividing shrub cover up into different height layers (0-1, 1-2, ..., 6-9.9 meters), the midpoint of the layer that had the greatest cover was assigned as the average shrub canopy height.

V8 – % Dominance of salt cedar and mesquite in shrub canopy

Calculated in the vegetation model as the total amount of cover for mesquite + saltcedar in the shrub + tree layers (although both were typically < 10 m tall).

Botteri's Sparrow

V1 – Major Community Type

This was calculated in the vegetation model by assigning suitability metrics based on patch type, with sacaton grassland the best (1), forbland next (0.6), mixed open habitats next (0.2), shrublands next (0.05), and woodlands and forests assigned a score of 0.

V2 – Sacaton Dominance

Calculated as the modeled % cover of live sacaton in the patch.

V3 – Mean Height of Sacaton

This variable could not be estimated using the vegetation model and was, therefore, excluded from the analysis.

V4 – Density of Sacaton

Estimated in the vegetation model by summing the the total live cover and dead cover of herbaceous plants (not just sacaton), using the following cutoffs:

>80% cover = very dense

>=50% cover = dense

<50% cover = sparse

While some of the output from the vegetation model could not be included in the HSI models without some modification of the HSI variables, and while a small number of HSI variables had to be excluded because they could not be accommodated in the vegetation model, we believe that the results reported below are not substantially affected.

Results

In general, the projected changes in HSI scores for each of the three study species follow the trends identified in the EPA and San Pedro Vulnerability frameworks. That is that the species that is most dependent on the cottonwood/willow gallery forest, yellow-billed cuckoo, shows the most marked projected decreases in HSI scores (Figures 4-3 through 4-5). This is most apparent in the only one of the study sites (Palominas) that currently supports relatively high quality cuckoo habitat (Figure 4-5). In contrast, and as projected by both the EPA and the San Pedro Vulnerability Frameworks, Botteri's sparrow habitat may increase in quality over the next century, especially at Kolbe and Palominas (Figures 4-9 through 4-11). The results for willow flycatcher (Figures 4-6 through 4-8) are intermediate in that no clear increasing or decreasing trends are evident. This is consistent with the results of the two framework analyses where this species, due to its independence from forested habitats but reliance on scrub habitats, could potentially benefit from the future scenarios.

It is interesting to note that even without incorporating climate change into future conditions (the no change scenario) marked changes in habitat quality are projected for the yellow-billed cuckoo and the Botteri's sparrow. This is because under the no change scenario, the existing cottonwood/willow forest will senesce and begin to contract about the middle of this century. This will result in a decrease in habitat for the cuckoo, but an increase in Botteri's sparrow habitat as the forest is replaced with grasslands and shrublands.

The other interesting point to note is the high degree of variability within species and scenarios. Much of this is due to the stochasticity introduced into the future projections by fire. Thus, while climate change will be a driver of future change in the habitat availability and quality for the three study species, it is likely that fire (either mediated through a changing climate or independently) and natural successional processes may be equally important in determining the future vegetative and wildlife habitat landscapes of the area.

The results reported thus far should be considered preliminary. Future runs of the vegetation and HSI models will include additional bird species (yellow and Wilson's warbler), increased model simulations, and simulations intended to explore the relative importance of the drivers (particularly climate change and fire) in determining future ecosystem conditions. Also, it was our original intent to include groundwater hydrology variables in our vegetation modeling. This has not yet proven possible due to unforeseen difficulties (see Attachment 4). However, it is our intent to include such variables in future runs.

Figure 4-3. Yellow-billed Cuckoo HSI Scores at Kolbe

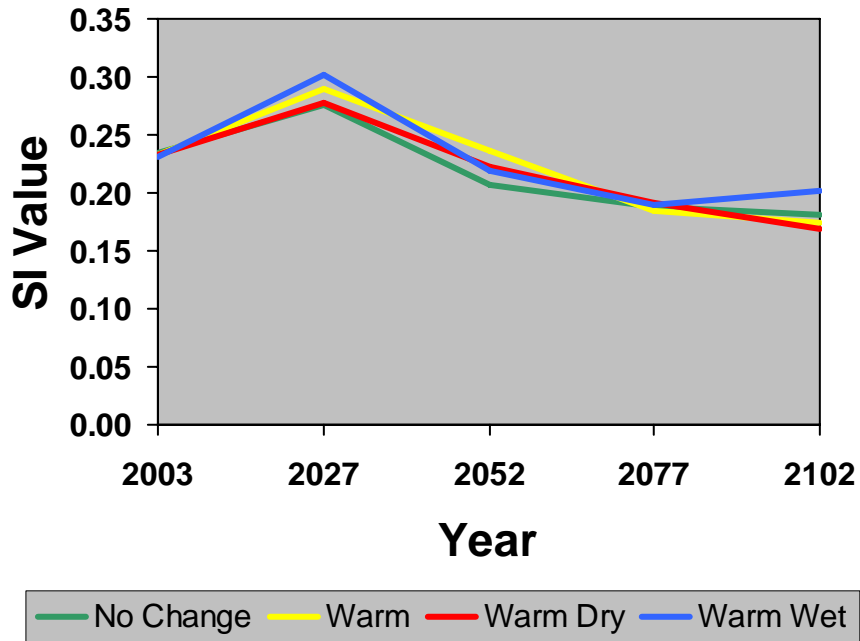


Figure 4-4. Yellow-billed Cuckoo HSI scores at Contention

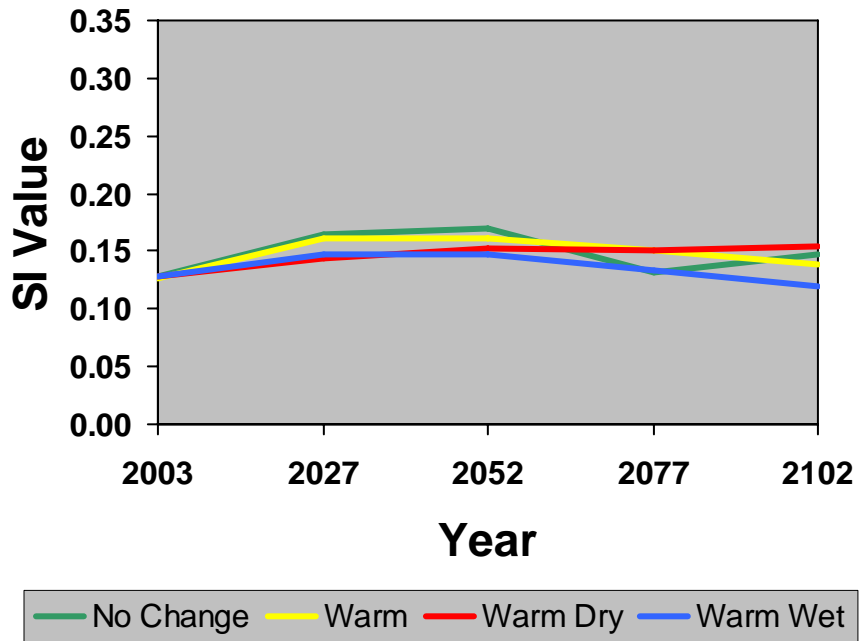


Figure 4-5. Yellow-billed Cuckoo HSI Scores at Palominas

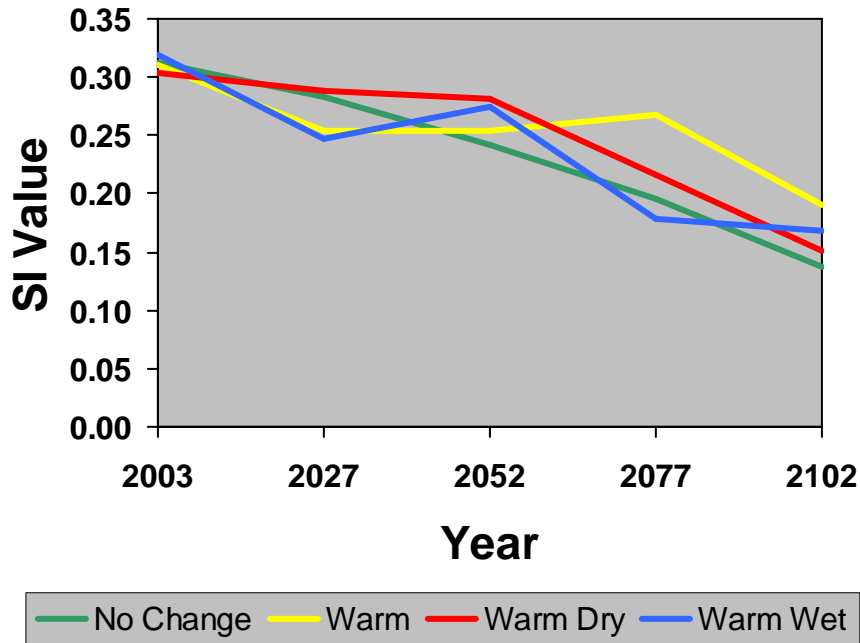


Figure 4-6. Willow Flycatcher HSI Scores at Kolbe

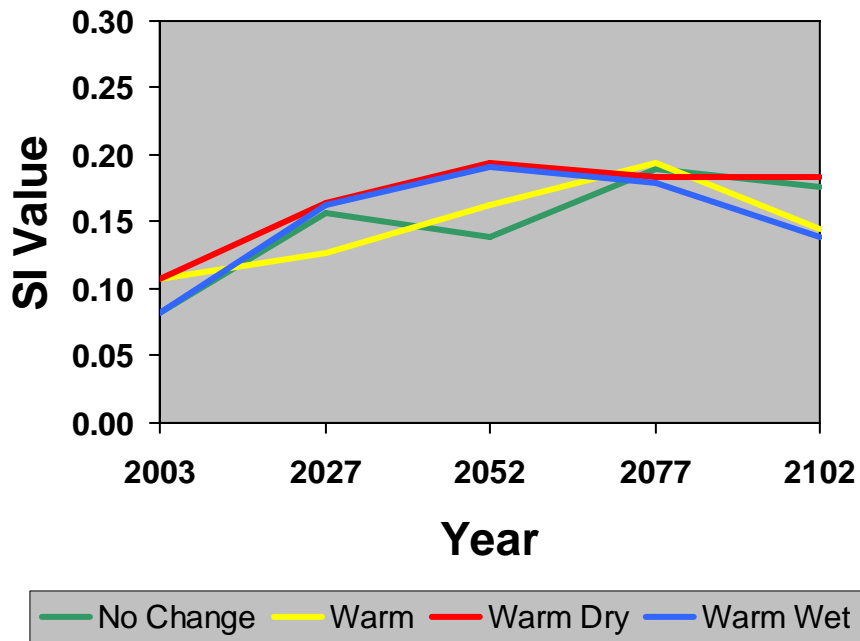


Figure 4-7. Willow Flycatcher HSI Scores at Contention

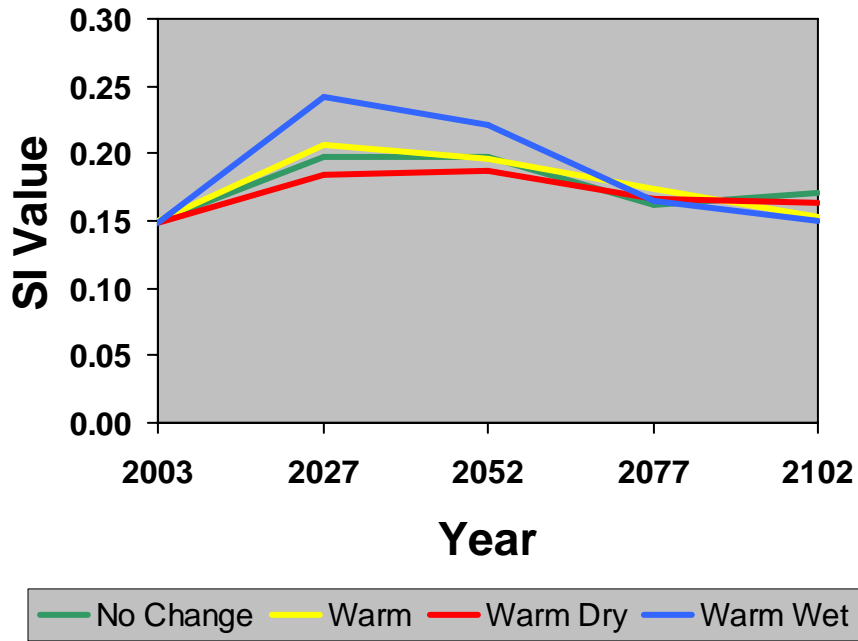


Figure 4-8. Willow Flycatcher HSI Scores at Palominas

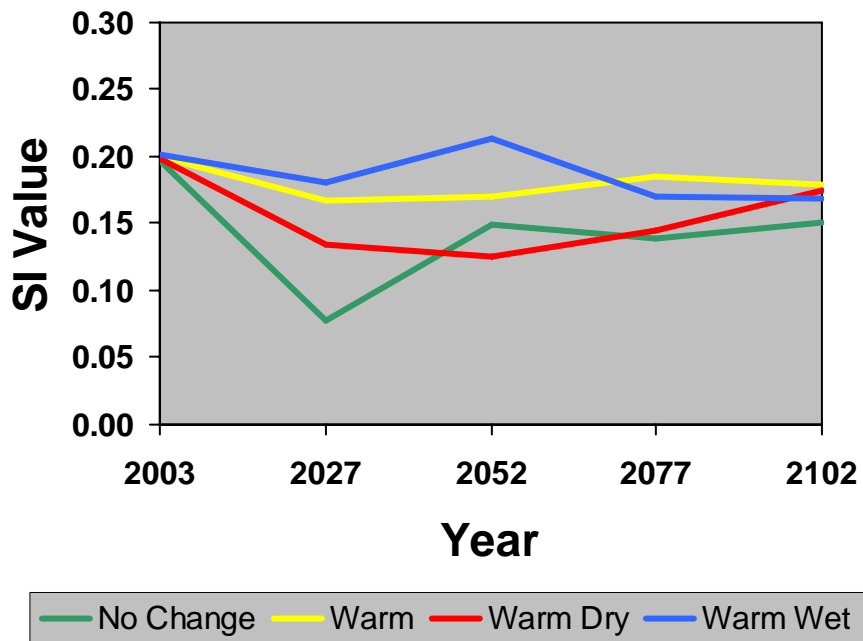


Figure 4-9. Botteri's sparrow at Kolbe

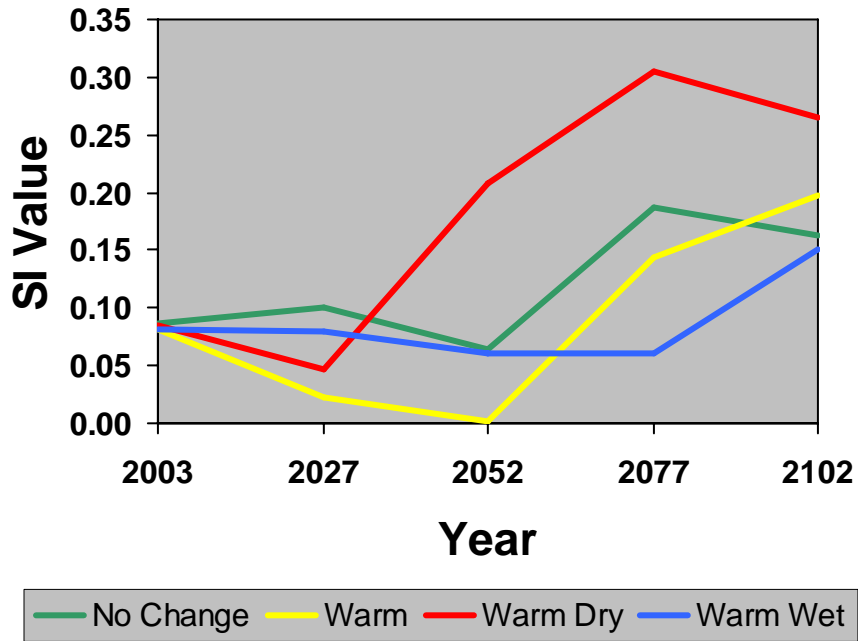


Figure 4-10. Botteri's sparrow at Contention

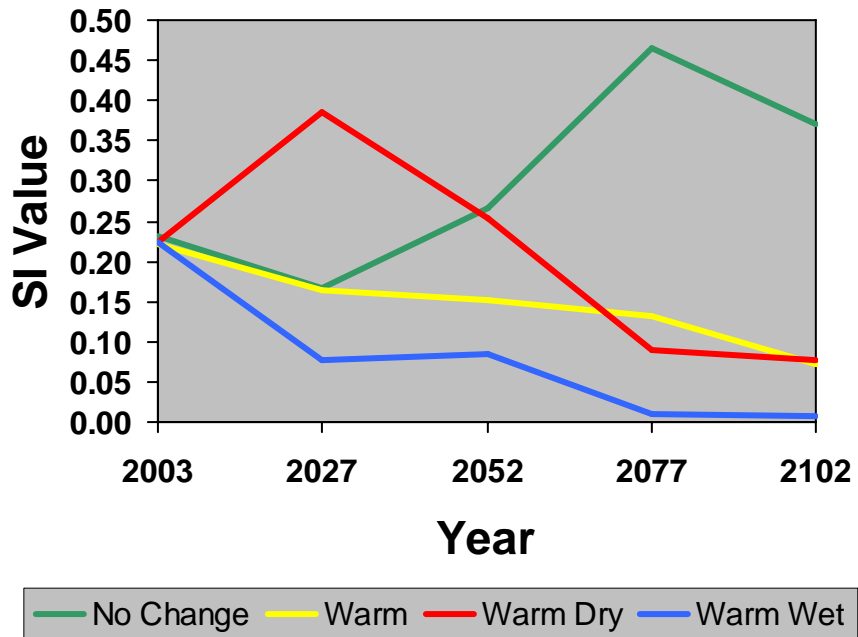
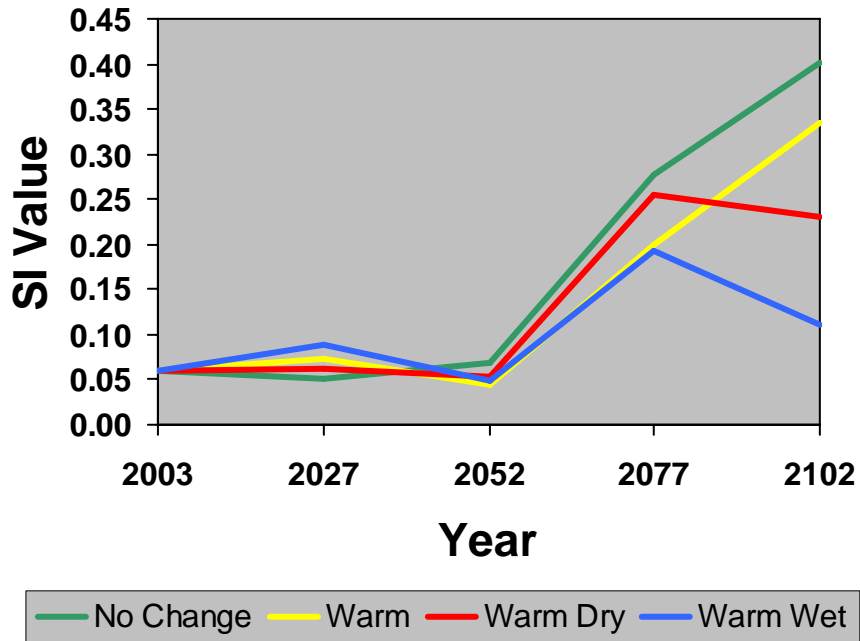


Figure 4-11. Botteri's sparrow at Palominas



4.4 Avian Bioenergetics as a Potentially Limiting Factor

Because of its location, the San Pedro is a corridor oasis within a harsh desert environment. The riparian zone along the river acts as one of the main “funnels” through which many Neotropical songbirds migrating along the Pacific flyway. This river valley is an important stopover site for the migrating birds to replenish their energy stores on their travel between their North American breeding grounds and their Central or South American wintering grounds.

A stopover site is defined as “...an area with the combination of resources (like food, cover, water) and environmental conditions (temperature, precipitation, presence and absence of predators and competitors) that promotes occupancy by individuals of a given species (or population) and allows those individuals to survive ...” (Morrison et al., 1992) during their journey. The importance of this habitat has unfortunately not been central to many conservation efforts, and thus many important stopover sites or “migrant traps”, have been unduly degraded. Additionally, the ecology at stopover sites has largely gone unstudied until rather recently.

Migration is a highly risky endeavor. Besides the expense and risk of the travel itself, each migrant must contend with finding appropriate habitat, even when there are unfavorable winds and weather. Usually they must find the stopover habitat at night, because almost all Neotropical migrants begin migration after sunset and stop before dawn, and often times before midnight. Indeed, the peak migration time for these songbirds is around 10:00 at night (Moore et al. 1995). Actually, at dawn migrants often will shift to a better, close-by habitat that has the ability to better meet their energetic needs (Moore et al. 1995).

Critical to successful migration is a stopover area where migrants can rest and replenish depleted stores of fat (Moore et al. 1995). Enough resources, in the form of insect prey, are needed to provide nutrients and energy for their existence and to allow fat to be stored for the next leg of the migratory journey. If the resources are not available in high enough abundance, then the margin of safety is lessened for the migrants at the stopover location and on the next leg of their journey. Hence, their physical condition could be damaged if they encounter bad weather, unexpected predators, lack of food at the next stopover site, or competitors who have more energy to out compete them for a necessary resource. They might not have the reserves to endure these maladies unscathed. Compromising their physical condition could manifest itself, for example, by losing territorial battles or by not attracting as dominant a mate as possible. Indeed, in the extreme case individuals could die. Hence, having the resources available at stopover sites to replenish depleted fat stores is critical to the overall fitness of the migrants. Even arriving late at the next stopover site could mean that resources there are depleted, which could mean that time spent searching for food would be increased. Thus, fat stores could again take longer to replenish, making arrival at the breeding grounds that much later, or they may not be able to be completely replenished and thereby continue to decrease the fitness of the migrants. This, in turn, could decrease the population abundance of migrant species.

The problem at hand is the concern that humans may be causing a drop in the water table, which in turn could easily result in the destruction of the riparian gallery forest (Arias 2000). There are three goals that need to be addressed for my portion of the San Pedro Project:

To assess the importance of the San Pedro National Conservation Area (SPRNCA), which includes the riparian habitat along the river from around the Mexican border north to near David City, as a stopover site for Neotropical migrant birds, many of which are already showing signs of population declines (Terborgh 1989),

To determine approximately the amount of nutrients (e.g., insects) needed to replenish the stored fat required to fuel the existence of the migrants while visiting the SPRNCA and the next leg of their migratory trips, and

To attempt to determine the minimum amount of habitat needed to provide the necessary number of insects to sustain a healthy population of migrants while visiting and when ready to impart on the next stage of their migratory journey.

4.4.1 Migratory Bird Use of the SPRNCA

To attain the first goal data are needed that indicate the species, along with their abundances, use of the San Pedro River Valley as a stopover site for migration. Data on the presences and relative abundances of birds using the SPRNCA, many of them migrants, were found and obtained. Only three years of these data (1999-2001) were found to be available. These included two different types of banding data. First are the data from the banding project taking place in the SPRNCA itself. These data began being collected in 1998, but were not consistently computerized until 1999. Therefore, we currently have data for 1999, 2000 and part of 2001. The second type of banding data is for the same three-year period from the USGS Bird Banding Lab (BBL) in Maryland. These data were collected from the US-Mexico border at 31.33° to the area around Escalante, Arizona, which is at 31.83° N Latitude and at the northern edge of the SPRNCA. Longitudinally the area brackets the river from 110° W Longitude, which is about 2.5 miles east of Tombstone, Arizona, to the west gate of Fort Huachuca, which is at 110.33° W Longitude.

These two sets of data provide information on 105 species, of which 12 are hummingbirds caught for a special project looking at their movements along the San Pedro River Valley. Given that most banding efforts use mesh sizes that are too big to effectively catch hummingbirds (Pardieck and Waide 1992), having these data are quite remarkable and valuable. A search of the literature found lists of riparian species for the San Pedro Valley or the neighboring Rio Grande Valley. The following studies investigated birds along the San Pedro River system: Skagen and co-authors (1998) recorded a total of 186 species and Krueper and co-authors (2003) provided a list of 61 species that are either showing declining or increasing populations. Hanson (2001) provides the checklist of the 370 species that use the SPRNCA—ranging from Canada Geese to Rufous Hummingbirds.

In this checklist the summer and winter residence along with the spring/fall migrants are denoted. Wang and Finch (2002) recorded 197 species in the Rio Grande Valley. Table 4-17 lists all of these species along with their sources. All three of these studies (not the checklist in Hanson's publication) used censusing and mist netting as means of identifying the species in the riparian forests. Consequently, these species lists contain species that are rarely captured in mist nets due to mesh size of the nets used (Pardieck and Waide 1992), the habits of the birds (e.g.,

aerial feeders, such as swallows, are rarely caught in mist nets), or both (e.g., large ground or aerial birds, such as Greater Roadrunner and Red-tailed Hawk). Table 4-17 provides abundance values for those species with data obtained from SPRNCA and BBL data. Abundance values are not available from the other studies. The checklist that Hanson (2001) provides does include a categorization of common, uncommon and rare for the various species. Even after extensive searching these are the only data that we could obtain. Therefore, the data available for this analysis are unfortunately quite sparse.

The number of birds reported in the SPRNCA and BBL data sets provide approximately the same representation of the underlying population. This can be seen in Figure 4-12, which plots the SPRNCA data on the X-axis and the BBL data on the Y-axis. The correlation coefficient between the two data sets is 0.74 with a $p < 0.001$. This is true even when the hummingbird data are included. The slope of the association is less than 1.0, which is expected, given that the SPRNCA data are much sparser than the BBL data.

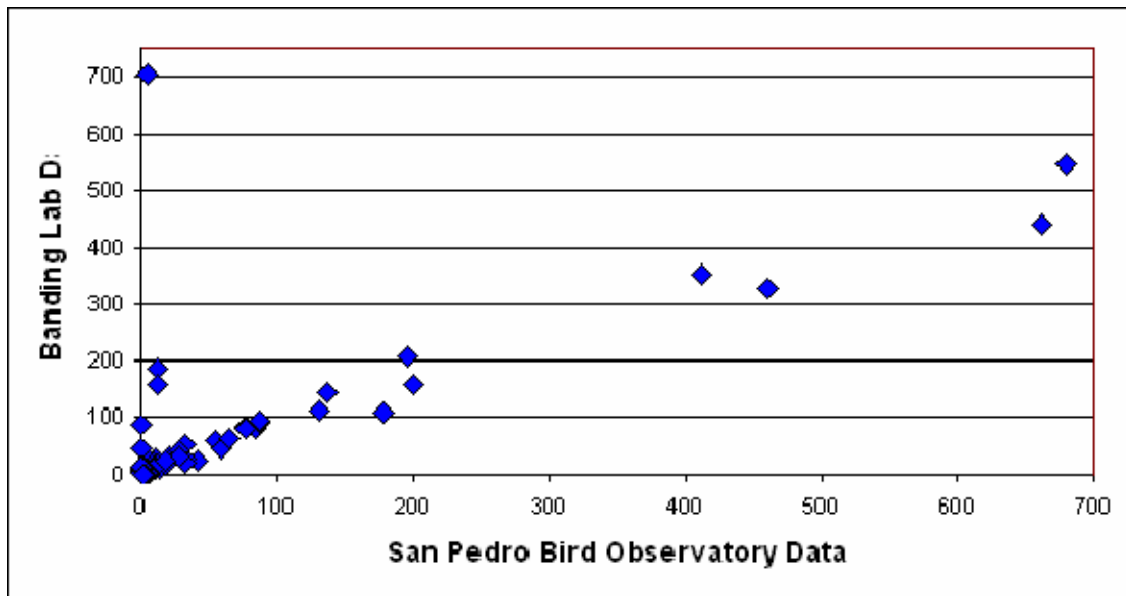


Figure 4-12: Relationship between the SPRNCA and BBL data. The correlation coefficient between the two data sets is 0.74 with a p value of < 0.001 .

The number of species for a given numbers of individuals is shown in Figure 4-13a & b. Due to the large size of the number of individuals we actually plotted the values of the log to the base 10 of these numbers. Figure 4-13a is for the SPRNCA data and 4-13b is for the BBL data. The shapes of both curves are the same, as expected.

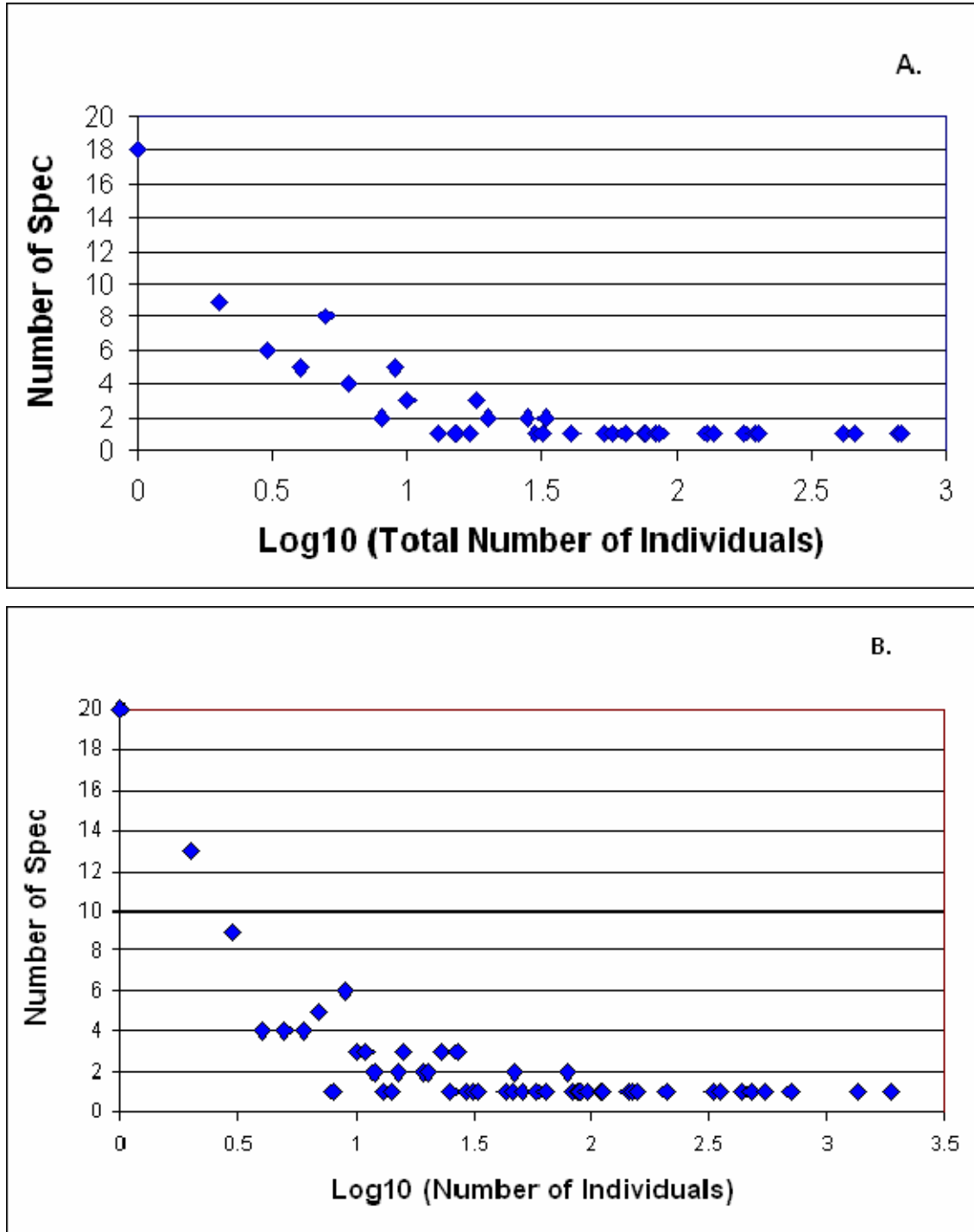


Figure 4-13. Phase plane of Log (total number of individuals) by species for SPRNCA (A.) and BBL (B.) data.

Figure 4-14a and b break down the data in Figure 4-13 by species and by year. The actual names of the species have been left off for clarity, but can be found on the legend of the Y-axis of figures 4-15 and 4-16. Both figures provide a histogram of the number of individuals per species

of birds by year, with Figure 4-15 plotting SPRNCA data and Figure 4-16 the BBL data. The total number of records for the species is also provided.

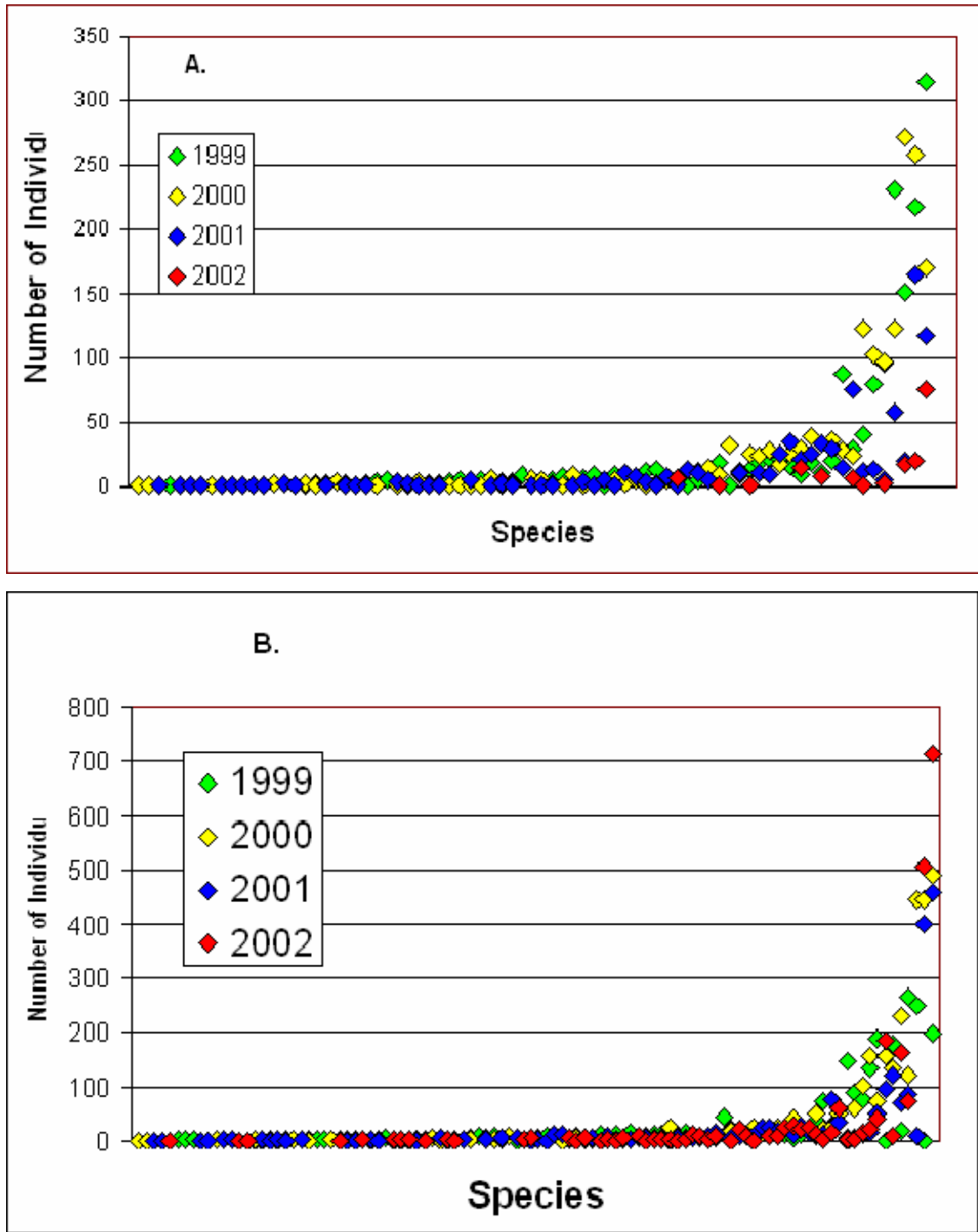


Figure 4-14. A break down by year of the number of individuals in each species in either the SPRNCA (A.) or BBL (B.) data set. These data are broken out with the species names in Figure 4-15 for SPRNCA data and Figure 4-16 for BBL data.

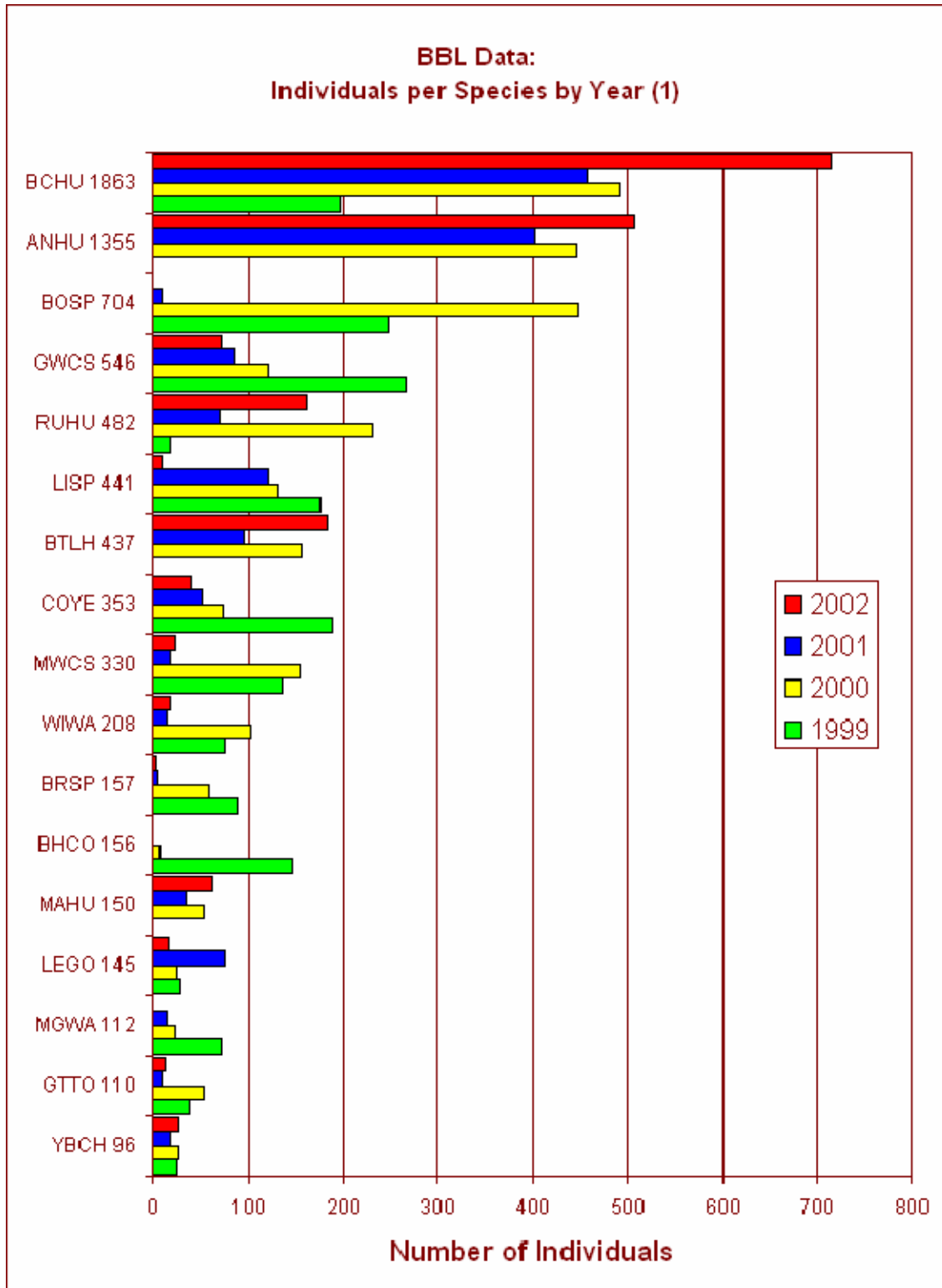


Figure 4-15. The first of 5 plots showing the number of individuals per year for each species recorded in the BBL data set. The species names are given in their standard four-letter code. The number after the code is the total number of species.

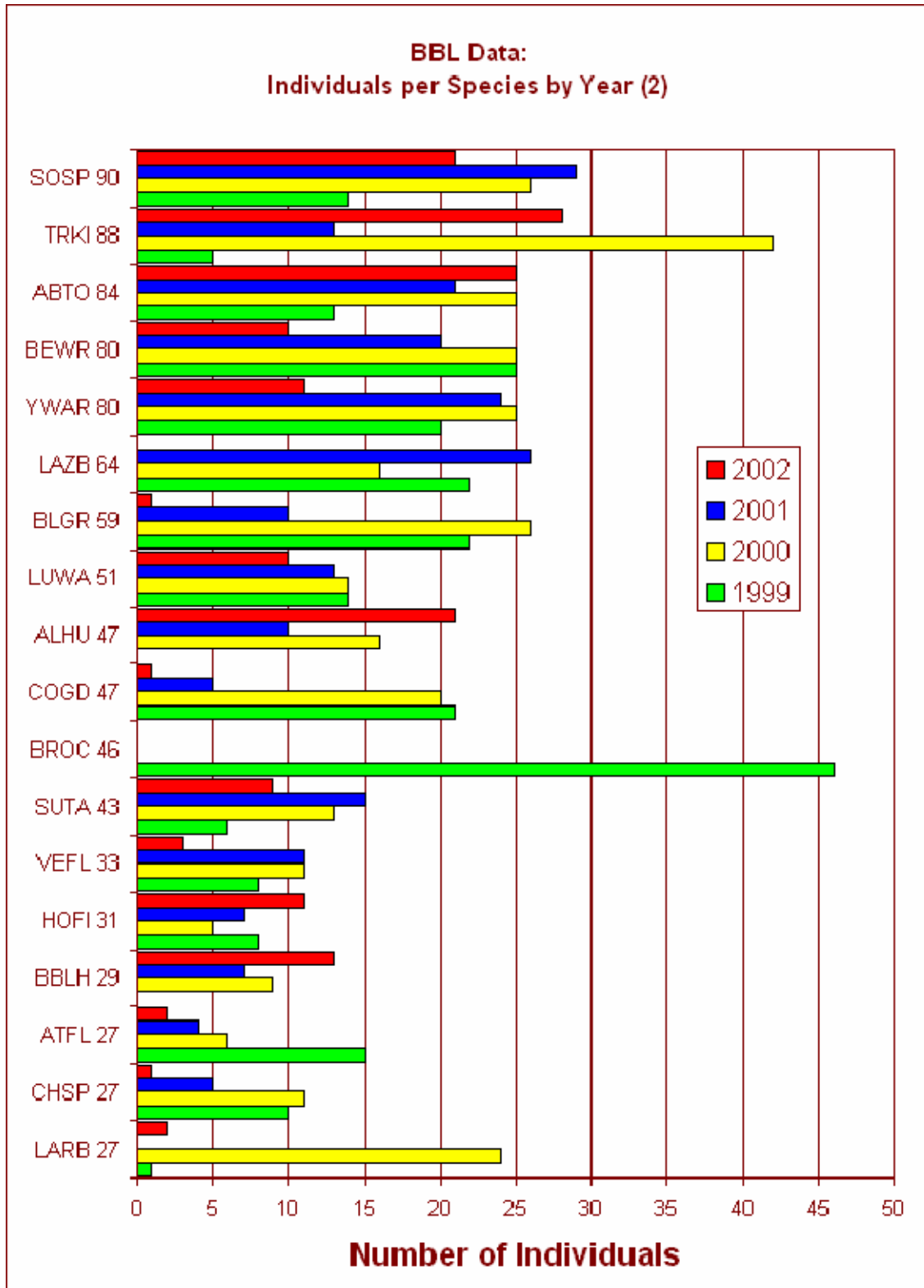


Figure 4-15 continued.

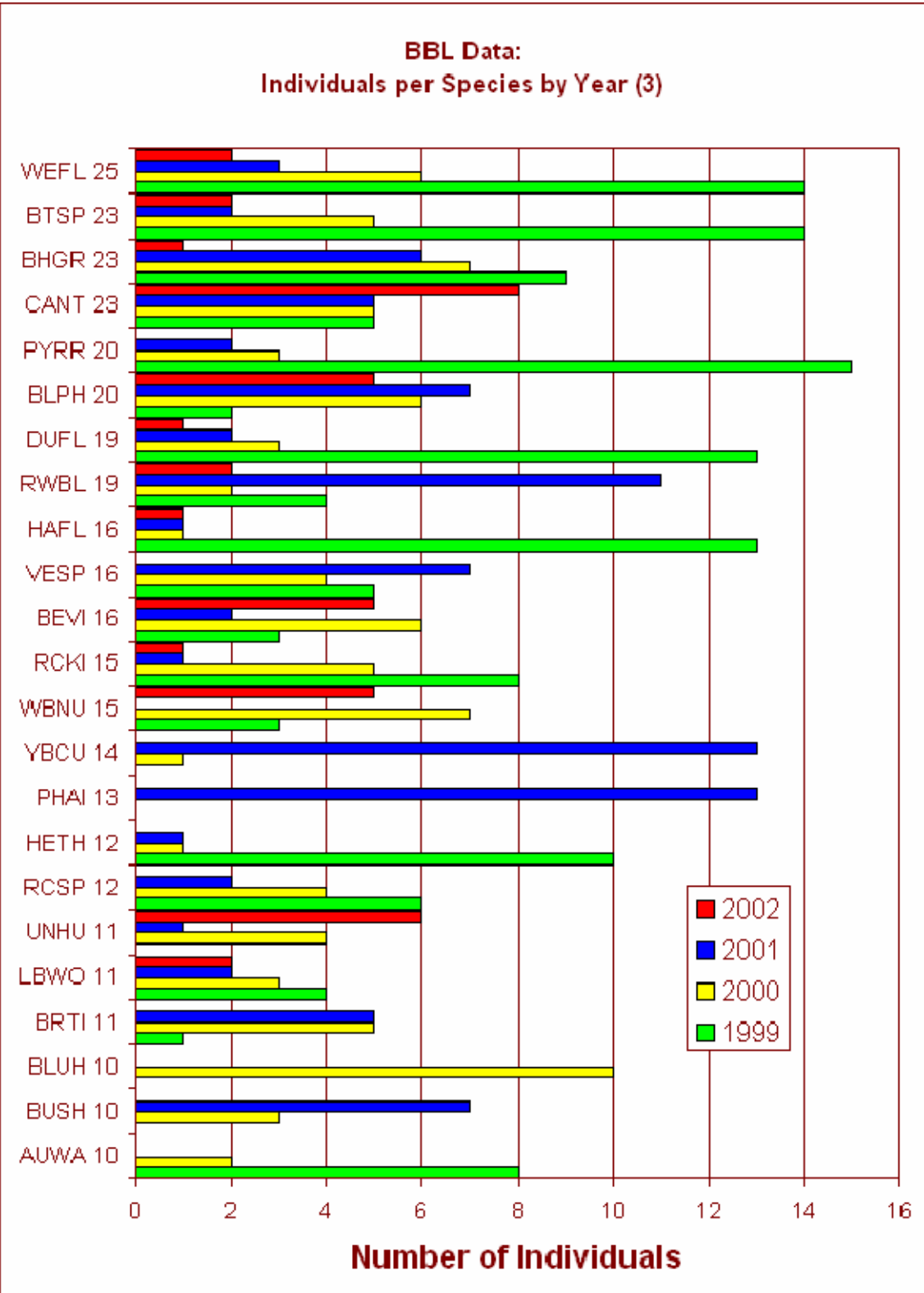


Figure 4-15 continued.

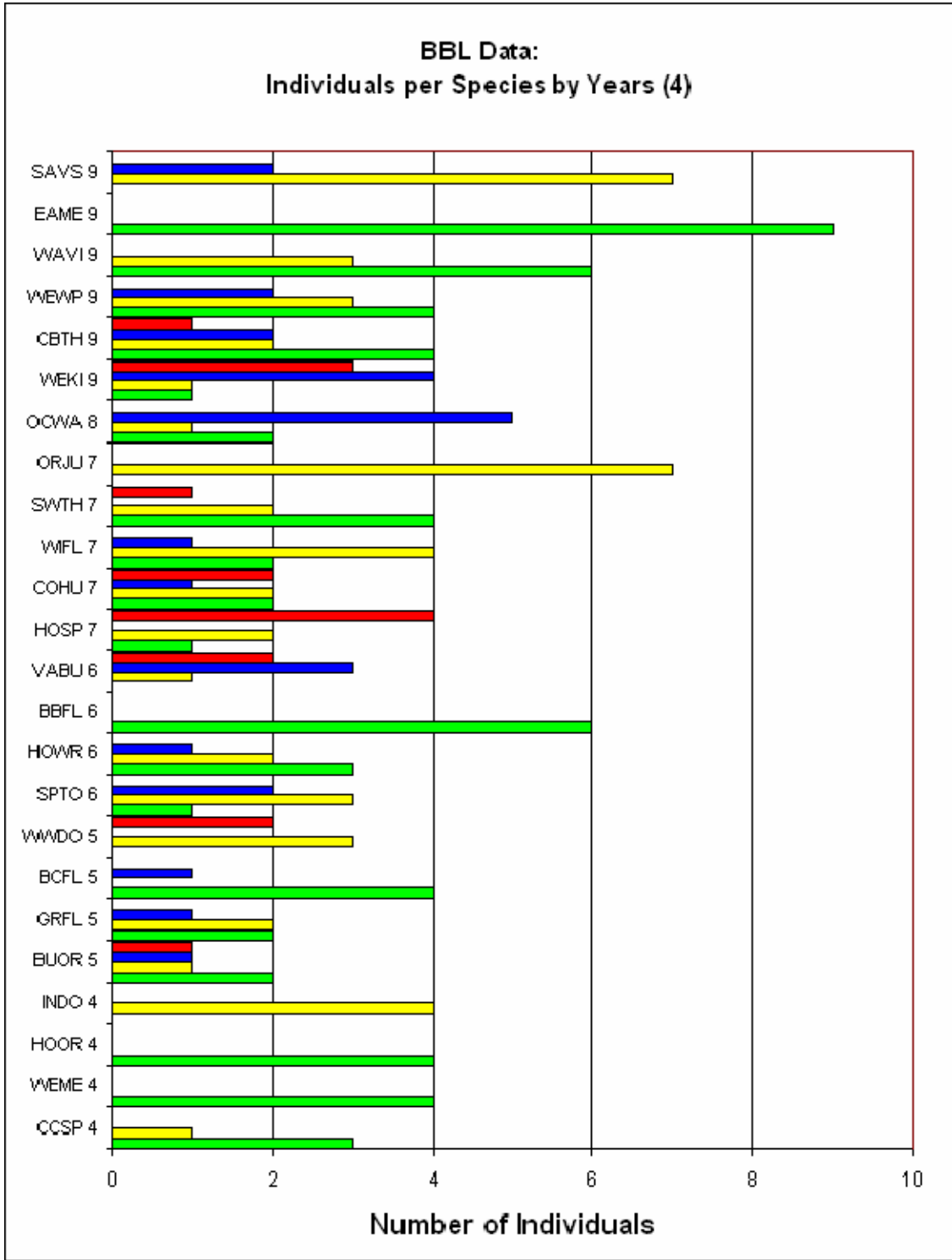


Figure 4-15 continued.

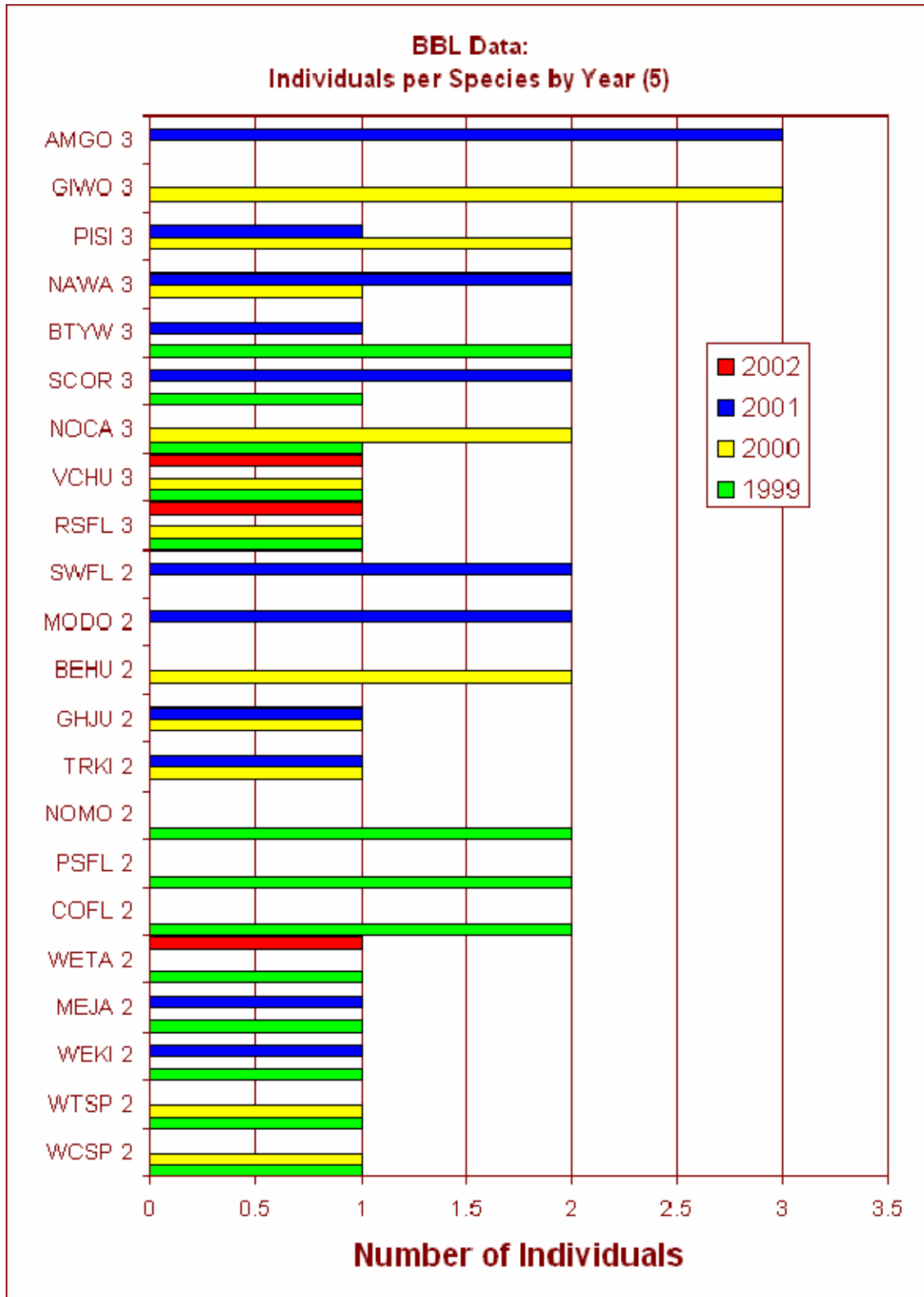


Figure 4-15 continued.

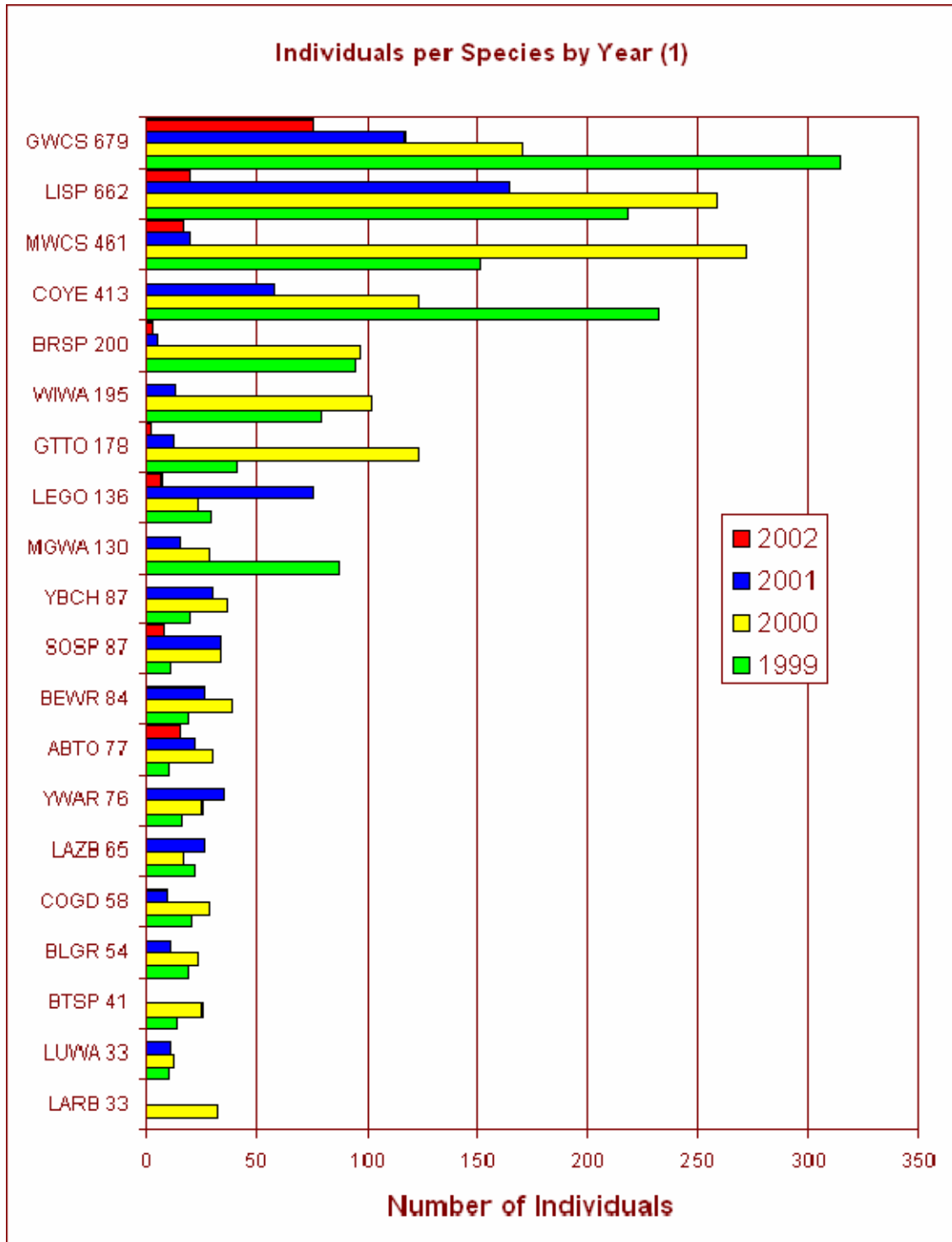


Figure 4-16. The first of 4 plots showing the number of individuals per year for each species recorded in the SPRNCA data set. The species names are given in their standard four-letter code. The number after the code is the total number of species.

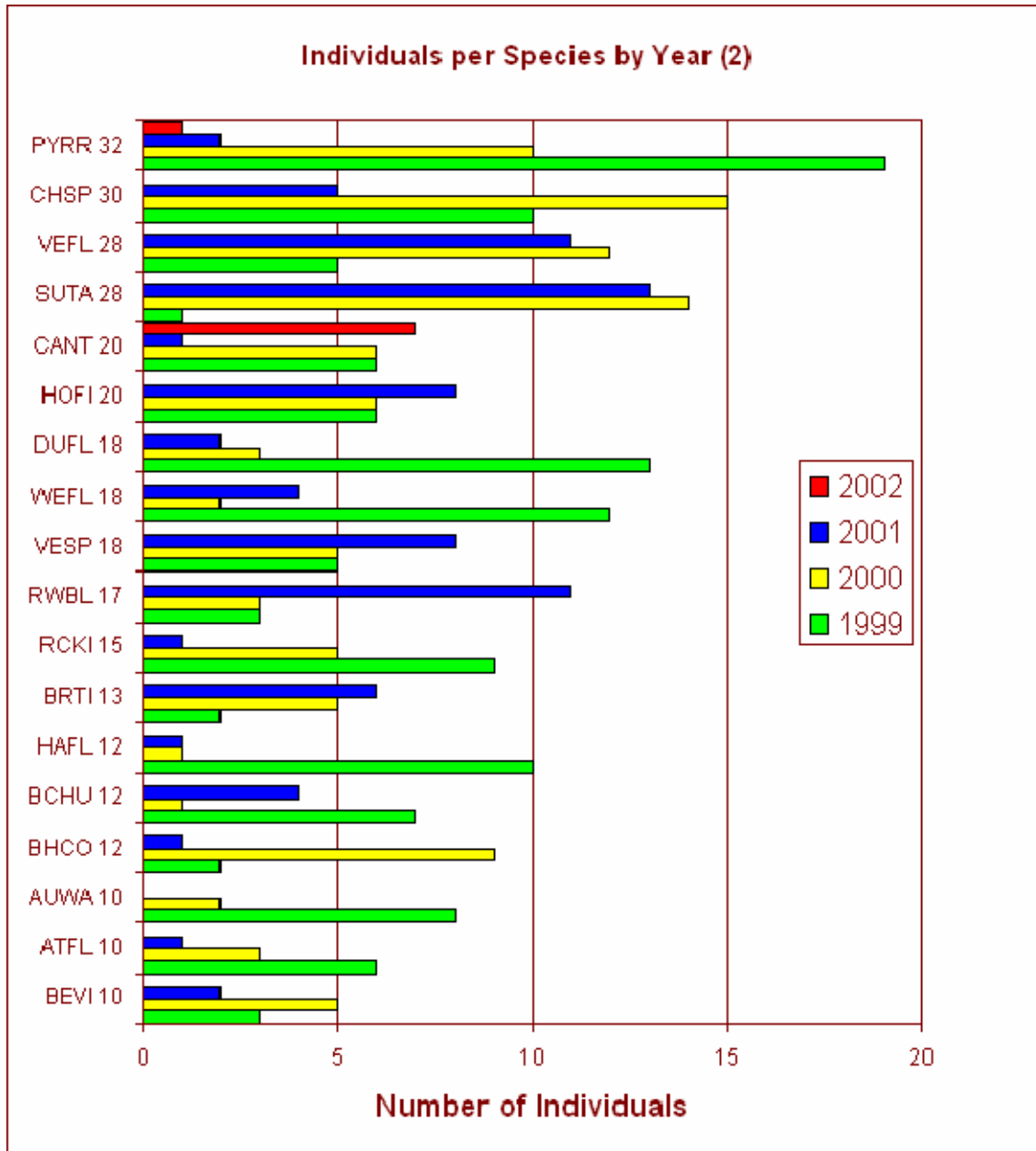


Figure 4-16 continued.

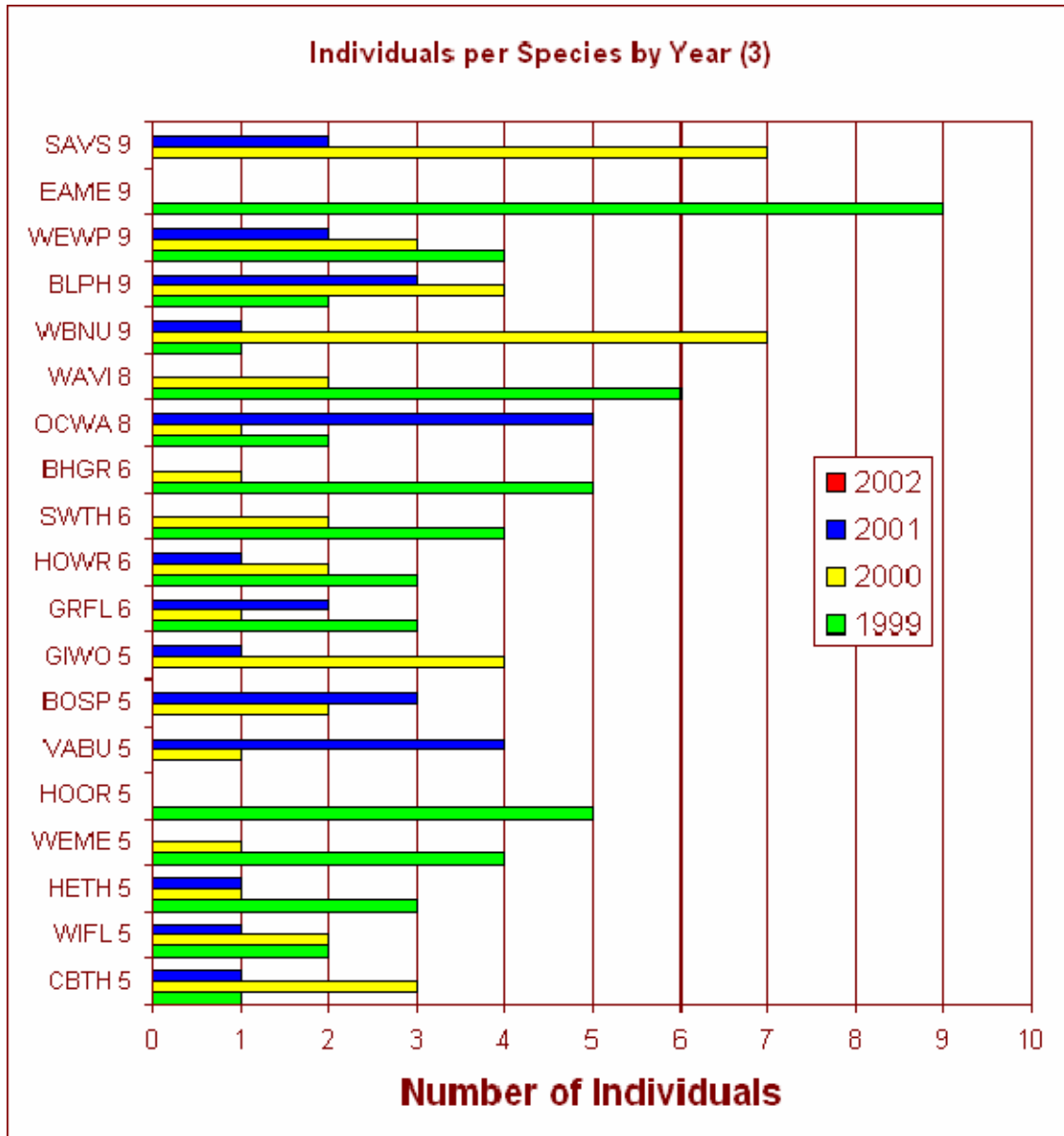


Figure 4-16 continued.

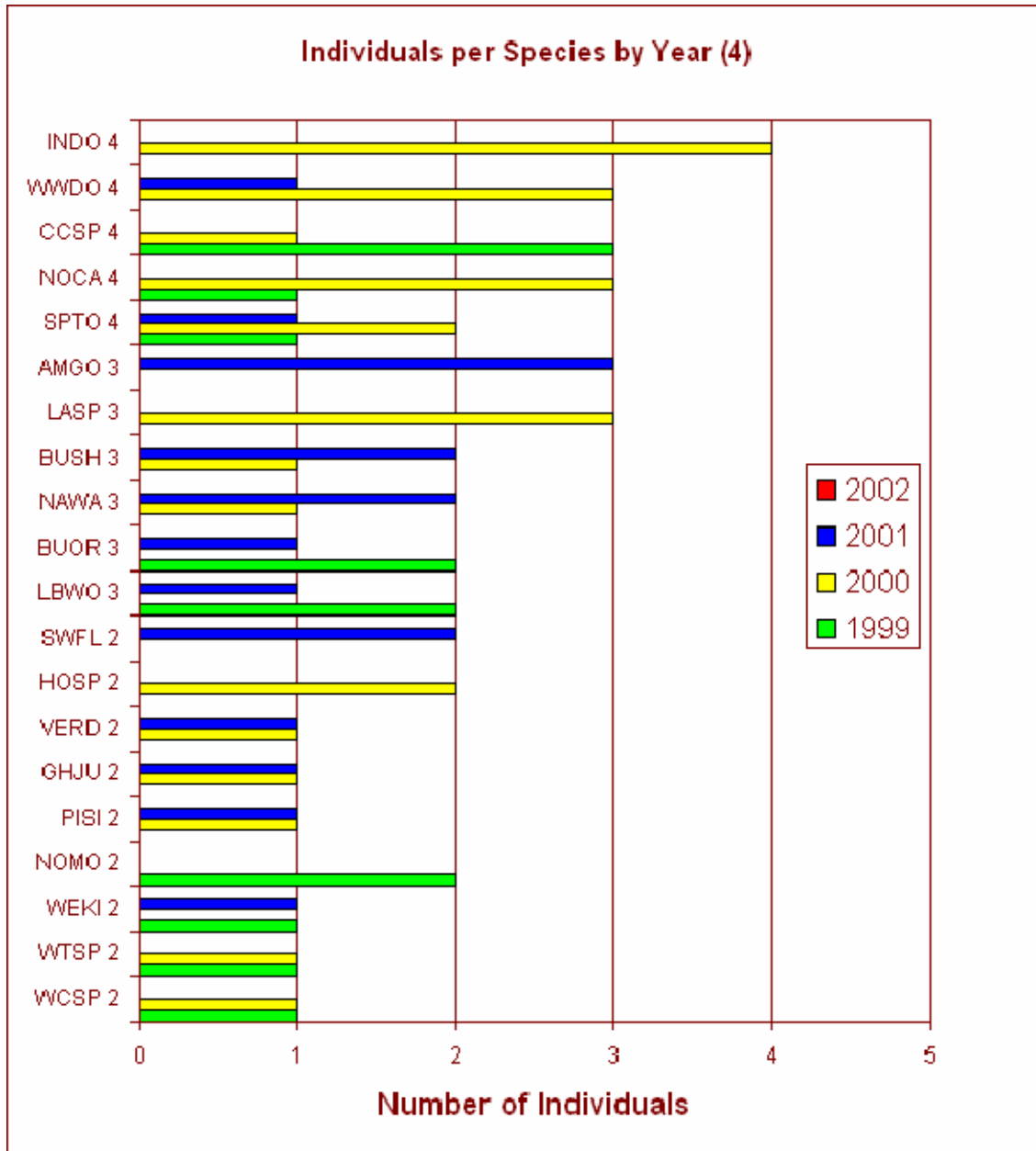


Figure 4-16 continued.

There is a debate in the literature about whether or not banding data can be used to estimate relative abundances of species communities. Scientists at Point Reyes Bird Observatory have shown that these data are a fairly good representation, but Remsen and Good (1996) wrote a theoretical article that showed, via a model, how the following aspects of species affects whether or not individuals are captured in a mist net. These factors include:

The height above the ground at which the bird flies. If it flies very low to the ground (below ~0.5m) or above about 3.5 m, then mist nets typically placed at heights from 0.5m to 3.0m, will not effectively capture species.

Territoriality. Birds that are territorial and thus have a restricted area within which they fly will be captured much less frequently than individuals not holding territories. This affect can be seen in the fact that by using mist netting information, species that forage along a trap line and thus fly around a lot and do not hold territories (e.g., manikins) are captured disproportionately more often than are territorial species.

Mean flight distance. Species with longer mean flight distances, even just 0.5m longer than another, have a higher probability of being captured than those with shorter mean flight distances.

Flight frequency. Species that move around on wing more often than not are more apt to be captured.

Catchability. MacArthur and MacArthur (1974) labeled this as “net avoidance.” This is a “catchall” category that includes situations such as species that are able for whatever reason to avoid mist nets. This could be due to keen eyesight and maneuverability that allow them to fly and avoid the nets. This could also be due to the wrong size of mesh being used to catch species of particular sizes. For example, species 16-25 g are easily caught in nets with mesh sizes of 30 to 36 mm, while birds >50g usually are not.

Be that as it may, it appears that at least at a fairly crude level, these mist-net data from both SPRNCA and BBL do provide the relative abundance distribution of the underlying population. We will return to this issue of whether or not these data presented in figures 4 and 5 are indeed representative of the relative abundance of the underlying population.

Using this combination of data we identified the principle migratory species and their relative abundance in the area. These species are listed in Table 1. We use these species in the next section to calculate the nutrient (i.e. insect biomass) requirements of migratory re-fueling.

It has been estimated that one to four million migrants pass through the SPRNCA annually (Hanson 2003). These include birds of prey, ducks, shorebirds, hummingbirds and songbirds. The majority of migrants, however, are Neotropical migratory songbirds of approximately 60 species. We concentrate our analyses on these species due to their prevalence and the importance of riparian-area-dependent insects to fueling their migratory journeys after crossing the Mexican desert.

To estimate the approximate number of individuals migrating through SPRNCA annually we used the following calculation. From Table 4-17 we know that there are 36 permanent resident species in the SPRNCA and 24 summer residents. For this exercise we assume that most of these species set up breeding territories and that the territories are on average around 150m² in size. The SPRNCA is approximately 2.35x10⁷ m². That means that there could be about 1.57x10⁵ territories within the boundaries of the SPRNCA.

From the checklist in Hanson (2001) we know the relative abundances of the species broken down into three categories: common, uncommon and rare. Common means that in the appropriate habitat a “moderate to large number” of birds occur annually, making them rather

easy to see. Uncommon means that again in proper habitats “small to moderate numbers” of birds occur annually, making them more difficult to find. Rare means that the birds occur “singly or in very small numbers annually or semiannually,” or that these species “breed extremely locally or in very small numbers.” We excluded those species that are extremely rare – irregular sightings of individuals every few years – and irruptive species. While of charismatic importance to bird-watching, these species do not depend on the SPRNCA for their migratory sustenance. For our analysis we defined common as three times as abundant as the rare species and uncommon as two times as abundant.

In the summer undoubtedly all of the area within the boundaries of SPRNCA are not suitable for birds to set up their territories. As a conservative estimate, we assume that only 75% of the habitat is suitable for territories that are 150 m². This could mean that there are areas that are uninhabitable, that there are areas that are not highly productive, or both, and thus require territories that are larger than 150 m². Hence, on average we assume the number of territories are $0.75 \times 1.57 \times 10^5 = 1.18 \times 10^5$. From Table 1 we see that there are a total of 46 common species breeding in the SPRNCA, 10 uncommon ones and 4 rare birds. Taking into account that we assume that the common species (C) are three times the rare (R) ones and uncommon species (U) are 2 times, we obtain the following equation:

$$46(3R) + 10(2R) + 4R = 1.18 \times 10^5$$

Therefore, R = ~750 individuals per species

$$C = \sim 2,300, \text{ and } U = \sim 1,500.$$

We can validate our estimate by looking at the wintering species. Again from Table 4-17 we see that there are a total of 39 common species, 23 uncommon ones and 11 are rare, giving a total of 73 species. These numbers are the combination of the values for the permanent residents (28, 6, 2, respectively) and the winter residents (11, 17, 9, respectively). Owing to the season, we assume *a priori* that 90% of the possible territories can be filled, on average. It is an average, because many of the species do not hold territories in the winter and instead forage in mixed species flocks. But the area covered by the flock can be estimated to be roughly equivalent to the number of territories of the number of species in the flock (e.g., 5 territories for a 5-species flock). Therefore, there is room for 1.41×10^5 territories (or individuals). This results in the following equation:

$$39(3R) + 23(2R) + R = 1.41 \times 10^5.$$

Therefore, R = ~810, which is close to 750!

$$C = \sim 2,440, \text{ which is close to } 2,300, \text{ and}$$

$$U = \sim 1,620, \text{ which is close to } 1,500.$$

To determine how many individuals migrates annually through SPRNCA we first need to know roughly how much room is left once the permanent residence are taken into account. The number of individual permanent residents is

$$28(2,350) + 6(1,550) + 2(775) = 7.67 \times 10^4.$$

This leaves room for $1.57 \times 10^5 - 7.67 \times 10^4 = 8.04 \times 10^4$ individuals, if we assume that an individual needs about the same amount of habitat that would be encompassed in a territory.

During peak migration time we can assume that 100% of the habitat is filled. While we do not have direct information on the migration time periods for these species' in the SPRNCA, we can

gain insight from research in surrounding areas. Wang and Finch (1997) assessed population trends of migrants along the middle Rio Grande watershed from 1980-1994. The Rio Grande and its associated riparian areas (similar to those of the SPRNCA) funnel migratory birds from a broad range of southern wintering habitat to a large geographic range of breeding grounds to the north. Thus, this southwestern “bottleneck” of riparian stopovers is critical to bird populations across North America and can be used to gauge broad population trends.

The migration window on the Rio Grande is from around the week of April 10 to around the week of June 11 (Wang and Finch 1998). If we assume that the individuals exhibit a normal distribution with the peak migration time, thus, being the week of May 9, then weeks 1 and 2 would each have 5% of the individuals pass through, week 3 10%, week 4 20%, week 5 40%, week 6 20%, week 7 10% and weeks 8 and 9 5% each. But week 5 the habitat is saturated with 8.04×10^4 individuals.

We know from Wang and Finch (1998) that migrants stay an average of around 2.3 days at a stopover site. Consequently, each week can be seen as having 3 distinct waves of migrants. The total number of spring migrants can then be calculated in the following manner:

$$\text{Week 5: } 3(8.04 \times 10^4) = 2.41 \times 10^5,$$

$$\text{Weeks 4 and 6: } 2(0.5(3(8.04 \times 10^4)) = 2.41 \times 10^5,$$

$$\text{Weeks 3 and 7: } 2(0.25(3(8.04 \times 10^4)) = 1.21 \times 10^5,$$

$$\text{Weeks 1, 2, 8 and 9: } 4(0.125(3(8.04 \times 10^4)) = 1.21 \times 10^5.$$

This results in finding that approximately 7.25×10^5 individuals use the SPRNCA as a stopover site on their migration from the wintering ground to their breeding sites. So we can say about 0.75×10^6 .

The fall migration period is from the week of August 7 to the week of October 5, again 9 weeks long (Wang and Finch 1998). Given the same assumptions as those in the spring, the number of individuals migrating through in the autumn is 0.75×10^6 . Therefore, annually the best guess as to how many individuals use the SPRNCA as a stopover site on migration either to or from their breeding sites is $\sim 1.5 \times 10^6$, and we should probably say that the actual number will be $\pm 0.5 \times 10^6$. Therefore, the answer to the first goal of this project is that the SPRNCA is vastly important to between 1×10^6 and 2×10^6 individual migrants annually.

Research indicates that the quality, though not necessarily the spatial extent, of local riparian habitat is important for species abundance. An assessment of the use of migratory corridors and oases along the San Pedro River concluded that all riparian patches in southeastern Arizona were important as stopover sites for migrants, regardless of size or connection to other patches (Skagen et al. 1998). Another study determined that local increases in habitat quality can create local increases in the abundance of birds despite declining regional trends (Krueper et al. 2003). While this particular research emphasized breeding habitat, the conclusions might be equally relevant to migratory habitat.

The fuel deposition rate at a stopover site is a critical factor in the determining the speed and success of migration (Schaub and Jenni 2000). We also note the importance of water to the migrants as recent studies have shown that dehydration can also be a significant limiting factor for migrants (Leberg et al. 1996). Consequently, good quality habitat for foraging and shelter

benefits birds both locally and beyond if that habitat is located on a migratory route. In the next section, we demonstrate the importance of the San Pedro riparian areas as migrant stopover sites and insect-fuel sources, extending the previous findings on their importance for breeding (i.e. Krueper et al. 2003).

The conclusions of these regional studies are supported by the widespread recognition of the importance of stopover habitat to migrants (e.g., Terborgh 1989; Weber et al. 1999). Riparian areas, as potentially high quality stopover sites, are important to migratory birds in the desert Southwest. Several bird species, including Yellow Warblers, Wilson's Warblers, and Yellow-rumped Warblers, are found in the SPRNCA at migration densities far exceeding those of their breeding populations (Skagen et al. 1998). This indicates that the San Pedro watershed is serving birds that breed far beyond its boundaries. Furthermore, the significance of the San Pedro River is amplified by the scarcity of habitat that it provides: the majority of riparian areas throughout the Southwestern US have been converted to other uses or diminished in quality due to particular land management practices, e.g. cattle grazing, draw-down of water from irrigation (Steintz et al. 2003). As the last free-flowing river in the region, we conclude that the San Pedro is likely to be one of most important riparian stopover sites in the region for the $1-2 \times 10^6$ migrating individuals comprised of several dozen species of migratory birds.

4.4.2 Determining Avian Energetic Needs

To determine approximately the amount of nutrients (e.g., insects) needed to replenish the stored fat required to fuel the existence of the migrants while visiting the SPRNCA and the next leg of their migratory trips, we assume the value of 1.5 million individuals using the SPRNCA annually as a stopover site. Willow Flycatchers at a stopover site on the Middle Rio Grande gained an average of 1.6%/day in body mass (Yong and Finch 1997). Indeed, migratory birds are capable of extraordinary insect consumption and fuel deposition rates during migratory periods; several studies estimate that net daily mass gains of greater than 10% lean body mass are not only possible, but commonplace (Bairlein 1990; Kvist and Ake 2003). The daily rates, however, are subject to allometric constraints (Klaassen 1996). Taking this into consideration, we sorted species into three categories according to their mass and energetic requirements. Group 1 includes the hummingbirds; group 2 includes species with a mass of 10-25g; and group 3 includes species with a mass of 25-40g. We assigned each group a mean daily insect mass consumption based upon the literature.

Bird energy requirements. The energy requirements of hummingbirds are high relative to their body weight. While nectar is a major component of their diet, insects are also a critical food source to supply protein (Ehrlich et al. 1988). Daily energy estimates are approximately 6 kcal/day (Nagy 1987). To be conservative, we assume that 50% of this is met by carbohydrates from nectar. Therefore, we use 3 kcal as the daily migratory energy requirement from insects. The second category of migrants (10-25g) includes mostly warblers and sparrows. Several studies examine the energy requirements of captive and free-living sparrows and warblers (e.g., Bairlein 1998; Graber and Graber 1983; Nagy 1987; Schaub and Jenni 2000). For birds of this size range, they estimate that maximum gross daily energy consumption, in the context of migratory re-fueling, is 15-19 kcal/day. This corresponds to ingesting 1.2-1.7 times their own

weight in insects per day (Graber and Graber 1983). We use the conservative estimate of 15 kcal/day for group two. Group three, including thrushes and orioles, have considerably higher energy requirements. Two independent studies of birds in the 25-40g range found maximum energy intake of 25-29 kcal/day (Bairlein 1990; Klaassen et al. 1997). We use the conservative estimate of 25 kcal/day.

We recognize that there is considerable debate on the composition of migratory fuel stores, i.e. fat versus protein (e.g., Lindstrom and Piersma 1993; McWilliams and Karasov 2001). Despite the lesser energy density of protein compared to fat, there is strong evidence that protein is an important component of migratory fueling (e.g., Klaassen 1996). Our calculations are agnostic to this issue. We only use gross energy intake for birds, and the gross caloric content of insects, and do not decompose the fat and protein components.

Insect energy content. From research by Graber and Graber (1983), we use the estimate of insect nutrition as 5 kcal/g *dry* insect. From their field data, an insect larva weighs on average 0.1g (wet mass). Insect larvae are 80% water, which means that an insect is 0.02g dry content or 100 calories (0.1 kcal). For group one, the hummingbirds, this produces a crude estimate of 3g of insects consumed per bird-day. For group two, the sparrows and warblers, approximately 15 g of insects are consumed per bird-day. For group three, approximately 25 g of insects are consumed per bird-day.

The values above are for *daily* energy intake for an individual. Stopover length, however, varies. The length of stopover varies by location, species, individual bird, and year; this is a subject of much theoretical discussion and debate (e.g., Kaiser 1999; Kuenzi et al. 1991; Schaub and Jenni 2001). Empirical studies of songbirds have suggested ranges of 1-7 days as the norm, with outliers to two weeks. The estimates from Morris (1996) and Kuenzi (1991), both of whom worked on North American spring migration, fit well with the empirical finding of the length of stopover along the Rio Grande was around 2.3 days (Yong et al 1998). For the following estimate we use this latter finding for all species. As a result, for each individual bird, we multiply the daily insect consumption by 2.3 to represent the total insects consumed while migrating through the SPRNCA.

Total insect consumption. We calculate the estimated total insect biomass consumed during migration as follows. The abundance category for each species in each size group (1, 2 or 3) is obtained from the second column of Table 1. For group 1 there is 1 common species, 3 uncommon ones and 2 rare species. These same values for those species in group 2 (mostly sparrow and warblers) are 40, 28 and 21, respectively, and for group 3 (blackbirds and orioles) they are 24, 5, and 6, respectively. Using the values estimated above for the number of individuals in each abundance category (i.e., common 2,350; uncommon 1,550; and rare 775) we can calculate that there are a total of 8,550 hummingbirds per day needing food, 155,000 sparrow- and warbler-sized individuals needing food each day during migration time, and finally, 68,800 larger birds per day will be in search of food. Combining these numbers with the number of grams each individual needs to eat and converting from dry mass back to wet mass leaves us with an estimate of 20,400 kg/day of insect mass needed to feed the migrants stopping over in the SPRNCA. Remembering the caveats and assumptions discussed above, these numbers then

convert into 204 billion 0.1 g insect larvae being eaten a day throughout SPRNCA during the week of peak migration.

4.4.3 Determining habitat requirements based on bioenergetics

To attempt to determine the minimum amount of habitat needed to provide the necessary number of insects to sustain a healthy population of migrants while visiting and when ready to impart on the next stage of their migratory journey, we assume that at least 20,400 kg of insects are needed each day during the peak migration week. The actual insect densities in the SPRNCA are unknown. Graber and Graber (1983) determined that an insect larval biomass of 0.70 g/m^3 was necessary for warblers to maintain a positive energy balance. Using this estimate, if 20,400 kg/day of insects are needed during migration, then approximately 29 million m^3 of SPRNCA habitat for insects is required. In order to translate this cubic measurement of insect density into a geographic area, it is necessary to estimate the “depth” of insect habitat. In the largest trees, there might be 10 m of foliage habitat, but the smaller trees might have only 5 m of foliage habitat. The range of insect habitat, assuming an “insect habitat depth” of 5-10 m is approximately 13-27 million m^2 or 1300 - 2700 ha. From Steinitz et al. (2003), there are currently about 3100 ha of cottonwood-willow forest (prime riparian habitat) in the SPRNCA. This is a remarkably good fit to the estimate of insect biomass required to support the current numbers of migratory birds. If mesquite, mixed broadleaf and tamarisk are also included, then the current total is 8100 ha of riparian habitat (Skagen et al. 1998). This estimate, however, includes area of much lower insect density. In order to more accurately apply the calculations of insect consumption by migratory birds, empirical estimates of insect density in different habitats in the SPRNCA would be valuable.

Table 4-16: Doves, hummingbirds, woodpeckers, cuckoos and songbirds that use the SPRNCA, excluding those species that are irregular visitors. Listed are data from Hanson (2001), the BBL data set, the SPRNCA data set, Krueper et al. (2003), Skagen et al. 1998, and Wang and Finch (2002). The columns for the Hanson entry are abundance category (C—common, U—uncommon, R—rare), when the SPCNA is used by the species (P—permanent resident, S—summer resident, W—winter resident, T—transient), and if the species is a migrant. Under the Krueper column the N indicates the species abundance is increasing and the D indicates it is decreasing. Under the Wang and Finch column the M indicates the species is known from mist netted individuals, the P means the species was recorded on a point count and the B means that both occurred.

Species	Hanson			BBL	SPRNC A	Krueper	Skagen	Wang & Finch
	Common Ground-Dove				47	58	N	
Inca Dove				4				
Mourning Dove	C	P	M	2		N	1	
White-winged Dove	C	S	M	5	4			
Broad-billed Hummingbird	R	T	M	29				B
Violet-crowned Hummingbird	R	T	M	3				B
Black-chinned Hummingbird	C	S	M	1868	12			B
Anna's Hummingbird	U	P		1355				
Calliope Hummingbird	R	T	M	7		N	3	B
Broad-tailed Hummingbird	U	T	M	437				
Rufous Hummingbird	U	T	M	482		N	3	M
Allen's Hummingbird				47				
Berylline Hummingbird				2				
Blue-throated Hummingbird				10				
Magnificent Hummingbird				150				
Acorn Woodpecker	R	T	M					
Gila Woodpecker	C	P		3		N	2	B
Red-naped Sapsucker	U	W	M			N	2	B
Ladder-backed Woodpecker	C	P		11				B
Yellow-billed Cuckoo				14		N		B
Northern Flicker	U	P		3		N	3	
Northern Beardless-Tyrannulet	U	S	M					
Buff-bellied Flycatcher				6				
Olive-sided Flycatcher	R	T	M				3	B
Greater Wood-Peevee	R	T	M					
Western Wood-Peevee	C	S	M	9	9			B
Cordillerian Flycatcher				2				
Western Flycatcher				25	18			
Southwestern Willow Flycatcher				2	2			
Willow Flycatcher	R	T	M	7		D		B
Hammond's Flycatcher	U	W	M	16		N		B

Dusky Flycatcher	U	W	M	19					B
Gray Flycatcher	U	W	M	5	6	N			
Pacific-slope Flycatcher	C	T	M	2					P
Black Phoebe	C	P		20					B
Eastern Phoebe	R	W	M					1	
Say's Phoebe	C	P	M						
Vermillion Flycatcher	C	S	M	33					
Dusky-capped Flycatcher	U	S	M						
Ash-throated Flycatcher	C	S	M	27					B
Brown-crested Flycatcher	C	S	M	5		N		3	B
Cassin's Kingbird	C	S	M			N		2	B
Tropical Kingbird				88					
Western Kingbird	C	S	M	9	2	N		3	B
Mexican Jay				2					
Bridled Titmouse	U	W	M	11	13	D		1	B
Verdin	C	P		2	2	D			M
Bushtit	C	P		10	3				
White-breasted Nuthatch	C	P		15	9	D			B
Brown Creeper	U	W	M						
Cactus Wren	C	P				N		3	P
Rock Wren	C	P				N			M
Canyon Wren	U	P						4	P
Bewick's Wren	C	P		80	84				
House Wren	U	W	M	6				4	B
Winter Wren	R	W	M			N		2	B
Marsh Wren	U	W	M			D			M
Ruby-crowned Kinglet	C	W	M	15					
Blue-gray Gnatcatcher	U	T	M						B
Black-tailed Gnatcatcher	U	T	M			N			
Western Bluebird	U	W	M			D			
Mountain Bluebird	U	W	M						
Swainson's Thrush	R	T	M	7	6	D		1	
Hermit Thrush	U	W	M	12	5	N		1	
Northern Mockingbird	C	P		2					
Sage Thrasher	R	W	M						B
Bendire's Thrasher	R	P	M						M
Curve-billed Thrasher	C	P		9	5				
Crissal Thrasher	C	P							B
American Pipit	U	W	M					4	B
Cedar Waxwing	U	W	M						B
Phainopepla	U	P	M	13					B
Loggerhead Shrike	C	P	M						
European Starling	C	P				N		3	P
Bell's Vireo	C	S	M	16	10	N		1	B
Gray Vireo	R	T	M			D			
Solitary Vireo	C	T	M						B

Hutton's Vireo	U	T	M						
Warbling Vireo	C	T	M	9		N			B
Orange-crowned Warbler	C	T	M	8	8	N	1		B
Nashville Warbler	U	T	M	3					B
Virginia's Warbler	R	T	M						B
Lucy's Warbler	C	S	M	51			5		B
Yellow Warbler	C	S	M	80	76	N	2		B
Yellow-rumped Warbler	C	W	M	10	10		2		B
Black-throated Gray Warbler	U	T	M	3					P
Townsend's Warbler	U	T	M			N	3		B
Hermit Warbler	R	T	M						B
Black-and-white Warbler	R	T	M						B
American Redstart	R	T	M						P
Northern Waterthrush	R	T	M			N	2		B
MacGillivray's Warbler	U	T	M	112					B
Common Yellowthroat	C	S	M	353	413	N			
Wilson's Warbler	C	T	M	208	195	D	1		
Painted Redstart	R	T	M			D	2		B
Yellow-breasted Chat	C	S	M	96	87	D			B
Summer Tanager	C	S	M	43	28				B
Western Tanager	C	T	M	2					B
Northern Cardinal	U	P	M	3	4				B
Pyrrhuloxia	C	P	M	20					B
Black-headed Grosbeak	C	T	M	23					M
Blue Grosbeak	C	S	M	59					P
Lazuli Bunting	C	T	M	64		N			P
Indigo Bunting	R	S	M				4		B
Varied Bunting	R	S	M	6					M
Painted Bunting	R	T	M						B
Green-tailed Towhee	C	W	M	110		N			B
Spotted Towhee				6					B
Canyon Towhee	C	P		23					B
Abert's Towhee	C	P		84			2		B
Botteri's Sparrow	C	S	M	704	5				
Cassin's Sparrow	C	S	M						P
Rufous-crowned Sparrow	U	P		12					M
Chipping Sparrow	C	W	M	27	30				B
Brewer's Sparrow	C	W	M	157					B
Black-chinned Sparrow	R	T	M						
Vesper Sparrow	C	W	M	16					B
Clay-colored Sparrow				4					B
Lark Sparrow	U	W	M	3		N	2		B
Black-throated Sparrow	C	P		23	41	N	3		B
Lark Bunting	U	W	M	27	33				B
Savannah Sparrow	U	W	M	9	9				M
Baird's Sparrow	R	W	M						B

Grasshopper Sparrow	R	W	M					
Song Sparrow	C	P		90		D		B
Lincoln's Sparrow	C	W	M	441	662	N	2	P
Swamp Sparrow	R	W						B
White-throated Sparrow	R	W		2				
White-crowned Sparrow	C	W	M	2	2			B
Gray-headed Junco				2				B
Oregon Junco				7				
Chestnut-collared Longspur	R	W	M					B
Red-winged Blackbird	C	P	M	19	17			P
Eastern Meadowlark	C	P		9		D	3	B
Western Meadowlark	C	W	M	4				B
Yellow-headed Blackbird	C	W	M					B
Brewer's Blackbird	C	W	M			N		B
Great-tailed Grackle	C	P				N	1	B
Bronzed Cowbird	R	P	M	46			4	B
Brown-headed Cowbird	C	P	M	156				B
Hooded Oriole	U	S	M	4	5	N	2	B
Bullock's Oriole	C	S	M	5	3			B
Scott's Oriole	U	S	M	3			5	B
House Finch	C	P	M	31	20			M
Pine Siskin	U	W	M	3	2	N	3	B
Lesser Goldfinch	C	P	M	145	136	N	3	B
American Goldfinch	R	W	M	3	3			B
House Sparrow	C	P	M	7			2	B
GWCS ?				546				
MWCS ?				330				

4.5 Bioclimatic Modeling of Avian Range Changes

The biogeographic distribution of animals has long been thought to be limited by climate (Andrewartha and Birch 1954; Ricklefs 1979; Krebs 1985). Still, very few studies have examined large-scale distributions of North American birds and their association with climate. Paradoxically, much of the work examining climate as a limiting factor took place near the beginning of the twentieth century. As the century progressed, studies focused more on habitat and species interactions, usually in a small area. Even with the advent of consistently run continentwide bird surveys and inexpensive computers, few quantitative studies examining associations between climate and avian distributions have been performed.

Much of the work examining associations between climate and distribution has been qualitative rather than quantitative. In a study of the niche relationships of the California Thrasher (*Toxostoma redivivum*), Grinnell (1917) found that this species' range was limited to the Upper Sonoran life zone. Within this climate-delimited area, he found a direct correspondence between rainfall and the occurrence of three thrasher subspecies. Similarly, Bent (1946) observed that the range of the Black-billed Magpie (*Pica pica*) closely matched the distribution of the Cold Type Steppe Dry Climate of Russell (1931). More recently, Johnson (1978) examined bird species distribution within the Intermountain Region of the western United States. This area contains several mountain ranges separated by large expanses of desert. Within the mountain ranges, Johnson found that the northwestern distribution of Grace's Warbler (*Dendroica graciae*) appeared to be limited by environmental conditions. Other species he found to be associated with environmental variables included: Downy Woodpecker (*Picoides pubescens*) and Ladder-backed Woodpecker (*P. scalaris*) separated by temperature and moisture; and Mountain Bluebird (*Sialia currucoides*) and Western Bluebird (*S. mexicana*) separated by average spring and summer temperatures.

One of the earliest quantitative studies on the relationship between climate and bird distributions was an examination of the role of the environment in limiting the eastern distribution of House Wren (*Troglodytes aedon aedon*). Kendeigh (1934) found the distribution of this species represented an interplay among environmental conditions, behavioral adaptations, and the species' anatomy and physiology. Environmental factors were found to be associated with both the northern limit (average minimum daily temperature) and southern limit (average maximum daily temperature) of the distribution.

More recent work includes a series of smaller-scale studies examining the relationship between changes in avian density and climate (Cody 1985). While not strictly a study of distributional limits, correlations between climate and the densities of some grassland species were found. These included a positive correlation between Eastern Meadowlark density and spring rainfall at a tallgrass prairie site in Kansas; and correlations between five climate variables and densities of Clay-colored Sparrow, Savannah Sparrow, Western Meadowlark, Grasshopper Sparrow, Bobolink, and Baird's Sparrow at a mixed-grass prairie site in North Dakota (scientific names for these species can be found in Table 1). Finally, a study in western North Dakota found that densities of six of eight common species declined during a drought period in 1988 (George *et. al.* 1992).

The most complete examination, to date, of the association between North American continentwide bird distributions and environmental factors was undertaken by Root (1988a, 1988b). Data collected on the Christmas Bird Count were used to create relative abundance maps of bird species wintering in North America (Root 1988b). These maps were then compared with maps of six environmental factors. The northern range limits for more than 60% of the species were found to be associated with climate (average minimum January temperature). Climate (mean annual precipitation) was also associated with the eastern range boundaries of 39.7% of the species, and the western range boundaries of 36% of the species (Root 1988a).

Of the 51 passerine species found to have their northern range limit associated with temperature, published information on winter physiology was available for 14 (Root 1988c). Based on this published information, Root was able to calculate the basal metabolic rate of these species at their northern distributional edge (northern basal metabolic rate - NBMR). This value consistently came out to be approximately 2.5 times the basal metabolic rate (BMR) of the species. Estimating the BMR for the remaining species based on their body mass, Root found the NBMR to be approximately 2.6 times the BMR. This research demonstrates a strong link between physiology and the early winter northern distributional limits of some passerine birds. Changes in climate will bring about changes in species' distributions. To project the extent of these distributional changes, it is first necessary to understand the association between climate and species' current distributions. Of the studies mentioned above, only Root's could be used to develop quantitative estimates of potential change. However, there are a number of techniques that can be used to associate a species' range with climate. Collectively, these are frequently referred to as biogeographical or bioclimatic analyses. Two of the more prevalent techniques used are climate-envelope studies, often used to analyze plant distributions, and generalized linear statistical models such as logistic regression analyses. There have been a number of studies using these techniques to look at bird distributions but the most comprehensive of them have been performed by Price (1995, 2000a-f, 2001, in press, Price and Glick 2002, Price and Root 2001,2000).

The BBS has been run throughout North America since 1967. For this study, models were developed using data from routes run between 1985 and 1989. The short, five-year, time period was chosen in order to minimize potential effects from large-scale habitat changes and from the more pronounced climatic changes that occurred the 1990s (IPCC 2001). These years were chosen because they encompassed a drought year (1988), a relatively wet year (1987), and three fairly 'normal' climatic years (1985, 1986, 1989) for a range of climatic variability.

Data sources -

Bird Data

The BBS is an annual survey, performed by skilled volunteers, to estimate population trends of many of the species occurring in summer in the United States and Canada. It does not detect breeding birds *per se*, but most species detected along a route are probably breeding in the area. Begun in 1965, the BBS currently consists of approximately 3000 routes.

BBS survey routes' starting point and direction were placed, at random, along roadways, within each one-degree block of latitude and longitude. The number of routes per block varies from one in areas of the West to 16 in areas of the East. Once a route has been planned, efforts are taken to minimize changes in the survey route and to find volunteers to run that route every year. Some BBS routes have been run consistently for over 20 years while others have been run only once.

Each survey route is composed of a series of 50 point counts, spaced evenly 800m (0.5 miles) apart, largely along the 40 km (24.5 mile) length of a secondary road. The duration of each point-count is 3 minutes with observers driving between points. At each point, all species seen within 400 m (0.25 mile), and heard at any distance from the observer are recorded (Robbins et al 1986). Surveys begin 0.5 hour before sunrise and are run once per year during the height of the breeding season. Thus, the survey is run in different months depending upon latitude. In the southern United States, many of the surveys are run in late May. In the northern United States, routes are not run until mid- to late June, with some routes in parts of Canada and Alaska not run until early July. There are a number of problems typically associated with the BBS. These include differential detectability between species, roadside bias in detectability and bird use, differences in capabilities among volunteers running routes, and influences from weather and extraneous noise. To minimize problems, the surveys are run according to strict guidelines. Any bias these issues introduce remains largely consistent among years. An overview of some of the possible problems and biases associated with the BBS can be found in Ralph and Scott (1981) and Sauer and Droege (1990).

Once the BBS data were obtained from the U.S. Fish and Wildlife Service they were checked for errors. First, the data were used to create a list of the species seen in each of the states and provinces. These lists were compared against the Distributional Checklist of North American Birds (DeSante and Pyle 1986). Discrepancies were reported to the BBS office, where they were checked against original data sheets. Those determined to be errors were corrected whenever possible or the data were deleted from the database. Second, the data were checked for errors in route coordinates. The BBS office provided latitudes and longitudes of the starting point for each route. These coordinates were checked to see if they lay within the boundaries of the appropriate state or province. Errors were checked against the original route maps and the necessary corrections were made.

To determine if the BBS routes for the years 1985-1989 sampled points within the published range of each species, relative abundance maps were created following the techniques of Price et al (1995) summarized below. These maps were visually compared with the relative abundance maps in the "Summer Atlas of North American Birds" (Price et al 1995) and with range maps in the "Field Guide to the Birds of North America" (National Geographic Society 1987). The maps in Price et al (1995) are similar to those used in this study except the data there encompassed a longer time period, more data points were used in map development, and some post-processing corrections were made to the edges of some species' ranges. The distribution maps in field guides are the result of intensive research and consultation with experts on the avifauna of each region. By their very nature the mapped distributions tend to be more spatially uniform than the actual distributions. They also tend to depict a somewhat broader range for most species than occurs in most years. These maps often include areas where the species are

only present sporadically. Nevertheless, maps created from the BBS data often agree closely with those published elsewhere. All species in this study appear to be adequately sampled (geographically) by the BBS. That is, BBS routes where the species was detected were scattered throughout the range of the species. For some species, portions of the range, especially portions in Mexico or the Arctic, were not included in the study as there were no BBS data available for those areas.

Climate Data

United States climate data were derived from the TD-3200 Summary of the Day Cooperative Observer Network database of the National Climate Data Center. This database was obtained from Climatedata, distributed by EarthInfo, Inc., Boulder, CO. The Cooperative Observer Network is composed of thousands of observers who collect weather data and submit them daily to the National Climate Data Center. Most stations collect data on at least minimum and maximum temperatures and precipitation. Some stations collect additional information such as snow depth, humidity, and pan evaporation. The Climatedata database consists of all of the collected weather data, as well as summary information for each weather station (e.g., latitude, longitude, and elevation). Data were extracted from this database for each of the study years, composited into monthly averages and converted to metric units.

Geographic coordinates for each weather station were then checked against a second, updated data base, obtained from the National Climate Data Center. In a few cases, discrepancies in latitude, longitude, or elevation were found. These data were checked against published records. In cases where coordinate concordance could not be obtained, the station's data were deleted from the database. The final database contained latitude, longitude, and monthly weather data for stations throughout the United States for the years 1985-1989.

Monthly summarized weather data for Canada were obtained from Canadian Climate Centre, Environment Canada, for 1985-1989. These data were provided in metric units, with geographic coordinates and elevation. No secondary source was available to use in checking the geographic coordinates of these weather stations.

The combination of the two databases resulted in an average of 12,000 - 15,000 monthly data points for each weather variable. The difference in the number of data points varied by time of year, year, and variable. More data were typically available for summer because of data reported from seasonal fire lookout stations. Similarly, there were slightly more weather stations reporting precipitation data than temperature data because of seasonal fire lookout stations and agricultural reporting stations. Finally, there was a decline in the number of weather stations between 1985 and 1989.

Locations of weather stations were plotted and compared with the distribution of BBS routes. The distribution of the weather stations was similar to that of the BBS routes, with several weather stations located near each BBS route. Like the BBS, there were more stations in the East and fewer stations in the West, northern Ontario, and Quebec. In all years, the number of weather stations exceeded the number of BBS routes.

Weather data were also examined for gross errors (e.g., elevations of greater than 20,000 m in Nebraska, monthly precipitation values of greater than 2,000 cm) and obvious errors were deleted. The possibility of additional errors (outliers) in the data also existed. Outliers were identified by examining plots of each weather variables. As it was not possible to identify which outliers might represent correct data, all outliers were removed from the data base.

Not all stations collected data on all weather variables. Only data on temperature and precipitation were regularly collected at most stations over a broad geographic area. For that reason, variables used in this study were derived solely from temperature and precipitation.

Data Interpolation

Neither weather stations nor BBS routes were uniformly distributed in time or space. Some weather stations were in operation only during certain seasons, others had been moved between years, had stopped collecting data for some of the variables, or had missing data for a given variable in a given month. The weather station closest to a given BBS route varied depending upon month, year, or variable of interest. It would have been possible to restrict weather stations used in this study to those that did not move and had consistent coverage for all weather parameters. This would have meant that the distance between some BBS route and the closest weather station sometimes would exceed 80 km (50 miles). In parts of the West, this would have led to problems due to elevational gradients. For example, one BBS route begins near Pagosa Springs, CO (elevation about 2280 m [7500 feet]). The closest weather station with consistent data was located at Wolf Creek Pass (above timberline, elevation approximately 3300 m [10,850 feet]). Thus, weather at the station would have been substantially different from weather along the route. For these reasons, spatial interpolation was used to estimate the values of the climate parameters for all BBS route locations.

Spatial interpolation takes advantage of the autocorrelated nature of these data. It estimates the value of points on a regularly spaced grid based on the values from known data points. In a study of rainfall patterns in south Florida, kriging was found to be one of the best spatial interpolation techniques (Abteu et al 1993). Kriging is a geostatistical technique developed to predict the average grade of gold ore in a mining block, based on data from nearby mining blocks (Cressie 1990). It is one of the better spatial interpolation techniques in that it is linear, an unbiased estimator (predictor) of the value at a point, and it minimizes error variance (Isaaks and Srivastava 1989; Cressie 1989). Kriging provides a weighted linear average for a given point to be estimated, based on the spatial relationship and covariation of the surrounding data.

Kriging begins with known, usually irregularly spaced, data points. A decision is then made as to the proper grid spacing to use. This grid is composed of the regularly spaced points to be estimated. If the grid is too coarse, information will be lost and the estimated values will have a greater variance. If the grid is too fine the estimated points present more information than the data can support. The ideal grid size is the one producing the smallest residual values, calculated by:

$$Z_{\text{res}} = Z_{\text{dat}} - Z_{\text{grid}}$$

Where: Z_{res} is the residual; Z_{dat} is the actual data value at a known point (equivalent to $z(x_i)$ above); and Z_{grid} is the estimated value at the grid node closest to that point (equivalent to $Z^*(X_0)$ above).

Surfer (Golden Software, Inc.) was used for kriging all climate variables and species' distributions in this study. Surfer uses an assumed linear variogram in the calculation of the weights of the kriging model. This model has been found to provide accurate estimates except in cases where severe anisotropy, caused by directional data, is present (T. Bresnahan, Golden Software, oral commun.). For example, in a species restricted to a straight, narrow riparian corridor the positive values would have direction relative to the negative values. While data with some direction can be modeled with this approach, the more severe the direction the poorer the estimates become.

The grid used for all of the interpolation in this study had a spacing of 50 km (31 miles), or slightly longer than the length of a BBS route. The 10 nearest known points were used in the estimation of the value at each grid node. For each grid node, the known values were weighted such that those closer, and with a similar covariance, provided more weight than those farther away. Even though the same 10 values might have been used for more than one grid node, the weighting factors, and thus the estimate for the node, differed. The more observations there were near the point to be estimated, the better the overall estimation.

Using the parameters above, kriging was used to create a climate surface grid for minimum temperature, maximum temperature, and precipitation for each month in each year of the study (a total of 180 grids). The latitude and longitude of the start point of each BBS route then were used to extract the estimated value for each of the variables for each of the BBS routes. This was done by locating the grid node whose coordinates were closest to the coordinates of the BBS route. These values then were used to produce a database of average monthly climate values for the period 1985-1989 for each BBS route.

Deriving Climate Variables

Climate variables used in this study were derived from monthly temperature and precipitation variables. The monthly values were first combined to produce seasonal temperature (average) and precipitation (total) variables. The seasons were as follows:

- Summer - June, July, August
- Fall - September, October, November
- Winter - December, January, February
- Spring - March, April, May.

The final database, used in all analyses, contained the seasonal variables, as well as variables for climatic extremes, range, and various combinations of temperature and precipitation.

Climate variables selected for this study were chosen with the understanding that climate would be acting as a surrogate for many possible limiting factors. While some climatic variables might act directly (e.g., on physiology), others (especially those in fall and winter) would be act indirectly (e.g., on food resources or habitat). The variables selected covered a range of average

and extreme conditions and were selected after a review of similar biogeographic studies (Austin et al 1990; Busby 1986; Lindenmayer et al 1991; Nix 1986; Walker and Cocks 1991).

Developing and Validating Models

Breeding Bird Survey routes run during 1985-1989 were split into two groups, training and validation. The training group, used in model development, consisted of all routes run every year (1173 routes). The validation (or test) group consisted of all routes run at least once (1077 routes) and provided an independent group to use in testing the models. Once the models had been developed, they were used to predict the values in the validation group. Cross-classification was used to test the goodness-of-fit between the values predicted by the model and the observed values of the validation group.

Logistic Regression Models

A model should provide the simplest, best fitting, and most biologically meaningful description of the relationship between the response variable and the explanatory variables (Hosmer and Lemeshow 1989). Regression analyses have often been used to model relationships between species and their environment. In any given area a species is either present or absent. The binary nature of the response variable suggests logistic regression as an appropriate statistical modeling technique. Several studies examining the relationship between a species' distribution and environmental variables have used multiple logistic regression models (e.g., Pereira and Itami 1991; Austin et al 1990; Brennan et al 1986; Dawson et al 1993; Robbins et al 1989). Logistic regression is an appropriate technique to use when the response variable is binary (Hosmer and Lemeshow 1989).

Organisms frequently respond to their environment in a nonlinear fashion (Johnson 1981). Additionally, measured environmental variables often have a skewed or kurtotic distribution (Brennan et al 1986). Even in cases where the response variable is linear, it is possible the relationships among explanatory variables may be nonlinear (Johnson 1981). For these reasons, Johnson (1981, U.S. geological Survey, oral commun.) suggested nonlinear relationships be considered in developing environmental models.

Quadratic regression is a commonly used alternative to linear regression in wildlife studies (Johnson 1981; Marzluff 1986). Quadratic regression includes the squares of explanatory variables in the modeling procedure. This produces a curvilinear relationship possibly capturing some of the nonlinearity. In this study, the eighteen climate variable, as well as their squares, were used as explanatory variables. The quadratic terms in the equations are identified with an S before the variable name.

PROC LOGISTIC (SAS Institute 1992) was used to develop logistic models relating species' distributions to climate. The response variable was the species' presence or absence on a given BBS route. All routes recording the species at least once during any of the five-years were scored 1 (present) otherwise they were scored 0 (absent). Explanatory variables were the 18 climate variables and their quadratics.

Choosing the “best” logistic regression model was done by assessing the new model’s fit against the existing model’s fit by examining how much the addition, or deletion, of a variable changed the model. A number of tests can be used to assess a model’s significance. These include the -2 Log Likelihood test, Akaike Information Criteria, Schwartz Criterion, Wald test, and Score test (Hosmer and Lemeshow 1989). Each test differs in its assumptions and computational efficiency. Of these, the Score test (ST) is one of the most computationally efficient and was the one used here. The model with the best fit was the one with the highest ST.

Once a model had been selected, its initial predictive ability was tested by examining the rank correlation between predicted probabilities and observed responses (Norusis 1988). A positive relationship between predicted and observed exists if most pairs are concordant. This study used the Goodman-Kruskall Gamma index as a measure of association based on the probability of predicting one value given the other. The closer the value is to one, the closer the relationship between the ranks of predicted probabilities and observed responses (Agresti 1990).

Model Validation

The logistic regression model, coupled with the climate data for a given BBS route, provided the probability of a species' presence or absence on a given route. To validate the models, probabilities first had to be converted into binary variables. The cut-off point used to convert logistic regression probabilities to binary variables is often arbitrarily set at 0.5. If this cut-off point is set too high or too low then the mis-classification rate will be high. For this study, the optimal cut-off point was found to be 0.4 (e.g., 40% probability of occurrence). This was determined by comparing the results from cross-classification studies done with cut-off points of 0.2, 0.4, 0.5, and 0.6. All routes with a 0.4 or greater probability of a species' occurrence were classified as 1 (present). All other routes were classified as 0 (absent).

Cross-classification uses a 2 X 2 classification table and the chi-square statistic to measure the goodness-of-fit of models. The statistical null hypothesis is that the predicted values are independent of the observed values. If the null hypothesis is rejected, the model is considered to provide a good fit. The cross-classification rates for most of the logistic regression models were statistically significant (most with $p < 0.00001$). In addition to the chi-square statistic, the classification rate (percentage of correct classification) was also calculated for each model.

These analyses were performed on both the training and validation data sets. Gamma index values for the validation set were compared with those of the training set. Classification rates for the validation set were also compared with the training set. This validation step demonstrated that most of the logistic regression models were adequate in predicting the presence or absence of a species based on these climate variables.

Graphical Analyses

Logistic regression provided an equation predicting the probability of a species occurring on a given BBS route, given the climate on that route. Validation tests provided an indication of how well the models fit the validation data sets. No model correctly classified all routes. On

some routes, a species was predicted to occur where it was not known to occur (error of commission). On other routes, the species occurred yet was predicted to be absent (error of omission).

Logistic regression models do not depict any spatial element of the distribution. There are many possible explanations if an area was incorrectly classified as containing (or not containing) a species. For example, if the mis-classification fell within a species' published range, but the species had not been detected on that route, the possibilities include: 1) the species occurred in the area but was not detected on the route; 2) the climate was suitable for the species but the habitat was not; 3) the microclimate in that area was not suitable for the species; or 4) the climate and the habitat were suitable but the species was absent from the area for other reasons. If the mis-classification fell outside of the published range of the species (commission error) the possibilities include: 1) the species was present in that area but had not been detected by the survey; 2) the climate was suitable, but some other requirement was lacking; or 3) the model is inadequate (this includes differences due to variation among subspecies).

Maps were created to assess the spatial component of the models. These maps were then compared with published sources and the original relative abundance map of the species. This process involved creating several different types of maps, each containing different patterns of shading. These map types included: 1) relative abundance maps where the shades correspond to the relative abundance of the species in the area, and 2) logistic regression maps where the shades represent the probability of a species occurring in the area, based on the modeled species' distribution).

Developing Maps of Avian Relative Abundance Patterns

A number of decisions must be made in order to create a map from a regularly spaced grid. The first has to do with the contour interval. On a topographic map, the contour interval is regularly spaced (e.g., every 10 meters). The abundance of biological organisms often is not regularly distributed; most sites will have few individuals and a few sites will have many individuals. For that reason, a regularly spaced scale is not appropriate. For this study the scale used in the avian relative abundance maps has the following levels: < 5; 5 - 20; 20 - 50; and > 50 individuals per route, per year.

A second decision has to do with defining the edge of a species' distribution. It is difficult to determine the actual edge of any species' distribution. From day to day, and especially from year to year, the edge of the distribution may differ. While zero might be a logical choice, this would potentially lead to the inclusion of areas where the species is rarely seen. This could include areas that have been over-interpolated (e.g., areas where the species has never been detected but where the interpolation algorithm estimates the species to be present in low numbers). For maps in this study, the edge of the distribution was set at 0.5 birds per route per year (i.e., about one individual of that species seen on that route every other year).

The relative abundance maps created for this study were then visually compared with those in Price et al (1995) and other sources (National Geographic Society 1987; Peterson 1980, 1990). Particular attention was paid to the position of the range edge and the homogeneity of the distribution, providing a measure of how well BBS routes used in this study sampled the species within its range. The relative abundance maps also were used in comparisons with the graphical representations of the logistic regression models.

Logistic Regression Maps

The logistic regression model, linked with the climate values for each route, generated a probability of a species' occurrence on that route. These probabilities were then used, with the methods described above, to generate a map showing the probabilities of occurrence for most of the species in this study. Like the validation process, 0.4 was typically used as the cut-off for a species being present or absent. All shaded areas on the map represent the predicted distribution of the species. The scale used on most maps has the following levels: 40% - 60%, 60% - 80%, and > 80% probability of occurrence. For some species (e.g., Sprague's Pipit) the scale was lowered to 20% in the map depicting the projected species' range. This was done to show that the climate for the species does have a small probability of suitability for the species.

Logistic regression map often comes close to matching both the relative abundance map and maps in published sources. These models could be considered as representing the qualitative climate realized niche (*sensu* the qualitative environmental realized niche of Austin et al [1990]).

The geographic scale on all of these maps is relatively coarse, representing estimated values for blocks with a dimension of 50 km x 50 km (31 miles x 31 miles). This should be interpreted as meaning the species is likely to be found, along a road, in the proper habitat; or the climate will have this average value; or the average probability of occurrence has this value; somewhere within this block. Therefore, any 'point' on the maps should actually be considered to have a spatial resolution of a 50 km x 50 km block.

General Circulation Model Output

Equilibrium atmospheric general circulation models (GCM) make specific predictions as to the magnitude of changes to temperature and precipitation likely, often under a scenario of doubled carbon dioxide (2 X CO₂) (Smith and Tirpak 1990). Although the models themselves are relatively coarse, the differences between output from the current conditions model and the 2 X CO₂ model can be spatially interpolated in a manner similar to that described above.

In order to estimate changes in bird distributions, a model must first be able to adequately predict the current distribution. Similarly, in order to estimate climate change, a GCM must first be able to adequately predict current climate. For this study, the choice of GCM output was restricted by several factors. First, it had to be readily available. Second, it had to include the variables used in the original bird-climate models. Finally, due to computational limitations, it needed to represent a climatic endpoint rather than the entire climatic transition state. After consultation with the National Center for Atmospheric Research (D. Joseph, National Center for Atmospheric Research, Boulder, Colorado, oral commun.), the condensed North American

subset of the Canadian Climate Centre Second-Generation General Circulation Model (hereafter referred to as CCC) was chosen.

The CCC is an equilibrium model, predicting the climate for a given set of conditions (e.g., a doubling of carbon dioxide), but not for the transition between the current climate and those conditions. The North American subset of this model consists of several different climate variables computed for each of 570 grid nodes (approximately 3.75° apart) between 20° - 90° N latitude, and 150° - 40° W longitude. The variables included average daily precipitation, maximum daily temperature, and minimum daily temperature condensed into monthly means (Boer et al 1992). Model output provided average climate values based on 10 years of simulated climate under current conditions, and 10 years of simulated climate under 2 X CO₂ conditions.

A complete review of the details of the CCC can be found in McFarlane et al (1992). Of importance to this study is how reliably the model simulates the current climate. In general, simulated winter (December - February) precipitation matches observed values within the geographic boundaries of this study. However, simulated summer precipitation in parts of the west was greater (approx. 4-6 mm day⁻¹) than observed values. Simulated temperatures in parts of the west were approximately 5° C cooler than observed temperatures. These deficiencies were primarily found in areas with high orographic relief (McFarlane et al 1992). They do not have a major impact on this study as few BBS routes are found in regions with rapid changes in elevation.

Output from CCC, run under conditions of doubled carbon dioxide, deals only with the equilibrium state once a doubled level has been reached. The complete results of the Canadian Climate Centre's greenhouse gas climate change experiment can be found in Boer et al (1992). The CCC predicts a mean annual increase in temperature of 4.4° C over land areas, with an increase in precipitation of 0.9%. Overall temperature increases are predicted to be greater in winter than summer, and summer precipitation is predicted to decrease by 0.5%. These are global averages. Changes within the study area range from 1° to 9° C increases in average winter temperature, and from 2° to 6° C increases in average summer temperature. The model predicts increases, decreases, and shifts in precipitation patterns. Within the study area, changes in total precipitation range from 45 mm drier to greater than 100 mm wetter in winter, with large areas showing no change. In summer, most areas are predicted to be drier, with changes ranging from 85 mm drier to more than 40 mm wetter.

Modeling Projected Impacts of Climate Change

CCC output represents the average of all of the area surrounding a given grid point, not data for the point itself (Canadian Climate Centre 1990). Examining changes in the climate at each BBS route required several steps. First, the differences between the current climate model output and 2 X CO₂ model outputs (anomalies) were calculated for each grid node for each variable. This difference represented the average change in climate in that area due to a doubling of atmospheric carbon dioxide. Second, kriging was used to interpolate this difference onto the same size grid used for all baseline climate variables. Third, the values for each BBS route were extracted from these grids. Finally, these differences were applied to the original BBS-climate database to create a new doubled carbon dioxide BBS-climate database.

These new data were then used, with the models developed above, to project changes in the climatic ranges of each species associated with a doubling of carbon dioxide. This included developing graphical representations coupling the logistic regression model with doubled carbon dioxide output (logistic regression coupled model) for each of the species. These graphical representations were then used to investigate the potential vulnerability of each species to climate change. A species' vulnerability was assessed by examining the extent of distributional change within the geographic boundaries of the study. Besides showing predicted changes in climatic ranges of a species' distribution, the maps also indicated areas where the species is currently found that might also contain the species under this doubled carbon dioxide scenario. These areas are important in that they might represent refugia for these species. As such they merit increased conservation attention.

Results

The methods described above were used to provide information on nearly 200 species. This information includes a discussion of any potential limitations in the sample. Statistical information on the logistic regression model is then provided, including the equation and its accompanying Score test (ST) statistics, goodness of fit statistics, and a comparison of concordance for training and test data sets. An assessment of the graphical representation of the logistic regression model under current climate conditions (map B in the figures, see attachment 7) follows. This map depicts the species' distribution based on climate variables alone, where different shades represent probabilities of occurrence. This map is then compared with the relative abundance map and published sources. Finally, an estimate of the vulnerability of the species to the climate change predicted by the CCC is provided. This is done by examining the graphical representation (map C in the figures, see attachment 7) of the logistic regression model coupled with the climate output from the CCC. This graphical representation is compared with the other maps and the results are summarized. Shaded regions in these maps also represent the probability of the species occurrence in that area.

Climate and Distribution

Associations between climate and species distributions can be related to direct effects, indirect effects, or a combination of the two. A direct effect would occur when the distribution was limited by physiology, biology, or behavior of a species. This includes physiological limits of adults, newly hatched, or juvenile birds, or limits on nest placement (relative to climate/microclimate) or incubation requirements for the species. Possible indirect effects include climate acting upon habitat (species composition, structure, vigor, or physiognomy of species in the plant community), or on food resources of the species (seed set, onset of flowering, insect development or activity rates). Some of the associations found in this study involved winter climate variables. As many of the study species are migratory, or partially migratory, these associations must represent indirect effects. Most of the associations, however, were related to spring or summer variables. These could represent either direct or indirect effects. Given Root's (1988c) research linking physiology with winter distributions (of some species), and some recent work possibly linking macroclimate with microclimate/habitat (see below),

physiology likely plays a role as a factor limiting the biogeographic distributions of at least some of the species considered in this study.

Summer bird ranges are often assumed to be tightly linked to particular habitats. This is only partially true. While certain species are usually only found in specific habitats (e.g., Kirtland's Warbler breeding in jack pines), others are more flexible in their habitat use. Species found in a particular habitat type throughout their summer range may not be found in apparently equivalent habitat north or south of their current distribution. Birds are also limited in their distributions by their physiology and food availability. The link between physiology and the winter distributions of many species is well known (Kendeigh 1934, Root 1988a, 1988b) and recent research shows that physiology plays a role in limiting summer distributions as well (Dawson 1992, T. Martin, *pers. comm.*). Often, the choice of a specific habitat may be to provide a microclimate suitable for a species' physiology. While habitat selection, food availability, and competition may all play a role in influencing *local* distributions of a given bird species, looking at a species' overall distribution often yields different results. Building on earlier work that found that many winter bird distributions were associated with climate (Root 1988a, 1988b), this study examined the association between summer bird distributions and climate and how these distributions may change with climate change.

A great deal of research has examined the role of habitat in defining bird distributions (e.g., work summarized in Cody 1985). Some species are closely linked with specific tree species or local habitat types. For example, Kirtland's Warbler (*Dendroica kirtlandii*) is found only in a relatively narrow band of jack pine (*Pinus banksiana*) forest in central and northern Michigan (Botkin et al 1991). With few exceptions, much of the work on habitat and bird distributions has been performed over relatively small scales. No habitat data are collected along BBS routes. The only consistent source of habitat data for routes is remote sensing satellites. Several studies, currently in progress, are attempting to use remote sensing data to categorize habitat along BBS routes. When complete, these studies may provide a coarse overview of habitat types along some BBS routes. Until these data become readily available, it is not possible to directly relate bird distributions to habitat over the continentwide scale of the BBS.

There are a number of difficulties involved in trying to understand the factors limiting a species' distribution. Teasing out all of the relationships would require a multi-year/multi-scale study examining the year-round climate (both macroclimate and microclimate); amount of soil moisture; floristic composition and structure; phenology of growth, flowering, and seed set; number of seeds and/or flowers produced; identity and enumeration of invertebrate prey; and presence and interactions with other vertebrate species (avian and otherwise). A study of this magnitude has yet to be attempted. Instead, a typical study examines avian presence or density with, at most, the number and species of major plants, and possibly a measure of the vertical and horizontal structure of those plants. Without taking into account any of the abiotic, or some of the other biotic, factors, it is impossible to make absolute statements as to the factors limiting the distribution of a species.

Distributional models and distributional maps have been developed for almost all North American passerine birds. What these maps actually show are areas projected to have the proper climate for the species, or *climatic range*, under conditions derived from the CCC model. While

the results of the models cannot be used to look at the fine points of how a given species' distribution might change, they can provide an impression of the possible direction and potential magnitude of the change in the suitable climate for the species. The following list of potential changes to the avifauna of the SPRNCA was prepared by comparing the maps of projected summer bird climatic ranges with the information found in *The Birds of Arizona* (Monson and Phillips 1964). Until such times as models are completed for species breeding in Mexico, a conservative biogeographic rule of thumb of a northward shift of approximately 100 km for every 1° C temperature increase was used to provide an estimate of which species breeding in Mexico might colonize Arizona. For this study, species whose ranges extended to approximately 200 km of the border, according to the maps in *The Birds of Sonora* (Russell and Monson 1998) and whose habitats (as described in the book) appear to currently exist in Arizona, were included. It does not take into account habitat conversion in Mexico that might make it more difficult for species to colonize northward. The maps in *The Birds of Sonora* were also used to modify projections of which species might be extirpated from the SPRNCA as opposed to strictly going off of the data in the maps (see attachment 7).

Ultimately, the greatest impact on wildlife and vegetation may not come from climate change itself, but rather from the rate of change. Given enough time, many species would likely be able to adapt to climatic shifts, as they have done in the past. However, the current projected rate of warming is thought to be greater than has occurred at any time in the last 10,000 years (IPCC 1996). This rate of change could ultimately lead to many changes in the SPRNCA's Nongame avifauna.

Species whose future climatic ranges might exclude the SPRNCA, Arizona (i.e., possibly extirpated as summer residents) - Lazuli Bunting, Indigo Bunting, Say's Phoebe, Ash-throated Flycatcher, Horned Lark, Purple Martin, House Wren, Yellow Warbler, Common Yellowthroat, Summer Tanager, Northern Cardinal, Grasshopper Sparrow, Song Sparrow, Eastern Meadowlark, Western Meadowlark and Yellow-headed Blackbird.

Species whose future climatic summer ranges might include the SPRNCA, Arizona - Elegant Quail, Nutting's Flycatcher, Cave Swallow, Sinaloa Martin, Sinaloa Wren, Blue Mockingbird, Painted Bunting, Rusty Sparrow and Black-vented Oriole.

Scale Issues - Macroclimate Versus Microclimate

This (and similar) studies have all examined associations between macroclimate and the continentwide distribution of birds based on data averaged over 50 km x 50 km blocks. A BBS route is 40 km (24.5 miles) long and typically runs through many different habitat types. Thus, the number of birds detected per BBS route is an average collected from all of the habitats the route traverses. The climate variables used in this study represent the average climate for the entire block. Thus, a single climate applies to all habitats in the block. Even though the models are based on the macroclimate of the species, there is evidence that some of the general relationships are also valid in much smaller areas.

Lanyon (1956) examined the sympatric distribution of Eastern and Western Meadowlarks in the north central United States. The zone of overlap between these species increased from

1900 to 1950, largely due to Western Meadowlark spreading east. In areas where distributions overlap, Lanyon found Eastern Meadowlarks occurring in more mesic lowlands and Western Meadowlarks in more xeric uplands. This relationship held throughout the zone of overlap, whether it was in Kansas, Missouri, or Wisconsin. As both species were detected in a variety of plant associations, habitat alone could not be responsible for the differences noted. Lanyon examined the role of climate and discovered a strong correlation between average spring precipitation and the species' preferred habitats. This finding is in concordance with results from previously developed climate-envelope models (Price 1995) - Eastern Meadowlarks were found in areas with an average total spring precipitation of 87 mm; Western Meadowlarks in areas with an average total spring precipitation of 52 mm.

Wiens (1969) studied habitat use among seven species of grassland birds in a 32.4 ha plot in Fitchburg Township, Wisconsin, and noted a relationship between increasing habitat density (both vegetation and litter density) and species use of the habitat. Wiens ranked the habitats from lower density (drier) to higher density (wetter). The species use of these habitats were as follows: Western Meadowlark - Vesper Sparrow - Savannah Sparrow, Grasshopper Sparrow, Eastern Meadowlark - Bobolink - Henslow's Sparrow. The range of differences between these species was small, and considerable overlap occurred. Nevertheless, this ranking is very similar to the climate envelope results presented in Price (1995). When overall average summer precipitation values (averaged across the range of the species where it occurred) are ranked, the resulting species list is as follows: Western Meadowlark - Vesper Sparrow - Savannah Sparrow - [Bobolink] - Grasshopper Sparrow - [Henslow's Sparrow] - Eastern Meadowlark. In comparison to Wiens' ranking, only Bobolink and Henslow's Sparrow are out of position, and the BBS data for Henslow's Sparrow are probably too sparse to accurately rank the species.

These findings suggest there may be a general relationship between microclimate/habitat use and overall macroclimate as determined in this study. This relationship appears to hold for non-grassland species as well. Ongoing research has found a general agreement between local microclimate/habitat use and macroclimate models for Orange-crowned (*Vermivora celata*) and Virginia's Warbler (*V. virginiae*) (T. Martin, U.S. Geological Survey, Missoula, Montana, oral commun.; J. Price, unpub. data); and Blue-winged (*V. pinus*) and Golden-winged Warbler (*V. chrysoptera*) (Confer and Knapp 1981; J. Price, unpub. data). In both of these cases the microclimate used by the species (open, slightly more xeric habitats used by one species versus closed, slightly more mesic habitats used by the other), corresponded with differences in average summer precipitation found between the species pairs. These examples are drawn from species found on many of the same BBS routes; the overall differences in their distributions corresponding to microclimate/habitat differences found where the two overlap in the same field or study area. Few studies have quantitatively measured the localized or microclimate where species are found relative to their overall distribution. Hopefully, these early results will encourage other researchers to measure microclimate in addition to habitat use. This could help determine whether the relationship between macroclimate and microclimate/habitat use is real or coincidental.

The list of potential changes to the avifauna of the SPRNCA are not all-inclusive, since results obtained from models of some species were not adequate to assess how their climatic

ranges might change. Nor do the lists include those species whose climatic ranges may undergo little change. Finally, these lists are based on output from a single, commonly used climate model. There are different models, and results vary between them. While the magnitude of the temperature increase is somewhat similar between models, the projected precipitation changes are often different. Using output from different climate models may therefore yield somewhat different results. In addition, the geographic scale of these models, like those of the underlying climate change model, is relatively coarse. As such, the models are unable to take into account localized topographic changes and the possible existence of suitable microclimates – along rivers, for example. Therefore, some of the species whose *climatic* ranges are projected as shifting out of Illinois may be able to persist if a suitable microclimate is available, especially in montane areas, on north facing slopes, or along riparian areas.

It is helpful to consider how species' ranges may change to know what sorts of changes to look for in the future. Observed evidence and model projections both show that warming is/will be more pronounced by increases in minimum temperatures than maximum (although these will increase as well). Thus, species might be expected to show northward range expansions (including colonization) before they show declines/extirpations in the southern portions of their range. Furthermore, while the average temperature (climate) increases, weather still occurs and some years will be cooler and others warmer than otherwise expected. So, colonization will most likely occur in fits and starts before a species can truly be considered to be established as part of Illinois's breeding avifauna. In some cases, a species may start appearing as a vagrant, off and on, for several years before breeding is attempted. In other cases a species may start breeding in an area, then become extirpated, and then resume breeding – possibly in greater numbers than before.

How quickly distributional changes might occur is unknown. The rate of change will largely depend on whether limits to a given species' distribution are more closely linked with climate (especially temperature), vegetation, or some other factor. The rate of change will also likely be tied to the rate of change of the climate itself. If the climate changes relatively slowly, then species may be able to adapt to the new climate. However, many changes could (and are) occurring relatively quickly. One pilot study found that the average latitude of occurrence of some species of neotropical migrants has already shifted significantly farther north in the last 20 years, by an average distance of almost 60 miles (100 km) (Price, unpublished data). In another study, the arrival date of 20 species of migratory birds was found to be 21 days earlier in 1994 than in 1965 (Root, unpublished data, Price and Root 2000). Many other species have been found to be arriving and breeding earlier, not only in the US but in Europe and elsewhere (Root et al. 2003).

Shifts in individual species' distributions are only part of the story. It is unlikely that ranges of coexisting species will shift in concert. Bird communities, as we currently know them, may look quite different in the future. As species move, they may have to deal with different prey, predators and competitors. So-called "optimal" habitats may no longer exist, at least in the short term. The potential rates-of-change of birds and the plants that shape their habitats are often quite different. While many birds may be able to respond quickly to a changing climate, some plant ranges may take from decades to centuries to move (Davis and Zabiniski 1992).

Thus, some species may face a bottleneck with physiological limits pressing them to move but having no habitat available to move into. This may be especially true for the grassland birds.

Conservation

The BBS was established to monitor trends in the populations of birds summering in the United States and Canada. Conservation plans are currently being prepared by Partners in Flight for many bird species and their habitats. These plans include attempts to identify reasons for population declines, identification of critical habitat for the species, and recommendations of possible steps that could be taken to minimize further declines. Recovery efforts to reverse population declines often center on acquisition of tracts of suitable habitat, or reserves, for the species. As many species are projected potentially to undergo northward shifts in their ranges with changes in the climate. This further complicates the design of reserves. Areas where a species is currently present may not contain the species in the future. Peters (1992) reviewed the difficulties of establishing reserves in the face of habitat loss and climate change. He recommended that reserves be designed and established now, using the best available information. If reserve planning waits until the climate has changed, the habitat may be too fragmented to support the species. However, planned reserves should take into account projected impacts from climate change. If a reserve is placed based on current climate conditions, the conditions could become unsuitable for the species. For many species it is now possible to identify geographic areas that are projected to be climatically suitable for the species both now and under climate change conditions. Preferentially placing reserves in those areas might help offset some of the impacts of climate change. Even with proper planning, it might be necessary to take an active role in the preservation of the species. This could include establishing proper habitat, as well as translocating species into new, more climatically suitable, areas (Peters 1992). However, such efforts are expensive and carry their own risks (IPCC 2001).

Other Climate Models

There are many different general circulation models, each differing in their predictions as to the changes expected with a doubling of carbon dioxide. Most models agree as to the direction of change in temperature, and as to how these changes may differ across the continent (IPCC 1990). However, they disagree as to the extent and, sometimes, the direction of changes in precipitation (NAO 2000). The results presented here were based on output from the CCC. If output from a different GCM were used, the predicted distributions would differ. For species with ranges largely associated with temperature, the differences would most likely be relatively minor (e.g., the distribution might not shift as far north). For species with ranges largely associated with precipitation, the differences could potentially lead to results opposite of those presented here. The results of this study should not be taken as firm projections as to how these species' distributions might change. Rather, they should be viewed as first approximations of the types of changes in avian distributions likely to occur under climate change. The logistic regression models presented here are not restricted to a single GCM. They could be coupled with any GCM that provided monthly summary output for maximum temperature, minimum temperature, and precipitation. As GCMs improve, and their results begin to converge, the output can be used to refine the predictions of how bird distributions might change. Projected

changes in distribution presented here are based on a doubling of atmospheric carbon dioxide, the value that atmospheric modelers frequently incorporate into GCMs. Greater increases in greenhouse gases would lead to greater temperature increases and other climate changes. This, in turn, would lead to even greater impacts on avian distributions.

Projected future rapid climate change is of major concern, especially when viewed in concert with other already well-established population stresses (e.g., habitat conversion, pollution, invasive species). Research and conservation attention needs to be focused not only on each stressor by itself, but also on the synergies of multiple stressors acting together. These synergistic stresses are likely to prove to be the greatest challenge to wildlife conservation in the 21st Century. Because anticipation of changes improves the capacity to manage, it is important to understand as much as possible about the responses of animals to a changing climate.

Managers may ultimately need to adapt not only in terms of wildlife conservation but also to replace lost ecological services normally provided by wildlife. For example, it may be necessary to develop adaptations to losses to natural pest control, pollination and seed dispersal. While replacing providers of these services may sometimes be possible, the alternatives may be costly. Finding a replacement for other services, such as contributions to nutrient cycling and ecosystem stability/biodiversity are much harder to imagine. In many cases, losses of the values of wildlife associated with subsistence hunting, cultural and religious ceremonies, any attempt at replacement may represent a net loss.

SECTION 5 CHANGES IN ECOSYSTEM SERVICES

5.1 Ecosystem Services - General

Ecosystem goods and services are “the conditions and processes through which natural ecosystems ... sustain and fulfill human life”, (Daily, 1997). Important examples include soil renewal, pest control by predators, water purification, mitigation of floods and droughts by wetlands, insect pollination of crops, and harvestable biota. These and other goods and services are essential components of the human life-support system, most of which would be technically and financially impossible to artificially replicate.

Ecosystem services may be *extrinsic*, that is they are the “products” of ecosystem processes and/or characteristics that directly benefit humans, for example harvestable plants or wildlife. They can also be *intrinsic*, that is they are important in supporting ecosystem processes or conditions that may directly benefit humans. Examples of the latter may include ecosystem features that support biodiversity, which, in turn, may facilitate harvesting of plants or wildlife or other such extrinsic services.

Despite their great value, the human record of stewardship of ecosystem goods and services has often been poor. Largely out of a lack of understanding, or through knowingly ignoring or underestimating their real value, humans have often destroyed or impaired the ability of ecosystems to continue providing important services. In some areas, society now finds itself attempting to turn back the clock and restore, often at great cost and with limited success, services once freely available (e.g., efforts to reforest mountain ranges, restore wetlands, or eliminate invasive species from communities that previously provided erosion control, wildlife habitat, or any number of other services (Mooney and Hobbs, 2000; NRC, 1992; Strange et al., 2002).

Several attempts have been made to calculate the economic value of these goods and services. Although the accuracy and precision of these attempts may be debatable, they have merit in that they draw attention to and emphasize their enormous economic importance. Previous estimates include: between US\$8,977 and \$17,000 (1983 dollars) for the goods and services provided by each acre of Louisiana wetlands (Costanza et al., 1989), and between US\$19 million and US\$70 million per year for a 45-mile stretch of the Platte River, Colorado (Loomis et al., 2000). Finally, Costanza et al. (1988) estimated the total annual value of the biosphere’s goods and services to be between US\$16 trillion and US\$54 trillion in 1994 dollars. Regardless of the degrees of precision or accuracy that can be assigned to these estimates, the economic importance of maintaining functioning ecosystems is obvious.

In human-modified landscapes, the survival and condition of ecosystems and their services is often the result of accommodations among competing users (accommodations meaning explicit or implicit agreements among resource users where no one entity is allowed unlimited exploitative rights over a resource, so that other entities may also participate in the use). For example, many services provided by riparian and aquatic ecosystems may only survive in some areas if societal and/or governmental decisions are made to allocate a portion of the key resource

(water) to ecosystem functioning, and not direct it all to (for example) agricultural, or municipal use. The accommodations that result in the protection of ecosystems are, in many cases, renegotiable; this renders ecosystems and the services that they provide vulnerable to changes in stressors.

Human stewardship of ecosystem goods and services has been poor. Largely out of a lack of understanding, or through knowingly ignoring or underestimating their real value, the abilities of ecosystems to continue providing important services have often been impaired or destroyed. In some cases, attempts are now being belatedly made to turn back the clock and restore, often at great cost and with limited success, services that previously were freely available (e.g., current efforts to reforest mountain ranges, reduce contaminants, restore wetlands, or eliminate invasive species from communities that previously provided erosion control, wildlife habitat, biological diversity, or any number of other services [Mooney and Hobbs, 2000; NRC, 1992; Strange et al., 2002]).

Historically, natural systems have been destroyed or impaired by the “traditional” stressors: habitat destruction, overexploitation, contaminants, and the introduction of exotic species. However, the recent advent of another potentially important stressor - global climate change, has greatly increased the penalties for failing to take ecosystem and service protection seriously (Peters and Lovejoy, 1992; Malcolm and Pitelka, 2000). This new stressor is being applied to systems already under considerable pressure from the traditional stressors and that may survive only because of fragile accommodations. This raises important questions: how might climate change, in conjunction with traditional stressors, affect the relevance of these accommodations among users of (for example) water? How might it affect the robustness and resilience of systems that are already stressed by overuse of natural resources, in which biodiversity has been reduced, or that are pervasively contaminated? Above all, how will these interactions affect the abilities of ecosystems to continue providing vital goods and services?

5.2 Ecosystem Services in the SPRNCA

In the studies reported in this document we have attempted to project the future effects of climate change on ecosystem processes and conditions in the riparian habitat of the SPRNCA. This is an area that provides highly valued ecosystem services (specifically, habitat support for high levels of biodiversity, species that are rare or restricted in their status and distribution, and habitat and attractive species that encourage human recreational use). We have projected the future effects of various climate change scenarios on the components of the SPRNCA ecosystem that support the provision of these services, specifically the riparian gallery forest, shrub/forest, and wetlands. In this final section we qualitatively evaluate how the projected changes might affect the important ecosystem services.

5.2.1 Projected ecological changes and their potential effects on ecosystem services

Our projections of future riparian habitat conditions in the SPRNCA are a function of the climate change scenario under consideration: the no change, warmer, and warmer and drier scenarios that we modeled all result in losses of riparian forest and wetlands and their replacement by more

mesic or xeric vegetation communities. What effects would such alterations have on the ecosystem services currently provided by the SPRNCA? First, the high levels of vertebrate, particularly avian, biodiversity in the SPRNCA is due to its juxtaposition of two major habitat types: riparian gallery forest and wetland in a matrix of desert scrub and grassland. Loss or diminution of either of these habitats would reduce the biodiversity that the SPRNCA supports. Thus, the projected loss of the riparian hydrophytic habitats will have an adverse impact on the diversity of species. The San Pedro vulnerability analysis reported in Section 4 indicates that up to about 26% of the bird species that currently inhabit the SPRNCA would be vulnerable to the projected changes. Given the projected vegetation changes, these birds would be replaced by species that are current occupiers of the desert shrub matrix in which the SPRNCA is located. While climate change might also facilitate the expansion of some species north out of Mexico into the SPRNCA area, there are few such species that are not already found there. Thus, there would be a major net loss of avian biodiversity.

The biodiversity numbers, alone, do not tell the full story of how ecosystem services might be affected by the no change, warmer, and warmer and drier climate change scenarios. Many of the species that comprise the 26% that we have identified as potentially harmed are birds that are otherwise rare, restricted, and vulnerable in their North American ranges. Green kingfisher, grey hawk, yellow-billed cuckoo are all relatively rare within the contiguous states. Thus the impacts of climate change on avian biodiversity would be greatest on species that are already threatened for various reasons and for which the San Pedro currently provides one of their rare refuges.

The services discussed thus far could be considered “intrinsic” (see above). However, the SPRNCA also provides important “extrinsic” services – services directly valued and used by humans. As discussed in Section 1, the SPRNCA is a major attraction to wildlife viewers in Arizona, from throughout the U.S. and from abroad. As an example of the latter, it is one of the areas typically included in the itineraries of guided parties of birders from Europe and is well-known among such enthusiasts as a “must-visit” area. The main reason that such visitors are attracted by the SPRNCA is its high avian biodiversity and the presence of species that are difficult to see elsewhere, particularly green kingfisher, grey hawk, and, to a lesser extent, yellow-billed cuckoo, the very species most vulnerable to future climate change.

Another attraction of the SPRNCA to local residents and visitors from further afield is the relative uniqueness of the habitat. Riparian ecosystems elsewhere in North America have been so adversely affected by human land use that areas where mature riparian gallery forest can be experienced and appreciated are few and far between. The SPRNCA is probably the best such area in North America. Thus, visitors are attracted by the sheer impressiveness of the habitat and also by the shaded, cool, walking conditions that the gallery forest provides in an otherwise hot exposed desert environment. If, as projected under the three driest climate change scenarios, this gallery forest were to be fragmented or lost entirely, the attractiveness of the area to the public (one of its ecosystem services) would be reduced.

If future climate conditions more resemble the warm and wet and the warm and very wet scenario, the ecosystem services currently provided by the SPRNCA might be maintained (because of the adequate water supply to the ecosystem under these conditions). However, it is

not possible to predict which of the three drier or the two wetter climate scenarios are most likely.

SECTION 6 REFERENCES

- Abtew, W., J. Obeysekera, and G. Shih. 1993. Spatial analysis for monthly rainfall in south Florida. *Water Resources Bulletin* 29: 179-188.
- Agresti, A. 1990. *Categorical data analysis*. John Wiley & Sons, New York.
- Amlin, N.M. and S.B. Rood. 2001. Comparative tolerances of riparian willows and cottonwoods to water-table decline. *Wetlands* 22: 338-346.
- Amlin, N.M. and S.B. Rood. 2002. Comparative tolerances of riparian willows and cottonwoods to water-table decline. *Wetlands* 22: 338-346.
- Andrade, E.R., Jr., and W.D. Sellers. 1988. El Niño and its effect on precipitation in Arizona and western New Mexico. *Journal of Climatology* 8:403-410.
- Andrewartha, H.G. and L.C. Birch. 1954. *The distribution and abundance of animals*. University of Chicago Press, Chicago.
- Ansley, R.J., D.L. Jones, T.R. Tunnell, B.A. Kramp, and P.W. Jacoby. 1998. Honey mesquite canopy responses to single winter fires: Relation to herbaceous fuel, weather and fire temperature. *International Journal of Wildland Fire* 8:241-252.
- Archer, S., C. Scifres, C.R. Bassham, and R. Maggio. 1988. Autogenic succession in a subtropical savanna conversion of grassland to thorn woodland. *Ecological Monographs* 58:111-128.
- Archer, S., D.S. Schimel, and E.A. Holland. 1995. Mechanisms of shrubland expansion – land-use, climate or CO₂. *Climatic Change* 29:91-99.
- Arias Rojo, H.M. 2000 International groundwaters: The Upper San Pedro River Basin case. *Natural Resources Journal* 40:199-221.
- Arias Rojo, H.M., G. Thomas, J.D. Bredehoeft, R. Lacewell, J. Price, and J.C. Stromberg. 1999. *Sustaining and Enhancing Riparian Migratory Bird Habitat on the Upper San Pedro River*. Commission for Environmental Cooperation. Montreal, Canada.
- Arnold, J.G., J.R. Williams, R. Srinivasan, K.W. King, and R.H. Griggs. 1994. *SWAT: Soil Water Assessment Tool*. USDA, Agricultural Research Service, Grassland, Soil and Water Research Laboratory, Temple, TX.
- Auble, G.T., J.M. Friedman, and M.L. Scott. 1994. Relating riparian vegetation to present and future streamflows. *Ecological Applications* 4:544-554.

- Auble, G.T. and M.L. Scott. 1998. Fluvial disturbance patches and cottonwood recruitment along the upper Missouri River, Montana. *Wetlands* 18:546-556.
- Austin, M.P., A.O. Nicholls, and C.R. Margules. 1990. Measurement of the realized qualitative niche: environmental niches of five *Eucalyptus* species. *Ecological Monographs* 60: 161-177.
- Bagstad, K. 2003. *Herbaceous plants as bioindicators of groundwater decline, San Pedro River, Arizona*. M.S. Thesis, Arizona State University, Tempe, AZ.
- Bahre, C.J. 1991. *A legacy of change – historic human impact on vegetation in the Arizona borderlands*. University of Arizona Press, Tucson.
- Bahre, C.J. and M.L. Shelton. 1993. Historic vegetation change, mesquite increase, and climate in southeastern Arizona. *Journal of Biogeography* 20:489-504.
- Bairlein, F. 1990. Nutrition and Food Selection in Migratory Birds. In: Gwinner E. (ed.) *Bird migration: Physiology and ecophysiology*. Springer-Verlag Berlin, Heidelberg, pp 198 – 213.
- Bairlein F. 1998. The effect of diet composition on migratory fuelling in Garden Warblers *Sylvia Borin*. *Journal of Avian Biology* 29:546 – 551.
- Baron, J.S., M.D. Hartman, T.G.F. Kittel, L.E. Band, D.S. Ojima, and R.B. Lammers. 1998. Effects of land cover, water redistribution, and temperature on ecosystem processes in the South Platte basin. *Ecological Applications*, 84:1037-1051.
- Bendix, J. 1994. Scale, direction, and pattern in riparian vegetation-environment relationships. *Annals of the Association of American Geographers* 84:2977-2990.
- Bent, A.C. 1946. *Life histories of North American jays, crows, and titmice*. United States National Museum Bulletin, 191.
- Birds of North America*. Life Histories for the 21st Century. (A. Poole and F. Gill, eds). The Birds of North America, Inc., Philadelphia, PA.
- Bock, C.E. and J.H. Bock. 1978. Response of birds, small mammals, and vegetation to burning sacaton grasslands in southeastern Arizona. *Journal of Range Management* 31:296-300.
- Boer, G.J., N.A. McFarlane and M. Lazare. 1992. Greenhouse gas-induced climate change simulated with the CCC second-generation general circulation model. *Journal of Climate* 5:1045-1077.
- Botkin, D.P., D.A. Woodby and R.A. Nisbet. 1991. Kirtland's Warbler habitat: a possible early indicator of climate warming. *Biological Conservation* 56: 63-78.
- Brennan, L.A., W.M. Block and R.J. Gutierrez. 1986. The use of multivariate statistics for developing habitat suitability index models, in Verner, J. et al. (eds.). *Wildlife 2000: modeling habitat relationships of terrestrial vertebrates*. University of Wisconsin Press, Madison, WI.

Brown, D.E. (ed.). 1994. *Biotic communities of the American Southwest – United States and Mexico*. University of Utah Press, Salt Lake City, UT.

Bryan, K. 1928. Change in plant associations by change in ground water level. *Ecology* 9:474-478.

Burgess, T.L. 1995. Desert grassland, mixed shrub savanna, shrub steppe, or semidesert grassland? Pages 31-67 in M.P. McClaran and T.R. Van Devender, (eds.). *The Desert Grassland*. The University of Arizona Press, Tucson, AZ.

Busby, J.R. 1986. A biogeoclimatic analysis of *Nothofagus cunninghamii* Hook Oerst in south-eastern Australia. *Australian Journal of Ecology* 11: 1-7.

Busch, D.E. 1995. Effects of fire on southwestern riparian plant community structure. *Southwest Naturalist* 40:259-267.

Busch, D.E. and S.D. Smith. 1995. Mechanisms associated with decline of woody species in riparian ecosystems of the southwestern US. *Ecological Monographs* 65:347-370.

Canadian Climate Centre. 1990. *Application of the Canadian Climate Centre general circulation model output for regional climate impact studies - guidelines for users, version 1*. Canadian Climate Centre, Atmospheric Environment Centre, Downsview, Ontario.

Center for Biological Diversity (CBD). 1998. Petition to list the yellow-billed cuckoo as a federally endangered species. Petition to Mr. Bruce Babbitt, Secretary of the Interior.

Cody, M.L. 1985. Habitat selection in grassland and open-country birds, pp. 191-226 in Cody, M.L., ed., *Habitat selection in birds*. Academic Press, San Diego, CA.

Confer, J.L. and K. Kapp. 1981. Golden-winged Warblers and Blue-winged Warblers: the relative success of a habitat specialist and a generalist. *Auk* 98: 108-114.

Cooper, D.J., D.C. Andersen, and R.A. Chimner. 2003. Multiple pathways for woody plant establishment on floodplains at local to regional scales. *Journal of Ecology* 91:182-196.

Costanza, R., S.C. Farber, and J. Maxwell. 1989. Valuation and management of wetland ecosystems. *Ecological Economics*, 1:335-361.

Costanza, R., R. d'Arge, R. de root, S. Farber, M. Grasso, B. Hannon, K. Limburg, S. Naeem, R.V. O'Neill, J. Paruelo, R.G. Raskin, P. Sutton, and M. van den Belt. 1997. The value of the world's ecosystem services and natural capital. *Nature*, 387:253-260.

Cox, J., H.L. Morton, J.T. LaBaume, and K.G. Renard. 1983. Reviving Arizona's rangelands. *Journal of Soil and Water Conservation* 38:342-345.

- Cox, J.R. and H.L. Morton. 1986. Big sacaton (*Sporobolus wrightii*) riparian grassland management: annual winter burning, annual winter mowing, and spring-summer grazing. *Applied Agricultural Research* 1:105-111.
- Cox, J.R. 1988. Seasonal burning and mowing impacts on *Sporobolus-wrightii* grasslands. *Journal of Range Management* 41:12-15.
- Cressie, N. 1989. Geostatistics. *American Statistician* 43: 197-202.
- Cressie, N. 1990. The origins of kriging. *Mathematical Geology* 22: 239-252.
- Dahm, C.N. and M.C. Molles, Jr. 1992. Streams in semi-arid regions as sensitive indicators of global climate change. Pages 250-260 in P. Firth and S. Fisher, (eds.). *Global Climate Change and Freshwater Ecosystems*, Springer-Verlag, New York, NY.
- Daily, G.C. 1997. Introduction: what are ecosystem services? In: *Nature's Services. Societal Dependence on Natural Ecosystems*. G.C. Daily (ed.), Island Press, Washington, DC.
- Davis, G.P., Jr. 1982. *Man and wildlife in Arizona – the American exploration period 1824-1865*. The Arizona Game and Fish Department, Phoenix, AZ.
- Davis, M.B. and C. Zabinski. 1992. Changes in geographical range resulting from greenhouse warming: effects on biodiversity in forests. Pp. 297-308 in R. L. Peters and T. E. Lovejoy. *Global Warming and Biological Diversity*. Yale University Press, New Haven, CT.
- Dawson, D.K., L.J. Darr and C.S. Robbins. 1993. Predicting the distribution of breeding forest birds in a fragmented landscape. *Transactions of the North American Wildlife and Natural Resources Conference* 58: 35-43.
- DeCamps, H. 1993. River margins and environmental change. *Ecological Applications* 3:441-445.
- DeSante, D. and P. Pyle. 1986. *Distributional checklist of North American birds*. Artemisia Press, Lee Vining, CA.
- Dixon, M.D. and W.C. Johnson. 1999. Riparian vegetation along the middle Snake River, Idaho: zonation, geographical trends, and historical changes. *Great Basin Naturalist*
- Dixon, M. D. 2003a. *Prototype Model of Riparian Vegetation Dynamics for the Upper San Pedro River*. 4th Quarter 2002 Report to American Bird Conservancy.
- Dixon, M.D. 2003b. *Sample Runs of Riparian Vegetation Model for the Upper San Pedro River*. 1st Quarter 2003 Report to the American Bird Conservancy.
- Dixon, M.D. 2003c. *Estimates of Channel Migration Rates for the Upper San Pedro River*. 2nd Quarter 2003 Report to the American Bird Conservancy.

- Doherty, R. and L.O. Mearns. 1999. *A comparison of simulations of current climate from two coupled atmosphere-ocean global climate models against observations and evaluation of their future climates*. Report to the National Institute for Global Environmental Change (NIGEC), Boulder, CO.
- Drewa, P.B. 2003. Effects of fire season and intensity on *Prosopis glandulosa* Torr. var. *glandulosa*. *International Journal of Wildland Fire* 12:147-157.
- Dunning, J.B., R.K. Bowers, S.J. Suter, and C.E. Bock 1999. Cassin's sparrow. *The Birds of North America. Life Histories for the 21st Century. No. 471* (A. Poole and F. Gill, eds). The Birds of North America, Inc., Philadelphia, PA.
- Easterling, D.R., G.A. Meehl, C. Parmesan, S.A. Changnon, T.R. Karl, and L.O. Mearns. 2000. Climate extremes: observations, modeling, and impacts. *Science* 289:2068-2074.
- Ellis, L.M. 2001. Short-term response of woody plants to fire in a Rio Grande riparian forest, central New Mexico, USA. *Biological Conservation* 97:159-170.
- Fenner, P., W. W. Brady, and D. R. Patton. 1985. Effects of regulated water flows on regeneration of Fremont cottonwood. *Journal of Range Management* 38:135-138.
- Friedman, J.M., W.R. Osterkamp, and W.M. Lewis. 1996. Channel narrowing and vegetation development following a Great Plains flood. *Ecology* 77:2167-2181.
- Galbraith, H., and J.Price. 2002. *Predicting the potential risk of climate change to animals listed under the Endangered Species Act*. Report to U.S. EPA, Office of Research and Development, January, 2002.
- Galbraith, H., K. LeJeune, and J. Lipton. 1996. Metal and Arsenic Impacts to Soils, Vegetation Communities, and Wildlife Habitat in Southwest Montana Uplands Contaminated by Smelter Emissions: I Field Evaluation. *Environmental Toxicology and Chemistry*. 14:1895-1903.
- Gao, Q. and J.F. Reynolds. 2003. Historical shrub-grass transitions in the northern Chihuahuan Desert: modeling the effects of shifting rainfall seasonality and event size over a landscape gradient. *Global Change Biology* 9:1475-1493.
- Gardner, R. H., W. W. Hargrove, M. G. Turner, and W. H. Romme. 1996. Climate change, disturbances and landscape dynamics. Pp. 149-172 In: B. Walker and W. Steffen (eds.). *Global change and terrestrial ecosystems*. Cambridge University Press, Cambridge, U.K.
- George, T.L., A.C. Fowler, R.L. Knight and L.C. McEwen. 1992. Impacts of a severe drought on grassland birds in western North Dakota. *Ecological Applications* 2: 275-284.

- Giorgi, F., L.O. Mearns, C. Shields, and L. McDaniel. 1998. Regional nested model simulations of present day and 2 X CO₂ climate over the Central Plains of the U.S. *Climatic Change* 40:457-493.
- Glassy, J.M. and S.W. Running. 1994. Validating diurnal climatology of the MT-CLIM model across a climatic gradient in Oregon. *Ecological Applications* 4:248-257.
- Glendening, C.E. and H.A. Paulsen. 1955. *Reproduction and establishment of velvet mesquite as related to invasion of semidesert grasslands*. USDA Technical Bulletin 1127:1-50.
- Glinski, R. L. and D.E. Brown. 1982. Mesquite (*Prosopis juliflora*) response to severe freezing in southeastern Arizona, USA. *Journal of the Arizona Academy of Science* 17:15-18.
- Glinski, R.L. 1977. Regeneration and distribution of sycamore and cottonwood trees along Sonoita Creek, Santa Cruz County, Arizona. Pp. 116-123 In: *Importance, Preservation and Management of Riparian Habitat: A Symposium*. USDA Forest Service General Technical Report RM-43.
- Goode, T.C., and T. Maddock. Undated. *Simulation of groundwater conditions in the upper San Pedro Basin for the evaluation of alternative futures*. Report from Department of Hydrology and Water Resources, University of Arizona, Tucson, AZ.
- Goode, T.C., T. Maddock III. 2000. *Simulation of groundwater conditions in the Upper San Pedro Basin for the evaluation of alternative futures*. University of Arizona Department of Hydrology and Water Resources and Research Laboratory for Riparian Studies report HWR 00-030, Tucson, Arizona.
- Goodrich, D.C., R. Scott, J. Qi., B. Goff, C.L. Unkrich, M.S. Moran, D. Williams, S. Schaeffer, K. Snyder, R. Mac Nish, T. Kaddock, D. Pool, A. Chehbouni, D.I. Cooper, W.E. Eichinger, W.J. Shuttleworth, Y. Kerr, R. Marsett, and W. Ni. 2000. Seasonal estimates of riparian evapotranspiration using remote and *in-situ* measurements. *Agricultural and Forest Meteorology* 105(1-3): 281-309.
- Graber J.W., and R.R. Graber. 1983. Feeding rates of warblers in spring. *Condor* 85:139-150.
- Grabherr, G., M. Gottfried, and H. Pauli. 1994. Climate effects on mountain plants. *Nature* 369: 448.
- Graf, W.L. 1985. *The Colorado River – Instability and Basin Management*. Resource Publications in Geography, State College, Pennsylvania.
- Griffiths, D. 1901. *Range improvement in Arizona: Cooperative experiments with the Arizona Experiment Station*. USDA Bureau of Plant Industry – Bulletin No. 4. Government Printing Office, Washington DC, 31 p.

Grimm, N.B., A. Chacon, C.N. Dahm, S.W. Hostetler, O.T. Lind, P.L. Starkweather, and W.W. Wurtsbaugh. 1997 Sensitivity of aquatic ecosystems to climatic and anthropogenic changes: The Basin and Range, American Southwest and Mexico. *Hydrological Processes* 11:1023-1041.

Grinnell, J. 1917. The niche-relationships of the California Thrasher. *Auk* 34: 427-433.

Grover, H.D. and H.B. Musick. 1990. Shrubland encroachment in southern New Mexico, USA: An analysis of desertification processes in the American Southwest. *Climatic Change* 17:305-330.

Halterman, M.D. 1991. *Distribution and habitat use of the Yellow-billed Cuckoo on the Sacramento River, California, 1987-1990*. MS Thesis, California State University, Chico.

Hamlet, A.F and D.P. Lettenmaier. 1999 Effects of climate change on hydrology and water resources in the Columbia River basin. *Journal of the American Water Resources Association* 35:1597-1623.

Hanson, J. 2003. River of birds. *The Nature Conservancy*, pp 76-80.

Hanson, R.B. 2001. *The San Pedro River: A Discovery Guide*. University of Arizona Press, Tucson, AZ.

Hastings, J. R. 1959. Vegetation change and arroyo cutting in southeastern Arizona. *Journal of the Arizona Academy of Science* 1:60-67.

Hastings, J.R. and R.M. Turner. 1965. *The changing mile: an ecological study of vegetation change with time in the lower mile of an arid and semiarid region*. University of Arizona Press, Tucson, AZ.

Hendrickson, D.A. and W.L. Minckley. 1984. Cienegas – Vanishing climax communities of the American Southwest. *Desert Plants* 6:131-175.

Hereford, R. 1993. *Entrenchment and widening of the Upper San Pedro, Arizona*. Geological Society of America Special Paper 282, 46 p.

Hernandez, M., S.N. Miller, D.C. Goodrich, B.F. Goff, W.G. Kepner, C.M. Edmonds, and K.B. Jones. 2000. Modeling runoff response to land cover and rainfall spatial variability in semi-arid watersheds. *Environmental Monitoring and Assessment* 64:285-298.

Hernandez, M., W.G. Kepner, D.J. Semmens, D.W. Ebert, D.C. Goodrich, and S.N. Miller. 2003. *Integrating a landscape/hydrologic analysis for watershed assessment*. The First Interagency Conference on Research in the Watersheds, 27-30 October 2003, Benson, AZ.

Horton, J.L. and J.L. Clark 2001. Water table decline alters growth and survival of *Salix gooddingii* and *Tamarix chinensis* seedlings. *Forest Ecology and Management* 140:239-247.

Horton J.L., T.E. Kolb and S.C. Hart. 2001. Responses of riparian trees to interannual variation in groundwater depth in a semi-arid river basin. *Plant, Cell and Environment* 24:293-304.

Horton, J.S. 1977. The development and perpetuation of the permanent tamarisk type in the phreatophyte zone of the Southwest. Pp. 124-127 In: *Importance, Preservation and Management of Riparian Habitat: A Symposium*. USDA Forest Service General Technical Report RM-43.

Hosmer, D.W. and S. Lemeshow. 1989. *Applied logistic regression*. John Wiley & Sons, New York

Houghton, J.T., Y. Ding, D.J. Griggs, M. Noguer, P.T. van der Linden, X. Dai, K. Maskell, and C.A Johnson. 2001. *Climate Change 2001: The Scientific Basis*. Cambridge University Press, Cambridge, UK. 944 p.

Huckleberry, G. 1994. Contrasting channel response to flooding on the middle Gila River, Arizona. *Geology* 22:1083-1086.

Huckleberry, G. 1996. *Historical channel changes on the San Pedro River, southeastern Arizona*. Arizona Geological Survey Open File Report 96-15.

Hughes, J.M. 1999. *Yellow-billed cuckoo*. The Birds of North America. Life Histories for the 21st Century. No. 418 (A. Poole and F. Gill, eds). The Birds of North America, Inc., Philadelphia, PA.

Hunt, A.G. 1999. Understanding a possible correlation between El Niño occurrence frequency and global warming. *Bulletin of the American Meteorological Society* 80:297-300.

Idso, S.B. 1992. Shrubland expansion in the American Southwest. *Climatic Change* 22:85-86.

Intergovernmental Panel on Climate Change [IPCC], 1990, *Climate change: the IPCC Scientific Assessment*. Cambridge University Press, Cambridge, England.

Intergovernmental Panel on Climate Change [IPCC], 2001, *Climate change 2001: the IPCC Scientific Assessment, Third Assessment Report*. Cambridge University Press, Cambridge, England,

Isaaks, E.H. and R.M. Srivastava. 1989. *An introduction to applied geostatistics*. Oxford University Press, Oxford, U.K.

Johnson, D.H. 1981. The use and misuse of statistics in wildlife habitat studies, Pp. 11-19 in Capen, D.E., ed., *The use of multivariate statistics in studies of wildlife habitat*. U.S. Dept. of Agriculture, Forest Service, General Technical Report RM-87. Rocky Mountain Forest Range Experimental Station. Fort Collins, CO.

- Johnson, N.K. 1978. Patterns of avian geography and speciation in the intermountain region. *Great Basin Naturalist Memoirs* 2: 137-159.
- Judd, J.B., J.M. Laughlin, H.R. Guenther, and R. Handergrade. 1971. The lethal decline of mesquite on the Casa Grande National Monument. *Great Basin Naturalist* 31:153-159.
- Kalischuk, A.R., S.B. Rood, and J.M. Mahoney. 2001. Environmental influences on seedling growth of cottonwood species following a major flood. *Forest Ecology and Management* 144:75-89.
- Kauffman, J.B. and W.C. Krueger. 1984. Livestock impacts on riparian ecosystems and streamside management implications: a review. *Journal of Range Management* 37:430-437.
- Kaiser A. 1999. Stopover strategies in birds: a review of methods for estimating stopover length. *Bird Study* 46:299-308.
- Kaufman, K. 1996. *Lives of North American Birds*. Houghton Mifflin Company. Boston.
- Keane, R.E., P. Morgan, and S.E. Running. 1996. *FIRE-BGC: a mechanistic ecological process model for simulating fire succession on coniferous forest landscapes of the northern Rocky Mountains*. USDA Forest Service Research Paper INT-484.
- Kendeigh, S.C. 1934. The role of environment in the life of birds. *Ecological Monographs*, 4: 297-417.
- Kepner, W.G., C.J. Watts, C.E. Edmonds, J.K. Maingi, S.E. Marsh, and G. Luna. 2000. A landscape approach for detecting and evaluating change in a semi-arid environment. *Environmental Monitoring and Assessment* 645:179-195.
- Kepner, W.G., C.M. Edmonds, and C.J. Watts. 2002. *Remote sensing and geographic information systems for decision analysis in public resource administration: a case study of the 25 years of landscape change in a southwestern watershed*. EPA/600/R-02/039, US-EPA, Office of Research and Development, National Exposure Research Laboratory, Las Vegas, NV.
- Kepner, W.G., D.J. Semmens, S.D. Bassett, D.A. Mouat, and D.C. Goodrich. 2004. Scenario analysis for the San Pedro River, analyzing hydrological consequences of a future environment. *Environmental Monitoring and Assessment* 94:115-117.
- Kimball, J.S., S.W. Running, and R. Nemani. 1997. An improved method for estimating surface humidity from daily minimum temperature. *Agricultural and Forest Meteorology* 85:87-98.
- Kitzberger, T., T.W. Swetnam, and T.T. Veblen. 2001. Inter-hemispheric synchrony of forest fires and the El Niño-Southern Oscillation. *Global Ecology and Biogeography* 10: 315-326.
- Klaassen M. 1996. Metabolic constraints on long-distance migration in birds. *Journal of Experimental Biology* 199:57-64.

- Klaassen M, A. Lindstrom, and R. Zijlstra. 1997. Composition of fuel stores and digestive limitations to fuel deposition rate in the long-distance migratory thrush nightingale, *Luscinia luscinia*. *Physiological Zoology* 70:125 – 133.
- Knopf, F.L., R.R. Johnson, T. Rich, F.B. Samson, and R.C. Szaro. 1988. Conservation of riparian ecosystems in the United States. *Wilson Bulletin*, 100:272-284.
- Knutson, M.G., J.P. Hoover, and E.E. Klaas. 1996. The importance of floodplain forests in the conservation and management of neotropical migratory birds in the Midwest. In F.R. Thompson (ed.) *Management of mid-western landscapes for the conservation of neotropical migratory birds*. U.S. Forest Service General Technical Report NC-187.
- Krebs, C.J. 1985. *Ecology: the experimental analysis of distribution and abundance* (3d ed.). Harper & Row, New York.
- Krueper D., J.Bart, and T.D. Rich. 2003. Response of vegetation and breeding birds to the removal of cattle on the San Pedro River, Arizona (USA). *Conservation Biology* 17: 607-615.
- Krueper, D. 1997. *Annotated Checklist to the Birds of the Upper San Pedro River Valley*. Unpublished report – Bureau of Land Management. San Pedro Riparian National Conservation Area.
- Kuenzi, A.J., F.R. Moore, and T.R. Simons. 1991. Stopover of neotropical landbird migrants on East Ship Island following trans-gulf migration. *Condor* 93:869 – 883.
- Kvist, A., and L. Ake. 2003. Gluttony in migratory waders -- unprecedented energy assimilation rates in vertebrates. *Oikos* 103:397-402.
- Lanyon, W.E. 1956. Ecological aspects of the sympatric distribution of meadowlarks in the North-Central States. *Ecology*, 37: 98-108.
- Larsen, E.W. and S. E. Greco. 2002. Modeling channel management impacts on river migration: a case study of Woodson Bridge State Recreation Area, Sacramento River, California. *Environmental Management* 30(2):209-224.
- Laymon. S.A. 1980. *Feeding and nesting behavior of the yellow-billed cuckoo in the Sacramento Valley Wildlife Management Branch Administration Rep.* 80-2. California Department of Fish and Game, Sacramento.
- Laymon, S.A. and M.D. Halterman. 1987. Can the western subspecies of Yellow-billed Cuckoo be saved from extinction? *Western Birds* 18:19-25.
- Leberg P.L., T.J. Spengler, and W.C. Barrow. 1996. Lipid and water depletion in migrating passerines following passage over the Gulf of Mexico. *Oecologia* 106:1-7.

- Leenhouts, J. 2003. *San Pedro River, AZ, Gila River Basin, Part 9 – 2002 – Regular Station Flood-inundation Analysis (unpublished report)*.
- Lesica P. and S. Miles. 2001. Tamarisk growth at the northern margin of its naturalized range in Montana, USA. *Wetlands* 21: 240-246.
- Lindenmayer, D.B., H.A. Nix, J.P. McMahon, M.F. Hutchinson and M.T. Tanton. 1991. The conservation of Leadbeater's Possum, *Gymnobelideus leadbeateri* (McCoy): a case study in the use of bioclimatic modeling. *Journal of Biogeography*, 18: 371-383.
- Lindstrom A., and T. Piersma. 1993. Mass changes in migrating birds - the evidence for fat and protein storage reexamined. *Ibis* 135:70 – 78.
- Lite S.J. 2003. *San Pedro River riparian vegetation across water availability and flood disturbance gradients*. PhD dissertation. Arizona State University, Tempe, Arizona.
- Loomis, J., P. Kent, L. Strange, K. Fausch, and A. Covich. 2000. Measuring the total economic value of restoring ecosystem services in an impaired river basin: results from a contingent valuation study. *Ecological Economics*, 33:103-117.
- Mace, G. and Stuart, S. 1994. Draft IUCN Red List categories. *Species*, 21-22:13-24.
- Mahoney J.M. and S.B. Rood. 1998. Streamflow requirements for cottonwood seedling recruitment - an integrative model. *Wetlands* 18: 634-645.
- Makings, E. In press. Flora of the San Pedro River National Conservation Area, Cochise County, Arizona. In Proceedings of the 2nd Conference on Biodiversity and Management of the Madrean Archipelago.
- Malcolm, J.R., and L.F. Pitelka. 2000. *Ecosystems and Global Climate Change. A Review of Potential Impacts on U.S. Terrestrial Ecosystems and Biodiversity*. Pew Center on Global Climate Change, Arlington, VA.
- Mantua, N.J., S.R. Hare, Y. Zhang, J.M. Wallace, and R.C. Francis. 1997. A Pacific interdecadal climate oscillation with impacts on salmon production. *Bulletin of the American Meteorological Society* 78:1069-1079.
- Martinez, A. and J. Lopez-Portillo. 2003. Allometry of *Prosopis glandulosa* var *torreyana* along a topographic gradient in the Chihuahuan desert. *Journal of Vegetation Science* 14:111-120.
- Marzluff, J.M. 1986. Assumptions and design of regression experiments: the importance of lack-of-fit testing, Pp/ 165-170 in Verner, J., and others, eds., *Wildlife 2000: Modeling habitat relationships of terrestrial vertebrates*. University of Wisconsin Press, Madison, Wisconsin.

- McAuliffe, J.R. 2003. The interface between precipitation and vegetation: The importance of soils in arid and semiarid environments. Chapter 2, pages 9-27 in *Changing Precipitation Regimes and Terrestrial Ecosystems: A North American Perspective*, J.F. Weltzin and G.R. McPherson, eds., The University of Arizona Press, Tucson, AZ.
- McCabe, G.J., M.A. Palecki, and J.L. Betancourt. 2004. Pacific and Atlantic Ocean influences on multidecadal drought frequency in the United States. *Proceedings of the National Academy of Science, USA* 101:4136-4141.
- McFarlane, N.A., G.J. Boer, J.-P. Blanchet and M. Lazare. 1992. The Canadian Climate Centre second-generation general circulation model and its equilibrium climate. *Journal of Climate*, 5: 1013-1044.
- McWilliams S.R., and W. Karasov. 2001. Phenotypic flexibility in digestive system structure and function in migratory birds and its ecological significance. *Comparative Biochemistry and Physiology Part A* 128:579-593.
- McPherson G.R. 1995. The role of fire in the desert grasslands. In: *The desert grassland*. M.P. McClaran and T.R. VanDevender, eds. University of Arizona Press, Tucson, AZ.
- Mearns, L.O., I. Bogardi, F.Giorgi, I. Matyasovzsky, and M. Palecki. 1999. Comparison of climate change scenarios generated from regional climate model experiments and statistical downscaling. *Journal of Geophysical Research* 104:6603-6621.
- Miller, C. and D.L. Urban. 1999. A model of surface fire, climate, and forest pattern in the Sierra Nevada, California. *Ecological Modelling* 114:113-135.
- Miller, S.N., W.G. Kepner, M.H. Mehaffey, M. Hernandez, R.C. Miller, D.C. Goodrich, K.K. Devonald, D.T. Heggem, and W.P. Miller. 2002. Integrating landscape assessment and hydrologic modeling for land cover change analysis. *Journal of the American Water Resources Association* 38(4):915-929.
- Minckley, W.L. and T.O. Clark. 1984. Formation and destruction of a Gila River mesquite bosque community. *Desert Plants* 6:23-30.
- Mooney, H.A., and R.J. Hobbs. 2000. *Invasive species in a changing world*. Island Press, Washington, DC.
- Morris, S.R. 1996. Mass loss and probability of stopover by migrant warblers during spring and fall migration. *Journal of Field Ornithology* 67:456 – 462.
- Mosconi, S.L., and R.L. Hutto. 1982. The effects of grazing on land birds of a western Montana riparian habitat. In: *Wildlife-livestock Relationships Symposium: Proc. 10*, Univ. Idaho Forest Wildlife Range Exp. Station, Moscow, ID.

- Nagy, K.A. 1987. Field metabolic rate and food requirement scaling in mammals and birds. *Ecological Monographs* 57:111-128.
- Naiman, R.J. and H. Decamps. 1997. The ecology of interfaces: riparian zones. *Annual Review of Ecology and Systematics* 28:621-658.
- Naiman, R.J., H. Decamps, and M. Pollock. 1993. The role of riparian corridors in maintaining regional biodiversity. *Ecological Applications* 3:209-212.
- Naiman, R.J., G. Pinay, C.A. Johnston, and J. Pastor. 1988. Alteration of North American streams by beaver. *BioScience* 38:73-76.
- National Assessment Synthesis Team [NAST]. 2000. *Climate change impacts on the United States: the potential consequences of climate variability and change*. Cambridge University Press, Cambridge, U.K..
- National Geographic Society. 1987. *Field guide to the birds of North America* (2d ed.): National Geographic Society, Washington, DC.
- National Research Council (NRC). 1992. *Restoration of Aquatic Ecosystems. Science, Technology and Public Policy*. National Academy Press, Washington, DC.
- Neilson, R.P., and R.J. Drapek. 1998. Potentially complex biosphere responses to transient global warming. *Global Change Biology* 4:505-521.
- Neitsch, S.L., J.G. Arnold, J.R. Kiniry, J.R. Williams, and K.W. King. 2002. *Soil and Water Assessment Tool Theoretical Documentation. Version 2000*. Texas Water Resources Institute, College Station, Texas. TWRI Report TR-191.
- Nix, H.A. 1986. *BIOCLIM - a bioclimatic analysis and prediction system*. C.S.I.R.O. Division Water and Land Resources Research Annual Report, C.S.I.R.O., Canberra, Australia.
- Noble, I.R., G.A.V. Bary, and A.M. Gill. 1980. McArthur fire-danger meters expressed as equations. *Australian Journal of Ecology* 5:201-203.
- Norusis, M.J. 1988. *The SPSS guide to data analysis for SPSS/PC+*. SPSS Inc., Chicago.
- Noss, R.R., E.T. Laroe, and J.M. Scott. 1995. *Endangered ecosystems of the United States: a preliminary assessment of loss and degradation*. National Biological Service Biological Report 28. Washington, DC.
- Pardieck K, and B.B. Waide. 1992. Mesh size as a factor in avian community studies using mist nets. *Journal of Field Ornithology* 63:250-255.
- Patten, D.T. 1998. Riparian ecosystems of semi-arid North America: diversity and human impacts. *Wetlands* 18:498-512.

- Pereira, J.M.C. and R.M. Itami. 1991. GIS-based habitat modeling using logistic multiple regression: a study on the Mt. Graham red squirrel. *Photogrammetric Engineering and Remote Sensing*, 57: 1475-1486.
- Peters, R.L. 1992. Conservation of biological diversity in the face of climate change, Pp. 15-30 in Peters, R., and Lovejoy, T., eds., *Global warming and biological diversity*. Yale University Press, New Haven, CT.
- Peters, R.L., and T.E. Lovejoy. 1992. *Global Warming and Biodiversity*. Yale University Press. New Haven.
- Peterson, R.T. 1980. *A field guide to the birds of eastern and central North America*. Houghton Mifflin, Boston.
- Peterson, R.T. 1990. *A field guide to western birds*. Houghton Mifflin, Boston.
- Philips, A. J. Marshall, and G. Monson. 1964. *The Birds of Arizona*. University of Arizona Press, Tucson.
- Phillips, W.S. 1963. Depth of roots in soil. *Ecology* 44:424.
- Pockman, W.T. and J.S. Sperry. 2000. Vulnerability to xylem cavitation and the distribution of Sonoran desert vegetation. *American Journal of Botany* 87:1287-1299.
- Pool, D.R. and A.L. Coes. 1999. *Hydrogeologic investigations of the Sierra Vista subwatershed of the Upper San Pedro Basin, Cochise County, Southeast Arizona*. Water-Resources Investigations Report 99-4197.
- Price, J. T. In press. *Potential Impacts of Climate Change on the Summer Distributions of Some North American Grassland Birds*. U.S.G.S. Technical Report.
- Price, J. 2001. Modeling the potential impacts of climate change on the summer distributions of Georgia's nongame birds. *The Oriole* 66(2): 1-8.
- Price, J. 2000a. Climate change and bird distributions in the Mid-Atlantic Region. Page 32 in A. Fisher et al., (eds). *Preparing for a Changing Climate: Mid-Atlantic Overview for the National Assessment on the Potential Consequences of Climate Change for the United States*. Mid-Atlantic Regional Assessment Report, The Pennsylvania State University, University Park, PA.
- Price, J. 2000b. Modeling the potential impacts of climate change on the summer distributions of Ohio's non-game birds. *Ohio Birds and Natural History* 2(1): 32-39.
- Price, J. 2000c. Modeling the potential impacts of climate change on the summer distributions of Massachusetts' passerines. *Bird Observer* 28(4): 224-230.

- Price, J. 2000d. Modeling the potential impacts of climate change on the summer distributions of Michigan's nongame birds. *Michigan Birds and Natural History* 7(1): 3-13.
- Price, J. 2000e. Modeling the potential impacts of climate change on the summer distribution of Colorado's nongame birds. *Journal of the Colorado Field Ornithologists* 34:160-167.
- Price, J. 2000f. Climate change and Minnesota birds. *Minnesota Birding* 37(2): 14-15.
- Price, J. T. 1995. *Potential Impacts of Global Climate Change on the Summer Distributions of Some North American Grassland Birds*. Ph.D. Dissertation, Wayne State University, Detroit, MI.
- Price, J. T. and P. L. Glick. 2002. *The Birdwatcher's Guide to Global Warming*. National Wildlife Federation and American Bird Conservancy, 36 pp. plus CD-ROM of state fact sheets. Available online at www.abcbirds.org/climatechange/statepage.htm or www.nwf.org/climate/
- Price, J. T. and T. L. Root. 2001. Climate change and Neotropical migrants. *Transactions of the 66th North American Wildlife and Natural Resources Conference*, pp. 371-379.
- Price, J.T. and T.L. Root, 2000. Focus: Effects of climate change on bird distributions and migration patterns. *Pages 65-68 in P.J. Sousounis and J.M. Bisanz (eds.) Preparing for a Changing Climate: The Potential Consequences of Climate Variability and Change*. University of Michigan, Atmospheric, Oceanic, and Space Sciences Dept., Ann Arbor, Michigan.
- Price, J., S. Droege, and A. Price, 1995. *The summer atlas of North American birds*. Academic Press, London.
- Ralph, C.J. and J.M. Scott. 1981. Estimating numbers of terrestrial birds. *Studies in Avian Biology*, 6.
- Reichardt, K.L., B. Schladweiler, and J.L. Sterling. 1978. *An inventory of riparian habitats along the San Pedro River*. Unpublished report submitted to The Nature Conservancy by the Office of Arid Lands Studies, University of Arizona.
- Ricklefs, R.E. 1979. *Ecology* (2d ed.): Chiron Press, NY.
- Robbins, C.S., D. Bystrak and P.H. Geissler. 1986. *The Breeding Bird Survey: its first fifteen years, 1965-1979*. U.S. Fish and Wildlife Service, Resource Publication.
- Robbins, C.S. D.K. Dawson and B.A. Powell. 1989. Habitat area requirements of breeding forest birds in the middle Atlantic states. *Wildlife Monographs*, 103: 1-34.
- Rood, S.B., S. Patiño, K. Coombs, and M.T. Tyree. 2000. Branch sacrifice: cavitation-associated drought adaptation of riparian cottonwoods. *Trees* 14:248-257.
- Rood, S.B., J.H. Braatne, and F.M.R. Hughes. 2003. Ecophysiology of riparian cottonwoods: stream flow dependency, water relations and restoration. *Tree Physiology* 23:1113-1124.

- Root, T.L. 1988a. Environmental factors associated with avian distributional boundaries. *Journal of Biogeography*, 15: 489-505.
- Root, T.L. 1988b. *Atlas of wintering North American birds*. University of Chicago Press, Chicago.
- Root, T.L. 1988c. Energetic constraints on avian distributions and abundances. *Ecology* 69: 330-339.
- Rothermel, R.C. 1972. *A mathematical model for predicting fire spread in wildland fuels*. USDA Forest Service General Technical Report INT-143.
- Russell, R.J. 1931. *Dry climates of the United States*. University of California Publications in Geology, v. 4, p. 1-41.
- Ryan, K.C. and E.D. Reinhardt. 1988. Predicting postfire mortality of seven western conifers. *Canadian Journal of Forest Research* 18:1291-1297.
- Sala, O.E., W.K. Lauenroth, and W.J. Parton. 1992. Long-term soil water dynamics in the shortgrass steppe. *Ecology* 73(4):1175-1181.
- Samuelson, G.M. and S.B. Rood. 2004. Differing influences of natural and artificial disturbances on riparian cottonwoods from prairie to mountain ecoregions in Alberta, Canada. *Journal of Biogeography* 31:435-450.
- SAS Institute Inc. 1992. *SAS/STAT software: changes and enhancements, release 6.07*. SAS technical report P-229, SAS Institute Inc., Cary, NC.
- Sauer, J.R. and S. Droege (eds.). 1990. *Survey designs and statistical methods for the estimation of avian population trends*. U.S. Fish and Wildlife Service Biological Report 90(1).
- Schaub M., and L. Jenni. 2000. Fuel deposition of three passerine bird species along the migration route. *Oecologia* 122:306 – 317.
- Schaub M., and L. Jenni. 2001. Variation of fuelling rates among sites, days and individuals in migrating passerine birds. *Functional Ecology* 15:584 – 594.
- Schneider, S.H. 1993. Scenarios of global warming. Pp. 9-23 in Kingsolver, J., Kareiva, P., and R. Huey (eds.). *Biotic interactions and global change*. Sinauer Associates, Sunderland, MA.
- Schneider, S.H., and T.L. Root. 2002. *Wildlife responses to climate change*. Island Press, Washington, DC.
- Scholes, R.T. and S.R. Archer. 1997. Tree-grass interactions in savannas. *Annual Review of Ecology and Systematics* 28:517-544.

- Scott, R., D. Goodrich, D. Williams, J. Stromberg, and J. Leenhouts. 2002. *San Pedro Riparian National Conservation Area (SPRNCA) Water Needs Study, Year 2001 Progress Report*.
- Scott, R.L., W.J. Shuttleworth, D.C. Goodrich, and T. Maddock, III. 2000. The water use of two dominant vegetation communities in a semiarid riparian ecosystem. *Agricultural and Forest Meteorology* 105:241-256.
- Scott, R.L., C. Watts, J.G. Payan, E. Edwards, D.C. Goodrich, D. Williams, and W.J. Shuttleworth. 2003. The understory and overstory partitioning of energy and water fluxes in an open canopy, semiarid woodland. *Agricultural and Forest Meteorology* 114:127-139.
- Scott, M.L., J.M. Friedman, and G.T. Auble. 1996. Fluvial process and the establishment of bottomland trees. *Geomorphology* 14:327-339.
- Scott M.L., P.B. Shafroth and G.T. Auble. 1999. Responses of riparian cottonwoods to alluvial water table declines. *Environmental Management* 23: 347-358.
- Scott M.L., G.C. Lines and G.T. Auble. 2000. Channel incision and patterns of cottonwood stress and mortality along the Mojave River, California. *Journal of Arid Environments* 44: 399-414.
- Sedgwick, J.A. 2000. *Willow Flycatcher*. The Birds of North America. Life Histories for the 21st Century. No. 533 (A. Poole and F. Gill, eds). The Birds of North America, Inc., Philadelphia, PA.
- Segelquist, C.A., M.L. Scott, and G.T. Auble. 1993. Establishment of *Populus deltoides* under simulated alluvial groundwater declines. *American Midland Naturalist* 130:275-285.
- Sferra, S.J., T.E. Corman, C.E. Paradzick, J.W. Rourke, J.A. Spencer, and M.W. Sumner. 1997. *Arizona Partners in Flight southwestern willow flycatcher survey: 1993-1996 summary report*. Arizona Game and Fish Department. Nongame technical Report 113. Phoenix.
- Shafroth, P.B., J.M. Friedman, and L.S. Ischinger. 1995. Effects of salinity on establishment of *Populus fremontii* (cottonwood) and *Tamarix ramosissima* (saltcedar) in southwestern United States. *Great Basin Naturalist* 55:58-65.
- Shafroth P.B., G.T. Auble, J.C. Stromberg, and D.T. Patten. 1998. Establishment of woody riparian vegetation in relation to annual patterns of streamflow, Bill Williams River, Arizona. *Wetlands* 18: 577-590.
- Shafroth P.B., J.C. Stromberg and D.T. Patten. 2000. Woody riparian vegetation response to different alluvial water table regimes. *Western North American Naturalist* 60:66-76.
- Sheppard, P.R., A.C. Comrie, G.D. Packin, K. Angersbach, and M.K. Hughes. 2002. The climate of the US Southwest. *Climate Research* 21:219-238.

Skagen S.K., C.P. Melcher, W.H. Howe, and F.L. Knopf. 1998. Comparative use of riparian corridors and oases by migrating birds in southeast Arizona. *Conservation Biology* 12: 896-909.

Skirvin, S.M., S.E. Drake, M.P. McClaran, S.E. Marsh, and D.M. Meko. 2000. Climate change and land tenure: Potential impacts on vegetation and development in the San Pedro watershed, southeastern Arizona. *4th International Conference on Integrating GIS and Environmental Modeling (GIS/EM4): Problems, Prospects and Research Needs*. Banff, Alberta, Canada, September 2 - 8, 2000. <http://www.colorado.edu/research/cires/banff/pubpapers/23/>

Smith, J.B. and D.A. Tirpak. 1990. *The potential effects of global climate change on the United States*. Hemisphere Publishing Corp., NY.

Smith S.D., D.A. Devitt, A. Sala, J.R. Cleverly, and D.E. Busch. 1998. Water relations of riparian plants from warm desert regions. *Wetlands* 18: 687-696.

Snyder K.A. and D.G. Williams. 2000. Water sources used by riparian trees varies among stream types on the San Pedro River. *Journal of Agricultural and Forest Meteorology* 105: 227-240.

Sogge, M.K., and R.M. Marshall, 2000. A survey of current breeding habitats. In: *Status, Ecology, and Conservation of the Southwestern Willow Flycatcher*. USDA, Forest Service General Report RMRS-GTR-60.

SRAG (Southwest Regional Assessment Group). 2000. *Preparing for a changing climate: the potential consequences of climate variability and change*. <http://www.ispe.arizona.edu/research/swassess/pdf/complete.pdf>

Steinitz, C., H. Arias, S. Bassett, M. Flaxman, M. Goode, T. Maddock, D. Mouat, R. Peiser, and A. Shearer. 2003. *Alternative Futures for Changing Landscapes, the Upper San Pedro Basin in Arizona and Sonora*. Island Press, Washington, D.C.

Strange, E., H. Galbraith, S. Bickel, D. Mills, D. Beltman, and J. Lipton. 2002. Determining ecological equivalence in service-to-service scaling of salt marsh restoration. *Environmental Management*, 29:290-300.

Stromberg, J.C., D.T. Patten, and B.D. Richter. 1991. Flood flows and dynamics of Sonoran riparian forests. *Rivers* 2:221-235.

Stromberg, J.C., J. Fry, and D.T. Patten. 1997. Marsh development after large floods in an alluvial, arid-land river. *Wetlands* 17:292-300.

Stromberg, J., S. Lite, T. Rychener, and E. Makings. 2003. *San Pedro Water Needs Report*

Stromberg J.C., J.A. Tress, S.D. Wilkins, and S. Clark. 1992. Response of velvet mesquite to groundwater decline. *Journal of Arid Environments* 23:45-58

- Stromberg J.C. 1993. Riparian mesquite forests: a review of their ecology, threats, and recovery potential. *Journal of the Arizona-Nevada Academy of Science* 27:111-124.
- Stromberg J.C., B.D. Richter, D.T. Patten, and L.G. Wolden. 1993a. Response of a Sonoran riparian forest to a 10-year return flood. *Great Basin Naturalist* 53: 118-130.
- Stromberg J.C., S.D. Wilkins, and J.A. Tress. 1993b. Vegetation-hydrology models as management tools for velvet mesquite (*Prosopis velutina*) riparian ecosystems. *Ecological Applications* 3: 307-314.
- Stromberg J.C., R. Tiller, and B. Richter. 1996. Effects of groundwater decline on riparian vegetation of semi-arid regions: The San Pedro River, Arizona. *Ecological Applications* 6: 113-131.
- Stromberg, J.C. 1997. Growth and survivorship of Fremont cottonwood, Goodding willow, and salt cedar seedlings after large floods in central Arizona. *Great Basin Naturalist* 57(3)198-208.
- Stromberg J.C. 1998a. Dynamics of Fremont cottonwood (*Populus fremontii*) and saltcedar (*Tamarix chinensis*) populations along the San Pedro River, Arizona. *Journal of Arid Environments* 40:133-155.
- Stromberg J.C. 1998b. Functional equivalency of saltcedar (*Tamarix chinensis*) and Fremont cottonwood (*Populus fremontii*) along a free-flowing river. *Wetlands* 18: 675-676.
- Swetnam, T.W. and J.L. Betancourt. 1990. Fire-southern oscillation relations in the southwestern United States. *Science* 249:1017-1020.
- Swetnam, T.W. and J.L. Betancourt. 1998. Mesoscale disturbance and ecological response to decadal climate variability in the American Southwest. *Journal of Climate* 11:3128-3147.
- Tellman, B., R. Yarde, and M.G. Wallace. 1997. *Arizona's Changing Rivers: How People have Affected the Rivers*. University of Arizona: Water Resources Center.
- Terborgh, J. 1989. *Where have all the birds gone?* Princeton University Press, Princeton, NJ.
- Thornton, P.E. and S.W. Running. 1999. An improved algorithm for estimating incident daily solar radiation from measurements of temperature, humidity, and precipitation. *Agricultural and Forest Meteorology* 93:211-228.
- Tiller R.L., J.C. Stromberg, D.G. Williams, and K. Snyder. In prep. Productivity and water source use of *Sporobolus wrightii* (big sacaton) along gradients of soil moisture.
- Timmerman, A., J. Oberhuber, A. Bacher, M. Esch, M. Latif, and E. Roeckner. 1999. Increased El Niño frequency in a climate model forced by future greenhouse warming. *Nature* 398:694-697.

Tucker, G.M. and M.F. Heath. (1996). *Birds in Europe: their conservation status*. Cambridge, U.K.: Birdlife International (Birdlife Conservation Series No. 3).

Turnage, W.V. and A.L. Hinckley. 1938. Freezing weather in relation to plant distribution in the Sonoran Desert. *Ecological Monographs* 8:529-550.

U.S. Fish and Wildlife Service, 1997. *Final determination of critical habitat for the southwestern willow flycatcher*. Federal Register 62:39129-39146 (July 22, 1997).

U.S. Fish and Wildlife Service, 2001. *Southwestern willow flycatcher – draft recovery plan*. U.S. Fish and Wildlife Service, Albuquerque, New Mexico.

Van Auken, O.W. 2000. Shrub invasions of North American semiarid grasslands. *Annual Review of Ecology and Systematics* 31:197-215.

Van Wagner, C.E. 1973. Height of crown scorch in forest fires. *Canadian Journal of Forest Research* 3:373-378.

Vionnet, L.B. and T. Maddock. 1992. *Modeling of ground-water flow and surface/ground-water interaction for the San Pedro River basin. Part I. Cananea, Mexico to Fairbank, Arizona*. University of Arizona Department of Hydrology and Water Resources Report HWR 92-010, Tucson, AZ.

Walker, P.A. and K.D. Cocks. 1991. HABITAT: a procedure for modelling a disjoint environmental envelope for a plant or animal species. *Global Ecology and Biogeography Letters* 1: 108-118.

Webb, E.A., and C.E. Bock. 1996. *Botteri's sparrow*. The Birds of North America. Life Histories for the 21st Century. No. 216 (A. Poole and F. Gill, eds). The Birds of North America, Inc., Philadelphia, PA.

Webb, R.H. and J.L. Betancourt. 1992. *Climatic variability and flood frequency of the Santa Cruz River, Pima County, Arizona*. U.S. Geological Survey Water-Supply Paper 2379, 40 p.

Weber T.P., A.I. Houston, B.J. Ens. 1999. Consequences of habitat loss at migratory stopover sites: a theoretical investigation. *Journal of Avian Biology* 30:416 – 426.

Weltzin, J.F. and G.R. McPherson. 1997. Spatial and temporal soil moisture partitioning by trees and grasses in a temperate savanna, Arizona, USA. *Oecologia* 112:156-164.

Westerling, A.L., A. Gershunov, T.J. Brown, D.R. Cayan, and M.D. Dettinger. 2003. Climate and wildfire in the western United States. *Bulletin of the American Meteorological Society* 84:595-603.

- Whitfield, M.J., and K.M. Enos, 1996. *A brown-headed cowbird control program and monitoring for the southwestern willow flycatcher, South Fork Kern River, California, 1996*. California Department of Fish and Game, Sacramento.
- Wiens, J.A. 1969. An approach to the study of ecological relationships among grassland birds. *Ornithological Monographs* 8: 1-93.
- Wood, M. L. 1997. *Historical channel changes along the lower San Pedro River, southeastern Arizona*. Arizona Geological Survey Open-File Report 97-21, 39 p.
- Wright, J.R. and C.L. Hanson. 1990. Crop coefficients for rangeland. *Journal of Range Management* 43:482-485.
- Wu, I.P. 1997. *A simple evapotranspiration model for Hawaii: The Hargreaves model*. Cooperative Extension Service, College of Tropical Agriculture and Human Resources, University of Hawaii at Manoa, CTAHR Fact Sheet, Engineer's Notebook no. 106.
- Xiong S.J., C. Nilsson, M.E. Johansson, and R. Jansson. 2001. Responses of riparian plants to accumulation of silt and plant litter: the importance of plant traits. *Journal of Vegetation Science* 12 (4): 481-490.
- Yong, W. and D.M. Finch. 2002. Consistency of mist netting and point counts in assessing landbird species richness and relative abundance during migration. *Condor* 104: 59-72.
- Yong, W. and D.M. Finch. 1997. Population trends of migratory landbirds along the middle Rio Grande. *Southwestern Naturalist* 42: 137-147.
- Yong W., and D.M. Finch. 1997. Migration of the Willow Flycatcher along the middle Rio Grande. *Wilson Bulletin* 109:253-268.
- Yong W, D.M. Finch, F.R. Moore, and J.F. Kelly. 1998. Stopover ecology and habitat use of migratory Wilson's Warblers. *Auk* 115:829-842.
- Yuncevich, G.M. 1993. *The San Pedro Riparian National Conservation Area*. USDA Forest Service General Technical Report RM 226:369-372.

ATTACHMENT 1 - SIMULATED VEGETATION TRANSITIONS

Attachment 1.1 Simulated vegetation transitions on plots at Contention transect under four climate scenarios.

Site	Plot	Scenario	Patch Type by Year of Simulation				
			2003	2027	2052	2077	2102
Content	10 W	Nochange	mature mesquite shrubs	Sacaton grassland	sacaton grassland	mature mesquite shrubs	old mesquite woods
Content	10 W	Warm	mature mesquite shrubs	Mature mesquite woods	old mesquite shrubs	old mesquite woods	old mesquite woods
Content	10 W	Warmdry	mature mesquite shrubs	Mature mesquite woods	old mesquite woods	old mesquite shrubs	old mesquite woods
Content	10 W	Warmwet	mature mesquite shrubs	Sacaton grassland	mature mesquite shrubs	mature mesquite woods	mature mesquite woods
Content	9W	Nochange	mature2 willow forest	Sacaton grassland	sacaton grassland	sacaton grassland	sacaton grassland
Content	9W	Warm	mature2 willow forest	Sacaton grassland	mature mesquite shrubs	old mesquite forest	old mesquite forest
Content	9W	Warmdry	mature2 willow forest	Mature mesquite woods	old mesquite woods	old mesquite woods	old mesquite forest
Content	9W	Warmwet	mature2 willow forest	mature mesquite woods	old mesquite forest	old mesquite forest	mature mesquite forest
Content	7.5 W	Nochange	sacaton grassland	mature mesquite shrubs	old mesquite woods	old mesquite forest	old mesquite woods
Content	7.5 W	Warm	mixed open	mature mesquite	mature mesquite	old mesquite woods	mature mesquite shrubs

				shrubs	shrubs		
Content	7.5 W	Warmdry	mixed open	mature mesquite woods	old mesquite forest	mature mesquite forest	mature mesquite shrubs
Content	7.5 W	Warmwet	mixed open	mature mesquite woods	old mesquite forest	old mesquite forest	old mesquite woods
Content	6W	Nochange	mixed open	sacaton grassland	sacaton grassland	sacaton grassland	sacaton grassland
Content	6W	Warm	mixed open	sacaton grassland	sacaton grassland	sacaton grassland	mature mesquite shrubs
Content	6W	Warmdry	mixed open	sacaton grassland	sacaton grassland	sacaton grassland	mature mesquite shrubs
Content	6W	Warmwet	mixed open	sacaton grassland	old mesquite shrubs	old mesquite forest	old mesquite woods
Content	5W	Nochange	mixed open	mature mesquite woods	mature mesquite shrubs	sacaton grassland	sacaton grassland
Content	5W	Warm	mixed open	mature mesquite woods	mature mesquite woods	mature mesquite woods	mature mesquite woods
Patch Type by Year of Simulation							
Site	Plot	Scenario	2003	2027	2052	2077	2102
Content	5W	Warmdry	mixed open	sacaton grassland	mature mesquite shrubs	mature mesquite woods	old mesquite woods
Content	5W	Warmwet	mixed open	mature mesquite woods	old mesquite woods	old mesquite forest	mature mesquite woods
Content	4W	Nochange	mixed open	sacaton grassland	sacaton grassland	sacaton grassland	sacaton grassland
Content	4W	Warm	mixed open	mature1 saltcedar shrubs	mature mesquite forest	old mesquite forest	mature mesquite woods

Content	4W	Warmdry	mixed open	mature1 saltcedar shrubs	mature mesquite woods	mature mesquite forest	sacaton grassland
Content	4W	Warmwet	mixed open	sacaton grassland	mature mesquite forest	mature mesquite forest	mature mesquite woods
Content	3W	Nochange	sacaton grassland	Mature2 saltcedar forest	old saltcedar forest	sacaton grassland	sacaton grassland
Content	3W	Warm	sacaton grassland	mature2 saltcedar forest	old saltcedar forest	mature mesquite woods	mature mesquite woods
Content	3W	Warmdry	sacaton grassland	mature1 saltcedar woods	mature2 saltcedar woods	sacaton grassland	mature mesquite shrubs
Content	3W	Warmwet	sacaton grassland	mature2 saltcedar forest	old saltcedar forest	old mesquite forest	old mesquite forest
Content	2.5 W	Nochange	mixed open	sacaton grassland	mature mesquite shrubs	mature1 saltcedar woods	mature2 saltcedar woods
Content	2.5 W	Warm	mixed open	mature1 saltcedar shrubs	mature2 saltcedar forest	mature2 saltcedar forest	old mesquite forest
Content	2.5 W	warmdry	mixed open	mature1 saltcedar shrubs	mature mesquite shrubs	mature mesquite shrubs	mature mesquite forest
Content	2.5 W	warmwet	mixed open	mature1 saltcedar shrubs	mature mesquite woods	mature mesquite woods	mature mesquite shrubs
Content	1E	nochange	mature1 saltcedar shrubs	sacaton grassland	sacaton grassland	mature1 saltcedar forest	mature2 saltcedar forest
Content	1E	warm	mature1 saltcedar	young saltcedar	mature2 saltcedar woods	mature mesquite forest	mature mesquite woods

			shrubs	woods			
Content	1E	warmdry	mature1 saltcedar shrubs	old saltcedar woods	sacaton grassland	mature mesquite woods	sacaton grassland
Content	1E	warmwet	mature1 saltcedar shrubs	old saltcedar woods	mature mesquite woods	old mesquite woods	old mesquite forest
Patch Type by Year of Simulation							
Site	Plot	Scenario	2003	2027	2052	2077	2102
Content	2.5 E	nochange	mixed open	mature1 saltcedar shrubs	mature mesquite woods	old mesquite shrubs	sacaton grassland
Content	2.5 E	warm	mixed open	sacaton grassland	mature2 saltcedar shrubs	sacaton grassland	sacaton grassland
Content	2.5 E	warmdry	mixed open	sacaton grassland	sacaton grassland	mature mesquite shrubs	mature mesquite woods
Content	2.5 E	warmwet	mixed open	mature1 saltcedar woods	mature mesquite forest	mature mesquite woods	mature mesquite woods
Content	4.5 E	nochange	sacaton grassland	mature mesquite woods	mature mesquite shrubs	old mesquite shrubs	old mesquite woods
Content	4.5 E	warm	sacaton grassland	mature mesquite woods	mature mesquite shrubs	sacaton grassland	mature mesquite woods
Content	4.5 E	warmdry	sacaton grassland	mature mesquite woods	mature mesquite woods	mature mesquite woods	old mesquite forest
Content	4.5 E	warmwet	sacaton grassland	mature mesquite woods	sacaton grassland	mature mesquite forest	mature mesquite forest

Content	6E	nochange	mature mesquite shrubs	mature mesquite woods	old mesquite woods	sacaton grassland	sacaton grassland
Content	6E	warm	mature mesquite shrubs	mature mesquite woods	mature mesquite woods	old mesquite woods	old mesquite forest
Content	6E	warmdry	mature mesquite shrubs	mature mesquite woods	old mesquite woods	mature mesquite shrubs	mature mesquite woods
Content	6E	warmwet	mature mesquite shrubs	mature mesquite woods	old mesquite woods	old mesquite woods	old mesquite woods
Content	4.5 E	warmwet	sacaton grassland	mature mesquite woods	sacaton grassland	mature mesquite forest	mature mesquite forest
Content	6E	nochange	mature mesquite shrubs	mature mesquite woods	old mesquite woods	sacaton grassland	sacaton grassland
Content	6E	warm	mature mesquite shrubs	mature mesquite woods	mature mesquite woods	old mesquite woods	old mesquite forest
Content	6E	warmdry	mature mesquite shrubs	mature mesquite woods	old mesquite woods	mature mesquite shrubs	mature mesquite woods
Content	6E	warmwet	mature mesquite shrubs	mature mesquite woods	old mesquite woods	old mesquite woods	old mesquite woods

Attachment 1.2. Simulated vegetation transitions on new plots formed by channel migration at Contention transect under four climate scenarios. Blank cells indicate that plots had not been initiated yet. “First Year” corresponds to initiation year (flood year) of plot.

Site	First Year	Scenario	Patch Type by Simulation Year			
			2027	2052	2077	2102
Content	2007	nochange	sacaton grassland	mature2 saltcedar woods	Sacaton grassland	mixed open
Content	2007	warm	mature1 saltcedar woods	mature2 saltcedar forest	mature1 saltcedar forest	mature2 saltcedar woods
Content	2007	warmdry	mature1 saltcedar woods	mature2 saltcedar woods	mature mesquite forest	mature mesquite shrubs
Content	2007	warmwet	sacaton grassland	mature1 saltcedar woods	mature2 saltcedar woods	mature mesquite woods
Content	2019	warmwet	sacaton grassland	mature2 saltcedar forest	old saltcedar forest	old saltcedar forest
Content	2029	nochange		forbland	mature2 saltcedar woods	mature mesquite woods
Content	2029	warmwet		mature1 saltcedar forest	mature2 saltcedar woods	mature mesquite forest
Content	2035	warmwet		sacaton grassland	mature2 saltcedar woods	mature mesquite woods
Content	2045	nochange		forbland	Sacaton grassland	Forbland
Content	2045	warm		forbland	mature2 saltcedar woods	mature2 saltcedar forest
Content	2045	warmwet		forbland	mature1 saltcedar woods	mature2 saltcedar forest
Content	2052	nochange		forbland	Sacaton grassland	mixed open
Content	2052	warm		forbland	mature1 saltcedar woods	mature1 saltcedar forest
Content	2052	warmwet		forbland	mature1 saltcedar woods	mature2 saltcedar woods

Content	2059	nochange			Sacaton grassland	mature2 saltcedar woods
Content	2059	warm			mature1 saltcedar woods	mature2 saltcedar forest
Content	2059	warmdry			mature1 saltcedar woods	old saltcedar forest
Content	2059	warmwet			mature1 saltcedar shrubs	mature2 saltcedar forest
Content	2071	warmwet			Forbland	mature2 saltcedar forest
Content	2081	nochange				mixed open
Content	2081	warmwet				mature1 saltcedar woods
Content	2082	warmwet				mature1 saltcedar forest
Content	2087	warmwet				mixed open
Content	2097	nochange				mixed open
Content	2097	warm				mixed open
Content	2097	warmwet				mixed open
Content	2098	warmwet				mixed open

Attachment 1.3 Simulated vegetation transitions on plots at Kolbe transect under four climate scenarios.

Site	Plot	Scenario	Patch Type by Year of Simulation				
			2003	2027	2052	2077	2102
Kolbe	2W	Nochange	mature1 willow forest	mature2 willow forest	mature mesquite woods	old mesquite woods	old mesquite woods
Kolbe	2W	Warm	mature1 willow forest	mature2 willow forest	mature mesquite woods	mature mesquite woods	old mesquite forest
Kolbe	2W	Warmdry	mature1 willow forest	mature2 willow forest	sacaton grassland	mature mesquite woods	mature mesquite woods
Kolbe	2W	Warmwet	mature1 willow forest	mature2 willow forest	old mesquite forest	old mesquite woods	old mesquite woods
Kolbe	1W	Nochange	mixed open	sacaton grassland	mature mesquite shrubs	old mesquite forest	old mesquite woods
Kolbe	1W	Warm	mixed open	mature1 saltcedar woods	mature mesquite forest	mature mesquite woods	mature mesquite shrubs
Kolbe	1W	Warmdry	mixed open	mature1 saltcedar woods	old saltcedar forest	mature mesquite woods	mature mesquite woods
Kolbe	1W	Warmwet	mixed open	sacaton grassland	mature mesquite woods	mature mesquite forest	old mesquite woods
Kolbe	1E	Nochange	young willow forest	mature1 willow forest	mature2 cottonwood forest	old cottonwood forest	old cottonwood forest
Kolbe	1E	Warm	young willow forest	mature1 willow forest	mature2 willow forest	old cottonwood forest	old cottonwood forest
Kolbe	1E	Warmdry	young willow forest	mature2 willow forest	mature2 willow forest	old cottonwood woods	old cottonwood woods
Kolbe	1E	Warmwet	young willow forest	mature2 willow forest	mature2 cottonwood forest	old cottonwood forest	old cottonwood forest
Kolbe	2E	Nochange	mature1 willow forest	mature2 willow forest	mature2 willow woods	sacaton grassland	old mesquite shrubs

Kolbe	2E	Warm	mature1 willow forest	mature2 willow forest	mature2 willow woods	sacaton grassland	mature mesquite woods
Kolbe	2E	warmdry	mature1 willow forest	mature2 willow forest	mature2 willow woods	mature mesquite shrubs	mature mesquite shrubs
Kolbe	2E	warmwet	mature1 willow forest	mature2 willow forest	mature2 willow forest	mature mesquite woods	old mesquite woods
Kolbe	3E	nochange	mature1 cottonwood forest	old cottonwood forest	old cottonwood forest	sacaton grassland	sacaton grassland
Kolbe	3E	warm	mature1 cottonwood forest	old cottonwood forest	old cottonwood forest	old cottonwood woods	sacaton grassland
Patch Type by Year of Simulation							
Site	Plot	Scenario	2003	2027	2052	2077	2102
Kolbe	3E	warmdry	mature1 cottonwood forest	old cottonwood forest	old cottonwood forest	sacaton grassland	sacaton grassland
Kolbe	3E	warmwet	mature1 cottonwood forest	old cottonwood forest	old cottonwood forest	old cottonwood woods	mature mesquite shrubs
Kolbe	4E	nochange	mixed open	ash woods	ash forest	ash forest	ash forest
Kolbe	4E	warm	mixed open	ash forest	ash forest	ash forest	mature mesquite forest
Kolbe	4E	warmdry	mixed open	ash forest	ash forest	ash forest	ash woods
Kolbe	4E	warmwet	mixed open	ash woods	ash shrubs	mature mesquite woods	mature mesquite woods
Kolbe	5E	nochange	sacaton grassland	sacaton grassland	sacaton grassland	mature mesquite shrubs	mature mesquite shrubs
Kolbe	5E	warm	forbland	mature2 willow shrubs	mature mesquite woods	mature mesquite shrubs	mature mesquite woods
Kolbe	5E	warmdry	forbland	sacaton	sacaton	sacaton	mature mesquite shrubs

				grassland	grassland	grassland	
Kolbe	5E	warmwet	forbland	mature2 willow shrubs	mature mesquite woods	old mesquite woods	sacaton grassland
Kolbe	6E	nochange	old cw/wi forest	old cottonwood forest	mature mesquite woods	old mesquite shrubs	old mesquite shrubs
Kolbe	6E	warm	old cw/wi forest	old cottonwood forest	old cottonwood woods	sacaton grassland	sacaton grassland
Kolbe	6E	Warmdry	old cw/wi forest	old cottonwood forest	old cottonwood woods	sacaton grassland	sacaton grassland
Kolbe	6E	Warmwet	old cw/wi forest	old cottonwood forest	old cottonwood woods	sacaton grassland	mixed open
Kolbe	7E	Nochange	cottonwood forest	old cottonwood woods	mature mesquite woods	old mesquite woods	mature mesquite woods
Kolbe	7E	Warm	cottonwood forest	old cottonwood woods	old cottonwood woods	old mesquite woods	mature mesquite shrubs
Kolbe	7E	Warmdry	cottonwood forest	old cottonwood woods	sacaton grassland	sacaton grassland	sacaton grassland
Kolbe	7E	Warmwet	cottonwood forest	old cottonwood woods	mature mesquite woods	mature mesquite woods	sacaton grassland

Attachment 1.4 Simulated vegetation transitions on new plots formed by channel migration at Kolbe transect under four climate scenarios. Blank cells indicate that plots had not been initiated yet. “First Year” corresponds to initiation year (flood year) of plot.

Site	First Year	Scenario	Patch Type by Simulation Year			
			2027	2052	2077	2102
Kolbe	2007	nochange	sacaton grassland	mature mesquite woods	mature mesquite forest	old mesquite woods
Kolbe	2007	warm	mature1 cw/wi forest	mature2 saltcedar forest	old saltcedar forest	old cottonwood woods
Kolbe	2007	warmdry	mature1 cw/wi woods	mature mesquite shrubs	mature mesquite shrubs	mature mesquite shrubs
Kolbe	2007	warmwet	mature1 cottonwood woods	mature2 cottonwood forest	old cottonwood woods	old cottonwood forest
Kolbe	2019	warmwet	young willow forest	mature2 willow forest	old cottonwood forest	old cottonwood forest
Kolbe	2029	nochange		mature1 willow forest	mature2 cottonwood forest	old cottonwood woods
Kolbe	2029	warmwet		mature1 cottonwood forest	mature2 cottonwood forest	old cottonwood forest
Kolbe	2035	warmwet		mature1 cottonwood forest	mature2 cottonwood forest	old cottonwood forest
Kolbe	2045	nochange		sapling cottonwood forest	mature1 cottonwood forest	mature2 cottonwood forest
Kolbe	2045	warm		young willow forest	mature2 cottonwood forest	old cottonwood forest
Kolbe	2045	warmwet		young cottonwood forest	mature2 cottonwood forest	old cottonwood forest
Kolbe	2052	nochange		Forbland	mature1 cottonwood forest	mature2 cottonwood forest
Kolbe	2052	warm		Forbland	mature1 cottonwood forest	old cottonwood forest

Kolbe	2052	Warmwet		Forbland	mature1 cottonwood forest	old cottonwood forest
Kolbe	2059	Nochange			young willow forest	mature2 saltcedar forest
Kolbe	2059	Warm			mature1 saltcedar forest	old saltcedar forest
Kolbe	2059	Warmdry			sacaton grassland	mature2 saltcedar woods
Kolbe	2059	Warmwet			mature1 saltcedar woods	mature2 saltcedar woods
Kolbe	2071	Warmwet			young willow forest	mature2 cw/wi forest

Site	First Year	Scenario	Patch Type by Simulation Year			
			2027	2052	2077	2102
Kolbe	2081	nochange				mature1 cottonwood woods
Kolbe	2081	warmwet				mature1 willow forest
Kolbe	2082	warmwet				mature1 cottonwood forest
Kolbe	2087	warmwet				mature1 cottonwood forest
Kolbe	2097	nochange				sapling cottonwood shrubs
Kolbe	2097	warm				sapling cottonwood woods
Kolbe	2097	warmwet				young willow forest
Kolbe	2098	warmwet				sapling willow shrubs

Attachment 1.5 Simulated vegetation transitions on plots at Palominas UA transect under four climate scenarios.

Site	Plot	Scenario	Patch Type by Year of Simulation				
			2003	2027	2052	2077	2102
PaloUA	6W	nochange	mature1 cottonwood shrubs	mature2 cottonwood woods	ash forest	ash woods	ash woods
PaloUA	6W	warm	mature1 cottonwood shrubs	mature2 cottonwood woods	ash woods	ash shrubs	sacaton grassland
PaloUA	6W	warmdry	mature1 cottonwood shrubs	mature2 cottonwood woods	ash forest	ash forest	ash woods
PaloUA	6W	warmwet	mature1 cottonwood shrubs	mature2 cottonwood woods	ash forest	ash woods	mature mesquite shrubs
PaloUA	5W	nochange	mature1 cottonwood woods	mature2 cottonwood forest	old cottonwood woods	sacaton grassland	sacaton grassland
PaloUA	5W	warm	mature1 cottonwood woods	mature2 cottonwood forest	old cottonwood woods	sacaton grassland	old mesquite shrubs
PaloUA	5W	warmdry	mature1 cottonwood woods	mature2 cottonwood forest	old cottonwood woods	sacaton grassland	sacaton grassland
PaloUA	5W	warmwet	mature1 cottonwood woods	mature2 cottonwood woods	old cottonwood woods	sacaton grassland	old mesquite woods
PaloUA	4W	nochange	mature1 cottonwood forest	mature2 cottonwood forest	old cottonwood forest	old cottonwood forest	sacaton grassland
PaloUA	4W	warm	mature1 cottonwood	mature2 cottonwood	old cottonwood	old cottonwood forest	sacaton grassland

			forest	forest	forest		
PaloUA	4W	warmdry	mature1 cottonwood forest	mature2 cottonwood forest	old cottonwood forest	old cottonwood forest	old cottonwood woods
PaloUA	4W	warmwet	mature1 cottonwood forest	mature2 cottonwood woods	old cottonwood forest	mature mesquite forest	sacaton grassland
PaloUA	3W	nochange	mature2 cottonwood forest	old cottonwood forest	sacaton grassland	sacaton grassland	mature mesquite woods
PaloUA	3W	warm	mature2 cottonwood forest	old cottonwood forest	sacaton grassland	mature1 saltcedar woods	old saltcedar woods
PaloUA	3W	warmdry	mature2 cottonwood forest	old cottonwood forest	old saltcedar woods	mature1 saltcedar forest	mature2 saltcedar woods
PaloUA	3W	warmwet	mature2 cottonwood forest	old cottonwood forest	sacaton grassland	sacaton grassland	mature mesquite woods
Patch Type by Year of Simulation							
Site	Plot	Scenario	2003	2027	2052	2077	2102
PaloUA	2W	nochange	young cottonwood forest	mature2 cottonwood forest	Old cottonwood forest	old cottonwood forest	sacaton grassland
PaloUA	2W	warm	young cottonwood woods	sacaton grassland	mature2 saltcedar forest	mature mesquite woods	mature mesquite woods
PaloUA	2W	warmdry	young cottonwood forest	mature2 cottonwood forest	old cottonwood forest	mature mesquite forest	mature mesquite woods
PaloUA	2W	warmwet	young	mature2	old	old	sacaton grassland

			cottonwood forest	cottonwood forest	cottonwood forest	cottonwood forest	
PaloUA	1W	nochange	young cottonwood woods	mature1 cottonwood forest	mature1 saltcedar forest	old saltcedar forest	sacaton grassland
PaloUA	1W	warm	young cottonwood forest	mature2 cottonwood forest	old cottonwood forest	old cottonwood forest	old cottonwood forest
PaloUA	1W	warmdry	young cottonwood woods	mature2 cottonwood forest	old cottonwood forest	old cottonwood forest	old cottonwood forest
PaloUA	1W	warmwet	young cottonwood forest	young saltcedar shrubs	mature2 saltcedar forest	mature mesquite forest	mature mesquite woods
PaloUA	1E	nochange	young cottonwood shrubs	mature2 cottonwood forest	old cottonwood forest	old cottonwood forest	old mesquite forest
PaloUA	1E	warm	young cottonwood shrubs	mature2 cottonwood woods	old cottonwood woods	old cottonwood forest	sacaton grassland
PaloUA	1E	warmdry	young cottonwood shrubs	mature2 cottonwood forest	old cottonwood forest	old cottonwood forest	old mesquite woods
PaloUA	1E	warmwet	young cottonwood shrubs	mature2 cottonwood woods	old cottonwood forest	old cottonwood forest	mature mesquite woods
PaloUA	2E	nochange	young saltcedar shrubs	mature1 saltcedar forest	old saltcedar forest	sacaton grassland	sacaton grassland
PaloUA	2E	warm	young saltcedar shrubs	mature1 saltcedar forest	old saltcedar forest	old saltcedar forest	sacaton grassland
PaloUA	2E	warmdry	young	mature2	old saltcedar	sacaton	mature mesquite woods

			saltcedar shrubs	saltcedar forest	forest	grassland	
PaloUA	2E	warmwet	young saltcedar shrubs	mature1 saltcedar forest	old saltcedar woods	mature mesquite woods	mature mesquite woods
PaloUA	3E	nochange	mature1 saltcedar woods	mature2 saltcedar forest	old saltcedar woods	sacaton grassland	sacaton grassland
Patch Type by Year of Simulation							
Site	Plot	Scenario	2003	2027	2052	2077	2102
PaloUA	3E	warm	mature1 saltcedar woods	mature2 saltcedar forest	Old saltcedar woods	old mesquite shrubs	sacaton grassland
PaloUA	3E	warmdry	mature1 saltcedar woods	sacaton grassland	mature2 saltcedar woods	mature mesquite shrubs	sacaton grassland
PaloUA	3E	warmwet	mature1 saltcedar woods	mature2 saltcedar woods	old saltcedar woods	mature mesquite shrubs	mature mesquite shrubs
PaloUA	4E	nochange	dryshrub shrubs	sacaton grassland	sacaton grassland	sacaton grassland	sacaton grassland
PaloUA	4E	warm	dryshrub shrubs	sacaton grassland	mature mesquite shrubs	mature mesquite shrubs	old mesquite shrubs
PaloUA	4E	warmdry	dryshrub shrubs	sacaton grassland	sacaton grassland	sacaton grassland	sacaton grassland
PaloUA	4E	warmwet	dryshrub shrubs	sacaton grassland	mature mesquite shrubs	mature mesquite shrubs	old mesquite woods

Attachment 1.6 Simulated vegetation transitions on new plots formed by channel migration at Palominas UA transect under four climate scenarios. Blank cells indicate that plots had not been initiated yet. “First Year” corresponds to initiation year (flood year) of plot.

Site	First Year	Scenario	Patch Type by Simulation Year			
			2027	2052	2077	2102
PaloUA	2007	nochange	sacaton grassland	mature2 saltcedar woods	mature1 saltcedar forest	mature1 saltcedar forest
PaloUA	2007	Warm	sacaton grassland	mature1 saltcedar woods	mature2 saltcedar woods	old saltcedar woods
PaloUA	2007	warmdry	mature1 saltcedar forest	mature2 saltcedar forest	mature mesquite forest	old mesquite forest
PaloUA	2007	warmwet	sacaton grassland	sacaton grassland	mature mesquite woods	mature mesquite forest
PaloUA	2019	warmwet	young willow forest	mature2 cottonwood forest	old cottonwood forest	old cottonwood forest
PaloUA	2029	nochange		mature1 cottonwood forest	mature2 cottonwood forest	old cottonwood forest
PaloUA	2029	warmwet		mature1 cottonwood forest	mature2 cottonwood forest	mature mesquite forest
PaloUA	2035	warmwet		mature1 cottonwood forest	mature2 cottonwood forest	old cottonwood forest
PaloUA	2045	nochange		young willow forest	mature1 cottonwood forest	mature2 cottonwood forest
PaloUA	2045	Warm		young cottonwood woods	mature1 cottonwood forest	old cottonwood forest
PaloUA	2045	warmwet		young cottonwood forest	mature1 cottonwood forest	old cottonwood forest
PaloUA	2052	nochange		forbland	mature1 cottonwood forest	mature2 cottonwood forest
PaloUA	2052	Warm		forbland	mature1 cottonwood forest	old cottonwood forest
PaloUA	2052	warmwet		forbland	mature1 cottonwood woods	mature2 cottonwood forest

PaloUA	2059	nochange			mature1 saltcedar shrubs	mature2 saltcedar woods	
PaloUA	2059	warm			mature1 saltcedar woods	old cottonwood woods	
PaloUA	2059	warmdry			mature1 saltcedar woods	old saltcedar woods	
PaloUA	2059	warmwet			mature1 cottonwood woods	mature mesquite forest	
PaloUA	2071	warmwet			young willow forest	mature1 saltcedar forest	
Site	First Year	Scenario	2027	Patch Type by Simulation Year			2102
				2052	2077		
PaloUA	2081	nochange				mature1 willow forest	
PaloUA	2081	warmwet				mature1 cottonwood forest	
PaloUA	2082	warmwet				mature1 cottonwood forest	
PaloUA	2087	warmwet				mature1 cottonwood forest	
PaloUA	2097	nochange				sapling cottonwood shrubs	
PaloUA	2097	warm				Young willow forest	
PaloUA	2097	warmwet				sapling cottonwood forest	
PaloUA	2098	warmwet				sapling cottonwood shrubs	

ATTACHMENT 2 – Modified EPA Framework

MODULE 1 - CATEGORIZING THE "BASELINE" VULNERABILITY (Vb) OF WILLOW FLYCATCHER IN

THE SPRNCA. Bold scores represent "best estimates" others are alternate scores.

Current population size in SPRNCA:		Score		Likely future non-climate stressor trends:	Score	
	<50	1	1	increase	1	
	50-100	2		stable	2	2
	>100	3		reduction	3	3
				high (3)		
Certainty	high (3)		3	medium (2)		2
	medium (2)			low (1)		
	low (1)					
Regional population trend in last 50 years:		Score		Replacement time for individuals:	Score	
	>50% reduction	1	1	> 5 years	1	
	>20% reduction	2	2	2-5 years	2	
	Apparently stable	3		<2 years	3	3
	Increasing	4		<1 year	4	4
				high (3)		3
Certainty:	high (3)		3	medium (2)		
	medium (2)			low (1)		
	low (1)					
Current regional population trend:		Score		Likely future vulnerability to stochastic events:	Score	
	rapid decline	1		vulnerable	1	
	slow decline	2	2	not vulnerable	2	2
	stable	3	3	benefiting	3	3
	increasing	4		high (3)		
Certainty:	high (3)			medium (2)		2
	medium (2)		2	low (1)		
	low (1)					
Regional range trend in last 50 years		Score		Likely future vulnerability to policy/management change	Score	
	>50% reduction	1	1	Highly vulnerable	1	1
	>20%reduction	2	2	vulnerable	2	2
	apparently stable	3		not vulnerable	3	
	increasing	4		high (3)		3
Certainty:	high (3)		2	medium (2)		
	medium (2)			low (1)		

	low (1)	
Current regional range trend:		Score
	rapid reduction	1
	slow reduction	2
	stable	3
	increasing	4
Certainty:	high (3)	3
	medium (2)	
	low (1)	

		Likely future vulnerability to natural stressors		Score
		Highly vulnerable	1	
	2	vulnerable	2	2
	3	not vulnerable	3	3
		high (3)		
	3	medium (2)		2
		low (1)		

TOTAL SCORE	22	(17 - 25)
Baseline vulnerability scores:		
Vb1	<16	Highly vulnerable
Vb2	16-21	Vulnerable
Vb3	22-27	Least Vulnerable
Vb4	>27	Not Vulnerable
Species score:	Vb3 (Vb2)	

CUMULATIVE CERTAINTY SCORE:	26
Max. score	30
Min. score	10

MODULE 2 - CATEGORIZING THE VULNERABILITY OF WILLOW FLYCATCHERS IN THE SPRNCA TO CLIMATE CHANGE (Vc). Bold scores represent "best estimates" others are alternate scores.

Physiological vulnerability to temperature increase:		Score	Likely extent of habitat change due to climate change		Score
	Likely highly sensitive	1		all or most (>50%)	1
	Likely moderately sensitive	2	2	some (20-50%)	2
	Likely insensitive	3	3	no change	3
	likely to benefit	4		some gain (20-50%)	4
Certainty:	high (3)			large gain (>50%)	4
	medium (2)		2		5
	low (1)			Certainty: high (3)	5
Physiological vulnerability to precipitation change:		Score		medium (2)	2
	Likely highly sensitive	1		low (1)	
	Likely moderately sensitive	2	2	Dependence on temporal inter-relations:	
	Likely insensitive	3	3	highly dependent	Score 1
	Likely to benefit	4		moderately dependent	2 2
Certainty:	high (3)			independent	3 3
	medium (2)		2	Certainty: high (3)	
	low (1)			medium (2)	2
Vulnerability to change in frequency/degree of extreme weather events:		Score		low (1)	
	Likely highly sensitive	1		Dependence on other species:	
	Likely moderately sensitive	2	2	highly dependent	Score 1
	Likely insensitive	3	3	moderately dependent	2 2
	likely to benefit	4		independent	3 3
Certainty:	high (3)			Certainty: high (3)	
	medium (2)		3	medium (2)	2
	low (1)			low (1)	
Recolonization capability:		Score		Ability to utilize mesic or xeric species	
	Low	1		Not able	1 1
	Moderate	2		Able	2 2
	High	3	3	Certainty: high (3)	3
				medium (2)	

Certainty: high (3)
medium (2)
low (1)

Degree of habitat specialization: Score
Highly specialized 1
Moderately specialized 2
Generalist 3

Certainty: high (3)
medium (2)
low (1)

TOTAL	32 (26 - 36)
Climate change vulnerability scores:	
Vc1	<17 Highly vulnerable
Vc2	17-23 Vulnerable
Vc3	24-30 Not vulnerable
Vc4	>30 May benefit
Species score:	Vc4 (Vc3, Vc4)

CUMULATIVE CERTAINTY SCORE:	29
Max. score	36
Min. score	12

3 low (1)
Ability to utilize non-native vegetation
Not able 1 1
Able 2 2
Certainty: high (3) 3
medium (2)
low (1)

Dependence on gallery forest
3 Highly dependent 1
Somewhat dependent 2
Independent 3 3
Certainty: high (3) 3
medium (2)
low (1)

Dependence on wetland, or standing or flowing water
Highly dependent 1
Somewhat dependent 2 2
Independent 3 3
Certainty: high (3)
medium (2) 2
low (1)

MODULE 3 - COMBINING BASELINE AND CLIMATE VULNERABILITY SCORES FOR WILLOW FLYCATCHER INTO OVERALL VULNERABILITY SCORE (Vo)

Bold and italics show "best estimate" and "alternate" scores, respectively.

	Vb1	Vb2	Vb3	Vb4	
Vc1	Vo1	Vo1	Vo2	Vo2	Vo1 - Highly Vulnerable
Vc2	Vo1	Vo1	Vo2	Vo3	Vo2 - Vulnerable
Vc3	Vo1	Vo2	Vo3	Vo4	Vo3 - Least Vulnerable
Vc4	Vo2	Vo3	Vo4	Vo4	Vo4 - Not Vulnerable

Species score: Vo4 (Vo2)

MODULE 4 - CERTAINTY/UNCERTAINTY ANALYSIS FOR WILLOW FLYCATCHER

	Max. Scores
Module 1	30
Module 2	36
Both Modules	66
Total Score	Certainty Evaluation
22-32	Low
33-45	Medium
>45	High

	Module 1	Module 2	Both	
Total score	25	30	55	Certainty Score - High

MODULE 1 - CATEGORIZING THE "BASELINE" VULNERABILITY (Vb) OF YELLOW-BILLED CUCKOO IN THE SPRNCA. Bold scores represent "best estimates" others are alternate scores.

Current population size in SPRNCA:		Score		Likely future non-climate stressor trends:	Score	
	<50	1	1	increase	1	1
	50-100	2	2	stable	2	2
	>100	3		reduction	3	
Certainty:	high (3)		3	Certainty:	high (3)	
	medium (2)				medium (2)	2
	low (1)				low (1)	
Regional population trend in last 50 years:		Score		Replacement time for individuals:	Score	
	>50% reduction	1	1	> 5 years	1	
	>20% reduction	2	2	2-5 years	2	2
	Apparently stable	3		<2 years	3	3
	Increasing	4		<1 year	4	
Certainty:	high (3)			Certainty:	high (3)	3
	medium (2)		2		medium (2)	
	low (1)				low (1)	
Current regional population trend:		Score		Likely future vulnerability to stochastic events:	Score	
	rapid decline	1		vulnerable	1	1
	slow decline	2	2	not vulnerable	2	2
	stable	3	3	benefiting	3	
	increasing	4		Certainty:	high (3)	
Certainty:	high (3)				medium (2)	2
	medium (2)		2		low (1)	
	low (1)					
Regional range trend in last 50 years		Score		Likely future vulnerability to policy or management changes	Score	
	>50% reduction	1	1	Highly vulnerable	1	
	>20%reduction	2	2	vulnerable	2	2
	apparently stable	3		not vulnerable	3	3
	increasing	4		Certainty:	high (3)	3
Certainty:	high (3)				medium (2)	2
	medium (2)		2			
	low (1)					

Current regional range trend:		Score
rapid reduction		1
slow reduction		2
stable		3
increasing		4
Certainty:	high (3)	3
	medium (2)	
	low (1)	

TOTAL SCORE	20 (14 - 24)	
Baseline vulnerability scores:		
Vb1	<16	Highly vulnerable
Vb2	16-21	Vulnerable
Vb3	22-27	Least Vulnerable
Vb4	>27	Not Vulnerable
Species score:	Vb3 (Vb1, Vb3)	

		low (1)	
Likely future vulnerability to natural stressors:			Score
	Highly vulnerable		1
	vulnerable		2
	not vulnerable		3
Certainty:	high (3)		
	medium (2)		2
	low (1)		

CUMULATIVE CERTAINTY SCORE:	24
Max. score	30
Min. score	10

MODULE 2 - CATEGORIZING THE VULNERABILITY OF YELLOW-BILLED CUCKOO IN THE SPRNCA TO CLIMATE CHANGE (Vc). Bold scores represent "best estimates" others are alternate scores.

Physiological vulnerability to temperature increase:		Score		Likely extent of habitat change due to climate change	Score	
	Likely highly sensitive	1	1		1	1
	Likely moderately sensitive	2	2	all or most (>50%)	1	1
	Likely insensitive	3		some (20-50%)	2	2
	likely to benefit	4		no change	3	
Certainty:	high (3)			some gain (20-50%)	4	
	medium (2)			large gain (>50%)	5	
	low (1)		1			
Physiological vulnerability to precipitation change:		Score		Certainty:	high (3)	
	Likely highly sensitive	1			medium (2)	2
	Likely moderately sensitive	2	2		low (1)	
	Likely insensitive	3		Dependence on temporal inter-relations:		
	Likely to benefit	4		highly dependent	1	1
Certainty:	high (3)			moderately dependent	2	2
	medium (2)			independent	3	
	low (1)		1			
Vulnerability to change in frequency/degree of extreme weather events:		Score		Certainty:	high (3)	
	Likely highly sensitive	1	1		medium (2)	2
	Likely moderately sensitive	2	2		low (1)	
	Likely insensitive	3		Dependence on other species:		
	likely to benefit	4		highly dependent	1	1
Certainty:	high (3)			moderately dependent	2	2
	medium (2)			independent	3	
	low (1)		1			
Recolonization capability:		Score		Certainty:	high (3)	
	Low	1			medium (2)	2
	Moderate	2			low (1)	
	High	3	3	Ability to utilize mesic or xeric species		
				Not able	1	1
				Able	2	
				Certainty:	high (3)	3
					medium (2)	

Certainty:	high (3)	3
	medium (2)	
	low (1)	
Degree of habitat specialization:		Score
	Highly specialized	1
	Moderately specialized	2
	Generalist	3
Certainty:	high (3)	3
	medium (2)	
	low (1)	

TOTAL	19 (16 - 22)
Climate change vulnerability scores:	
Vc1	<17 Highly vulnerable
Vc2	17-23 Vulnerable
Vc3	24-30 Not vulnerable
Vc4	>30 May benefit
Species score:	Vc2 (Vc1)

CUMULATIVE CERTAINTY SCORE:	27
Max. score	36
Min. score	12

	low (1)	
Ability to utilize non-native vegetation		
	Not able	1
	Able	2
Certainty:	high (3)	3
	medium (2)	
	low (1)	
Dependence on gallery forest		
	Highly dependent	1
	Somewhat dependent	2
	Independent	3
Certainty:	high (3)	3
	medium (2)	
	low (1)	
Dependence on wetland, or standing or flowing water		
	Highly dependent	1
	Somewhat dependent	2
	Independent	3
Certainty:	high (3)	2
	medium (2)	
	low (1)	

MODULE 3 - COMBINING BASELINE AND CLIMATE VULNERABILITY SCORES FOR YELLOW-BILLED CUCKOO INTO OVERALL VULNERABILITY SCORE (Vo)

(bold and italics show "best estimate" and "alternate" scores, respectively)

	Vb1	Vb2	Vb3	Vb4	
Vc1	Vo1	Vo1	V02	Vo2	Vo1 - Highly Vulnerable
Vc2	Vo1	Vo1	Vo2	Vo3	Vo2 - Vulnerable
Vc3	Vo1	Vo2	Vo3	Vo4	Vo3 - Least Vulnerable
Vc4	Vo2	Vo3	Vo4	Vo4	Vo4 - Not Vulnerable

Species score: Vo2 (Vo1)

MODULE 4 - CERTAINTY/UNCERTAINTY ANALYSIS FOR YELLOW-BILLED CUCKOO

	Max. Scores
Module 1	30
Module 2	36
Both Modules	66

Total Score	Certainty Evaluation
23-32	Low
33-45	Medium
>45	High

	Module 1	Module 2	Both	
Total score	24	27	51	Certainty Score - High

MODULE 1 - CATEGORIZING THE "BASELINE" VULNERABILITY (Vb) OF BOTTERI'S SPARROWS IN THE SPRNCA. Bold scores represent "best estimates" others are alternate scores.

Current population size in SPRNCA:		Score	Likely future non-climate stressor trends:		Score	
	<50	1		increase	1	1
	50-100	2	2	stable	2	2
	>100	3	3	reduction	3	
Certainty	high (3)					
	medium (2)		2	Certainty:	high (3)	
	low (1)				medium (2)	2
Regional population trend in last 50 years:		Score		Replacement time for individuals:	Score	
	>50% reduction	1		> 5 years	1	
	>20% reduction	2		2-5 years	2	
	Apparently stable	3	3	<2 years	3	3
	Increasing	4		<1 year	4	4
Certainty:	high (3)					
	medium (2)		1	Certainty:	high (3)	3
	low (1)				medium (2)	
Current regional population trend:		Score		Likely future vulnerability to stochastic events:	Score	
	rapid decline	1		vulnerable	1	
	slow decline	2		not vulnerable	2	2
	stable	3	3	benefiting	3	3
	increasing	4				
Certainty:	high (3)			Certainty:	high (3)	
	medium (2)		2		medium (2)	2
	low (1)				low (1)	
Regional range trend in last 50 years		Score		Likely future vulnerability to policy or management changes	Score	
	>50% reduction	1		Highly vulnerable	1	
	>20%reduction	2		vulnerable	2	2
	apparently stable	3	3	not vulnerable	3	3
	increasing	4				
Certainty:	high (3)					

	medium (2)	
	low (1)	
Current regional range trend:		Score
rapid reduction		1
slow reduction		2
stable		3
increasing		4
Certainty:	high (3)	
	medium (2)	
	low (1)	

TOTAL SCORE	29 (25 - 30)	
Baseline vulnerability scores:		
Vb1	<16	Highly vulnerable
Vb2	16-21	Vulnerable
Vb3	22-27	Least Vulnerable
Vb4	>27	Not Vulnerable
Species score:	Vb4 (Vb3)	

1	Certainty:	high (3)	
		medium (2)	2
		low (1)	
3	Likely future vulnerability to natural stressors:		Score
	Highly vulnerable		1
	vulnerable		2
	not vulnerable		3
2	Certainty:	high (3)	3
		medium (2)	
		low (1)	2

CUMULATIVE CERTAINTY SCORE:	19
Max. score	30
Min. score	10

MODULE 2 - CATEGORIZING THE VULNERABILITY OF BOTTERI'S SPARROWS IN THE SPRNCA TO CLIMATE CHANGE (Vc). Bold scores represent "best estimates" others are alternate scores.

Physiological vulnerability to temperature increase:	Score		Likely extent of habitat change due to climate change	Score	
Likely highly sensitive	1		all or most (>50%)	1	
Likely moderately sensitive	2		some (20-50%)	2	
Likely insensitive	3	3	no change	3	
likely to benefit	4	4	some gain (20-50%)	4	4
Certainty: high (3)			large gain (>50%)	5	5
medium (2)			Certainty: high (3)		
low (1)		1	medium (2)		2
			low (1)		
Physiological vulnerability to precipitation change:	Score		Dependence on temporal inter-relations:	Score	
Likely highly sensitive	1	1	highly dependent	1	
Likely moderately sensitive	2	2	moderately dependent	2	2
Likely insensitive	3		independent	3	3
Likely to benefit	4		Certainty: high (3)		
Certainty: high (3)			medium (2)		2
medium (2)			low (1)		
low (1)		1	Dependence on other species:	Score	
Vulnerability to change in frequency/degree of extreme weather events:	Score		highly dependent	1	
Likely highly sensitive	1		moderately dependent	2	2
Likely moderately sensitive	2		independent	3	3
Likely insensitive	3	3	Certainty: high (3)		
likely to benefit	4	4	medium (2)		2
Certainty: high (3)			low (1)		
medium (2)			Ability to utilize mesic or xeric species		
low (1)		1	Not able	1	1
Recolonization capability:	Score		Able	2	2
Low	1		Certainty: high (3)		3
Moderate	2		medium (2)		
High	3	3			

Certainty:	high (3)		3
	medium (2)		
	low (1)		
Degree of habitat specialization:		Score	
	Highly specialized	1	1
	Moderately specialized	2	2
	Generalist	3	
Certainty:	high (3)		3
	medium (2)		
	low (1)		

TOTAL	32 (26 - 36)		
Climate change vulnerability scores:			
Vc1	<17	Highly vulnerable	
Vc2	17-23	Vulnerable	
Vc3	24-30	Not vulnerable	
		May benefit	
Vc4	>30		
Species score:	Vc4 (Vc3)		

	low (1)		
Ability to utilize non-native vegetation			
	Not able	1	1
	Able	2	2
Certainty:	high (3)		3
	medium (2)		
	low (1)		
Dependence on gallery forest			
	Highly dependent	1	
	Somewhat dependent	2	
	Independent	3	3
Certainty:	high (3)		3
	medium (2)		
	low (1)		
Dependence on wetland, or standing or flowing water			
	Highly dependent	1	
	Somewhat dependent	2	2
	Independent	3	3
Certainty:	high (3)		2
	medium (2)		
	low (1)		

CUMULATIVE CERTAINTY SCORE:	29
Max. score	
Min. score	

MODULE 3 - COMBINING BASELINE AND CLIMATE VULNERABILITY SCORES FOR BOTTERI'S SPARROW INTO OVERALL VULNERABILITY SCORE (Vo). Bold and italics show "best estimate" and "alternate" scores, respectively.

	Vb1	Vb2	Vb3	Vb4	
Vc1	Vo1	Vo1	Vo2	Vo2	Vo1 - Highly Vulnerable
Vc2	Vo1	Vo1	Vo2	Vo3	Vo2 - Vulnerable
Vc3	Vo1	Vo2	Vo3	Vo4	Vo3 - Least Vulnerable
Vc4	Vo2	Vo3	Vo4	Vo4	Vo4 - Not Vulnerable

Species score: Vo4 (Vo3)

MODULE 4 - CERTAINTY/UNCERTAINTY ANALYSIS FOR BOTTERI'S SPARROW

	Max. Scores
Module 1	30
Module 2	36
Both Modules	66
Total Score	
23-32	Certainty Evaluation
33-45	Low
>45	Medium
	High

	Module 1	Module 2	Both	
Total score	19	29	48	Certainty Score - High

ATTACHMENT 3 – HSI Models

**BREEDING HABITAT SUITABILITY INDEX MODEL FOR
BOTTERI'S SPARROW IN THE SAN PEDRO NCA**

Developed by:

Hector Galbraith PhD
Galbraith Environmental Sciences, LLC.
Boulder, Colorado

19 June 2003

1. INTRODUCTION

This document presents a breeding season Habitat Suitability Index (HSI) model for Botteri's sparrows (*Aimophila botterii arizonae*), intended for use in the San Pedro Riparian National Conservation Area (SPRNCA). This model, which quantifies the habitat relationships of the species, is the result of a review of the scientific literature, focusing mainly on those studies that address habitat use by the species in Arizona during the breeding season. The resulting draft model was tested in the San Pedro in areas where the breeding densities of Botteri's sparrow had been quantified in previous surveys. The model will be used, in conjunction with vegetation community and climate modeling predictions, to evaluate the potential effects of global climate change on the ability of the SPRNCA to provide breeding habitat for this species in the future.

1.1 Breeding Botteri's sparrows in North America and the SPRNCA

Currently the Botteri's sparrow is limited as a breeding species in North America to two distinct and non-contiguous areas: southeastern Arizona and southwestern New Mexico, and coastal south Texas. There is evidence that its historical breeding distribution may have been more extensive (though confined to the arid southwest and Texas) but contracted due to habitat fragmentation and loss through overgrazing by livestock (Webb and Bock, 1996). The wintering range of the Arizona subpopulation (*A. b. arizonae*) is not known but is probably in central and southern Mexico.

Within the SPRNCA, the species is a fairly common summer resident and breeder from Charleston south to Palominas (Kreuper, 1997). First arrivals in the spring are in late April and the birds usually leave the area in Sep-Oct (Kreuper, 1997, Webb and Bock, 1996). Its breeding distribution in the SPRNCA and southeastern Arizona, in general, is confined to areas of tall native grasslands, primarily giant sacaton stands in relatively flat outwash areas (Jack Whetstone, BLM, *pers. comm.*). It differs from the closely related Cassin's sparrow (*Aimophila cassinii*) in that the latter prefers less tall and less dense grassland stands and can tolerate greater densities of shrubs such as mesquite (Dunning et al., 1999).

The species' timing of breeding is largely determined by the advent of the summer rains in southeastern Arizona, which typically occur from July to August. This timing allows the birds to exploit the seasonal flush of invertebrate biomass, particularly Orthopterans (Webb and Bock, 1996).

1.2 HSI models

HSI models evaluate the likely impacts of any actual or potential changes in habitat quality on carrying capacity (defined here as the habitat's capacity to support organisms) for either a single species, a guild of species, or biodiversity in general. HSI models achieve this by:

5. Identifying the critical habitat variables that affect the carrying capacity of habitat.
6. Establishing quantitative relationships between the occurrence of these variables and the carrying capacity of habitat. Each variable is assigned a suitability index (SI). This is a score of between 0 and 1, where the former is completely unsuitable habitat (i.e., minimal carrying capacity) and the latter is optimal habitat (i.e., greatest carrying capacity).

7. Developing metrics that can be used in the field to quantify the occurrence of the critical habitat components (and, therefore, the carrying capacity of the habitat)
8. Developing algorithms that combine the variable scores (SIs) into an expression of the overall carrying capacity of the habitat. This final score is the HSI and can be between 0 (unsuitable for species or guild) and 1 (optimal habitat).

Previous applications of HSI models have included the prediction of the possible effects of particular land management alternatives on biota (Brand *et al.*, 1986; Schamberger and Farmer, 1978), the quantification of past injuries to ecosystem wildlife carrying capacities (Galbraith *et al.*, 1996; LeJeune *et al.*, 1996), evaluating the potential effects of climate change and aquifer depletion on biota (Galbraith *et al.*, *in press*), and estimating the exposure to contaminants of wildlife species. If the structures, extents, and/or compositions of post-change vegetation communities can be predicted, it becomes possible to use HSI models to quantify and compare pre- and post-change habitat quality and potential carrying capacities.

U.S. Fish and Wildlife Service has developed approximately 160 HSI models. These include 85 terrestrial species (62 birds, 17 mammals, and 6 reptiles and amphibians). The remainder comprise marine and freshwater organisms. Most of the models have specific geographic, habitat, and seasonal areas of applicability. For example, the model for American woodcock, *Scolopax minor*, applies only to the species' wintering range in the southeastern states (Cade, 1985). In addition to the single-species HSI models, U.S. Fish and Wildlife has also developed a few models that quantify the carrying capacity of habitat for groups of species, for example habitat guild models (Short, 1983), or for wildlife diversity in general (Short, 1984).

No previously developed HSI model exists for Botteri's sparrow. This model has been developed for the species in its breeding range in southern Arizona and it might not be applicable, without modification, elsewhere in its breeding range.

1.3 Approach used in the development of this HSI model

The components and structure of this model were based on a literature review of the habitat preferences Botteri's sparrows in their breeding habitat in southeastern Arizona. The literature sources are cited in section 5. The resulting draft model was then tested in the SPRNCA in areas of known sparrow density. Based on these results, the model was modified and finalized.

1.4 Seasonal and geographical applicability of this HSI model

This model is intended for use only during the breeding season (May – September) and in grassland habitat in southeastern Arizona. Without modification, it might not be applicable to breeding sites elsewhere.

2. HABITAT INFORMATION

2.1 General

Botteri's sparrow is confined as a breeding bird in southern Arizona to stands of grasslands, particularly to giant sacaton stands. Densities are highest in those sacaton stands that are tall and

dense with a high representation of senescent plants (Webb and Bock, 1996). They generally avoid areas of high shrub density or grasslands that are dominated by non-native species. Thus, overgrazing of native grasslands, and their reduced density or replacement by invasive species reduces their attractiveness to Botteri's sparrows. This may have been responsible for the range fragmentation and habitat loss that occurred in the past in the southwest. When overgrazed or disturbed areas have been reseeded with native species of grasses, Botteri's sparrows may recolonize (Webb and Bock, 1996).

The grassland stands most favored by Botteri's sparrows are to a great extent limited by topography, occurring only on relatively flat and poorly drained outwash areas, or on riparian flats. Better drained, steeper grasslands tend to be dominated by less lush growths of other grass species.

2.2 Specific habitat requirements/preferences

The specific habitat features in this section are based on the published scientific literature, particularly on the results obtained by Webb (1985) and reported in Webb and Bock (1996). The specific features are identified below:

V1. Major Community Type in 100m radius of sampling point. Breeding Botteri's sparrows in southeastern Arizona are confined to grasslands. Within that broad habitat type they can breed in areas with emergent shrubs (e.g., mesquite and ocotillo), but only at very low densities. This relationship is shown below and in Figure 1.

% GRASS COVER DOMINANCE	SUITABILITY INDEX
0-40%	0.05
40-60%	0.2
60-80%	0.6
>80%	1.0

V2. Giant Sacaton Dominance in 20 m. radius of sampling point. Grasslands dominated by giant sacaton (*Sporobolus wrightii*) comprise the preferred habitat in southeastern Arizona (Webb and Bock, 1996). They will also breed in other grasslands, for example those with a high representation of tobosa (*Hilaria mutica*), but at lower densities.. This relationship is shown below and presented graphically in Figure 2.

% SACATON DOMINANCE	SUITABILITY INDEX
<40%	0.1
40-60%	0.5
60-80%	0.8
>80%	1.0

V3. *Mean Height of Sacaton in 20 m. radius of sampling point.* Based on information in Webb and Bock (1996), the following sacaton stand height and habitat suitability categorization has been hypothesized (presented graphically in Figure 3):

MEAN HEIGHT (M)	SUITABILITY INDEX (SI)
<0.2	0.1
0.2-0.5	0.3
0.5-1.0	0.7
>1.0	1.0

V4. *Density of sacaton in 20m radius of sampling point.* Based on information from Webb and Bock (1996), the following sacaton density and habitat suitability categorization has been developed:

MEAN DENSITY	SUITABILITY INDEX (SI)
Sparse (easy to see >5m at waist height)	0.2
Dense (easy to see >3m at waist height)	0.6
Very dense (cannot see >2m at waist height)	1.0

This relationship is presented graphically in Figure 4.

V5. *Sacaton senescense.* Based on information from Webb and Bock (1996), the following sacaton density and habitat suitability categorization has been developed:

% COVER SENESCENT GRASS IN 10M RADIUS	SUITABILITY INDEX
<10%	0.1
10-30%	0.3
30-50%	0.6
>50%	1.0

This relationship is presented graphically in Figure 5.

V6. *Percent forbs or non-native grasses in 20 m radius of sampling point).* Based on information in Webb and Bock (1996), the following forb/non-native grass species cover and habitat suitability categorization has been developed:

% COVER	SUITABILITY INDEX (SI)
>30%	0.05
20-30%	0.2
10-20%	0.6
<10%	1.0

This relationship is presented graphically in Figure 6.

Micro-climate. There is some evidence that Botteri's sparrows select nest sites that provide optimal micro-climatic conditions (Webb and Bock, 1996), by selecting sites that are shaded from the direct heat of the sun. Also, the breeding season of the species is determined by the timing of monsoonal rains. In these two ways, therefore, climate and variability in weather influence the breeding ecology of the species. If sacaton grasslands were to become more open due to climate change (or any other stressor, such as overgrazing) it could affect nest site habitat quality. This eventuality would be detected and addressed by the variables described above. Thus, by focusing on grass density, height and senescence, the model already addresses the potential outcomes of this habitat variable. A change in the timing or severity of the monsoonal rains would not be incorporated by the model, but would be addressed separately in the overall evaluation of climate change on the species' ecology.

3. MODEL APPLICATION

The six variables described above are combined into an index of the overall assessment of the habitat suitability (HSI) of a particular patch of grassland habitat using the following 6th root algorithm:

$$HSI = (V1 \times V2 \times V3 \times V4 \times V5 \times V6)^{1/6}$$

The HSI values obtained using this equation range between 0 and 1.0 (lowest and highest estimates of suitability, respectively).

4. FIELD TEST RESULTS

The Botteri's sparrow draft model was tested in June, 2003 at sites on the San Pedro River where Bureau of Land Management surveys had quantified densities of singing males in each year between 1986 and 1990. In the absence of visual evidence to the contrary, it was assumed that little or no habitat change had occurred between the survey years and the present. The results of the field test of the model are presented in Figure 7. These results show that the predictions of the HSI model regarding habitat suitability are accurate (if it is assumed that breeding density is a reflection of at least short term habitat quality), except at sites where HSI values are less than about 0.3. Apparently, Botteri's sparrows in the San Pedro do not consider such sites as providing habitat. Thus, the HSI model developed for this study is a reasonable predictor of breeding habitat quality for the study species

5. REFERENCES

Brand, G.J., S.R. Shifley, and L.F. Ohman. 1986. Linking wildlife and vegetation models to forecast the effects of management. In: J. Verner, M.L. Morrison, and C.J. Ralph (eds), *Wildlife 2000: modeling habitat relationships of terrestrial vertebrates*. University of Wisconsin Press, Madison, Wisconsin.

Cade, B.S. 1985. Habitat suitability index models: American woodcock (wintering). U.S. Fish Wildl. Serv. Biol. Rep. 82(10.105). Ft. Collins, Colorado.

Dunning, J.B., R.K. Bowers, S.J. Suter, and C.E. Bock 1999. Cassin's sparrow. The Birds of North America. Life Histories for the 21st Century. No. 471 (A. Poole and F. Gill, eds). The Birds of North America., Inc., Philadelphia, PA.

Galbraith, H., K. LeJeune, and J. Lipton. 1996. Metal and Arsenic Impacts to Soils, Vegetation Communities, and Wildlife Habitat in Southwest Montana Uplands Contaminated by Smelter Emissions: I Field Evaluation. *Environmental Toxicology and Chemistry*. 14:1895-1903.

Galbraith, H. Kapustka, L. and M. Luxon. *In press*. Incorporating habitat quality in ecological risk assessments: role of HSI models, Proceedings of ASTM Symposium on landscape ecology and ecological risk assessment, Kansas City, April, 2003.

Krueper, D. 1997. Annotated Checklist to the Birds of the Upper San Pedro River Valley. Unpublished report – Bureau of Land Management. San Pedro Riparian National Conservation Area.

LeJeune, K., H. Galbraith, J. Lipton, and L.A. Kapustka. 1996. Effects of Metals and Arsenic on Riparian Soils, Vegetation Communities, and Wildlife Habitat in Southwest Montana. *Ecotoxicology*. 5:297-312.

Schamberger, M., and A. Farmer. 1978. The habitat evaluation procedures: their application in project planning and impact evaluation. North American Natural Resources Conference, 43:274-283.

Sedgwick, J.A. 2000. Willow Flycatcher. The Birds of North America. Life Histories for the 21st Century. No. 533 (A. Poole and F. Gill, eds). The Birds of North America., Inc., Philadelphia, PA.

Short, H.L. 1983. Wildlife guilds in Arizona desert habitats. U.S. Fish and Wildlife Service, Ft. Collins, CO. BLM Technical Note 362.

Short, H. L. 1984. Habitat suitability index models: the Arizona Guild and Layers of Habitat models. U.S. Fish and Wildlife Service, Ft. Collins, CO. FWS/OBS-82/10.70

Webb, E.A., and C.E. Bock. 1996. Botteri's sparrow. The Birds of North America. Life Histories for the 21st Century. No. 216 (A. Poole and F. Gill, eds). The Birds of North America., Inc., Philadelphia, PA.

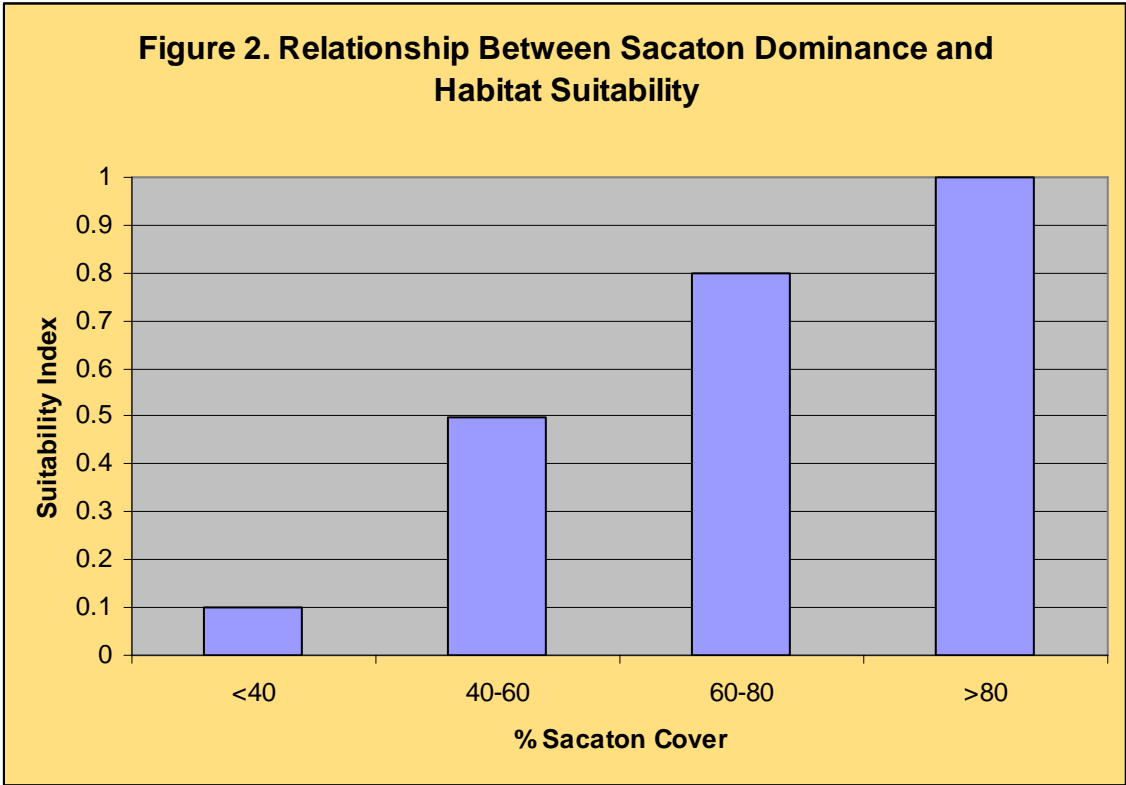
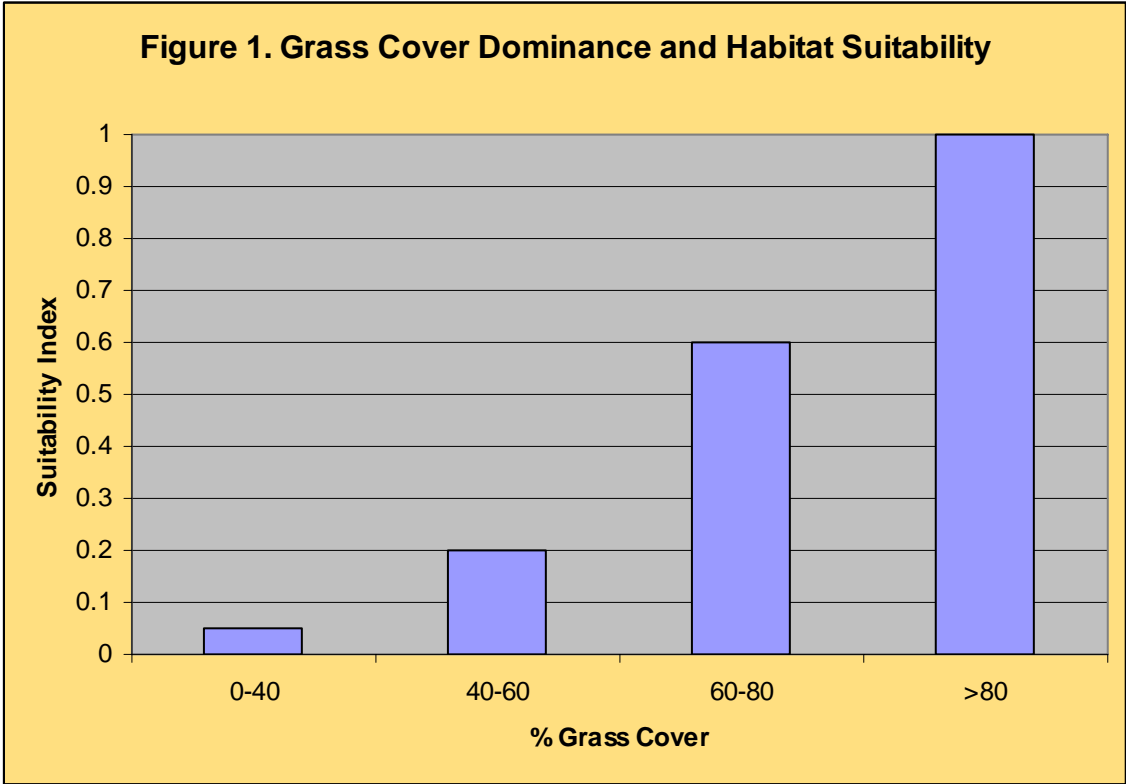


Figure 3. Relationship Between Sacaton Height and Suitability Index

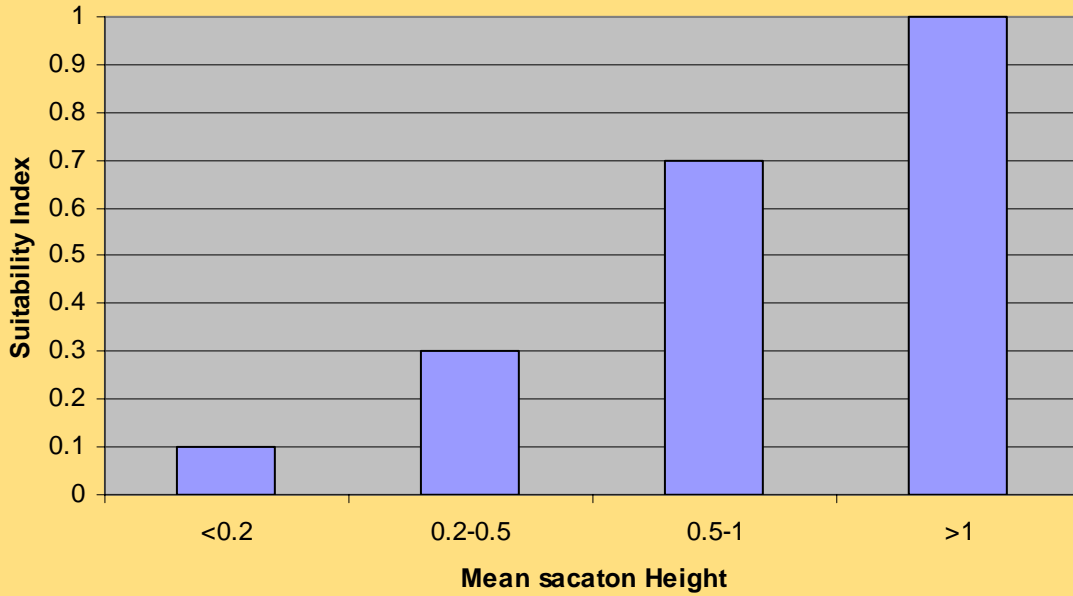


Figure 4. Relationship Between Sacaton Density and Habitat Suitability

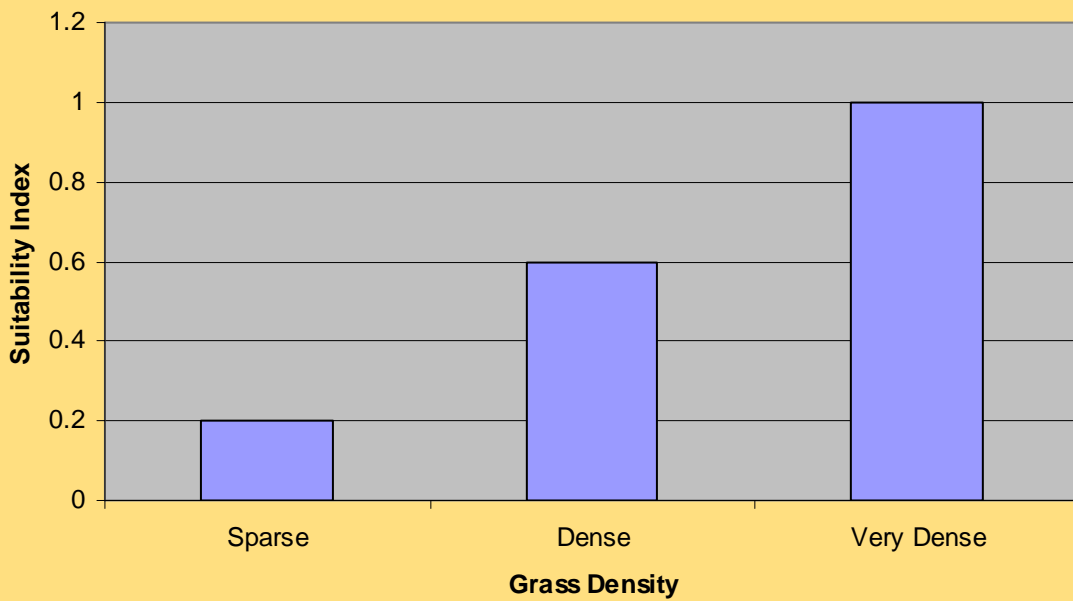


Figure 5. Cover of Senescent Sacaton and Habitat Suitability

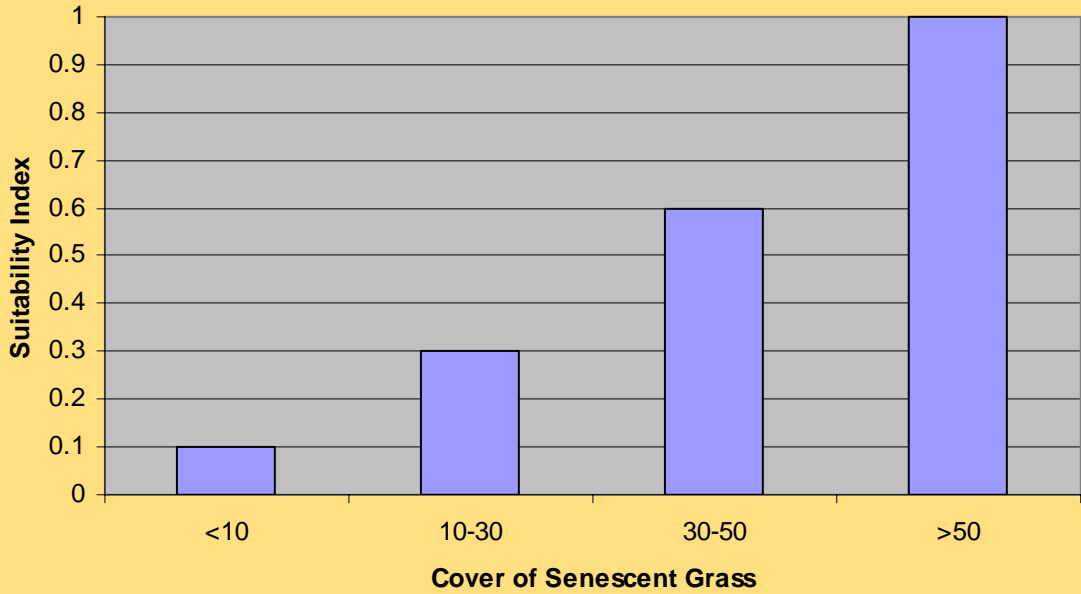


Figure 6. Relationship Between Cover of Forbs or Non-native grasses and Habitat Suitability

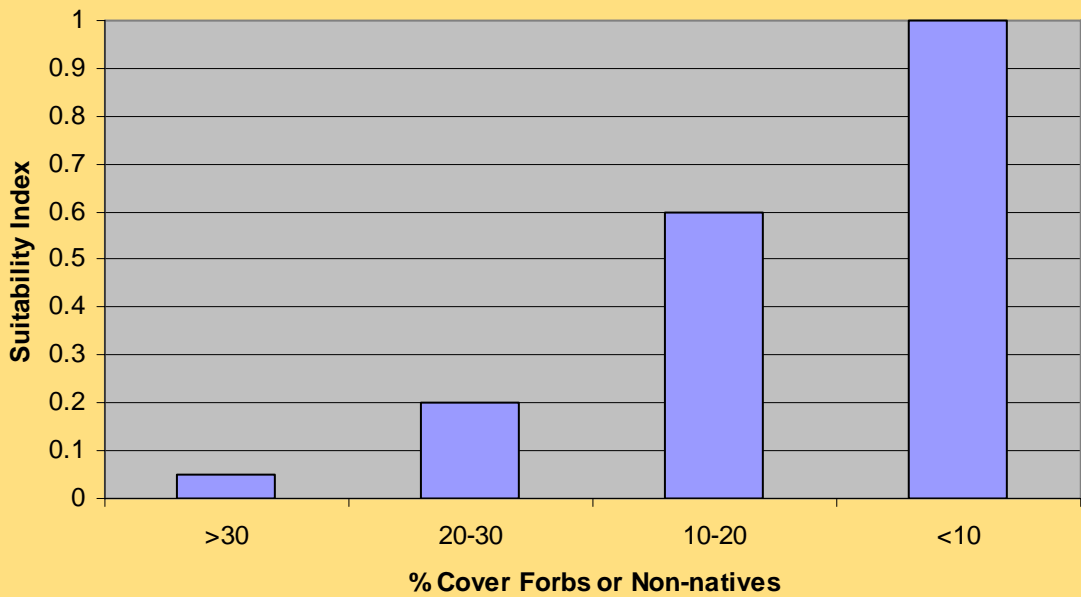
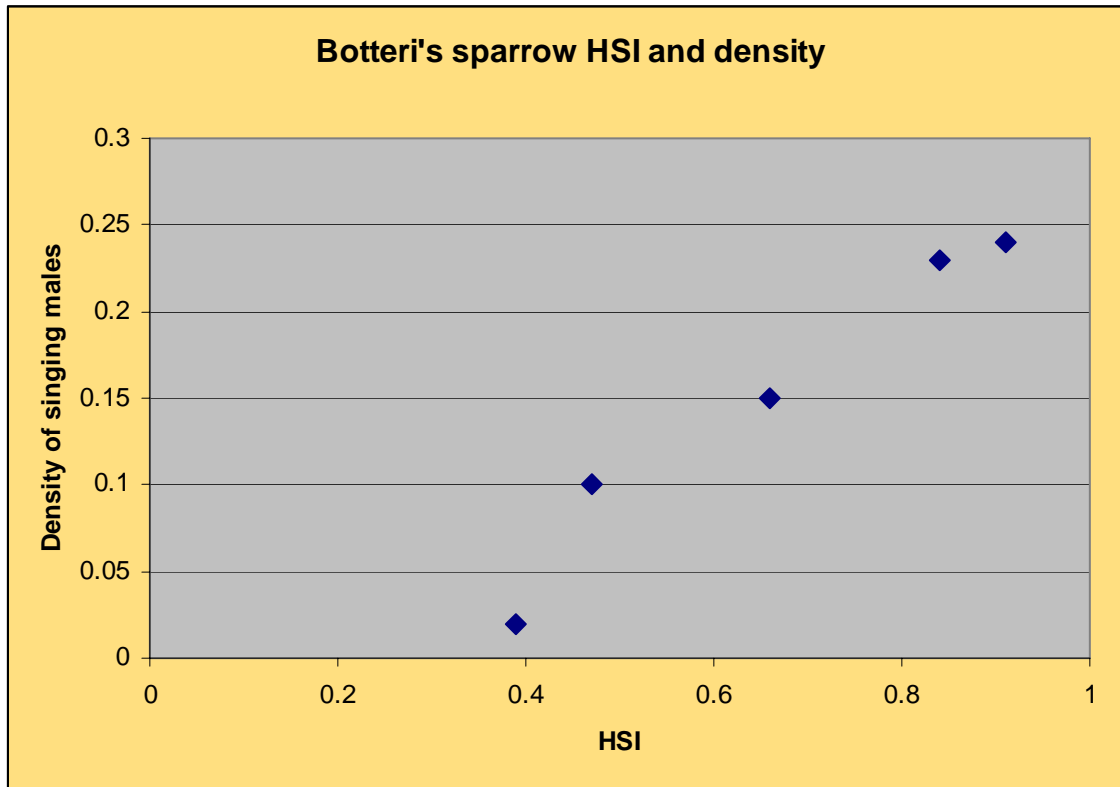


Figure 7. Results of field test of Botteri's sparrow model.



**HABITAT SUITABILITY INDEX MODEL FOR
SOUTHWESTERN WILLOW FLYCATCHER**

Developed by:

Hector Galbraith PhD
Galbraith Environmental Sciences, LLC.
Boulder, Colorado

4th August 2002

1. INTRODUCTION

This document presents a Habitat Suitability Index (HSI) model for the southern Arizona population of the southwestern willow flycatcher, *Empidonax traillii extimus*. It is intended for use in the San Pedro Riparian National Conservation Area (SPRNCA). This model, which quantifies the habitat relationships of the species, is the result of field testing a previous draft version of the model (Galbraith, 2002) and incorporating comments on that previous version by Arizona willow flycatcher researchers. This resulting model will be used, in conjunction with vegetation community and climate modeling predictions, to evaluate the potential effects of global climate change on the ability of the SPRNCA to provide habitat for this species in the future.

1.1 Current and historical distribution, habitat, and status of the southwestern willow flycatcher

The southwestern willow flycatcher is a summer visitor to North America. Mainly because of identification difficulties, little is known about the migration and wintering areas of this race of willow flycatcher, though the species as a whole probably winters in Central and South America, south to Panama and northern Colombia (Finch et al., 2000; Sedgwick, 2000).

Throughout most of its breeding range the willow flycatcher is confined to brushy thickets associated with standing or slow-moving water (Sedgwick, 2000). The southwestern willow flycatcher is largely restricted as a breeding species to riparian shrubby thickets in an otherwise arid or semi-desert landscape (Sogge and Marshall, 2000; U.S. Fish and Wildlife Service, 1997; U.S. Fish and Wildlife Service, 2001; Arizona Game and Fish Department unpublished data; Paradzick and Woodward, in press; Allison et al., in press).

The breeding distribution of the southwestern willow flycatcher once included most of the riparian river reaches in the southwestern states (California, Arizona, Utah, New Mexico, Colorado, Nevada, and Texas). However, the status and distribution of the species has been greatly altered during the late 19th and 20th centuries by human land use patterns. Widespread destruction of riparian habitat by agriculture, mining, dams, water withdrawals, and urbanization has led to the eradication of many subpopulations and a radical reduction in range and numbers. Throughout its breeding range there are now likely to be fewer than 850 occupied territories, with about 341 at 91 sites in Arizona, 224 at 65 sites in California, 263 at 32 sites in New Mexico, and 37 at 5 sites in Colorado (the remainder are in Utah and Nevada) (Sogge et al., 2001). In response to these low numbers and to continuing anthropogenic threats to the subspecies' habitats, U.S. Fish and Wildlife Service listed the subspecies under the Endangered Species Act as "endangered" in 1995.

Southwestern willow flycatchers have bred or have been reported occupying territories in the SPRNCA: at Charleston in 1977 and Hereford in 1989 (Krueper, 1997); at Gray Hawk ranch in 1994 and two territories in the "upper San Pedro" in 1996, and one in 1997 (Paradzick and Woodward, in review). They may be considered intermittent and rare breeders in the area.

1.2 HSI models

HSI models evaluate the likely impacts of any actual or potential changes in habitat quality on carrying capacity (defined here as the habitat's capacity to support organisms) for either a single species, a guild of species, or biodiversity in general. HSI models achieve this by:

9. Identifying the critical habitat variables that affect the carrying capacity of habitat.
10. Establishing quantitative relationships between the occurrence of these variables and the carrying capacity of habitat. Each variable is assigned a suitability index (SI). This is a score of between 0 and 1, where the former is completely unsuitable habitat (i.e., minimal carrying capacity) and the latter is optimal habitat (i.e., greatest carrying capacity).
11. Developing metrics that can be used in the field to quantify the occurrence of the critical habitat components (and, therefore, the carrying capacity of the habitat)
12. Developing algorithms that combine the variable scores (SIs) into an expression of the overall carrying capacity of the habitat. This final score is the HSI and can be between 0 (unsuitable for species or guild) and 1 (optimal habitat).

Previous applications of HSI models have included the prediction of the possible effects of particular land management alternatives on biota (Brand *et al.*, 1986; Schamberger and Farmer, 1978), the quantification of past injuries to ecosystem wildlife carrying capacities (Galbraith *et al.*, 1996; LeJeune *et al.*, 1996), and estimating the exposure to contaminants of wildlife species (Galbraith *et al.*, 2001). If the structures, extents, and/or compositions of post-change vegetation communities can be predicted, it becomes possible to use HSI models to quantify and compare pre- and post-change habitat quality and potential carrying capacities.

U.S. Fish and Wildlife Service has developed approximately 160 HSI models. These include 85 terrestrial species (62 birds, 17 mammals, and 6 reptiles and amphibians). The remainder comprise marine and freshwater organisms. Most of the models have specific geographic, habitat, and seasonal areas of applicability. For example, the model for American woodcock, *Scolopax minor*, applies only to the species' wintering range in the southeastern states (Cade, 1985). In addition to the single-species HSI models, U.S. Fish and Wildlife has also developed a few models that quantify the carrying capacity of habitat for groups of species, for example habitat guild models (Short, 1983; Schroeder, 1986), or for wildlife diversity in general (Short, 1984).

No HSI model exists for the southwestern willow flycatcher in any part of its breeding range. It is one of the objectives of this research project to develop and apply such a model in the San Pedro to evaluate the potential effects of climate change to the biota of the riparian systems.

1.3 Approach used in the development of this HSI model

The components and structure of this model were initially based on a literature review of the habitat preferences and patterns of use of southwestern willow flycatchers. This resulted in a draft model (Galbraith, 2002). This provided a focus for discussions with southwestern willow flycatcher researchers in Arizona, and model modification and testing in the field. Chuck Paradzick and April Woodward, willow flycatcher researchers with Arizona Game and Fish

Department, commented on the draft model. It was then tested along the lower San Pedro and Gila Rivers at Paradzick and Woodward study sites with known flycatcher densities. Based on the comments of Paradzick and Woodward and the field test results the draft model was modified, resulting in this version.

1.5 Seasonal and geographical applicability of this HSI model

This model is intended for use only during the breeding season and in riparian habitat in southern Arizona. It need not necessarily be applicable to sites elsewhere where willow flycatcher habitat preferences may be different.

2. HABITAT INFORMATION

2.3 General

Currently the southwestern willow flycatcher breeds from near sea level to over 8,000 feet above sea level in California, New Mexico, Colorado, Arizona, Utah, Texas, and Nevada (U.S. Fish and Wildlife Service, 2001). In Arizona and the other states within its breeding range, the species is almost entirely confined as a breeding species to riparian shrub habitats and forests with well-developed shrub understories, particularly those dominated by willows (*Salix* spp.) and by salt cedar (*Tamarix chinensis*) (Sogge and Marshall, 2000; U.S. Fish and Wildlife Service, 1997; U.S. Fish and Wildlife Service, 2001; Sedgwick, 2000). It shows a strong preference throughout its range for denser, lush shrub canopies, particularly at nest site height (typically 3-5 meters), and avoids sparser cover.

The species does not seem to need a tree canopy (i.e., older or mature willows and cottonwoods greater than 10m in height) at its nesting sites. Many sites are shrub-dominated, with few or no trees present. At other sites, birds do nest in riparian forest, but only where there is a lush shrub understory. Thus, it appears that it is the shrub habitat layer that is most important to the nesting birds. In Arizona, the two breeding sites with the largest populations, Roosevelt Lake and the Gila/San Pedro River confluence, are largely shrub dominated with only scattered tree canopies (Paradzick and Woodward, in press). Between them, these two sites held over 70% of the total Arizona breeding population in 2000 (Paradzick and Woodward, in press).

While, historically, southwestern willow flycatchers were largely confined to salix-dominated habitats, they, apparently, are able to inhabit and successfully breed in habitats with high proportions, or even dominated by, invasive shrubs (especially salt cedar). At many areas in the two main breeding sites in Arizona (Lake Roosevelt and the Gila/San Pedro River confluence) salt cedar is an important co-dominant (with willow), or is dominant (Paradzick and Woodward, in press). Nesting success does not appear to be impaired by nesting in salt cedar-dominated habitats: in Arizona between 1993 and 1999, percent nest success (the percentage of nests that fledged one or more young) was 54% in salt cedar-dominated habitats and 39% in native spp.-dominated habitats (U.S. Fish and Wildlife Service, 2001).

2.4 Specific habitat requirements/preferences

The specific habitat features in this section are based on the published scientific literature, conversations with southwestern willow flycatcher researchers and observations in the field at breeding sites on the Lower San Pedro and the Gila rivers where nesting habitat typically comprises dense shrub cover (where shrubs are defined as woody vegetation up to approximately 10 m in height, e.g., saltcedar, willow, and cottonwood saplings).

Shrub Patch size. Nesting southwestern willow flycatchers have occurred in isolated shrub patches as small as 0.6 ha and as large as 100 ha (U.S. Fish and Wildlife Service, 2001). In New Mexico on the Gila River, occupied patch size ranged down to 0.9 ha (Skaggs, 1996). Breeding success and productivity in the smallest patch sizes have not been reported, it is possible, however, that nesting in smaller patches (with shorter interior-edge distances, may make flycatchers vulnerable to cowbird parasitism and to predation).

Although small shrub patches (<1 ha) may be used by flycatchers, this occurs mainly in areas where other such patches exist in close proximity (Paradzick and Woodward *pers comm*). Thus the landscape matrix within which the patch exists is important. Small isolated patches (i.e., no other patches within 100m) are not likely to comprise as acceptable breeding habitat.

Patch width. According to U.S. Fish and Wildlife Service (2001), southwestern willow flycatchers do not generally nest in riparian patches with widths of less than 10 meters. Nesting in narrower patches might also expose the flycatchers to greater nest predation/parasitism risk.

Shrub canopy height. Higher shrub canopies are preferred as nesting sites by flycatchers. Allison et al. (*in press*) found in Arizona that each additional meter of canopy height more than tripled the probability that a site would be occupied. Paradzick and Woodward (*in press*) found that sites with median canopy heights within 6-12 meters were preferred by flycatchers. Thus 6 to 10 meters appears to be the typical range in shrub canopy height that provides suitable habitat for flycatchers in the study region.

Shrub canopy cover. Southwestern willow flycatchers typically nest in areas of shrub cover that are almost continuous, but that also have interspersed breaks in the canopy (either patches bare of shrubs or areas where there the canopy cover is thin). These more open areas could be important as feeding sites and as song perches for the males (Allison *et al.*, *in press*).

Shrub density at 3-5 meters. Studies in Arizona and elsewhere have shown a clear preference for nesting in shrub patches where foliage density at about 5 meters and below is high (U.S. Fish and Wildlife Service, 2001; Allison et al., *in press*). Presumably, this is an adaptation to minimize nest losses to predators and brood-parasites. Sparse shrub vegetation is avoided as a nesting habitat.

Tree canopy cover. As previously stated, southwestern willow flycatchers do not apparently require a tree canopy layer in their breeding habitats. However, due to shading, there is likely to be an inverse relationship between tree canopy cover and shrub density, and, therefore habitat suitability: areas with denser tree canopies are likely to have sparser shrub canopies and, therefore, lower habitat suitability.

Distance to standing or slow-moving water. Being a riparian obligate species, southwestern willow flycatchers are found only in areas close to standing or slowly-moving water. However,

within such sites, there is some evidence that flycatchers prefer areas closer to water as nest sites. Marshall (2000) states that territories are seldom more than a “few dozen meters” from water or saturated soil, and often nests are placed over water (Whitfield and Enos, 1996; Sferra et al., 1997). The highest densities of nesting willow flycatchers at the lower San Pedro and Gila study sites have consistently been in areas immediately adjacent (i.e., within 10 m) to the river channel or where the habitat is flooded either by beaver activity or irrigation (Paradzick and Woodward *pers comm*, Galbraith *pers obs.*). During the summer drought of 2002, such areas were among the few in which flycatchers persisted in their breeding attempts and that were successful in raising young. In such areas, the soil moisture content typically ranges from moist to permanently or intermittently saturated.

Micro-climate. Being a riparian species, southwestern willow flycatchers typically inhabit shaded humid areas in an otherwise arid matrix. However, it is unknown whether this is a direct preference for such conditions or a consequence of requiring riparian shrub habitat (which is generally shaded and humid). The main Arizona breeding sites for southwestern willow flycatcher are at Roosevelt lake and the Gila/San Pedro River confluence, which are 3000 feet lower in elevation than the SPRNCA and where average maximum June/July temperatures are about 10°F higher than on the SPRNCA, and where rainfall is generally 6-10 inches less [data obtained from the Internet (<http://www.wrdc.dri.edu/cgi-bin/cliRECtM.pl?azwink>) from weather stations at Fort Huachuca, Maricopa, Winkelman, Sacaton, and Florence]. Thus, if climate change were to result in hotter and more arid conditions prevailing on the SPRNCA, this might not necessarily adversely affect its suitability as a habitat for flycatchers.

3. MODEL COMPONENTS

Based on this review of the habitat preferences of southwestern willow flycatchers, the draft HSI model will incorporate eight variables (patch area and degree of isolation, width of habitat patch, shrub canopy cover, shrub foliage density at 3-5 meters, shrub canopy height, tree canopy cover, distance to standing or slow-moving water, soil moistness). The model does not include a micro-climatic variable (see Section 2.2).

The numerical relationships between each of the variables and habitat suitability are the core of the habitat model. These are given below.

VI. Area and degree of isolation of riparian shrub patch. A riparian shrub or forest patch is defined as a shrub vegetation community (either with or without a tree canopy), generally less than 10 m in height, and dominated by willows and/or salt cedar. Based on data presented in U.S. Fish and Wildlife Service (2001), Skaggs (1996), and conversations with Paradzick and Woodward, the following patch size, patch isolation and habitat suitability categorization has been developed:

PATCH SIZE (ha)	SUITABILITY INDEX (SI)
<1 (and no other patches within 100m)	0.05
<1 (and one or more patches within 100m)	0.2
1-2	0.3
2-5	0.5

>5

1.0

It is assumed in this categorization that patches smaller than 1 ha do not provide habitat for the species unless within a landscape of small patches, that small and medium size patches (1-2 and 2-5 ha, respectively) provide increasing levels of suitability and that patches larger than 5 ha are optimal for the species. This relationship is presented graphically in Figure 1.

V2. *Width of riparian patch.* Based on information presented in U.S. Fish and Wildlife Service (2001), the following patch width and habitat suitability categorization has been hypothesized:

PATCH WIDTH (m)	SUITABILITY INDEX (SI)
<10	0.1
10-50	0.5
>50	1.0

It is assumed in this categorization that the relationship between patch width and habitat suitability is approximately linear and that riparian strips narrower than 10 m do not provide habitat for the species. This relationship is presented graphically in Figure 2.

V3. *Percent shrub canopy cover in 20 m radius of sampling point.* Based on the results reported in U.S. Fish and Wildlife Service (2001), Allison et al. (*in press*), and Paradzick and Woodward unpublished results, the following shrub cover and habitat suitability categorization has been developed:

% COVER	SUITABILITY INDEX (SI)
<50%	0.05
50-60%	0.1
61-80%	0.5
81-90%	1.0
>90%	0.8

It is assumed in this categorization that the relationship between % cover and habitat suitability is approximately linear, except at very high percent shrub covers where continuous shrub cover eliminates the presence of canopy breaks, another important habitat feature for the species. It is also assumed that shrub cover that is less than 50% does not provide habitat for flycatchers. This relationship is presented graphically in Figure 3.

V4. *Shrub foliage density at 3-5 meters.* Based on data presented in U.S. Fish and Wildlife Service (2001), Paradzick and Woodward (*in press*), Marshall (2000), and Sedgwick (2000), the following relationship between shrub foliage density at 3-5 m and habitat suitability has been developed:

FOLIAGE DENSITY	SUITABILITY INDEX (SI)
-----------------	------------------------

Sparse	0.1
Moderately dense	0.3
Dense	0.6
Very dense	1.0

Sparse equates with a site where it is possible to clearly see more than 20 m at 3-5 m elevation above ground level from the sampling point for the majority of 360°. Moderately dense equates with visibility between 10 and 20m. Dense equates with visibility between 5 and 10 m. Very dense equates with visibility less than 5m. This relationship is presented graphically in Figure 4.

V5. Average shrub canopy height within 20 m radius of sampling point. Based on the information reported in Paradzick and Woodward (in press), Marshall (2000), and suggestions by Paradzick, the following mean shrub canopy height and habitat suitability categorization has been developed:

AVERAGE SHRUB CANOPY HEIGHT (m)	SUITABILITY INDEX (SI)
<4	0.1
4-5	0.3
5-6	0.7
>6	1.0

It is assumed in this categorization that canopy heights of less than 4 meters do not provide habitat for flycatchers, and that optimal habitat is reached at 6 meters. This relationship is presented graphically in Figure 5.

V6. Tree canopy cover within 20 m radius of sampling point. Based on the relationships among tree cover, shading and shrub growth, the following tree canopy (woody vegetation > 10m in height) and habitat suitability categorization has been hypothesized:

% TREE CANOPY COVER	SUITABILITY INDEX (SI)
<10	1.0
10-25	0.7
26-50	0.4
51-75	0.2
>75	0

It is assumed in this categorization that at high levels of tree canopy cover (>51%) shading is such that the surviving shrub layer will probably not be dense enough to provide high quality habitat. This relationship is presented graphically in Figure 6.

V7. Distance to standing or slow-moving water. Based on information presented in Marshall (2000), Whitfield and Enos (1996), and Sferra et al. (1997), and personal observations on the

lower San Pedro and Gila rivers, the following distance to water (defined as standing or slow moving water greater than 5 meters in diameter or 2 meters in width) and habitat suitability categorization has been developed:

DISTANCE (m)	SUITABILITY INDEX (SI)
<5	1.0
5-10	0.6
11-20	0.4
>20	0.2

It is assumed in this categorization that even sites distant from water may provide low quality flycatcher habitat. This relationship is presented graphically in Figure 7.

V8. Degree of soil waterlogging. On the lower San Pedro River and its confluence with the Gila River, southwestern willow flycatchers prefer nesting habitat that has at least moist soils, or, optimally, wet or waterlogged soils (Paradzick and Woodward pers comm.). Based on this the following variable categorization has been developed:

SOIL MOISTNESS	SUITABILITY INDEX (SI)
completely dry	0.1
generally damp	0.3
wet	0.6
saturated	1.0

This relationship is presented graphically in Figure 8.

4. MODEL APPLICATION

The eight variables described above will be combined into an index of the overall assessment of the habitat suitability (HSI) of a particular patch of riparian habitat using the following 8th root algorithm:

$$HSI = (V1 \times V2 \times V3 \times V4 \times V5 \times V6 \times V7 \times V8)^{1/8}$$

The HSI values obtained using this equation will range between 0 and 1.0 (lowest and highest estimates of suitability, respectively).

5. FIELD TEST RESULTS

The results of the field test of the southwestern willow flycatcher model are presented in the Attachment A to this document. These results show that the predictions of the HSI model regarding habitat suitability are generally accurate (if it is assumed that breeding density is a reflection of at least short term habitat quality). Thus the HSI model developed for this study is a reasonable predictor of breeding habitat quality for the study species.

6. REFERENCES

- Allison, L. J., C.E. Paradzick, J.W. Rourke, and T.D. McCarthey. In press. A characterization of vegetation in nesting and non-nesting plots for southwestern willow flycatchers in central Arizona. *Studies in Avian Biology*.
- Brand, G.J., S.R. Shifley, and L.F. Ohman. 1986. Linking wildlife and vegetation models to forecast the effects of management. In: J. Verner, M.L. Morrison, and C.J. Ralph (eds), *Wildlife 2000: modeling habitat relationships of terrestrial vertebrates*. University of Wisconsin Press, Madison, Wisconsin.
- Cade, B.S. 1985. Habitat suitability index models: American woodcock (wintering). U.S. Fish Wildl. Serv. Biol. Rep. 82(10.105). Ft. Collins, Colorado.
- Finch, D.M., J.F. Kelly, and J-L. E. Cartron. 2000. Migration and winter ecology. In: *Status, Ecology, and Conservation of the Southwestern Willow Flycatcher*. USDA, Forest Service General Report RMRS-GTR-60.
- Galbraith, H. 2002. Draft habitat suitability index model for the southwestern willow flycatcher. Unpublished report to American Bird Conservancy. 18th April, 2002.
- Galbraith, H., K. LeJeune, and J. Lipton. 1996. Metal and Arsenic Impacts to Soils, Vegetation Communities, and Wildlife Habitat in Southwest Montana Uplands Contaminated by Smelter Emissions: I Field Evaluation. *Environmental Toxicology and Chemistry*. 14:1895-1903.
- Galbraith, H. Kapustka, L. and M. Luxon. 2001. Incorporating habitat quality in ecological risk assessments: selecting assessment species, SETAC Annual Conference, Baltimore, MD, November, 2001.
- Hatten, J.R., and C.E. Paradzick. In press. A multi-scaled model of southwestern willow flycatcher breeding habitat.
- Krueper, D. 1997. Annotated Checklist to the Birds of the Upper San Pedro River Valley. Unpublished report – Bureau of Land Management. San Pedro Riparian National Conservation Area.
- LeJeune, K., H. Galbraith, J. Lipton, and L.A. Kapustka. 1996. Effects of Metals and Arsenic on Riparian Soils, Vegetation Communities, and Wildlife Habitat in Southwest Montana. *Ecotoxicology*. 5:297-312.
- Marshall, R.M. 2000. Population status on breeding grounds. In: *Status, Ecology, and Conservation of the Southwestern Willow Flycatcher*. USDA, Forest Service General Report RMRS-GTR-60.

- Paradzick, C.E., and A.A. Woodward. In press. Distribution, abundance, and habitat characteristics of southwestern willow flycatchers (*Empidonax traillii extimus*) in Arizona, 1993-2000. *Studies in Avian Biology*.
- Schamberger, M., and A. Farmer. 1978. The habitat evaluation procedures: their application in project planning and impact evaluation. *North American Natural Resources Conference*, 43:274-283.
- Schroeder, R.L. 1986. Habitat suitability index models: wildlife species richness in shelterbelts. U.S. Fish and Wildlife Service Biological Report 82. Fort Collins, Colorado.
- Sedgwick, J.A. 2000. Willow Flycatcher. *The Birds of North America. Life Histories for the 21st Century*. No. 533 (A. Poole and F. Gill, eds). The Birds of North America, Inc., Philadelphia, PA.
- Sferra, S.J., T.E. Corman, C.E. Paradzick, J.W. Rourke, J.A. Spencer, and M.W. Sumner. 1997. Arizona Partners in Flight southwestern willow flycatcher survey: 1993-1996 summary report. Arizona Game and Fish Department. Nongame technical Report 113. Phoenix.
- Short, H.L. 1983. Wildlife guilds in Arizona desert habitats. U.S. Fish and Wildlife Service, Ft. Collins, CO. BLM Technical Note 362.
- Short, H. L. 1984. Habitat suitability index models: the Arizona Guild and Layers of Habitat models. U.S. Fish and Wildlife Service, Ft. Collins, CO. FWS/OBS-82/10.70
- Skaggs, R.W. 1996. Population size, breeding biology, and habitat of willow flycatchers in the Cliff-Gila Valley, New Mexico. New Mexico department of Fish and game Report.
- Sogge, M.K., and R.M. Marshall, 2000. A survey of current breeding habitats. In: *Status, Ecology, and Conservation of the Southwestern Willow Flycatcher*. USDA, Forest Service General Report RMRS-GTR-60.
- Sogge, M.K., Sferra, S.J., McCarthy, T., Williams, S.O., and B.E. Kus. 2001. Southwestern willow flycatcher breeding site and territory summary – 2000. US Fish and Wildlife Service, Region 2, Albuquerque, NM.
- U.S. Fish and Wildlife Service, 1997. Final determination of critical habitat for the southwestern willow flycatcher. *Federal Register* 62:39129-39146 (July 22, 1997).
- U.S. Fish and Wildlife Service, 2001. Southwestern willow flycatcher – draft recovery plan. U.S. Fish and Wildlife Service, Albuquerque, New Mexico.
- Whitfield, M.J., and K.M. Enos, 1996. A brown-headed cowbird control program and monitoring for the southwestern willow flycatcher, South Fork Kern River, California, 1996. California Department of Fish and Game, Sacramento.

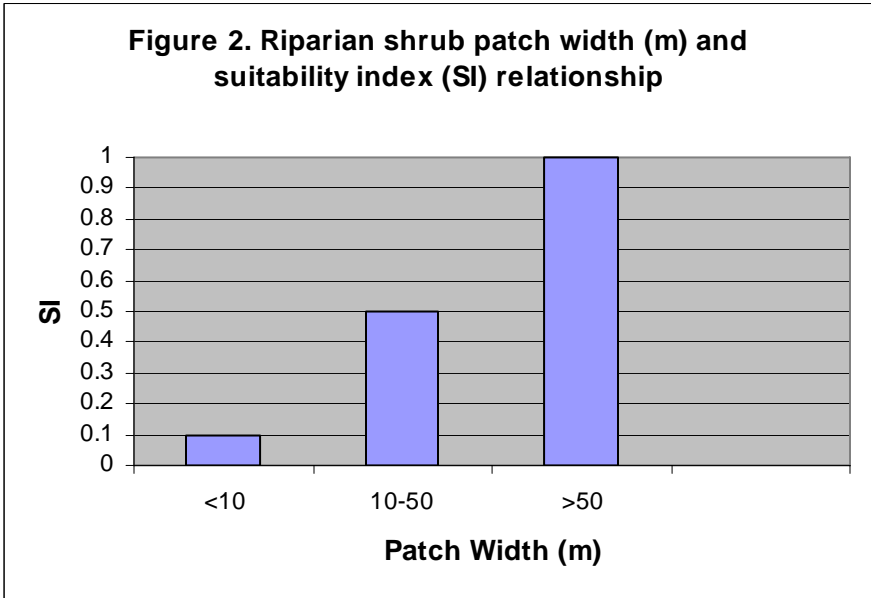
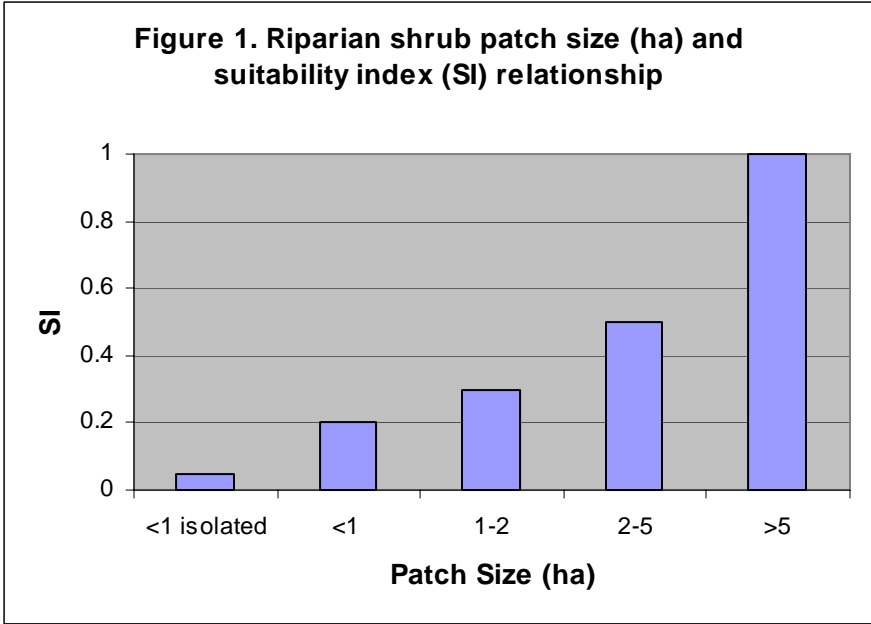


Figure 3. Percent shrub canopy cover and suitability index (SI) relationship

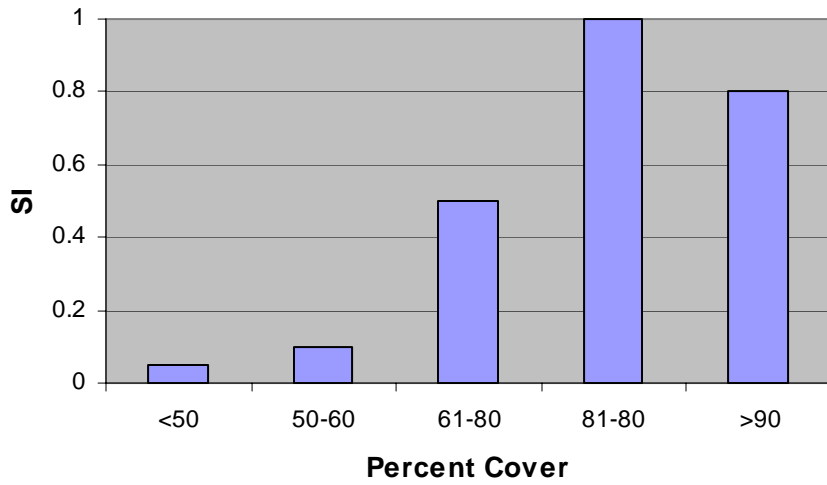


Figure 4. Shrub foliage density and suitability index (SI) relationship

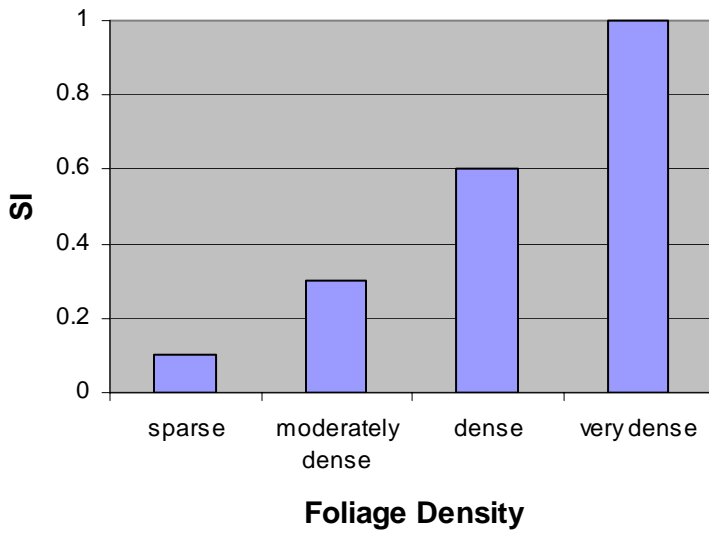


Figure 5. Mean shrub canopy height (m) and suitability index (SI) relationship

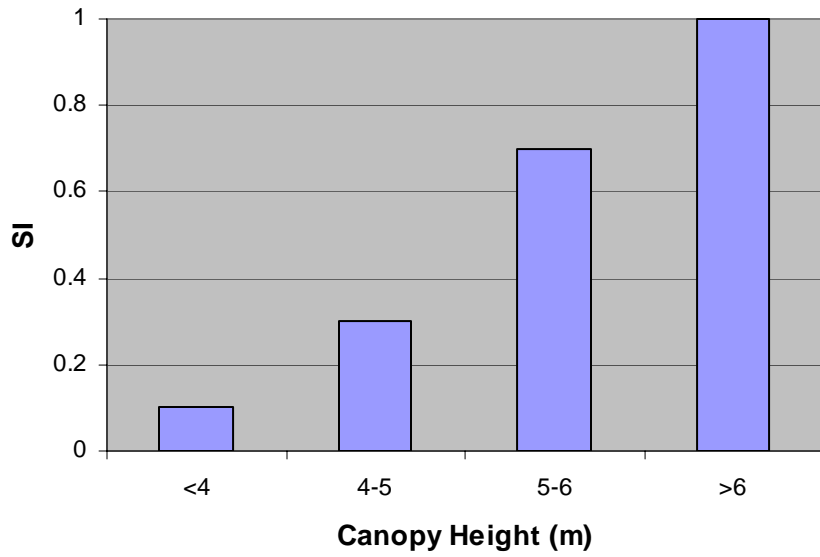
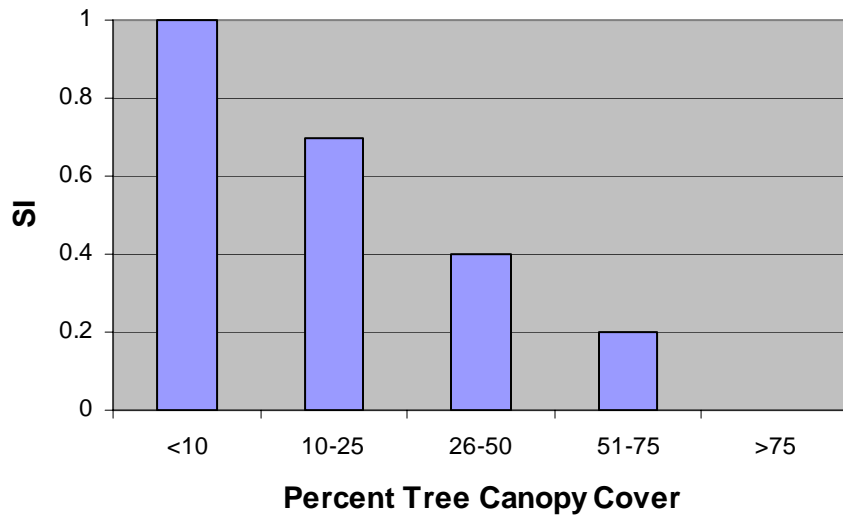
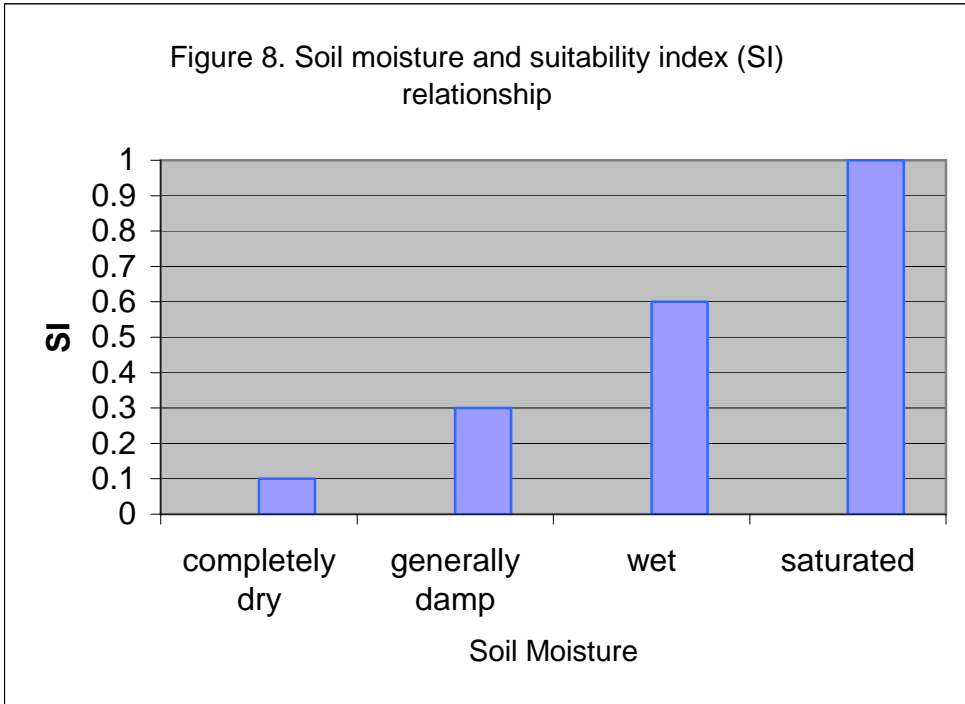
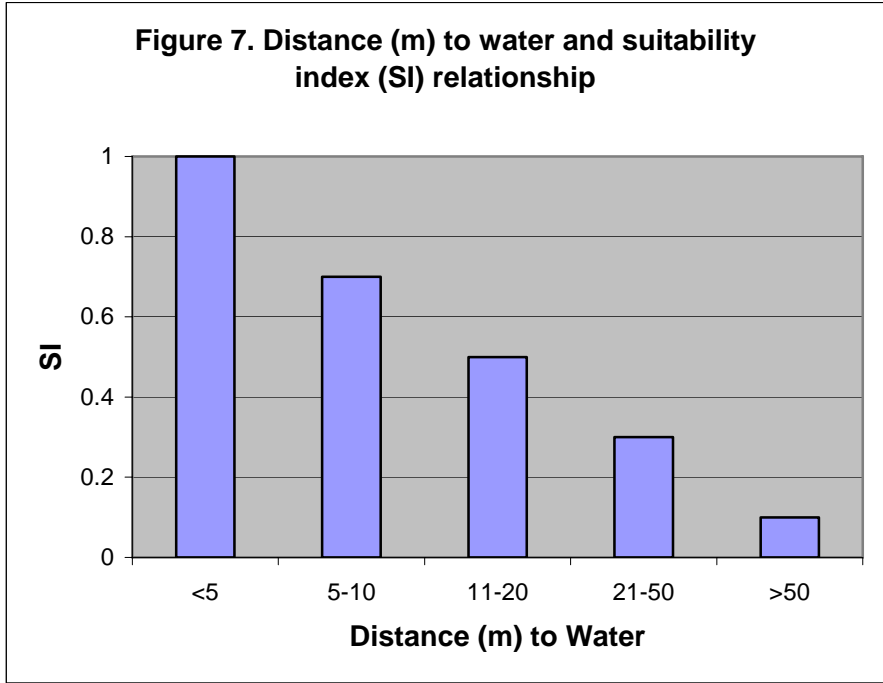


Figure 6. Tree canopy cover and suitability index (SI) relationship





Attachment A – Results of Field Tests of Willow Flycatcher Model

Table A1 shows the results of surveying southwestern willow flycatcher breeding habitat quality at seven sites of differing breeding densities on the lower San Pedro and Gila rivers. The resulting HSI scores are plotted against known breeding density in Figure A1. These results show that the predictions of the HSI model regarding habitat suitability are generally accurate (if it is assumed that breeding density is a reflection of at least short term habitat quality). Thus the HSI model developed for this study is a reasonable predictor of breeding habitat quality for the study species.

The data in Table A1 show most variation between sites for variable V3, V4, V7, and V8. Thus, it is largely shrub canopy cover and density and proximity to standing water and soil water that drive the differences in HSI scores among sites. Figure A2 shows a site with comparatively low quality habitat (site GS-7). This is a salt cedar dominated site with generally low to moderate shrub density, more than 20 m from standing water and, since it is perched on a bench 5 m above the river, completely dry soil. At this site, the breeding density was only 1.7 territories/ha.

In contrast, Figures A3 and A4 show a site (Wheat) of high breeding density (9.9 territories/ha). At this salt cedar dominated site the shrub canopy is very dense and the site is in close proximity (<5 m) to the river. Furthermore, the site is regularly flooded by excess irrigation water from an adjacent cotton field. Therefore, the site is kept permanently wet. This combination of a dense shrub layer and wet conditions create optimal flycatcher habitat.

Table A1. SI and HSI scores and breeding densities for southwestern willow flycatcher sites visited in July 2002.

Site	V1	V2	V3	V4	V5	V6
ARVN 1	1	1	0.5	0.6	1	1
GN18	1	1	0.5	0.6	1	1
KRNYPD	1	1	1	1	1	1
ARVN 2	1	1	0.1	0.3	1	0.2
San Pedro Aravaipa confluence	1	1	0.05	0.1	0.7	0.4
Wheat	1	1	0.5	1	1	1
GS 7	1	1	0.1	0.3	0.7	1

Table A1 continued

Site	V7	V8	HSI	Density (territories/ha)
ARVN 1	0.2	0.3	0.60	6.4
GN18	0.4	0.1	0.57	6.1
KRNYPD	0.6	0.6	0.88	10.8
ARVN2	0.6	0.3	0.42	3.8
San Pedro Aravaipa confluence	0.4	0.3	0.33	2.7
Wheat	1	1	0.92	9.9
GS 7	0.2	0.1	0.37	1.7

Figure A1. HSI scores and breeding densities of southwestern willow flycatchers on San Pedro and Gila rivers

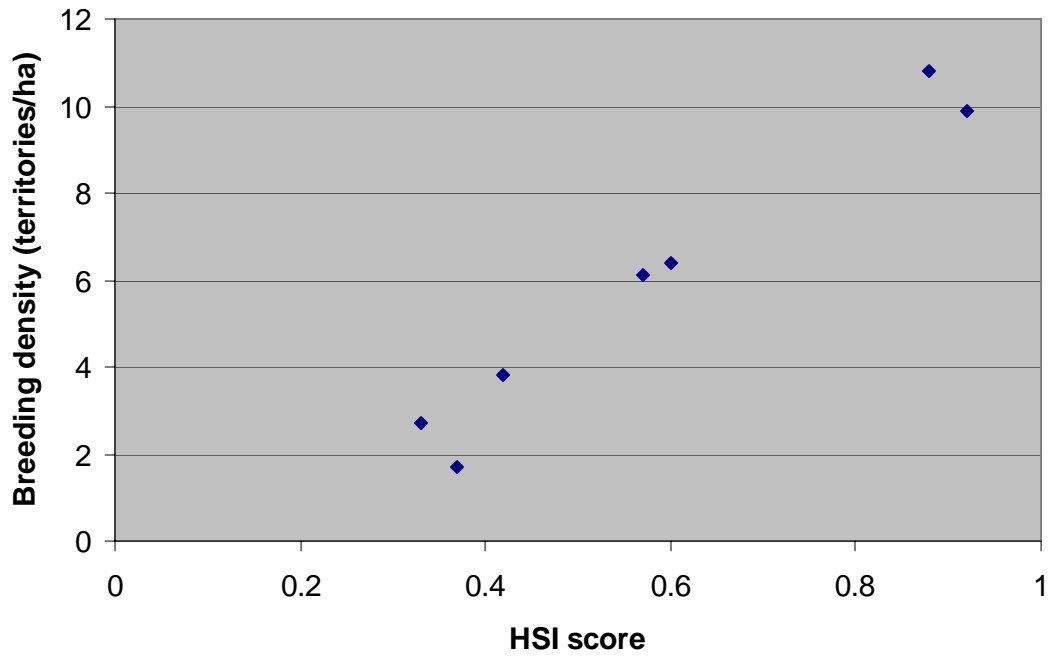




Figure A2. GS-7 Site. The southwestern willow flycatchers breed in the salt cedar scrub on the left bank perched about 3 metres above the river.



Figure A3. Interior of GS-7 site showing the comparatively open shrub layer and the complete lack of standing water or soil moisture. Because of these attributes, this site has a low density of breeding flycatchers.



Figure A4. Wheat site on lower San Pedro River. The southwestern willow flycatchers breed in the thick salt cedar scrub to the left of the river channel.



Figure A5. Interior of Wheat site on the lower San Pedro River. The area beyond the person in the picture is kept wet or flooded by releases of irrigation water from a cotton field that is to the left of the site. Also, the river is less than 8 m to the left of the area shown in the photograph. This site combines several essential attributes of flycatcher breeding habitat: a dense shrub layer and a more or less wetland cover type.

**HABITAT SUITABILITY INDEX MODEL FOR
WILSON'S WARBLERS MIGRATING IN SPRING THROUGH THE SAN PEDRO
NATIONAL CONSERVATION AREA**

Developed by:

Hector Galbraith PhD
Galbraith Environmental Sciences, LLC.
Boulder, Colorado

19 June 2003

1. INTRODUCTION

This document presents a spring migration season Habitat Suitability Index (HSI) model for Wilson's warblers (*Wilsonia pusilla*), intended for use in the San Pedro Riparian National Conservation Area (SPRNCA). This model, which quantifies the habitat relationships of the species, is the result of a review of the scientific literature, focusing mainly on those studies that concern the habitat use by the species during spring migration. The model was tested in areas of the San Pedro where previous survey work has quantified Wilson's warbler density. The model will be used, in conjunction with vegetation community and climate modeling predictions, to evaluate the potential effects of global climate change on the ability of the SPRNCA to provide spring migration habitat for this species in the future.

1.1 Spring migration of Wilson's warblers in the SPRNCA

Wilson's warbler is a common spring migrant in the SPRNCA (Kreuper, 1997), where densities of as high as 480/km² have been recorded (Skagen et al., 1998). The first migrants (generally males) appear at the SPRNCA in early to mid-March and numbers peak in early May, declining by mid-May. Wilson's warbler does not breed in the SPRNCA (Kreuper, 1997)

While the total numbers of Wilson's warblers that migrate into North America in spring are unknown, it is highly likely that a substantial proportion of the birds that subsequently breed in the western part of their breeding range pass through the SPRNCA. It is, therefore, an important migration stopover site for this species.

1.2 HSI models

HSI models evaluate the likely impacts of any actual or potential changes in habitat quality on carrying capacity (defined here as the habitat's capacity to support organisms) for either a single species, a guild of species, or biodiversity in general. HSI models achieve this by:

13. Identifying the critical habitat variables that affect the carrying capacity of habitat.
14. Establishing quantitative relationships between the occurrence of these variables and the carrying capacity of habitat. Each variable is assigned a suitability index (SI). This is a score of between 0 and 1, where the former is completely unsuitable habitat (i.e., minimal carrying capacity) and the latter is optimal habitat (i.e., greatest carrying capacity).
15. Developing metrics that can be used in the field to quantify the occurrence of the critical habitat components (and, therefore, the carrying capacity of the habitat)
16. Developing algorithms that combine the variable scores (SIs) into an expression of the overall carrying capacity of the habitat. This final score is the HSI and can be between 0 (unsuitable for species or guild) and 1 (optimal habitat).

Previous applications of HSI models have included the prediction of the possible effects of particular land management alternatives on biota (Brand *et al.*, 1986; Schamberger and Farmer, 1978), the quantification of past injuries to ecosystem wildlife carrying capacities (Galbraith *et al.*, 1996; LeJeune *et al.*, 1996), evaluating the potential effects of climate change and aquifer

depletion on biota (Galbraith et al., *in press*), and estimating the exposure to contaminants of wildlife species. If the structures, extents, and/or compositions of post-change vegetation communities can be predicted, it becomes possible to use HSI models to quantify and compare pre- and post-change habitat quality and potential carrying capacities.

U.S. Fish and Wildlife Service has developed approximately 160 HSI models. These include 85 terrestrial species (62 birds, 17 mammals, and 6 reptiles and amphibians). The remainder comprise marine and freshwater organisms. Most of the models have specific geographic, habitat, and seasonal areas of applicability. For example, the model for American woodcock, *Scolopax minor*, applies only to the species' wintering range in the southeastern states (Cade, 1985). In addition to the single-species HSI models, U.S. Fish and Wildlife has also developed a few models that quantify the carrying capacity of habitat for groups of species, for example habitat guild models (Short, 1983), or for wildlife diversity in general (Short, 1984).

No HSI models exist for the Wilson's warbler in any parts of its range. Thus, a new HSI model has been developed. It is tailored to the specific needs of quantifying habitat during spring migration in the SPRNCA.

1.3 Approach used in the development of this HSI model

The components and structure of this provisional model were based on a literature review of the habitat preferences and patterns of use of Wilson's warblers during their spring migration in the Western U.S. The literature sources are cited in Section 6. The resulting draft model was then tested against empirical data (singing male densities in spring) from the SPRNCA and modified where necessary.

1.6 Seasonal and geographical applicability of this HSI model

This model is intended for use only during the spring migration season and in riparian habitat in southern Arizona. It may be applicable to sites elsewhere where Wilson's warbler migration habitat preferences may be different.

2. HABITAT INFORMATION

2.5 General

During spring migration in the western U.S., the Wilson's warbler typically occurs in wetland shrub and forested habitats (Kaufman, 1996; Dunn and Garrett, 1997; Amon and Gilbert, 1999). Along the Rio Grande River in New Mexico, Yong et al (1998) found the species to be most abundant in spring in riparian shrub habitat (willow), less abundant in riparian cottonwood forest, and least abundant in shrub habitat dominated by salt cedar or Russian olive. Thus, unlike the yellow warbler, Wilson's warblers apparently are not strongly tied to communities with a tree canopy, and they avoid communities dominated by the two invasive shrubs listed above.

2.6 Specific habitat requirements/preferences

The specific habitat features in this section are based on the published scientific literature, and communications with Wilson's warbler researchers on the San Pedro (Susan Skagen of USGS and Jack Whetstone of BLM). The specific features are identified below:

Forest/Shrub Patch size. Studies in southern Arizona (Skagen et al., 1998) have shown that migrating Wilson's warblers are not confined to the largest, most contiguous habitat patches, and that they may also utilize smaller habitat fragments. The smallest habitat patches investigated by Skagen et al. (1998) were about 40 ha in extent, while the largest exceeded 2,000 ha. Densities of birds did not differ between these two size categories. Nevertheless, there is no doubt a minimum size at which a patch will not provide suitable habitat for migrating yellow warblers. Based on the Skagen et al., (1998) results, this patch size must be less than 40 ha.

Presence of Tree Canopy Layer. Unlike the yellow warbler, Wilson's warblers during spring migration (and on their breeding range [Amon and Gilbert, 1999]) are not confined to riparian vegetation with a vertical tree layer, but prefer lower shrub dominated vegetation. This preference is reflected in the fact that they typically forage closer to the ground than other warblers: <2m (Hutto, 1981)

% Dominance in Shrub Layer by Hydrophytes. The preferred foraging habitats for Wilson's warblers comprise medium sized to tall hydrophytic shrubs, willows (Yong et al., 1998). Hutto (1985) found that in southern Arizona spring densities of Wilson's warblers were low in vegetation communities dominated by mesquite, acacia, or other such xeric species. Yong et al. (1998) determined that during spring stopover on the Rio Grande, daily weight gains were highest among birds foraging in willow, and lower in other communities, particularly when dominated by salt cedar and Russian olive. Thus the representation of hydrophytic shrubs is an important habitat characteristic for Wilson's warblers.

Heights of Shrub and Tree Canopy Layers. Wilson's warblers typically forage closer to the ground than yellow warblers. Hutto (1981) found that the mean foraging height in summer in Wyoming was less than 1.5 m (compared to 2.6 m for yellow warbler). Thus, taller shrubs, whether or not a tree canopy is present, comprises suitable habitat.

Exotic shrub species. Yong et al. (1998) found in riparian habitat in New Mexico that Wilson's warblers occurred at relatively low densities in shrub communities with a high representation of the exotic shrubs salt cedar and Russian olive. When foraging in such habitats, daily weight gains were lower than in preferred willow shrub. Thus, salt cedar dominated habitat must be considered sub-optimal habitat.

3. MODEL COMPONENTS

Based on this review of the habitat preferences of Wilson's warblers, the draft HSI model will incorporate five variables (see below). The numerical relationships between each of the variables and habitat suitability are the core of the habitat model. These are given below.

VI. Riparian forest/shrub patch size. A riparian shrub or forest patch is defined as a shrub vegetation community (either with or without a tree canopy), dominated by cottonwoods or

willows. Based on data presented in Skagen et al. (1998), and conversations with Susan Skagen, the following patch size and habitat suitability categorization has been developed:

PATCH SIZE (ha)	SUITABILITY INDEX (SI)
<1 (and no other patches within 100m)	0.05
<1 (and one or more patches within 100m)	0.1
1-20	0.3
21-40	0.5
>40	1.0

It is assumed in this categorization that patches smaller than 1 ha do not provide habitat for the species unless within a landscape of small patches, that small and medium size patches (1-20 and 21-40 ha, respectively) provide increasing levels of suitability and that patches larger than 40 ha are optimal for the species. This relationship is presented graphically in Figure 1.

V2. *Percent shrub canopy cover in 20 m radius of sampling point*). Based on information from the scientific literature, the following shrub cover and habitat suitability categorization has been developed:

% COVER	SUITABILITY INDEX (SI)
<30%	0.05
30-50%	0.2
50-70%	0.5
70-100%	1.0

It is assumed in this categorization that the relationship between % cover and habitat suitability is approximately linear. It is also assumed that shrub cover that is less than 30% provides only poor quality habitat for Wilson’s warblers. This relationship is presented graphically in Figure 2.

V3. *% Cover in shrub canopy of cottonwood or willow in 20m radius of sampling point*. Based on information from the scientific literature, the following relationship between shrub canopy cover and habitat suitability has been developed:

% COVER	SUITABILITY INDEX (SI)
<20%	0.1
20-40%	0.3
40-60%	0.6
>60%	1.0

This relationship is presented graphically in Figure 3.

V4. *Mean shrub canopy height in 20 m radius of sampling point*. Based on information from the scientific literature, the following relationship between shrub canopy height and habitat suitability has been developed (only where no tree canopy exists):

MEAN SHRUB CANOPY HEIGHT (m)	SUITABILITY INDEX (SI)
<0.5	0.05
0.5-1	0.3
1-1.5	0.8
>1.5	1.0

This relationship is presented graphically in Figure 4.

V5. % dominance in shrub canopy by salt cedar in 20 m radius of sampling point. Based on information from the scientific literature, the following relationship habitat suitability for Wilson's warblers and salt cedar has been developed:

% DOMINANCE	SUITABILITY INDEX (SI)
<5	1.0
5-20	0.7
20-30	0.6
30-40	0.3
>40	0.1

This relationship is presented graphically in Figure 5.

4. MODEL APPLICATION

The five variables described above are combined into an index of the overall assessment of the habitat suitability (HSI) of a particular patch of riparian habitat using the following 5th root algorithm:

$$HSI = (V1 \times V2 \times V3 \times V4 \times V5)^{1/5}$$

The HSI values obtained using this equation will range between 0 and 1.0 (lowest and highest estimates of suitability, respectively).

5. FIELD TEST RESULTS

The Wilson's warbler draft model was tested in June, 2003 by visiting sites on the San Pedro River where Bureau of Land Management surveys had quantified densities of singing males in each year between 1986 and 1990. In the absence of visual evidence to the contrary, it was assumed that little or no habitat change had occurred between the survey years and the present. The results of the field test of the model are presented in Figure 6. These results show that the predictions of the HSI model regarding habitat suitability are generally accurate (if it is assumed that breeding density is a reflection of at least short term habitat quality, except at sites where the HSI values are less than about 0.3. Apparently, Wilson's warblers migrating through the San Pedro do not consider such sites as providing habitat. Thus, the HSI model developed for this study is a reasonable predictor of breeding habitat quality for the study species.

6. REFERENCES

- Amon, E.M., and W.M. Gilbert. Wilson's warbler (*Wilsonia pusilla*). In *The Birds of North America*, No. 478 (A. Poole and F. Gill, eds). The Birds of North America, Inc. Philadelphia, PA.
- Brand, G.J., S.R. Shifley, and L.F. Ohman. 1986. Linking wildlife and vegetation models to forecast the effects of management. In: J. Verner, M.L. Morrison, and C.J. Ralph (eds), *Wildlife 2000: modeling habitat relationships of terrestrial vertebrates*. University of Wisconsin Press, Madison, Wisconsin.
- Cade, B.S. 1985. Habitat suitability index models: American woodcock (wintering). U.S. Fish Wildl. Serv. Biol. Rep. 82(10.105). Ft. Collins, Colorado.
- Dunn, J., and K. Garrett. 1997. *Peterson Field Guides: warblers*. Houghton Mifflin, Boston.
- Galbraith, H. 2002. Draft habitat suitability index model for the southwestern willow flycatcher. Unpublished report to American Bird Conservancy. 18th April, 2002.
- Galbraith, H., K. LeJeune, and J. Lipton. 1996. Metal and Arsenic Impacts to Soils, Vegetation Communities, and Wildlife Habitat in Southwest Montana Uplands Contaminated by Smelter Emissions: I Field Evaluation. *Environmental Toxicology and Chemistry*. 14:1895-1903.
- Galbraith, H., Kapustka, L. and M. Luxon. *In press*. Incorporating habitat quality in ecological risk assessments: role of HSI models, Proceedings of ASTM Symposium on landscape ecology and ecological risk assessment, Kansas City, April, 2003.
- Hutto, R.L. 1981. Seasonal variation in the foraging behavior of some migratory western wood warblers. *The Auk*, 98:765-777.
- Hutto, R.L. 1985. Seasonal changes in the habitat distribution of transient insectivorous birds in southeastern Arizona: competition mediated? *The Auk*, 102:120-132.
- Kaufman, K. 1996. *Lives of North American Birds*. Houghton Mifflin, Boston.
- Krueper, D. 1997. Annotated Checklist to the Birds of the Upper San Pedro River Valley. Unpublished report – Bureau of Land Management. San Pedro Riparian National Conservation Area.
- LeJeune, K., H. Galbraith, J. Lipton, and L.A. Kapustka. 1996. Effects of Metals and Arsenic on Riparian Soils, Vegetation Communities, and Wildlife Habitat in Southwest Montana. *Ecotoxicology*. 5:297-312.
- Schamberger, M., and A. Farmer. 1978. The habitat evaluation procedures: their application in project planning and impact evaluation. North American Natural Resources Conference, 43:274-283.

Short, H.L. 1983. Wildlife guilds in Arizona desert habitats. U.S. Fish and Wildlife Service, Ft. Collins, CO. BLM Technical Note 362.

Short, H. L. 1984. Habitat suitability index models: the Arizona Guild and Layers of Habitat models. U.S. Fish and Wildlife Service, Ft. Collins, CO. FWS/OBS-82/10.70

Skagen, S.K., C.P. Melcher, W.H. Howe, and F.L. Knopf. 1998. Comparative use of riparian corridors and oases by migrating birds in Southeast Arizona. *Cons. Biol.* 12:896-909.

Yong, W., D.M. Finch, F.R. Moore, and J.F. Kelly. 1998. Stopover ecology and habitat use of migratory Wilson's warblers. *The Auk*, 115:829-842.

Figure 1. Riparian forest/shrub patch size

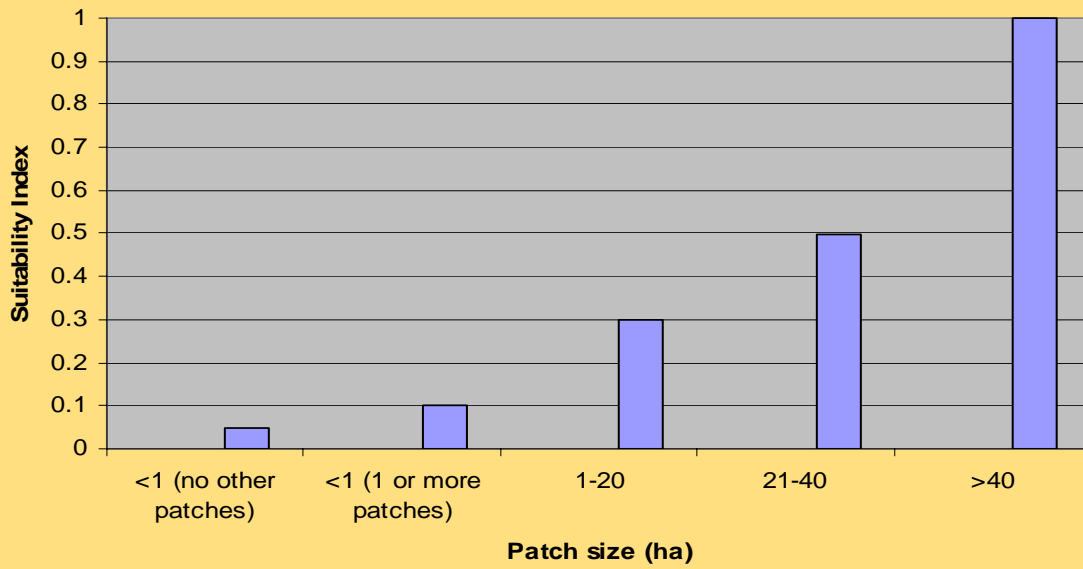
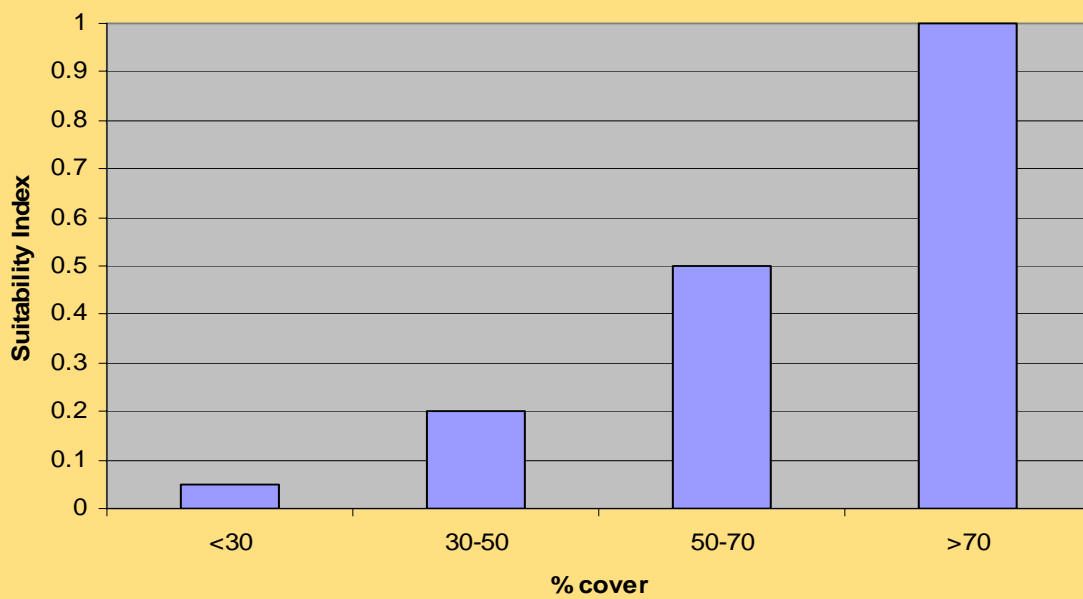


Figure 2. Shrub Canopy Cover and Habitat Suitability



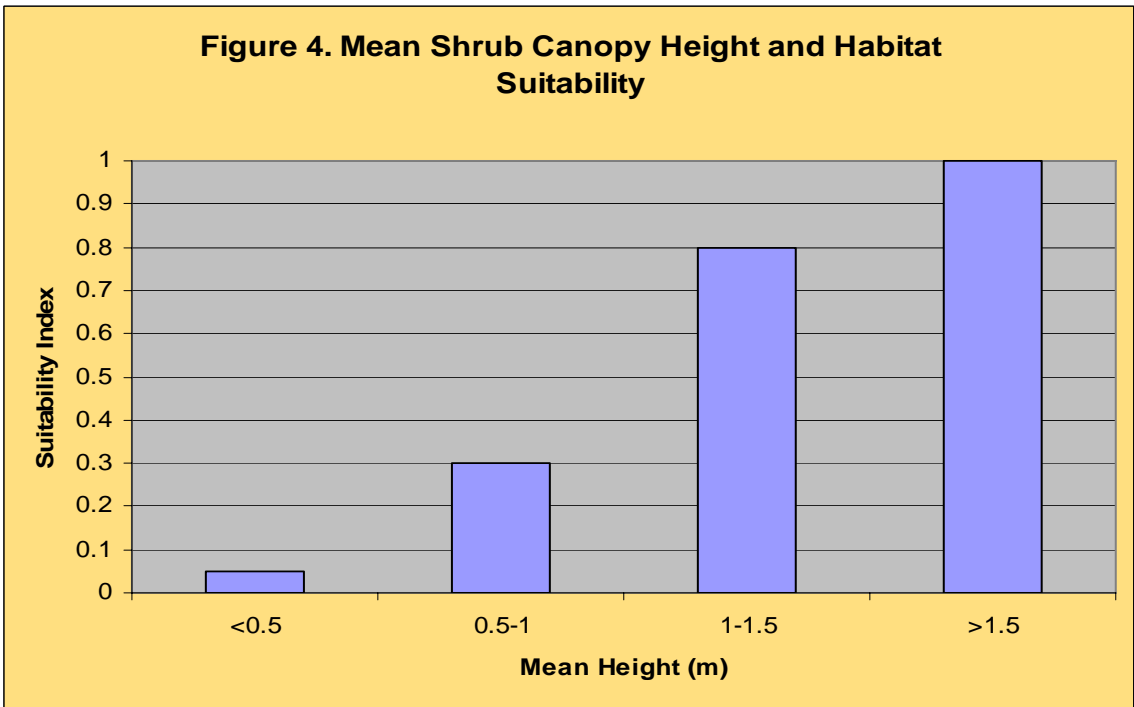
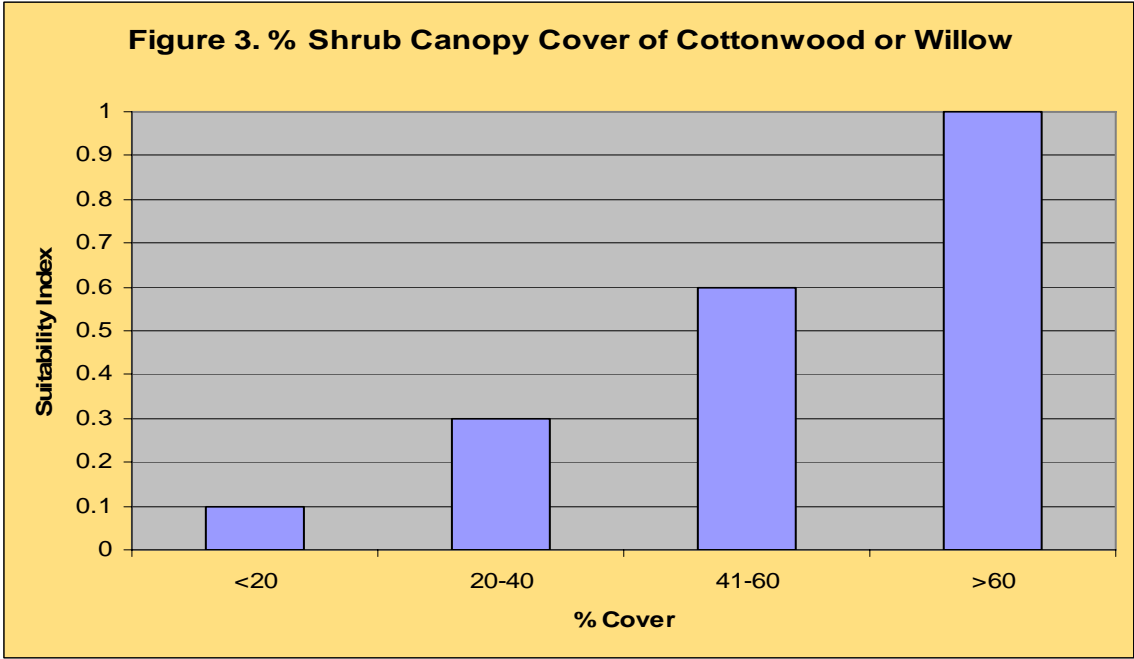


Figure 5. % Dominance of Salt Cedar in Shrub Canopy and Habitat Suitability

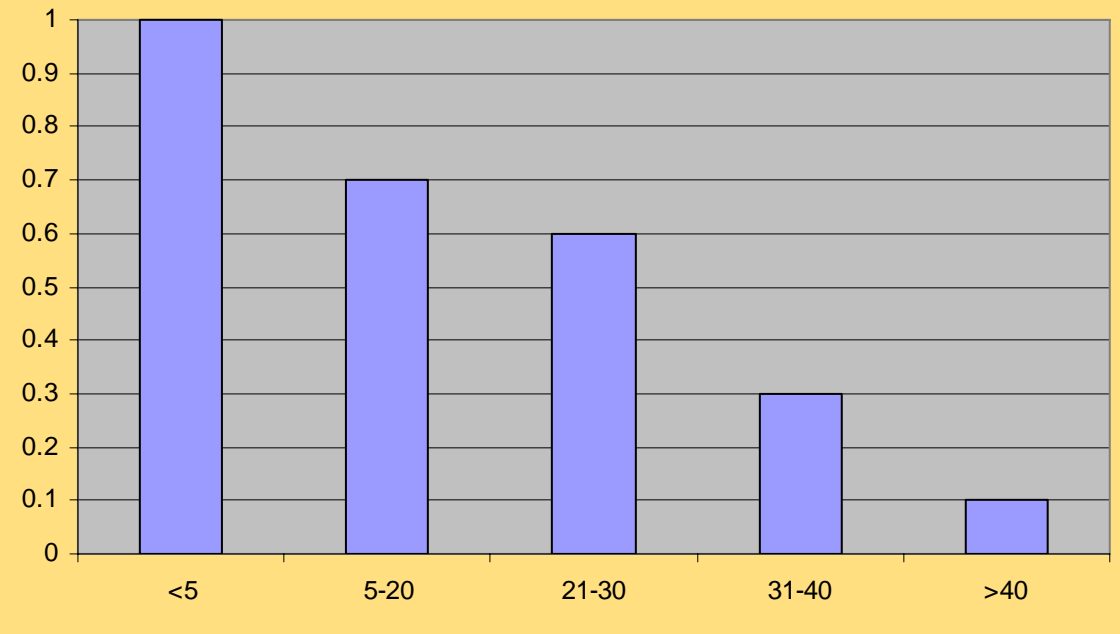
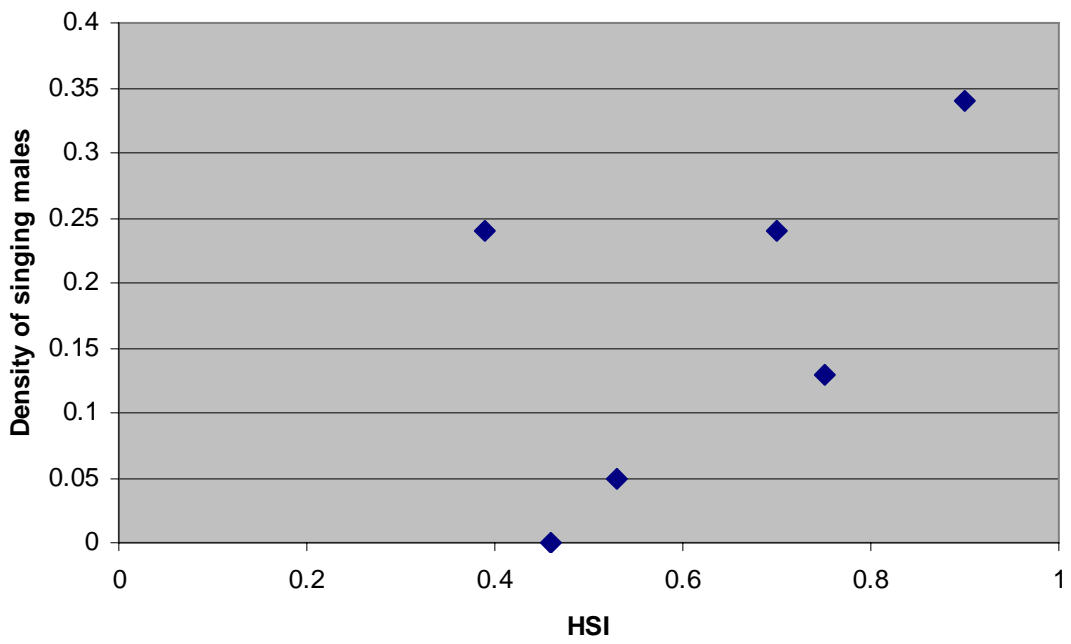


Figure 6. Wilson Warbler HSI and density



**HABITAT SUITABILITY INDEX MODEL FOR
WESTERN YELLOW-BILLED CUCKOO**

Developed by:

Hector Galbraith PhD
Galbraith Environmental Sciences, LLC
Boulder, Colorado

4th August 2002

1. INTRODUCTION

This document presents a Habitat Suitability Index (HSI) model for the southern Arizona population of the yellow-billed cuckoo, *Coccyzus americanus occidentalis*. It is intended for use in the San Pedro Riparian National Conservation Area (SPRNCA). This model, which quantifies the habitat relationships of the species, is the result of field-testing a previous draft version of the model (Galbraith, 2002), and incorporating comments on that previous version by Arizona yellow-billed cuckoo researchers. This resulting model will be used, in conjunction with vegetation community and climate modeling predictions, to evaluate the potential effects of regional climate change on the ability of the SPRNCA to provide habitat for this species in the future.

1.1 Current and historical distribution, habitat, and status of the western yellow-billed cuckoo

The yellow-billed cuckoo is a summer visitor to North America, wintering in Central and South America (Kaufman, 1996; Hughes, 1999). While the eastern populations of the species breed in many types of forested or scrub habitats, the western race is largely confined to riparian broad-leaved woodlands, particularly those dominated by mature cottonwoods or willows (Gaines, 1974; Hamilton and Hamilton, 1965; Hughes, 1999). They apparently avoid riparian habitats dominated by invasive salt cedar, *Tamarix pentandra* (Laymon and Halterman, 1987).

Prior to the beginning of the twentieth century, the breeding range of western yellow-billed cuckoos extended throughout western North America from southern Arizona and New Mexico north to British Columbia. However, widespread destruction of riparian habitat by agriculture, mining, dams, water withdrawals, and urbanization has led, since then, to a radical reduction in its range and numbers. Currently, the species no longer breeds in British Columbia, Washington, Idaho, or Oregon. It has been reduced drastically in numbers in more southern western states; for example in the Central Valley of California where thousands of pairs once bred there now are only a few tens of pairs (Halterman, 1991). In Arizona, yellow-billed cuckoos were relatively widespread 50 years ago (Phillips et al., 1964). However, they now breed regularly only in isolated populations along the Gila, San Pedro, Bill Williams, and Colorado Rivers. It is likely that, at most, 600 pairs now breed in Arizona, with 50-100 of these in the SPRNCA (Laymon and Halterman, 1987; Krueper, 1997). The rapid population decreases and range reductions of western yellow-billed cuckoos have recently prompted efforts (thus far unsuccessful) to have the race listed under the Endangered Species Act (e.g., CBD, 1998).

1.2 HSI models

HSI models evaluate the likely impacts of any actual or potential changes in habitat quality on carrying capacity (defined here as the habitat's capacity to support organisms) for either a single species, a guild of species, or biodiversity in general. HSI models achieve this by:

17. Identifying the critical habitat variables that affect the carrying capacity of habitat.

18. Establishing quantitative relationships between the occurrence of these variables and the carrying capacity of habitat. Each variable is assigned a suitability index (SI). This is a score of between 0 and 1, where the former is completely unsuitable habitat (i.e., minimal carrying capacity) and the latter is optimal habitat (i.e., greatest carrying capacity).
19. Developing metrics that can be used in the field to quantify the occurrence of the critical habitat components (and, therefore, the carrying capacity of the habitat)
20. Developing algorithms that combine the variable scores (SIs) into an expression of the overall carrying capacity of the habitat. This final score is the HSI and can be between 0 (unsuitable for species or guild) and 1 (optimal habitat).

Previous applications of HSI models have included the prediction of the possible effects of particular land management alternatives on biota (Brand *et al.*, 1986; Schamberger and Farmer, 1978), the quantification of past injuries to ecosystem wildlife carrying capacities (Galbraith *et al.*, 1996; LeJeune *et al.*, 1996), and estimating the exposure to contaminants of wildlife species (Galbraith *et al.*, 2001). If the structures, extents, and/or compositions of post-change vegetation communities can be predicted, it becomes possible to use HSI models to quantify and compare pre- and post-change habitat quality and potential carrying capacities.

U.S. Fish and Wildlife Service has developed approximately 160 HSI models. These include 85 terrestrial species (62 birds, 17 mammals, and 6 reptiles and amphibians). The remainder comprise marine and freshwater organisms. Most of the models have specific geographic, habitat, and seasonal areas of applicability. For example, the model for American woodcock, *Scolopax minor*, applies only to the species' wintering range in the southeastern states (Cade, 1985). In addition to the single-species HSI models, U.S. Fish and Wildlife has also developed a few models that quantify the carrying capacity of habitat for groups of species, for example habitat guild models (Short, 1983; Schroeder, 1986), or for wildlife diversity in general (Short, 1984).

No HSI model exists for yellow-billed cuckoo in any part of its breeding range. It is one of the objectives of this research project to develop and apply such a model in the San Pedro to evaluate the potential effects of climate change to the biota of the riparian systems.

1.3 Approach used in the development of this draft HSI model

The components and structure of this model were initially based on a literature review of the habitat preferences and patterns of use of western yellow-billed cuckoos in the southwestern states. This resulted in a draft model (Galbraith, 2002). This provided a focus for discussions with SPRNCA cuckoo researchers, Murrelet Halterman and Sean O'Connor, and model modifications. It was then tested in the SPRNCA at study sites with known breeding densities (unpublished information supplied by M. Halterman). Based on the comments received and the field test results, the draft model was modified, resulting in this version.

1.7 Seasonal and geographical applicability of this HSI model

This model is intended for use only during the breeding season and in riparian habitat in Arizona.

2. HABITAT INFORMATION

2.7 General

In the southwestern states, including Arizona, the yellow-billed cuckoo is confined as a breeding species to riparian forests, particularly those dominated by cottonwoods and willows (Hughes, 1999). Forests with a relatively lush, woody understory (either of willow or cottonwood saplings) are preferred (Gaines and Laymon, 1984). This type of habitat is generally found most extensively in functioning riparian systems where scour of vegetation due to floods and recolonization occurs. In areas where flow is controlled to prevent floods or where grazing has reduced shrub cover, such dense layered habitat is less prevalent. The species also avoids areas dominated by invasive species such as salt cedar. Thus the western yellow-billed cuckoo could be considered an indicator organism for functioning, healthy western riparian systems.

The western yellow-billed cuckoo generally builds its nest in shrubby vegetation, particularly denser patches of willows, between 1 and 6 metres above the ground (Hughes, 1999). While the birds nest in willows, much of the feeding by the adults occurs in the cottonwood canopy (Laymon, 1980). Thus, the species utilizes vertically layered habitats.

The configuration of riparian forest patches is an important factor contributing to their suitability for yellow-billed cuckoos. Gaines and Laymon (1984) and Laymon and Halterman (1989) found that larger and wider patches provided better habitat. Small and narrow patches were either marginal or not used by cuckoos.

2.8 Specific habitat requirements/preferences

Geographical continuity of riparian tree and shrub canopies. Observations at sites with known densities of yellow-billed cuckoos in the SPRNCA in July 2002 indicated that the linear geographical continuities of the tree and shrub canopies were important determinants of cuckoo habitat quality. River reaches that had continuous and unbroken tree canopies over a distance of 200 meters or more supported higher densities of breeding cuckoos, compared with reaches where the tree canopy was linearly fragmented. Cuckoos can persist, but at lower densities, in areas of fragmented tree canopy cover if the shrub understory remains continuous. However, in such areas, some tree canopy cover must survive if they are to constitute cuckoos habitat.

Width of riparian forest or shrub patches. Based on nesting density measurements in California, the width of a riparian forest patch is an important determinant of habitat quality. Linear patches that are less than 100 meters in width are not suitable habitat, while patches between 100 and 200 meters are marginal. Patches between 200 and 600 meters are suitable and those greater than 600 meters are optimal. In the SPRNCA, these habitat requirements are, apparently, less stringent: forest or shrub widths of 50 meters or less support few or no cuckoos; widths of 50-100 meters provide marginal habitat; widths of 100-200 and >200 are high and highest quality habitat, respectively (pers. obs.).

Shrub density. The density of the shrub layer of riparian forest is an important determinant of nest site habitat quality through its relationship with foliage density and nest crypticity. Most sightings of yellow-billed cuckoos in California were in areas of shrub canopy cover of between

30 and 90% (Gaines and Laymon, 1984; Laymon, 1980). Tree canopy cover is probably less important except that in forest of taller trees, the shrub canopy may be denser.

Tree canopy height. At two sites in California, tree canopy height at nesting sites ranged between 4.3 and 19.5 meters and averaged 8.2 to 9.1 meters (Laymon et al., 1997). As noted above, tree canopy characteristics may be less important than the shrub canopy. However, a canopy of cottonwoods is necessary for feeding habitat, and that canopy should be at least 10 meters in height and the taller the better (since this allows the development of a shrub layer).

Cottonwood/willow dominance in tree canopy. Western yellow-billed cuckoos show a strong preference for mature riparian cottonwood and willow forests. In Arizona, the most important tree species are Fremont cottonwood, *Populus fremontii*, and Gooding willow, *Salix goodingii*. The invasive salt cedar is avoided.

Dominance in the shrub layer. In the southwestern states the preferred shrub layer species are, apparently, cottonwood and willow saplings, with ash (*Fraxinus* spp.), walnut (*Juglans* spp.), and seep willow (*Baccharis*) also being important. The invasive salt cedar is avoided.

Representation of salt cedar or mesquite in the shrub canopy. Areas dominated by salt cedar appear to be avoided by nesting yellow-billed cuckoos (CBD, 1998). In the lower San Pedro River, where salt cedar stands are widespread and important community attributes, few or no yellow-billed cuckoos nest (Paradzick pers comm.). While mesquite is sometimes used as a feeding habitat by cuckoos on the SPRNCA (Halterman pers comm., pers. obs.), it is unlikely that the extensive representation of mesquite in the shrub layer would comprise suitable cuckoo habitat.

Distance to waterbodies. Western yellow-billed cuckoo nesting habitat is invariably associated with riparian systems and, therefore, waterbodies.

Micro-climate. Being a riparian species, western yellow-billed cuckoos typically inhabit shaded humid areas in an otherwise arid matrix. However, it is unknown whether this is a direct preference for such conditions or a consequence of requiring riparian forest habitat (which is generally shaded and humid). In addition to nesting on the SPRNCA where the average maximum June/July temperature is 90°F and annual rainfall is 15.6 inches, the species also nests 3000 feet lower in elevation on the Gila River where average maximum June/July temperatures reach 102-107°F and rainfall is generally less than 12 inches [data obtained from the Internet (<http://www.wrdc.dri.edu/cgi-bin/cliRECTM.pl?azwink>) from weather stations at Fort Huachuca, Maricopa, Winkelman, Sacaton, and Florence]. Thus, while yellow-billed cuckoos nest in comparatively cool, moist habitat in the SPRNCA, they also nest in hotter, drier areas further downriver on the Gila. This suggests that the availability of riparian forest is the most important factor, of which the micro-climatic conditions may be a consequence. It should also be noted that at one time the species nested as far north as British Columbia and as far south as Mexico, indicating, a degree of flexibility in its climatic requirements.

3. MODEL COMPONENTS

Based on this review of the habitat preferences of western yellow-billed cuckoos, the HSI model incorporates eight variables (continuity and width of habitat patch, shrub density (canopy cover), tree and shrub canopy heights, cottonwood/willow dominance in tree canopy, cottonwood/willow/ash/walnut/Baccharis dominance in shrub canopy, salt cedar and/or mesquite dominance in the shrub understory).

The numerical relationships between each of the variables and habitat suitability are the core of the habitat model. These are given below.

V1. Linear continuity of riparian forest or shrub habitat. In the SPRNCA, riparian shrub or tree linear patches that are relatively unbroken over at least 200 meters provide higher quality cuckoo habitat than more fragmented habitats. To accommodate this, the following categorization has been developed:

LINEAR CONTINUITY (%)	SUITABILITY INDEX (SI)
>90%	1.0
70-90%	0.7
50-70%	0.5
30-50%	0.3
<30%	0.05

Linear continuity is estimated at the scale of 200-meter strips of the riparian zone. This relationship is presented graphically in Figure 1.

V2. Width of riparian forest patch. Based on data presented in Laymon and Halterman (1989) and observations at sites of known breeding density in the SPRNCA, the following patch width and habitat suitability categorization has been developed:

PATCH WIDTH (m)	SUITABILITY INDEX (SI)
<50	0.1
51-100	0.3
101-200	0.6
>200	1.0

It is assumed in this categorization that the relationship between patch width and habitat suitability is approximately linear and that riparian strips narrower than 50 m do not provide good habitat for the species. This relationship is presented graphically in Figure 2.

V3. Percent shrub canopy cover in 50 m radius of sampling point). Based on the results reported in Gaines and Laymon (1984) and observations at sites with known breeding densities of cuckoos on the SPRNCA, the following shrub cover and habitat suitability categorization has been developed:

% COVER	SUITABILITY INDEX (SI)
----------------	-------------------------------

<10%	0.05
10-25%	0.1
26-50%	0.4
51-75%	0.6
>75%	1.0

In this variable, shrub canopy is defined as the canopy of the understory (mainly cottonwood and willow saplings and seep willow) up to 10 meters in height. It is assumed in this categorization that the relationship between % cover and habitat suitability is approximately linear except at very low percent shrub covers where a further reduction will result in a disproportionate effect on habitat suitability. This relationship is presented graphically in Figure 3.

V4. Average shrub canopy height within 50 m radius of sampling point. Based on observations made at the SPRNCA in areas of known cuckoo breeding density, the following shrub canopy height and habitat suitability categorization has been developed:

SHRUB CANOPY HEIGHT (m)	SUITABILITY INDEX (SI)
<2	0.1
2-3	0.5
>3	1.0

This relationship is presented graphically in Figure 4.

V5. Average tree canopy height within 50 m radius of sampling point. Based on the results reported in Gaines (1977), Gaines and Laymon (1984), and observations made at the SPRNCA in areas of known cuckoo breeding density, the following tree canopy height and habitat suitability categorization has been developed:

TREE CANOPY HEIGHT (m)	SUITABILITY INDEX (SI)
<10	0.1
10-15	0.5
>15	1.0

It is assumed in this categorization that the relationship between tree canopy height and habitat suitability is approximately linear. It is also assumed that even low canopy heights may have some habitat value. This relationship is presented graphically in Figure 5.

V6. Cottonwood/willow dominance in tree canopy within 50 m radius of sampling point. Based on the results reported in Laymon and Halterman (1985), the following cottonwood/willow dominance in the tree canopy and habitat suitability categorization has been developed:

% DOMINANCE	SUITABILITY INDEX (SI)
<10	0.05
10-25	0.1
26-50	0.3
51-75	0.6
>75	1.0

It is assumed in this categorization that the relationship between % dominance and habitat suitability is approximately linear. It is also assumed that very low representations of these species (<10%), provide at best marginal habitat for yellow-billed cuckoos. This relationship is presented graphically in Figure 6.

V7. Cottonwood/willow/ash/walnut/seep willow percent dominance (relative cover) in shrub layer within 50 m radius of sampling point. Based on the results reported in Gaines and Laymon (1984) and observations made at the SPRNCA in areas of known cuckoo breeding density, the following shrub cover and habitat suitability categorization has been developed:

% DOMINANCE	SUITABILITY INDEX (SI)
<10	0.05
10-25	0.1
26-50	0.3
51-75	0.6
>75	1.0

It is assumed in this categorization that the relationship between % dominance and habitat suitability is approximately linear except at very low percent shrub covers where a further reduction will result in a disproportionate effect on habitat suitability. It is also assumed that less than 10% dominance, provides only extremely marginal habitat for yellow-billed cuckoos. This relationship is presented graphically in Figure 7.

V8. Percent dominance (relative cover) of salt cedar and/or mesquite in the shrub canopy within 50 m radius of sampling point. The following relationship between representation of salt cedar and/or mesquite in the vegetation community and habitat suitability is hypothesized:

% DOMINANCE	SUITABILITY INDEX (SI)
<10	1.0
10-30	0.7
31-50	0.5
51-70	0.2
>70	0.05

It is assumed in this categorization that the relationship between % dominance of salt cedar/mesquite and habitat suitability is not linear but that increasing dominance by salt cedar or mesquite has a disproportionate effect on habitat suitability. It is also assumed that the highest

dominance by salt cedar and/or mesquite (>70%) will constitute extremely marginal habitat for yellow-billed cuckoos. This relationship is presented graphically in Figure 8.

4. MODEL APPLICATION

The eight variables described above will be combined into an index of the overall assessment of the habitat suitability (HSI) of a particular patch of riparian forest habitat using the following 8th root algorithm:

$$HSI = (V1 \times V2 \times V3 \times V4 \times V5 \times V6 \times V7 \times V8)^{1/8}$$

The HSI values obtained using this equation will range between 0 and 1.0 (lowest and highest estimates of suitability, respectively).

5. FIELD TEST RESULTS

The results of the field test of the western yellow-billed cuckoo model are presented in Attachment A to this document. These results show that the predictions of the HSI model regarding habitat suitability are generally accurate (if it is assumed that breeding density is a reflection of at least short term habitat quality). Thus the HSI model developed for this study is a reasonable predictor of breeding habitat quality for the study species.

6. REFERENCES

- Brand, G.J., S.R. Shifley, and L.F. Ohman. 1986. Linking wildlife and vegetation models to forecast the effects of management. In: J. Verner, M.L. Morrison, and C.J. Ralph (eds), *Wildlife 2000: modeling habitat relationships of terrestrial vertebrates*. University of Wisconsin Press, Madison, Wisconsin.
- Cade, B.S. 1985. Habitat suitability index models: American woodcock (wintering). U.S. Fish Wildl. Serv. Biol. Rep. 82(10.105). Ft. Collins, Colorado.
- Center for Biological Diversity (CBD). 1998. Petition to list the yellow-billed cuckoo as a federally endangered species. Petition to Mr. Bruce Babbitt, Secretary of the Interior.
- Gaines, D. 1974. Review of the status of the Yellow-billed Cuckoo in California: Sacramento Valley populations. *Condor* 76:204-209.
- Galbraith, H. 2002. Draft HSI model for Yellow-billed Cuckoo. Unpublished report to American Bird Conservancy.
- Galbraith, H., K. LeJeune, and J. Lipton. 1996. Metal and Arsenic Impacts to Soils, Vegetation Communities, and Wildlife Habitat in Southwest Montana Uplands Contaminated by Smelter Emissions: I Field Evaluation. *Environmental Toxicology and Chemistry*. 14:1895-1903.

Galbraith, H. Kapustka, L. and M. Luxon. 2001. Incorporating habitat quality in ecological risk assessments: selecting assessment species, SETAC Annual Conference, Baltimore, MD, November, 2001.

Halterman, M.D. 1991. Distribution and habitat use of the Yellow-billed Cuckoo on the Sacramento River, California, 1987-1990. MS Thesis, California State University, Chico.

Hamilton, W.J., and M.E. Hamilton. 1965. Breeding characteristics of Yellow-billed Cuckoos in Arizona. *Proc. Calif. Acad. Sci.* 32:405-432.

Hughes, J.M. 1999. Yellow-billed cuckoo. *The Birds of North America. Life Histories for the 21st Century.* No. 418 (A. Poole and F. Gill, eds). The Birds of North America, Inc., Philadelphia, PA.

Kaufman, K. 1996. *Lives of North American Birds.* Houghton Mifflin Company. Boston.

Krueper, D. 1997. Annotated Checklist to the Birds of the Upper San Pedro River Valley. Unpublished report – Bureau of Land Management. San Pedro Riparian National Conservation Area.

Laymon, S.A. 1980. Feeding and nesting behavior of the yellow-billed cuckoo in the Sacramento Valley Wildlife Management Branch Administration Rep. 80-2. California Department of Fish and Game, Sacramento.

Laymon, S.A. and M.D. Halterman. 1987. Can the western subspecies of Yellow-billed Cuckoo be saved from extinction? *Western Birds* 18:19-25.

Laymon, S.A. and M.D. Halterman. 1989. A proposed habitat management plan for yellow-billed cuckoos in California. USDA Forest Service GTR PSW-110.

Laymon, S.A. and M.D. Halterman. 1990. Distribution and habitat requirements of the yellow-billed cuckoo in California. Report to The Nature Conservancy, Sacramento, California.

Laymon, S.A., P.L. Williams, and M.D. Halterman. 1997. Breeding status of the yellow-billed cuckoo in the South Fork Kern River Valley, Kern County, California. Report to the USDA Forest Service Sequoia National Forest.

LeJeune, K., H. Galbraith, J. Lipton, and L.A. Kapustka. 1996. Effects of Metals and Arsenic on Riparian Soils, Vegetation Communities, and Wildlife Habitat in Southwest Montana. *Ecotoxicology.* 5:297-312.

Philips, A. J. Marshall, and G. Monson. 1964. *The Birds of Arizona.* University of Arizona Press, Tucson.

Schamberger, M., and A. Farmer. 1978. The habitat evaluation procedures: their application in project planning and impact evaluation. *North American Natural Resources Conference,* 43:274-283.

Schroeder, R.L. 1986. Habitat suitability index models: wildlife species richness in shelterbelts. U.S. Fish and Wildlife Service Biological Report 82. Fort Collins, Colorado.

Short, H.L. 1983. Wildlife guilds in Arizona desert habitats. U.S. Fish and Wildlife Service, Ft. Collins, CO. BLM Technical Note 362.

Short, H. L. 1984. Habitat suitability index models: the Arizona Guild and Layers of Habitat models. U.S. Fish and Wildlife Service, Ft. Collins, CO. FWS/OBS-82/10.70

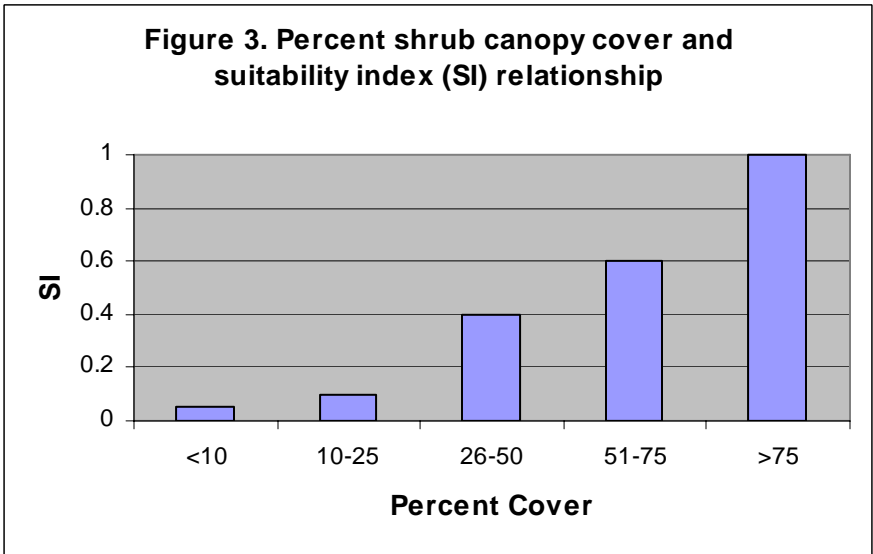
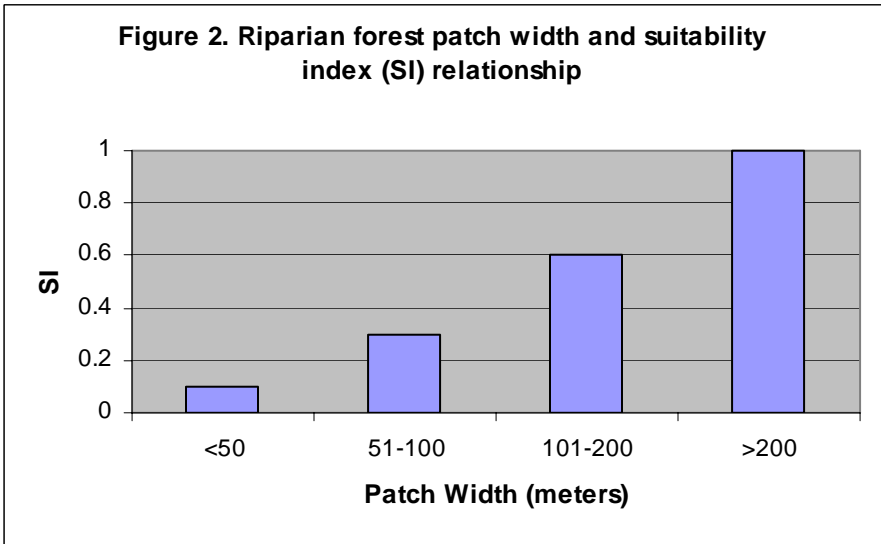
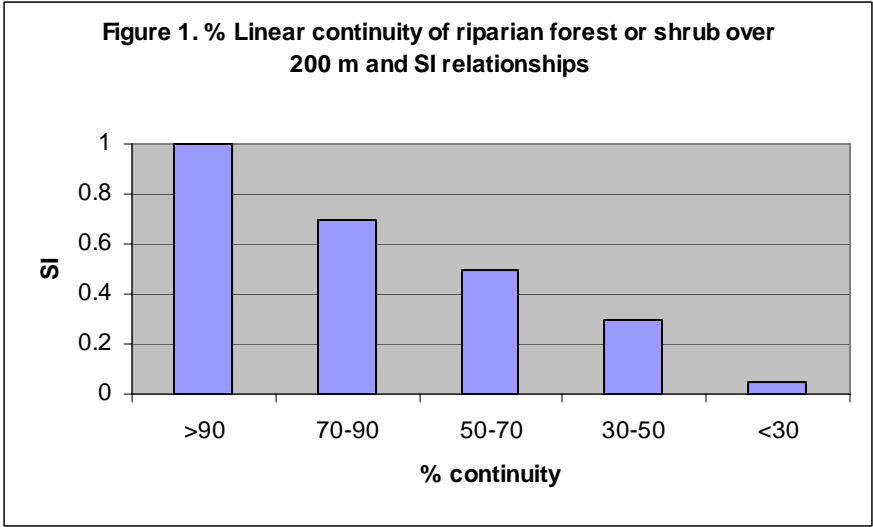


Figure 4. Average shrub canopy height and suitability index (SI) relationship

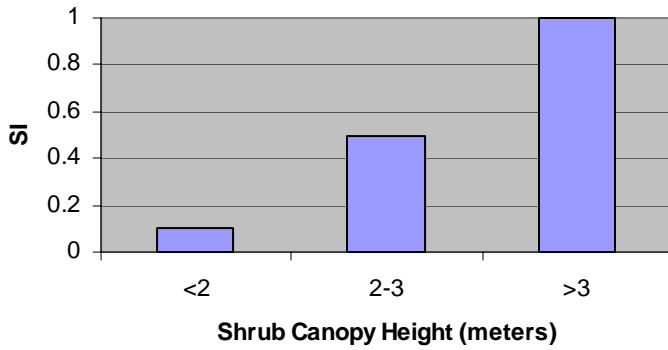


Figure 5. Average tree canopy height and suitability index (SI) relationship

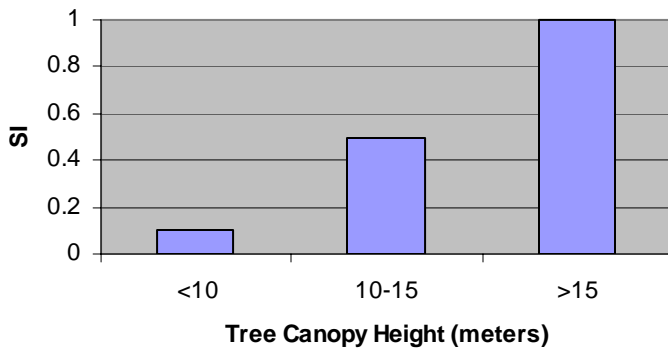
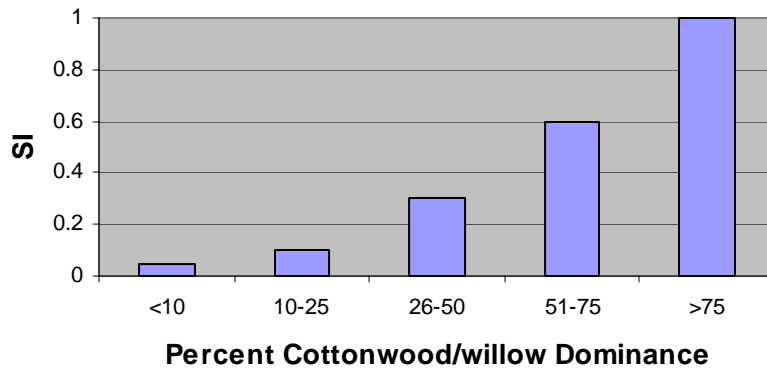
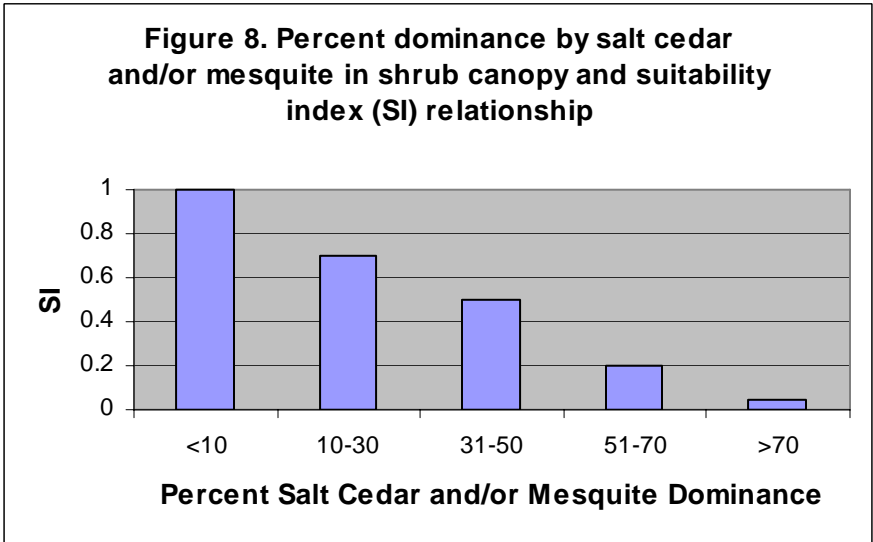
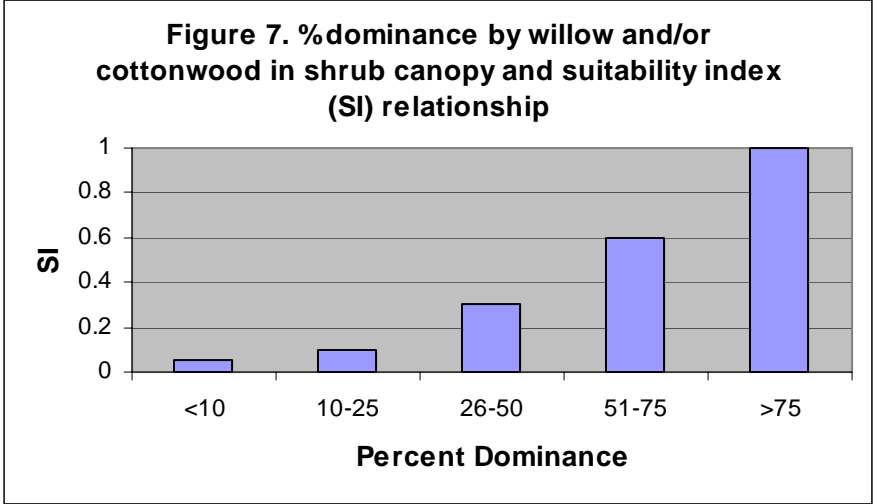


Figure 6. Cottonwood/willow dominance in tree canopy and suitability index (SI) relationship





Attachment A. Results of Field Tests of Yellow-billed Cuckoo HSI Model

Table A1 shows the results of surveying yellow-billed cuckoo breeding habitat quality at six sites of known differing breeding densities on the SPRNCA. The resulting HSI scores are plotted against known breeding density in Figure A1. These results show that the predictions of the HSI model regarding habitat suitability are generally accurate (if it is assumed that breeding density is a reflection of at least short term habitat quality). However, Figure A1 also shows that low HSI scores (<0.3) may overestimate the ability of an area of habitat on the SPRNCA to support cuckoos. This should be borne in mind when interpreting future vegetation scenarios. In general, above HSI scores of 0.3, the HSI model developed for this study is a reasonable predictor of breeding habitat quality for the study species. Scores of <0.3 should be regarded as indicating marginal habitat.

The data in Table A1 show most variation between sites for variable V1 and V2. Thus, it is largely spatial variability in the linear continuity and width of riparian patches that drive the differences in HSI scores among sites. Figures A2 and A3 show a site with high cuckoo breeding densities and high HSI scores (Charleston south 2). This is an area where the riparian zone is comparatively wide (generally >100 m), where it is totally continuous, and where the understory of willow and seep willow is dense. At this site, the breeding density was 2.7 pairs/km. This is optimal cuckoo habitat on the San Pedro.

In contrast, Figures A4 and A5 show a site (Hereford north A) where cuckoo breeding density was medium (0.6 pairs/km) and where the HSI score was 0.77. At this site, fire had reduced the width of the riparian zone and its linear continuity. Nevertheless, enough of a shrub layer survived (with some tree canopy) to maintain cuckoo habitat.

Table A1. SI and HSI scores and breeding densities of yellow-billed cuckoos at SPRNCA sites visited in July 2002.

Site	V1	V2	V3	V4	V5	V6
Charleston south 1	0.7	0.05	0.4	1	1	0.6
Charleston south 2	1	1	0.6	1	1	1
Hereford north 1A	0.3	0.3	0.4	0.5	0.1	1
Hereford north 1B	1	1	0.6	1	1	0.6
Hereford north 2	0.7	0.3	0.6	1	1	1
San Pedro House north	0.7	0.6	0.4	1	1	1

Table A1 continued

Site	V7	V8	HSI	Density (pairs/km)
Charleston south 1	0.6	0.5	0.47	0.6
Charleston south 2	1	1	0.94	2.7
Hereford north 1A	1	1	0.45	0
Hereford north 1B	1	1	0.88	2.5
Hereford north 2	1	1	0.77	0.6
San Pedro House north	1	1	0.8	1.3

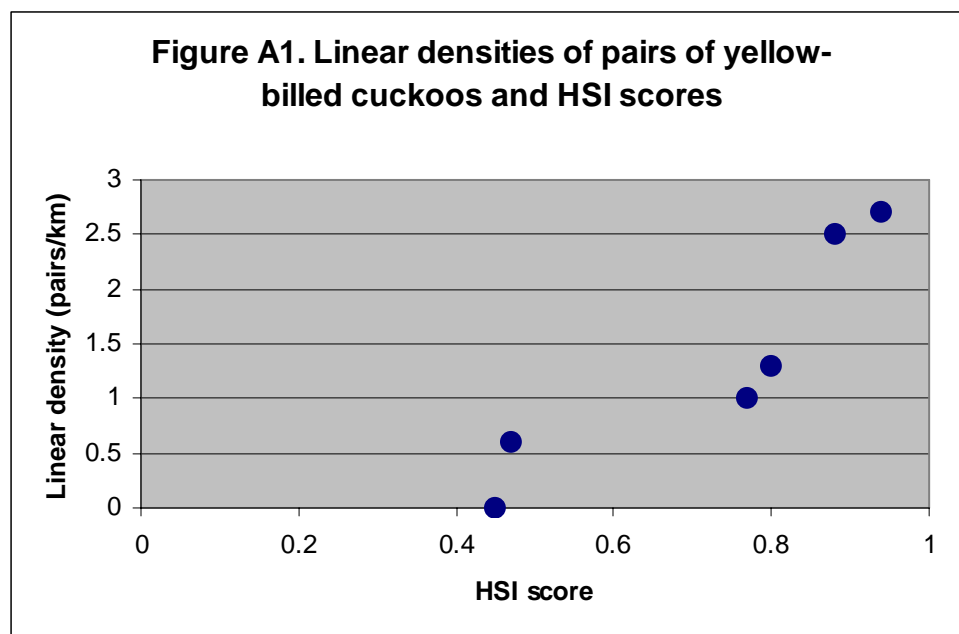




Figure A2. The riparian zone in the SPRNCA at Charleston south showing high-density yellow-billed cuckoo breeding habitat. Note the relatively wide and linearly continuous riparian forest.



Figure A3. Charleston south – an area of high cuckoo breeding density. Note the tall cottonwood/willow tree canopy and the dense willow and seep willow shrub understory.



Figure A4. Hereford north A on the SPRNCA. In this area a fire in March 1998 reduced to the width and linear continuity of the riparian forest, resulting in cuckoo habitat of only medium quality.



Figure A5. A wider view of Hereford north A showing the impacts caused to habitat linear continuity and width caused by fire.

**HABITAT SUITABILITY INDEX MODEL FOR
YELLOW WARBLERS MIGRATING IN SPRING THROUGH THE SAN
PEDRO NATIONAL CONSERVATION AREA**

Developed by:

Hector Galbraith PhD
Galbraith Environmental Sciences, LLC.
Boulder, Colorado

19 June 2003

1. INTRODUCTION

This document presents a spring migration season Habitat Suitability Index (HSI) model for yellow warblers (*Dendroica petechia*), intended for use in the San Pedro Riparian National Conservation Area (SPRNCA). This model, which quantifies the habitat relationships of the species, is the result of a review of the scientific literature, focusing mainly on those studies that concern the habitat use by the species in Western North America and during spring migration. The model was tested in areas of the San Pedro where previous survey work has quantified yellow warbler density. The model will be used, in conjunction with vegetation community and climate modeling predictions, to evaluate the potential effects of global climate change on the ability of the SPRNCA to provide spring migration habitat for this species in the future.

1.1 Spring migration of yellow warblers in the SPRNCA

The yellow warbler is the most abundant spring migrant in the SPRNCA (Kreuper, 1997), where singing male densities of as high as 4,800/km² have been recorded (Skagen et al., 1998). The first migrants (generally males) appear at the SPRNCA in early to mid-March and numbers peak in late April and early May, declining by mid-May. A relatively small number of birds stay to breed on the SPRNCA (at about 570 birds/km² [Kreuper reported in Skagen et al., 1998]), however, these breeding birds are vastly outnumbered by migrants during the spring.

While the total numbers of yellow warblers that migrate into North America in spring are unknown, it is highly likely that a substantial proportion of the birds that subsequently breed in the western part of their breeding range pass through the SPRNCA. Based on the total numbers of all migrants moving through the San Pedro in spring and singing male densities in Skagen et al. (1998), it is likely that in excess of one million yellow warblers pass through the SPRNCA. It is, therefore, an important migration stopover site for this species.

1.2 HSI models

HSI models evaluate the likely impacts of any actual or potential changes in habitat quality on carrying capacity (defined here as the habitat's capacity to support organisms) for either a single species, a guild of species, or biodiversity in general. HSI models achieve this by:

21. Identifying the critical habitat variables that affect the carrying capacity of habitat.
22. Establishing quantitative relationships between the occurrence of these variables and the carrying capacity of habitat. Each variable is assigned a suitability index (SI). This is a score of between 0 and 1, where the former is completely unsuitable habitat (i.e., minimal carrying capacity) and the latter is optimal habitat (i.e., greatest carrying capacity).
23. Developing metrics that can be used in the field to quantify the occurrence of the critical habitat components (and, therefore, the carrying capacity of the habitat)
24. Developing algorithms that combine the variable scores (SIs) into an expression of the overall carrying capacity of the habitat. This final score is the HSI and can be between 0 (unsuitable for species or guild) and 1 (optimal habitat).

Previous applications of HSI models have included the prediction of the possible effects of particular land management alternatives on biota (Brand *et al.*, 1986; Schamberger and Farmer, 1978), the quantification of past injuries to ecosystem wildlife carrying capacities (Galbraith *et al.*, 1996; LeJeune *et al.*, 1996), evaluating the potential effects of climate change and aquifer depletion on biota (Galbraith *et al.*, *in press*), and estimating the exposure to contaminants of wildlife species. If the structures, extents, and/or compositions of post-change vegetation communities can be predicted, it becomes possible to use HSI models to quantify and compare pre- and post-change habitat quality and potential carrying capacities.

U.S. Fish and Wildlife Service has developed approximately 160 HSI models. These include 85 terrestrial species (62 birds, 17 mammals, and 6 reptiles and amphibians). The remainder comprise marine and freshwater organisms. Most of the models have specific geographic, habitat, and seasonal areas of applicability. For example, the model for American woodcock, *Scolopax minor*, applies only to the species' wintering range in the southeastern states (Cade, 1985). In addition to the single-species HSI models, U.S. Fish and Wildlife has also developed a few models that quantify the carrying capacity of habitat for groups of species, for example habitat guild models (Short, 1983), or for wildlife diversity in general (Short, 1984).

Although an HSI model exists for the yellow warbler in its breeding habitat (Schroeder, 1982), no migration season model exists. Also, the breeding season model was developed for shrub dominated riparian habitats, rather than the gallery forest that is prevalent in the SPRNCA. For these reasons, a new HSI model has been developed and, while this new model incorporates some of the variables of the existing breeding season model, it is tailored to the specific needs of quantifying habitat during spring migration in the SPRNCA.

1.3 Approach used in the development of this HSI model

The components and structure of this provisional model were based on a literature review of the habitat preferences and patterns of use of yellow warblers during their spring migration in the Western U.S. The literature sources are cited in section 6. The resulting draft model was then tested against empirical data (singing male densities in spring) from the SPRNCA and modified where necessary.

1.8 Seasonal and geographical applicability of this HSI model

This model is intended for use only during the spring migration season and in riparian habitat in southern Arizona. It may not be applicable to sites elsewhere where yellow warbler migration habitat preferences may be different.

2. HABITAT INFORMATION

2.9 General

While on migration, the yellow warbler typically occurs in habitats that are similar to its breeding habitats: deciduous forested and shrub wetlands and riparian areas (Lowther *et al.*,

1999; Kaufman, 1996). In the east, its habitat preferences may be broader and residential suburban and a variety of other habitat types may be used (Dunn and Garrett, 1997). However, in the Western U.S. it is largely confined to riparian and wetland areas, which occur as isolated patches in the otherwise relatively arid landscapes. A few studies (Saab, 1999; Lowther et al., 1999) have suggested that the species has a preference for edge habitats during both the breeding and migration seasons.

Riparian habitats used by migrating yellow warblers in the west are often dominated by cottonwoods (*Populus* spp.) or willows (*Salix* spp.). No information was found that indicated that yellow warblers avoided exotic tree or shrub species such as salt cedar.

2.10 Specific habitat requirements/preferences

The specific habitat features in this section are based on the published scientific literature, and communications with yellow warbler researchers on the San Pedro (Susan Skagen of USGS and Jack Whetstone of BLM). The specific features are identified below:

Forest/Shrub Patch size. Studies in southern Arizona (Skagen et al., 1998) have shown that migrating yellow warblers are not confined to the largest, most contiguous habitat patches, and that they may also utilize smaller habitat fragments. The smallest habitat patches investigated by Skagen et al. (1998) were about 40 ha in extent, while the largest exceeded 2,000 ha. Densities of birds did not differ between these two size categories. Nevertheless, there is no doubt a minimum size at which a patch will not provide suitable habitat for migrating yellow warblers. Based on the Skagen et al., (1998) results, this patch size must be less than 40 ha.

Presence of Tree Canopy Layer. Various studies have shown that in comparison to other warblers that migrate through the SPRNCA, yellow warblers forage at greater height from the ground, typically utilizing the tree canopy or taller shrubs (Scott et al *in press*; Hutto, 1981; Frydendall, 1967 reported in Lowther et al., 1999). Other studies have indicated the importance of a vertically stratified foraging habitat, including tall shrub and tree canopy layers (Saab, 1999; Hutto, 1981)

% Dominance in Tree Canopy and Shrub Layers by Hydrophytes. The preferred foraging habitats for yellow warblers comprise medium sized to tall hydrophytic shrubs and trees, particularly cottonwoods (*Populus* spp.) and willows (*Salix* spp.) (Saab, 1999; Scott et al., *in press*; Lowther et al., 1999; Finch, 1989). Hutto (1985) found that in southern Arizona spring densities of yellow warblers were low in vegetation communities dominated by mesquite, acacia, or other such xeric species. Thus the representation of such shrub and tree species, and, conversely, of xerophytic species such as mesquite, is an important habitat characteristic for yellow warblers.

Heights of Shrub and Tree Canopy Layers. Yellow warblers typically forage at greater heights than, for example, Wilson's warblers (Hutto, 1981). Hutto found that the mean foraging height in summer in Wyoming exceeded 2.6 m, while in winter in Mexico it exceeded 4 m. Thus, taller shrubs, particularly where no tree canopy is present, may comprise more attractive habitat.

3. MODEL COMPONENTS

Based on this review of the habitat preferences of yellow warblers, the draft HSI model will incorporate seven variables. The numerical relationships between each of the variables and habitat suitability are the core of the habitat model. These are given below.

V1. Riparian forest/shrub patch size. A riparian shrub or forest patch is defined as a shrub vegetation community (either with or without a tree canopy), dominated by cottonwoods or willows. Based on data presented in Skagen et al. (1998), and conversations with Susan Skagen, the following patch size and habitat suitability categorization has been developed:

PATCH SIZE (ha)	SUITABILITY INDEX (SI)
<1 (and no other patches within 100m)	0.05
<1 (and one or more patches within 100m)	0.1
1-20	0.3
21-40	0.5
>40	1.0

It is assumed in this categorization that patches smaller than 1 ha do not provide habitat for the species unless within a landscape of small patches, that small and medium size patches (1-20 and 21-40 ha, respectively) provide increasing levels of suitability and that patches larger than 40 ha are optimal for the species. This relationship is presented graphically in Figure 1.

V2. Tree Canopy cover in 20 m. radius of sampling point. Based on information from the scientific literature, the following patch width and habitat suitability categorization has been hypothesized:

% COVER	SUITABILITY INDEX (SI)
<10	0.1
10-50	0.5
50-75	1.0
>75	0.6

It is assumed in this categorization that the relationship between % tree canopy cover and habitat suitability is approximately linear, except at very high percent covers where continuous tree canopy cover is likely to result in shading that eliminates the presence of a shrub layer, another important habitat feature for the species. This relationship is presented graphically in Figure 2.

V3. Percent shrub canopy cover in 20 m radius of sampling point). Based on information from the scientific literature, the following shrub cover and habitat suitability categorization has been developed:

% COVER	SUITABILITY INDEX (SI)
----------------	-------------------------------

<30%	0.05
30-50%	0.2
50-70%	0.5
70-90%	1.0
>90%	0.8

It is assumed in this categorization that the relationship between % cover and habitat suitability is approximately linear, except at very high percent shrub covers where continuous shrub cover eliminates the presence of edge habitat, another important habitat feature for the species. It is also assumed that shrub cover that is less than 30% provides only poor quality habitat for yellow warblers. This relationship is presented graphically in Figure 3.

V4. % Cover in tree canopy of cottonwood or willow in 20m radius of sampling point. Based on information from the scientific literature, the following relationship between tree canopy cover and habitat suitability has been developed:

% COVER	SUITABILITY INDEX (SI)
<20%	0.1
20-40%	0.3
40-60%	0.6
>60%	1.0

This relationship is presented graphically in Figure 4.

V5. % Cover in shrub canopy of cottonwood or willow in 20 m radius of sampling point. Based on information from the scientific literature, the following relationship between tree canopy cover and habitat suitability has been developed:

% COVER	SUITABILITY INDEX (SI)
<20%	0.1
20-40%	0.3
40-60%	0.6
>60%	1.0

This relationship is presented graphically in Figure 5.

V6. Mean shrub canopy height (if no tree canopy present) in 20 m radius of sampling point. Based on information from the scientific literature, the following relationship between shrub canopy height and habitat suitability has been developed (only where no tree canopy exists):

MEAN SHRUB CANOPY HEIGHT (m)	SUITABILITY INDEX (SI)
<1	0.05
1-2	0.3
2-3	0.7
>3	1.0

This relationship is presented graphically in Figure 6.

V7. % dominance in tree or shrub canopy by meso- or xerophytic species in 20 m radius of sampling point. Based on information from the scientific literature, the following relationship between meso- and xerophytic species in the tree or shrub canopy and habitat suitability has been developed:

% DOMINANCE	SUITABILITY INDEX (SI)
<5	1.0
5-20	0.7
20-40	0.6
40-60	0.3
>60	0.1

This relationship is presented graphically in Figure 7.

4. MODEL APPLICATION

The seven variables described above are combined into an index of the overall assessment of the habitat suitability (HSI) of a particular patch of riparian habitat using the following 7th root algorithm:

$$HSI = (V1 \times V2 \times V3 \times V4 \times V5 \times V6 \times V7)^{1/7}$$

The HSI values obtained using this equation will range between 0 and 1.0 (lowest and highest estimates of suitability, respectively).

5. FIELD TEST RESULTS

The yellow warbler draft model was tested in June, 2003 on sites on the San Pedro River where Bureau of Land Management surveys had quantified densities of singing males in each year between 1986 and 1990. In the absence of visual evidence to the contrary, it was assumed that little or no habitat change had occurred between the survey years and the present. The results of the field test of the yellow warbler model are presented in Attachment A to this document. These results show that the predictions of the HSI model regarding habitat suitability are generally accurate (if it is assumed that breeding density is a reflection of at least short term habitat quality) except at sites where the HSI value is less than about 0.4. Apparently, yellow warblers migrating through the San Pedro regard such sites as not providing habitat. Thus, the HSI model developed for this study is a reasonable predictor of breeding habitat quality for the study species.

6. REFERENCES

Brand, G.J., S.R. Shifley, and L.F. Ohman. 1986. Linking wildlife and vegetation models to forecast the effects of management. In: J. Verner, M.L. Morrison, and C.J. Ralph (eds), Wildlife

2000: modeling habitat relationships of terrestrial vertebrates. University of Wisconsin Press, Madison, Wisconsin.

Cade, B.S. 1985. Habitat suitability index models: American woodcock (wintering). U.S. Fish Wildl. Serv. Biol. Rep. 82(10.105). Ft. Collins, Colorado.

Dunn, J., and K. Garrett. 1997. Peterson Field Guides: warblers. Houghton Mifflin, Boston.

Finch, D.M. 1989. Habitat use and habitat overlap of riparian birds in three elevational zones. *Ecology*, 70:866-880.

Frydenhall, M.J. 1967. Feeding ecology and territorial behavior of the yellow warbler. Ph.D. diss., Utah State University, Logan, UT.

Galbraith, H. 2002. Draft habitat suitability index model for the southwestern willow flycatcher. Unpublished report to American Bird Conservancy. 18th April, 2002.

Galbraith, H., K. LeJeune, and J. Lipton. 1996. Metal and Arsenic Impacts to Soils, Vegetation Communities, and Wildlife Habitat in Southwest Montana Uplands Contaminated by Smelter Emissions: I Field Evaluation. *Environmental Toxicology and Chemistry*. 14:1895-1903.

Galbraith, H. Kapustka, L. and M. Luxon. *In press*. Incorporating habitat quality in ecological risk assessments: role of HSI models, Proceedings of ASTM Symposium on landscape ecology and ecological risk assessment, Kansas City, April, 2003.

Hutto, R.L. 1981. Seasonal variation in the foraging behavior of some migratory western wood warblers. *The Auk*, 98:765-777.

Hutto, R.L. 1985. Seasonal changes in the habitat distribution of transient insectivorous birds in southeastern Arizona: competition mediated? *The Auk*, 102:120-132.

Kaufman, K. 1996. Lives of North American Birds. Houghton Mifflin, Boston.

Krueper, D. 1997. Annotated Checklist to the Birds of the Upper San Pedro River Valley. Unpublished report – Bureau of Land Management. San Pedro Riparian National Conservation Area.

LeJeune, K., H. Galbraith, J. Lipton, and L.A. Kapustka. 1996. Effects of Metals and Arsenic on Riparian Soils, Vegetation Communities, and Wildlife Habitat in Southwest Montana. *Ecotoxicology*. 5:297-312.

Lowther, P.E., C. Celada, N.K. Klein, C.C. Rimmer, and D.A. Spector. 1999. Yellow warbler (*Dendroica petechia*). In *The Birds of North America*, No. 454 (A. Poole and F. Gill, eds). The Birds of North America, Inc. Philadelphia, PA.

Saab, V. 1999. Importance of spatial scale to habitat use by breeding birds in riparian forests: a hierarchical analysis. *Ecological Applications*, 9:135-151.

Schamberger, M., and A. Farmer. 1978. The habitat evaluation procedures: their application in project planning and impact evaluation. *North American Natural Resources Conference*, 43:274-283.

Schroeder, R.L. 1982. Habitat suitability index models: yellow warbler. U.S. Dept. Int., Fish Wildl. Serv. FWS/OBS-82/10.27.

Scott, M.L., S.K. Skagen, and M.F. Merigliano. *In press*. Relating geomorphic change, vegetation structure, and avian diversity in riparian forests. *In press Cons. Biol*

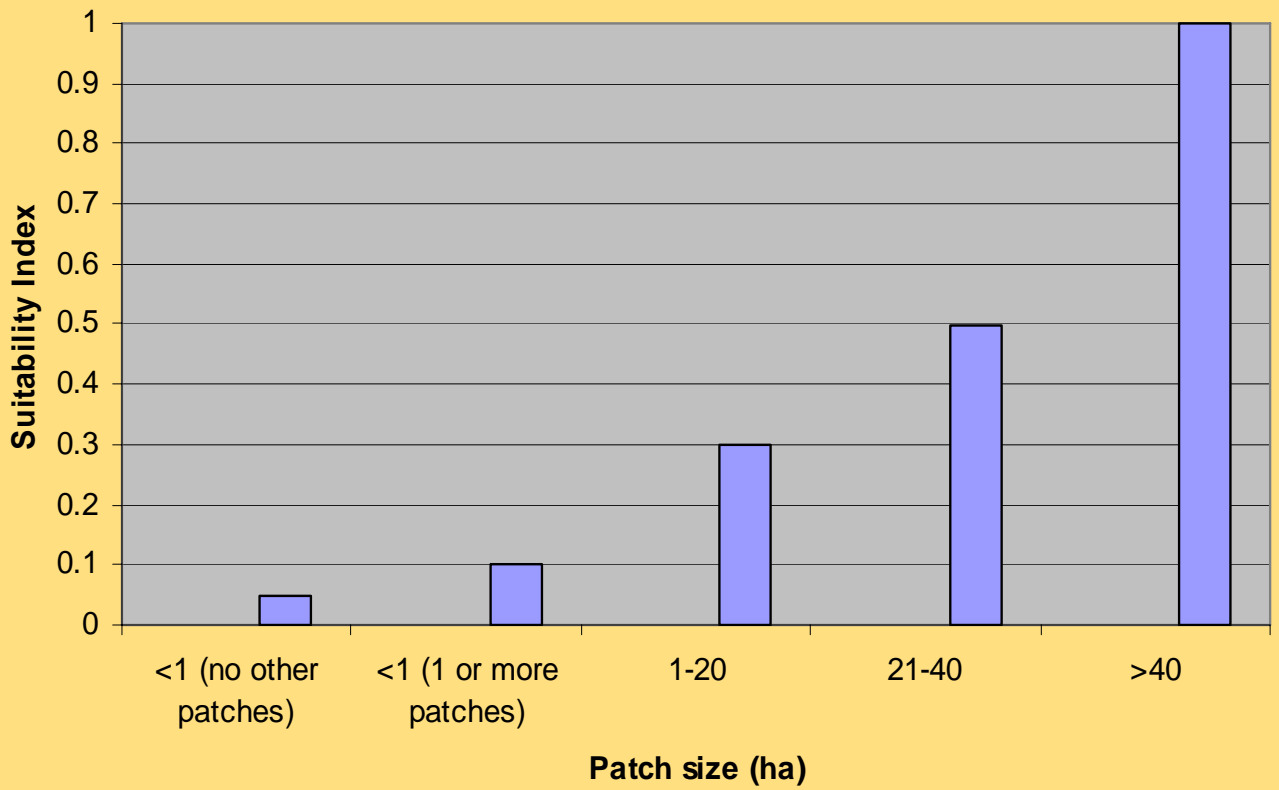
Sedgwick, J.A. 2000. Willow Flycatcher. *The Birds of North America. Life Histories for the 21st Century*. No. 533 (A. Poole and F. Gill, eds). The Birds of North America, Inc., Philadelphia, PA.

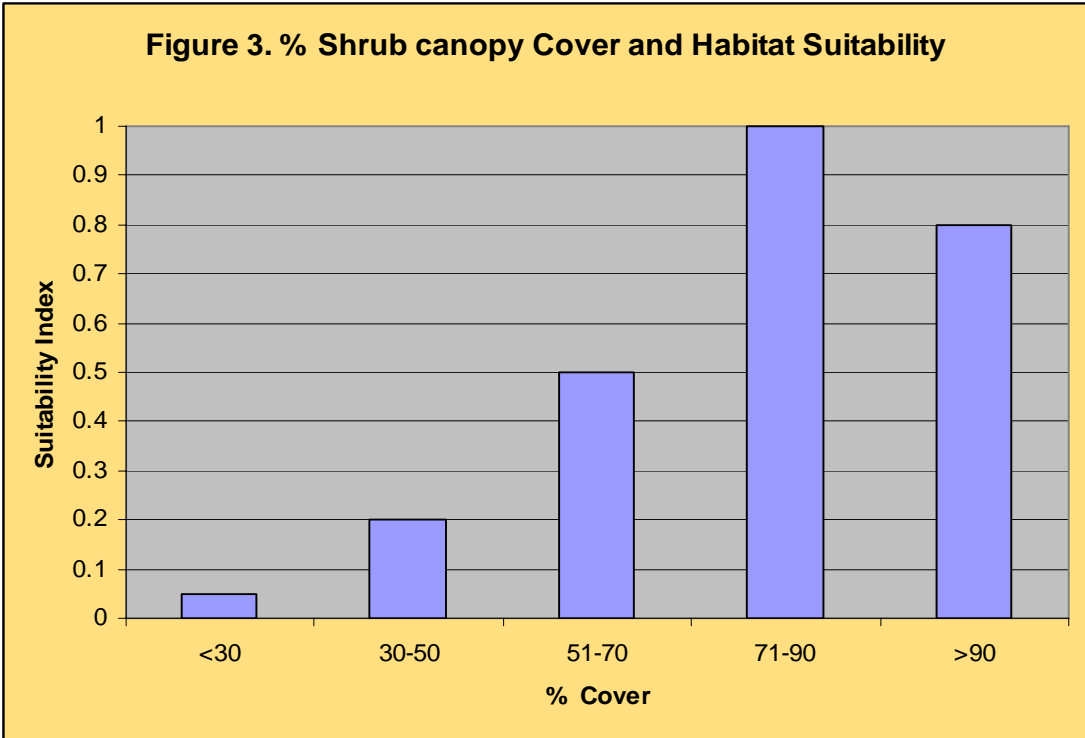
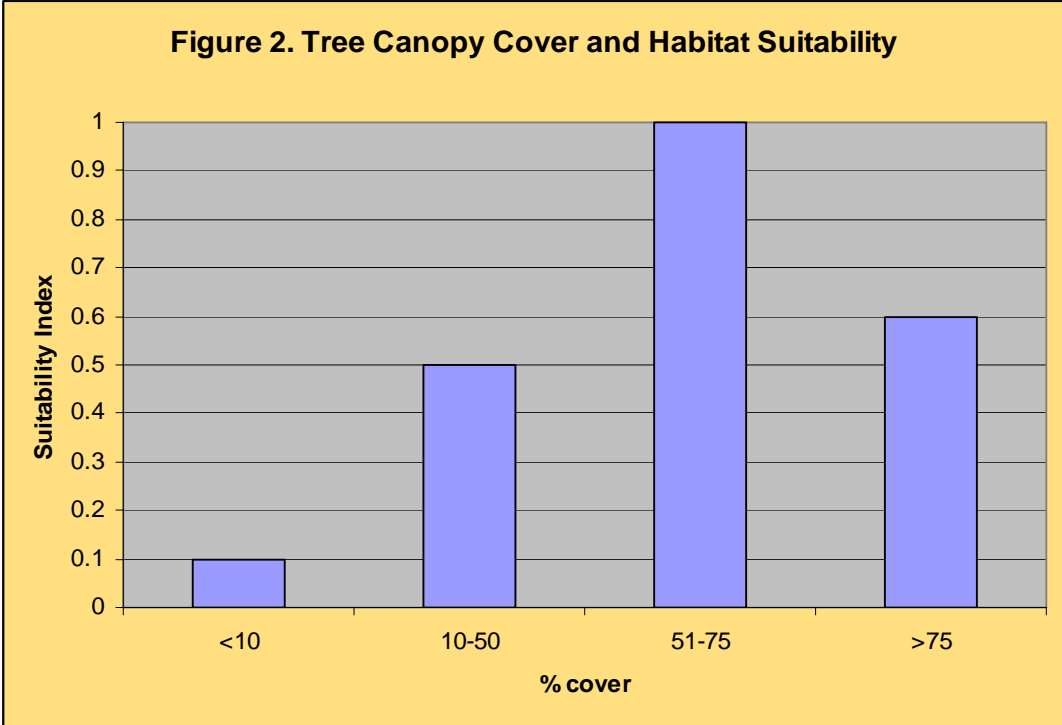
Short, H.L. 1983. Wildlife guilds in Arizona desert habitats. U.S. Fish and Wildlife Service, Ft. Collins, CO. BLM Technical Note 362.

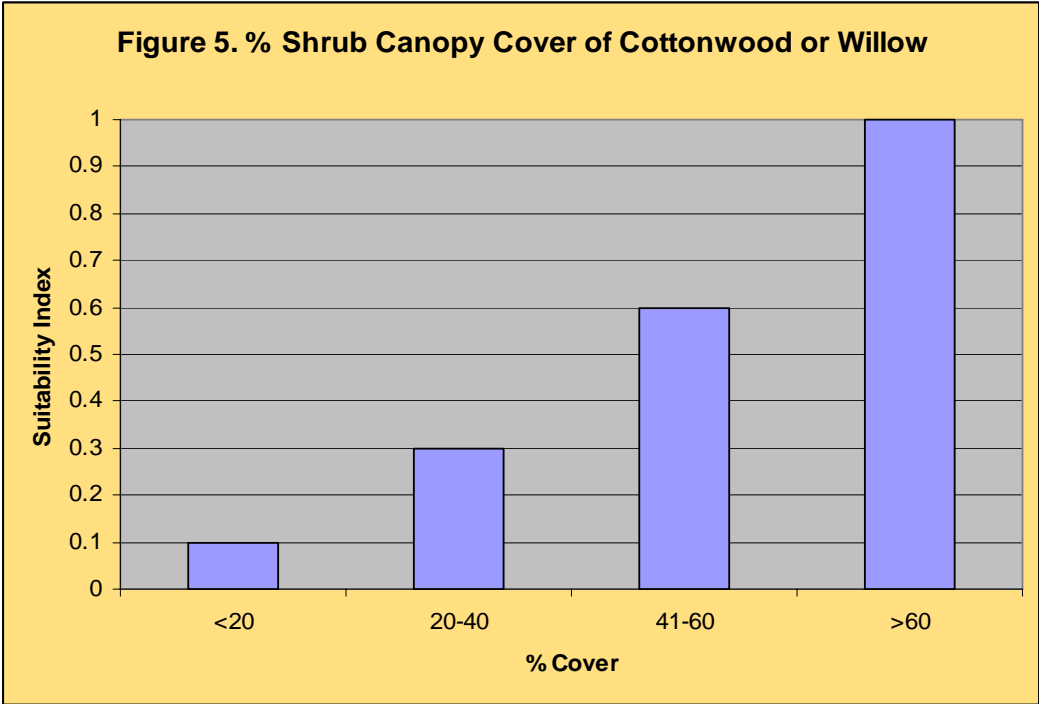
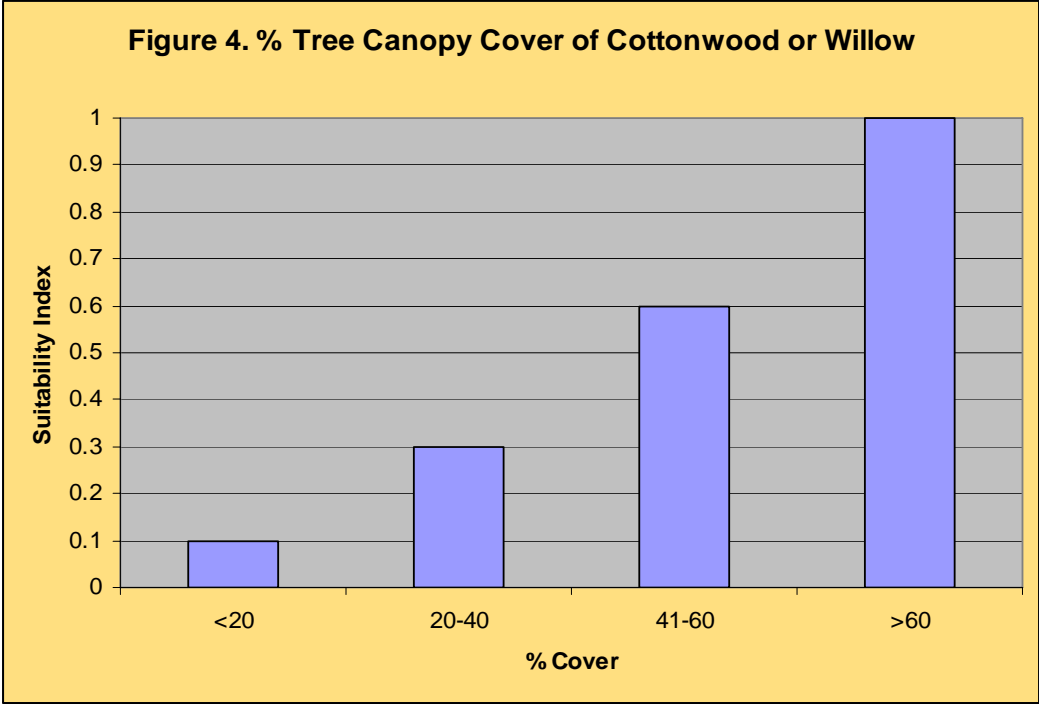
Short, H. L. 1984. Habitat suitability index models: the Arizona Guild and Layers of Habitat models. U.S. Fish and Wildlife Service, Ft. Collins, CO. FWS/OBS-82/10.70

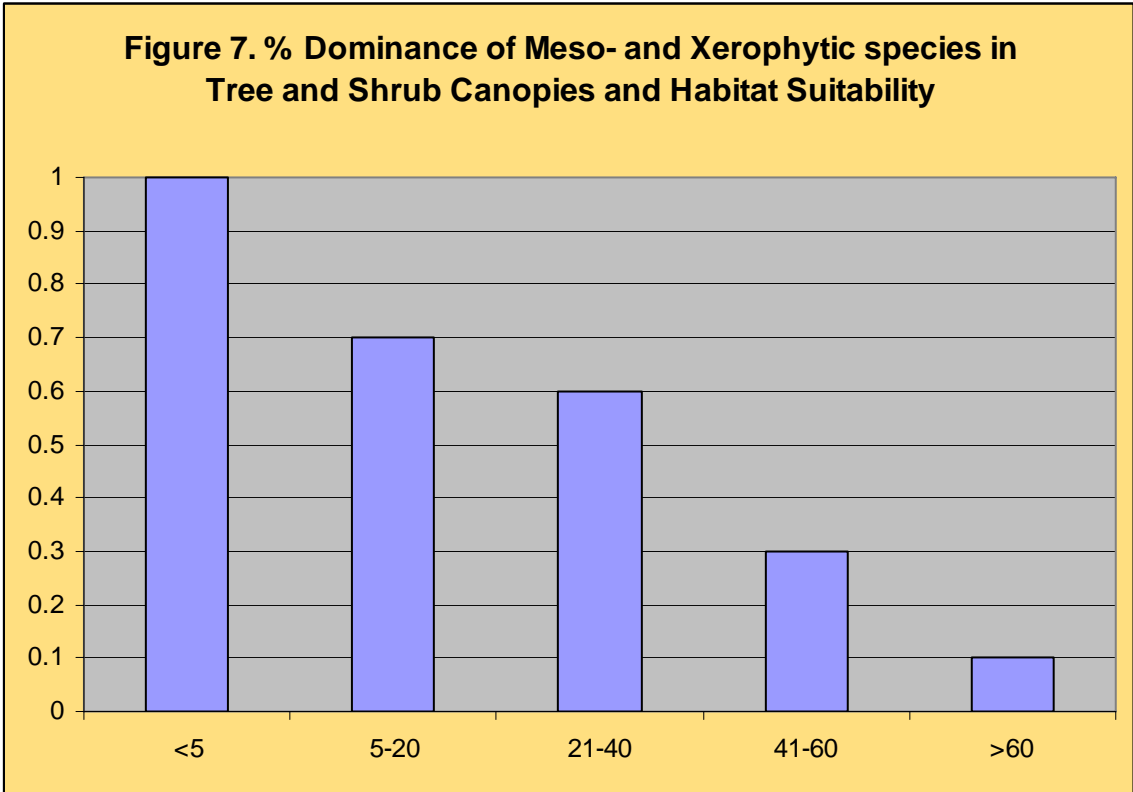
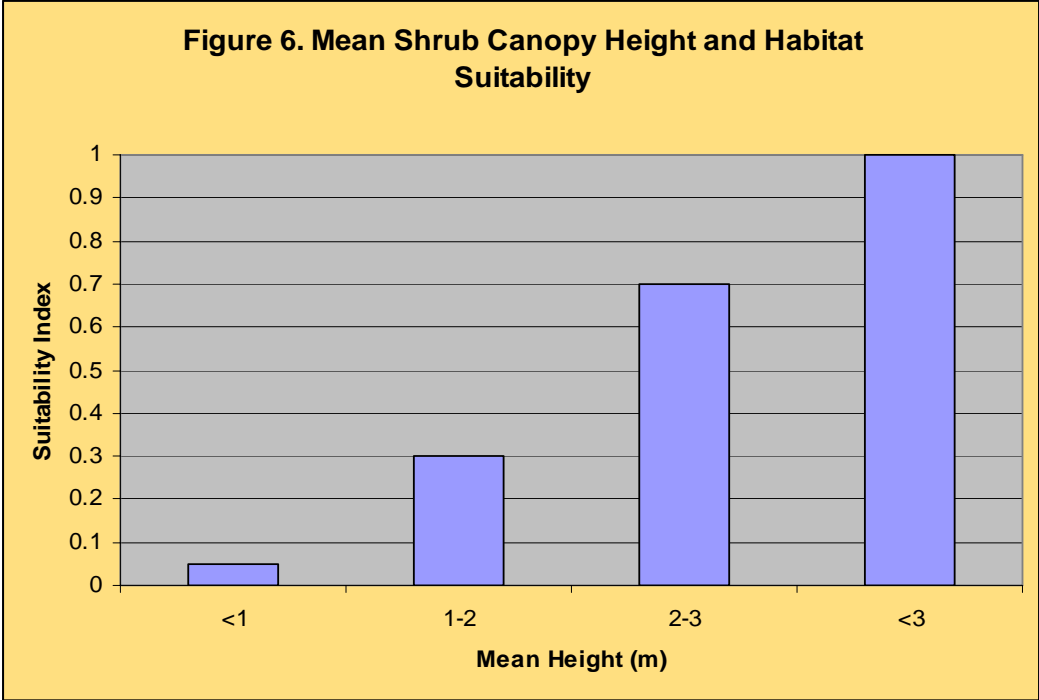
Skagen, S.K., C.P. Melcher, W.H. Howe, and F.L. Knopf. 1998. Comparative use of riparian corridors and oases by migrating birds in Southeast Arizona. *Cons. Biol.* 12:896-909.

Figure 1. Riparian forest/shrub patch size

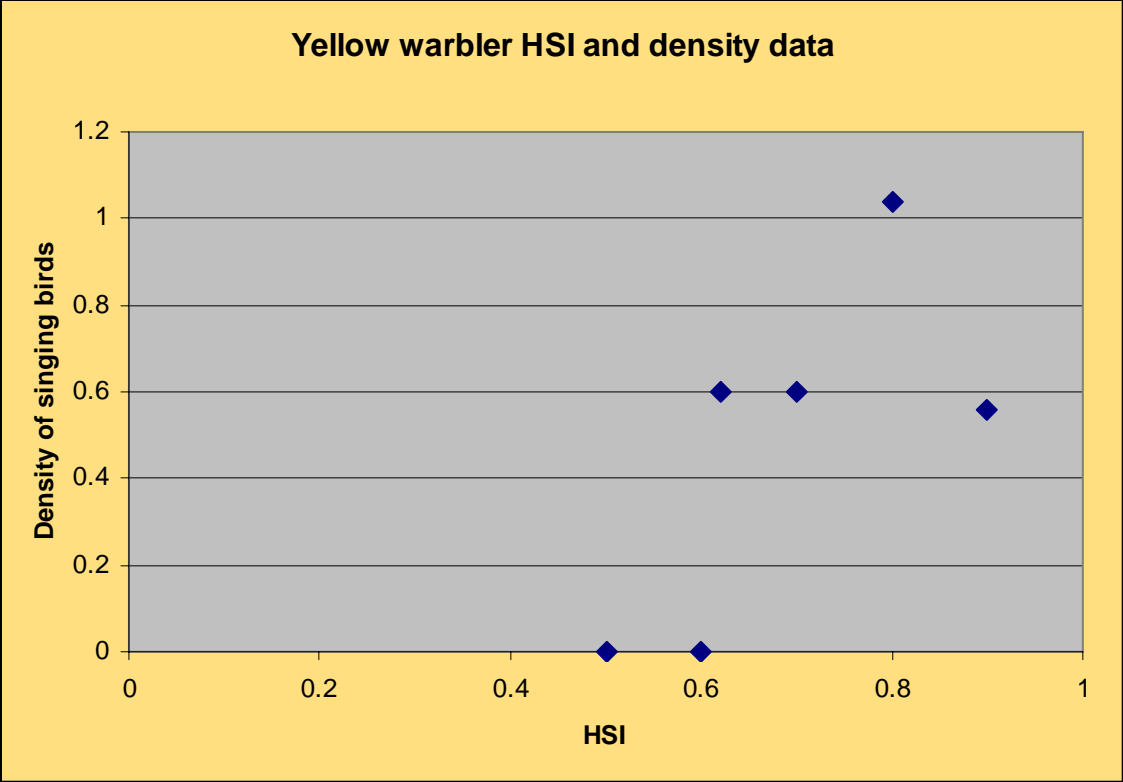








Attachment A. Results of Field Tests of Yellow Warbler HSI Model



ATTACHMENT 4 – Publications on the HSI model

Hector Galbraith¹, Jeff Price², Mark Dixon³, and Julie Stromberg³

Title of paper: Development of HSI models to evaluate risks to riparian wildlife habitat from climate change and urban sprawl

Reference Block: Galbraith, H., Price, J., Dixon, M., Stromberg, J. " **Development of HSI models to evaluate risks to riparian wildlife habitat from climate change and urban sprawl**" *Landscape Ecology and Wildlife Habitat Evaluation: Critical Information for Ecological Risk Assessment, Land-Use Management Activities, and Biodiversity Enhancement Practices, ASTM STP 1458*, L. A. Kapustka, H. Galbraith, M. Luxon, G. R. Biddinger, Eds., ASTM International, West Conshohocken, PA 2004.

Abstract: Hitherto, HSI models have largely been utilized to quantify the quality of existing habitat for wildlife species, without reference to how that habitat may have been altered in the past or how it might be altered in the future. In this study, we are using HSI models as part of an integrated modeling approach to estimate the risk of habitat quality gain or loss for a variety of indicator species due to future climate change and aquifer management decisions at the San Pedro Riparian National Conservation Area (SPRNCA). Current anthropogenic stressors, including agricultural and municipal water use, are having adverse impacts on the extent and quality of riparian habitat in the SPRNCA. Future climate change, through its potential effects on hydrology and water demand by local communities, may exacerbate these effects. Because of these current and potential future changes, vertebrates that depend on riparian habitats for their breeding, wintering or migration sites are at risk. Combining climate, hydrology, and vegetation modeling with HSI models allows us to predict the effects these risks.

¹Galbraith Environmental Sciences LLC, 289 Wiswall Hill Rd., Newfane, VT 05345.

²American Bird Conservancy, Boulder, CO.

³Department of Plant Biology, Arizona State University, Tempe, AZ.

Keywords: Biodiversity, Riparian habitat, Hydrology, Water use, Climate change, HSI models

Introduction

The upper San Pedro Riparian National Conservation Area (SPRNCA) ecosystem in southeastern Arizona and northern Sonora is of critical importance in maintaining regional biodiversity at the ecotone between the Sonoran and Chihuahuan deserts and the Plains grassland. It contains one of the richest assemblages of species and supports one of the most important western migratory bird habitats in North America (Arias Rojo et al. 1999). For its size, the SPRNCA has one of the highest avian diversities found anywhere in the U.S. Almost 390 bird species have been recorded there, of which 250 are migrants that winter in Central or South America and depend on the San Pedro as a staging post on their journeys to and from their breeding areas in the U.S. and Canada. Between one and four million songbirds use the SPRNCA as a migratory corridor each year.

Riparian ecosystems are fragile, especially those found in arid climates. Water is the lifeblood of these communities and the abundance, diversity and health of these ecosystems are strongly influenced by the hydrologic regime, particularly depth to groundwater and the amount, timing and pattern of surface flow. A water table within a few feet of the ground surface is an essential prerequisite for the growth and survival for riparian tree species and other vegetation, while frequent and strong surface flows are essential for the recruitment of tree species such as cottonwoods and willows (Stromberg et al., 1996; Stromberg, 1998; Auble et al., 1994).

The hydrologic regime in the SPRNCA depends on both the local climate (evaporation rates, rainfall) and the state of the groundwater system. Groundwater pumping to provide water for agricultural, industrial, and municipal uses impacts the state of the groundwater system. Models developed by the Arizona Department of Water Resources and others (*in* Arias Rojo et al. 1999) indicate that groundwater pumping in the nearby city of Sierra Vista area has already impacted baseflow in the river. The population of Sierra Vista has grown at an annual rate of 2.4% over the last 20 years and is projected to continue at that rate for the foreseeable future. This has already resulted in an increase in the depth to groundwater in the shallow aquifer. Groundwater modeling indicates that as the population continues to grow, the baseflow of the river may be further affected (Vionnet et al., 1992). This, in turn, could lead to reductions in the extent of the riparian vegetation, invasion by xerophytic species such as mesquite and non-natives (e.g., salt cedar) and to a reduction in faunal biodiversity in the area (Stromberg *et al.*, 1996).

Previous hydrologic models, while taking into account human population growth in the area around the Upper San Pedro River, have not taken into account potential changes that could accompany climate change resulting from an increase in greenhouse gases. Models prepared for the western megaregion of the U.S. National Assessment show potential average temperature increases of around 1.8° C by 2030 and of between 4° and 5.3° C by the year 2095 (VEMAP 2000). Even with precipitation increases, the overall amount of soil moisture will likely decrease. These climatic changes could lead to direct changes to the riparian biodiversity and exacerbate changes brought about by anthropogenic impacts to the water regime.

In this EPA-funded project we are integrating hydrologic, climatic, and vegetation modeling with wildlife habitat models in an attempt to predict the potential effects of future human population growth (and water extractions) and climate change on the riparian vegetation communities of the SPRNCA, and their ability to support important wildlife communities. In this paper, we describe how wildlife Habitat Suitability Index (HSI) models are being developed and how they are to be

integrated with the overall modeling process, and the vegetation models in particular, to evaluate the risk of habitat change and loss.

Problem Identification and HSI Model Development

Previous applications of HSI models have included the prediction of the possible effects of particular land management alternatives on biota (Brand *et al.*, 1986; Schamberger and Farmer, 1978), the quantification of past injuries to ecosystem wildlife carrying capacities (Galbraith *et al.*, 1996; LeJeune *et al.*, 1996), and estimating the exposure to contaminants of wildlife species (Galbraith *et al.*, 2001). If the structures, extents, and/or compositions of post-change vegetation communities can be predicted, it becomes possible to use HSI models to quantify and compare pre- and post-change habitat quality and potential carrying capacities. HSI models achieve this by:

- 25. Identifying the critical habitat variables that affect the carrying capacity of habitat.
- 26. Establishing quantitative relationships between the occurrence of these variables and the carrying capacity of habitat. Each variable is assigned a suitability index (SI). This is a score of between 0 and 1, where the former is completely unsuitable habitat (i.e., minimal carrying capacity) and the latter is optimal habitat (i.e., greatest carrying capacity).
- 27. Developing metrics that can be used in the field to quantify the occurrence of the critical habitat components (and, therefore, the carrying capacity of the habitat)
- 28. Developing algorithms that combine the variable scores (SIs) into an expression of the overall carrying capacity of the habitat. This final score is the HSI and can be between 0 (unsuitable for species or guild) and 1 (optimal habitat).

A fifth component, that is not often performed, should be the testing and validation of HSI models in the field.

To anticipate the effects of depth to groundwater changes on vegetation and wildlife habitat we are developing a hydrophytic model and a number of HSI models (Table 1). HSI models are being developed for species that are likely to lose habitat if the changes described above occur. However, they are also being developed for species that may not be adversely affected or, indeed, may benefit from the expected phytoecological changes.

Table 1. HSI models being developed and rationale for each.		
Model species	Habitat gain or loss	Rationale for model
Southwestern willow flycatcher	Potential gain	Species, while riparian, is not dependent on native gallery forest but breeds successfully in the region in salt cedar and other riparian scrub
Yellow-billed cuckoo	Potential loss	In region this species is obligate of shady riparian gallery forest

Yellow and Wilson's warblers	Potential loss	Large migratory populations passing through the SPRNCA feed largely in willow and cottonwood canopy
Botteri's sparrow	Potential gain	Species characteristic of mesic or xerophytic grasslands bordering SPRNCA riparian forest. May benefit as former replaces latter.

The developmental and field-validation processes of two of these models are illustrated below by focusing on two individual models (southwestern willow flycatcher and yellow-billed cuckoo). Space does not permit the description of all five models.

Southwestern Willow Flycatcher.

The southwestern willow flycatcher, *Empidonax traillii extimus*, is a summer visitor to southern Arizona, wintering in Central and South America, south to Panama and northern Colombia (Finch et al., 2000; Sedgwick, 2000).

Throughout most of its breeding range the willow flycatcher is confined to brushy thickets associated with standing or slow-moving water (Sedgwick, 2000). The southwestern race is largely restricted as a breeding species to riparian shrubby thickets in an otherwise arid or semi-desert landscape (Sogge and Marshall, 2000; U.S. Fish and Wildlife Service, 1997; U.S. Fish and Wildlife Service, 2001; Arizona Game and Fish Department unpublished data; Paradzick and Woodward, in press; Allison et al., in press). In response to anthropogenic impacts to the subspecies' habitats (agriculture, mining, etc.) and to population declines, U.S. Fish and Wildlife Service listed the subspecies under the Endangered Species Act as "endangered" in 1995.

Southwestern willow flycatchers have bred or have been reported occupying territories in the SPRNCA in 1977 and 1989 (Krueper, 1997). At present, they may be considered intermittent and rare breeders in the area which may benefit if riparian forests are replaced by shrubbier habitats, including salt cedar stands.

No previous HSI model exists for the southwestern willow flycatcher in any part of its breeding range. Therefore, one was developed for this project. The components and structure of this model were initially based on a literature review of the habitat preferences and patterns of use of southwestern willow flycatchers. This resulted in a draft model, which provided a focus for discussions with southwestern willow flycatcher researchers in Arizona, and model testing and modification in the field (along the lower San Pedro and Gila Rivers at long-term Arizona Game and Fish Department study sites with known flycatcher densities). Based on the comments of species experts and the field test results, the draft model was modified, resulting in this version.

The final southwestern willow flycatcher HSI model incorporates eight variables (patch area and degree of isolation, width of habitat patch, shrub canopy cover, shrub foliage density at 3-5 meters, shrub canopy height, tree canopy cover, distance to standing or slow-moving water, soil moistness). The numerical relationships between each of the variables and habitat suitability are the core of the habitat model. These were developed from information in the scientific literature (e.g., U.S. Fish and Wildlife Service, 2001; Skaggs, 1996; Sedgwick, 2000; Marshall, 2000), and from conversations and field visits with

Arizona Department of Game and Fish willow flycatcher researchers C. Paradzick and A. Woodward. They are described below and in Figures 1 through 8.

V1. Area and degree of isolation of riparian shrub patch. A riparian shrub or forest patch is defined as a shrub vegetation community (either with or without a tree canopy), generally less than 10 m in height, and dominated by willows and/or salt cedar. The patch size, patch isolation and habitat suitability scores that were developed are shown in Figure 1. It is assumed that patches smaller than 1 ha do not provide habitat for the species unless within a landscape of small patches, that small and medium size patches (1-2 and 2-5 ha, respectively) provide increasing levels of suitability and that patches larger than 5 ha are optimal for the species.

V2. Width of riparian patch. The patch width and habitat suitability scores that were developed are shown in Figure 2. It is assumed that the relationship between patch width and habitat suitability is approximately linear and that riparian strips narrower than 10 m do not provide habitat for the species.

V3. Percent shrub canopy cover in 20 m radius of sampling point. The shrub cover and habitat suitability scores that were developed are shown in Figure 3. It is assumed that the relationship between % cover and habitat suitability is approximately linear, except at very high percent shrub covers where continuous shrub cover eliminates the presence of canopy breaks, another important habitat feature for the species. It is also assumed that shrub cover that is less than 50% does not provide habitat for flycatchers.

V4. Shrub foliage density at 3-5 meters. The relationships between shrub foliage density at 3-5 m and habitat suitability are shown in Figure 4. Sparse equates with a site where it is possible to clearly see more than 20 m at 3-5 m elevation above ground level from the sampling point for the majority of 360°. Moderately dense equates with visibility between 10 and 20m. Dense equates with visibility between 5 and 10 m. Very dense equates with visibility less than 5m.

V5. Average shrub canopy height within 20 m radius of sampling point. The mean shrub canopy height and habitat suitability categorization are shown in Figure 5. It is assumed in this categorization that canopy heights of less than 4 meters do not provide habitat for flycatchers, and that optimal habitat is reached at 6 meters.

V6. Tree canopy cover within 20 m radius of sampling point. Based on the relationships among tree cover, shading and shrub growth, the tree canopy (woody vegetation > 10m in height) the habitat suitability scores shown in Figure 6 were developed. It is assumed that at high levels of tree canopy cover (>51%) shading is such that the surviving shrub layer will probably not be dense enough to provide high quality habitat.

V7. Distance to standing or slow-moving water. The distance to water (defined as standing or slow moving water greater than 5 meters in diameter or 2 meters in width) and habitat suitability scores shown in Figure 7 were developed. It is assumed that even sites distant from water may provide low quality flycatcher habitat. This relationship is presented graphically in Figure 7.

V8. Degree of soil waterlogging. **On the lower San Pedro River and its confluence with the Gila River, southwestern willow flycatchers prefer nesting habitat that has at least moist soils, or, optimally, wet or waterlogged soils (Paradzick and Woodward pers comm.). Based on this the variable categorization shown in Figure 8 was developed:**

Figure 1. Riparian shrub patch size (ha) and suitability index (SI) relationship

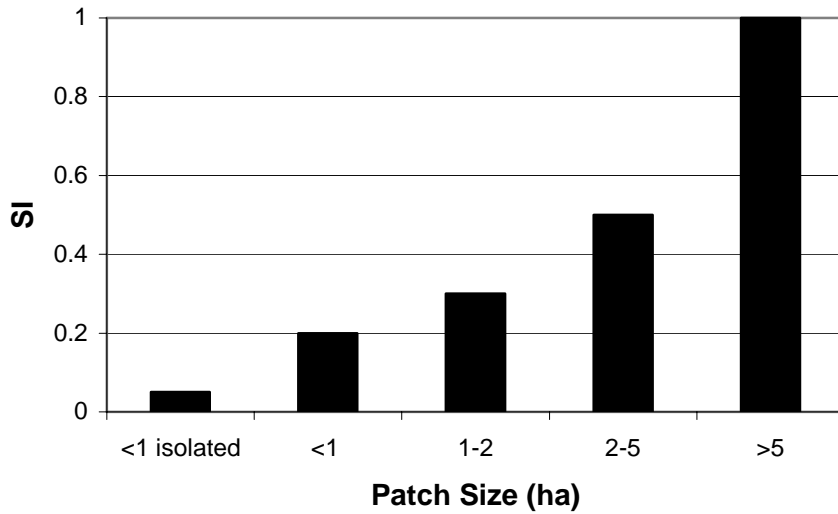


Figure 2. Riparian shrub patch width (m) and suitability index (SI) relationship

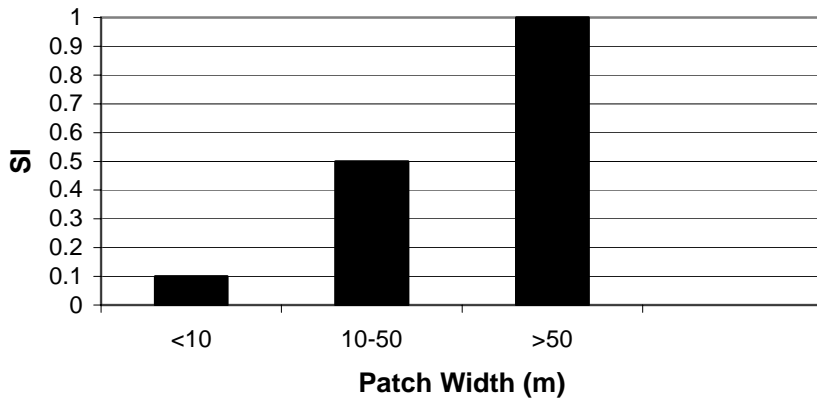


Figure 3. Percent shrub canopy cover and suitability index (SI) relationship

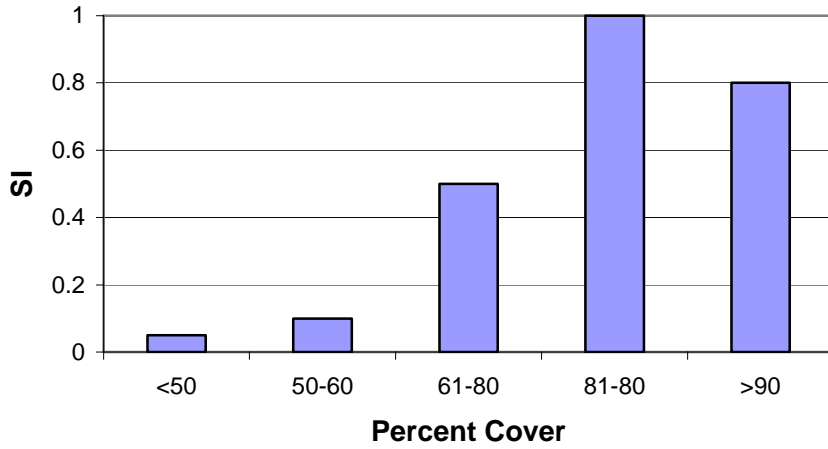
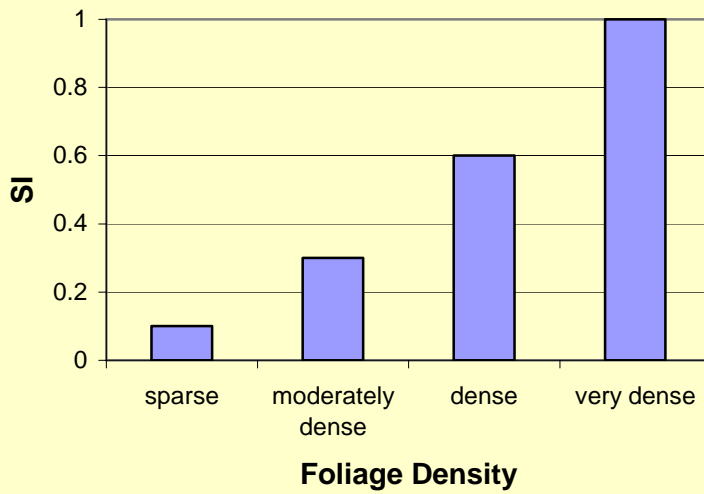
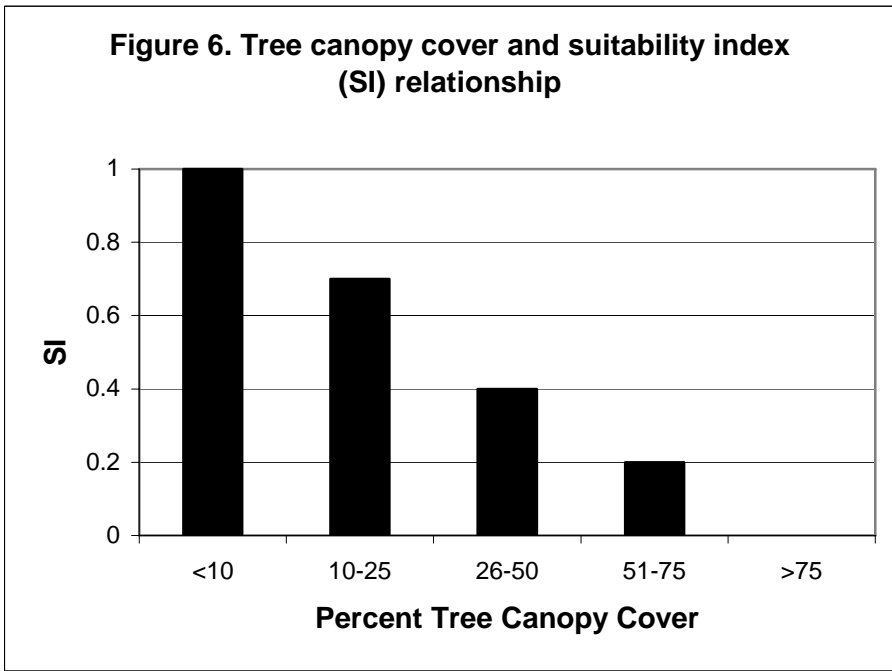
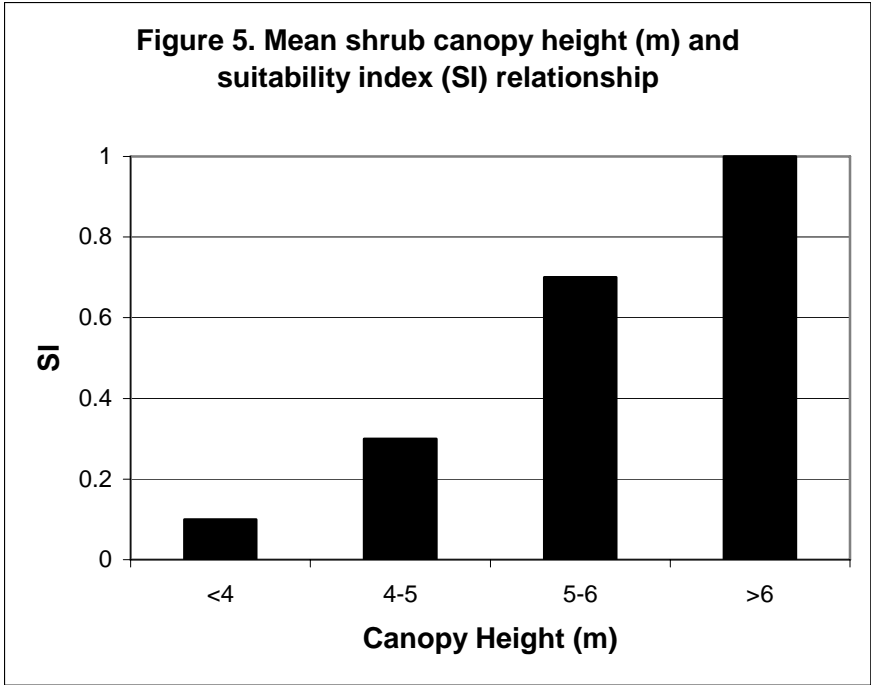
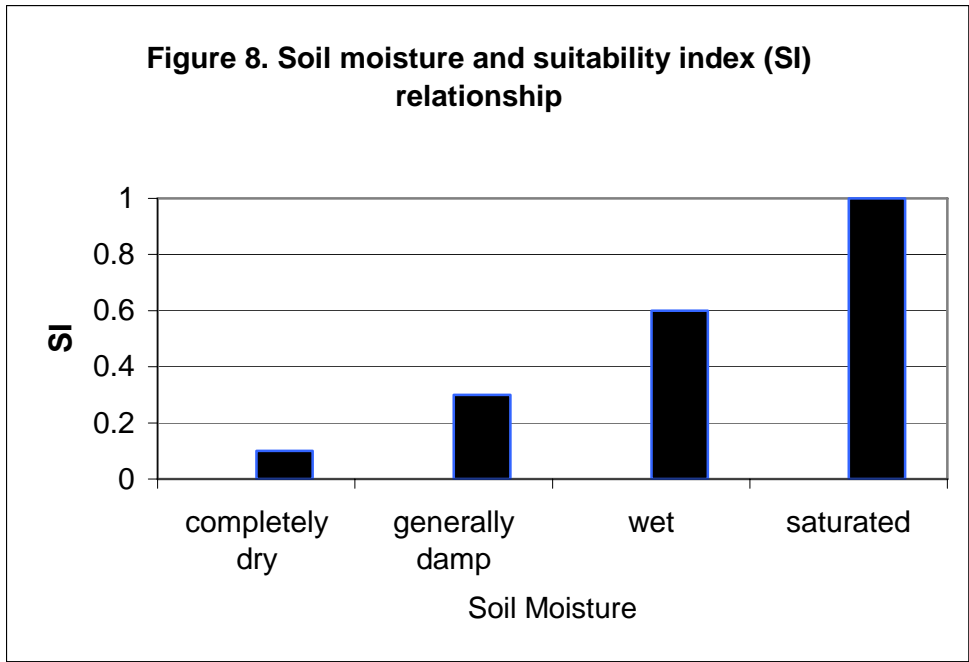
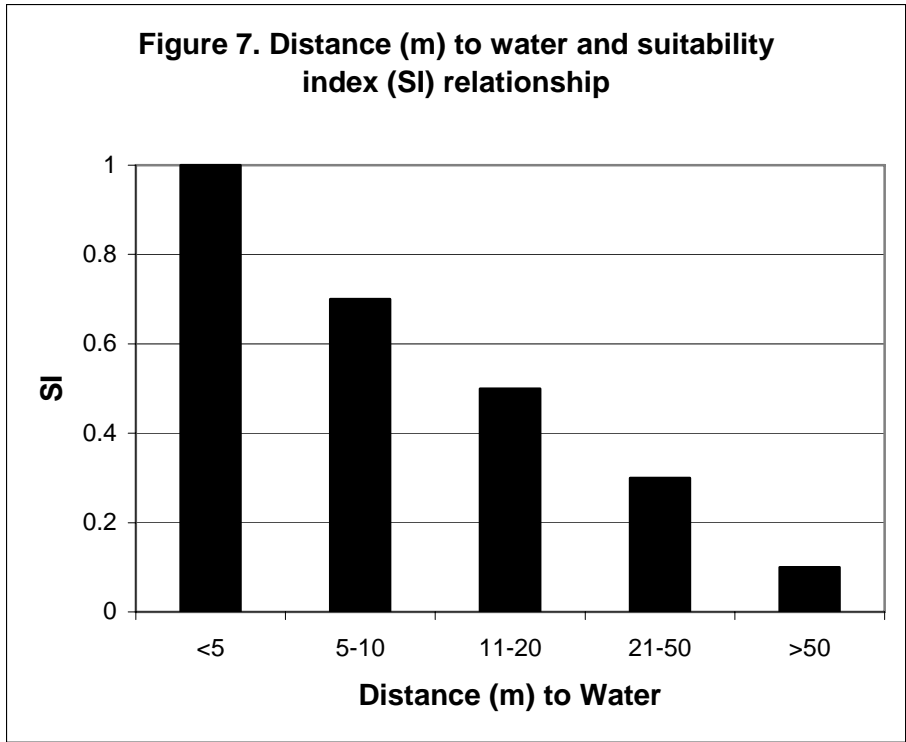


Figure 4. Shrub foliage density and suitability index (SI) relationship







Model application

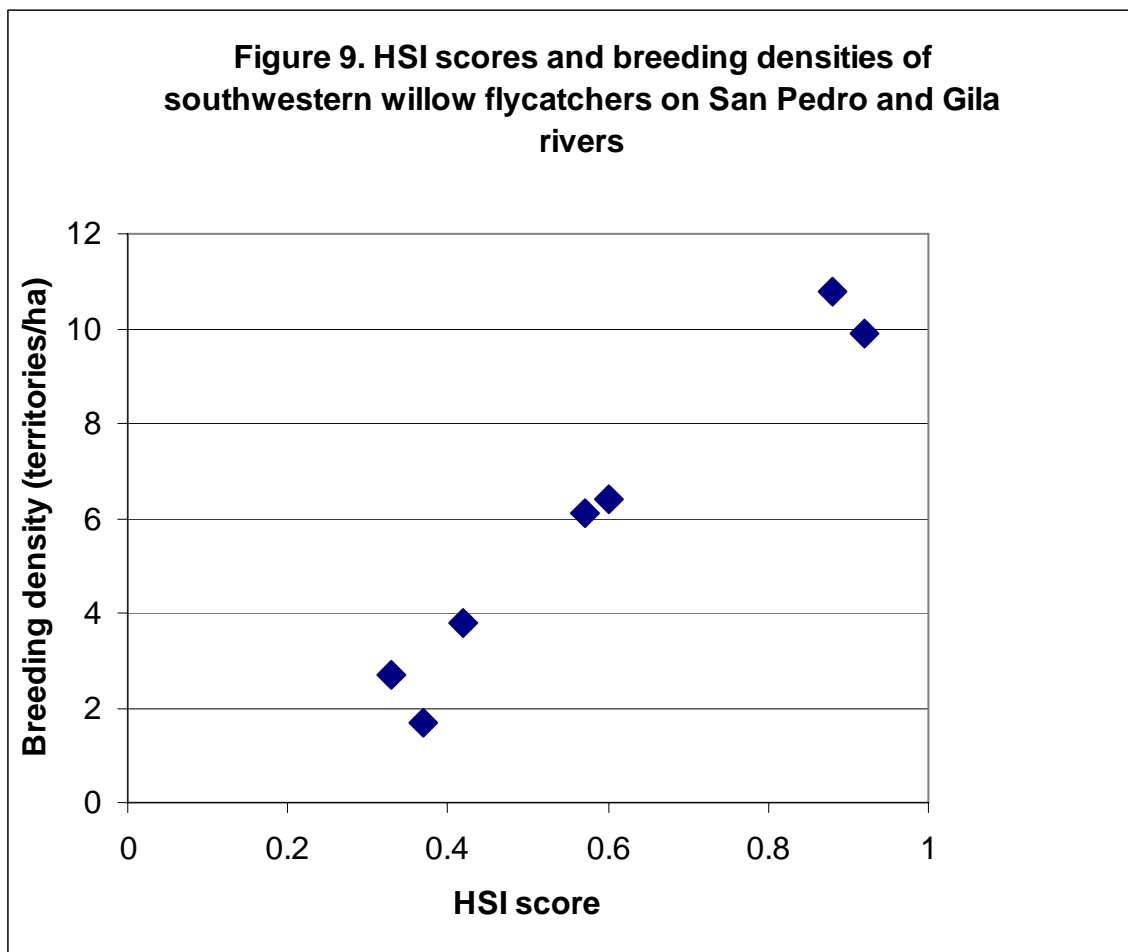
The eight variables described above were combined into an index of the overall assessment of the habitat suitability (HSI) of a particular patch of riparian habitat using the following 8th root algorithm (to limit the HSI scores to between 0 and 1):

$$HSI = (V1 \times V2 \times V3 \times V4 \times V5 \times V6 \times V7 \times V8)^{1/8}$$

The HSI values obtained using this equation range between 0 and 1 (lowest and highest estimates of suitability, respectively).

Field test results

The draft HSI model was tested in the field in areas of known willow flycatcher breeding density (unpublished data – C. Paradzick and A. Woodward, Arizona Game and Fish Department). The results of the field test of the southwestern willow flycatcher model are presented in Figure 9. These results show that the predictions of the HSI model regarding habitat suitability are generally accurate (if it is assumed that breeding density is a reflection of at least short term habitat quality). Thus the HSI model developed for this study is a reasonable predictor of breeding habitat quality for the study species.



Yellow-billed Cuckoo

The yellow-billed cuckoo is a summer visitor to North America, wintering in Central and South America (Kaufman, 1996; Hughes, 1999). The western race is largely confined to riparian broad-leaved woodlands, particularly those dominated by mature cottonwoods or willows (Gaines, 1974; Hamilton and Hamilton, 1965; Hughes, 1999). They apparently avoid riparian habitats dominated by invasive salt cedar, *Tamarix pentandra* (Laymon and Halterman, 1987).

It is likely that, at most, 600 pairs of yellow-billed cuckoos breed in Arizona, with 50-100 of these in the SPRNCA (Laymon and Halterman, 1987; Krueper, 1997). Rapid population decreases and range reductions of western yellow-billed cuckoos have recently prompted efforts (thus far unsuccessful) to have the race listed under the Endangered Species Act.

No previous HSI models existed for yellow-billed cuckoo in any part of its breeding range. Therefore, a model was developed to evaluate the potential effects of climate change to the biota of the riparian systems of the SPRNCA. The components and structure of this model were initially based on a literature review of the habitat preferences and patterns of use of yellow-billed cuckoos. This resulted in a draft model which provided a focus for discussions with researchers in Arizona, and model modification in the field. It was then tested in the SPRNCA at sites with known cuckoo breeding densities. Based on the comments of species experts and the field test results, the draft model was modified, resulting in this version.

The final yellow-billed cuckoo HSI model incorporates eight variables: continuity and width of habitat patch, shrub density (canopy cover), tree and shrub canopy heights, cottonwood/willow dominance in tree canopy, cottonwood/willow/ash/walnut/Baccharis dominance in shrub canopy, salt cedar and/or mesquite dominance in the shrub understory. The numerical relationships between each of the variables and habitat suitability are the core of the habitat model. These were developed from information in the scientific literature (e.g., Hughes, 1999; Gaines and Laymon, 1984; Laymon et al., 1997; Laymon and Halterman, 1989), and from conversations and field visits with yellow-billed cuckoo researchers working in the SPRNCA. They are described below and in Figures 10 through 17.

V1. Linear continuity of riparian forest or shrub habitat. In the SPRNCA, riparian shrub or tree linear patches that are relatively unbroken over at least 200 meters provide higher quality cuckoo habitat than more fragmented habitats. To accommodate this, the categorization shown in Figure 10 was developed.

V2. Width of riparian forest patch. Based on data presented in Laymon and Halterman (1989) and observations at sites of known breeding density in the SPRNCA, the patch width and habitat suitability categorizations shown in Figure 11 were developed. It is assumed that the relationship between patch width and habitat suitability is approximately linear and that riparian strips narrower than 50 m do not provide good habitat for the species.

V3. Percent shrub canopy cover in 50 m radius of sampling point. Based on the results reported in Gaines and Laymon (1984) and observations at sites with known breeding densities of cuckoos on the SPRNCA, the shrub cover and habitat suitability categorizations shown in Figure 12 were developed. It is assumed in this categorization that the relationship between % cover and habitat suitability is approximately linear except at very low percent shrub covers where a further reduction will result in a disproportionate effect on habitat suitability.

V4. Average shrub canopy height within 50 m radius of sampling point. Based on observations made at the SPRNCA in areas of known cuckoo breeding density, the shrub canopy height and habitat suitability categorizations shown in Figure 13 were developed.

V5. Average tree canopy height within 50 m radius of sampling point. **Based on the results reported in Gaines (1977), Gaines and Laymon (1984), and observations made at the SPRNCA in areas of known cuckoo breeding density, the tree canopy height and habitat suitability categorization shown in Figure 14 were developed. It is assumed that the relationship between tree canopy height and habitat suitability is approximately linear. It is also assumed that even low canopy heights may have some habitat value.**

V6. Cottonwood/willow dominance in tree canopy within 50 m radius of sampling point. **Based on the results reported in Laymon and Halterman (1985), the cottonwood/willow dominance in the tree canopy and habitat suitability categorizations shown in Figure 15 were developed. It is assumed that the relationship between % dominance and habitat suitability is approximately linear. It is also assumed that very low representations of these species (<10%), provide at best marginal habitat for yellow-billed cuckoos.**

V7. Cottonwood/willow/ash/walnut/seep willow percent dominance (relative cover) in shrub layer within 50 m radius of sampling point. **Based on the results reported in Gaines and Laymon (1984) and observations made at the SPRNCA in areas of known cuckoo breeding density, the shrub cover and habitat suitability categorizations shown in Figure 16 were developed. It is assumed that the relationship between % dominance and habitat suitability is approximately linear except at very low percent shrub covers where a further reduction will result in a disproportionate effect on habitat suitability. It is also assumed that less than 10% dominance, provides only extremely marginal habitat for yellow-billed cuckoos.**

V8. Percent dominance (relative cover) of salt cedar and/or mesquite in the shrub canopy within 50 m radius of sampling point. **The relationships between representation of salt cedar and/or mesquite in the vegetation community and habitat suitability shown in Figure 17 are assumed. It is assumed in this categorization that the relationship between % dominance of salt cedar/mesquite and habitat suitability is not linear but that increasing dominance by salt cedar or mesquite has a disproportionate effect on habitat suitability. It is also assumed that the highest dominance by salt cedar and/or mesquite (>70%) will constitute extremely marginal habitat for yellow-billed cuckoos.**

Figure 10. % Linear continuity of riparian forest or shrub over 200 m and SI relationships

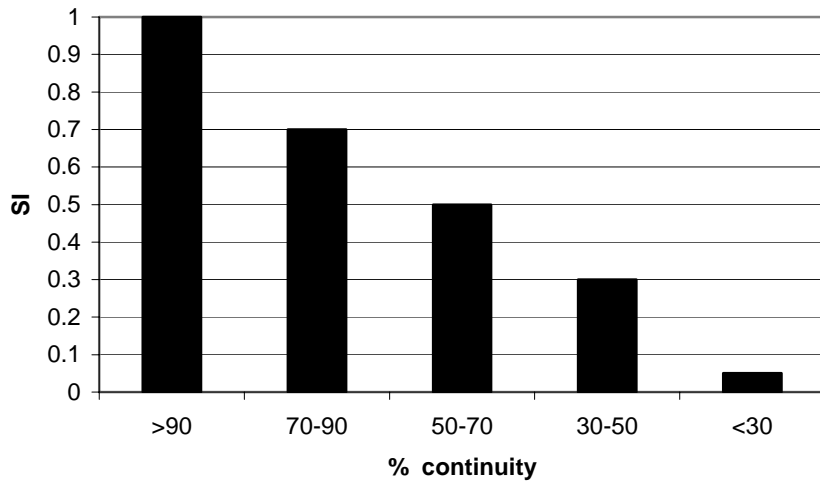


Figure 11. Riparian forest patch width and suitability index (SI) relationship

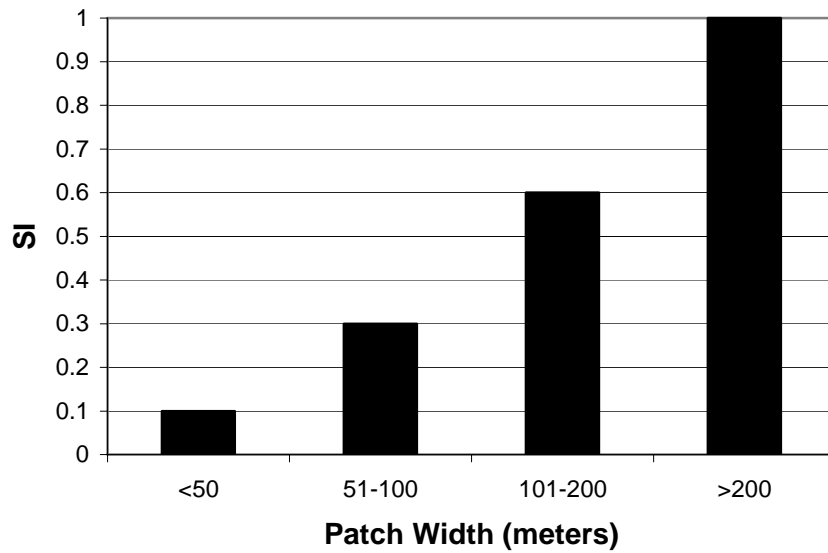


Figure 12. Percent shrub canopy cover and suitability index (SI) relationship

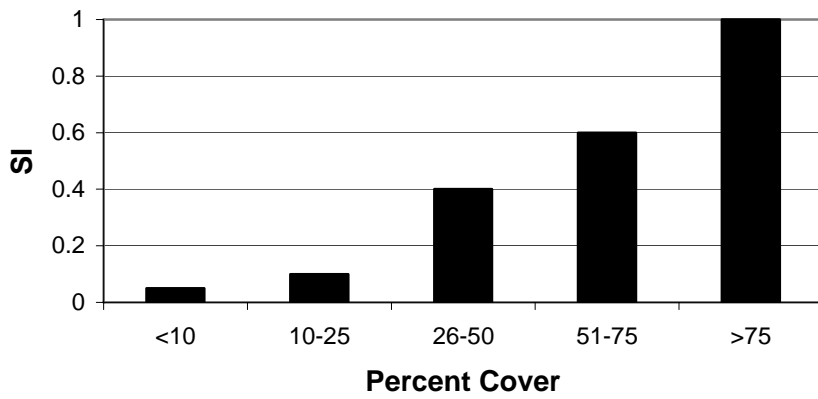


Figure 13. Average shrub canopy height and suitability index (SI) relationship

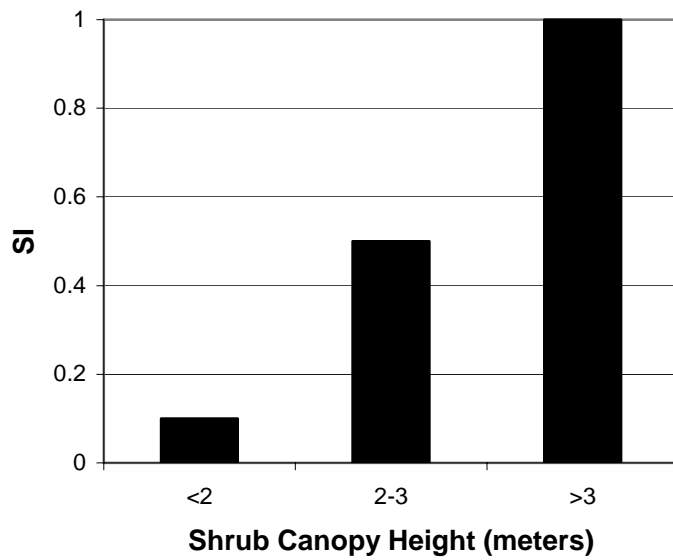


Figure 14. Average tree canopy height and suitability index (SI) relationship

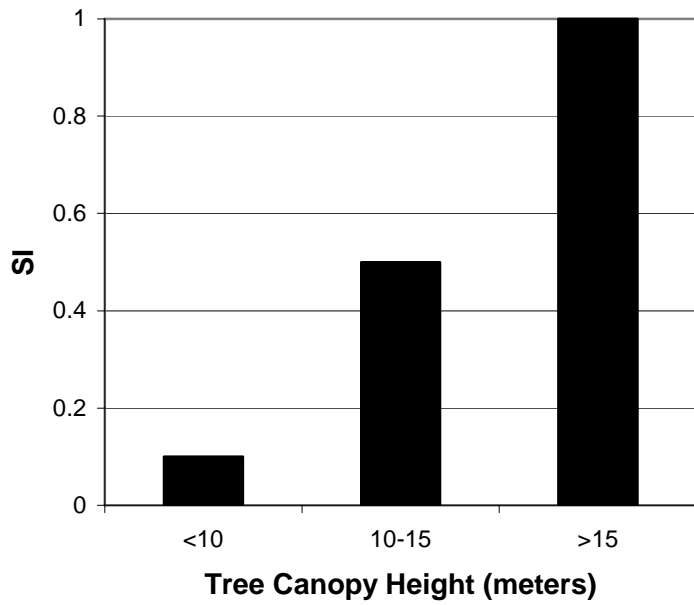
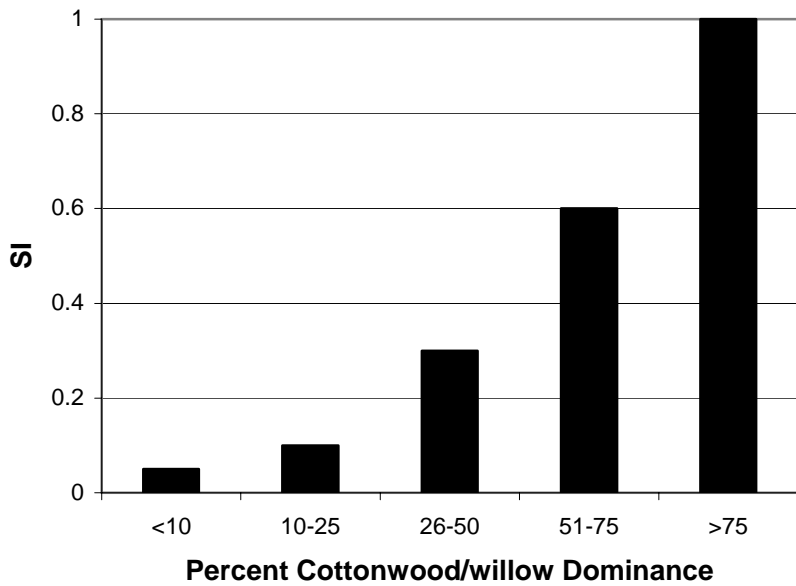
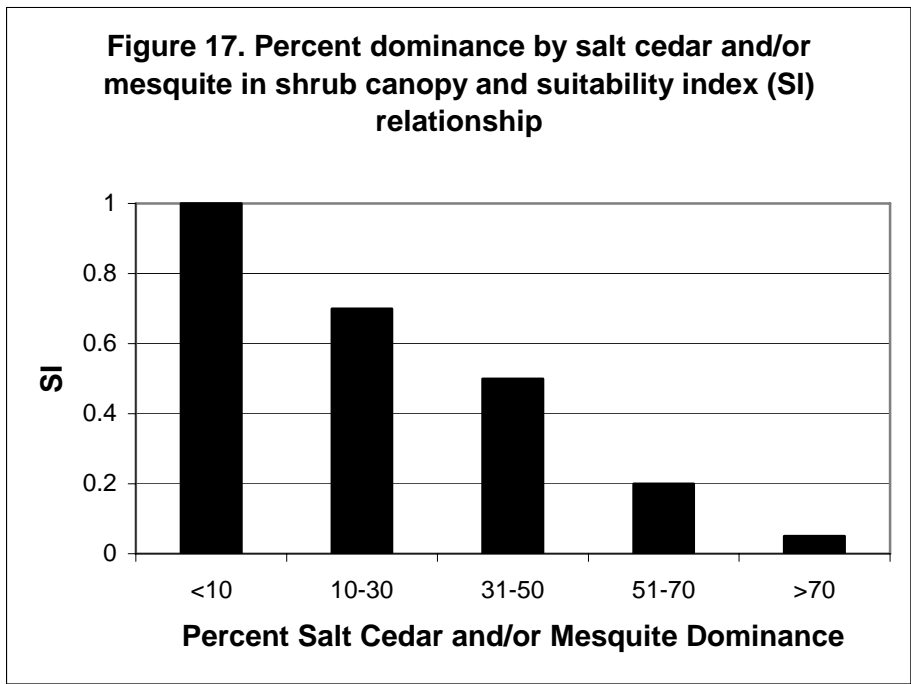
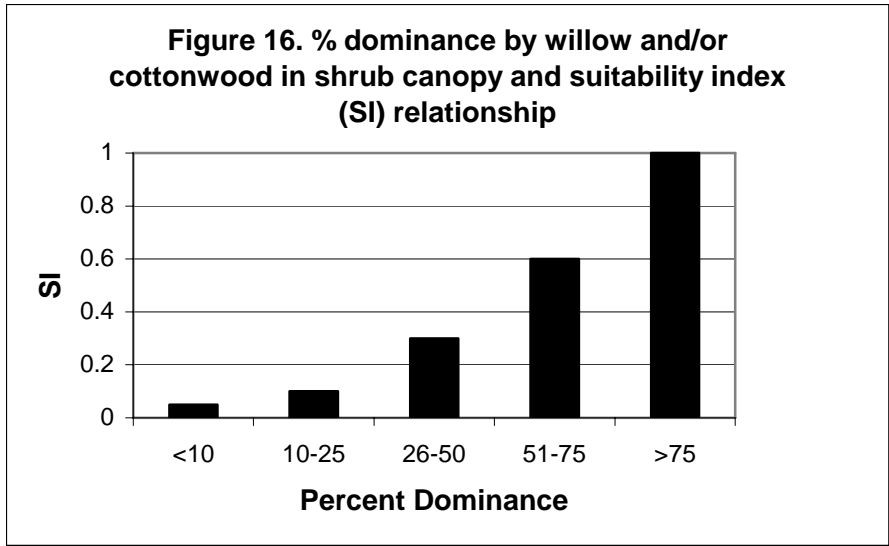


Figure 15. Cottonwood/willow dominance in tree canopy and suitability index (SI) relationship





Model application

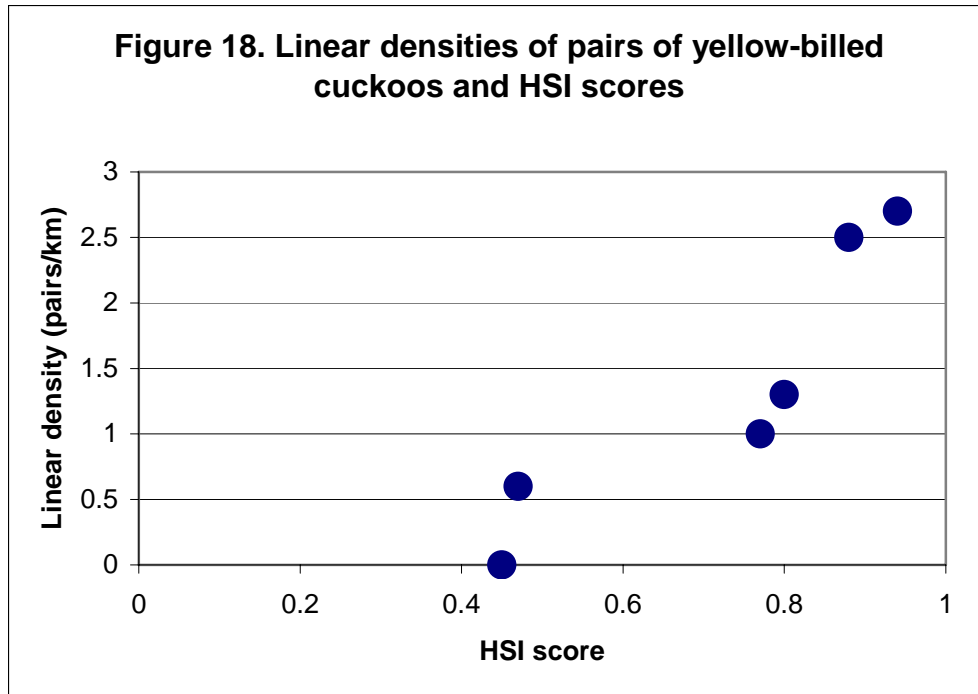
The eight variables described above will be combined into an index of the overall assessment of the habitat suitability (HSI) of a particular patch of riparian forest habitat using the following 8th root algorithm (to limit the HSI scores to between 0 and 1):

$$HSI = (V1 \times V2 \times V3 \times V4 \times V5 \times V6 \times V7 \times V8)^{1/8}$$

The HSI values obtained using this equation will range between 0 and 1 (lowest and highest estimates of suitability, respectively).

Field test results

The draft yellow-billed cuckoo HSI model was tested in the SPRNCA in areas of known yellow-billed cuckoo breeding density (unpublished data – M. Halterman, Bureau of Land Management). The results of the field test of the western yellow-billed cuckoo model are presented in Figure 18. These results show that the predictions of the HSI model regarding habitat suitability are generally accurate (if it is assumed that breeding density is a reflection of at least short term habitat quality). Thus the HSI model developed for this study is a reasonable predictor of breeding habitat quality for the study species.



Conclusions

Hitherto, HSI models have largely been utilized to quantify the quality of existing habitat for wildlife species, without reference to how that habitat may have been altered in the past or how it might be altered in the future. In this study, we are using HSI models as part of an integrated modeling approach to estimate the habitat quality gain or loss for a variety of indicator species due to future climate change and aquifer management decisions. In effect, the HSI models are being utilized as part of an ecological risk assessment (ERA), except that the stressors are not the traditional ERA contaminants but are climatic changes and land-use policies, and the outcomes are not toxicity or physiological impairment but changes in habitat quality and carrying capacity. Other reports in this volume detail how HSI might be used as part of traditional ERA, however, the experience of this project has identified a number of areas in which these models could be profitably integrated into the process. These include:

- Determining the extent that wildlife may actually use, or avoid, the site or contaminated portions thereof, and therefore, their exposure risk.

- Determining the extent to which existing wildlife habitat may be altered by site remediation.
- Focusing remediation on areas of lower habitat value.
- Evaluating the extent to which proposed remediation activities might incur net benefits (due to contamination being removed) or costs (due to loss of habitat) through remediation.

One of the main limitations of the HSI models that are currently available is that relatively few have been developed. Also, most of those that have been developed have not been field-tested. Nevertheless, the development and testing of HSI models for ERA (focussed on species that typically occur in such assessments) could be accomplished relatively easily and quickly.

References

Auble, G.T., J.M. Friedman and M.L. Scott. 1994. Relating riparian vegetation to present and future streamflows. *Ecological Applications*, 4:544-554.

Brand, G.J., S.R. Shifley, and L.F. Ohman. 1986. Linking wildlife and vegetation models to forecast the effects of management. In: J. Verner, M.L. Morrison, and C.J. Ralph (eds), *Wildlife 2000: modeling habitat relationships of terrestrial vertebrates*. University of Wisconsin Press, Madison, Wisconsin.

Finch, D.M. 1989. Habitat use and habitat overlap of riparian birds in three elevational zones. *Ecology*, 70:866-880.

Gaines, D. 1974. Review of the status of the Yellow-billed Cuckoo in California: Sacramento Valley populations. *Condor* 76:204-209.

Galbraith, H., K. LeJeune, and J. Lipton. 1996. Metal and Arsenic Impacts to Soils, Vegetation Communities, and Wildlife Habitat in Southwest Montana Uplands Contaminated by Smelter Emissions: I Field Evaluation. *Environmental Toxicology and Chemistry*. 14:1895-1903.

Galbraith, H. Kapustka, L. and M. Luxon. 2001. Incorporating habitat quality in ecological risk assessments: selecting assessment species, SETAC Annual Conference, Baltimore, MD, November, 2001.

Halterman, M.D. 1991. Distribution and habitat use of the Yellow-billed Cuckoo on the Sacramento River, California, 1987-1990. MS Thesis, California State University, Chico.

Hamilton, W.J., and M.E. Hamilton. 1965. Breeding characteristics of Yellow-billed Cuckoos in Arizona. *Proc. Calif. Acad. Sci.* 32:405-432.

Hughes, J.M. 1999. Yellow-billed cuckoo. *The Birds of North America. Life Histories for the 21st Century*. No. 418 (A. Poole and F. Gill, eds). The Birds of North America, Inc., Philadelphia, PA.

- Kaufman, K. 1996. Lives of North American Birds. Houghton Mifflin Company. Boston.
- Krueper, D. 1997. Annotated Checklist to the Birds of the Upper San Pedro River Valley. Unpublished report – Bureau of Land Management. San Pedro Riparian National Conservation Area.
- Laymon, S.A. and M.D. Halterman. 1987. Can the western subspecies of Yellow-billed Cuckoo be saved from extinction? *Western Birds* 18:19-25.
- Laymon, S.A., P.L. Williams, and M.D. Halterman. 1997. Breeding status of the yellow-billed cuckoo in the South Fork Kern River Valley, Kern County, California. Report to the USDA Forest Service Sequoia National Forest.
- LeJeune, K., H. Galbraith, J. Lipton, and L.A. Kapustka. 1996. Effects of Metals and Arsenic on Riparian Soils, Vegetation Communities, and Wildlife Habitat in Southwest Montana. *Ecotoxicology*. 5:297-312.
- Marshall, R.M. 2000. Population status on breeding grounds. In: *Status, Ecology, and Conservation of the Southwestern Willow Flycatcher*. USDA, Forest Service General Report RMRS-GTR-60.
- Roja, H.A., J. Bredehoeft, R. Lacewell, J. Price, J. Stromberg, G.A. Thomas. 1998. *Sustaining and enhancing riparian migratory bird habitat on the Upper San Pedro River*. Report to the Commission for Environmental Cooperation.
- Schamberger, M., and A. Farmer. 1978. The habitat evaluation procedures: their application in project planning and impact evaluation. *North American Natural Resources Conference*, 43:274-283.
- Sedgwick, J.A. 2000. Willow Flycatcher. *The Birds of North America. Life Histories for the 21st Century*. No. 533 (A. Poole and F. Gill, eds). The Birds of North America, Inc., Philadelphia, PA.
- Skaggs, R.W. 1996. Population size, breeding biology, and habitat of willow flycatchers in the Cliff-Gila Valley, New Mexico. New Mexico department of Fish and game Report.
- Sogge, M.K., and R.M. Marshall, 2000. A survey of current breeding habitats. In: *Status, Ecology, and Conservation of the Southwestern Willow Flycatcher*. USDA, Forest Service General Report RMRS-GTR-60.
- Stromberg, J.C. 1998. Dynamics of Fremont cottonwood (*Populus fremontii*) and saltcedar (*Tamarix chinensis*) populations along the San Pedro River, Arizona. *Journal of Arid Environments*, 40:133-155.
- Stromberg, J.C., R. Tiller, and B. Richter. 1996. Effects of groundwater decline on riparian vegetation of semiarid regions: the San Pedro, Arizona. *Ecological Applications*, 6:113-131.

U.S. Fish and Wildlife Service, 1997. Final determination of critical habitat for the southwestern willow flycatcher. Federal Register 62:39129-39146 (July 22, 1997).

U.S. Fish and Wildlife Service, 2001. Southwestern willow flycatcher – draft recovery plan. U.S. Fish and Wildlife Service, Albuquerque, New Mexico.

VEMAP, 1995. Vegetation/ecosystem modeling and analysis project: Comparing biogeography and biochemistry models in a continental-scale study of terrestrial ecosystem responses to climate change and CO₂ doubling. *Global Biogeochemical Cycles*, 9:407-437.

Vionnet, L.B., and T. Maddock. 1992. Modeling of ground-water flow and surface/ground-water interaction for the San Pedro Basin – Part 1- Mexican border to Fairbank, Arizona. Department of Hydrology and Water Resources, University of Arizona, Phoenix.

ATTACHMENT 5 – Hydrologic Modeling

Final Report

This document is a final report that describes the hydrologic work activities undertaken through a contract with the American Bird Conservancy on a project entitled “Potential Effects of Climate Change on Biodiversity and Riparian Wildlife Habitat of the Upper San Pedro River.” The work includes a series of tasks to modify an existing groundwater flow model developed under the Alternative Futures Study (Steinitz et al., 2003). The modifications have been made to allow the groundwater flow model to be used to evaluate climate change conditions on the groundwater system of the Upper San Pedro River Basin.

This document describes the study area, the existing Alternative Futures Model, the modifications made to that Alternative Futures model to enhance its use for climatic change evaluation, and the development of the software necessary to carry out the modifications (an example of the software documentation is included in an Appendix).

Ultimately, the major modeling packages were seasonalized but due to spatial scale issues the model was not fine enough within the riparian/river area to accurately predict depth to groundwater maps at the scale required for the avian analysis. To achieve this level of spatial detail, a new model (using the Alternative Futures model as its bases) is required. The development of a new model is beyond the scope of this project. However, work on this model is underway but lack of funding is delaying its completion. At the present time, the new groundwater flow model for climatic change evaluation could be ready for scenario application by August 2006.

Study Area

The San Pedro Basin is located in the northern portion of Sonora, Mexico and southeastern Arizona (Figure 1). The basin is traditionally divided into two sections, the

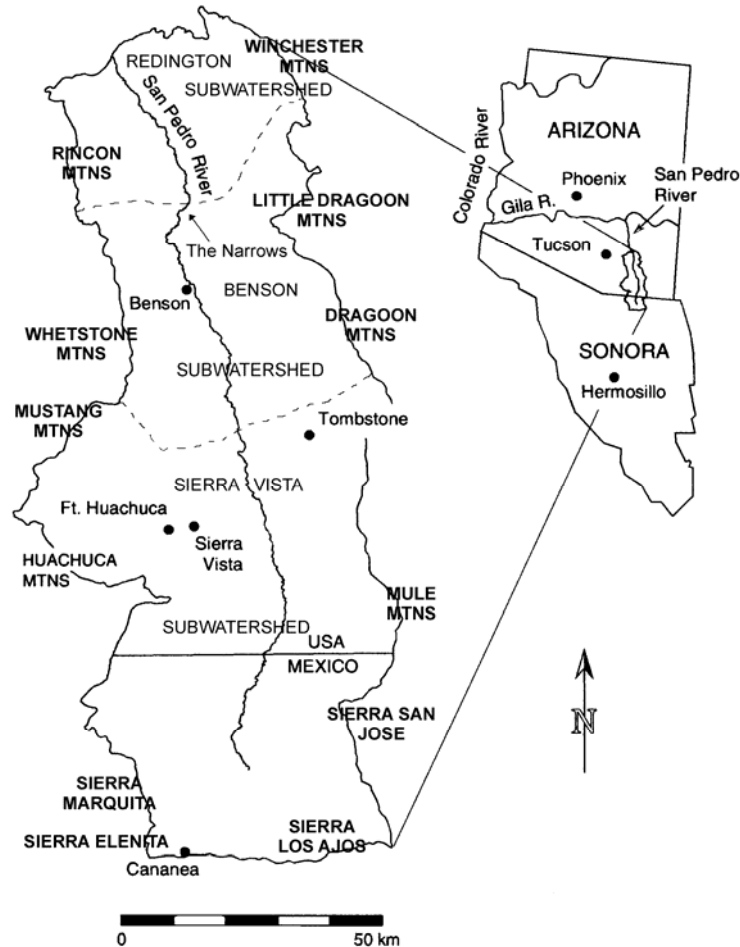


Figure 1. Location of study area (adapted from MacNish et al., 2000)

Upper and Lower San Pedro Basins, which are separated by the geologic formation known as “The Narrows.” This study includes the Upper San Pedro Basin and a portion of the Lower San Pedro Basin. The Upper San Pedro Basin is that portion of the watershed elevated above “The Narrows” extending southward into Mexico. The portion of the Lower San Pedro Basin included in the study extends north from “The Narrows” to the Redington stream gauge, also known as the Redington sub-basin.

The San Pedro River, beginning with its headwaters in northern Sonora, Mexico, near the city of Cananea, flows northwards from Mexico into the southeastern portion of Arizona, to its confluence with the Gila River. The river is perennial in many places and intermittent in others. A major tributary, the Babocomari River, is also perennial in places. A few small intermittent streams also contribute to the San Pedro River, but the majority of contributing drainages are ephemeral.

Existing Model

Only a portion of the watershed of Upper San Pedro Basin was modeled because a good portion of the basin is mountainous and composed of non-aquifer materials. In Figure 2 the red outlined area is the watershed boundary and the blue areas are the modeled areas.

Conceptual and Numerical Models

The groundwater model of the Upper San Pedro Basin (Goode and Maddock, 1999) required two developmental phases: the creation of a conceptual and numerical model.

Conceptual Model

The creation of the conceptual model was accomplished through the utilization of Geographic Information System (GIS) software, namely ArcView, used primarily to view and create point, line, and polygonal shapes. The conceptual model was conceived as having four layers.

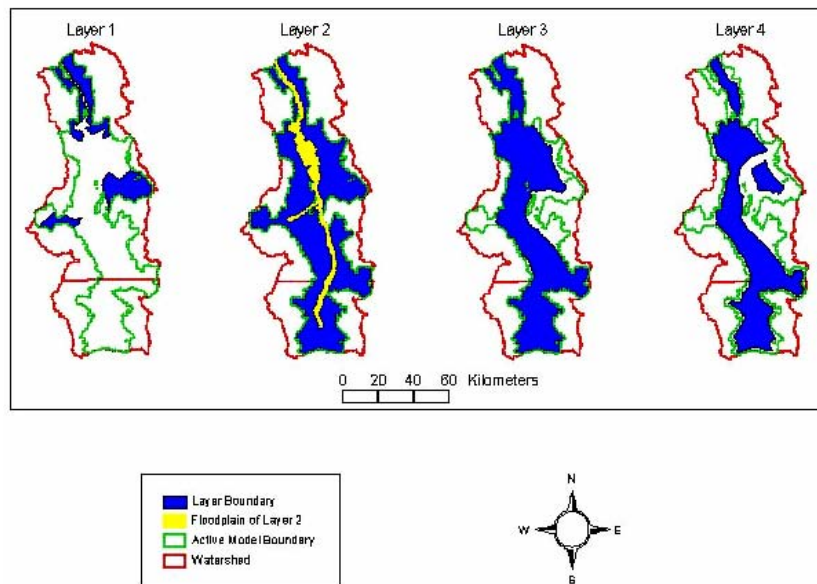


Figure 2. Conceptual model layers of the Upper San Pedro Basin

Layer 1 consisted of the hill slope areas away from riparian areas. Layer 2 includes both the Upper Basin fill of the regional aquifer, and the floodplain aquifer. Layer 3 loosely corresponds to the lower basin fill of the regional aquifer system. Layer 4 represents the consolidated sediments 305 meters (~1000 feet) below the ground surface.

Numerical Model

The creation of a numerical model was accomplished by the infusion of the conceptual model into a 3D finite difference grid used in MODFLOW groundwater software from the U.S. Geological Survey (Harbough and McDonald, 1996). MODFLOW computes the water mass balance and the hydraulic head (water level) for each cell within the grid. The infusion of the two models (conceptual and numerical) was allowed through the use of Department of Defense Groundwater Modeling System (GMS, 1999) software.

Stress Periods

The time period for groundwater modeling began with predevelopment conditions, or “steady state.” Steady state conditions were assumed to exist in 1940. The steady state was used as the initial condition for the subsequent transient analysis. The transient simulation applied historical and current information of pumping stresses to the system from 1940 to 1997 aggregated into twenty three stress periods (Table 1).

Table 1. Stress periods

Stress Period	Years
1	1940-41
2	1942-45
3	1946-50
4	1951-63
5	1964-66
6	1967
7	1968
8	1969-72
9	1973-76
10	1977
11	1978-85
12	1986
13	1987
14	1988
15	1989
16	1990
17	1991
18	1992
19	1993
20	1994
21	1995
22	1996
23	1997

Model Areal Recharge

The primary sources of areal recharge into the San Pedro Basin are from mountain front recharge and infiltration of irrigation waters.

Mountain Front Recharge

The groundwater recharge into the San Pedro Basin occurs along the mountain front. Mountain front recharge is the water that infiltrates into the zone of coarse alluvium that extends from the

base of the mountain into the basin. Water flows downward through the unsaturated zone in a broad band paralleling the mountain front. The width of the recharge zone is dependent on the nature and magnitude of the runoff from the consolidated rock areas. Infiltration takes place in the coarse grained unconsolidated sediments. For the Alternative Future study, an equation developed by Anderson et al (1992) was used to determine regional mountain front recharge amounts. Figure 3 present the distribution of precipitation to the watershed and rates of mountain front recharge assigned to the boundary cells of the groundwater flow model. Agricultural Recharge

Agricultural Recharge

Agriculture is a major water user in the basin, especially along the floodplain where water is used mostly for irrigation. The water used for irrigation may be applied in a number of ways including flood, furrow, and sprinkler methods. Each of these methods provides water for plant use as well as water evaporation. The water not consumed by plants and evaporation percolates through the soil and recharges the aquifer beneath. For the Alternative Future study, it was assumed that the ratio for consumed water to recharged water is 70:30, where 70% of irrigation water is consumed and 30% of the water is recharged into the underlying aquifer.

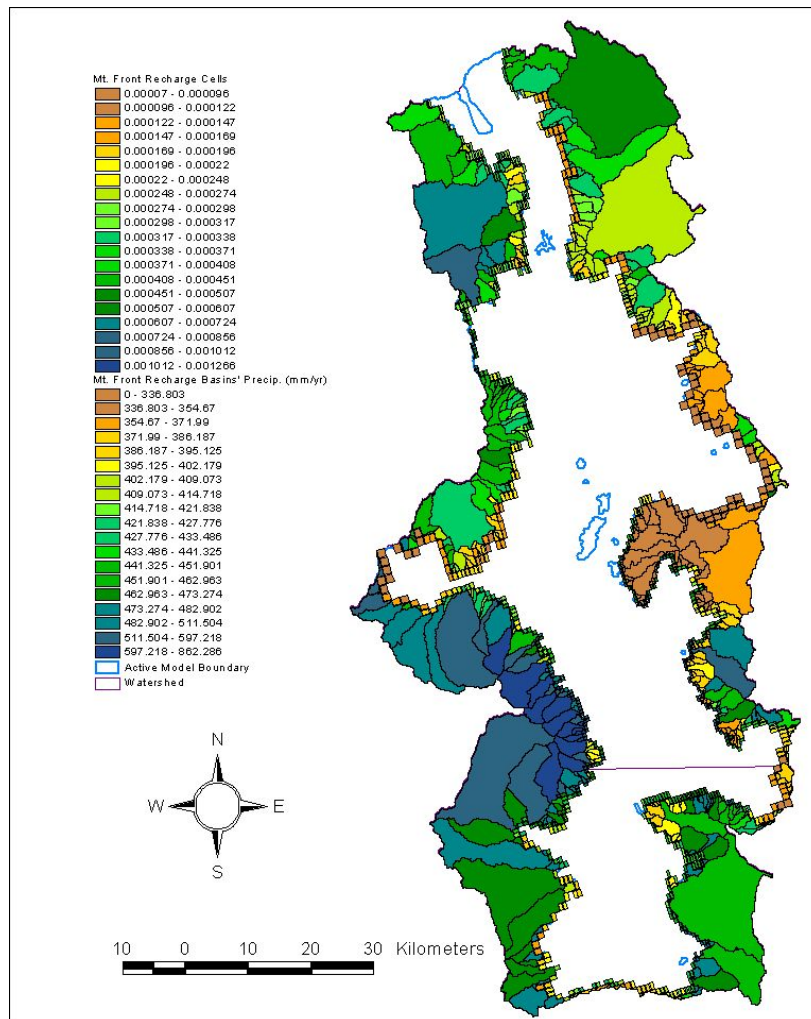


Figure 3. Mountain front recharge cells and contributing basins

For the Alternative Future study, the agricultural lands where recharge occurs were determined by 1997 satellite coverage information concerning land use. Agricultural lands are seen as polygons. These polygons include both currently active agricultural lands as well as those lying fallow.

A recharge rate for each polygon was computed using the pumping rate for all irrigation wells within 300 meters of a polygon. The pumping rate for all of these wells were added together and then divided by the area of their associated polygon. This irrigation rate was then reduced by 70%, leaving 30% of the total irrigation rate to be applied to the polygon as recharge.

For the Alternative Future study, all agricultural recharge cells were located in layer 2 of the model. Figure 4 shows the irrigation wells, agricultural polygons, and agricultural recharge cells and their respective locations within the Upper San Pedro Basin.

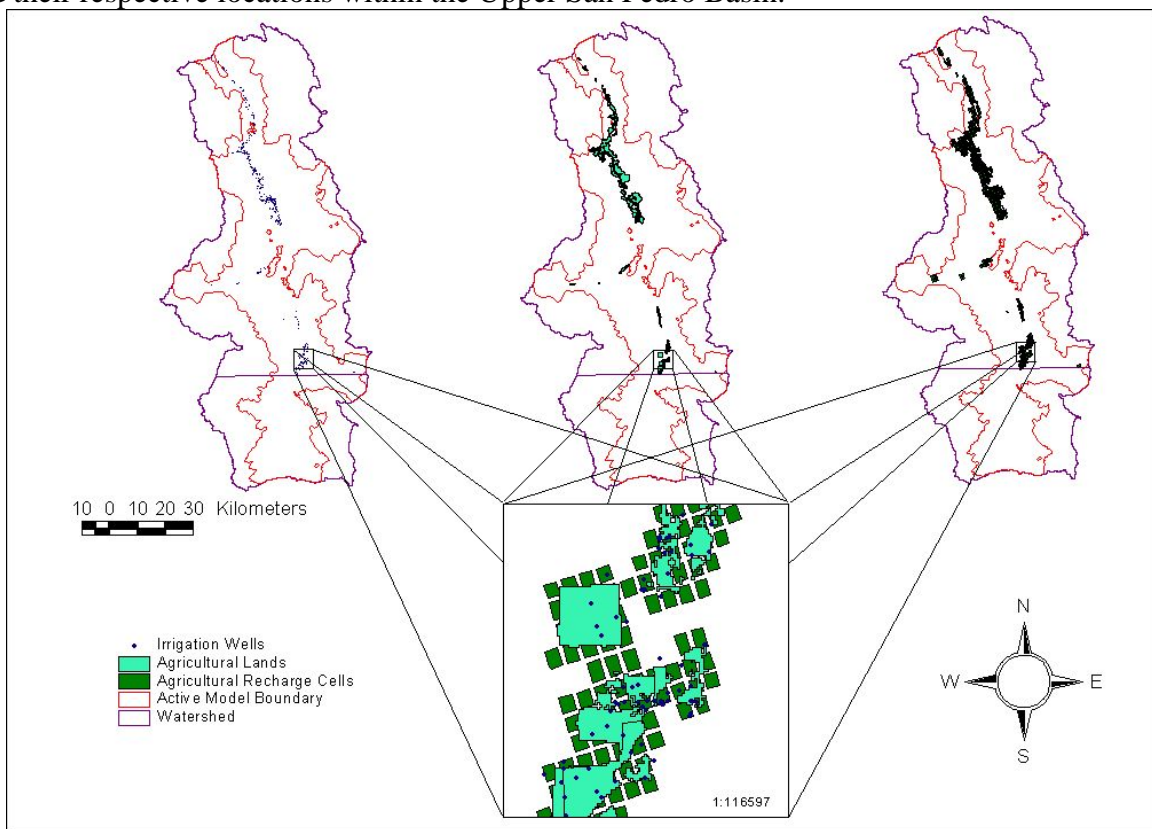


Figure 4. Agricultural recharge cells with associated pumping wells and recharge polygons

Riparian Evapotranspiration

Riparian areas exist along the floodplain of the San Pedro River. For the Alternative Future study, the areal extent of the riparian area was determined from satellite coverages of the San Pedro Basin from 1997 (the extent of the riparian area in 1940 is assumed to be the same as 1997). It is generally accepted that phreatophytes, groundwater-using plants, only exist along the floodplain due to the relatively shallow water table conditions. There are three types of phreatophytic vegetative cover,

significant to this study, defined within the riparian area: cottonwood-willow (*Populus fremontii* and *Salix gooddingii*), Mesquite bosque (*Prosopis velutina*), and a mixture of the two types. There are other types of vegetation suspected of using groundwater along the floodplain, namely tamarisk and saccaton grass, however they are not considered within Alternative Future study as they were deemed insignificant on the regional scale.

Figure 5 presents the distribution of riparian and agricultural vegetation for the Alternative Futures modeled area. The Alternative Future study assumed that evapotranspiration is modeled as an annual flux term. The evapotranspiration is treated as head-dependent in a piecewise linear fashion that starts at an extinction depth and monotonically approaches a maximum evapotranspiration rate (see Figure 6).

The evapotranspiration rates for each vegetative type were assigned to their respective polygons. Evapotranspiration rates were assigned to model cells based on the percentage of that polygon type contained within the model cell. The percentage was then multiplied by the evapotranspiration rate, giving the evapotranspiration rate for that particular cell. This process was completed for all cells containing any portion of riparian vegetation polygons. Figure 7 shows the model cells overlain by riparian vegetation polygons.

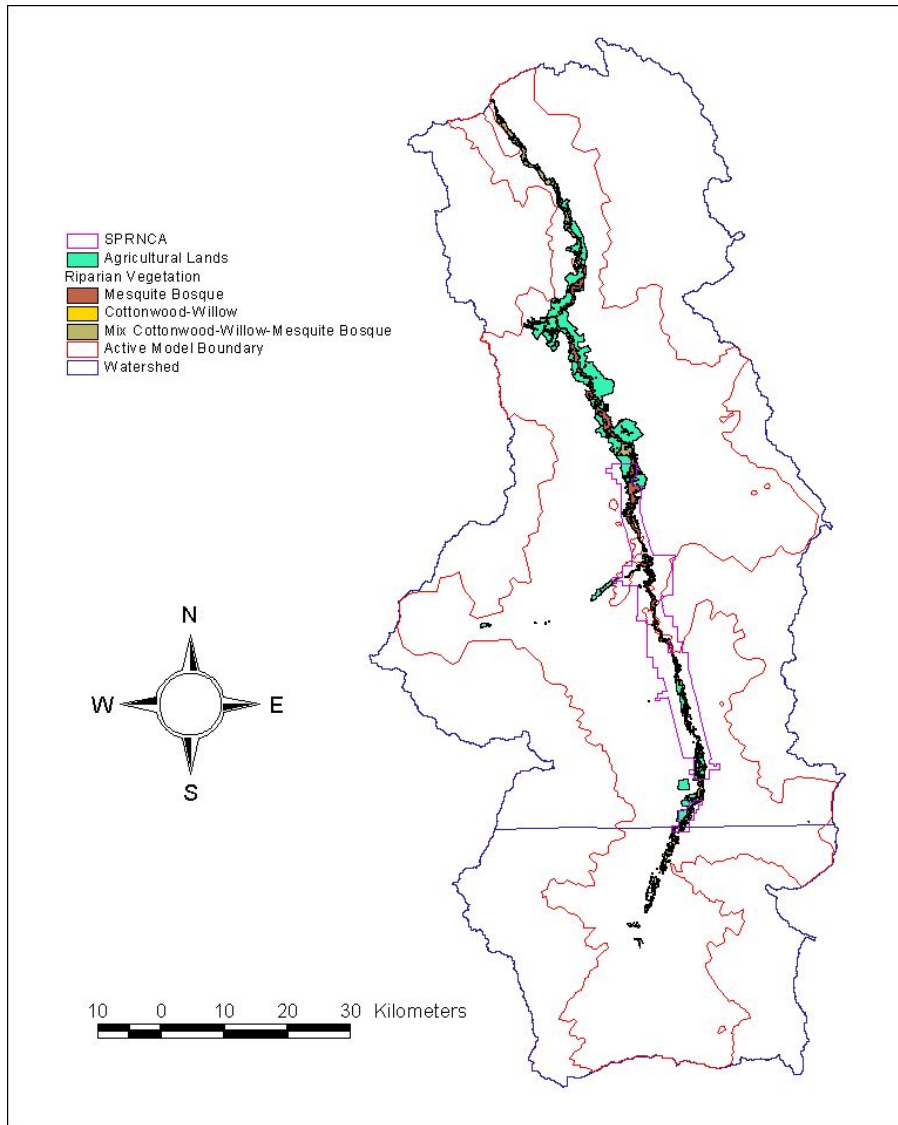


Figure 5. Riparian and agricultural areas

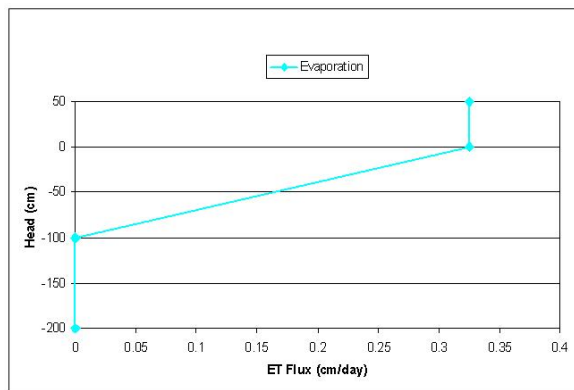


Figure 6. Traditional MODFLOW flux curve for evapotranspiration

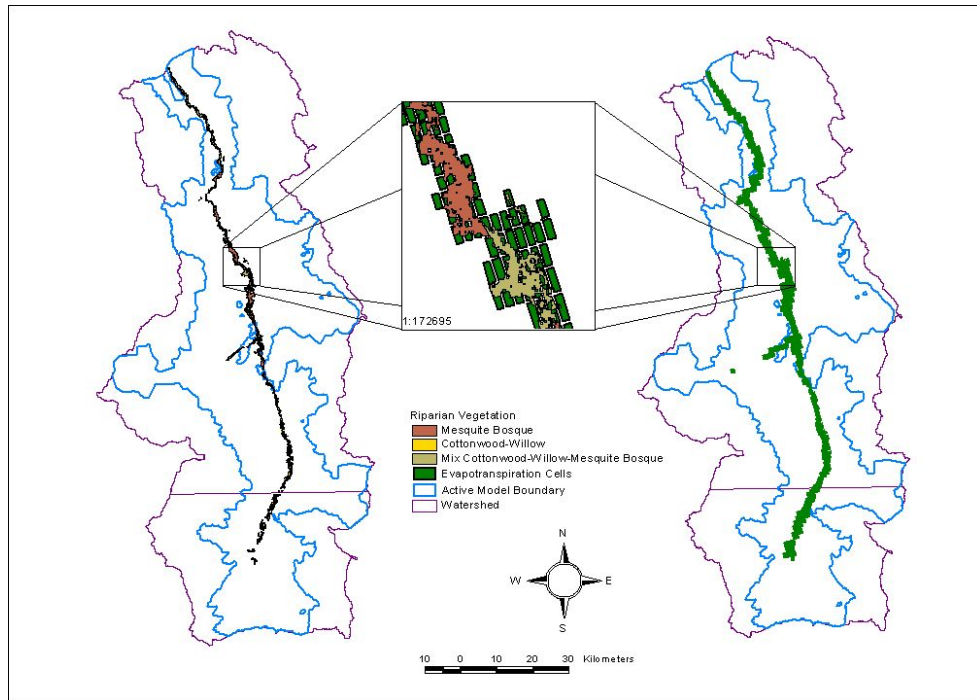


Figure 7. Evapotranspiration cells and associated riparian vegetation polygons

The actual extinction depth of the root zone in the riparian area is five meters, however, to compensate for the large cell size, an additional five meters was added to compensate for the averaging of vertical elevation variances within each cell. An extinction depth of ten meters was assigned for the riparian areas. Figure 8 gives a schematic representation of this procedure. This procedure increases the availability for water in the riparian area, but created an improper extinction depth that was never exceeded.

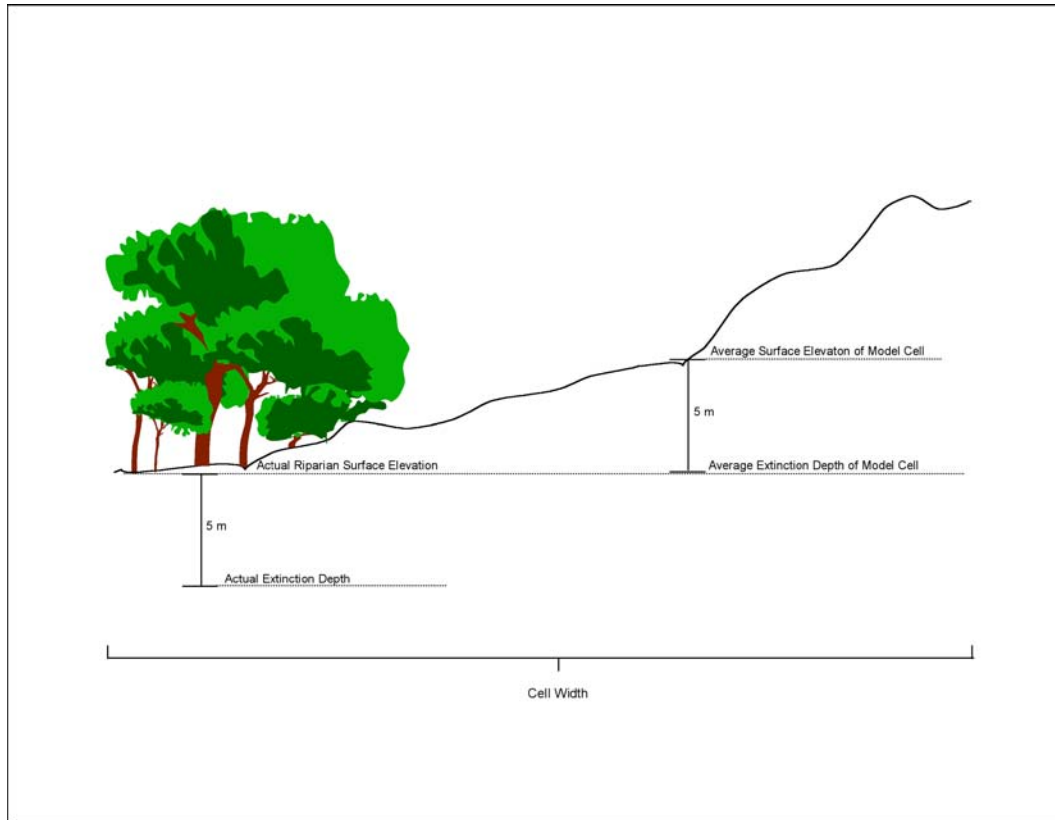


Figure 8. Adjustment of extinction depth for evapotranspiration cells

Groundwater Pumping

The distribution of groundwater pumped wells is presented in Figure 9. The different colored dots in the figure represent different water use types within the basin. The water use types used in the basin are stated below.

- **Public Supply Wells**
- **Irrigation Wells**
- **Domestic Wells**
- **Stock Wells**
- **Industrial Wells**
- **Commercial Wells**
- **Institutional Wells**

The pumping rates for all types of well were average annual values.

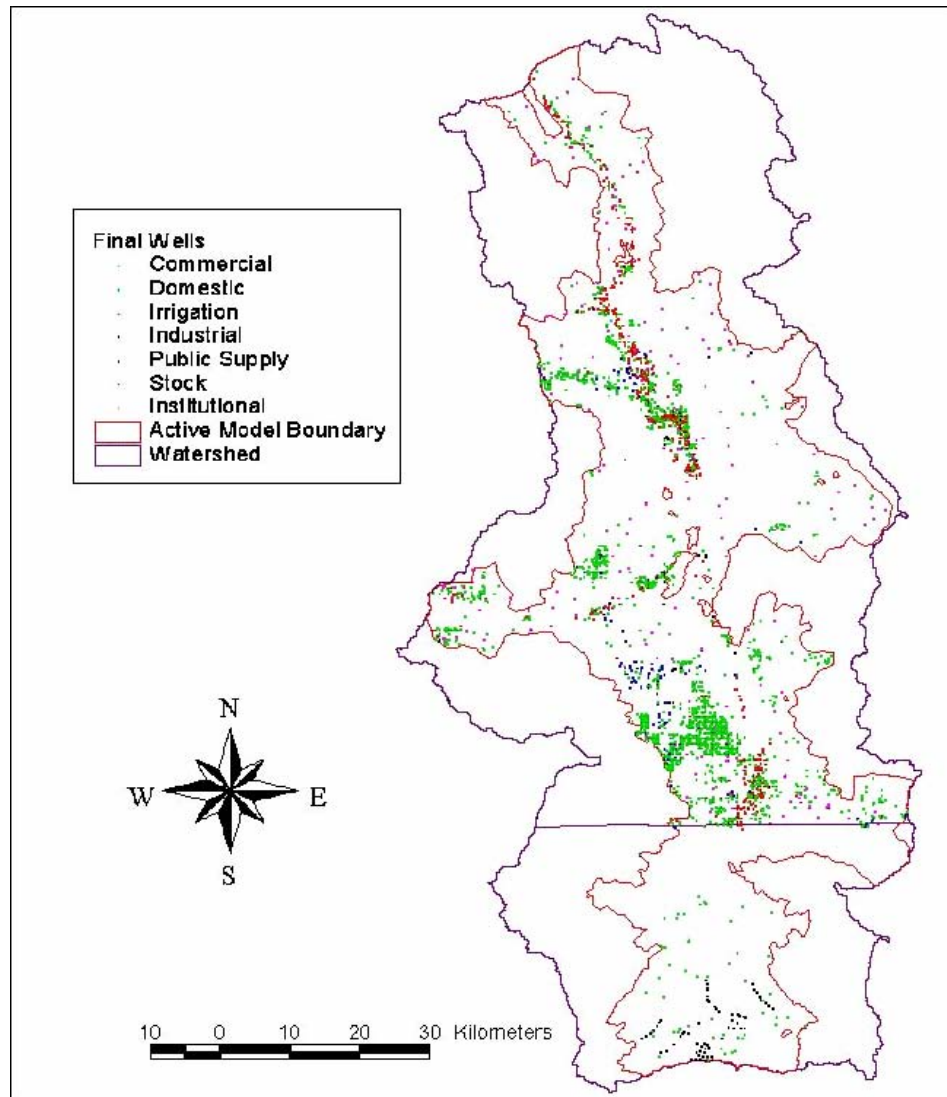


Figure 9. Distribution of well by type used for simulation

Modifications to Existing Model

Seasonalizing the annual groundwater model for the Upper San Pedro basin allows for a more accurate estimation of water budget, and better assessment of anthropogenic and climatic changes on riparian vegetation.

Seasonalization

Climate change can exhibit trends that produce long term variation in boundary conditions over the years, and/or by seasonal changes that redistribute the inflows or outflows of the boundary conditions within the annual cycle. The long term variations can be treated by trend analyses, however, to redistribute seasonal inflows and outflows, the model must be seasonal.

The Alternative model was not seasonal; instead, it was based on aggregated annual averages for stream base flow, evapotranspiration, mountain front recharge, and groundwater pumping. Examination of precipitation records indicates that the Upper San Pedro Basin has four seasons: rainy seasons in the summer and winter, and dry seasons in the fall and spring. Based on this information the annual Alternative futures model was converted into a four season model. The seasons are defined in table 2.

Table 2. Upper San Pedro groundwater model seasons

Season	Months
Spring	April - May
Summer	June - September
Fall	October - November
Winter	December - March

Seasonal values for stream base flow, and agricultural pumping were initially determined by factoring the annual-averaged volumes into seasonal averaged volume components based on local climatic conditions, and converting these components to multiplicative seasonal scale factors (Maddock and Vionnet, 1998). The product of the seasonal scale factor times the annual average rate produces the seasonal rate. Figures 10, 11 and 12 present the seasonal scale factors for streamflow and agricultural pumping.

The seasonal variations in base flow, evapotranspiration and agricultural groundwater pumping reoccur from year-to-year, and produce a wave like behavior. The lateral penetration of the wave is dampened within the porous media by an affect know as skin depth (Maddock and Vionnet, 1998) which is a function of hydraulic conductivity of the porous material. For most aquifer systems, short term waves like those produced by seasonal variation dampen out with in five to ten miles of the wave source. Because of the distance between where the mountain front recharge enters the Upper San Pedro Basin and the riparian areas is greater than ten miles, mountain front recharge does not affect the periodicity of the riparian unit and was not initially treated as being seasonal.

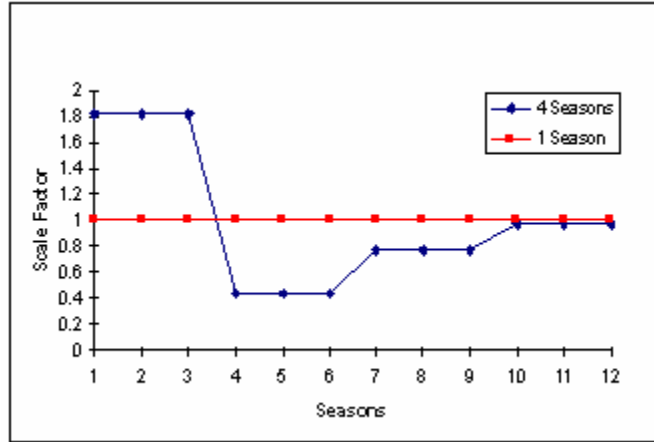


Figure 10. Four season scale factors for streamflow

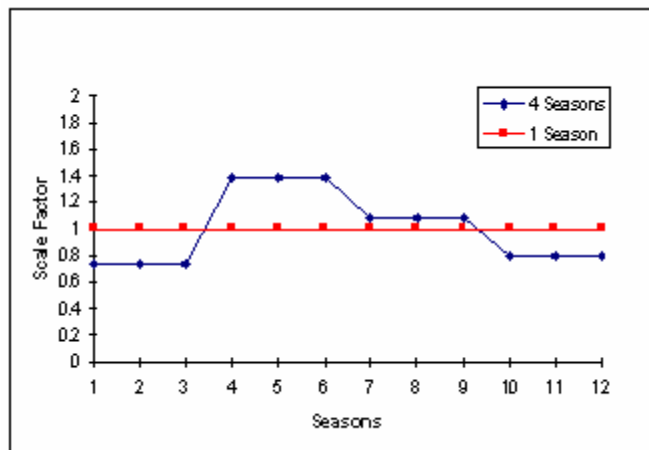


Figure 11. Four season scale factors for evapotranspiration

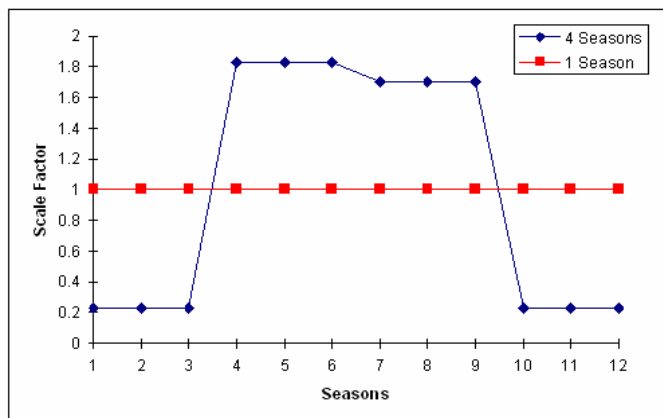


Figure 12. Four season scale factors for agricultural groundwater pumping

The climatic change of seasonal variation can be simulated by adjusting the scale factor curves under the constraint that the area under the readjusted curve is equal to the area under the one

season or annual curve. Increase in annual climatic condition is treated separately using trend analysis.

Steady Oscillatory

The predevelopment steady-state analysis performed in the Alternative Futures Study to serve as initial conditions for the transient analysis is no longer valid. In particular, the steady state analysis produces a single hydraulic head and mass balance for the numerical model's cells. Since there are four seasons, four initial states of the flow system are needed, one for each season. To determine the four initial states, we assumed that the natural recharge process vary through the four seasons, but repeat from year to year. A transient flow model is used to impose the four season period conditions over a large number of cycles. As the numerical model processes through the cycles, any non periodic portions diminish and the periodic solution becomes more dominant. When the non-periodic portions are absent, the seasonal heads and fluxes begin to repeat from cycle to cycle, a steady-oscillatory solution is said to be achieved.

For this project, a steady oscillatory solution was determined assuming periodic stream base flow, agricultural pumping and evapotranspiration. The first attempt at the steady oscillatory solution assumed the traditional MODFLOW approach to evapotranspiration described in a previous section of this report.

Modified Stress Periods

The starting point for analysis of climatic change is assumed to be the year 2000. The historical flow processes from the years 1940 through 2000 had to be simulated, because during this period of time, regardless of seasonalization, the Upper San Pedro Basin is in transient states due to the groundwater development. Therefore, a historical seasonal analysis was undertaken using the steady oscillatory solution for the seasonal initial condition. Thus the number of stress period jumped from 23 (which started in 1940 and ended in 1997) to 240 (four seasons from 1940 to 2000). The 240 stress period solution is used as the initial condition to the climatic change simulation.

Data Entry Programs

The data entry requirements for the climatic change groundwater flow model are horrendous and required development of a number of data entry software. These data entry software are called preprocessors. All of the preprocessors were developed within the Windows® environment. The preprocessor for evapotranspiration will be discussed in a later section.

PreProSTR

The first preprocessor to be developed was **PreProSTR**, a software that provides easy of data entry into the Stream-Aquifer Module of MODFLOW. In particular, the software allow the easy entering of periodic seasonal stream flow data and expedites the determination of oscillatory solutions, particularly since it may take as may as 400 cycles (1600 stress periods) to achieve a steady oscillatory solution.

PreProWEL

This software provides easy entry into the Well Module of MOFLOW. There are seven classifications of wells used by our study: Public Supply Wells, Irrigation Wells, Domestic Wells, Stock Wells, Industrial Wells, Commercial Wells, and Institutional Wells. In addition, any specified flux boundary condition is simulated by wells. The software categorizes the wells by type, and provides easy entry of location and amount of pumping. This software, like PreProSTR, allows the easy entering of periodic seasonal data and expedites the determination of oscillatory solutions.

PreProRCH

This software provides easy entry into the Recharge Module of MOFLOW. The application of water for agricultural will produce periodic recharge to the aquifer. The software provides easy entry of location and amount of recharge to the aquifer. This software, like PreProSTR and PreProWEL, allow the easy entering of periodic seasonal data and expedites the determination of oscillatory solutions.

Modifications of Evapotranspiration Module

Because riparian and wetland systems contain a disproportionate share of regional biodiversity and play a dominant role in the regional water and energy balance, if these ecologically significant systems are to be modeled, a MODFLOW package that properly reflects the eco-physiology of riparian and wetland ecosystems needed to be developed. Traditionally, the ET source term is treated as head-dependent in a piecewise linear fashion that starts at an extinction depth and monotonically approaches a maximum ET rate. While this quasi-linear relationship may hold true for evaporation, it does not accurately reflect the relationship between riparian transpiration and groundwater conditions. Furthermore, ET processes generally vary between plant types, making it necessary to determine variations by type. To improve the ability to determine riparian evapotranspiration and predict ecosystem response to changing environmental conditions, a Riparian ET (RIP-ET) package for MODFLOW-96 (Harbough and McDonald, 1996) was developed that attempts to simulate evapotranspiration from the water table that lies beneath riparian/wetland systems in a manner that reflects their ecology and physiology.

Plant Functional Groups

Riparian and wetland ecosystems are composed of a variety of plant types and species. The identification and use of plant functional groups can assist in reducing the enormous complexity of individual species and populations into a relatively small number of general recurrent patterns. This technique has emerged as a useful way to organize plant species that have similar impacts on ecosystem processes into manageable and meaningful categories (Williams et al., 1998). Plant functional groups are defined as non-phylogenetic groupings of plant species that exhibit similar responses to environmental conditions and have similar effects on the dominant ecosystem processes. In the Riparian ET package, plant functional groups are used to elucidate the interactive processes of plants (and plant ET) with groundwater conditions. The model is designed to be flexible, with the user determining which sets of plant functional groups are

appropriate for the simulation and geographic region of the riparian/wetland system to be modeled.

In the development of the Riparian ET Package, five basic functional groups are defined based on transpiration rates and processes, plant rooting depth, and drought tolerance. While the groups presented here are for semi-arid environments, the methodology can be applied universally. The generalized plant functional groups are: obligate wetland, shallow-rooted riparian, deep-rooted riparian, transitional riparian and bare ground/open water. The last category, while not a plant functional group, must be included to accurately model evaporation (non-transpiration) from the cell or active modeling area. The evapotranspiration rates and range of groundwater elevations over which these groups exist differ for each plant functional group.

Plant Functional Subgroups

Plant size and density also play roles in determining evapotranspiration rates. Large woody plants have different maximum rooting depths, hydraulic architecture and transpiration rates than smaller. Furthermore, areas with dense configurations of both woody and herbaceous plants may show increased transpiration rates compared to sparse configurations. Taken together, the plant functional group and plant size or density comprise a plant functional subgroup (PFSG). Examples of possible plant functional subgroups are: transitional riparian-large or wetlands-medium density. Table 3 presents the possible plant functional subgroups for this example. This table is by no means exhaustive and is meant to be illustrative.

Table 3. Subgroupings for plant functional groups, by size and density.

Plant Group	Size	Densities	Species Examples
Obligate Wetland	N/A	Low, medium, high	Cattail, Bulrush
Shallow-rooted Riparian	N/A	Low, medium, high	Curly dock, Cocklebur, Deer grass
Deep-rooted Riparian	Small, medium, large	Low, medium, high	Cottonwood, Willow, Mesquite (bosque)
Transitional Riparian	Small, medium, large	Low, medium, high	Walnut, Hackberry, Sacaton, Sycamore

Evapotranspiration rates and the range of groundwater elevations over which these groups exist differ for each plant functional group (Figure 13). Streamside riparian corridors typically consist of multiple plant functional subgroups, each reacting differently to the hydrologic conditions. A deeper water table may be ideal for a transitional riparian group, but near fatal to a wetland or herbaceous, shallow-rooted group. Similarly, a high water table conducive to a wetland group may drown out the trans-riparian. Even so, it is quite likely that a MODFLOW cell covering a riparian system will comprise a number of compatible plant functional groups. Thus, the evapotranspiration loss from a riparian/wetland system is dependent on the plant functional subgroups present and on the groundwater depth. Furthermore, as the region near the riparian system is urbanized, results of that development (such as increased groundwater pumping) may affect each group differently.

ET Flux Rate Curves

The ET rate per area is called the ET flux rate. Due to differences in sensitivity to water availability and rooting depth, ET flux rates in plant species and thus in the subgroups vary with groundwater depths. Based on a literature review, field measurements and researcher input, preliminary ET flux rate curves were developed for the basic set of plant functional groups (Figure 13), (Maddock and Baird, 2003). These curves provide the ET flux rate as a function of water table conditions (or hydraulic head).

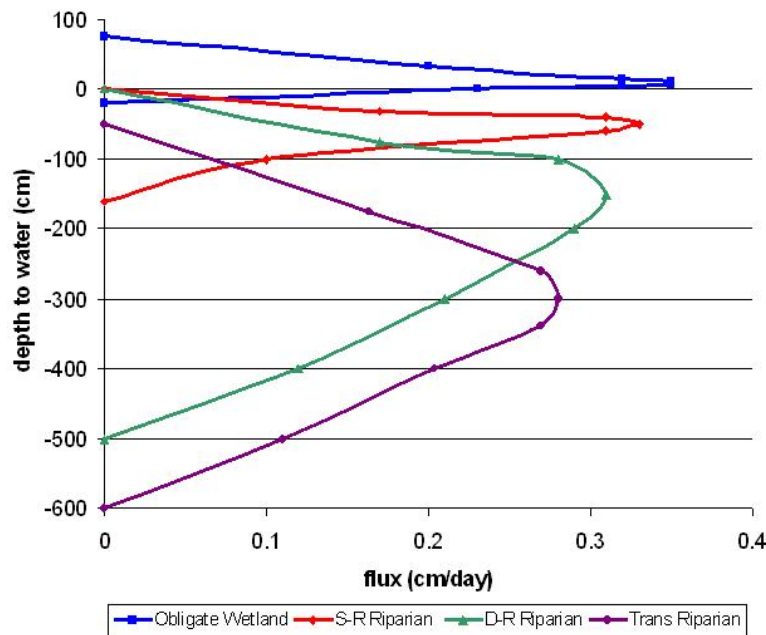


Figure 13. Average ET flux rate curves for four plant functional groups: obligate wetland, shallow rooted (S-R) riparian, deep-rooted (D-R) riparian and transitional (Trans) riparian.

Figure 14 illustrates a representative ET flux rate curve. For each plant functional subgroup there is a water table elevation or extinction depth elevation (H_{xd} in Figure 14) below which the roots can not obtain water and ET is nonexistent. When the water table rises and water becomes available to the root system, the ET rates rise until they reach an average maximum ET flux (R_{max}). At higher water table elevations, the root systems become oxygen deficient and ET rates decline until the plants die of anoxia. The water table elevation associated with plant death is the saturation extinction depth elevation (H_{sxd} in Figure 14). The decrease in ET flux rates resulting from high water tables has not been considered in previous MODFLOW Evapotranspiration Packages. Although Figure 14 shows H_{sxd} below the land surface elevation, it need not be; it can be at, or above the land surface elevation for some subgroups. For example, some wetland species may tolerate as much as a meter of standing water above the land surface.

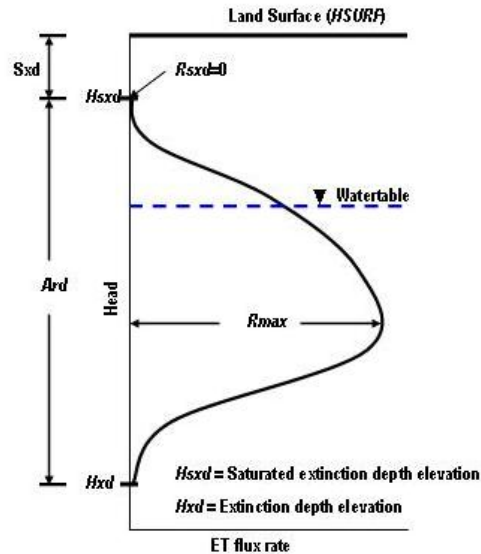


Figure 14. Generic ET flux rate curve

For the purpose of modeling, the distance between the two extinction depths is called the active root zone depth (Ard). The saturated extinction depth (Sxd) is measured with respect to the land surface elevation, HSURF. If H_{sxd} is below the land surface elevation, Sxd is positive; if it is above, Sxd is negative.

The maximum ET flux rate (R_{max}) is the measured average head-dependent ET rate, not a measured peak ET rate. For plants that have a saturation extinction depth, $R_{sxd} = 0$. For bare ground or open water, R_{sxd} equals the evaporation rates, and a shallow, more appropriate, extinction depth should be applied.

ET Flux Rate Curve Linear Interpolation

The Riparian ET Package does not use the continuous curve of Figure 14, but instead uses an approximation based on linear segments as illustrated in Figure 15. The ET flux rates reported in the literature are in various sets of units (e.g. cm/sec, feet/day, liters/day, kg/(m²-sec); the latter units need to be adjusted by the density of water to be dimensionally correct). To help alleviate problems that might occur with a particular choice of units, the curve segments are read into the RIP as dimensionless. They are converted during the simulation to units consistent with other MODFLOW packages based on the units of R_{max} and Ard . The R_{max} (L/T) and Ard (L) units must match the length and time units used elsewhere in the simulation. A more detail description of the package can be found in the user manual (Maddock and Baird, 2003).

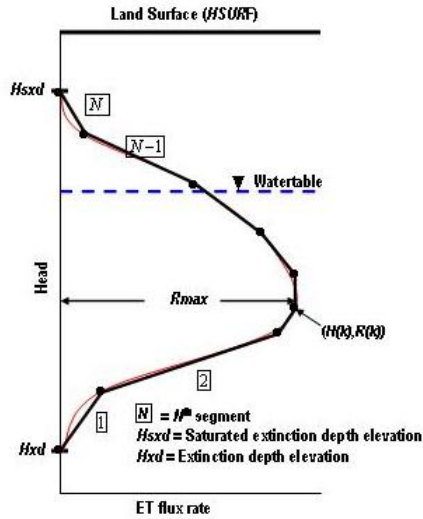


Figure 15. Hypothetical segmented ET flux curve.

Plant Coverage

The use of this package requires having information about the distribution of the plant functional subgroups within the active modeling areas. Not all of a MODFLOW cell is likely to contain active riparian or wetland habitat, nor is a cell likely to contain all of the possible plant functional subgroups. Furthermore, the amount of canopy coverage (or coverage of flux area) may change from cell to cell. The Riparian ET Package requires a fractional coverage for each of the plant functional subgroups present for a cell to simulate the mixture. For bare areas not supported by shallow water tables, ET rates can be excluded from the cell area or assigned flux rates of zero (e.g. the non-habitat area in Fig. 16). The fractional cover within a cell has three components: 1) fraction of active habitat, 2) fraction of plant functional subgroup, and 3) fraction of plant canopy or flux area.

Fraction of active habitat

The fraction of active habitat refers to the fraction of the cell that contains wetland or riparian habitat. Since cell sizes in MODFLOW may be quite large (e.g., square kilometer), only a fraction of cell will contain the habitat (see Figure 16). The fraction of active habitat (f_{AH}) is defined as

$$f_{AH} = \frac{\text{area of active habitat}}{\text{area of cell}}$$

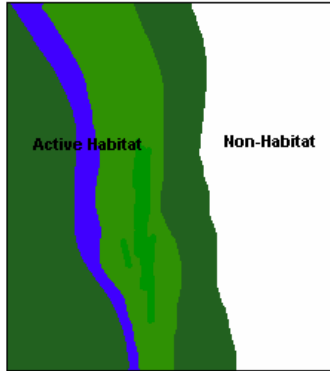


Figure 16. Area of active habitat in a cell

Fraction of a subgroup in the cell

The active habitat area in a cell may be composed of a variety of plant functional subgroups (see Figure 17). The fraction of i^{th} plant functional subgroup is defined as

$$fSG(i) = \frac{\text{area subgroup } i}{\text{area of active habitat}}$$

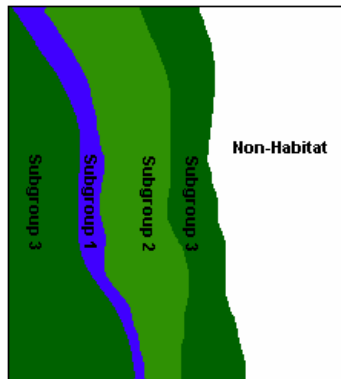


Figure 17. Area associated with plant functional subgroups

Fraction of plant canopy or flux area

Within any habitat, plant functional subgroup canopy or plant cover rarely equals 100 percent (Figure 18). Percent canopy or plant cover may vary, depending on habitat type and resource availability. To accurately determine ET the area of canopy cover or plant cover is required, as most flux rates are evaluated on canopy or plant cover. Note that for open water areas the fraction of plant coverage is equal to one. The fraction of plant coverage is defined as,

$$fPC(i) = \frac{\text{canopy area for subgroup } i}{\text{area subgroup } i}$$

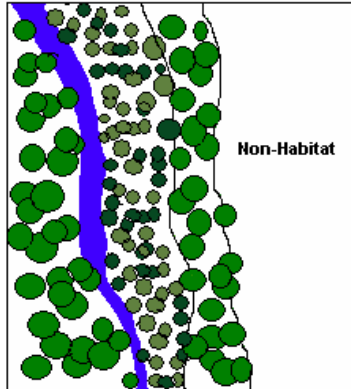


Figure 18. Area associated with canopy

Fractional Coverage

The fractional coverage of the i^{th} plant functional subgroup in a cell ($fCov(i)$) is given by the equation,

$$fCov(i) = fAH \times fSG(i) \times fPC(i)$$

The components of fractional cover can be determined using a combination of GIS techniques, aerial photography and ground verification. If a plant functional subgroup is not present in a cell, its fraction is entered as zero. Fractional cover has not been included as a variable in previous MODFLOW Evapotranspiration packages.

Land Surface Elevations

Within the model area, the land surface elevation ($HSURF$) will vary from cell to cell. It may also vary within a cell. The magnitude of this change is important. If $HSURF$ varies on the same order of magnitude as the extinction depths within the cell, the ET calculations will be affected. The user has an option of either assigning a single $HSURF$ for the average surface elevation of the cell, or assigning an $HSURF$ value for each plant functional group within a cell. If a single value of $HSURF$ is used, the average surface elevation of the cell is used to calculate Hxd (see Figure 8). If $HSURF$ is assigned for each plant functional subgroup, the actual surface elevation of the habitat within the cell is used to calculate Hxd . It should be noted that a MODFLOW model assumes that the water table elevation is constant within the cell boundary.

Status

The evapotranspiration package, which is called RIPET, is now complete and fully documented. The American Bird Conservancy has been supplied with copies of the software, examples and the documentation of this program.

Preprocessor for Evapotranspiration

The preprocessor for the new riparian evapotranspiration package is called PreRipET, and is a Windows program. PreRipET designed to help you create a riparian evapotranspiration module data file for MODFLOW-96 or MODFLOW-2000. The documentation for PreRipET is complete and included in Appendix A.

Evapotranspiration Package for the San Pedro

The original MODFLOW ET package is being replaced by RIP-ET to determine seasonal ET. Updating the ET package required two steps. The first task was to determine the appropriate plant functional groups for the river and then to develop ET curves for these groups. Based on data collected by ARS, our work, and literature values, seasonal curves were developed for the following plant functional groups:

- Cottonwood/Willow
- Mesquite
- Sacaton
- Saltcedar
- Emergent
- Evaporation (summer and winter).

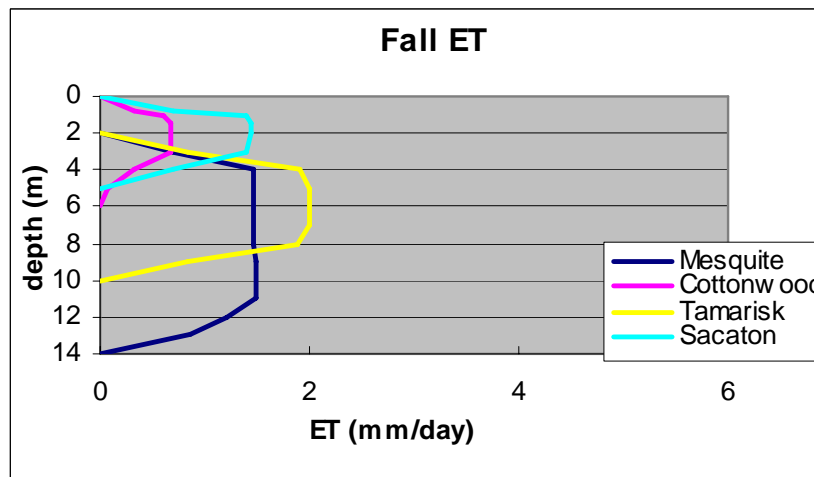
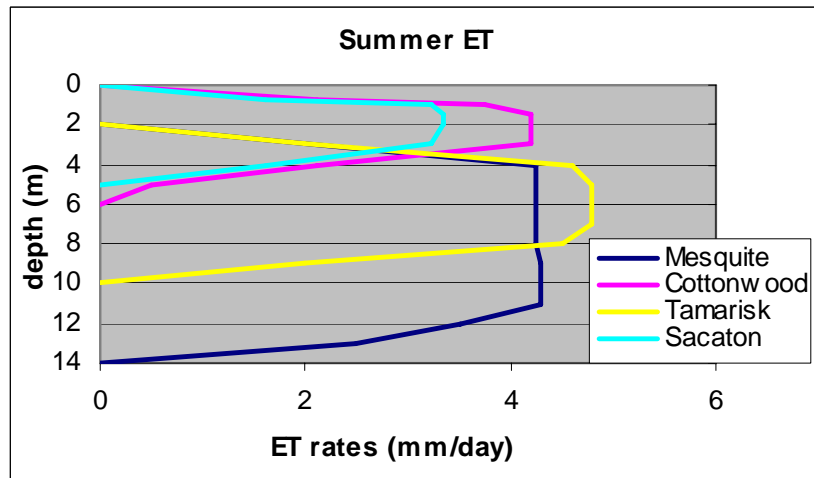
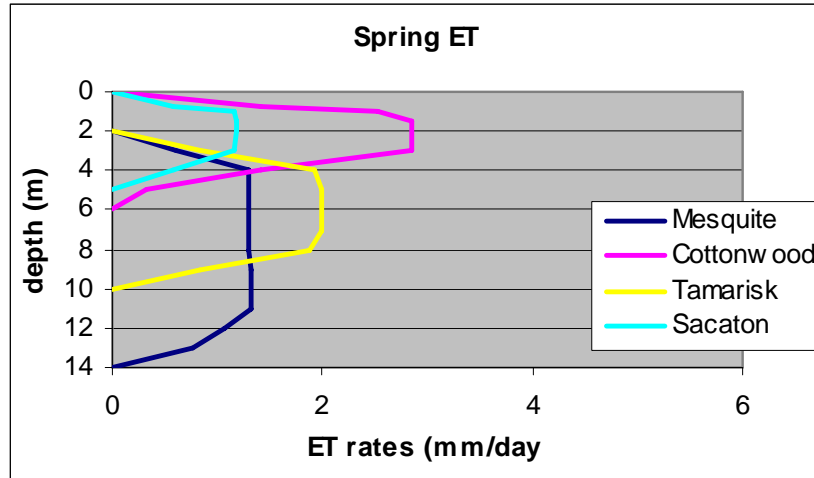
Table 4 shows the calculated seasonal ET rates (in mm/day) for these groups. Figures 19 through 21 illustrate their correlation with groundwater depth.

Table 4. Seasonal ET rates for Upper San Pedro plant functional groups.

	Mesquite	Cottonwood	Saltcedar	Sacaton	Evap	Emergent
	mm/day					
April/May	1.31	2.84	2.00	1.19	7.48	3.00
June/Sept	4.29	4.20	4.80	3.34	6.73	3.50
Oct/Nov	1.48	0.68	2.00	1.45	4.29	1.50
Dec/March	0.00	0.00	0.00	0.00	3.77	0.00

Next a vegetation map of the entire upper San Pedro basin needed to be created. This task turned out not to be a trivial undertaking. Within the SPRNCA relatively good mapping exists. However, the SPRNCA represents only a small portion of the basin. Maps from BLM, and EPA were merged with the SPRNCA maps to form one coverage file. The vegetation data associated with these coverages then needed to be converted into coverage data for the appropriate plant functional groups.

These tasks completed, PRE-RIP-ET was used to generate the new ET package. This package is complete and ready to be employed in the new model.



Figures 19-21. Seasonal transpiration rates for the dominate USP plant functional groups. Scales are equivalent to better show seasonal changes.

Additional Modifications

Prior to the seasonalization of this model, an improved version of the groundwater program, MODFLOW-2000 was released. To use MODFLOW-2000 the basic MODFLOW package needed to be modified, adding top and bottom elevations to the aquifer layers and converting various flow parameters such as transmissivity to conductance. These changes were completed and new layer coverages created and imported into MODFLOW. A MODFLOW-2000 steady-state oscillatory model with the new values was completed and the groundwater budget values checked against the original Goode and Maddock model and found to be in agreement. It was at this point that problems with scale and ground elevations were determined. The original model was completed with MODFLOW-96. In this version of MODFLOW, surface elevation aren't used, instead the program uses layer thickness. In converting to MODFLOW-2000, it became apparent that the stream surface elevations did not coincide with the ground surface elevations.

Using more recent 10 meter DEMs, river elevations were sampled and a new stream coverage file created. Additional river nodes were added for more accuracy. This file was imported into MODFLOW, the existing river diversion and tributaries were joined to the river and corrections made.

Monthly stream gage records were obtained for 1943 to present. The annual stream flow values used in the Goode and Maddock model were then allocated seasonally based on weighted averages of the monthly stream gage records. The original annual flow value and the subsequent seasonal flow values for San Pedro River and tributaries are illustrated in table 5.

Table 5. Annual and seasonal base flow values for San Pedro River and tributaries.

	Annual m ³ /day	April/May m ³ /day	June/Sept m ³ /day	Oct/Nov m ³ /day	Dec/March m ³ /day
Ash	978.6302	81.20417	2039.195	415.1892	645.7699
Hot Springs	6238.768	517.6766	12999.87	2646.831	4116.784
Paige	978.6302	81.20417	2039.195	415.1892	645.7699
San Pedro	0				
Babo	0				

A Problem of Scale

The finite difference grid applied to the original model region paralleled the predominant flow direction of the San Pedro River with finer resolution near the river and near high-density well occurrences. The cell sizes ranged from $2.26 \times 10^5 \text{ m}^2$ to $2.09 \times 10^6 \text{ m}^2$ in areal extent. The discretization of the system was developed for a different set of concerns and questions. These cell sizes were more than adequate for the original purpose of the model. To address the current concerns of avian nesting and depth to groundwater at very fine scales the model proved to be inadequate. To accurately predict depth to water at the scale required to answer these concerns a new model is required. Development of a new San Pedro model is beyond the scope and monetary support of this grant.

Due to the discrepancy between the model scale and the “question” scale, it was necessary to produce an interim product. Sufficient changes to the annual model were completed to make the resulting groundwater elevations comparable to the river elevations. The 2001 conditions were then projected into the future.

A New Seasonal Model

While the creation of the new model is beyond the scope of this project, the need for this model is obvious. Using the existing Goode and Maddock model as the bases, a new four season model with finer resolution is currently being constructed. To complete this model, new data sets need to be created for the mountain front recharge and well packages. The evapotranspiration and stream packages described above will be used with some modifications. A new steady oscillatory model must first be developed to establish the predevelopment state and then seasonal pumping can be applied.

Mountain Front Recharge

The annual model of the Upper San Pedro basin uses an average rainfall rate rather than rates that reflect the oscillation of the seasons. Riparian and wetland plants along the San Pedro are dependent upon groundwater levels remaining within the active root zone of the plant. Annual rates can mask the true seasonal water stress of the San Pedro’s riparian and wetland species. In addition to the temporal variation in rainfall, there is also a spatial variation to precipitation resulting in unequal distribution of recharge. Therefore, a new data set based on historical precipitation data was created rather than attempt to modify the existing data

PRISM precipitation data was obtained for the United States portion of the basin. Within the Mexican portion of the basin, original precipitation values were used as no other source was located. Using the CRWR-Prepro program the major streams and sub-basins within the Upper San Pedro basin were delineated. One of the most difficult parts of determining mountain front recharge is determining what portion of the precipitation actually recharges the groundwater aquifer. The Anderson equation is considered the best approach for the San Pedro. The original Anderson Equation is:

$$\text{Log } Q_{\text{recharge}} = - 1.40 + 0.98\text{Log } P$$

where P is the precipitation in excess of 8 inches per year. The equation is designed for large, high elevation basins.

Several methods of applying a seasonal factor to this equation were explored. The first was to determine the amount of excess precipitation that fell within the entire valley and allocate that amount based on weighted seasonal averages for each sub-basin. The second was to break down the minimal eight inches of precipitation into seasons by getting the inches per day ($8/365=.0219178$) and then multiplying by the number of days in each season. The seasonal equivalent to the annual 8 inches then becomes:

- Spring = 61 days > 1.337 inches/season or 3.400 cm/season
- Summer = 122 days >2.674 inches/season or 6.792 cm/season

- Fall = 61 days >1.337 inches/season or 3.400 cm/season
- Winter = 121.25 days >2.658 inches/season or 6.750 cm/season.

The two methods yielded similar total recharge volumes but different allocation patterns. The second method was chosen and resulted in recharge in the winter, summer and fall seasons. Seasonalizing the recharge resulted in a 12% reduction in recharge from the Goode and Maddock model. Using a Recharge program created by C. Drago the excess volume of water per individual sub-basins is applied to the adjacent MODFLOW recharge cells.

Well Package

Seasonalizing the well package is a major undertaking. Each of the various well types has a different seasonal pattern. Work on seasonalizing this package is still in the early stages.

Calibration

Once the new packages have been completed the seasonal model will need to be calibrated. At the present time, the new groundwater flow model for climatic change evaluation could be ready for scenario application by August 2006.

ATTACHMENT 6 – Evapotranspiration/Hydrology Publications

6.1 – Simulation riparian evapotranspiration: a new methodology and application for groundwater models



Simulating riparian evapotranspiration: a new methodology and application for groundwater models

Kathryn J. Baird*, Thomas Maddock III

University of Arizona, Tucson, AZ 85721, USA

Received 14 August 2003; revised 9 February 2005; accepted 11 February 2005

Abstract

This paper describes the development and application of a new methodology to simulate riparian and wetland evapotranspiration (ET) in groundwater models. Traditional approaches for modeling ET are based on quasi-linear relationship between ET flux rate and hydraulic head (groundwater elevation). The approach presented here uses multiple non-linear, segmented flux curves that reflect the ecophysiology of the plant species in these systems. Five plant functional groups (PFGs) based on water tolerance ranges and rooting depths are used to elucidate the interactive processes of plant transpiration with groundwater conditions. ET flux rate curves set the extinction and saturation extinction depths and define the group's ET flux rate as a function of water table depth relative to the ground surface. The calculated ET loss from a riparian or wetland system is dependent on the contributing area of each plant functional subgroup present and water table conditions. The new methodology requires a fractional coverage for each of the PFGs present within the groundwater model cell and allows for more accurate assignment of land surface elevations. Model results for a case-study show significant differences in predicted ET and subsequent depth to groundwater between the new and the traditional approaches. The development of physiologically based transpiration curves combined with the traditional linear curve for bare soil/open water results in more accurate determinations of riparian ET and improved basin scale water budgets. The use of PFGs in combination with the new RIP-ET package provides an explicit link between groundwater and riparian/wetland habitat conditions and offers an opportunity to better manage and restore riparian and wetland systems.

© 2005 Elsevier B.V. All rights reserved.

Keywords: Evapotranspiration; Groundwater modeling; Riparian; Wetlands

1. Introduction

Riparian ecosystems play a dominant role in regional water and energy balances and contain

a disproportionate share of biodiversity in arid and semi-arid areas (Naiman and Decamps, 1997; Williams et al., 1998; Horton et al., 2001). Being intricately coupled to ambient groundwater and surface water regimes, these systems are extremely sensitive to groundwater and surface water perturbations (Stromberg, 1993; Busch et al., 1992; Grimm et al., 1997). As early as 1927, Meinzer (1927) warned that changes in water table depth had the potential to

* Corresponding author. Tel.: +1 520 621 7115; fax: +1 520 621 1422.

E-mail addresses: kbaird@hwr.arizona.edu (K.J. Baird), maddock@hwr.arizona.edu (T. Maddock).

- McDonald, M.G., Harbaugh, A.W., 1996. Programmer's documentation for MODFLOW-96, an update to the US Geological Survey Modular Finite-difference Ground-Water Flow Model. US Geological Survey, Open-File Report 96-486.
- Meinzer, F.C., Andrade, J.L., Goldstein, G., Holbrook, N.M., Cavelier, J., Jackson, P., 1997. Control of transpiration from the upper canopy of a tropical forest: the role of stomatal layer and hydraulic architecture components. *Plant, Cell and Environment* 20, 1242–1252.
- Mienzer, O.E., 1927. Plants as indicators of groundwater, Water Supply Paper 577. United States Geological Survey, Washington, DC.
- Munoz-Reinoso, J.C., 2001. Vegetation changes and groundwater abstraction in SW Donana, Spain. *Journal of Hydrology* 242, 197–209.
- Nagler, P.L., Glen, E.P., Thompson, G.L., 2003. Comparison of transpiration rates among saltcedar, cottonwood and willow trees by sap flow and canopy temperature methods. *Agricultural and Forest Meteorology* 116, 73–89.
- Naiman, R.J., Decamps, H., 1997. The ecology of interfaces: riparian zones. *Annual Review of Ecology and Systematics* 28, 621–658.
- Oren, R., Phillips, N., Ewers, B.E., Pataki, D.E., Magonigal, J.P., 1999. Sap-flux-scaled transpiration responses to light, vapor pressure deficit, and leaf area reduction in a flooded *Taxodium distichum* forest. *Tree Physiology* 19, 337–347.
- Richter, B.D., Baumgartner, J.V., Wigington, R., Braun, D.P., 1997. How much water does a river need?. *Freshwater Biology* 37, 231–249.
- Schaeffer, S.M., Williams, D.G., Goodrich, D.C., 2000. Transpiration of cottonwood/willow forest estimated from sap flux. *Agricultural and Forest Meteorology* 105, 257–270.
- Scott, R.L., Shuttleworth, W.J., Goodrich, D.C., 1998. Water use of two dominant riparian vegetation communities in southeastern Arizona. In: Wood, E.F., Chehbouni, A.G., Goodrich, D.C., Seo, D.J., Zimmerman, J.R. (Eds.), *Proceedings from the Special Symposium on Hydrology*. American Meteorological Society, Boston, MA, pp. 43–48.
- Seo, D.J., Zimmerman, J.R. (Eds.), *Proceedings from the Special Symposium on Hydrology*. American Meteorological Society, Boston, MA, pp. 173–175.
- Shiple, B., Keddy, P.A., Moore, R.J., Lemky, K., 1989. Regeneration and establishment strategies of emergent macrophytes. *Journal of Ecology* 77, 1093–1110.
- Shuttleworth, W.J., 1991. Evaporation models in hydrology. In: Schmugge, T.J., André, J. (Eds.), *Land Surface Evaporation*. Springer, New York, pp. 93–120.
- Snyder, K.A., Williams, D.G., 2000. Water sources used by riparian trees varies among stream types on the San Pedro River, Arizona. *Agricultural and Forest Meteorology* 105, 227–240.
- Stromberg, J.C., 1993. Fremont cottonwood-Goodding willow riparian forests: a review of their ecology, threats, and recovery potential. *Journal of the Arizona-Nevada Academy of Science* 26 (3), 97–110.
- Stromberg, J.C., 2001. Restoration of riparian vegetation in the south-western United States: importance of flow regimes and fluvial dynamism. *Journal of Arid Environments* 49, 17–34.
- Stromberg, J.C., Tiller, R., Richter, B., 1996. Effects of groundwater decline on riparian vegetation of semiarid regions: the San Pedro, Arizona. *Ecological Applications* 6 (1), 113–131.
- Symstad, A.J., Siemann, E., Haarstad, J., 2000. An experimental test of the effect of plant functional group diversity on arthropod diversity. *OIKOS* 89, 243–253.
- Wever, L.A., Flanagan, L.B., Carlson, P.J., 2002. Seasonal and interannual variation in evapotranspiration, energy balance and surface conductance in a northern temperate grassland. *Agricultural and Forest Meteorology* 112, 31–49.
- Williams, D.G., Brunel, J.-P., Schaeffer, S.M., Snyder, K.A., 1998. Biotic controls over the functioning of desert riparian ecosystems. In: Wood, E.F., Chehbouni, A.G., Goodrich, D.C., Seo, D.J., Zimmerman, J.R. (Eds.), *Proceedings from the Special Symposium on Hydrology*. American Meteorological Society, Boston, MA, pp. 43–48.

alter the structure of riparian forests. Today we recognize that surface water regimes and groundwater depths can strongly influence species composition, community structure and biological diversity (Stromberg et al., 1996; Ehleringer and Dawson, 1992; Munoz-Reinoso, 2001). As the economic value of water increases and municipal, industrial, and agricultural uses are evaluated, the linkage between hydrological factors and riparian plant community function is becoming increasingly important (Busch et al., 1992).

Sustaining riparian and wetland ecosystem functions while providing a dependable water supply for urban, agricultural, and industrial needs is a major challenge. In the western United States, urban population growth is increasing the regional demand for water. For many Southwest communities, water from regional aquifers has become the largest single source of fresh water (Scott et al., 1998). The development of new water sources increasingly involves the conjunctive use of surface water and groundwater. The effects of excessive and unsustainable groundwater development may not be immediately evident but ultimately can and is threatening natural resources and causing serious user conflicts (Cooper et al., 2003).

One of the main objectives of modern land planning is the protection of ecologically valuable areas and land-use that supports integrated water management with special attention being given to the protection of groundwater systems, especially in wetland and riparian areas (Batelaan et al., 2003). Improving water management and developing reliable and accurate methods for preserving and restoring ecologically significant ecosystems has become critical. The use of regional groundwater models to quantify and simulate hydrologic conditions can be part of the solution, if accurate estimates of boundary conditions can be determined. One of the most critical but poorly quantified groundwater boundary condition is seasonal riparian evapotranspiration (Goodrich et al., 2000).

The complex hydrology and the narrow, heterogeneous nature of riparian zones hinder the understanding and quantification of the evapotranspiration (ET) processes from these systems (Hipps et al., 1998). Controlled by the interaction of both environmental and biological factors evapotranspiration influences such ecosystem parameters and processes

as soil moisture content, vegetation productivity, and ecosystem nutrient and water budgets (Jarvis and McNaughton, 1986; Wever et al., 2002). In tightly coupled riparian and wetland ecosystems or in groundwater systems where ET accounts for a substantial fraction of the water budget, the method used to model evapotranspiration can affect the calculated ET quantities, simulated depths to groundwater, and resulting interpretations regarding ecosystem dynamics (Banta, 2000). The problem is intensified in arid and semi-arid regions where anthropogenic-caused water shortages continue to threaten critical riparian and wetland ecosystems (Maddock et al., 1998).

In the present state of groundwater modeling, evapotranspiration is modeled as an annual source term (Maddock et al., 1998). This ET source term is treated as head dependent in a piecewise linear fashion that monotonically approaches a maximum ET rate. While this linear relationship may be appropriate for evaporation, it does not accurately reflect the relationship between riparian and wetland plant transpiration and groundwater conditions.

To improve the ability to determine riparian ET, estimate ecosystem water requirements, and predict riparian vegetation response to changing water availability, a new method for estimating riparian/wetland ET was developed. The new methodology simulates evapotranspiration from riparian/wetland systems in a manner that reflects the ecophysiology of the plant species in these systems. This approach is applied in a new seasonal ET package, a Riparian Evapotranspiration Package for MODFLOW-96 and MODFLOW-2000 (RIP-ET) (Maddock and Baird, 2003). Beyond introducing RIP-ET, the objectives of this paper are to describe the ways in which the new modeling method/package overcomes the limitations of traditional ET modeling approaches and discuss implications and applications of the model.

2. Modeling methods

2.1. Plant functional groups (PFGs)

Transpiration rates vary with groundwater depth and between plant species due to morphological differences in root architecture (including rooting depth)

and physiological sensitivities to water availability. Reductionist studies of selected species and specific environments are not likely to produce general predictive models given the vast numbers of species involved and the even greater range of possible environments. To develop such models, it is necessary to abandon taxonomic units and, instead, use attributes such as resource use patterns that are generalized beyond taxonomic boundaries (Shipley et al., 1989; Hills et al., 1994).

Plant functional groups are non-phylogenetic groupings of plant species that exhibit similar responses to environmental conditions and have similar effects on the dominant ecosystem processes (Lavorel et al., 1997). Identifying and using plant functional groups can assist in reducing the enormous complexity of individual species and populations, and has emerged as a useful way to organize plant species into meaningful yet manageable categories (Leishman and Westoby, 1992; Williams et al., 1998).

For purposes of this analysis and in the development of RIP-ET, plant functional groups are used to elucidate the interactive processes of plant (and plant ET) with groundwater conditions. Four basic plant functional groups are defined based on transpiration rates, plant rooting depths, and the upper and lower range of seasonal groundwater tolerance. These groups are obligate wetland, shallow-rooted riparian, deep-rooted riparian, and transitional riparian. A fifth group, bare ground/open water, is included to model the evaporation portion of ET. In the RIP-ET package, the user determines the suite of plant functional groups appropriate for the simulation and geographic region of the riparian/wetland system to be modeled. While the functional groups presented here are relevant for semi-arid environments, the methodology can be applied universally.

The first plant functional group, obligate wetland, contains plants that require saturated soil conditions or standing water. Most species in this category are herbaceous, generally with shallow root systems. In the southwestern United States, species such as *Typha* spp. (cattail), *Scirpus* spp. (bulrush) and *Juncus* spp. (rushes) typify this group.

Herbaceous riparian species such as *Rumex crispus* (curly dock), *Muhlenbergia rigens* (deer grass), *Xanthium* sp. (cocklebur) and *Mimulus guttatus* (monkey flower) comprise the shallow-rooted riparian

plant functional group. Species in this functional group require a shallow groundwater table and, like the deep-rooted riparian species, use groundwater as their dominant water source. At the same time, these species have limited tolerance for extended periods of saturated soil conditions. In areas receiving significant amounts of summer rainfall, it may be useful to differentiate perennial species from annual species that may be relying on flood water as their major water source.

The deep-rooted riparian group contains drought-intolerant phreatophytes such as *Populus* spp. (cottonwoods), and *Salix* spp. (willows) that rely primarily on shallow groundwater for establishment, growth and transpiration (Busch et al., 1992; Stromberg, 1993; Snyder and Williams, 2000). In some studies, multiple deep-rooted riparian PFGs may be useful, depending upon the suite of species present. This would allow distinction between the more deeply-rooted species, such as *Prosopis velutina* (bosque mesquite trees), from the less deeply-rooted cottonwood and willow trees. Some species in this category may have the ability to escape flooded conditions with temporary dormancy. However, generally species in this group have limited seasonal tolerance for extended seasonal saturated soil conditions.

The last plant functional group, transitional (or facultative) riparian, have water requirements that exceed those of the surrounding upland environment but do not require as shallow of water table as the preceding group. These species often grow along the outer edges of perennial riparian systems or along ephemeral streams supported by perched groundwater tables. Species in this category may include *Sambucus* sp. (elderberry), *Juglans* spp. (walnut), *Celtis* sp. (hackberry) and *Sporobolus wrightii* (sacaton).

2.2. Plant functional subgroups (PFGs)

In modeling evapotranspiration from an area, plant size and/or stand density may also play a role in determining transpiration rates. Large woody plants have different maximum rooting depths, hydraulic architecture and transpiration rates than smaller trees (Meinzer et al., 1997). Furthermore, areas with a dense cover of woody and herbaceous plants may have higher transpiration rates than sparsely covered areas. Taken together, the plant functional group,

Table 1
Illustrative plant functional subgroups composed of PFG, size and density

Plant group	Plant size	Densities	Species examples
Obligate wetland	N/A	Low, medium, high	Cattail, bulrush
Shallow-rooted riparian	N/A	Low, medium, high	Curly dock, cocklebur
Deep-rooted riparian	Small, medium, large	Low, medium, high	Cottonwood, willow, mesquite (bosque)
Transitional riparian	Small, medium, large	Low, medium, high	Walnut, hackberry, elderberry

and plant size or density defines a plant functional subgroup (PFG). Examples of possible plant functional subgroups are presented in Table 1.

Evapotranspiration rates and the range of groundwater elevations over which these groups exist differ for each plant functional subgroup. Most riparian corridors are composed of a combination of plant functional subgroups with different hydrologic requirements and ET rates. Thus, evapotranspiration from a riparian/wetland system is determined by the combination of plant functional subgroups present and the local, ambient groundwater depth.

2.3. Traditional modeling approaches

The traditional approach to modeling ET processes in a groundwater model (such as MODFLOW (McDonald and Harbaugh, 1988, 1996)) assumes a piecewise linear relationship between the ET flux rate and hydraulic head (Fig. 1). Here, if the water table is below the model extinction depth, H_{xd} , the ET rate is assumed to be zero. If on the other hand, the groundwater level is at or above a maximum elevation, H_{max} , the ET rate is assumed to be constant at the maximum rate or R_{max} . The distance between H_{xd} and H_{max} is called the extinction depth, d . Between H_{xd} and H_{max} , the ET rate is assumed to vary linearly with hydraulic head with a slope of R_{max}/d . In ETS1, an ET package for MODFLOW 2000, Banta (2000) replaces the linear slope with a segmented function (Fig. 1). This function allows for some flexibility but still assumes a constant R_{max} above the maximum ET surface elevation (generally assumed to be land surface).

These two approaches are problematic in several ways. First, a single ET curve is assumed to represent all vegetated conditions present in a cell or the active model area. Secondly, no allowance is made for a reduction in ET due to exceedance of the upper water

tolerance of the plant. Third, current methodologies apply a single flux rate to the entire area of the designated cell not allowing for fractional habitat coverage. And last, a single surface elevation is assigned to the entire cell despite the high surface variability characteristic of many riparian systems.

By developing new transpiration curves, the modeling approach presented in this paper allows for variability in vegetative conditions, the reduction in transpiration with elevated water tables, and separate representation of evaporation from transpiration. Furthermore, based on the types and coverage of

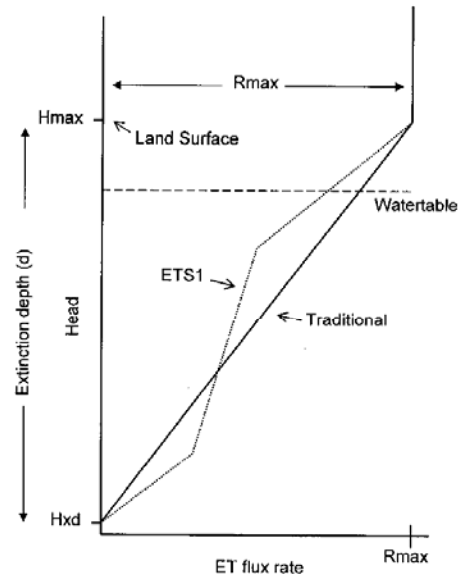


Fig. 1. Traditional linear (MODFLOW 96) and ETS1 segmented function (MODFLOW 2000) ET curves. H_{xd} , extinction depth elevation; d , extinction depth; R_{max} , maximum ET rate; H_{max} , maximum ET surface elevation.

plant functional subgroups present in the cell, multiple ET curves and surface elevations can be applied in a single model cell.

2.4. Development of new ET curves

Transpiration rates in plants depend upon external atmospheric conditions such as incoming solar radiation, wind speed and vapor pressure deficit, on soil water status, and on internal factors such as tree physiological and biometrical conditions (Bosveld and Bouten, 2001). When soil moisture conditions are not limiting, meteorological and vegetation conditions dominate the ET process (Shuttleworth, 1991). However in semi-arid and arid environments where potential ET is greater than precipitation, ET is thought to be limited by soil moisture (Kurc and Small, 2004). Each seasonal ET curve developed for use in RIP-ET represents a set averaged climate condition. This can vary from a single annualized ET average to four or more specific seasonal curves for each PFSG depending upon the model time step. Since, RIP-ET focuses on the link between groundwater and ET, the researcher or modeler must deal with climatic changes external to the model by creating a set of curves for each condition or season.

The first step in developing new transpiration-groundwater curves is to decouple the physical process of evaporation and from the biophysical process of transpiration and then define a generalized curve shape that simulates the response of plants to different groundwater elevations (Fig. 2). For each plant functional subgroup, there is an extinction depth elevation (Hxd) or water table elevation below which the roots are unable to obtain water and ET is zero. As the water table rises, water becomes available to the root system and ET rates increase until a maximum average ET flux (Rmax) is reached. This maximum ET flux rate is the measured or estimated maximum average daily ET rate, not the peak daily ET flux rate.

At higher water table elevations, the root systems in plants other than obligate wetland species, become oxygen deficient and ET rates decline until the plants die of anoxia. In obligate wetland plants, the upper limit of water depth tolerance is determined by additional factors such as light availability. The water table elevation associated with plant death is the saturated extinction depth elevation (Hsxd).

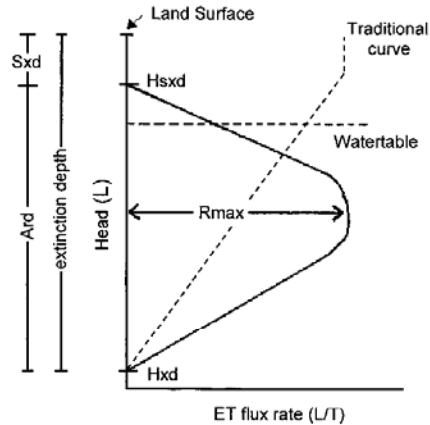


Fig. 2. Generic ET flux rate curve for a plant functional group in RIP-ET. Sxd, saturated extinction depth (L); Ard, active rooting depth (L); Hsxd, saturation extinction depth elevation; Hxd, extinction depth elevation; HSURF, land surface elevation; Rmax, maximum ET rate.

Although Fig. 2 shows Hsxd to be below the land surface elevation, it need not be. It can be at, or even above, the ground surface elevation as some wetland species tolerate as much as a meter of standing water.

The distance between the two extinction depths is called the active root zone depth (Ard). The saturated extinction depth (Sxd) is the distance [L] between the saturated extinction depth elevation and the surface. If Sxd is at or below ground surface, Ard represents the physical rooting zone of the representative plants. If Sxd is above the land surface, Ard is the physical root zone plus the depth of standing water. For modeling purposes, the relationship between the flux rates and water table levels need to be defined as depths [L] or distances relative to the land surface (HSURF). The elevations (Hsxd and Hxd) are then calculated within the program based on the specific land surface elevations inputs.

By definition, the ET flux rates at saturated extinction depth and at extinction depth are zero. Extinction depths can be approximated from the maximum rooting depth of the species within the PFSG in question. These values can be obtained through field studies, literature research or a combination of both. At the other extreme, saturated

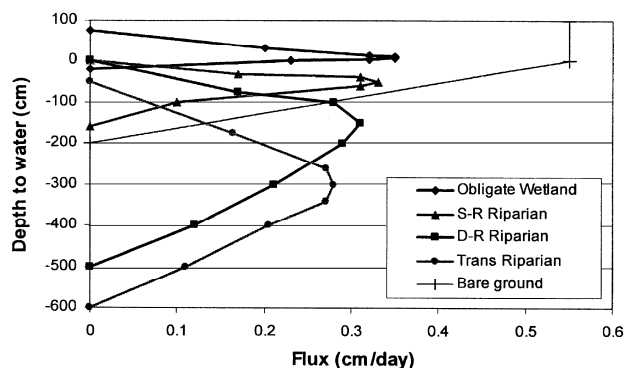


Fig. 3. Mean daily ET canopy flux (cm/day) curves for PFGs. Positive numbers denote standing water.

extinction depths are based on correlations between plant species occurrences and water table elevations. While these values may not be precise they provide a good starting point by representing the upper and lower range of water tolerance for the species in question.

The shape of the transpiration curves between the two extremes is again determined from measured or estimated transpiration rates associated with specific water table depths for each PFG. Due to differences in sensitivity to water availability and rooting depth, transpiration flux rates in plant species and thus in the subgroups vary with groundwater depths. Unfortunately, there are few estimates of the magnitude or the spatial and temporal heterogeneity of transpiration fluxes in arid and semi-arid riparian species (Schaeffer et al., 2000).

Based on literature review, field measurements and researcher input, summer ET flux rate curves were developed for the basic plant functional groups (Fig. 3). Sap flow measurements were used to quantify transpiration in 42 individual willow and cottonwood trees over the course of three growing seasons: two at the South Fork Kern River in central California and one in the San Pedro River basin in southern Arizona. The trees were divided up into the following four DBH size classes: <15, 15–30, 30–45, and >45 cm. Simultaneous groundwater depths and meteorological parameters were measured at both locations. In the San Pedro, a controlled pumping experiment was performed specifically to measure the response of tree

transpiration to declining water tables. Data from both sites formed the basis for this set of seasonal deep-rooted riparian ET curves (Fig. 4). While these curves are based on the best available data, they should be regarded as preliminary and would benefit from refinement. The authors invite other researchers to provide input and data towards developing additional curves and/or refining these curves.

The traditional ET curve, illustrated in Fig. 2, is now used exclusively to model evaporation from bare soil or open water. Consequently, the extinction depth is set to the depth of measurable evaporation for bare soil. As before, R_{max} is set to the land surface elevation and assumed to be constant value above that point.

2.5. A new ET modeling package

The approach outlined above is applied in a new seasonal ET package: a Riparian Evapotranspiration Package for MODFLOW-96 and MODFLOW-2000 (Maddock and Baird, 2003). In this package, the continuous curve shown in Fig. 2, is replaced with an approximation based on linear segments. Curve segments are specified in RIP-ET as being dimensionless and are converted during the simulation into units consistent with other MODFLOW packages following the units of R_{max} and Ard . Fig. 5 illustrates the resulting segmented, ET flux rate curve. The curve segments (labeled 1–7 in Fig. 5) are defined by the vertices ($h(k)$, $R(k)$) and determine the shape of

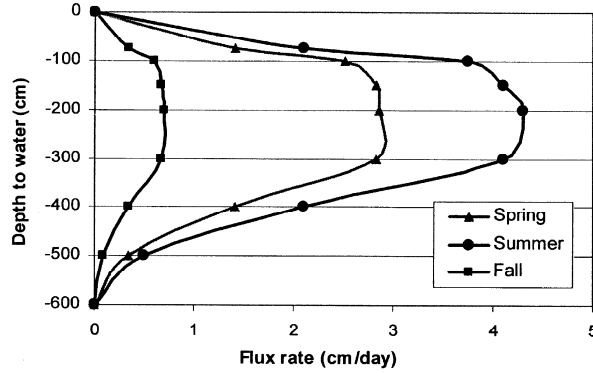


Fig. 4. Seasonal mean daily canopy flux rate curves (cm/day) for deep-rooted riparian PFG: spring, summer and fall.

the curve. $d(1)...d(N)$, represent the change in head over each segment (in length units), while $dR(1)...dR(N)$ represent the change in flux over the segment (in flux rate units).

The process for producing the dimensionless, segmented curves is conducted external to the RIP-ET package. To build the dimensionless curves, the parameters $d(k)$ and $dR(k)$, where $k=1...N$ are computed as follows. In general, for N segments where $1 \leq k \leq N$,

$$d(k) = h(k + 1) - h(k)$$

and

$$dR(k) = dR(k + 1) - dR(k).$$

For each functional subgroup curve, the fractional change in head ($fdh(k)$) and flux rate ($fdR(k)$) are defined for each dimensionless segment as:

$$fdh(k) = \frac{d(k)}{Ard}$$

and

$$fdR(k) = \frac{dR(k)}{Rmax}$$

with:

$$\sum_{k=1}^N fdh(k) = 1$$

and

$$\sum_{k=1}^N fdR(k) = \frac{R_{sxd}}{R_{max}}$$

Consequently, within a simulation, $fdh(k)$ and $fdR(k)$ are known constants for each plant functional subgroup and, when multiplied by Ard and $Rmax$, the segment variables $d(k)$ and $dR(k)$ are recovered.

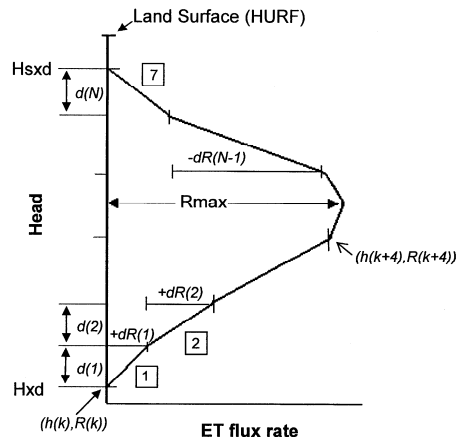


Fig. 5. Segmented ET flux curve illustrating linear interpolation using $d(N)$ s and $dR(N)$ s.

Within the RIP-ET package, the individual user may develop application specific flux curves. However, the $fdh(k)$ and $fdR(k)$ values for the curves illustrated in Fig. 3 and the four DBH size classes for deep-rooted riparian have been provided in the RIP-ET manual. The segmented curve (Fig. 5) and the values for $fdh(k)$ and $fdR(k)$ can also be created using PRE-RIP-ET, a pre-processor developed to aid in preparing RIP-ET (Baird et al., 2004). RIP-GIS requires the following input to develop the curve: extinction depth, saturation extinction depth, and preferably at least three ET rates at specific ground-water depths.

2.6. Land surface elevation

Given the linear nature and high variability in surface elevations within and along riparian corridors, a single average model cell elevation is not likely to be representative of surface-groundwater relationship required to accurately estimate ET. If the within cell variability in surface elevation (HSURF) is of the same order of magnitude as the PFG's extinction depths, the ET calculations will be adversely affected. RIP-ET offers the option of assigning a single surface elevation per cell, the only option available in the traditional ET packages, or assigning a unique HSURF value for each plant functional group or designated area within a cell. If a single value of HSURF is used, the average land surface elevation in the cell is used to calculate the extinction depth elevations for all PFGs. With the second option, the surface elevations for each individual PFSG area or polygon are used to calculate extinction depths. Using RIP-GIS, a GIS pre-and post-processor embedded in PRE-RIP-ET, assigning elevations for each PFSG polygon can be automated using data from any type of digital elevation grid such as a digital elevation models (DEMs). In many locations, 10-m or smaller resolution DEMs are currently available.

2.7. Determination of ET flux rates and scaling factors

There are numerous techniques for measuring or estimating ET fluxes depending upon the plant community and terrain being examined. Ultimately, most measuring techniques yield a specific flux per specified unit area (e.g. xylem area, basal area, canopy

area or ground area). One possible technique, sap flow measurements, provides a practical technique for estimating the water use of individual trees and is often the only feasible alternative for measuring forest and woodland transpiration (Hatton et al., 1995). If sap flow is measured for a sufficiently large numbers and size range of individuals, the resulting data can be scaled up to stand level (Meinzer et al., 1997; Hatton et al., 1995).

A common approach for scaling sap flux measurements to stand level water use involves obtaining a mean flux to a mean canopy area ratio at the population level, making canopy area the scaling factor. Detailed measurements of crown cover are helpful in accurately estimating tree leaf area, as forest inventories show a large spatial variation in tree ground cover (Oren et al., 1999; Granier et al., 2000). A second approach relies on the relationship of sapwood to tree diameter at breast height (DBH). Cienciala et al. (2000) reported a strong linear relationship between sapwood area and DBH in *Acacia*. In this case, total basal area would be the specified unit area. In the calculation of ET presented below, this specified unit area is applied as a scaling factor. The modeling method used in the RIP-ET package can accommodate multiple techniques including micrometeorological providing R_{max} and the subsequent flux curves match the scaling factor applied.

2.8. Determination of PFSG and scaling areas

Within a groundwater model, volumetric ET [L^3/T] is determined by multiplying the ET flux rate [L/T] by the cell area [L^2]. Cell sizes in a groundwater model are generally quite large (e.g. square kilometers) so only a portion of the cell is likely to contain active habitat (Fig. 6a). Since few riparian or wetland areas are monotypic, a cell is also likely to contain a mixture of plant functional subgroups. The new ET estimation methodology allows for fractional coverage or multiple flux rates within a cell. To accomplish this, information about the distribution of plant functional subgroups within the active modeling areas is required.

To calculate the ET flux from a cell, the coverage area of each subgroup must first be determined.

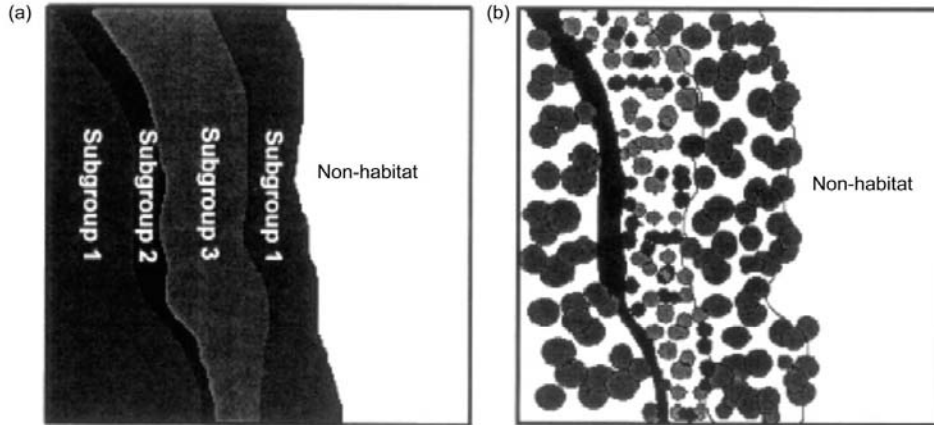


Fig. 6. (a) Active plant functional group areas within a groundwater model cell and (b) plant canopy cover within each plant functional subgroup area.

The fraction of the i th subgroup ($fSG_{(i)}$) is defined as:

$$fSG_{(i)} = \frac{\text{area of PFSG}_{(i)}}{\text{total cell area}}$$

Next the area associated with the appropriate scaling factor needs to be calculated. In this example, the scaling factor is canopy or plant cover. Within any habitat or PFSG area, canopy or plant cover varies depending upon habitat type and resource availability but rarely equals 100% (Fig. 6b). The fraction of plant coverage, $fPC_{(i)}$, is defined as:

$$fPC_{(i)} = \frac{\text{canopy area}_{(i)}}{\text{area of PFSG}_{(i)}}$$

Therefore, the area of the i plant functional subgroup contributing to ET or $fCov_{(i)}$ equals:

$$fCov_{(i)} = fSG_{(i)} \times fPC_{(i)}$$

The fractional covers ($fCov$) for each plant functional subgroup are required for each cell. The components of fractional cover can be determined using a combination of GIS techniques, aerial photography with ground verification or from detailed field surveys. These aerial determinations and calculations are more easily performed in a GIS platform. The pre-processor in RIP-GIS automates the steps

required to complete a riparian theme for those with ARC-VIEW capabilities.

2.9. ET calculations

Consider one of the plant functional subgroups present in the cell. If $(h(k), R(k))$ and $(h(k+1), R(k+1))$ are the coordinates of consecutive vertices that define the k th segment for that plant functional subgroup, and if h is the head in the cell, then the ET flux rate for the subgroup, $R(h)$ is given by (Hadley, 1964),

$$R(h) = R(k) + \frac{h - h(k)}{h(k+1) - h(k)} (R(k+1) - R(k))$$

for $h(k) \leq h \leq h(k+1)$.

The initial values are,

$$h(1) = \text{HSURF} - \text{Sxd} - \text{Ard}$$

and,

$$R(1) = 0.$$

The higher k valued vertices are given by,

$$h(k+1) = h(k) + \text{fdh}(k)\text{Ard}$$

and

$$R(k+1) = R(k) + \text{fdR}(k)\text{Rmax}.$$

To calculate the volumetric ET rate for the PFSG, $R(h)$ is multiplied by the cell area (Area) and the fractional coverage (fCov):

$$ET(h) = R(h)(Area)fCov$$

These calculations are then repeated for each plant functional subgroup present in a cell, and for each cell designated as containing habitat. The volumetric ET rate for each plant functional subgroups is summed to give the total volumetric ET rate within a cell and each cell is summed to obtain the global volumetric ET rate.

3. Results

To illustrate the utility of the methodology described in this paper, we compared the model results from the traditional and RIP-ET packages on a sample case from the South Fork Kern River basin. Within this semi-arid basin, a mixture of wet sedge and marsh areas intermix with cottonwood-willow forest habitat supporting populations of two endangered species. The effects of pumping wells on the protected riparian habitat need to be ascertained. A detailed water budget is required to address issues of water availability for human needs, water requirements for the existing riparian vegetation, and to project future changes in both.

Pre-development conditions were simulated using a two-season (summer and winter), steady-oscillatory state model (Maddock and Vionnet, 1998). Well pumping was added and the simulation run for 10 years. The basin-scale, summer ET estimated from both models is shown in Fig. 7. On average, the traditional modeling approach estimated 489% more ET than is predicted by the RIP-ET approach. A comparison of cell areas contributing to the two models revealed that the traditional model overestimated the area contributing to basin wide ET by 51%. After adjusting for this discrepancy, the traditional ET model still over-estimated riparian and wetland ET by 238% relative to the new approach.

The difference between the techniques is also crucial in terms of the simulated heads (i.e. groundwater elevation) and thus in predicating the potential distribution and health of the various habitats within the ecosystem. By relating PFSG rooting depths, ET rates and groundwater levels

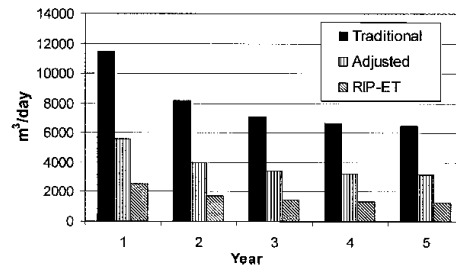


Fig. 7. Estimated basin scale ET rates from (a) traditional MODFLOW ET package, (b) area adjusted MODFLOW package and (c) RIP-ET package.

within a spatially based model it is possible to identify potential habitat types, predict habitat response to changes in land or water use, or to ascertain the potential plant stress of existing PFG from a groundwater perspective. The post-processor portion of RIP-GIS, links the resulting head distribution from MODFLOW with the surface elevations to determine the depth to groundwater throughout the basin. These results can then be mapped at the resolution required to identify the potential PFSG distributions based on user defined PFSG-depths to groundwater categories.

The two models predict different pre- and post-development potential habitat distributions. In the pre-development phase, the RIP-ET method predicts more water remaining in the system with less ET, resulting in higher water table elevations compared to the traditional ET method (Fig. 8). RIP-ET predicts a much larger wetland marsh area and areas suitable for small deep-rooted trees than the traditional method. Post-development predictions continue to show significant difference in the models. After only 3 years of pumping, the traditional model predicts the loss of riparian forest over a much large portion of the valley. Ultimately both models predict significant habitat loss, however, the timing and location of losses are different.

The method applied in RIP-ET will not always predict less ET from a given area, rather the idea is more accurate estimations. In another instance, a small (13.51 mi²) cienega in southern Arizona was modeled using both methods. Measured water table depths placed water levels at the lower portion of

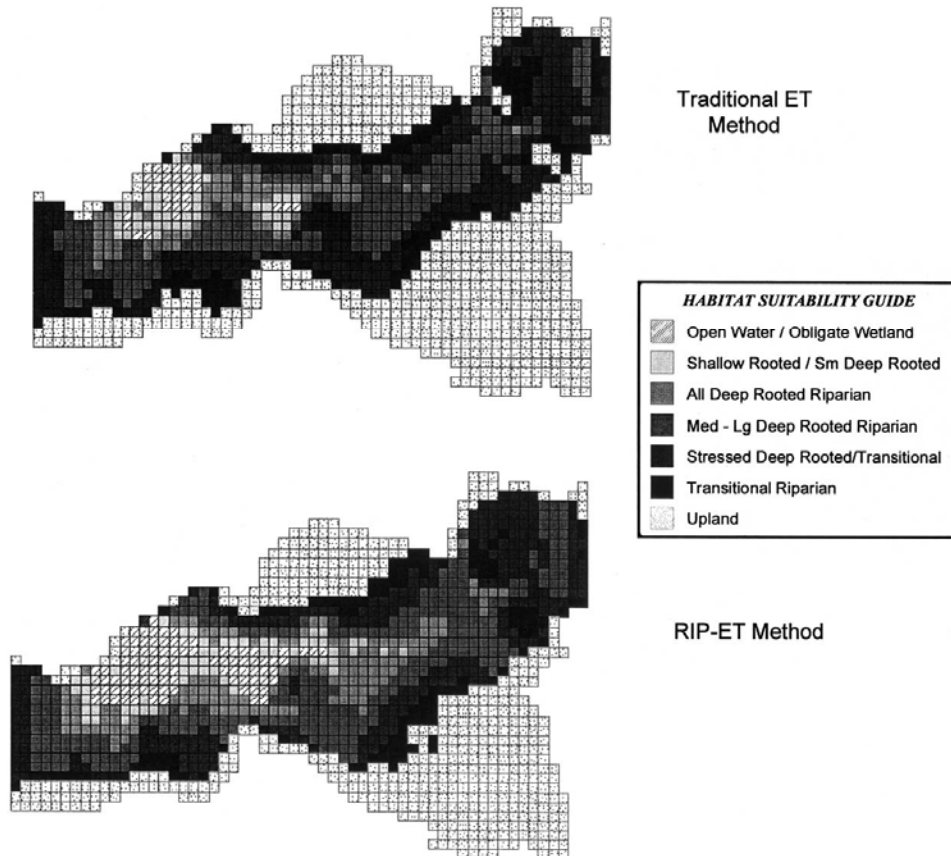


Fig. 8. Pre-development habitat distribution/groundwater depths predicted from the traditional ET and RIP-ET methods.

the traditional curve, and closer to the maximum rates for the species present. Consequently, ET estimates using RIP-ET were 37% higher than estimated with the traditional method.

4. Discussion

The use of plant functional groups based on water tolerance ranges and rooting depths in combination with the new RIP-ET package

provides an explicit link between groundwater and riparian/wetland habitat conditions and improves upon traditional groundwater modeling techniques with several innovations. First, the single, monotonically increasing ET flux curve used in traditional modeling packages is replaced with a set of eco-physiologically based curves. Each of the multiple transpiration curves reflects a particular plant functional group, thus reflecting the variability in vegetative conditions present in the system. For each plant functional group,

the transpiration curve not only reflects transpiration declines at deep water levels, but also reflects the reduction in transpiration that occurs due to anoxic soil conditions that develop under conditions of elevated water tables.

In addition to the physical factors that govern evaporation, transpiration responds to a set of physiological and biometrical conditions. By decoupling the two processes, with the traditional linear curve being retained to model evaporation better estimates can be obtained for both. Third, RIP-ET improves accuracy by more effectively dealing with spatial issues of plant and water table distribution. It replaces the single-cell, single-ET-elevation value approach with multiple ET curves, and associated fractional coverages with variable surface elevations. ET rates can now be calculated by determining the area of all habitat types present and then applying multiple ET curves to a single model cell. When accompanied with RIP-GIS or PRE-RIP-ET, detailed information can be incorporated on the distribution of plant functional groups across land surface elevations. This effectively captures the range of ET responses across the topographic-hydrologic gradients.

4.1. Defining recruitment zones

Paramount to ecosystem conservation and sustainability is the ability of the dominant plant species to regenerate. Regeneration of cottonwood-willow riparian forests requires the combination of high water tables during the early summer months and spring floods of a characteristic intensity (Stromberg, 2001; Mahoney and Rood, 1998). Areas with the appropriate groundwater conditions for new plant establishment can be thought of as potential regeneration areas. In Fig. 8 the areas mapped as small deep-rooted PFSG are potential regeneration areas. Due to the difference in time scales, regional time scales for groundwater versus event driven floods, these results do not directly identify regeneration areas. For accurate mapping of recruitment areas MODFLOW with RIP-ET would need to be run using shorter time steps and results from a surface water model overlain on the groundwater map to identify the actual riparian recruitment zone.

4.2. Restoration and conservation planning

Restoration of riparian and wetland ecosystems has become a major enterprise in developed nations (Stromberg, 2001). Restoring these ecosystems depends upon restoring or preserving the groundwater and surface water conditions fundamental to these systems. Water conservation and riparian ecosystem restoration programs require knowledge of comparative water use characteristics of riparian plant species and their effect on the water balance of riparian corridors (Nagler et al., 2003). RIP-ET can aid in this endeavor in two ways. First, water requirements, quantities and groundwater elevations, for various habitat types and sizes can be more accurately estimated. These estimates then need to be incorporated into regional planning and conservation plans. Second, the program can be used as an interactive tool in the planning stage. While the initial water table elevations at the location to be restored are commonly known, the response of water table to the restored habitats has been difficult to predict. Using RIP-GIS, the area can be modeled and calibrated in the pre-restored condition. The restored habitats can then be simulated and the resulting groundwater levels determined. If water table elevations do not fall within the required ranges, the plan can be easily altered and the model re-run until the two parameters converge.

RIP-ET can also help discern the potential success of phreatophyte control projects in salvaging water. In the 1950s and 1960s, under the guise of water salvage projects, cottonwoods, willows and other phreatophytes suspected of having very high ET rates were cleared from waterways throughout the western United States. Although water savings did not always materialize, water salvage efforts continue today. The primary target is tamarisk, a riparian tree/shrub species which has become a dominant species in the West since being introduced in the late 1800s. Based on the assumption that such projects will enable more water to be available for direct human use, massive federal efforts are underway to eliminate tamarisk stands. Models such as RIP-ET which provide more accurate estimates of current and projected ET rates by plant type are critical to

determining whether alleged water salvage benefits have been overstated.

4.3. Model calibration

In systems where a sizable portion of the model area is affected by ET, the differences in these methods can affect the model calibration process. Model calibration depends upon comparing simulated heads to known heads. In many basins, scant information exists on historical or existing water table elevations. In many cases, historical and/or current photographs or records of habitat distribution do exist. If simulated heads fall outside the tolerance ranges of the past or current PFSG, further calibration is indicated. The authors recognize that this is not precise calibration tool rather a generalized method that can aid in areas of sparse information.

5. Conclusion

Increasing human modification of the Earth's surface requires an understanding of how the productivity and biotic diversity of both natural and managed riparian ecosystems can be sustained (Chapin et al., 1996). Simplifying the complex structure of plant communities into PFGs provides a framework for predicting ecosystem response to environmental change by using information on correlated traits in lieu of detailed species information to predict the response of vegetation (Dyer et al., 2001; Szymstad et al., 2000). The use of plant functional groups based on plant transpiration and rooting depths in combination with improved ET modeling is a first step in allowing researchers to link groundwater changes in semi-arid areas with changes in the riparian ecosystem.

The methodology and Riparian ET Package presented here does not use the traditional linear ET flux rate curve, but instead, uses a segmented curve based on the ecophysiology of the plant species within the ecosystems. The method requires a fractional coverage for each of the PFSG present within the groundwater model cell and allows for more accurate assignment of land surface elevations. The calculated evapotranspiration loss

from a riparian or wetland system is dependent on the contributing area of each plant functional subgroup present and water table conditions. While the curves presented here are preliminary, the authors hope that they serve to focus attention on the need for development of eco-physiologically based ET curves

Development of physiologically based transpiration curves combined with the traditional linear curve for bare soil/open water results in more accurate determinations of riparian ET, improved basin scale water budgets, and allows for the quantification of riparian water requirements. Given supporting modeling data, groundwater conditions can be simulated, potential plant groundwater stress ascertained and suitable habitat areas or changes in habitat areas identified.

The combined approach of using hydrologic models, vegetation mapping and GIS has proven to be an effective tool in characterizing groundwater systems (Batelaan et al., 2003). Conservation planners and regional water planners alike are seeking tools that enable them to make informed decisions regarding effects of water allocation decisions on environmental amenities (Richter et al., 1997). Development of linked hydrology-vegetation models will be a major step towards effective, science-based water allocation decision-making. Incorporating riparian ecosystem water needs in the modeling process can help ensure that decision makers include riparian water demands as a vital component of the water budget.

Acknowledgements

We thank W.J. Shuttleworth and J.C. Stromberg for their helpful review comments. Primary funding for the research and development presented in this paper was provided by EPA-NSF Star Grant number R827150/01. Additional funding was provided from the National Science Foundation's Science and Technology Center (STC) Program through the Center for Sustainability of semi-Arid Hydrology and Riparian Areas (SAHRA) under Agreement EAR-9876800.

References

- Baird, K.J., Dragoo, C.A., Maddock III, T., 2004. PRE-RIP-ET, A preprocessor for RIP-ET. Department of Hydrology and Water Resources, University of Arizona Research Laboratory for Riparian Studies, University of Arizona.
- Banta, E.R., 2000. MODFLOW-2000 the US Geological Survey modular ground-water model—documentation of packages for simulating evapotranspiration with a segmented function (ETS1) and drains with return flow (DRT1). US Geological Survey Open-File Report 00-466.
- Batelaan, O., De Smedt, F., Triest, L., 2003. Regional groundwater discharge: phreatophyte mapping, groundwater modelling and impact analysis of land-use change. *Journal of Hydrology* 275, 86–108.
- Bosveld, F.C., Bouten, W., 2001. Evaluation of transpiration models with observations over a Douglas-fir forest. *Agricultural and Forest Meteorology* 108, 247–264.
- Busch, D.E., Ingraham, N.L., Smith, S.D., 1992. Water uptake in woody riparian phreatophytes of the southwestern United States: a stable isotope study. *Ecological Applications* 2, 450–459.
- Chapin III, F.S., Torn, M.S., Taten, M., 1996. Principles of ecosystem sustainability. *American Naturalist* 148, 1016–1037.
- Cienciala, E., Kucera, J., Malmer, A., 2000. Tree sap flow and stand transpiration of two *Acacia mangium* plantations in Sabah, Borneo. *Journal of Hydrology* 236, 109–120.
- Cooper, D.J., D'Amico, D.R., Scott, M.L., 2003. Physiological and morphological response patterns of *Populus deltoids* to alluvial groundwater pumping. *Environmental Management* 31 (2), 215–226.
- Dyer, A.R., Goldberg, D.E., Turkington, R., Sayer, C., 2001. Effects of growing conditions and source habitat on plant traits and functional group definition. *Functional Ecology* 15, 85–95.
- Ehleringer, J.R., Dawson, T.E., 1992. Water uptake by plants: perspectives from stable isotope composition. *Plant, Cell and Environment* 15, 1073–1082.
- Goodrich, D.C., Scott, R., Qi, J., Goff, B., Unkrich, C.L., Moran, M.S., Williams, D.G., Schaeffer, S.M., Snyder, K.A., MacNish, R.D., Maddock, T., Pool, D., Chehbouni, A., Cooper, D.I., Eichinger, W.E., Shuttleworth, W.J., Kerr, Y., Marssett, R., Ni, W., 2000. Seasonal estimates of riparian evapotranspiration using remote and in situ measurements. *Agricultural and Forest Meteorology* 105, 281–309.
- Granier, A., Biron, P., Lemoine, D., 2000. Water balance, transpiration and canopy conductance in two beech stands. *Agricultural and Forest Meteorology* 100, 291–308.
- Grimm, N.B., Chacon, A., Dahm, C.N., Hostetler, S.W., Lind, O.T., Starkweather, P.L., Wurtsbaugh, W.W., 1997. Sensitivity of aquatic ecosystems to climatic and anthropogenic changes: the Basin and Range, American Southwest and Mexico. *Hydrological Processes* 11, 1023–1041.
- Hadley, G., 1964. *Nonlinear and Dynamic Programming*. Addison-Wesley, Reading, MA.
- Hatton, T.J., Moore, S.J., Reece, P.H., 1995. Estimating stand transpiration in a *Eucalyptus populnea* woodland with the heat pulse method: measurement errors and sampling strategies. *Tree Physiology* 15, 219–227.
- Hills, J.M., Murphy, K.J., Pulford, I.D., Flowers, T.H., 1994. A method for classifying European riverine wetland ecosystems using functional vegetation groups. *Functional Ecology* 8, 242–252.
- Hipps, L.E., Cooper, D.I., Eichinger, W., Williams, D.G., Schaeffer, S.M., Snyder, K.A., Scott, R., Chehbouni, A., Watts, C., Hartogensis, O., Lhomme, J.-P., Monteny, B., Brunel, J.-P., Boulet, G., Schieldge, J., DeBruin, H.A.R., Shuttleworth, W.J., Kerr, Y., 1998. A summary of processes which are connected to evaporation of riparian and heterogeneous upland vegetation in arid regions. In: Wood, E.F., Chehbouni, A.G., Goodrich, D.C., Seo, D.J., Zimmerman, J.R. (Eds.), *Proceedings from the Special Symposium on Hydrology*. American Meteorological Society, Boston, MA, pp. 43–48.
- Horton, J.L., Kolb, T.E., Hart, S.C., 2001. Physiological response to groundwater depth varies among species and with river flow regulation. *Ecological Applications* 11, 1046–1059.
- Jarvis, P.G., McNaughton, K.G., 1986. Stomatal control of transpiration: scaling up from leaf to region. *Advances in Ecological Research* 15, 1–49.
- Kurc, S.A., Small, E.E., 2004. Dynamics of evapotranspiration in semiarid grassland and shrubland ecosystems during the summer monsoon season, central New Mexico. *Water Resources Research* 40 (W09305), 1–15.
- Lavorel, S., McIntyre, S., Landsberg, J.J., Forbes, T.D.A., 1997. Plant functional classifications: from general groups to specific groups based on response to disturbance. *Tree* 12, 474–478.
- Leishman, M.R., Westoby, M., 1992. Classifying plants into groups on the basis of associations of individual traits—evidence from Australian semi-arid woodlands. *Journal of Ecology* 80, 417–424.
- Maddock III, T., Baird, K.J., 2003. A riparian evapotranspiration package for MODFLOW-96 and MODFLOW-2000. HWR No. 02–03. Department of Hydrology and Water Resources, University of Arizona Research Laboratory for Riparian Studies, University of Arizona.
- Maddock III, T., Vionnet, L.B., 1998. Groundwater capture processes under a seasonal variation in natural recharge and discharge. *Hydrogeology Journal* 6, 24–32.
- Maddock III, T., MacNish, R.D., Goodrich, D.C., Williams, D.G., Shuttleworth, W.J., Goff, B.A., Scott, D.F., Moran, M.S., Cooper, D.I., Hipps, L.E., Chehbouni, A.G., 1998. The overview of atmospheric and surface water coupling to regional groundwater models in semi-arid basins. In: Wood, E.F., Chehbouni, A.G., Goodrich, D.C., Seo, D.J., Zimmerman, J.R. (Eds.), *Proceedings from the Special Symposium on Hydrology*. American Meteorological Society, Boston, MA, pp. 38–42.
- Mahoney, J.M., Rood, S.B., 1998. Streamflow requirements for cottonwood seedling recruitment—an integrative model. *Wetlands* 18, 634–645.
- McDonald, M.G., Harbaugh, A.W., 1988. A modular three-dimensional finite-difference ground-water flow model. US Geological Survey TWI 6-A1, 1988.

6.2 Linking riparian dynamics and groundwater: an ecohydrological approach to modeling groundwater and riparian vegetation

- Shafroth, P. B., J. R. Cleverly, T. L. Dudley, J. P. Taylor, C. van Riper III, E. P. Weeks, and J. N. Stuart. 2005. Control of *Tamarix spp.* in the western U.S.: Implications for water salvage, wildlife use, and riparian restoration. *Environmental Management* 35:231–246.
- Shafroth, P. B., J. C. Stromberg, and D. T. Patten. 2000. Woody riparian vegetation response to different alluvial water table regimes. *Western North American Naturalist* 60:66–76.
- Snyder, K. A., and D. G. Williams. 2000. Water sources used by riparian trees varies among stream types on the San Pedro River, Arizona. *Agricultural and Forest Meteorology* 105:227–240.
- Springer, A. E., J. M. Wright, P. B. Shafroth, J. C. Stromberg, and D. T. Patten. 1999. Coupling groundwater and riparian vegetation models to simulate riparian vegetation changes due to a reservoir release. *Water Resources Research* 35(12):3621–3630.
- Steinitz, C., H. Arias, S. Bassett, M. Flaxman, T. Goode, T. Maddock, D. Mouat, R. Peiser, and A. Shearer. 2003. Alternative futures for changing landscapes, the Upper San Pedro Basin in Arizona and Sonora. Island Press, Washington, D.C.
- Stromberg, J. C. 1993. Fremont cottonwood-Goodding willow riparian forests: A review of their ecology, threats, and recovery potential. *Journal of the Arizona-Nevada Academy of Science* 26(3):97–110.
- Stromberg, J. C. 2001. Restoration of riparian vegetation in the south-western United States: importance of flow regimes and fluvial dynamism. *Journal of Arid Environments* 49:17–34.
- Symstad, A. J., E. Siemann, and J. Haarstad. 2000. An experimental test of the effect of plant functional group diversity on arthropod diversity. *OIKOS* 89:243–253.
- Wever, L. A., L. B. Flanagan, and P. J. Carlson. 2002. Seasonal and interannual variation in evapotranspiration, energy balance and surface conductance in a northern temperate grassland. *Agricultural and Forest Meteorology* 112:31–49.
- Winter T. C., J. W. Harvey O. L. Franke and W. M. Alley. 1998. Groundwater and surface water: A single resource. U.S. Geological Survey Circular 1139, Denver, Colorado.
- Wurster, F. C., D. J. Cooper, and W. E. Sanford. 2003. Stream/aquifer interactions at Great Sand Dunes National Monument, Colorado: Influences on interdunal wetland disappearance. *Journal of Hydrology* 271:77–100.

Linking Riparian Dynamics and Groundwater: An Ecohydrologic Approach to Modeling Groundwater and Riparian Vegetation

KATHRYN J. BAIRD*

Department of Hydrology and Water Resources
University of Arizona
P.O. Box 210011
Tucson, Arizona, 85721-0011

JULIET C. STROMBERG

School of Life Sciences
Arizona State University
P.O. Box 874501
Tempe, Arizona 85287-4501

THOMAS MADDOCK, III

Department of Hydrology and Water Resources
University of Arizona
P.O. Box 210011
Tucson, Arizona, 85721-0011

model programs (RIP-ET and PRE-RIP-ET), the single, monotonically increasing evapotranspiration flux curve in traditional groundwater models is replaced with a set of ecophysiological based curves, one for each plant functional group present. For each group, the curve simulates transpiration declines that occur both as water levels decline below rooting depths and as waters rise to levels that produce anoxic soil conditions. Accuracy is further improved by more effective spatial handling of vegetation distribution, which allows modeling of surface elevation and depth to water for multiple vegetation types within each large model cell. The use of RIP-ET in groundwater models can improve the accuracy of basin scale estimates of riparian evapotranspiration rates, riparian vegetation water requirements, and water budgets. Two case studies are used to demonstrate that RIP-ET produces significantly different evapotranspiration estimates than the traditional method. When combined with vegetation mapping and a supporting program (RIP-GIS), RIP-ET also enables predictions of riparian vegetation response to water use and development scenarios. The RIP-GIS program links the head distribution from MODFLOW with surface digital elevation models, producing moderate- to high-resolution depth-to-groundwater maps. Together with information on plant rooting depths, these can be used to predict vegetation response to water allocation decisions. The different evapotranspiration outcomes produced by traditional and RIP-ET approaches affect resulting interpretations of hydro-vegetation dynamics, including the effects of groundwater pumping stress on existing habitats, and thus affect subsequent policy decisions.

ABSTRACT / The growing use of global freshwater supplies is increasing the need for improved modeling of the linkage between groundwater and riparian vegetation. Traditional groundwater models such as MODFLOW have been used to predict changes in regional groundwater levels, and thus riparian vegetation potential attributable to anthropogenic water use. This article describes an approach that improves on these modeling techniques through several innovations. First, evapotranspiration from riparian/wetland systems is modeled in a manner that more realistically reflects plant ecophysiology and vegetation complexity. In the authors'

Riparian Ecosystems and Water Resources

Freshwater ecosystems play an integral role in human society, affecting fields as diverse as commerce, transportation, health, and recreation. For centuries, human populations have exploited freshwater ecosys-

tems without understanding the basic environmental principles that allow these systems to maintain their inherent health and vitality (Naiman and others 2002). Consequently, overengineering, overabstraction of resources, pollution, and ineffective management practices have dramatically altered these ecosystems (Nienhuis and Leuven 2001). Many of the world's greatest rivers have been reduced from complex systems of floodplains and meandering, braided channels to single channels that support only a fraction of their original biodiversity and abundance (Kingsford 2000). Despite the mounting evidence of adverse effects and

KEY WORDS: Riparian evapotranspiration; Ecohydrologic model; Groundwater; plant functional group; MODFLOW

Published online August 29, 2005.

*Author to whom correspondence should be addressed; *email:* kbaird@hwr.arizona.edu

lack of success, radical river regulation measures continue today (Nienhuis and Leuven 2001).

Global demands on water resources are increasing as populations and material needs grow. The pressure for water resource development is particularly acute in arid regions where water is already in short supply. In the arid western United States, irrigation needs still largely govern river management priorities and objectives, but urban population growth is increasing regional water demands. Surface water resources, diverted for urban and agricultural uses, often are entirely appropriated by existing state, interstate, and international compacts and treaties. Groundwater often is the only new or untapped water resource (Cooper and others 2003). Unsustainable groundwater development, although not always immediately obvious, threatens natural resource values and is becoming a major source of user conflict (Cooper and others 2003; Glennon and Maddock 1994; Steinitz and others 2003).

Riparian systems, the dominant freshwater ecosystem throughout the western United States, typically occur where groundwater is in close proximity to the soil surface or where a direct connection exists between groundwater and surface water. These groundwater-surface water interfaces support greater biomass and often greater species diversity than the surrounding landscape, and in semiarid and arid environments function as critical oases for plants, animals, and humans (Wurster and others 2003). Intricately coupled to both groundwater and surface water regimes, riparian ecosystems are sensitive to perturbations in either (Busch and others 1992; Grimm and others 1997; Stromberg 1993).

Riparian biota are dependent on the dynamic characteristics of the surface water regime, described in terms of magnitude, frequency, timing, duration, and rate of change (Naiman and others 2002; Poff and others 1997; Richter and Richter 2000). Surface water, however, forms only the visible part of a continuous hydrologic system. Water in the surface stream, vadose zone, and groundwater aquifer collectively sustains riparian ecosystems (Hancock 2002). Water from the capillary fringe of the alluvial groundwater table is the major water source for many riparian tree species in arid and semiarid regions (Shafroth and others 2000; Snyder and Williams 2000). Lowering groundwater tables can have widespread ecologic consequences, including the conversion of perennial stream flows to intermittent flows and the alteration of vegetation composition and cover. Even short-term declines in alluvial groundwater tables can change the distribution and abundance of riparian plant associations, leading to the decline of phreatophytes (Cooper and others

2003; Shafroth and others 2000). Identifying the vulnerability of riparian and wetland ecosystems to anthropogenic activities and climatic variation necessitates a thorough understanding of the groundwater-surface water interactions that maintain them (Winter and others 1998; Wurster and others 2003).

Role of Groundwater Models in Protecting Riparian Ecosystems

In regions where anthropogenic water use disrupts recharge and discharge processes, creating groundwater or surface water deficits, balancing the need for water against the conservation of natural ecosystems present a daunting challenge. To protect riparian ecosystems, special attention must be given to the protection of groundwater systems and to the effects of land use changes on the hydrologic cycle (Batelaan and others 2003). Consequently, conservation and regional water planners alike require tools that allow them to make informed decisions regarding the effects of land use development and water allocation on freshwater ecosystems (Richter and others 1997). Groundwater models that simulate regional groundwater behavior can be useful tools.

Water use decisions often affect large geographic areas, making their impacts difficult to characterize. Regional models, which focus on broad landscape elements, allow us to understand and predict the effects of water management decisions and climate changes at relevant scales (Elmore and others 2003; Nilsson and Svedmark 2002). When coupled with mechanistic models of wetland or riparian ecology and with sufficient field monitoring, regional groundwater models can provide a tool for predicting both the vulnerability of wetland and riparian habitat to water table decline and the future status of created or restored ecosystems (Mitsch and Wilson 1996; Springer and others 1999). They also can aid in the quantification of basin or reach scale water requirements for key habitat types in the riparian landscape.

Regional groundwater models are used widely to estimate water budgets as part of the local water allocation decision-making process. The accuracy and applicability of these groundwater models is, of course, dependent on accurate representations of the processes they simulate. One of the most critical but poorly simulated processes is seasonal riparian evapotranspiration (ET) (Goodrich and others 2000). The narrow, heterogeneous nature of riparian zones, coupled with their complex hydrology, hinders our understanding and quantification of ET processes in these systems (Hippis and others 1998). Controlled by

the interaction of both abiotic and biotic factors, ET is strongly linked with such ecosystem parameters and processes as soil moisture content, nutrient flows, and vegetation productivity (Jarvis and McNaughton 1986; Wever and others 2002).

The method used to model ET affects the calculated water budget and simulated depths to groundwater, and thus the resulting interpretations regarding ecosystem dynamics. In the current state of groundwater modeling, ET is appropriately defined as a function of hydraulic head or groundwater depth in an alluvial aquifer. Unfortunately, the manner in which it is modeled does not accurately reflect the relationship between riparian or wetland plant transpiration and groundwater conditions.

To improve ability to calculate riparian and wetland ET, estimate vegetation water requirements, and aid in predicting vegetation response to changing water availability, we developed a new method for modeling riparian and wetland ET. This methodology is applied in a Riparian Evapotranspiration Package (RIP-ET) for MODFLOW-96 and MODFLOW 2000 (Maddock and Baird 2003). The RIP-ET package is designed to be coupled with MODFLOW (McDonald and Harbaugh 1988; 1996), one of the most widely used groundwater flow models in the fields of consulting and research (Romero and Maddock 2003). In addition, two pre-processing programs were developed to aid the user in RIP-ET data preparation. The first, RIP-GIS, is a geographic information system (GIS) pre- and postprocessor that automates the steps required to complete a riparian coverage file for those with ArcView capabilities (Dragoo and others 2004). The second preprocessor, PRE-RIP-ET (Baird and others 2004), sets up the desired ET curves, reads the fractional coverage information from RIP-GIS, assigns surface elevations (see following sections) and, using the MODFLOW grid, writes the riparian ET file required by MODFLOW.

The modeling and mathematical details of RIP-ET are described in Maddock and Baird (2003). The goal of this article is to bring the model to the attention of ecologists, conservationists, and land/water managers. The objectives are twofold: to describe the ways in which the new modeling method overcomes the limitations of traditional ET modeling approaches, and to demonstrate and discuss some conservation applications of the model.

Development of a New Modeling Methodology

Plant Functional Groups

The largest source of error in traditional approaches to ET modeling is the use of a single ET curve to

represent both evaporation and transpiration regardless of the species assemblages present and their vigor and density. Not only is evaporation a unique physically based process and transpiration a biologic process, but ET rates also vary widely between plant species because of morphologic differences in root architecture, including rooting depth, and physiologic sensitivities to water availability (Horton and others 2001; Shafroth and others 2000). Our first steps were to decouple the process of evaporation from transpiration and then develop individual transpiration curves for the species or vegetation types being modeled.

Given the complexity of freshwater ecosystems, the creation of transpiration curves for all riparian and wetland species is not feasible. To address this issue, we incorporated the concept of plant functional groups (PFGs) into the ET model. Plant functional groups are defined as nonphylogenetic associations of plant species that exhibit similar responses to environmental conditions and have similar effects on the dominant ecosystem processes (Lavorel and others 1997). Typically, these are groups of species with similar morphologic, physiologic, or phenologic traits that vary predictably along environmental gradients. Using information on correlated traits in lieu of detailed species information simplifies the complex structure of plant communities and provides a framework for predicting ecosystem response to environmental change (Dyer and others 2001; Symstad and others 2000).

In the Riparian Evapotranspiration Package, PFGs are the units used to elucidate the interaction of plant ET with groundwater depth. We defined a set of PFGs relevant for semiarid environments on the basis of transpiration rates, rooting depths, and the upper and lower range of seasonal groundwater depth tolerance. These basic groups are obligate wetland, shallow-rooted riparian, deep-rooted riparian, and transitional riparian species. Working definitions are provided in Maddock and Baird (2003). To decouple evaporation from transpiration, we included a fifth group: bare ground/open water.

Evapotranspiration rates and the occupied range of groundwater elevations differ between PFGs. Because most riparian corridors comprise a mixture of PFGs, each with different hydrologic requirements and ET rates, total ET is determined from the combination of PFGs present and the ambient groundwater levels. To make the methodology, and thus the program, broadly applicable, users can develop the set of PFGs relevant to their geographic region and model area.

Plant population traits such as health and age can affect rooting depths, limits of water tolerance, and transpiration rates (Meinzer and others 1997). Com-

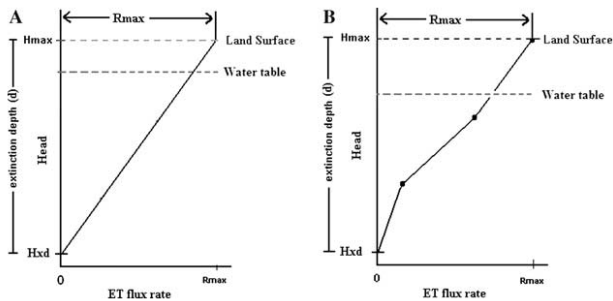


Figure 1. (a) Traditional linear (MODFLOW 96) and (b) segmented function (ETS1) package (MODFLOW 2000) evapotranspiration (ET) curves. Hxd, extinction depth elevation; d, extinction depth; Rmax, maximum ET rate; Hmax, maximum ET surface elevation.

munity traits such as plant density and cover also can affect transpiration rates, as can abiotic factors such as soil salinities. Any number of these or other such factors may be used as modifiers to create plant functional subgroups (PFSGs), and thus to refine further our ability to model plant ET in response to environmental conditions.

A New Transpiration Curve

A second source of error in traditional ET models involves the assumed shape of the curve relating ET rates to groundwater depths. The traditional approach to modeling ET in MODFLOW-96 (McDonald and Harbaugh 1988; 1996) assumes a quasilinear relationship between the ET flux rate and the hydraulic head or groundwater depth in an unconfined aquifer (Figure 1A). With this approach, if the water table is below the model extinction depth (Hxd) the ET rate is assumed to be zero. As the water table rises above this depth, the ET rate is assumed to increase linearly until it reaches a maximum rate (Rmax) at a user-defined maximum elevation (Hmax). The distance between Hxd and Hmax is called the extinction depth (d). Over this depth, the ET rate varies linearly with hydraulic head and is described by the slope of $\frac{R_{max}}{d}$.

In an ET package for MODFLOW 2000, Banta (2000) replaces the linear slope with a segmented function (ETS1) (Figure 1B). This function allows for limited flexibility, but assumes a constant Rmax above the maximum ET surface elevation, which in most modeling exercises is set equal to the land surface.

These quasilinear relationships may be useful for modeling evaporation, but do not accurately reflect the relationship between plant transpiration and groundwater conditions in that no allowance is made for the reduction in plant transpiration that occurs as the groundwater table approaches the upper horizons of the plant's rhizosphere. There is evidence that at high

water table elevations, the root systems of plants other than obligate wetland species become oxygen deficient, causing transpiration rates to decline until the plants eventually die of anoxia (Hughes 1997).

With RIP-ET, we simulate transpiration from riparian/wetland systems in a manner that more realistically reflects the ecophysiology of the component plant species (Figure 2). For each user-defined PFSG, as in the traditional approach, there is an extinction depth elevation (Hxd) (i.e., water table elevation below which the roots are unable to obtain water) at which transpiration is zero. As water table levels increase above the extinction depth, water becomes increasingly available to the root system and transpiration rates increase to a maximum average transpiration flux (Rmax) at a water table depth some distance below land surface. (This maximum transpiration flux rate is designed to be a measured or estimated maximum average daily transpiration rate, not the peak daily transpiration flux rate.) As water table elevations increase further, the root zone of nonobligate wetland groups becomes saturated, and increasingly less of the root system is capable of water uptake. Consequently, transpiration rates decline. The water table elevation associated with plant death from anoxia is the saturated extinction depth elevation (Hsxd). The transpiration flux rates for both the extinction and saturated extinction depths are by definition zero. The distance between these points is the active root zone depth (Ard). The traditional ET curve, illustrated in Figure 2 for comparative purposes, is used exclusively to model evaporation from bare soil or open water.

In the Riparian Evapotranspiration Package, we approximate the continuous curve shape with a series of small linear segments. Figure 3 illustrates the resulting segmented ET flux rate curve. The curve segments (labeled 1 through 7), defined by the vertices $h(h)$ and $R(h)$, determine the shape of the curve. The

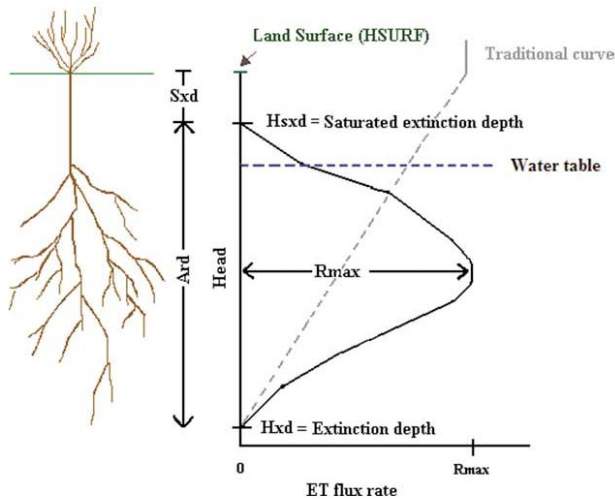


Figure 2. Generic evapotranspiration (ET) flux rate curve for a plant functional group in RIP-ET with associated plant schematic. Sxd, saturated extinction depth (L); Ard, active rooting depth (L); Hsxd, saturation extinction depth elevation; Hxd, extinction depth elevation; HSURF, land surface elevation; Rmax, maximum ET rate.

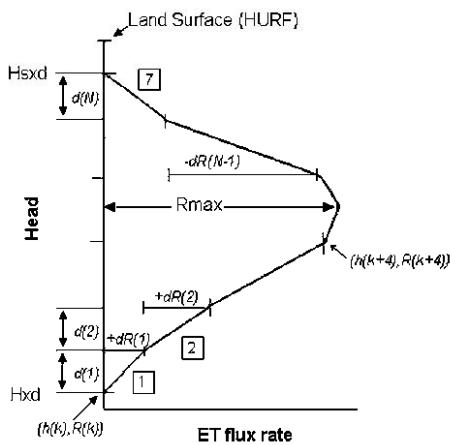


Figure 3. Segmented evapotranspiration flux curve illustrating linear interpolation using $d(N)$ s and $dR(N)$ s.

functions $d(1) \dots d(N)$ represent the change in head over each segment (in length units), whereas $dR(1) \dots dR(N)$ represent the change in flux over the segment (in flux rate units). The curve segments are specified as dimensionless and converted into units consistent with the other MODFLOW packages during the modeling simulation. The process for producing the dimen-

sionless, segmented curves is conducted external to the RIP-ET package, and can be accomplished easily with PRE-RIP-ET. The following inputs are required for the development of an ET curve: extinction depth, saturation extinction depth, and preferably a minimum of three ET rates at specific groundwater depths.

Values of the extinction depth can be approximated by the maximum rooting depth of the species within each PFSG, as determined through field studies or literature research. Saturated extinction depth can be determined on the basis of experimental studies or correlations between plant species abundances and water table elevations. Between these extremes, the shape of the PFSG transpiration curves can be determined from measured or estimated transpiration rates associated with specific water table depths. For arid and semiarid riparian species, there are few estimates of the magnitude or the spatial and temporal heterogeneity of transpiration fluxes (Schaeffer and others 2000). However, even if available data are sparse, the use of an upper and lower water tolerance range for the species in question, combined with nonlinear curves (a more ecologically realistic scenario), provides for more realistic model outcomes.

Multiple Transpiration Curves

The third improvement in ET modeling methodology is the application of multiple transpiration curves within a single modeling cell. Traditional methods restrict the user to a single curve regardless of the com-

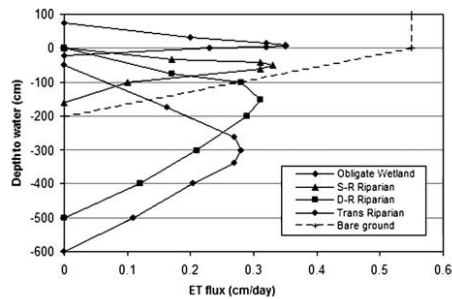


Figure 4. Mean daily evapotranspiration canopy flux (cm/day) curves for five plant functional groups. Positive numbers denote standing water.

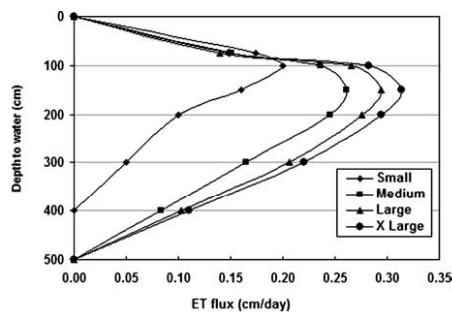


Figure 5. Mean daily canopy flux rates (cm/day) for four stem size classes of plants within the deep-rooted riparian plant functional group.

plexity of the system being modeled. With the traditional ET modeling approach, even when there is a range of plant species, age classes, and densities in the riparian landscape, the evaporation and transpiration rates must be averaged to a single value. With RIP-ET, the use of multiple ET curves, one for each PFSG, allows for a more realistic simulation of mixed plant assemblages and multistoried habitats.

On the basis of field ET measurements, literature review, and the expert opinion of researchers, preliminary transpiration–groundwater curves were developed for the riparian PFSGs and evaporation curve (bare ground) presented in the RIP-ET package (Figure 4). Sap flow measurements were used to quantify transpiration in a set of willow (*Salix* spp.) and cottonwood (*Populus fremontii*) trees at the South Fork

Kern River in central California and in the San Pedro River basin of southern Arizona. Simultaneous groundwater depths and meteorologic parameters were measured at both locations. At San Pedro, a controlled pumping experiment was performed specifically to measure the response of tree transpiration to declining water tables. Data from both sites formed the basis for the deep-rooted riparian canopy ET curves (Figure 5). We hope the preliminary curves we present serve to focus attention on the need for the development of ecophysiologically based ET curves. Refinement of these PFG curves and the development of additional curves will greatly benefit ET modeling efforts.

Fractional Coverages

Having modified the manner in which ET–groundwater relationships are defined, and having introduced habitat complexity into the model, we next focus on determining accurate aerial estimates of PFG cover. The fourth RIP-ET innovation is the incorporation of a process for accurate quantification of distinct ET areas from vegetationally complex mapping units. In regional groundwater models, model cells are generally quite large, often exceeding a square kilometer. Given the narrow linear nature of riparian zones, only a fraction of the cell is likely to contain riparian or wetland habitat. Furthermore, this fraction of a habitat is likely to comprise a mixture of PFSGs (Figure 6).

Because volumetric ET (L^3/T) is determined by multiplying the ET flux rate (L/T) by the cell area (L^2), estimations of the area covered by each habitat type or PFSG within a cell are required for accurate ET estimates. With RIP-ET, the contribution of each PFSG to a cell's ET is determined as follows. The areal extent of the i^{th} subgroup within a cell or the fraction of the i^{th} subgroup ($fSG_{(i)}$) is defined as $fSG_{(i)} = \frac{\text{area of PFSG}_{(i)}}{\text{total cell area}}$. The fraction of this area associated with the scaling factor ($fPC_{(i)}$) is defined as $fPC_{(i)} = \frac{\text{average area}_{(i)}}{\text{area of PFSG}_{(i)}}$. Therefore, the area of the i PFSG contributing to ET within a cell or $fCov_{(i)}$ equals $fCov_{(i)} = fSG_{(i)} \times fPC_{(i)}$. Numerically, total plant coverage within a cell can exceed 100% to allow for multistoried habitats.

To deal with the discrepancy between cell size and riparian habitat area with the traditional approach, the percentage of the area within each cell contributing to ET can be estimated manually, and the ET rate adjusted accordingly. This process is external to the model, laborious, and too often neglected. Because volumetric ET is calculated as cell area multiplied by the head-dependent transpiration rate, the error associated with using the entire cell as ET area can be

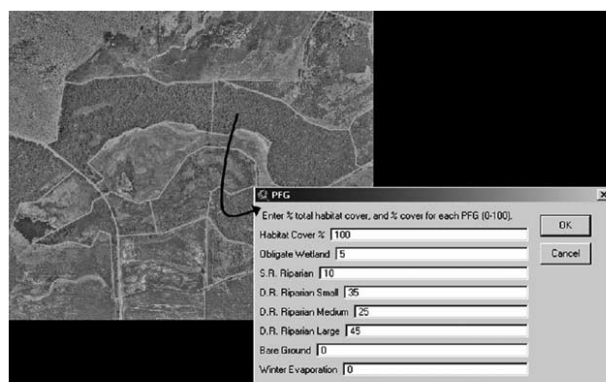


Figure 6. Digitized riparian polygons with RIP-GIS attribute table.

Table 1. Comparisons of groundwater model spatial information and areas of actively transpiring riparian habitat determined from the traditional-ET and RIP-ET modeling approaches^a

	Basin size (mi ²)	Cell size (m ²)	No. of cells	ET area traditional (m ²)	ET area RIP-ET (m ²)	% Difference
Unnamed AZ basin	13.5	150 × 150	1554	8,550,000	5,630,910	-34
South Fork Kern	22.6	150 × 150	2604	6,286,772	3,060,425	-51
Lower San Pedro	424.7	550 × 540	7363	171,922,038	57,684,161	-66

ET, evapotranspiration; RIP-ET, Riparian Evapotranspiration Package; AZ, Arizona

^aValues are shown for three semiarid basins.

substantial. Table 1 illustrates basin and cell dimensions for three groundwater model basins and the ET areas calculated using both methods.

Fractional coverage calculations must be performed for all active ET cells in the model. Hand calculation of values for the hundreds of cells that typify a MODFLOW model would be time consuming and error prone. Therefore, RIP-GIS, a GIS module, was developed. This GIS module is used to manage data while automating the fractional coverage section of PRE-RIP-ET. The standard in GIS desktop software is ArcView GIS from the Environmental Systems Research Institute. Riparian areas must be defined spatially within ArcView as polygons. Riparian polygons are most often identified and digitized using aerial photography, satellite images, topography maps such as digital elevation models, field surveys, or a combination of these sources. Once a new riparian polygon theme (shape file) is created, the required attribute fields are populated, and RIP-GIS prepares a text file that is then read by PRE-RIP-ET. Figure 6 illustrates a digitized riparian polygon containing multiple functional groups and the associated attribute table within RIP-GIS.

Depending on the plant community and terrain being studied, different measurement techniques may be used to estimate ET fluxes. Ultimately, most measuring techniques yield a specific flux (L/T: e.g., cm/sec) per specified unit area (L²: e.g., xylem area, basal area, canopy area, or ground area). To accommodate the various measurement techniques, we use a scaling factor to represent the unit area being measured. The units associated with the ET-flux curves must match the specified unit area or scaling factor.

Riparian ecosystems are dynamic, with plant cover and composition changing seasonally and annually. Over longer time scales, climate and atmospheric carbon dioxide concentration changes may alter the groundwater-transpiration relationship, requiring that a new set of ET curves be developed. Temporal changes in plant coverage or changes in transpiration-groundwater relationships are handled as separate time steps within MODFLOW. Each time step requires a separate fractional coverage or shape file. The PRE-RIP-ET program makes the preparation of seasonal coverages relatively easy. Historically, most groundwater models were based on annual time steps. However,

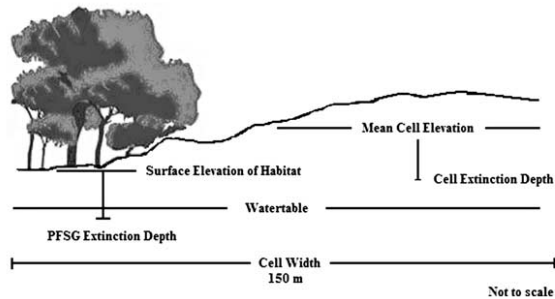


Figure 7. Schematic of a model cell showing the size of the cell, as compared with the riparian corridor width, and the effect of surface elevation variability on extinction depth.

seasonal models are strongly recommended if accurate groundwater–vegetation dynamics or estimates of ET are desired.

Land Surface Elevation

The fifth and final limitation we address deals with errors arising from the disparity between the variations in ground surface elevation and the assigned average cell elevation. Within the model domain, land surface elevation (HSURF) varies from cell to cell and within a cell. Because HSURF is one of the parameters used to calculate extinction depths for the PFGs, the magnitude of the within-cell variability of HSURF will have an important influence on ET. If the within-cell variation in land surface elevation is of the same magnitude as the extinction depths, it produces highly inaccurate ET calculations (Figure 7). There are two possible ways to avoid this problem: (1) make the model cell small enough to represent the variation in surface elevation or (2) allow for multiple surface elevations per cell. In most cases, option 1 is not feasible due to the large number of modeling cells this would require. Given the limitation on the number of cells in a model and the elevation changes inherent in many riparian ecosystems, the single average cell elevation used with the traditional method is not likely to produce meaningful estimates of riparian ET.

The RIP-ET program allows for multiple surface elevations per cell by providing the modeler with the option of assigning unique elevation values for each PFG or individual polygon within a cell. With RIP-GIS, a weighted-average elevation is calculated for each PFSG polygon using data from any type of digital elevation grid such as a digital elevation model. In many locations, fine-resolution digital elevation models (10 m or smaller) are now available. The extinction depths for the PFSGs are calculated according to the elevation of their associated polygons rather than the average

elevation for the entire cell. The accuracy of HSURF and thus the extinction depths are now controlled by the user-determined polygon size and the resolution of the elevation data rather than by the model cell size.

Computational and convergence limitations are the major reasons why most basins or watersheds cannot be modeled with cell sizes small enough to capture accurately the variability of vegetation type and surface elevations in riparian systems. Groundwater flow models are represented by a partial differential equation. Cell size and number are dictated largely by the numeric approximation of this partial differential equation. In a groundwater flow simulation, the replacement of the continuous partial differential equation for ground water flow into a set of discrete cells is not straightforward process. Determining the number of model cells involves a trade-off between the costs (data preparation and ability to run the model and solve the matrix) and the benefits (accuracy). Sufficient detail is required to represent the hydraulic properties (Ks), hydraulic stresses (i.e., pumping, ET), and complexities of the flow field for the objectives of the study. However, this must be balanced by limitation in central processing unit (CPU) time and memory. For most solvers, the CPU time required for convergence is a function of n^3 , where n is the number of nodes (cells). Increasing the number of nodes incurs a large penalty on the solver and convergence rates as instability develops. Convergence and instability are further exacerbated as the K field becomes more heterogeneous (Reilly and Harbaugh 2004).

Model Results

Are the results of this new method for estimating and predicting ET different from traditional methods? And are these differences substantial enough to alter interpretations of ecosystem dynamics and plant group distributions? As one test, we calculated model results

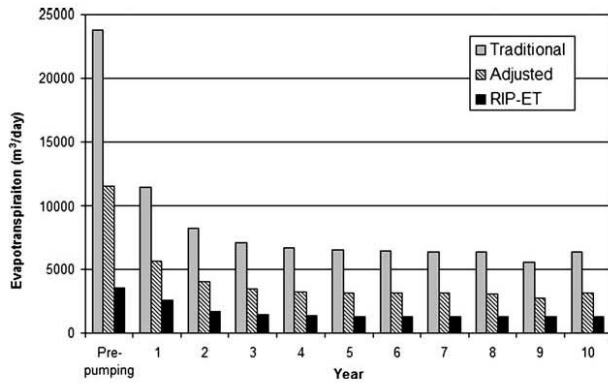


Figure 8. Estimated basin scale evapotranspiration (ET) rates from (a) the traditional MODFLOW ET package, (b) the area-adjusted MODFLOW package, and (c) the RIP-ET package.

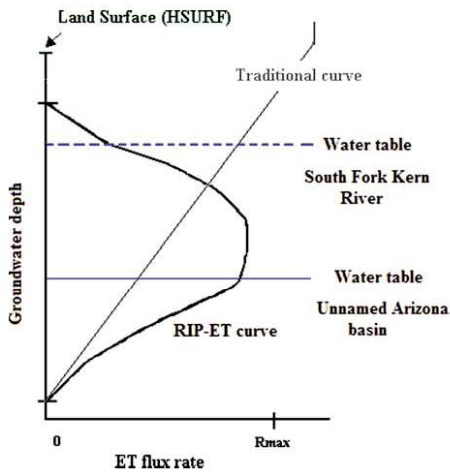


Figure 9. Average groundwater depths for South Fork Kern and no name basin in relation to the evapotranspiration curve for the dominant plant functional group.

from traditional and RIP-ET packages for two rivers. The first of these was the South Fork Kern River basin (California). Within this semiarid basin, wet sedge and marsh areas (obligate wetland and shallow rooted riparian PFGs) were intermixed with cottonwood-willow (deep-rooted riparian PFG) forest habitat along the length of the small river. Using physical modeling parameters developed for a regional groundwater model of the South Fork Kern River valley, we simulated conditions using a two-season (summer and

winter) steady-oscillatory state model (Maddock and Vionnet 1998). To make the comparisons as equitable as possible, ET estimates within the traditional method were based on a weighted average of the ET flux rates for the PFGs present.

At South Fork Kern River, there is concern over the potential loss of the endangered species riparian habitat attributable to changes in groundwater depths from increased agricultural pumping and proposed residential development. To impose development conditions, pumping was activated from a series of agricultural and domestic wells throughout the valley, and the model was run for a period of 10 years. All changes in ET are the result of changing groundwater elevations. No change in vegetation cover was simulated for these years. The resulting basin-scale summer ET estimates from both models (RIP-ET and traditional) are illustrated in Figure 8. The traditional modeling approach estimated 489% more ET than predicted by the RIP-ET approach. Much of this discrepancy was attributable to cell size effects (RIP-ET improvement number 4). The traditional model overestimated the riparian transpirational area by 51%. Although the South Fork Kern riparian habitat is extensive for a small river, few model cells were completely covered by riparian habitat. Most cells contained a mixture of riparian habitat, agricultural fields, and fallow pasture lands.

After adjustment for this discrepancy, the traditional ET model still overestimated riparian and wetland ET by 238% relative to the new approach. Factors contributing to the overestimation of ET included a high water table over much of the area that created water stress in the trees and reduced ET rates below the maximum. Field observations confirmed that this was

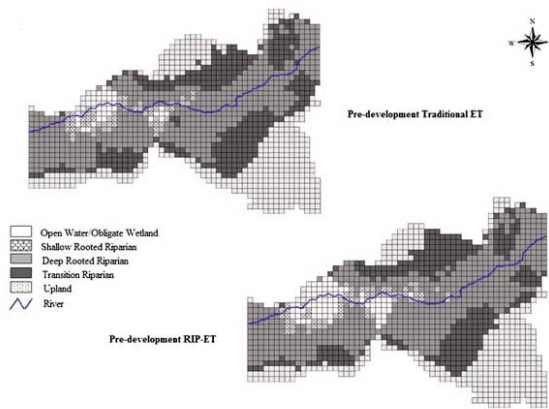


Figure 10. Predevelopment habitat distribution (based on modeled groundwater depths) as predicted using traditional evapotranspiration and RIP-ET methods.

in fact what the vegetation was experiencing, because the area is immediately upstream of a reservoir and experiences prolonged flooding for portions of the growing season. The traditional curve placed maximum ET rates at the upper part of the curve, whereas the maximum rates for most of the PFSG were at greater depths (Figure 9).

In addition to producing estimates of riparian ET and water needs that are more realistic and thus likely to be more accurate, RIP-GIS produces moderate to high resolution depth-to-groundwater maps based on the improved surface-groundwater modeling methods in RIP-ET. The postprocessor portion of RIP-GIS links the resulting head distribution from the MODFLOW simulation with surface elevations taken from a surface digital elevation model to determine depth to groundwater throughout the basin. These results then can be mapped at the resolution required to identify potential PFSG distribution based on user-defined water tolerance ranges. By relating PFSG rooting depths, ET rates, and groundwater levels within a spatially based model, it is possible to predict vegetation and habitat response to changes in land or water use, or to ascertain the level of plant stress that may arise from projected groundwater changes within the ecosystem.

In the South Fork Kern River example, the two methods of simulating ET resulted in substantially different habitat distribution maps. In the predevelopment phase, RIP-ET, with smaller ET losses, predicted higher water table elevations and consequently a much larger wetland area and more areas suitable for shallow-rooted and small deep-rooted trees than the traditional ET method (Figure 10). Postdevelopment

predictions continue to show a significant difference in the models. After only 3 years of pumping, the traditional model predicts the loss of riparian forest over a much larger portion of the valley. Ultimately, both models predict significant habitat loss, but the timing and location of losses differ. The resulting groundwater budgets can be used to estimate water requirements for riparian vegetation and water availability for human needs.

The RIP-ET program will not always predict lower ET quantities, as evidenced by our second case study river. In this case, a small basin (13.51 square miles) in southern Arizona was modeled using both methods. Measured water table depths were at the lower portion of the traditional ET flux curve, and closer to the maximum rates for the species present, as modeled by RIP-ET (Figure 9). Consequently, ET estimates using RIP-ET were 37% higher than the estimates derived with the traditional method.

Discussion

Use of RIP-ET in Restoration and Conservation

Techniques such as RIP-ET, which incorporate plant-functional-group-specific transpiration curves, can aid in conservation and restoration efforts by increasing the accuracy with which we model plant-hydrology interactions. The incorporation of PFGs based on water tolerance ranges and rooting depths into the RIP-ET package provides an explicit link between groundwater and riparian/wetland habitat conditions and allows the effects of land use decisions or

increased water development on freshwater habitats to be ascertained. When this is combined with a probabilistic vegetation model, such as that developed by Rains and others (2004), changes in community types attributable to changes in groundwater/surface water regimes can be simulated.

Distinct transpiration curves for the various PFGs and the use of detailed spatial information on their distribution and elevation should improve estimates of basin-scale ET, water budgets, and environmental water needs. Ideally, incorporation of riparian ecosystem water needs into the modeling process will help to ensure that decision makers include riparian water demands as a vital component of the water budget. These estimates can then be incorporated into regional planning and conservation plans.

River rehabilitation or restoration has become a hot topic for water authorities, river managers, governmental regulators, and nature conservation groups throughout the world. In developed nations, ecosystem restoration has become (for better or worse) a major enterprise (Stromberg 2001). If restoration or conservation is to be successful, the natural hydrologic processes that govern ecosystem dynamics must operate effectively (Henry and others 2002). Knowledge of hydrology-vegetation interactions and the comparative water use characteristics of the target plant species as well as their effect on the local water balance is fundamental to the success of wetland and riparian restoration (Kolka and others 2000; Nagler and others 2003).

The RIP-ET and PRE-RIP-ET programs can help guide restoration when used as interactive tools during the planning stage. Existing or initial conditions can be used to calibrate a MODFLOW model of the area to be restored. Groundwater maps can be used to identify areas suitable initially for the target species. The groundwater levels produced by a restoration action and the effects on the proposed habitat or habitats then can be simulated using RIP-ET. If groundwater elevations do not stay within the required ranges of the desired plant groups, the plan can be altered and the model run until the simulated groundwater levels stay within appropriate ranges. The RIP-ET program also will show locations of areas that lack sufficient water resources for restoration, helping to avoid costly restoration failures.

Conservation efforts benefit by identifying and protecting key plant regeneration zones. The ability of riparian or wetland species to regenerate is imperative for ecosystem sustainability (Springer and others 1999). Regeneration of numerous riparian species requires spring floods of a characteristic intensity com-

bined with high water tables during the early summer months (Mahoney and Rood 1998; Stromberg 2001). Areas with the appropriate groundwater conditions for tree establishment (e.g., the areas mapped as small deep-rooted PFG in Figure 10) can be thought of as potential regeneration areas. To identify riparian recruitment zones, river-specific regenerative flood intensity needs to be determined and the results from a surface water model overlain on the groundwater map. These data can be coupled with models such as the "recruitment box" model (Mahoney and Rood 1998) for further enhancement of our ability to predict recruitment success and area.

The RIP-ET program also can enlighten managers regarding the potential for phreatophyte control projects to increase downstream stream flow rates. In western United States, particularly in the 1950s and 1960s, cottonwoods, willows, and other phreatophytes suspected of having very high ET rates were cleared from waterways under the guise of water salvage. Although water savings did not always materialize, water salvage efforts continue today. The primary target is tamarisk, a riparian tree/shrub species that has become a dominant species in the West since its introduction to the United States in the late 1800s. Large-scale federal efforts are underway to eliminate tamarisk stands, partly under the assumption that such efforts will enable more water to be available for direct human use (Shafroth and others 2005). Models such as RIP-ET may prove valuable in providing accurate estimates of current and projected ET rates under various scenarios of vegetation replacement, and thus in determining whether alleged water salvage benefits are realistic or have been overstated.

Conclusion

Groundwater models traditionally have been used to characterize or simulate regional groundwater systems and predict changes in groundwater attributable to anthropogenic water use. The method used to model ET rates in these groundwater models can affect the calculated water budget, the simulated depths to groundwater, and the resulting interpretations regarding riparian ecosystem dynamics. We describe an approach that should increase the accuracy of these models, primarily by incorporating more realistic plant-hydrology interaction terms into the models. When combined with vegetation mapping and GIS, these ecohydrology models further increase our ability to understand and effectively manage riparian and wetland ecosystem responses, a matter of vital concern given the present milieu of increasing societal de-

mands for freshwater. This combined approach not only increases our understanding of ecohydrologic relationships, but also helps set the framework for more detailed research on the functioning of specific systems (Batelaan and others 2003).

The Riparian Evapotranspiration Package improves on traditional groundwater modeling techniques through numerous innovations. First, it uses a modeling approach that simulates ET from riparian/wetland systems in a manner that more accurately reflects both the ecophysiology of the component plant species and habitat complexity. The single, monotonically increasing ET flux curve used in traditional modeling packages is replaced with a set of ecophysiological based curves. Each of the multiple transpiration curves reflects a particular PFG, thus capturing the inherent variability in the vegetation. For each PFG, the transpiration curve not only reflects transpiration declines at deep water levels, but also reflects declines that occur when shallow water levels produce anoxic soil conditions throughout the root zone. Furthermore, the package provides for separate representation of evaporation and transpiration, with retention of the traditional linear curve to model the evaporation process from bare soil or open water.

The Riparian Evapotranspiration Package also improves accuracy by more effectively dealing with spatial issues of plant and water table distribution. It replaces the single-cell, single ET value approach with multiple ET curves and associated fractional coverage. In other words, ET rates can now be calculated by determining the area of all plant assemblages (or habitat types) present and then applying multiple ET curves to a single model cell. When this is accompanied with RIP-GIS or PRE-RIP-ET, detailed information can be incorporated on the distribution of PFGs across land surface elevations. This effectively captures the range of ET responses across the topographic-hydrologic gradients.

The use of RIP-ET in groundwater models should result in more accurate determinations of riparian ET rates and thus of basin scale water budgets, which is of great value for water planning purposes. Depending on the attributes of the riparian ecosystem, RIP-ET may produce higher or lower ET values than traditional methods, as demonstrated through two case studies. By allowing for the quantification of riparian vegetation water requirements within a river segment, RIP-ET enables determination of environmental water needs. It also allows for predictions of riparian vegetation response to water use and development scenarios. For example, RIP-GIS links the head distribution from MODFLOW with surface digital elevation models to produce moderate- to high-resolution depth-to-

groundwater maps. These maps then can be used, together with known plant rooting depths and tolerance ranges, to predict habitat response to changes in land use or water allocation decisions. Used as an interactive tool, RIP-ET can increase the success rate of restoration projects and help avoid costly restoration failures by identifying areas with insufficient water resources to recruit or sustain target plant communities. Finally, the models can be used to simulate water budget changes expected from phreatophyte control projects, thus helping managers to determine the legitimacy of such projects.

Literature Cited

- Baird, K. J., C. A. Dragoo, and T. Maddock III. 2004. PRE-RIP-ET: A preprocessor for RIP-ET. Department of Hydrology and Water Resources, University of Arizona, Tucson, Arizona.
- Banta, E. R. 2000. MODFLOW-2000: The U.S. Geological Survey modular groundwater model: Documentation of packages for simulating evapotranspiration with a segmented function (ETS1) and drains with return flow (DRT1). U.S. Geological Survey Open-File Report 00-466 USGS, Reston, Virginia.
- Batelaan, O., F. De Smedt, and L. Triest. 2003. Regional groundwater discharge: Phreatophyte mapping, groundwater modeling, and impact analysis of land use change. *Journal of Hydrology* 275:86–108.
- Busch, D. E., N. L. Ingraham, and S. D. Smith. 1992. Water uptake in woody riparian phreatophytes of the southwestern United States: A stable isotope study. *Ecological Applications* 2:450–459.
- Cooper, D. J., D. R. D'Amico, and M. L. Scott. 2003. Physiological and morphological response patterns of *Populus deltoides* to alluvial groundwater pumping. *Environmental Management* 31:215–226.
- Dragoo, C. A., T. Maddock III, and K. J. Baird. 2004. RIPGIS user's manual: An ArcView GIS pre- and post-processor for the MODFLOW Riparian Evapotranspiration Package. Department of Hydrology and Water Resources, University of Arizona, Tucson, Arizona.
- Dyer, A. R., D. E. Goldberg, R. Turkington, and C. Sayre. 2001. Effects of growing conditions and source habitat on plant traits and functional group definition. *Functional Ecology* 15:85–95.
- Elmore, A. J., J. F. Mustard, and S. J. Manning. 2003. Regional patterns of plant community responses to changes in water: Owens Valley, California. *Ecological Applications* 13:443–460.
- Glennon, R. J., and T. Maddock III. 1994. In search of sub-flow: Arizona's futile effort to separate groundwater from surface water. *Arizona Law Review* 36(3):567–610.
- Goodrich, D. C., R. Scott, J. Qi, B. Goff, C. L. Unkrich, M. S. Moran, D. G. Williams, S. M. Schaeffer, K. A. Snyder, R. D. MacNish, T. Maddock, D. Pool, A. Chehbouni, D. I. Cooper, W. E. Eicinger, W. J. Shuttleworth, Y. Kerr, R. Marssett,

- and W. Ni. 2000. Seasonal estimates of riparian evapotranspiration using remote and in situ measurements. *Agricultural and Forest Meteorology* 105:281–309.
- Grimm, N. B., A. Chacon, C. N. Dahm, S. W. Hostetler, O. W. Lind, P. L. Starkweather, and W. W. Wurtsbaugh. 1997. Sensitivity of aquatic ecosystems to climatic and anthropogenic changes: The basin and range, American Southwest and Mexico. *Hydrological Processes* 11:1023–1041.
- Hancock, P. J. 2002. Human impacts on the stream-groundwater exchange zone. *Environmental Management* 29:763–781.
- Henry, C. P., C. Amoros, and N. Roset. 2002. Restoration ecology of riverine wetlands: A 5-year postoperation survey on the Rhône River, France. *Ecological Engineering* 18:543–554.
- Hipps, L. E., D. I. Cooper, W. Eichinger, D. G. Williams, S. M. Schaeffer, K. A. Snyder, R. Scott, A. Chehbouni, C. Watts, O. Hartogensis, J. -P. Lhomme, B. Monteny, J. -P. Brunel, G. Boulet, J. Schieldge, H. A. R. DeBruin, W. J. Shuttleworth, and Y. Kerr. 1998. A summary of processes which are connected to evaporation of riparian and heterogeneous upland vegetation in arid regions. Pages 43–48 in E. F. Wood, A. G. Chehbouni, D. C. Goodrich, D. J. Seo, J. R. Zimmerman (eds.). Proceedings from the Special Symposium on Hydrology American Meteorological Society, 11–16 January 1998. Phoenix, Arizona.
- Horton, J. L., T. E. Kolb, and S. C. Hart. 2001. Physiological response to groundwater depth varies among species and with river flow regulation. *Ecological Applications* 11:1046–1059.
- Hughes, R. M. R. 1997. Floodplain biogeomorphology. *Progress in Physical Geography* 21:501–529.
- Jarvis, P. G., and K. G. McNaughton. 1986. Stomatal control of transpiration: Scaling up from leaf to region. *Advances in Ecological Research* 15:1–49.
- Kingsford, R. T. 2000. Protecting rivers in arid regions or pumping them dry? *Hydrobiologia* 427:111.
- Kolka, R. K., J. H. Singer, C. R. Coppock, W. P. Casey, and C. C. Trettin. 2000. Influence of restoration and succession on bottomland hardwood hydrology. *Ecological Engineering* 15:S131–S140.
- Lavorel, S., S. McIntyre, J. J. Landsberg, and T. D. A. Forbes. 1997. Plant functional classifications: from general groups to specific groups based on response to disturbance. *Tree* 12:474–478.
- Maddock III, T., and K. J. Baird. 2003. A riparian evapotranspiration package for MODFLOW-96 and MODFLOW-2000. HWR No. 02-03. Department of Hydrology and Water Resources, University of Arizona Research Laboratory for Riparian Studies, University of Arizona, Tucson, Arizona.
- Maddock III, T., and L. B. Vionnet. 1998. Groundwater capture processes under a seasonal variation in natural recharge and discharge. *Hydrogeology Journal* 6:24–32.
- Mahoney, J. M., and S. B. Rood. 1998. Streamflow requirements for cottonwood seedling recruitment: An integrative model. *Wetlands* 18:634–645.
- McDonald, M. G., and A. W. Harbaugh. 1988. A modular three-dimensional finite-difference groundwater flow model. U.S. Geological Survey TWI 6-A1, 1988 USGS, Reston, Virginia.
- McDonald, M. G., and A. W. Harbaugh. 1996. Programmer's documentation for MODFLOW-96, an update to the U.S. Geological Survey Modular Finite-Difference Groundwater Flow Model. U.S. Geological Survey, Open-File Report 96-486 USGS, Reston, Virginia.
- Meinzer, F. C., J. L. Andrade, G. Goldstein, N. M. Holbrook, J. Cavellier, and P. Jackson. 1997. Control of transpiration from the upper canopy of a tropical forest: The role of stomatal layer and hydraulic architecture components. *Plant, Cell and Environment* 20:1242–1252.
- Mitsch, W. J., and R. F. Wilson. 1996. Improving the success of wetland creation and restoration with know-how, time, and self-design. *Ecological Applications* 6:77–83.
- Nagler, P. L., E. P. Glen, and G. L. Thompson. 2003. Comparison of transpiration rates among saltcedar, cottonwood, and willow trees by sap flow and canopy temperature methods. *Agricultural and Forest Meteorology* 116:73–89.
- Naiman, R. J., S. E. Bunn, C. Nilsson, G. E. Petts, G. Pinay, and L. C. Thompson. 2002. Legitimizing fluvial ecosystems as user of water: an overview. *Environmental Management* 30:455–467.
- Nienhuis, P. H., and R. S. E. W. Leuven. 2001. River restoration and flood protection: Controversy or synergism? *Hydrobiologia* 444:85–99.
- Nilsson, C., and M. Svedmark. 2002. Basic principles and ecological consequences of changing water regimes: Riparian plant communities. *Environmental Management* 30:468–480.
- Poff, N. L., J. D. Allan, M. B. Bain, J. R. Karr, K. L. Prestegard, B. D. Richter, R. E. Sparks, and J. C. Stromberg. 1997. The natural flow regime: A paradigm for river conservation and restoration. *Bioscience* 47:769–784.
- Rains, M. C., J. F. Mount, and E. W. Larsen. 2004. Simulated changes in shallow groundwater and vegetation distributions under different reservoir operations scenarios. *Ecological Applications* 14(1):192–207.
- Reilly, T. E., and A. W. Harbaugh. 2004. Guidelines for evaluating groundwater flow models: U.S. Geological Survey Scientific Investigations Report 2004-5038 USGS, Reston, Virginia.
- Richter, B. D., J. V. Baumgartner, R. Wigington, and D. P. Braun. 1997. How much water does a river need?. *Freshwater Biology* 37:231–249.
- Richter, B. D., and H. E. Richter. 2000. Prescribing flood regimes to sustain riparian ecosystems along meandering rivers. *Conservation Biology* 14:1467–1478.
- Romero D. M., and T. Maddock III. 2003. MODFLOW: A finite-difference groundwater flow model or an integrated finite-difference groundwater flow model? in E. Poeter, C. Zheng, M. Hill (eds.). MODFLOW and More 2003: Understanding through modeling. International Ground Water Modeling Center, 16–19 September 2003. Colorado School of Mines, Golden, Colorado. pp 116–120.
- Schaeffer, S. M., D. G. Williams, and D. C. Goodrich. 2000. Transpiration of cottonwood/willow forest estimated from sap flux. *Agricultural and Forest Meteorology* 105:257–270.

6.3 Rip-ET Evapotranspiration Users Manual

A RIPARIAN EVAPOTRANSPIRATION PACKAGE FOR MODFLOW-96 AND MODFLOW-2000

By
Thomas Maddock III
And
Kathryn J. Baird

Department of Hydrology and Water Resources
University of Arizona Research Laboratory for Riparian studies
University of Arizona
Tucson, Arizona 85721

December 2003

Table of Contents

Table of Contents	ii
Figures	iii
Tables	iii
Aknowledgements	v
Abstract	vi
1.0 Introduction	1
2.0 Plant Functional Groups	2
3.0 Plant Functional Subgroups	3
4.0 ET Flux Rate Curves	4
5.0 ET Flux Rate Curve Linear Interpolation	5
6.0 Plant Coverage	8
6.1 Fraction of active habitat	8
6.2 Fraction of a subgroup in the cell	8
6.3 Fraction of plant canopy or flux area	9
7.0 Fractional Coverage	10
8.0 Alternative approaches	10
9.0 Land Surface Elevations	10
10.0 ET Calculations	11
11.0 Summary	13
12.0 Input Instructions for Riparian Package	13
13.0 Explanation of Variables Read by the RIP Package	14
14.0 Example	16
14.1 Data Sets For Example	19
14.2 Riparian Data Set	21
14.3 Abridged Results	23
15.0 Module Documentation for the Riparian Package	26
15.1 RIP2AL	27
15.2 Listing for RIP2AL Module	28
15.3 RIP2RP1	32
15. 4 Listing for RIP2RP1 Module	32
15.5 RIP2RP2	34
15.6 Listing for RIP2RP2 Module	34
15.7 RIP2FM	37
15.8 Listing for RIP2FM Module	38
15.9 RIP2BD	41
15.10 Listing for RIP2BD Module	42

15.11 HCOFtrm and RHStrm	46
15.12 Listing for HCOFtrm and RHStrm Functions.....	46
16.0 References	48
Appendix A, Plant Functional Subgroup Curves	50
Appendix B, Adapting RIP-ET to MODFLOW-2000.....	55

Figures

Figure 1: Average ET flux rate curves for four plant functional groups:	4
Figure 2: Generic ET flux rate curve.....	5
Figure 3: Hypothetical segmented ET flux cure	6
Figure 4: Linear interpolation of ET flux—d's	6
Figure 5: Linear interpolation of ET flux—dR's.....	6
Figure 6: Area of active habitat in a cell	8
Figure 8: Area associated with plant functional subgroup.....	9
Figure 8: Area associated with canopy.....	9
Figure 9: Average surface elevation and actual habitat surface elevation.....	11
Figure 10: Aerial view of Dry Alkaline Valley.....	16
Figure 11: Seasonal canopy-area ET curves for the three size classes.....	17
Figure 12: Traditional MODFLOW flux curve for evaporation.....	18
Figure A1: ET flux rates for Obligate wetlands.....	50
Figure A2: ET flux rates for Shallow-rooted riparian PFG.....	51
Figure A3: ET flux rates for Average deep-rooted riparian PFG.....	52
Figure A4: ET flux rates for Transitional riparian PFG.....	53
Figure A5: ET flux rates for small, medium, large and X-large deep-rooted riparian PFG	54

Tables

Table 1: Illustrative PFSG composed of plant functional groups, size or density.....	3
Table 2: Fractional coverage for plant functional subgroups per model cell.....	17
Table 3: Vertices for the ET rate flux functions (cm/day) for the deep rooted riparian subgroups.....	18
Table 4: Dimensionless fdh and fdR for deep rooted riparian subgroups.....	18
Table 5: List of variables in module RIP2AL.....	31
Table 6: List of variables in module RIP2RP1.....	34
Table 7: List of variables in module RIP2RP2.....	37
Table 8: List of variables in module RIP2FM.....	41
Table 9: List of variables in module RIP2BD.....	45
Table 10: List of variables in functions HCOFtrm and RHStrm.....	47
Table A1: Head, ET flux rates for Obligate wetland PFG.....	50

Table A2: <i>fdhs</i> and <i>fdRs</i> for Obligate wetland PFG	50
Table A3: Head, ET flux rates for Shallow-rooted riparian PFG	51
Table A4: <i>fdhs</i> and <i>fdRs</i> Shallow-rooted riparian PFG	51
Table A5: Head, ET flux rates for average Deep-rooted riparian PFG	52
Table A6: <i>fdhs</i> and <i>fdRs</i> for average Deep-rooted riparian PFG	52
Table A7: Head, ET flux rates for Transitional PFG	53
Table A8: <i>fdhs</i> and <i>fdRs</i> for Transitional PFG	53
Table A9: Head, ET flux rates for Deep-rooted riparian size classes	54
Table A10: <i>fdhs</i> and <i>fdRs</i> for Deep-rooted riparian size classes	54

Acknowledgements

This research was supported in part by two grants. The first was an EPA-NSF Star Grant entitled "Restoring and Maintaining Riparian Integrity in Arid Watersheds," number R827150/01, which funded field experiments in the South Fork of the Kern River in California and the San Pedro River in Arizona. The second was an NCEA Global Change Division CO-OP Agreement entitled "Potential Effects of Climate Change on Biodiversity and Riparian Wildlife Habitat of the Upper San Pedro River," which funded development of this software package. The views and conclusions contained in this document are those of the authors and should not necessarily be interpreted as representing official policies, (expressed or implied) of the EPA or NCEA.

We would like to thank our fellow grantees Julie Stromberg, Robert Glennon, and Bonnie Colby, who worked with us on the EPA-NSF project, and Jeff Price and again Julie Stromberg, who, worked with us on the NCEA project. A thank you also to our colleagues Bob MacNish, Phil Guertin, David Goodrich, Jim Shuttleworth, Paul Brooks and Ty Ferre. Thanks to the students that worked at the Kern River site: Asia Philben, Tom D. Maddock, Phil Bredfelt, Clair Tomkins and Chris Adams; and the students who worked at the tree torture site along the San Pedro River: Marla Odum, Kathleen McHugh, Asia Philben, Gerd Von Gliński, and Tom D. Maddock. We gratefully acknowledge the Palominas Trading Post without whose support, the San Pedro project could not have been completed. Thanks also to Reed Tollifson and Jeff King at the Audubon Kern River Preserve, and a special thank you to Carolyn Dragoo for her assistance and support.

A special thanks to Arlen W. Harbaugh for providing expertise to create a MODFLOW-2000 version of RIP-ET that is presented in Appendix B.

Abstract

A new evapotranspiration package for the U.S. Geological Survey's groundwater-flow model, MODFLOW, is documented. The Riparian Evapotranspiration Package (RIP-ET), provides flexibility in simulating riparian and wetland evapotranspiration (ET) not provided by the MODFLOW-96 Evapotranspiration (EVT) Package, nor by the MODFLOW-2000 Segmented Function Evapotranspiration (ETS1) Package. This report describes how the package was conceptualized and provides input instructions, listings and explanations of the source code, and an example simulation.

Traditional approaches to modeling ET processes assume a piecewise linear relationship between ET flux rate and hydraulic head. The Riparian ET Package replaces this traditional relationship with a segmented, nonlinear dimensionless curve that reflects the eco-physiology of riparian and wetland ecosystems. Evapotranspiration losses from these ecosystems are dependent not only on hydraulic head but on the plant types present. User-defined plant functional groups (PFGs) are used to elucidate the interactive processes of plant ET with groundwater conditions. Five generalized plant functional groups based on transpiration rates, plant rooting depth, and drought tolerance are presented: obligate wetland, shallow-rooted riparian, deep-rooted riparian, transitional riparian and bare ground/open water. Plant functional groups can be further divided into subgroups (PFSG) based on plant size and/or density.

The Riparian ET Package allows for partial habitat coverage and mixtures of plant functional subgroups to be present in a single model cell. This requires a determination of fractional coverage for each of the plant functional subgroups present in a cell to simulate the mixture of coverage types and resulting ET. The fractional cover within a cell has three components: 1) fraction of active habitat, 2) fraction of plant functional subgroup in a cell, and 3) fraction of plant canopy area. The Riparian ET package determines the ET rate for each plant functional group in a cell, the total ET in the cell, and the total ET rate over the region of simulation.

1.0 Introduction

The physical settings and dynamic processes of streams have changed dramatically over the past century (Stromberg, 2001). In the southwestern United States, many of the characteristic desert riparian habitats of cottonwood-willow galleries, cienegas and mesquite bosques that once lined the rivers are degrading and disappearing or have disappeared (Glennon and Maddock, 1994). The dynamics of riparian and wetland ecosystems are closely tied to groundwater and streamflow hydrology (Busch et al., 1992; Grimm et al., 1997). The pattern and quantity of surface and subsurface flows are the primary determinants of riparian ecosystem structure and function, while depth to groundwater and its rate of decline place important constraints on the distribution and vigor of different riparian vegetation types (Stromberg et al., 1996; Poff et al., 1997; Shafroth et al., 2000). Water is often the principle limiting resource for these critical systems, with surface water diversions and groundwater extractions greatly contributing to habitat degradation and loss (Stromberg, 1993).

Riparian and wetland systems contain a disproportionate share of regional biodiversity and play a dominant role in the regional water and energy balance, especially in arid and semi-arid regions (Williams et al., 1998). If these ecologically significant systems are to be preserved, the remaining systems and water resources must be carefully managed. Reliable and accurate methods for preserving and restoring these systems are essential. Regional groundwater models are a promising tool. However, if regional groundwater models are to be used, accurate estimates of boundary conditions are required. One of the most critical but poorly quantified groundwater boundary condition is seasonal riparian evapotranspiration (Goodrich et al., 2000). When modeling the flow in these systems, the method by which ET is simulated can affect calculated heads and thus the interpretations regarding system dynamics (Banta, 2000).

In the present state of groundwater modeling, both the stream and evapotranspiration are modeled as annual source terms (but are actually boundary conditions that have been converted to source terms). Traditionally, the ET source term is treated as head-dependent in a piecewise linear fashion that monotonically approaches a maximum ET rate. While this quazi-linear relationship may hold true for evaporation, it does not accurately reflect the relationship between riparian transpiration and groundwater conditions. Furthermore, ET processes generally vary seasonally and between plant types, making it necessary to determine seasonal variations and type. To improve the ability to determine riparian evapotranspiration (ET) and predict ecosystem response to changing environmental conditions, we developed Riparian ET (RIP-ET) packages for MODFLOW-96 (Harbaugh and McDonald, 1996) and MODFLOW-2000 (Harbaugh et al., 2000), which attempts to simulate evapotranspiration from the water table that lies beneath riparian/wetland systems in a manner that reflects their ecology and physiology. The MODFLOW-96 source codes are presented in the main body of this report and the conversion from MODFLOW-96 to MODFLOW-2000 is presented in an appendix.

2.0 Plant Functional Groups

Riparian and wetland ecosystems are composed of a variety of plant types and species. The identification and use of plant functional groups can assist in reducing the enormous complexity of individual species and populations into a relatively small number of general recurrent patterns. This technique has emerged as a useful way to organize plant species that have similar impacts on ecosystem processes into manageable and meaningful categories (Leishman and Westoby, 1992; Williams et al., 1998). Plant functional groups are defined as non-phylogenetic groupings of plant species that exhibit similar responses to environmental conditions and have similar effects on the dominant ecosystem processes (Lavorel et al., 1997). In the Riparian ET package, we use plant functional groups to elucidate the interactive processes of plants (and plant ET) with groundwater conditions. The model is designed to be flexible, with the user determining which sets of plant functional groups are appropriate for the simulation and geographic region of the riparian/wetland system to be modeled.

In the development of the Riparian ET Package, we defined five basic functional groups based on transpiration rates and processes, plant rooting depth, and drought tolerance. While the groups presented here are for semi-arid environments, the methodology can be applied universally. The generalized plant functional groups are: obligate wetland, shallow-rooted riparian, deep-rooted riparian, transitional riparian, and bare ground/open water. The last category, while not a plant functional group, must be included to accurately model evapotranspiration from the cell or active modeling area.

The obligate wetland plant functional group contains plants that require saturated soil conditions or standing water. Throughout most of the U.S., species in this category are herbaceous and have generally shallow root systems. In the southwestern U.S., species such as *Typha* spp. (cattail), *Scirpus* spp. (bulrush) and *Juncus* spp. (rushes) typify this group.

Riparian forests are composed of drought-intolerant phreatophytes that rely on shallow groundwater for establishment, growth and transpiration (Busch et al., 1992; Stromberg, 1993; Snyder et al., 2000). Due to the difference in rooting depths and transpiration rates, shallow-rooted and largely herbaceous riparian species (such as *Xanthium* sp. [cocklebur] and *Rumex crispus* [curly dock]) are categorized separately from and deep-rooted riparian plants such as *Populus* spp. (cottonwoods), and *Salix* spp. (willows). In some cases, multiple deep-rooted categories may be useful, depending upon the species present. For example, this refinement allows the distinction of *Prosopis velutina* (bosque mesquite trees) from cottonwood and willows. Neither the shallow nor the deep-rooted riparian group tolerates saturated conditions for extended periods of time.

The last plant functional group, transitional (or facultative) riparian, consists of species that while not strictly dependent upon a high water table, have water requirements that generally exceed the surrounding environment. These species generally exist along the outer edges of riparian systems and include *Sporobolus Wrightii* (sacaton), *Sambucus* sp. (elderberry), *Juglans* spp. (walnut), *Celtis* sp. (hackberry) and *Platanus* sp. (sycamore).

The evapotranspiration rates and range of groundwater elevations over which these groups exist differ for each plant functional group.

3.0 Plant Functional Subgroups

Plant size and density also play roles in determining evapotranspiration rates. Large woody plants have different maximum rooting depths, hydraulic architecture and transpiration rates than smaller trees (Meinzer et al., 1997). Furthermore, areas with dense configurations of both woody and herbaceous plants may show increased transpiration rates compared to sparse configurations. Taken together, the plant functional group and plant size or density comprise a plant functional subgroup (PFSG). Examples of possible plant functional subgroups are: transitional riparian-large or wetlands-medium density. Table 1 presents the possible plant functional subgroups for this example. This table is by no means exhaustive and is meant to be illustrative.

Table 1. Illustrative subgroupings for plant functional groups, by size and density.

Plant Group	Size	Densities	Species Examples
Obligate Wetland	N/A	Low, medium, high	Cattail, Bulrush
Shallow-rooted Riparian	N/A	Low, medium, high	Curly dock, Cocklebur, Deer grass
Deep-rooted Riparian	Small, medium, large	Low, medium, high	Cottonwood, Willow, Mesquite (bosque)
Transitional Riparian	Small, medium, large	Low, medium, high	Walnut, Hackberry, Sacaton, Sycamore

Evapotranspiration rates and the range of groundwater elevations over which these groups exist differ for each plant functional group (Fig. 1). Streamside riparian corridors typically consist of multiple plant functional subgroups, each reacting differently to the hydrologic conditions. A deeper water table may be ideal for a transitional riparian group, but near fatal to a wetland or herbaceous, shallow-rooted group. Similarly, a high water table conducive to a wetland group may drown out the trans-riparian. Even so, it is quite likely that a MODFLOW cell covering a riparian system will comprise a number of compatible plant functional groups. Thus, the evapotranspiration loss from a riparian/wetland system is dependent on the plant functional subgroups present and on the groundwater depth. Furthermore, as the region near the riparian system is urbanized, results of that development (such as increased groundwater pumping) may affect each group differently.

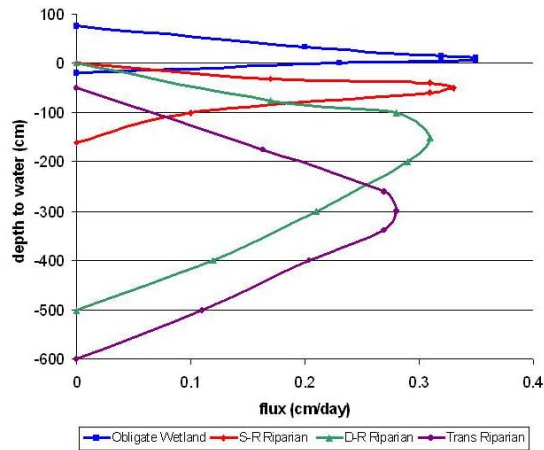


Figure 1: Average ET flux rate curves for four plant functional groups: obligate wetland, shallow rooted (S-R) riparian, deep-rooted (D-R) riparian and transitional (Trans) riparian.

4.0 ET Flux Rate Curves

The ET rate per area is called the ET flux rate. Due to differences in sensitivity to water availability and rooting depth, ET flux rates in plant species and thus in the subgroups vary with groundwater depths. Based on a literature review, field measurements and researcher input, preliminary ET flux rate curves were developed for the basic set of plant functional groups (Fig. 1), and for three deep-rooted riparian subgroups (Fig. 11) (Baird and Maddock, in preparation). These curves provide the ET flux rate as a function of water table conditions (or hydraulic head).

Figure 2 illustrates a representative ET flux rate curve. For each plant functional subgroup there is a water table elevation or extinction depth elevation (H_{xd} in Fig. 2) below which the roots can not obtain water and ET is nonexistent. When the water table rises and water becomes available to the root system, the ET rates rise until they reach an average maximum ET flux (R_{max}). At higher water table elevations, the root systems become oxygen deficient and ET rates decline until the plants die of anoxia. The water table elevation associated with plant death is the saturated extinction depth elevation (H_{sxd} in Fig. 2). The decrease in ET flux rates resulting from high water tables has not been considered in previous MODFLOW Evapotranspiration Packages (McDonald and Harbough, 1988; Harbough and McDonald, 1996; Banta, 2000). Although Figure 2 shows H_{sxd} below the land surface elevation, it need not be; it can be at, or above the land surface elevation for some subgroups. For example, some wetland species may tolerate as much as a meter of standing water above the land surface.

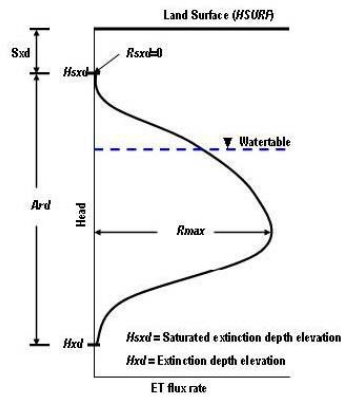


Figure 2: Generic ET flux rate curve

The distance between the two extinction depths is called the active root zone depth (Ard). The saturated extinction depth (Sxd) is measured with respect to the land surface elevation, $HSURF$. If $Hsxd$ is below the land surface elevation, Sxd is positive; if it is above, Sxd is negative. Since everything is relative to the land surface elevation, $HSURF$, the following relations hold:

and

$$Hsxd = HSURF - Sxd$$

$$Hxd = Hsxd - Ard$$

The user of the Rip package inputs the name ($RIPNM$) and the values of Sxd and Ard for each plant functional subgroup. The user also inputs the maximum ET flux rate ($Rmax$) and the ET flux rate at $Hsxd$ ($Rsxd$) for each plant functional subgroup. These values must be in units consistent with the MODFLOW simulation. The maximum ET flux rate ($Rmax$) is the measured average head-dependent ET rate, not a measured peak ET rate. For plants that have a saturated extinction depth, $Rsxd = 0$. For bare ground or open water, $Rsxd$ equals the evaporation rates, and a shallow, more appropriate, extinction depth should be applied.

5.0 ET Flux Rate Curve Linear Interpolation

The Riparian ET Package does not use the continuous curve of Fig. 2, but instead uses an approximation based on linear segments as illustrated in Fig. 3. The ET flux rates reported in the literature are in various sets of units (e.g. cm/sec, feet/day, liters/day, kg/(m²-sec); the latter units need to be adjusted by the density of water to be dimensionally correct). To help alleviate problems that might occur with a particular choice of units, the curve segments are read into the RIP as dimensionless. They are converted during the simulation to units consistent

with other MODFLOW packages based on the units of Rmax and Ard. The Rmax (L/T) and Ard (L) units must match the length and time units used elsewhere in the simulation.

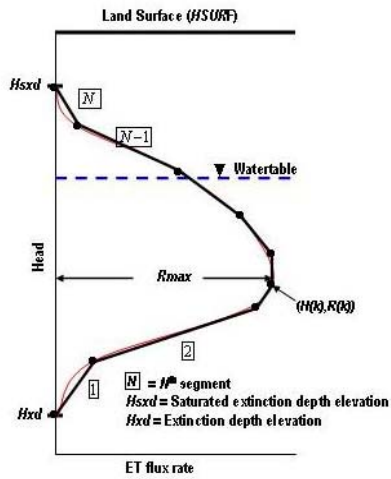


Figure 3: Hypothetical segmented ET flux curve.

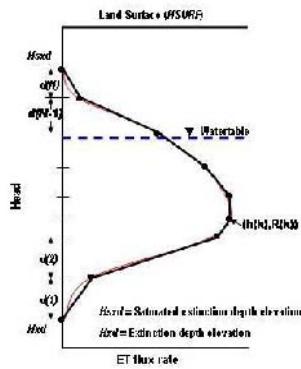


Figure 4: Linear interpolation of ET flux: d's

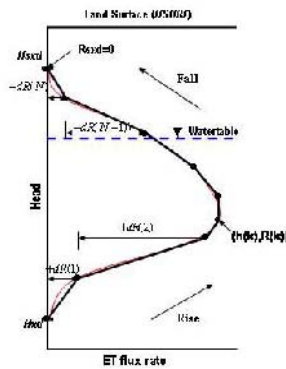


Figure 5: Linear interpolation of ET flux: dR's

The process for producing the dimensionless segmented curves is conducted externally to the RIP package by the user, and proceeds as follows. Figures 4 and 5 present the hypothetic, segmented ET

flux rate curve. Segments are defined by vertices $h(k)$, and $R(k)$ and are determined by the shape of the curve. In Fig. 4, $d(1)$, $d(2)\dots d(n)$, are in length units and represent the change in head over a segment, while in Fig. 5, $dR(1)$, $dR(2)\dots dR(n)$ are in flux rate units and represent the change in flux over a segment. The indices and segments must start at the extinction depth. If $h(1)$ and $R(1)$ are the head and the ET flux rate at the extinction depth; and $h(2)$ and $R(2)$ are the head and ET flux rate at the end of the first segment, then the d 's and dR 's are defined as, $d(1) = h(2) - h(1)$

and

$$dR(1) = R(2) - R(1)$$

In general, for N segments and $1 \leq k \leq N$, where the numbering of k moves upward toward the saturated extinction depth,

$$d(k) = h(k+1) - h(k)$$

and

$$dR(k) = R(k+1) - R(k)$$

For a functional subgroup, one must define the following dimensionless segment variables,

$$fdh(k) = \frac{d(k)}{Ard}$$

and

$$fdR(k) = \frac{dR(k)}{Rmax}$$

Note that for the N segments,

$$\sum_{i=1}^N fdh(i) = 1$$

and

$$\sum_{i=1}^N fdR(i) = \frac{R_{sxd}}{Rmax}$$

In Fig. 4, $R_{sxd} = 0$, but, as previously mentioned, R_{sxd} can be non-zero for other curves such as the curve for open water. Within a simulation, $fdh(k)$ and $fdR(k)$ are known constants for each plant functional subgroup, and when multiplied by Ard and $Rmax$ in their appropriate units, the segment variables $d(k)$ and $dR(k)$ are recovered.

The number of segments ($NuSeg$) for each plant functional subgroup, and the dimensionless segment variables ($fdh(k)$ and $fdR(k)$) are input for each segment and each plant functional subgroup by the RIP package user.

Values for $NuSeg$, $fdh(k)$ and $fdR(k)$ for four of the plant functional groups and three deep-rooted riparian size classes can be found in Appendix 1.

6.0 Plant Coverage

The use of this package requires having information about the distribution of the plant functional subgroups within the active modeling areas. Not all of the MODFLOW cell is likely to contain active riparian or wetland habitat, nor is a cell likely to contain all of the possible plant functional subgroups. Furthermore, the amount of canopy coverage (or coverage of flux area) may change from cell to cell. The Riparian ET Package requires a fractional coverage for each of the plant functional subgroups present for a cell to simulate the mixture. For bare areas not supported by shallow water tables, ET rates can be excluded from the cell area or assigned flux rates of zero (e.g. the non-habitat area in Fig. 6). The fractional cover within a cell has three components: 1) fraction of active habitat, 2) fraction of plant functional subgroup, and 3) fraction of plant canopy or flux area.

6.1 Fraction of active habitat

The fraction of active habitat refers to the fraction of the cell that contains wetland or riparian habitat. Since cell sizes in MODFLOW may be quite large (e.g., square kilometer), only a fraction of cell will contain the habitat (see Fig. 6). The fraction of active habitat (f_{AH}) is defined as

$$f_{AH} = \frac{\text{area of active habitat}}{\text{area of cell}}$$

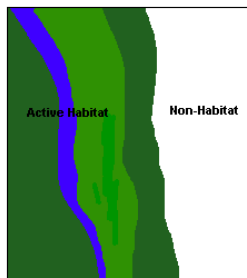


Figure 6: Area of active habitat in a cell

6.2 Fraction of a subgroup in the cell

The active habitat area in a cell may be composed of a variety of plant functional subgroups (see Fig. 7). The fraction of j^{th} plant functional subgroup is defined as

$$fSG(i) = \frac{\text{area subgroup } i}{\text{area of active habitat}}$$

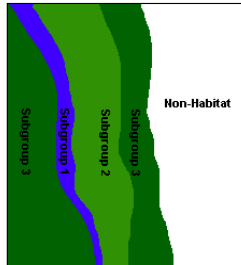


Figure 7: Area associated with plant functional subgroups

6.3 Fraction of plant canopy or flux area

Within any habitat, plant functional subgroup canopy or plant cover rarely equals 100 percent (Fig. 8). Percent canopy or plant cover may vary, depending on habitat type and resource availability. To accurately determine ET the area of canopy cover or plant cover is required, as most flux rates are evaluated on canopy or plant cover. Note that for open water areas the fraction of plant coverage is equal to one. The fraction of plant coverage is defined as

$$fPC(i) = \frac{\text{canopy area for subgroup } i}{\text{area subgroup } i}$$

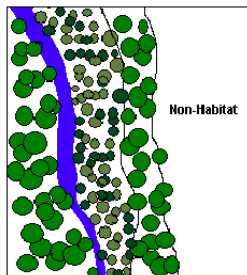


Figure 8: Area associated with canopy

7.0 Fractional Coverage

The fractional coverage of the i^{th} plant functional subgroup in a cell ($fCov(i)$) is given by the equation,

$$fCov(i) = fAH \times fSG(i) \times fPC(i)$$

The components of fractional cover can be determined using a combination of GIS techniques, aerial photography and ground verification. Along with the RIP package, a GIS preprocessor has been developed to guide the user through the process of quantifying these components for those with ARC-VIEW capabilities (Dragoo, Maddock, and Baird, in preparation). The fractional covers ($fCov$) are input into the RIP package for each plant functional subgroup for each cell. If a plant functional subgroup is not present in a cell, its fraction is entered as zero. Fractional cover has not been included as a variable in previous MODFLOW Evapotranspiration packages.

8.0 Alternative approaches

Woody plant transpiration (deep-rooted riparian and transitional riparian trees) can be estimated from measured xylem sap flux of individual trees, based on a variety of scaling approaches. A common approach to scale flux measurements to stand-level water use, relies on obtaining mean flux and a mean canopy-to-sapwood area ratio at the population level (Oren et al., 1999; Granier et al., 2000),

$$Canopy\ flux = \frac{Xylem\ flux \times Xylem\ area}{Canopy\ area}$$

The approach described in the previous analysis is based on canopy area and canopy flux.

A similar approach relies on the relationship of sapwood to tree diameter at breast height (DBH) or tree basal area. In this instance, the head dependent flux is multiplied by the fraction of basal area per subgroup area. If ET flux rates are measured as a flux per tree or tree within a size class, then the scaling factor should be density (i.e., number of trees) per unit area rather than coverage area. The RIP package can accommodate multiple approaches. The user is free to apply any approach as long as $Rmax$ and subsequent flux curves match the applied scaling factor.

9.0 Land Surface Elevations

Within the model area, the land surface elevation ($HSURF$) will vary from cell to cell. It may also vary within a cell. The magnitude of this change is important. If $HSURF$ varies on the same order of magnitude as the extinction depths within the cell, the ET calculations will be affected. The user has an option of either assigning a single $HSURF$ for the average surface elevation of the cell, or assigning an $HSURF$ value for each plant functional

group within a cell. If a single value of $HSURF$ is used, the average surface elevation of the cell is used to calculate Hxd (see Fig. 9). If $HSURF$ is assigned for each plant functional subgroup, the actual surface elevation of the habitat within the cell is used to calculate Hxd . If the terrain relief is small, the user is advised to set $HSURF$ to the single average surface elevation value. Furthermore, where there is considerable terrain relief within cells (as in Fig. 9), the user should consider a denser MODFLOW grid. It should be noted that the MODFLOW model assumes that the water table elevation is constant within the cell boundary.

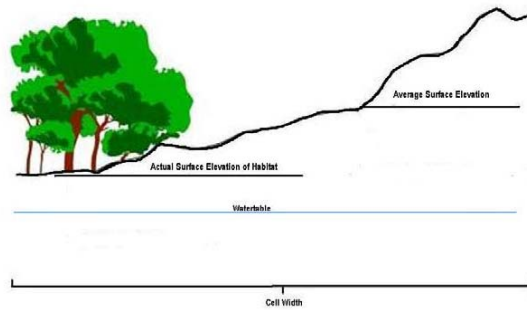


Figure 9: Average surface elevation and actual habitat surface elevation

10.0 ET Calculations

Consider a plant functional subgroup present in a cell. If $(h(k), R(k))$ and $(h(k+1), R(k+1))$ are the coordinates of consecutive vertices that define the k^{th} segment for that plant functional subgroup, and if H is the hydraulic head in the cell, then the ET flux rate for the subgroup, $R(H)$ is given by

$$R(H) = R(k) + \frac{H - h(k)}{h(k+1) - h(k)} (R(k+1) - R(k)) \quad \text{for } h(k) \leq H \leq h(k+1),$$

(Hadley, 1964). The initial values are the extinction depth values (Hxd in Fig. 3),

$$h(1) = Hxd = HSURF - Sxd - Ard$$

and

$$R(1) = 0$$

The higher k valued vertices are given by

$$h(k+1) = h(k) + fdh(k) \times Ard$$

and

$$R(k+1) = R(k) + fdR(k) \times Rmax .$$

To calculate the volumetric ET rate, $R(H)$ is multiplied by the cell area $[DEL C \times DEL R]$ and the fractional coverage, $fCov$, that is

$$ET(H) = R(H) \times [DEL C \times DEL R] \times fCov$$

$R(H)$ can be rewritten,

$$R(H) = \frac{R(k+1) - R(k)}{h(k+1) - h(k)} H + \frac{R(k)h(k+1) - R(k+1)h(k)}{h(k+1) - h(k)} \quad \text{for } h(k) \leq H \leq h(k+1).$$

A portion of $R(H)$ is dependent on the hydraulic head, H (first term), while the other portion is independent of hydraulic head (second term). Define $C1$ as the head dependent term adjusted for area, and $C2$ as the head independent term, also adjusted for area,

$$C1 = \frac{R(k+1) - R(k)}{h(k+1) - h(k)} \times [DEL C \times DEL R] \times fCov$$

$$C2 = \frac{R(k)h(k+1) - R(k+1)h(k)}{h(k+1) - h(k)} \times [DEL C \times DEL R] \times fCov$$

both for $h(k) \leq h \leq h(k+1)$. In the RIP package module RIP2FM, the variable $C1$ is loaded into the MODFLOW HCOF array, and $-C2$ (negative value) is loaded into the MODFLOW RHS array.

The above calculations are repeated in the formulation module, RIP2FM, for each plant functional subgroup present in a cell, and for each cell designated as containing habitat. The budget module RIP2BD, calculates, prints and stores the volumetric ET rate for a plant functional subgroup as

$$ET(h) = C1 \times h + C2$$

The volumetric ET rate can be summed over plant functional subgroups to give the total volumetric ET rate within a cell, and further summed over the cells to give a global value of the volumetric ET rate within the modeled region.

11.0 Summary

Traditional approaches to modeling ET processes within a groundwater model assume a piecewise linear relationship between the ET flux rate and hydraulic head (McDonald and Harbaugh, 1988; Harbaugh and McDonald, 1996a and 1996b; Banta 2000). These approaches are problematic in several ways. First, ET flux rates in plant species or PFSG vary with groundwater depths due to differences in rooting depths and plant physiology. Second, no allowance is made for a reduction in ET due to prolonged anoxic conditions. The methodology and Riparian ET Package presented here replaces the traditional linear relationship with a nonlinear dimensionless curve that reflects the ecophysiology of riparian and wetland plants.

The complex structure of wetland and riparian plant communities are simplified into a workable set of plant functional groups. While the groups presented here are for semi-arid environments, the methodology can be applied universally. The five plant functional groups presented in this report are: obligate wetlands, shallow-rooted riparian, deep-rooted riparian, transitional riparian and bare soil/open water. The groups can be further divided into subgroups based on plant size or density. Each subgroup has an ET flux curve that relates ET flux to water table elevation. A key characteristic of these flux curves is the existence of a saturated extinction depth along with the more traditional MODFLOW extinction depth, with the distance between them referred to as the active root depth. The ET flux curves are represented by a series of dimensionless, linear segments based on measured or approximated ET values.

RIP ET requires a fractional coverage for each of the plant functional subgroups present within the groundwater model cell. A MODFLOW cell from the finite difference formulation may contain several plant functional subgroups within its boundaries. Typically, not all of a cell contains habitat and only a portion of the habitat area has canopy or flux coverage. The fraction of habitat area within the cell, the fraction of PFSG area within the habitat, and the canopy or flux area within the PFSG constitute the fractional plant coverage within a cell. The product of PFSG's ET flux rate times the plant coverage times the surface area of the cell gives the PFSG's ET rate for the cell. Summing over the PFSG in the cell gives the ET rate for that cell; summing over all the riparian cells gives the global ET rate for the modeled region. The combination of physically based ET curves and plant coverage estimates provides more accurate estimates of riparian evapotranspiration and improves the modeling results. Directly linking groundwater conditions and plant functional groups offers the opportunity to better manage and restore these important ecosystems.

12.0 Input Instructions for Riparian Package

Input to the Riparian (RIP) Package is read from the file that has type "RIP" in the name file. The optional variable is shown in brackets. All variables are free format if the option "FREE" is specified in the BASIC Package input file; otherwise, variables have 10-character fields, or are specified.

FOR EACH SIMULATION

1. MAXRIP IRIPCB IRIPCB1 IHSURF [Option]
2. MAXTS MXSEG

Variables 3 are read for each plant functional subgroup.

3. RIPNM Sxd Ard Rmax Rxd NuSeg

The following sets of variables (4, and 5) are read for each plant functional subgroup

4. fdh(MAXTS,1) fdh(MAXTS,2) ... fdh(MAXTS,MXSEG)
5. fdR(MAXTS,1) fdR(MAXTS,3) ... fdR(MAXTS,MXSEG)

FOR EACH STRESS PERIOD

6. ITMP
7. The following data are read for each riparian cell.
If IHSURF = 0,
Layer Row Column HSURF fCov(1) fCov(2) ... fCov(MAXTS)

If IHSURF ≠ 0
Layer Row Column HSURF(1) fCov(1) HSURF(2) fCov(2) ... HSURF(MAXTS) fCov(MAXTS)

13.0 Explanation of Variables Read by the RIP Package

MAXRIP is the maximum number of riparian cells over all stress periods

IRIPCB is a cell-by-cell flow flag and unit number.

IRIPCB>0, unit number to which the total ET rate for each cell will be written when SAVE BUDGET or a non-zero value of ICBC is specified in output control.

IRIPCB=0, cell-by-cell terms not written

IRIPCB<0, the ET rate for each plant functional subgroup will be written to the LIST file by cell when SAVE BUDGET or a non-zero value of ICBCFL is specified in output control.

IRIPCB1 is a flag and unit number.

IRIPCB1>0, unit number to which the location, land surface elevation, ET rates for each plant functional subgroup and cell are saved.

IRIPCB1≤0, the values are not saved.

IHSURF is a flag to indicate that a single value of HSURF is read for a cell or multivalued (one for each active plant functional subgroups) are read for a cell.

[Option] is an optional character set, "CBCALLOCATE" or "CBC", that indicates memory should be allocated to store the total ET rate for each riparian cell.

MAXTS is the total number of plant functional subgroups. At present, MAXTS is maxed at 20.

MXSEG is the maximum number of segments in any plant functional subgroup for the interpolation of ET canopy flux rate as a function of hydraulic head.

RIPNM are the plant functional subgroup names, such as:

Obligate wetland: low, medium or high density

Shallow-rooted riparian: low, medium, or high density

Deep-rooted riparian: small, medium, or large size

Transitional-riparian: small, medium, or large size.

RIPNM is character*24 array and is dimensioned [20] (i.e., up to 20 plant functional subgroup names are allowed and a name can consist of up to 24 characters).

Sxd is the saturated extinction depth with respect to the surface elevation, and is dimensioned [MAXTS].

ARD is the active root depth, and is dimensioned [MAXTS].

Rmax is the maximum ET flux rate, and is dimensioned [MAXTS].

Rssd is the ET canopy flux rate at the saturated extinction depth, and is dimensioned [MAXTS].

NuSeg is the number of active segments to perform a linear interpolation for a plant functional subgroup, and is dimensioned [MAXTS].

Fdh is the active root depth segment factor, and is dimensioned [MAXTS, MXSEG].

fdR is the ET flux rate segment factor, and is dimensioned [MAXTS, MXSEG].

Layer is the layer number of the riparian cell.

Row is the row number of the riparian cell.

Column is the column number of the riparian cell.

HSURF is the land surface elevation of the riparian cell.

fCov is the fraction of land coverage of a plant functional subgroup for a cell; for each cell there is one value for each plant functional subgroup.

The values of Layer, Row, Column, and HSURF and the values of fCov are contained in the RIP array. If the CBC option is taken, the riparian cell aggregated ET rate is also stored in RIP.

ITMP is a flag or the number of riparian cells.

≥ 0 , number of riparian cells active during the current stress period.

< 0 , same riparian cells active during last stress period will be active during the current stress period.

14.0 Example

Dry Alkaline Valley extends over 200 square miles and is bounded to the north and south by mountain ranges that act as no-flow boundaries. The basin is underlain by a single unconfined aquifer with the hydraulic conductivity distribution and pertinent geometry given in Exmpl.bcf. A large lake to the northwest behaves hydrologically as a prescribed head boundary, and is the source of the river that transects the basin from west to east. The basin and the river both discharge to the east. Riparian habitats flourish along portions of the river (see Fig. 10). Dry Alkaline Valley has two seasons: a growing season from April to September and a dormant season from October to March. The stream inflow from the lake is assumed to be the same in both seasons. Stream data is given in Exmpl.str. The outflow from the eastern boundary is simulated as wells and is assumed to be the same for both seasons; its data is given in Exmpl.wel. Output control and the SIP solution packages are specified in Exmpl.oc and Exmpl.sip, respectively. The riparian evapotranspiration data set is called Exmpl1.rip.

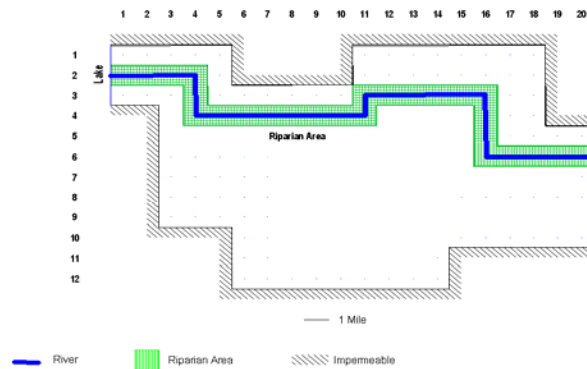


Figure 10: Aerial view of Dry Alkaline Valley

The Dry Alkaline Valley riparian habitat consists of a mixture of small, medium, and large deep-rooted riparian subgroups. A field survey of the Valley indicates that the active habitat area is composed of approximately 20% small, 30% medium, and 50% large trees. The model grid cells are 1 mile by 1 mile, and the fraction of active habitat in all cells is 0.125 on each side next to the river (.25 for the cell). The fraction of plant canopy for all three sizes was found to be 0.60. The deciduous trees are active for 6 months and dormant for 6 months. Bare ground or open water occupy the remaining 85% of surface area. The resulting coverage breakdown for each plant functional group is listed in Table 2. During the dormant season, the entire cell is modeled as bare ground. The average land surface elevation will be used for *HSURF* in each cell.

Table 2. Fractional coverage for plant functional subgroups per model cell

PFSG Type	Habitat area/cell	PFSG coverage	Canopy cover	Total Cover
Deep-rooted: Small	0.25	0.20	0.60	$0.25 \times 0.2 \times 0.6 = 0.030$
Deep-rooted: Medium	0.25	0.30	0.60	$0.25 \times 0.3 \times 0.6 = 0.045$
Deep-rooted: Large	0.25	0.50	0.60	$0.25 \times 0.5 \times 0.6 = 0.075$
Total PFSG coverage				0.15
Bare ground				0.85

During the first season (April to September), the habitat is active. Table 3 indicates that the maximum ET flux rates (R_{max}) are 0.2003 cm/day (7.61×10^{-8} ft/sec) for small trees, 0.2615 cm/day (9.91×10^{-8} ft/sec) for medium trees, and 0.2944 cm/day (1.12×10^{-7} ft/sec) for large trees. The active root depths (Ard) are 500 cm (16.40 ft) for the medium and large trees, and 400 cm (13.12 ft) for small trees (Fig. 11). The saturated extinction depth (Sxd) is at land surface for all the subgroups and is thus zero. The ET flux rate at the saturated extinction depth (R_{sxd}) is zero for all subgroups. Note that the ET flux rate in Table 3 is reported in cm/day, and the depth is in centimeters. Table 4 presents the fdh and fdR values calculated for the above curves. Recall that the fdh and fdR are dimensionless. Because the other MODFLOW data have units of length and time in feet and seconds, the values of Ard , Sxd , and R_{max} must also be in feet and feet/sec (given in parentheses above).

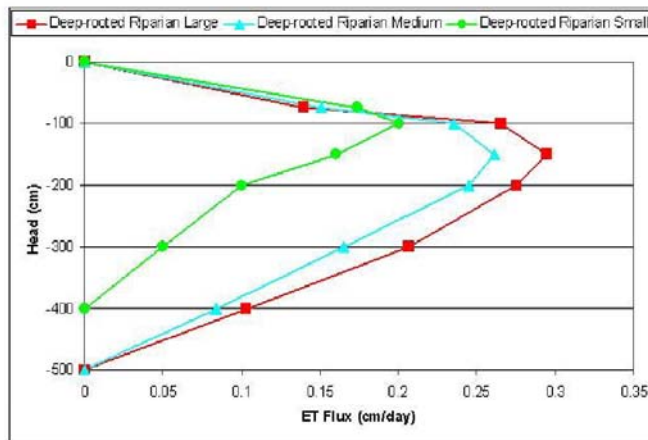


Figure 11: Seasonal canopy-area ET curves for the three size classes of deep-rooted riparian subgroups (cottonwood and willow).

Table 3. Vertices for the ET rate flux functions (cm/day) for the deep-rooted riparian subgroups (see Appendix 1)

Depth(cm)	Size (cm/day)		
	Small	Medium	Large
0.00	0.0000	0.0000	0.0000
-75.00	0.1742	0.1506	0.1400
-100.00	0.2003	0.2357	0.2653
-150.00	0.1602	0.2615	0.2944
-200.00	0.1001	0.2450	0.2759
-300.00	0.0501	0.1650	0.2064
-400.00	0.0000	0.0838	0.1032
-500.00	0.0000	0.0000	0.0000

Table 4. Dimensionless fdh and fdR for deep-rooted riparian subgroups (counting starts at extinction depth and proceeds toward land surface)

Small		Medium		Large	
fdh	fdR	fdh	fdR	fdh	fdR
0.25	0.2501	0.20	0.3218	0.20	0.3505
0.25	0.2496	0.20	0.3104	0.20	0.3505
0.125	0.3001	0.20	0.3065	0.20	0.2361
0.125	0.2002	0.10	0.0613	0.10	0.0629
0.0625	-0.1303	0.10	-0.0958	0.10	-0.0989
0.1875	-0.8697	0.05	-0.3257	0.05	-0.4256
		0.15	-0.5785	0.15	-0.4755

The ET flux curve for the bare ground/open water area during the first season and for the entire cell area the second season, follows the traditional MODFLOW form as shown in Fig. 12. The maximum ET flux rate (R_{max}) is assumed to be 0.325 cm/day (1.234×10^{-7} ft/sec), with an extinction depth of 100 cm (3.28 ft). The maximum ET surface coincides with the head at saturated extinction depth (H_{sxd}) and is assumed to be the land surface. The fdh and the fdR values for the traditional ET flux curves are both equal to 1.0.

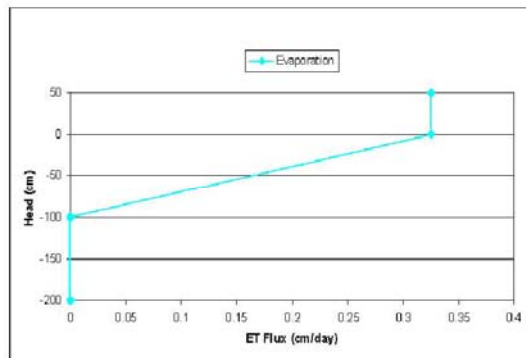


Figure 12: Traditional MODFLOW flux curve for evaporation

1	4	9	1	10	0.	0.	.0924	3750.	3760.
1	4	10	1	11	0.	0.	.0924	3747.	3757.
1	4	11	1	12	0.	0.	.0924	3743.	3753.
1	3	11	1	13	0.	0.	.0924	3742.	3752.
1	3	12	1	14	0.	0.	.0924	3739.	3749.
1	3	13	1	15	0.	0.	.0924	3736.	3746.
1	3	14	1	16	0.	0.	.0924	3732.	3742.
1	3	15	1	17	0.	0.	.0924	3728.	3738.
1	3	16	1	18	0.	0.	.0924	3727.	3737.
1	4	16	1	19	0.	0.	.0924	3726.	3736.
1	5	16	1	20	0.	0.	.0924	3725.	3735.
1	6	16	1	21	0.	0.	.0924	3724.	3734.
1	6	17	1	22	0.	0.	.0924	3721.	3731.
1	6	18	1	23	0.	0.	.0924	3717.	3727.
1	6	19	1	24	0.	0.	.0924	3714.	3724.
1	6	20	1	25	0.	0.	.0924	3710.	3720.
100.		.000568		.03					
100.		.000758		.03					
100.		.000189		.03					
100.		.000189		.03					
100.		.000379		.03					
100.		.000379		.03					
100.		.000947		.03					
100.		.000758		.03					
100.		.000758		.03					
100.		.000758		.03					
100.		.000568		.03					
100.		.000758		.03					
100.		.000189		.03					
100.		.000189		.03					
100.		.000568		.03					
100.		.000568		.03					
100.		.000758		.03					
100.		.000758		.03					
100.		.000189		.03					
100.		.000189		.03					
100.		.000189		.03					
100.		.000189		.03					
100.		.000568		.03					
100.		.000758		.03					
100.		.000568		.03					
100.		.000758		.03					
-1		0		0					

WEL File: Exmpl.wel

6	-1		
6			
1	5	20	-1.0
1	6	20	-1.0
1	7	20	-1.0
1	8	20	-1.0
1	9	20	-1.0
1	10	20	-1.0
-1			

SIP File: Exmpl.sip

100	5			
1.0000000	0.0001000	1	0.0	0

OC File: Exmpl.oc

```

HEAD PRINT FORMAT 7
HEAD SAVE FORMAT (10F8.1)
HEAD SAVE UNIT 30
PERIOD 1 STEP 1
PRINT HEAD
PRINT BUDGET
SAVE BUDGET
SAVE HEAD
PERIOD 2 STEP 1

```

PRINT HEAD
 PRINT BUDGET
 SAVE BUDGET
 SAVE HEAD

Initial Head File: Initial.hed

3800.0	3793.2	3787.5	3783.1	3780.8	-999.0	-999.0	-999.0	-999.0	-999.0
3743.6	3742.7	3741.3	3739.7	3738.1	3736.4	3734.9	3734.1	-999.0	-999.0
3800.0	3792.3	3785.9	3781.2	3778.6	-999.0	-999.0	-999.0	-999.0	-999.0
3744.7	3743.3	3741.6	3739.8	3737.9	3736.0	3734.5	3733.7	-999.0	-999.0
3800.0	3791.7	3782.7	3777.7	3773.5	3767.5	3762.8	3758.8	3754.9	3751.3
3747.5	3744.6	3742.2	3739.9	3737.6	3735.5	3733.7	3732.7	-999.0	-999.0
-999.0	-999.0	3775.3	3773.2	3770.1	3766.1	3762.2	3758.5	3754.9	3751.5
3748.2	3744.7	3742.0	3739.5	3737.1	3734.7	3732.5	3730.9	-999.0	-999.0
-999.0	-999.0	3770.3	3768.9	3766.6	3763.6	3760.4	3757.2	3753.9	3750.8
3747.8	3744.5	3741.7	3739.0	3736.2	3733.6	3730.8	3727.5	3723.3	3717.8
-999.0	-999.0	3766.6	3765.5	3763.7	3761.3	3758.6	3755.7	3752.9	3750.1
3747.3	3744.2	3741.4	3738.6	3735.5	3732.7	3729.5	3725.8	3721.7	3717.4
-999.0	-999.0	3763.8	3763.0	3761.5	3759.4	3757.0	3754.4	3751.9	3749.5
3746.8	3743.9	3741.1	3738.2	3735.0	3731.9	3728.6	3724.7	3720.7	3716.5
-999.0	-999.0	3762.1	3761.3	3759.8	3757.7	3755.4	3753.2	3751.1	3748.9
3746.5	3743.7	3741.0	3738.1	3734.7	3731.4	3727.9	3724.0	3720.0	3715.6
-999.0	-999.0	3761.2	3760.5	3758.8	3756.1	3754.0	3752.2	3750.4	3748.4
3746.2	3743.6	3741.1	3738.2	3734.7	3731.2	3727.6	3723.5	3719.5	3715.0
-999.0	-999.0	-999.0	-999.0	-999.0	3753.6	3752.6	3751.3	3749.8	3748.1
3746.1	3743.7	3741.4	3738.9	3734.8	3731.1	3727.4	3723.4	3719.2	3714.7
-999.0	-999.0	-999.0	-999.0	-999.0	3752.2	3751.6	3750.7	3749.4	3747.9
3746.1	3744.0	3742.2	3740.9	-999.0	-999.0	-999.0	-999.0	-999.0	-999.0
-999.0	-999.0	-999.0	-999.0	-999.0	3751.7	3751.2	3750.3	3749.2	3747.8
3746.1	3744.1	3742.6	3741.7	-999.0	-999.0	-999.0	-999.0	-999.0	-999.0
3800.0	3793.4	3787.8	3783.6	3781.4	-999.0	-999.0	-999.0	-999.0	-999.0
3745.4	3744.4	3742.9	3741.1	3739.3	3737.8	3736.6	3736.0	-999.0	-999.0
3800.0	3792.5	3786.2	3781.7	3779.2	-999.0	-999.0	-999.0	-999.0	-999.0
3746.5	3745.1	3743.2	3741.1	3739.2	3737.5	3736.2	3735.5	-999.0	-999.0
3800.0	3792.0	3783.3	3778.5	3774.5	3768.9	3764.4	3760.4	3756.7	3753.0
3749.2	3746.3	3743.8	3741.2	3738.8	3736.9	3735.3	3734.3	-999.0	-999.0
-999.0	-999.0	3776.4	3774.3	3771.4	3767.7	3763.9	3760.2	3756.7	3753.3
3749.8	3746.4	3743.5	3740.8	3738.3	3736.1	3733.9	3732.3	-999.0	-999.0
-999.0	-999.0	3771.4	3770.1	3767.9	3765.0	3761.9	3758.7	3755.5	3752.3
3749.2	3746.1	3743.2	3740.4	3737.6	3735.0	3732.1	3728.8	3723.5	3718.8
-999.0	-999.0	3767.7	3766.7	3765.0	3762.6	3759.9	3757.1	3754.3	3751.4
3748.5	3745.6	3742.7	3739.9	3737.0	3734.0	3730.8	3727.1	3722.9	3718.6
-999.0	-999.0	3765.0	3764.2	3762.7	3760.6	3758.2	3755.7	3753.2	3750.6
3747.9	3745.1	3742.3	3739.5	3736.4	3733.2	3729.8	3726.1	3722.0	3717.7
-999.0	-999.0	3763.3	3762.5	3760.9	3758.8	3756.6	3754.4	3752.2	3749.8
3747.4	3744.8	3742.1	3739.2	3736.1	3732.7	3729.2	3725.4	3721.3	3717.1
-999.0	-999.0	3762.4	3761.6	3759.9	3757.1	3755.2	3753.3	3751.3	3749.2
3747.0	3744.7	3742.1	3739.3	3736.0	3732.5	3728.8	3724.9	3720.9	3716.6
-999.0	-999.0	-999.0	-999.0	-999.0	3754.7	3753.7	3752.3	3750.6	3748.8
3746.8	3744.7	3742.5	3740.0	3736.1	3732.4	3728.6	3724.7	3720.7	3716.4
-999.0	-999.0	-999.0	-999.0	-999.0	3753.3	3752.7	3751.5	3750.1	3748.5
3746.7	3744.9	3743.3	3742.0	-999.0	-999.0	-999.0	-999.0	-999.0	-999.0
-999.0	-999.0	-999.0	-999.0	-999.0	3752.7	3752.2	3751.2	3749.9	3748.3
3746.7	3745.1	3743.7	3742.8	-999.0	-999.0	-999.0	-999.0	-999.0	-999.0

14.2 Riparian Data Set

The data set for Exmpl1.rip is as follows,

	25	-1	50	1	
"D.R. Riparian Small	4	7	0.00	13.12	0.761E-07 0.000E+00 6
"D.R. Riparian Medium			0.00	16.40	0.991E-07 0.000E+00 7
"D.R. Riparian Large			0.00	16.40	0.112E-06 0.000E+00 7
"Evaporation			0.00	3.28	0.123E-06 0.123E-06 1
0.25000	0.25000	0.12500	0.12500	0.06250	0.18750
0.25012	0.24963	0.30005	0.20020	-0.13030	-0.86970
0.20000	0.20000	0.20000	0.10000	0.10000	0.05000 0.15000
0.32184	0.31034	0.30651	0.06130	-0.09579	-0.32567 -0.57854

	0.20000	0.20000	0.20000	0.10000	0.10000	0.05000	0.15000		
	0.35054	0.35054	0.23607	0.06284	-0.09885	-0.42561	-0.47554		
	1.00000								
	1.00000								
	25								
0.85000	1	2	2	3793.00	0.03000	3793.00	0.04500	3793.00	0.07500 3793.00
0.85000	1	2	3	3786.00	0.03000	3786.00	0.04500	3786.00	0.07500 3786.00
0.85000	1	2	4	3782.00	0.03000	3782.00	0.04500	3782.00	0.07500 3782.00
0.85000	1	3	4	3781.00	0.03000	3781.00	0.04500	3781.00	0.07500 3781.00
0.85000	1	4	4	3780.00	0.03000	3780.00	0.04500	3780.00	0.07500 3780.00
0.85000	1	4	5	3778.00	0.03000	3778.00	0.04500	3778.00	0.07500 3778.00
0.85000	1	4	6	3776.00	0.03000	3776.00	0.04500	3776.00	0.07500 3776.00
0.85000	1	4	7	3771.00	0.03000	3771.00	0.04500	3771.00	0.07500 3771.00
0.85000	1	4	8	3767.00	0.03000	3767.00	0.04500	3767.00	0.07500 3767.00
0.85000	1	4	9	3763.00	0.03000	3763.00	0.04500	3763.00	0.07500 3763.00
0.85000	1	4	10	3760.00	0.03000	3760.00	0.04500	3760.00	0.07500 3760.00
0.85000	1	4	11	3756.00	0.03000	3756.00	0.04500	3756.00	0.07500 3756.00
0.85000	1	3	11	3755.00	0.03000	3755.00	0.04500	3755.00	0.07500 3755.00
0.85000	1	3	12	3752.00	0.03000	3752.00	0.04500	3752.00	0.07500 3752.00
0.85000	1	3	13	3749.00	0.03000	3749.00	0.04500	3749.00	0.07500 3749.00
0.85000	1	3	14	3745.00	0.03000	3745.00	0.04500	3745.00	0.07500 3745.00
0.85000	1	3	15	3741.00	0.03000	3741.00	0.04500	3741.00	0.07500 3741.00
0.85000	1	3	16	3740.00	0.03000	3740.00	0.04500	3740.00	0.07500 3740.00
0.85000	1	4	16	3739.00	0.03000	3739.00	0.04500	3739.00	0.07500 3739.00
0.85000	1	5	16	3738.00	0.03000	3738.00	0.04500	3738.00	0.07500 3738.00
0.85000	1	6	16	3737.00	0.03000	3737.00	0.04500	3737.00	0.07500 3737.00
0.85000	1	6	17	3734.00	0.03000	3734.00	0.04500	3734.00	0.07500 3734.00
0.85000	1	6	18	3730.00	0.03000	3730.00	0.04500	3730.00	0.07500 3730.00
0.85000	1	6	19	3727.00	0.03000	3727.00	0.04500	3727.00	0.07500 3727.00
0.85000	1	6	20	3723.00	0.03000	3723.00	0.04500	3723.00	0.07500 3723.00
0.85000	25								
1.00000	1	2	2	3793.00	0.00000	3793.00	0.00000	3793.00	0.00000 3793.00
1.00000	1	2	3	3786.00	0.00000	3786.00	0.00000	3786.00	0.00000 3786.00
1.00000	1	2	4	3782.00	0.00000	3782.00	0.00000	3782.00	0.00000 3782.00
1.00000	1	3	4	3781.00	0.00000	3781.00	0.00000	3781.00	0.00000 3781.00
1.00000	1	4	4	3780.00	0.00000	3780.00	0.00000	3780.00	0.00000 3780.00
1.00000	1	4	5	3778.00	0.00000	3778.00	0.00000	3778.00	0.00000 3778.00
1.00000	1	4	6	3776.00	0.00000	3776.00	0.00000	3776.00	0.00000 3776.00

1.00000	1	4	7	3771.00	0.00000	3771.00	0.00000	3771.00	0.00000	3771.00
1.00000	1	4	8	3767.00	0.00000	3767.00	0.00000	3767.00	0.00000	3767.00
1.00000	1	4	9	3763.00	0.00000	3763.00	0.00000	3763.00	0.00000	3763.00
1.00000	1	4	10	3760.00	0.00000	3760.00	0.00000	3760.00	0.00000	3760.00
1.00000	1	4	11	3756.00	0.00000	3756.00	0.00000	3756.00	0.00000	3756.00
1.00000	1	3	11	3755.00	0.00000	3755.00	0.00000	3755.00	0.00000	3755.00
1.00000	1	3	12	3752.00	0.00000	3752.00	0.00000	3752.00	0.00000	3752.00
1.00000	1	3	13	3749.00	0.00000	3749.00	0.00000	3749.00	0.00000	3749.00
1.00000	1	3	14	3745.00	0.00000	3745.00	0.00000	3745.00	0.00000	3745.00
1.00000	1	3	15	3741.00	0.00000	3741.00	0.00000	3741.00	0.00000	3741.00
1.00000	1	3	16	3740.00	0.00000	3740.00	0.00000	3740.00	0.00000	3740.00
1.00000	1	4	16	3739.00	0.00000	3739.00	0.00000	3739.00	0.00000	3739.00
1.00000	1	5	16	3738.00	0.00000	3738.00	0.00000	3738.00	0.00000	3738.00
1.00000	1	6	16	3737.00	0.00000	3737.00	0.00000	3737.00	0.00000	3737.00
1.00000	1	6	17	3734.00	0.00000	3734.00	0.00000	3734.00	0.00000	3734.00
1.00000	1	6	18	3730.00	0.00000	3730.00	0.00000	3730.00	0.00000	3730.00
1.00000	1	6	19	3727.00	0.00000	3727.00	0.00000	3727.00	0.00000	3727.00
1.00000	1	6	20	3723.00	0.00000	3723.00	0.00000	3723.00	0.00000	3723.00

14.3 Abridged Results

The results from the example above have been abridged to present only the riparian package and are as follows:

Following the stream/aquifer package allocation statement,

```

RIP2 - RIPARIAN PACKAGE, VERSION 2, 9/30/2002 INPUT READ FROM UNIT 20
MAXIMUM OF 25 RIPARIAN CELLS
THE ET RATE FOR EACH PLANT FUNCTIONAL SUBGROUP WILL BE WRITTEN TO THE LIST FILE
WHEN ICBCEL IS NOT 0
CELL LOCATION, SURFACE ELEVATION, AND PLANT FUNCTIONAL SUBGROUP ET RATES WILL BE
SAVED ON UNIT 50
HSURF IS READ AS FUNCTION OF BOTH CELL LOCATION AND PLANT FUNCTIONAL SUBGROUP
MAXIMUM NUMBERS OF PLANT FUNCTIONAL SUBGROUPS AND SEGMENTS
PLANT FUNCTIONAL SUBGROUPS = 4
MAXIMUM CURVE SEGMENTS = 7
908 ELEMENTS OF X ARRAY ARE USED BY RIP
5617 ELEMENTS OF X ARRAY USED OUT OF 1500000

```

Following SIP input echo,

RIPARIAN INFORMATION				
NAME	SATURATION EXTINCTION DEPTH	ACTIVE ROOT DEPTH	MAXIMUM ET FLUX	ET FLUX AT SATURATION EXTINCTION DEPTH
D.R. Riparian Small	0.0000	13.1200	0.7610E-07	0.0000E+00
D.R. Riparian Medium	0.0000	16.4000	0.9910E-07	0.0000E+00
D.R. Riparian Large	0.0000	16.4000	0.1120E-06	0.0000E+00
Evaporation	0.0000	3.2800	0.1230E-06	0.1230E-06

SEGMENT INFORMATION

NAME	SEGMENTS							
D.R. Riparian Small	fdh	0.2500	0.2500	0.1250	0.1250	0.0625	0.1875	
	fdR	0.2501	0.2496	0.3000	0.2002	-0.1303	-0.8697	
D.R. Riparian Medium	fdh	0.2000	0.2000	0.2000	0.1000	0.1000	0.0500	0.1500
	fdR	0.3218	0.3103	0.3065	0.0613	-0.0958	-0.3257	-0.5785
D.R. Riparian Large	fdh	0.2000	0.2000	0.2000	0.1000	0.1000	0.0500	0.1500
	fdR	0.3505	0.3505	0.2361	0.0628	-0.0988	-0.4256	-0.4755
Evaporation	fdh	1.0000						
	fdR	1.0000						

Following stream/aquifer package input echo for first stress period,

25 RIPARIAN CELLS.

RIPARIAN CELL INFORMATION

LAYER	ROW	COLUMN	SURFACE ELEVATION AND		FRACTIONAL COVERAGE OF PLANT			FUNCTIONAL SUBGROUPS		
			1	2	3	4	5	6		
1	2	2	3793.0	0.0300	3793.0	0.0450	3793.0	0.0750	3793.0	0.8500
1	2	3	3786.0	0.0300	3786.0	0.0450	3786.0	0.0750	3786.0	0.8500
1	2	4	3782.0	0.0300	3782.0	0.0450	3782.0	0.0750	3782.0	0.8500
1	3	4	3781.0	0.0300	3781.0	0.0450	3781.0	0.0750	3781.0	0.8500
1	4	4	3780.0	0.0300	3780.0	0.0450	3780.0	0.0750	3780.0	0.8500
1	4	5	3778.0	0.0300	3778.0	0.0450	3778.0	0.0750	3778.0	0.8500
1	4	6	3776.0	0.0300	3776.0	0.0450	3776.0	0.0750	3776.0	0.8500
1	4	7	3771.0	0.0300	3771.0	0.0450	3771.0	0.0750	3771.0	0.8500
1	4	8	3767.0	0.0300	3767.0	0.0450	3767.0	0.0750	3767.0	0.8500
1	4	9	3763.0	0.0300	3763.0	0.0450	3763.0	0.0750	3763.0	0.8500
1	4	10	3760.0	0.0300	3760.0	0.0450	3760.0	0.0750	3760.0	0.8500
1	4	11	3756.0	0.0300	3756.0	0.0450	3756.0	0.0750	3756.0	0.8500
1	3	11	3755.0	0.0300	3755.0	0.0450	3755.0	0.0750	3755.0	0.8500
1	3	12	3752.0	0.0300	3752.0	0.0450	3752.0	0.0750	3752.0	0.8500
1	3	13	3749.0	0.0300	3749.0	0.0450	3749.0	0.0750	3749.0	0.8500
1	3	14	3745.0	0.0300	3745.0	0.0450	3745.0	0.0750	3745.0	0.8500
1	3	15	3741.0	0.0300	3741.0	0.0450	3741.0	0.0750	3741.0	0.8500
1	3	16	3740.0	0.0300	3740.0	0.0450	3740.0	0.0750	3740.0	0.8500
1	4	16	3739.0	0.0300	3739.0	0.0450	3739.0	0.0750	3739.0	0.8500
1	5	16	3738.0	0.0300	3738.0	0.0450	3738.0	0.0750	3738.0	0.8500
1	6	16	3737.0	0.0300	3737.0	0.0450	3737.0	0.0750	3737.0	0.8500
1	6	17	3734.0	0.0300	3734.0	0.0450	3734.0	0.0750	3734.0	0.8500
1	6	18	3730.0	0.0300	3730.0	0.0450	3730.0	0.0750	3730.0	0.8500
1	6	19	3727.0	0.0300	3727.0	0.0450	3727.0	0.0750	3727.0	0.8500
1	6	20	3723.0	0.0300	3723.0	0.0450	3723.0	0.0750	3723.0	0.8500

Following stream/aquifer results for first stress period,

RIPARIAN ET PERIOD 1 STEP 1

LAYER	ROW	COLUMN	HEAD	CELL ET	SURFACE ELEVATION AND		FRACTIONAL COVERAGE OF PLANT			FUNCTIONAL SUBGROUPS		
					1	2	3	4	5	6		
1	2	2	3790.53415	0.96321E+00	3793.00	0.05541	3793.00	0.07222	3793.00	0.11200	3793.00	0.72350
1	2	3	3783.40908	-0.87471E+00	3786.00	-0.05668	3786.00	-0.07839	3786.00	-0.12728	3786.00	-0.61236
1	2	4	3779.05366	-0.62322E+00	3782.00	-0.06027	3782.00	-0.09594	3782.00	-0.17048	3782.00	-0.29652
1	3	4	3776.18462	-0.40798E+00	3781.00	-0.05172	3781.00	-0.12356	3781.00	-0.23270	3781.00	0.00000
1	4	4	3772.20286	-0.32675E+00	3780.00	-0.02582	3780.00	-0.10233	3780.00	-0.19861	3780.00	0.00000
1	4	5	3769.41265	-0.30042E+00	3778.00	-0.02199	3778.00	-0.09315	3778.00	-0.18529	3778.00	0.00000
1	4	6	3765.76028	-0.24204E+00	3776.00	-0.01398	3776.00	-0.07389	3776.00	-0.15417	3776.00	0.00000
1	4	7	3761.97375	-0.26580E+00	3771.00	-0.01986	3771.00	-0.08805	3771.00	-0.17789	3771.00	0.00000
1	4	8	3758.34640	-0.29822E+00	3767.00	-0.02167	3767.00	-0.09238	3767.00	-0.18417	3767.00	0.00000
1	4	9	3754.65783	-0.30859E+00	3763.00	-0.02318	3763.00	-0.09600	3763.00	-0.18942	3763.00	0.00000
1	4	10	3751.26747	-0.29559E+00	3760.00	-0.02128	3760.00	-0.09146	3760.00	-0.18284	3760.00	0.00000
1	4	11	3747.77997	-0.31266E+00	3756.00	-0.02377	3756.00	-0.09741	3756.00	-0.19148	3756.00	0.00000
1	3	11	3747.01879	-0.32062E+00	3755.00	-0.02492	3755.00	-0.10019	3755.00	-0.19551	3755.00	0.00000
1	3	12	3743.95323	-0.31843E+00	3752.00	-0.02461	3752.00	-0.09943	3752.00	-0.19440	3752.00	0.00000
1	3	13	3741.29724	-0.32989E+00	3749.00	-0.02627	3749.00	-0.10342	3749.00	-0.20020	3749.00	0.00000
1	3	14	3738.60208	-0.37206E+00	3745.00	-0.03370	3745.00	-0.11745	3745.00	-0.22091	3745.00	0.00000
1	3	15	3735.88289	-0.40442E+00	3741.00	-0.04861	3741.00	-0.12341	3741.00	-0.23241	3741.00	0.00000
1	3	16	3733.88154	-0.37912E+00	3740.00	-0.03695	3740.00	-0.11875	3740.00	-0.22342	3740.00	0.00000

1	4	16	3733.05875	-0.38360E+00	3739.00	-0.03901	3739.00	-0.11958	3739.00	-0.22501	3739.00	0.00000
1	5	16	3732.10746	-0.38483E+00	3738.00	-0.03958	3738.00	-0.11980	3738.00	-0.22545	3738.00	0.00000
1	6	16	3731.32611	-0.39036E+00	3737.00	-0.04213	3737.00	-0.12082	3737.00	-0.22741	3737.00	0.00000
1	6	17	3728.03487	-0.38300E+00	3734.00	-0.03874	3734.00	-0.11947	3734.00	-0.22480	3734.00	0.00000
1	6	18	3724.13541	-0.38554E+00	3730.00	-0.03991	3730.00	-0.11993	3730.00	-0.22570	3730.00	0.00000
1	6	19	3719.89733	-0.34989E+00	3727.00	-0.02918	3727.00	-0.11040	3727.00	-0.21031	3727.00	0.00000
1	6	20	3715.32316	-0.33076E+00	3723.00	-0.02640	3723.00	-0.10373	3723.00	-0.20064	3723.00	0.00000

Budget for first stress period:

VOLUMETRIC BUDGET FOR ENTIRE MODEL AT END OF TIME STEP 1 IN STRESS PERIOD 1

CUMULATIVE VOLUMES	L**3	RATES FOR THIS TIME STEP	L**3/T
IN:		IN:	
STORAGE =	39425952.0000	STORAGE =	2.4987
CONSTANT HEAD =	130673376.0000	CONSTANT HEAD =	8.2816
WELLS =	0.0000	WELLS =	0.0000
STREAM LEAKAGE =	170219808.0000	STREAM LEAKAGE =	10.7879
RIPARIAN ET =	0.0000	RIPARIAN ET =	0.0000
TOTAL IN =	340319136.0000	TOTAL IN =	21.5681
OUT:		OUT:	
STORAGE =	83008624.0000	STORAGE =	5.2608
CONSTANT HEAD =	0.0000	CONSTANT HEAD =	0.0000
WELLS =	94672800.0000	WELLS =	6.0000
STREAM LEAKAGE =	5289380.5000	STREAM LEAKAGE =	0.3352
RIPARIAN ET =	157342032.0000	RIPARIAN ET =	9.9717
TOTAL OUT =	340312832.0000	TOTAL OUT =	21.5677
IN - OUT =	6304.0000	IN - OUT =	4.0054E-04
PERCENT DISCREPANCY =	0.00	PERCENT DISCREPANCY =	0.00

Following stream/aquifer package input for second stress period,

25 RIPARIAN CELLS.

RIPARIAN CELL INFORMATION

LAYER	ROW	COLUMN	SURFACE ELEVATION AND		FRACTIONAL COVERAGE OF PLANT			FUNCTIONAL SUBGROUPS		
			1	2	3	4				
1	2	2	3793.0	0.0000	3793.0	0.0000	3793.0	0.0000	3793.0	1.0000
1	2	3	3786.0	0.0000	3786.0	0.0000	3786.0	0.0000	3786.0	1.0000
1	2	4	3782.0	0.0000	3782.0	0.0000	3782.0	0.0000	3782.0	1.0000
1	3	4	3781.0	0.0000	3781.0	0.0000	3781.0	0.0000	3781.0	1.0000
1	4	4	3780.0	0.0000	3780.0	0.0000	3780.0	0.0000	3780.0	1.0000
1	4	5	3778.0	0.0000	3778.0	0.0000	3778.0	0.0000	3778.0	1.0000
1	4	6	3776.0	0.0000	3776.0	0.0000	3776.0	0.0000	3776.0	1.0000
1	4	7	3771.0	0.0000	3771.0	0.0000	3771.0	0.0000	3771.0	1.0000
1	4	8	3767.0	0.0000	3767.0	0.0000	3767.0	0.0000	3767.0	1.0000
1	4	9	3763.0	0.0000	3763.0	0.0000	3763.0	0.0000	3763.0	1.0000
1	4	10	3760.0	0.0000	3760.0	0.0000	3760.0	0.0000	3760.0	1.0000
1	4	11	3756.0	0.0000	3756.0	0.0000	3756.0	0.0000	3756.0	1.0000
1	3	11	3755.0	0.0000	3755.0	0.0000	3755.0	0.0000	3755.0	1.0000
1	3	12	3752.0	0.0000	3752.0	0.0000	3752.0	0.0000	3752.0	1.0000
1	3	13	3749.0	0.0000	3749.0	0.0000	3749.0	0.0000	3749.0	1.0000
1	3	14	3745.0	0.0000	3745.0	0.0000	3745.0	0.0000	3745.0	1.0000
1	3	15	3741.0	0.0000	3741.0	0.0000	3741.0	0.0000	3741.0	1.0000
1	3	16	3740.0	0.0000	3740.0	0.0000	3740.0	0.0000	3740.0	1.0000
1	4	16	3739.0	0.0000	3739.0	0.0000	3739.0	0.0000	3739.0	1.0000
1	5	16	3738.0	0.0000	3738.0	0.0000	3738.0	0.0000	3738.0	1.0000
1	6	16	3737.0	0.0000	3737.0	0.0000	3737.0	0.0000	3737.0	1.0000
1	6	17	3734.0	0.0000	3734.0	0.0000	3734.0	0.0000	3734.0	1.0000
1	6	18	3730.0	0.0000	3730.0	0.0000	3730.0	0.0000	3730.0	1.0000
1	6	19	3727.0	0.0000	3727.0	0.0000	3727.0	0.0000	3727.0	1.0000
1	6	20	3723.0	0.0000	3723.0	0.0000	3723.0	0.0000	3723.0	1.0000

RIP2RP1—Reads data for variables that do not vary during a simulation run.

RIP2RP2—Reads data variable that vary over stress periods.

RIP2FM—Formulates terms needed to solve the groundwater flow equation simulating riparian evapotranspiration, and adds them to the head coefficient array (HCOF) and to the right-hand side array (RHS).

RIP2BD—Computes flow rates simulated as evapotranspiration from riparian systems and writes plant functional subgroup evapotranspiration rates or cell-by-cell flow rates if those options are selected.

The two functions are:

HCOFrm—Computes a component of the term added to head coefficient array (HCOF).

RHStrm—Computes a component of the term added to the right-hand side array (RHS).

Statements must be added to MODLFLW96.for, the main program to call the RIP package. There are five calls to the main module—RIP2AL, RIP2RP1, RIP2RP2, RIP2FM and RIP2BD. Add the RIP call statements as follows:

After the call to FHB1AL, add

```
IF (IUNIT(22) .GT. 0) CALL RIP2AL (ISUM, LENX, LCSxd, LCArd, LCRmax,
1  LCRsxd, LCNuSEG, LCFdh, LCFdR, LCRip, LCC1, LCC2,
2  LCETR, IUNIT(22), IOUT, IFREFM, MAXRIP, IRIPCB, IRIPCB1,
3  NRIPCL, NRIPVL, MAXTS, MXSEG, IRIPAL, IHSURF)
```

After the call to FHB1RP, add

```
IF (IUNIT(22) .GT. 0) CALL RIP2RP1 (X(LCSxd), X(LCArd), X(LCRmax),
1  X(LCRsxd), X(LCNuSEG), X(LCFdh), X(LCFdR), MAXTS, MXSEG,
2  RIPNM, IFREFM, IUNIT(22), IOUT)
```

After the call to CHD1RP, add

```
IF (IUNIT(22) .GT. 0) CALL RIP2RP2 (X(LCRIP), NRIPCL, NRIPVL, IRIPAL,
0.0 MAXRIP, MAXTS, IHSURE, IUNIT(22), IOUT, IFREFM)
```

After the call to FHB1FM, add

```
IF (IUNIT(22) .GT. 0) CALL RIP1FM (NRIPCL, NRIPVL, MAXRIP, MAXTS, IHSURF,
1  MXSEG, X(LCRIP), X(LCSxd), X(LCArd), X(LCRmax), X(LCRsxd),
2  X(LCNuSeg), X(LCFdh), X(LCFdR), X(LCC1), X(LCC2),
3  X(LCHNEW), X(LCHCOF), X(LCRHS), X(LCIBOU), NLAY,
4  NCOL, NROW, X(LCDELR), X(LCDELC))
```

After the call to FHB1BD, add

The above statements call the RIP package whenever the 22nd element of the IUNIT array is greater than zero. Another IUNIT element can be substituted if desired. To do this, replace IUNIT(22) in the "IF" statement and in the calling argument in the NAME File.

15.1 RIP2AL

The subroutine RIP2AL will read from the RIP file designated in the NAME file, allocates space in the X array, writes to the list file, and performs the following steps,

Step 1: Identifies the package as the Riparian Package, and initializes the number of active riparian cells (NRIPCL) to zero.

Step 2: Read in the maximum number of riparian cells (MAXRIP) allowed over all stress periods. Note that, NRIPCL, which is updated every stress period, is always $NRIPCL \leq MAXRIP$. Read in the IRIPCB, cell-by-cell flow flag or unit number, and IRIPCB1, the flag or unit number for plant functional subgroup ET rate storage. Read IHSURF, a flag to indicate whether HSURF has only one value for a cell or that it has the number of active plant functional subgroup per cell.

Step 3: Read CBC allocation flag, initialize IRIPAL to zero, and set IRIPAL = 1 if CBC is read as an option.

Step 4: Read in the maximum number of plant functional subgroups, MAXTS, and maximum number of segments used to interpolate the ET canopy flux rate function, MXSEG.

Step 5: Set NRIPVL, the size of the 1st dimension of the Rip array, to $NRIPVL = 4 + MAXTS + IRIPAL$ (the 4 is for layer, row, column and land surface elevation variables), and allocate space in the X vector of the main program of MODFLOW for the Sxd, Ard, Rmax, Rxd, NuSeg, fdh, fdR, Rip, HK, RK, C1, C2, and ETR arrays

Step 6: Print amount of space used by riparian package.

15.2 Listing for RIP2AL Module

```
!-----
!This package calculates riparian ET for a variety of riparian
!plant functional subgroups. Examples of subgroups are:
! Obligate Wetland (e.g. cattails & Dulrush)
! Shallow-rooted Riparian(e.g. cockleburn & sacaton)
! Deep-rooted Riparian (e.g. cottonwood & willow):small, medium,
! and large sizes.
! Transitional riparian (e.g. mesquite & sycamore):small,medium,
! and large sizes.
!
!-----
Subroutine RIP2AL(ISUM, LENX, LCSxd, LCArd, LCRmax, LCRsxd, LCNuSEG, LCfdh, &
                LCfGR, LCRip, LCC1, LCC2, LCETR, IN, IOUT, IFREFM, &
                MAXRIP, IRIPCB, IRIPCB1, NRIPCL, NRIPVL, MAXTS, &
                MXSEG, IRIPAL, IHSURF)
!
Implicit none
!
!-----
! This subroutine reads in dimension variables that remain constant
! over the simulation, and allocates array storage for riparian
! cells. The follow variables are used:
! IN is the unit number of input file.
! IOUT is the unit number of the LIST output file.
! LENX is the dimension of X array.
! ISUM is a pointer used to keep track of position in X array.
! LINE is the content of one line read from the input file.
! LLOC is a pointer used to keep track of position in LINE.
! ISTART is the starting position of parsed word.
! ISTOP is the ending position of parsed word.
! ISUM1 is the value ISUM-1.
! IFREFM is a flag indicating free format for data input.
! MAXRIP is the maximum number of riparian cells over all stress
! periods.
! IRIPCB is a cell-by-cell printing flag and unit number,
! IRIPCB1 is a flag to save cell values:location, surface elevation
! and ET rate for each plant functional subgroup.
! NRIPCL is the number of active riparian cells in a stress period.
! NRIPVL is the size of the first dimension of the array, RIP.
```

```

! MAXTS is the total number of plant functional subgroups for
! all cells.
! MXSEG is the maximum number of segments for interpolation of ET
! flux rate as a function of hydraulic head.
! IRIPAL is the dimension flag and increment for optional
! memory allocation.
! IHSURF is a flag to indicate that HSURF varies with just cells or
! with plant functional subgroup and cells.
! CSxd, LCArd, LCRmax, LCRsxd, LCNuSEG, LCFdh, LCFdR, LCRIP, LCC1,
! LCC2, LCETR are all pointers to partition the X array.
! N is a dummy integer variable.
! R is a dummy real variable.
! ISP is a counter.
-----
!
! Specifications
-----
Character(80)::Line
Integer:: ISUM, LENX, IFREFM, IN, IOUT, LLOC, ISTART, ISTOP, N, ISP, ISUM1
Integer:: NRIPCL, NRIPVL, MAXRIP, IRIPCB, IRIPCBI, MAXTS, MXSEG, IRIPAL
Integer:: IHSURF
Integer:: LCSxd, LCArd, LCRmax, LCRsxd, LCNuSEG, LCFdh, LCFdR
Integer:: LCRIP, LCC1, LCC2, LCETR
Real::R
!
!1-----Identify package and initialize NRIPCL
!
Write(IOUT,100) IN
100 Format(1x,/1x,'RIP2 - RIPARIAN PACKAGE, VERSION 2.', &
' 9/30/2002', ' INPUT READ FROM UNIT', I3)
!
NRIPCL=0
!
!2-----Read 1) maximum number of riparian cell, 2) a unit or flag
! for printing or storing ET terms, 3) an option value, if
! present, that allows storage in memory of the total ET Rate
! for each cell, and 4) A flag to indicate whether HSURF has
! only one value for a cell or that it has the number of active
! plant functional subgroup per cell.
!
Read(IN, '(A)') LINE
If (IFREFM == 0) Then
Read(LINE, '(3I10)') MAXRIP, IRIPCB, IRIPCBI, IHSURF
LLOC=41
Else
LLOC=1
CALL URWORD(LINE, LLOC, ISTART, ISTOP, 2, MAXRIP, R, IOUT, IN)
CALL URWORD(LINE, LLOC, ISTART, ISTOP, 2, IRIPCB, R, IOUT, IN)
CALL URWORD(LINE, LLOC, ISTART, ISTOP, 2, IRIPCBI, R, IOUT, IN)
CALL URWORD(LINE, LLOC, ISTART, ISTOP, 2, IHSURF, R, IOUT, IN)
Endif
Write(IOUT, 110) MAXRIP
110 Format(1x, 'MAXIMUM OF', I5, ' RIPARIAN CELLS')
If (IRIPCB < 0) then
write(IOUT, 120)
O.□ Format(1x, 'THE ET RATE FOR EACH PLANT FUNCTIONAL SUBGROUP WILL ', &
' BE WRITTEN TO THE LIST FILE WHEN ICBCFL IS NOT 0')
Elseif (IRIPCB > 0) then
write(IOUT, 130) IRIPCB
O.□ Format(1x, 'TOTAL ET RATE FOR EACH CELL WILL BE SAVED ON UNIT', I3)
Endif
If (IRIPCBI > 0) Then
Write(IOUT, 135) IRIPCBI
135 Format(1x, 'CELL LOCATION, SURFACE ELEVATION, AND PLANT ', &
' FUNCTIONAL SUBGROUP ET RATES WILL BE SAVED ', &
' ON UNIT', I3)
End if
If (IHSURF > 0) Then
Write(IOUT, 137)
137 Format(1x, 'HSURF IS READ AS A FUNCTION OF BOTH CELL ' &

```

```

'LOCATION AND PLANT FUNCTIONAL SUBGROUP')
Else
  write(IOUT,139)
  O. Format(1x,'HSURF IS A FUNCTION ONLY OF CELL LOCATION')
  End if
!
!3-----Read CEC allocation flag , initialize IRIPAL to zero, and
!   set IRIPAL = 1 if CBC is read as an option.
!
  IRIPAL=0
  Call URWORD(LINE,LLOC,ISTART,ISTOP,1,N,R,IOUT,IN)
  IF(LINE(ISTART:ISTOP)== 'CBCALLOCATE'.or. &
    LINE(ISTART:ISTOP)== 'CBC') Then
    IRIPAL=1
    Write(IOUT,140)
  O. Format(1x,'MEMORY IS ALLOCATED FOR CELL-BY-CELL TOTAL ', &
    'RIPARIAN ET TERMS')
  End if
!
!4-----Read and print maximum number of plant functional subgroups (MAXTS),
!   and the maximum of interpolation segments for the ET flux rate
!   function (MXSEG).
!
  If (IFREFM == 0) Then
    Read(IN,'(2I10)') MAXTS,MXSEG
  Else
    Read(IN,*) MAXTS,MXSEG
  Endif
  write(IOUT,150) MAXTS,MXSEG
150 Format(1x,'MAXIMUM NUMBERS OF PLANT FUNCTIONAL SUBGROUPS AND SEGMENTS ', &
  1x,'PLANT FUNCTIONAL SUBGROUPS =',I3,', &
  1x,'MAXIMUM CURVE SEGMENTS =',I3)
!
!5-----Set NRIPVL and allocate space in X vector. If IHSURF>0, HSURF has a
!   value for each active plant functional subgroup in a cell.If IHSURF=0,
!   HSURF has only one value for a cell
!
  If(IHSURF>0) Then
    NRIPVL=2*MAXTS+3+IRIPAL
  Else
    NRIPVL=MAXTS+4+IRIPAL
  End if
!
!5a-----Simulation variables, Sxd, Ard, Rmax, Rxd, fdh, fdR, NuSeg
!
  ISUM=ISUM
  LCSxd=ISUM
  ISUM=ISUM+MAXTS
  LCARD=ISUM
  ISUM=ISUM+MAXTS
  LCRmax=ISUM
  ISUM=ISUM+MAXTS
  LCRxd=ISUM
  ISUM=ISUM+MAXTS

  LCfdh=ISUM
  ISUM=ISUM+MAXTS*MXSEG
  LCFdR=ISUM
  ISUM=ISUM+MAXTS*MXSEG

  LCNuSEG=ISUM
  ISUM=ISUM+MAXTS
!
!5b-----Stress period variables, HK, RK, Rip, C1, C2, ETR
!
  LCRIP=ISUM
  ISUM=ISUM+NRIPVL*MAXRIP
  LCC1=ISUM
  ISUM=ISUM+MAXRIP*MAXTS*2
  LCC2=ISUM

```



```

ISUM=ISUM+MAXRIP*MAXTS*2
LCETR=ISUM
ISUM=ISUM+MAXRIP*MAXTS*2
!
!6-----Print amount of space used by the Riparian package.
!
ISP=ISUM-ISP
Write(IOUT,160) ISP
160 Format(1x,I10,' ELEMENTS OF X ARRAY ARE USED BY RIP')
ISUM1=ISUM-1
Write(IOUT,170) ISUM1,LENX
170 Format(1x,I10,' ELEMENTS OF X ARRAY USED OUT OF ',I10)
If(ISUM1 > LENX) Write(IOUT,180)
180 format(1x,' ***X ARRAY MUST BE MADE LARGER***')
!
!7-----Return
!
Return
End Subroutine RIP2AL

```

Table 5. List of variables in module RIP2AL

Variable	Scope	Definition
LINE	Module	Content of one line read from the input file
ISUM	Global	Pointer used to keep track of position in X array
LENX	Global	Dimension of X array
IFREFM	Global	Flag indicating if variables are to be read in free format
IN	Package	Unit number of input file
IOUT	Global	Unit number of LIST output file
LLOC	Module	Pointer used to keep track of position in LINE
ISTART	Module	Starting position of parsed word
ISTOP	Module	Ending position of parsed word
ISUM1	Module	The value ISUM-1
N	Module	Dummy integer variable
R	Module	Dummy real variable
NRIPCL	Package	Active number of riparian cells in a stress period
NRIPVL	Package	Dimensioning variable for RIP array
MAXRIP	Package	Maximum number of riparian cells
IRIPCB	Package	Cell-by-cell flag and unit number
IRIPCB1	Package	Save flag and unit number
MAXTS	Package	Maximum number of plant functional subgroups
MXSEG	Package	Maximum number of segments over all subgroups
IHSURF	Package	Flag for single or multiple HSURF in cells
IRIPAL	Package	Dimension increment and flag for the optional memory allocation
LCSxd	Package	Position in X array of first element of Sxd
LCArD	Package	Position in X array of first element of Ard
LCRmax	Package	Position in X array of first element of Rmax
LCRsxd	Package	Position in X array of first element of Rsxd
LCNuSeg	Package	Position in X array of first element of NuSeg
LCfdh	Package	Position in X array of first element of fdh
LCfdR	Package	Position in X array of first element of fdR
LCRIP	Package	Position in X array of first element of Rip
LCC1	Package	Position in X array of first element of C1
LCC2	Package	Position in X array of first element of C2
LCETR	Package	Position in X array of first element of ETR
ISP	Module	Counter

15.3 RIP2RP1

Subroutine RIP2RP1 performs the following steps:

Step 1: For each plant functional subgroup, read the name of the group, the saturated extinction depth, the maximum ET flux rate, the ET flux rate at the saturation extinction depth, the number of segment used to interpolate the ET flux rate curve, the active root depth segment factors, and the ET flux rate segment factor.

Step 2: For each plant functional subgroup, print the name of the group, the saturated extinction depth, the maximum ET flux rate, the ET flux rate at the saturation extinction depth, and the number of the segment used to interpolate the ET canopy flux rate curve.

Step 3: For each plant functional group, print the active root depth segment factors and the ET flux rate segment factors.

Step 4: Return.

15.4 Listing for RIP2RP1 Module

```
!.....
!
Subroutine RIP2RP1(Sxd,Ard,Rmax,Rsxd,NuSEG,fdh,fdR,MAXTS,MXSEG,RIPNM, &
                IFREFM,IN,IOUT)
!
Implicit none
!
!-----
! This subroutine reads array values that do not vary over the
! simulation:
! IN is the unit number of input file.
! IOUT is the unit number of the LIST output file.
! MAXTS is the total number of plant functional subgroups for
! all cells.
! MXSEG is the maximum number of segments for interpolation of
! ET flux rate as a function of hydraulic head.
! IFREFM is a flag indicating free format for data input.
! RIPNM is the plant functional subgroup names, may be up to
! 24 characters in length, and the maximum number of
! names is set to 20.
! Sxd is the saturation extinction depth with respect to land
! surface.
! Ard is the active root depth.
! Rmax is the maximum ET canopy flux rate.
! Rsxd is the ET canopy flux rate at the saturation extinction
! depth.
! NuSEG is the number of active segments for a plant functional
! subgroup.
! fdh is the active root depth segment factor.
! fdR is the maximum ET flux segment factor.
! Nfdh is the characters 'fdh'
! NfdR is the characters 'fdR'
! ITS and ISEG are counters.
!-----
!
! Specifications
!-----
Character*3::Nfdh='fdh',NfdR='fdR'
Character*24, Dimension(20)::RIPNM
Integer:: MAXTS,MXSEG,IFREFM
Integer IN,IOUT
Integer:: ITS,ISEG
Integer, Dimension(MAXTS)::NuSEG
Real, Dimension(MAXTS)::Sxd,Ard,Rmax,Rsxd
Real, Dimension(MAXTS,MXSEG)::fdh,fdR
```

```

!-----
!
!1a---For each plant functional subgroup, read the name, saturated extinction
! depth (measured from land surface), active root depth, maximum ET flux,
! ET flux rate at the saturation extinction depth, and the number of
! segments used to interpolate the ET flux rate curve.
!
Do ITS=1, MAXTS
  If (IFREFM == 0) then
    Read (IN, ' (A,3F10.0,I10) ' ) RIPNM (ITS), Sxd (ITS), Ard (ITS),      &
      Rmax (ITS), Rxxd (ITS), NuSEG (ITS)
  Else
    Read (IN, *) RIPNM (ITS), Sxd (ITS), Ard (ITS), Rmax (ITS), Rxxd (ITS),  &
      NuSEG (ITS)
  End if
End do
!
!1b--- For each plant functional subgroup, read the active root depth segment factors and ET      !
! flux rate segment factors.
!
Do ITS=1, MAXTS
  If (IFREFM == 0) then
    Read (IN, ' (10F10.4) ' ) (fdh (ITS, ISEG), ISEG=1, NuSEG (ITS))
    Read (IN, ' (10F10.4) ' ) (fdr (ITS, ISEG), ISEG=1, NuSEG (ITS))
  Else
    Read (IN, *) (fdh (ITS, ISEG), ISEG=1, NuSEG (ITS))
    Read (IN, *) (fdr (ITS, ISEG), ISEG=1, NuSEG (ITS))
  End if
End do
!
!2-----Print out plant functional subgroup name, saturated extinction depth
! (measured from land surface), active root depth, maximum ET flux,
! ET flux rate at saturation extinction depth.
!
Write (IOUT, 100)
100 Format (/, '
      RIPARIAN INFORMATION' //, &
      ' MAXIMUM     NAME     SATURATION     ACTIVE     ', &
      ' ET FLUX AT' //, &
      ' ET     SATURATION' //, &
      '     DEPTH     DEPTH     ', &
      ' FLUX     EXTINCTION DEPTH' )
!
Do ITS=1, MAXTS
  Write (IOUT, 110) RIPNM (ITS), Sxd (ITS), Ard (ITS), Rmax (ITS), Rxxd (ITS)
  O.□ Format (1x, A, T27, F10.4, T38, F10.4, T52, E11.4, T65, E11.4)
End do
!
!3-----Print out plant functional subgroup name and active root depth and ET
! flux rate segments.
!
Write (IOUT, 120)
120 Format (/, '
      SEGMENT INFORMATION' //, &
      ' NAME     SEGMENTS ' )
!
Do ITS=1, MAXTS
  Write (IOUT, 130) RIPNM (ITS), Nfdh, (fdh (ITS, ISEG), ISEG=1, NuSEG (ITS))
  130 Format (/, 1x, A, T27, A, 10F10.4)
  Write (IOUT, 140) Nfdr, (fdr (ITS, ISEG), ISEG=1, NuSEG (ITS))
  O.□ Format (1x, T27, A, 10F10.4)
End Do
!
!4-----Return
!
Return
End Subroutine RIP2RP1

```

Table 6. List of variables in module RIP2RP1

Variable	Scope	Definition
IFREFM	Global	Flag indicating if variables are to be read in free format
IN	Package	Unit number of input file
IOUT	Global	Unit number of LIST output file
MAXTS	Package	Maximum number of plant functional subgroups
MXSEG	Package	Maximum number of segments over all subgroups
RIPNM	Package	Names of plant functional subgroups
Sxd	Package	Saturation extinction depth
Ard	Package	Active root depth
Rmax	Package	Maximum ET canopy flux rate
Rsd	Package	ET canopy flux rate at saturation extinction depth
NuSeg	Package	Number of segments for a plant functional subgroup ET curve
fdh	Package	Active root depth segment factor
fdR	Package	Maximum ET flux segment factor
ITS	Module	Counter
ISEG	Module	Counter
Nfdh	Module	Characters 'fdh'
NfdR	Module	Characters 'fdR'

15.5 RIP2RP2

Subroutine RIP2RP2 performs the following steps:

Step 1: Read ITMP

Step 2: Test ITMP

If $ITMP \geq 0$, set $NRIPCL = ITMP$

If $ITMP < 0$, Return—use previous time period data.

Step 3: Test to make sure that $NRIPCL \leq MAXRIP$, if not, STOP.

Step 4: Printout number of active riparian cells for the stress period.

Step 5: If $NRIPCL = 0$ for the stress period, return.

Step 6: Initialize RIP array to zero.

Step 7: Printout headers for RIP data for $IHSURF = 0$. For each riparian cell, read and print location (Layer, Row, Column), a single land surface elevation, and the fractional coverage for each active plant functional subgroup.

Step 8: Print out headers for RIP data for $IHSURF \neq 0$. For each cell, read and print location (Layer, Row, Column). Read and print the land surface elevation and the fractional coverage of each plant functional subgroup within the cell.

Step 9: Return.

15.6 Listing for RIP2RP2 Module

```
! .....
!
Subroutine RIP2RP2 (RIP, NRIPCL, NRIPVL, IRIPAL, MAXRIP, MAXTS, IHSURF, &
IN, IOUT, IFREFM)
!
Implicit none
!-----
! This subroutine reads by stress period, the location of the riparian cells
! (layer, row, column), the land surface elevations, and the percentage
! coverage of each plant functional subgroup in each cell.
! IN is the unit number of input file.
```

```

! IOUT is the unit number of the LIST output file.
! IFREFM is a flag indicating free format for data input.
! ITMP is number of riparian cells or flag to repeat data from previous
! stress period.
! IHSURF=a flag to indicate that HSURF varies with just cells or
! with plant functional subgroup and cells.
! MAXRIP is the maximum number of riparian cells over all stress
! periods.
! NRIPCL is the number of active riparian cells in a stress period.
! NRIPVL is the size of the first dimension of the array, RIP.
! MAXTS is the total number of plant functional subgroups for
! all cells.
! IRIPAL is the dimension flag and increment for optional
! memory allocation.
! RIP is the RIP array with dimension (NRIPVL,MAXRIP), includes, by cell:
! layer,row, column, land surface elevation and fractional coverage
! for each plant functional subgroup.
! NRIPCL is the number of active riparian cells for the stress period
! HSURF is the land surface elevation that has either for one value for a
! cell, or the number of active plantfunctional subgroup per cell.
! K is the cell layer
! I is the cell row
! J is the cell column
! II,JJ,and NN are counters
!-----
!
! Specifications
!-----
Integer::IN,IOUT,IFREFM,ITMP,IHSURF
Integer:: NRIPCL,NRIPVL,IRIPAL,MAXRIP,MAXTS
Integer:: II,JJ,NN,K,I,J
Real::HSURF
Real, Dimension(NRIPVL,MAXRIP):: RIP
!
!1-----Read in ITMP (number of riparian cells or flag to reuse data).
!
!   If (IFREFM == 0) then
!     Read(IN,'(I10)') ITMP
!   Else
!     Read(IN,*) ITMP
!   Endif
!
!2-----Test ITMP.
!
!   If (ITMP < 0) Then
!2a-----If ITMP<0, reuse data from last stress period.
!     Write(IOUT,100)
!     O.□ Format(1x,/1x,'REUSING RIPARIAN CELL DATA FROM LAST STRESS PERIOD')
!     Return
!   Else
!2b-----If ITMP>=0, it is the number of riparian cells.
!     NRIPCL=ITMP
!   End if
!
!3-----If NRIPCL>MAXRIP then STOP.
!
!   If (NRIPCL > MAXRIP) Then
!     write(IOUT,110) NRIPCL,MAXRIP
!     O.□ Format(1x//,1x,'NRIPCL(',I4,') IS GREATER THAN MAXRIP(',I4,')')
!     Stop
!   Endif
!
!4-----Printout number of active riparian cells for the stress period.
!
!   write(IOUT,120) NRIPCL
!   O.□ Format(1x//,1x,I5,' RIPARIAN CELLS.')
```

```

      If(NRIPCL == 0) Return
!
!6-----Initialize RIP array.
!
      RIP = 0
!
!7-----IHSURF=0, one value of HSURF per cell, print out header
!
      If (IHSURF==0) Then
        Write(IOUT,130)
130      Format(1x/20x,'RIPARIAN CELL INFORMATION')
        Write(IOUT,140) (NN, NN=1,MAXTS)
140      format(1x,/,1x,'LAYER ROW COLUMN SURFACE SURFACE ELEVATION',/
              \ 'FRACTIONAL COVERAGE OF PLANT FUNCTIONAL SUBGROUPS',/
              \ 'ELEVATION',20I10/)
              \, &
              \, &
        Do II=1, NRIPCL
!
!7a----For each riparian cell,read and print location (Layer, row, column),
! surface elevation, and then fractional coverage for each plant
! functional subgroup.
!
          If(IFREFM == 0) then
            Read(IN,'(3I10)') K,I,J,HSURF,(RIP(JJ,II),JJ=5,NRIPVL-IRIPAL)
          Else
            Read(IN,*) K,I,J,HSURF,(RIP(JJ,II),JJ=5,NRIPVL-IRIPAL)
          Endif
          Write(IOUT,150) K,I,J,HSURF,(RIP(JJ,II),JJ=5,NRIPVL-IRIPAL)
0.□ Format(1x,I3,3x,I3,3x,I3,4x,F10.2,2x,20(F10.5) )
            RIP(1,II)=K
            RIP(2,II)=I
            RIP(3,II)=J
            RIP(4,II)=HSURF
          End do
        Else
!
!8-----IHSURF>0, MAXST values of HSURF per cell, print out header
!
          Write(IOUT,130)
          Write(IOUT,160) (NN, NN=1,MAXTS)
160      Format(1x,/,1x,'LAYER ROW COLUMN SURFACE ELEVATION AND FRACTIONAL \
              \ COVERAGE OF PLANT FUNCTIONAL SUBGROUPS'/
              \,20I18/)
              \, &
              \, &
          Do II=1, NRIPCL
!
!8a---For each riparian cell,read and print location (Layer, row, column),
! and land surface elevation and fractional coverage for each plant
! functional subgroup.
!
            If(IFREFM == 0) then
              Read(IN,'(3I10)') K,I,J,(RIP(JJ,II),JJ=4,NRIPVL-IRIPAL)
            Else
              Read(IN,*) K,I,J,(RIP(JJ,II),JJ=4,NRIPVL-IRIPAL)
            Endif
            Write(IOUT,170) K,I,J,(RIP(JJ,II),JJ=4,NRIPVL-IRIPAL)
0.□ Format(1x,I3,3x,I3,3x,I3,2x,20(3x,F6.1,3x,F6.5) )
              RIP(1,II)=K
              RIP(2,II)=I
              RIP(3,II)=J
            End do
          End if
!
!9-----Return.
!
          Return
End Subroutine RIP2RP2

```

Table 7. List of variables in module RIP2RP2

Variable	Scope	Definition
ITMP		Number of riparian cells or flag to reuse data
IFREFM	Global	Flag indicating if variables are to be read in free format
IN	Package	Unit number of input file
IOUT	Global	Unit number of LIST output file
MAXTS	Package	Maximum number of plant functional subgroups
MXSEG	Package	Maximum number of segments over all subgroups
MAXRIP	Package	Maximum number of riparian cells
IHSURF	Package	Flag for single or multiple HSURF in cells
NRIPCL	Package	Active number of riparian cells in a stress period
NRIPVL	Package	Dimensioning variable for RIP array : (4+MAXTS)
IRIPAL	Package	Dimension increment and flag for the optional memory allocation
RIP	Package	Array containing location, HSURF and percent coverage of plant functional subgroups
K	Module	Layer
J	Module	Column
I	Module	Row
HSURF	Module	Land surface elevation
II	Module	Counter
JJ	Module	Counter
NN	Module	Counter

15.7 RIP2FM

Subroutine RIP2FM performs the following steps:

Step 1: Check to see if there are riparian cells for this stress period, if not, return.

Step 2: Begin to process each cell in the riparian cell list.

Step 3: Get row, column and layer of riparian cell from RIP array.

Step 4: Check to see if cell is external, if so skip it and send a message that it is in an inactive cell (IBOUND=0).

Step 5: Set head for cell (HH=HNEW).

Step 6: Begin to process each plant functional subgroup in a cell, initialize C1 and C2, and determine which plant functional subgroups are active within a cell (RIP#0).

Step 7: If IHSURF = 0, HSURF a function of cell only. If IHSURF > 0, then HSURF is also a function of plant functional subgroups

Step 8: Determine cell non-zero fractional coverage for a plant functional subgroup, retrieve HSURF from Rip, calculate Hsxd and Hxd; and initialize the extinction depth segment end points, HK(1) to Hxd, and RK(1) to zero.

Step 9: Check to see if HH is beyond the ends of the ET flux curve; if HH <= Hxd, set both C1 and C2 to zero; or if HH >= Hsxd, set C1=0.0 and C2=-Rsxd*fCov*DELC(IR)*DELR(IC); in either case, cycle to the next plant functional subgroup.

Step 10: Loop through the ET flux rate function vertices and calculate the HKs and RKs as needed. Check to see if HK(KS)<HH≤HK(KS+1); when it is, calculate C1 and C2 using the functions HCOFtrm and RHStrm that are adjusted with fCov, DELR and DELC, i.e.,

$$C1=fCov*HCOFtrm*DELR*DELC$$

$$C2=fCov*RHStm*DELR*DELC.$$

Add C1 to HCOF, and subtract C2 from RHS.

Step 11: Return

15.8 Listing for RIP2FM Module

```

! .....
!
Subroutine RIP1FM(NRIPCL,NRIPVL,MAXRIP,MAXTS,IHSURF,MXSEG,RIP,      &
                Sxd,Ard,Rmax,Rsxd,NuSeg,fdh,fdR,C1,C2,HNEW,      &
                HCOF,RHS,IBOUND,NLAY,NCOL,NROW,DELR,DELC)
!
Implicit none
!
! -----
! Add riparian evapotranspiration to RHS and HCOF. The ET flux
! rate is estimated using a segmented interpolation structure.
! NLAY is the number of layers in the grid.
! NROW is the number of rows in the grid.
! NCOL is the number of columns in the grid.
! DELR is the cell dimension in row direction.
! DELC is the cell dimension in the column direction.
! HNEW is the most recent estimate of head in a cell.
! IBOUND is status of cell: <0, constant head;=0, inactive;>0, active.
! HCOF is the coefficient of head in the finite-difference equations.
! RHS is the right-hand side of the finite-difference equations.
! IL is the cell layer.
! IR is the cell row.
! IC is the cell column.
! Loc1 is a counter for fractional coverage values in a cell.
! Loc2 is a counter for land surface elevations in a cell, used
! only if IHSURF>0.
! HH is the hydraulic head in the cell.
! MAXRIP is the maximum number of riparian cells over all stress
! periods.
! NRIPCL is the number of active riparian cells in a stress period.
! NRIPVL is the size of the first dimension of the array, RIP.
! MAXTS is the total number of plant functional subgroups for
! all cells.
! MXSEG is the maximum number of segments for interpolation of ET
! flux rate as a function of hydraulic head.
! IHSURF is a Flag for HSURF. If positive, the HSURF for a cell
! has a value for each active plant functional subgroups,
! and is zero has only one HSURF per cell.
! HSURF is the land surface elevation that has either for one value for a
! cell, or the number of active plant functional subgroup per cell.
! Hxd is the extinction depth elevation.
! Hsxd is the saturated extinction depth elevation.
! Rmax is the maximum ET canopy flux rate.
! Rsxd is the ET canopy flux rate at the saturation extinction
! depth.
! fdh is the active root depth segment factor.
! fdR is the maximum ET flux segment factor.
! RIP is the RIP array with dimension (NRIPVL,MAXRIP), includes, by cell:
! layer,row, column, land surface elevation and fractional coverage
! for each plant functional subgroup.
! HK(N) is the head value at Nth vertex of the Ard segments.
! RK(N) is the ET canopy flux at Nth vertex of the R segments.
! C1 is the HCOF portion of ET rate.
! C2 is the RHS portion of ET rate.
! HCOFtrm is a function to calculate HCOF part of ET canopy flux.
! RHStm is a function to calculate RHS part of ET canopy flux.
! fCov is the fractional coverage in a cell by a plant functional
! subgroup.
! LC,KS,and NTS are counters.
! -----
!
! Specifications:

```



```

!-----
Integer::NLAY,NCOL,NROW
Integer::NRIPCL,NRIPVL,MAXRIP,MAXTS,MXSEG,IHSURF
Integer::IL,IR,IC
Integer::Loc1,Loc2
Integer::LC,KS,NTS
Integer, Dimension(MAXTS)::NuSEG
Double Precision, Dimension(NCOL,NROW,NLAY)::HNEW
Double Precision::HH
Double Precision, Dimension(MXSEG+1)::HK,RK
Double Precision, Dimension(MAXRIP,MAXTS)::C1,C2
Double Precision::HCOFtrm,RHStrm
Real, Dimension(NCOL,NROW,NLAY)::HCOF,RHS
Real, Dimension(NCOL)::DELR
Real, Dimension(NROW)::DELC
Real, Dimension(MAXTS)::Sxd,Ard,Rmax,Rsxd
Real, Dimension(MAXTS,MXSEG)::fdh,fdR
Real, Dimension(NRIPVL,MAXRIP)::RIP
Real::fCov,HSURF,Hxd,Hxd
Integer, Dimension(NCOL,NROW,NLAY)::IBOUND

!-----
!
!1-----If NRIPCL<=0, there are no riparian cells, return.
!
!   If (NRIPCL<=0) return
!
!2-----Process each cell in the riparian cell list.
!
Cell_Loop: Do LC=1,NRIPCL
!
!3-----Get column, row and layer from riparian cell array.
!
!       IL=RIP(1,LC)
!       IR=RIP(2,LC)
!       IC=RIP(3,LC)
!
!4-----If cell is external skip it and send a message to screen that cell
!         is inactive.
!
!       If (IBOUND(IC,IR,IL) == 0) Then
!         Write(*,'(A)') "***** Riparian cell is inactive *****"
!         Cycle Cell_Loop
!       End if
!
!5-----Set head for cell.
!
!       HH=HNEW(IC,IR,IL)
!
!6-----Process each plant functional subgroup, initialize C1 and C2,
!         and determine which plant functional subgroups are active
!         within in a cell.
!
!       TS_Loop:Do NTS=1,MAXTS
!         C1(LC,NTS)=0.0
!         C2(LC,NTS)=0.0
!
!7-----If IHSURF = 0, HSURF a function of cell only. If IHSURF > 0,
!         HSURF is also a function of plant functional subgroups
!
!       IF(IHSURF == 0) Then
!         Loc1=4+NTS           !retrieve fCov only
!       Else if (IHSURF > 0) Then
!         Loc1=3+2*NTS        !retrieves fCov
!         Loc2=3+2*NTS-1     !retrieves HSURF
!       End if
!       IF(RIP(Loc1,LC) /= 0.0) Then
!
!8-----Set cell non-zero fractional coverage for a plant functional subgroup,
!         retrieve HSURF from Rip, calculate Hxd and Hxd; and initialize
!         the extinction depth segment end points, HK(1) to Hxd, and RK(1)

```

```

!      to zero,
!
!      fCov=RIP(Loc1,LC)
!      If(IHSURF == 0) Then
!          HSURF=RIP(4,LC) !HSURF has only one value per cell
!      Else
!          HSURF=RIP(Loc2,LC) !HSURF has values for each plant
!      End if
!          !functional subgroup
!      Hxd=HSURF-Sxd(NTS)
!      Hxd=Hxd-Ard(NTS)
!      HK(1)=Hxd
!      RK(1)=0.0
!
!9-----Check to see if HH is beyond the ends of the ET flux curve;
!      If HH <= Hxd, set both C1 and C2 to zero; or if HH >= Hxd,
!      set C1=0.0 and C2=-Rxd*fCov*DELC(IR)*DELR(IC);
!      in either case, cycle to the next plant functional subgroup.
!
!          If(HH >= Hxd ) Then
!              C1(LC,NTS)=0.0
!              C2(LC,NTS)=-Rxd(NTS)*fCov*DELR(IC)*DELC(IR)
!              cycle TS_Loop
!          Else if(HH <= Hxd) then
!              C1(LC,NTS)=0.0
!              C2(LC,NTS)=0.0
!              cycle TS_Loop
!          End if
!
!10-----Loop through the ET flux rate function vertices.
!
!      Seg_Loop:DO KS=1, NuSeg(NTS)+1
!
!10A-----Calculate HKs and RKs as needed.
!
!          HK(KS+1)=Hk(KS)+fdh(NTS,KS)*Ard(NTS)
!          RK(KS+1)=RK(KS)+fdR(NTS,KS)*Rmax(NTS)
!
!10B-----Check to see if HK(KS)<HH<=HK(KS+1)
!
!          IF(HH > HK(KS) .and. HH <= HK(KS+1)) Then
!
!10C-----When it is, calculate C1 and C2 using the functions HCOFtrm and
!      RHStrm that are adjusted with fCov, DELR, and DELC.
!
!          C1(LC,NTS)=-fCov*HCOFtrm(HK(KS),HK(KS+1),      &
!              RK(KS),RK(KS+1))*DELR(IC)*DELC(IR)
!          C2(LC,NTS)=-fCov*RHStrm(HK(KS),HK(KS+1),      &
!              RK(KS),RK(KS+1))*DELR(IC)*DELC(IR)
!
!10D-----Add C1 to HCOF and subtract C2 from RHS.
!
!          HCOF(IC,IR,IL)=HCOF(IC,IR,IL)+C1(LC,NTS)
!          RHS(IC,IR,IL)=RHS(IC,IR,IL)-C2(LC,NTS)
!          EXIT Seg_Loop
!      End if
!      End do Seg_Loop
!      End if
!      End do TS_Loop
!      End do Cell_Loop
!
!11-----Return
!
!      Return
!
!      End Subroutine RIP1FM

```

Table 8. List of variables in module RIP2FM

Variable	Scope	Definition
NLAY	Global	Number of layers in the grid
NCOL	Global	Number of columns in the grid
NROW	Global	Number of rows in the grid
HNEW	Global	Most recent estimate of head in a cell
HCOF	Global	Coefficient of head in the finite-difference equations
RHS	Global	Right-hand side of the finite-difference equations
DELROW	Global	Cell dimension in row direction
DELC	Global	Cell dimension in column direction
IBOUND	Global	Status of cell: <0, constant head;=0, inactive;>0, active
NRIPCL	Package	Active number of riparian cells in a stress period
NRIPVL	Package	Dimensioning variable for RIP array : (4*MAXTS)
MAXRIP	Package	Maximum number of riparian cells
IHSURF	Package	IHSURF is a Flag for HSURF. If positive, the HSURF for a cell has a value for each active plant functional subgroups, and is zero has only one HSURF per cell.
MAXTS	Package	Maximum number of plant functional subgroups
MXSEG	Package	Maximum number of segments over all subgroups
HH	Module	Hydraulic head
HK	Package	Depth segment vertex component
RK	Package	ET Rate segment vertex component
Sxd	Package	Saturation extinction depth
Ard	Package	Active root depth
Rmax	Package	Maximum ET canopy flux rate
Rsxd	Package	ET canopy flux rate at saturation extinction depth
NuSeg	Package	Number of segments for a plant functional subgroup ET curve
fdh	Package	Active root depth segment factor
fdR	Package	Maximum ET flux segment factor
RIP	Package	Array containing location, HSURF and fractional coverage of plant functional subgroups
fCov	Module	Fractional coverage for a plant group
HSURF	Package	Land surface elevation
Hxd	Module	Extinction depth elevation
Hsxd	Module	Saturation extinction depth elevation
C1	Package	HCOF portion of ET rate
C2	Package	RHS portion of ET rate
LC	Module	Counter
IL	Module	Layer number
IR	Module	Row number
IC	Module	Column number
KS	Module	Counter
NTS	Module	Counter
Loc1	Module	Counter for fractional coverage values in a cell.
Loc2	Module	Counter for land surface elevations in a cell, used only if IHSURF>0.
HCOFtrm	Package	Function for HCOF portion of ET rate
RHStrm	Package	Function for RHS portion of ET rate

15.9 RIP2BD

Subroutine RIP2BD performs the following steps:

Step 1: Initialize the rate accumulator (RATOUT).

Step 2: Set cell-by-cell budget save flag (IBD) and clear buffer.

Step 3: Loop through each riparian cell (if NRIPCL > 0) and get row, column, layer, and surface elevation. Set HH=HNEW and initialize RATE to zero. Loop through plant functional groups, calculate ETR, and aggregate ETR to RATE, and load RATE to budget accumulator and to BUFF.

Step 4: If requested, print location, land surface elevation, head, cell ET rate and ET rate by plant functional subgroups. If IHSURF = 0, HSURF has only one value for a cell. If IHSURF ≠ 0, then HSURF has a value for each plant functional subgroups in a cell.

Step 5: If IRIPCB1>0, save the cell values: location, land surface elevation and ET rate for each plant functional subgroup. If IHSURF = 0, HSURF has only one value for a cell. If IHSURF ≠ 0, HSURF has a value for each plant functional subgroups in a cell.

Step 6: Copy cell ET rate to RIP if CBC option is set.

Step 7: Check to see if cell-by-cell flows are to be saved as a three-dimensional array.

Step 8: Move total riparian loss into VBVL for printing in BAS1OT.

Step 9: Add riparian ET (riparian ET rate times time's step length) to VBVL

Step 10: Move budget labels to VBNM for print by module BAS1OT.

Step 11: Increment Budget term counter.

Step 12: Return.

15.10 Listing for RIP2BD Module

```

!.....
!
Subroutine RIP1BD(C1,C2,RIP,ETR,MAXRIP,MAXTS,NRIPCL,NRIPVL,HNEW,NCOL,NROW,      &
                NLAY,DELT,VBVL,VBNM,MSUM,ICBCFL,IRIPCB,IRIPCBL,          &
                BUFF,IOUT,IRIPAL,KSTP,KPER,IHSURF)
!
Implicit none
!
!-----
! Calculates volumetric budgets for riparian cells,
! C1 is the HCOF portion of ET rate.
! C2 is the RHS portion of ET rate.
! RIP is the RIP array with dimension (NRIPVL,MAXRIP). includes, by cell:
! layer,row, column, land surface elevations and fractional coverage
! for each plant functional subgroup.
! ETR(c,p) is the ET rate for the pth plant functional subgroup
! in the cth cell.
! MAXRIP is the maximum number of riparian cells over all stress
! periods,
! MAXTS is the total number of plant functional subgroups for
! all cells
! NRIPCL is the number of active riparian cells in a stress period
! NRIPVL is the size of the first dimension of the array, RIP
! HNEW is the most recent estimate of head in a cell
! NLAY is the number of layers in the grid.
! NROW is the number of rows in the grid.
! NCOL is the number of columns in the grid.
! DELT is the length of current time step
! VBVL are the entries for volumetric budget.
! VBNM are the labels for entries in the volumetric budgets
! MSUM is the Counter for budget entries and labels in VBVL and VBNM
! ICBCFL is the flag for recording cell-by-cell flows
! IRIPAL is the dimension flag and increment for optional
! memory allocation.
! IRIPCB is a cell-by-cell save flag and unit number
! IRIPCBL is a flag to save cell values:location, surface elevation
! and ET rate for each plant functional subgroup.
! BUFF is a three dimensional array containing the RATE for each
! cell
! IOUT is the unit number of the LIST output file.
! IRIPAL is the dimension flag and increment for optional
! memory allocation.
! KSTP is a time step counter

```

```

! KPER is a stress period counter
! IHSURF is a flag to indicate that HSURF has only one value per
! cell, or that it has one value for each plant functional
! subgroups.
! IBD is a print or save flag.
! IBDLBL is a flag that indicate the first pass through a loop.
! RATE is plant functional subgroup aggregated ET rate for a cell,
! and is written to the RIP array if CBC is indicated under
! options.
! TEXT is a 16 character string, ' RIPARIAN ET' used in the
! budget.
! RATOUT is the Accumulator for total flow out of flow field
! to riparian ET.
! HH is the hydraulic head in a cell
! Zero is the number 0
! LC,NTS and II are counters
!-----
!
! Specifications:
!-----
Integer::MSUM
Character(16)::TEXT
Character(16), Dimension(MSUM)::VBNM
Integer::NCOL,NROW,NLAY,IBD,ICBCFL,IOUT,KSTP,KPER,IHSURF
Integer::IRIPCB,IRIPCB1,MAXRIP,MAXTS,NRIPCL,NRIPVL,IRIPAL,IBDLBL
Integer::IL,IC,IR,LC,NTS,II
Real::Zero,DELT,RATE,HSURF
Real, Dimension(4,MSUM)::VBVL
Real, Dimension(NRIPVL,MAXRIP)::RIP
Real, Dimension(NCOL,NROW,NLAY)::BUFF
Double Precision::RATOUT,HH
Double Precision, Dimension(NCOL,NROW,NLAY)::HNEW
Double Precision, Dimension(MAXRIP,MAXTS)::C1,C2,ETR
!
DATA TEXT /' RIPARIAN ET' /
!-----
!1-----Initialize the rate accumulator (RATOUT)
!
Zero=0.0
Ratout=zero
!
!2-----Set cell-by-cell budget save flag (IBD) and clear buffer
!
IBD=0
If (IRIPCB < 0 .and. ICBCFL /= 0) IBD=-1
If (IRIPCB > 0) IBD=ICBCFL
Do IL=1, NLAY
Do IR=1, NROW
Do IC=1, NCOL
BUFF(IC,IR,IL)=zero
End do
End do
!
!3-----Loop through each riparian cell if NRIPCL > 0.
!
If (NRIPCL > 0) Then
IBDLBL=0
Do LC = 1, NRIPCL
!3A-----Get row, column, layer, and surface elevation,
!
IL=RIP(1,LC)
IR=RIP(2,LC)
IC=RIP(3,LC)
!3B-----Set HH=HNEW, and initialize RATE to zero
!
HH=HNEW(IC,IR,IL)
RATE=zero

```

```

!
!3C-----Loop through plant functional subgroups, calculate ETR and
!         aggregate ETR to RATE
!
!         Do NTS=1,MAXTS
!           ETR(LC,NTS)=C1(LC,NTS)*HH+C2(LC,NTS)
!           RATE=RATE+ETR(LC,NTS)
!         End do
!
!3D-----Load RATE to budget accumulator and to BUFF
!
!         RATOUT=RATOUT+RATE
!         BUFF(IC,IR,IL)=BUFF(IC,IR,IL)+RATE
!
!4-----Print locations, head,surface elevations, cell ET rates and ET rate
!         by plant functional groups, if requested.
!
!         IF(IEB < 0)Then
!           IF(IEB=0) Write(IOUT,100) TEXT, KPER,KSTP
100         Format(1x,/,1x,A,' PERIOD',I3,' STEP',I3)
!
!4a----If IHSURF = 0, HSURF has only one value for a cell
!
!           IF(IHSURF == 0) Then
!             IF(IEB=0) Write(IOUT,120) (II, II=1,MAXTS)
120           format(1x,/,1x,' RIPARIAN ET',/ &
!             1x,' LAYER ROW COLUMN HEAD SURFACE ', &
!             ' CELL CELL ET RATE BY PLANT ', &
!             ' FUNCTIONAL GROUP',/ &
!             1x,' ELEVATION ', &
!             ' ET RATE ',10(I10),/)
!             HSURF=RIP(4,LC)
!             Write(IOUT,130) IL,IR,IC,HH,HSURF,RATE,(ETR(LC,NTS), &
!             NTS=1,MAXTS)
!           O.□ Format(1x,I3,3x,I3,3x,I3,2x,2F10.2,E14.5,5x,20(F10.5))
!
!4b----If IHSURF /= 0, HSURF has a value for each plant functional subgroup
!         in a cell.
!
!           Else if (IHSURF /= 0) Then
!             IF(IEB=0) Write(IOUT,140) (II, II=1,MAXTS)
140           Format(1x,/,1x,' RIPARIAN ET',/ &
!             1x,' LAYER ROW COLUMN HEAD CELL ', &
!             ' SURFACE ELEVATION AND FRACTIONAL COVERAGE OF ', &
!             ' PLANT FUNCTIONAL SUBGROUPS',/ &
!             ' ET ',10(I23))
!             Write(IOUT,150) IL,IR,IC,HH,RATE,((RIP(2+2*NTS,LC),ETR(LC, &
!             NTS)),NTS=1,MAXTS)
!           O.□ Format(1x,I3,3x,I3,3x,I3,2x,F10.2,E14.5,5x,20(F10.2,3x,F10.5))
!           End if
!           IBDL=1
!         End if
!
!5-----Save Cell values:location, surface elevation and ET rate for each plant
!         functional subgroup.
!
!         IF(IRIPCB1>0) then
!5a----IHSURF = 0, HSURF has only one value for a cell
!
!           IF(IHSURF== 0) Then
!             Write(IRIPCB1,160) IL,IR,IC,HSURF,(ETR(LC,NTS),NTS=1,MAXTS)
!           O.□ Format(3I5,F10.2,20E15.5)
!
!5b----IHSURF /= 0, HSURF has a value for each plant functional subgroup
!         in a cell.
!
!           ELSE
!             Write(IRIPCB1,170) IL,IR,IC,((RIP(2+2*NTS,LC),ETR(LC,NTS)) &
!             ,NTS=1,MAXTS)

```

```

0. Format(1x,I3,3x,I3,3x,I3,2x,20(F10.2,3x,F10.5))
      End if
      End if
!
!6-----Copy flow to RIP if CBC option is set.
!
      If(IRIPAL /= 0) RIP(NRIPVL,LC)=RATE
      End do
      End if
!
!7-----Check to see if cell-by-cell flows are to be saved as three-
!      dimensional array.
!
      If(IBD == 1) Then
        Call UBUDSV(KSTP,KPER,TEXT,IRIPCB,BUFF,NCOL,NROW,NLAY,IOUT)
      End if
!
!8-----Move total riparian loss into VEVL for printing in BASIOT.
!
      VBVL(3,MSUM)=Zero
      VBVL(4,MSUM)=RATOUT
!
!9-----Add riparian ET (riparian ET rate times time's step length)
!      to VEVL.
!
      VBVL(2,MSUM)=VEVL(2,MSUM)+RATOUT*DELTA
!
!10-----Move budget term labels to VBNM for printing by module BASIOT.
!
      VBNM(MSUM)=TEXT
!
!11-----Increment Budget term counter.
!
      MSUM=MSUM+1
!
!12-----Return
!
      Return
End Subroutine RIP1BD

```

Table 9. List of variables in module RIP2BD

Variable	Scope	Definition
NLAY	Global	Number of layers in the grid
NCOL	Global	Number of columns in the grid
NROW	Global	Number of rows in the grid
HNEW	Global	Most recent estimate of head in a cell
MSUM	Global	Counter for budget entries and labels in VBVL and VBNM
KSTP	Global	Time step counter
KPER	Global	Stress period counter
RATOUT	Module	Accumulator for total flow out of flow field to riparian ET
IBOUND	Global	Status of cell: <0, constant head;=0, inactive;>0, active
VBNM	Global	Labels for entries in the volumetric budgets
VBVL	Global	Entries for volumetric budget.
DELTA	Global	Length of current time step
RATE	Module	ET in cell aggregated over plant functional subgroups
ZERO	Module	The number 0
HH	Module	Hydraulic head
TEXT	Module	Label to be printed or recorded with array data.
BUFF	Global	Buffer used to accumulate information before printing it
IOUT	Global	Primary unit number for all printed output
IBD	Module	Flag for recording cell-by-cell flows
ICBCFL	Global	Flag for recording cell-by-cell flows
IRIPCB	Package	Flag for recording cell-by-cell flows
IRIPCB1	Package	Flag for list file printing
IRIPAL	Package	Dimension increment or flag for the optional memory allocation
NRIPCL	Package	Active number of riparian cells in a stress period
NRIPVL	Package	Dimensioning variable for RIP array : (4*MAXTS)
MAXRIP	Package	Maximum number of riparian cells

IHSURF	Module	a flag to indicate that HSURF has only one value per cell, or that is has one value for each plant functional subgroups.
MAXTS	Package	Maximum number of plant functional subgroups
IBDLBL	Module	A flag that indicate the first pass through a loop
RIP	Package	Array containing location, HSURF and percent coverage of plant functional subgroups
HSURF	Package	Land surface elevation
C1	Package	HCOF portion of ET rate
C2	Package	RHS portion of ET rate
ETR	Package	ET rate
IL	Module	Layer number
IC	Module	Row number
IR	Module	Column number
NTS	Module	Counters
II	Module	Counters

15.11 HCOFtrm and RHStrm

The functions HCOFtrm and RHStrm are based on a linear interpolation of the ET canopy flux rate function, $R(h)$, is given by the equation,

$$R(h) = R_k + \frac{(h - h_k)}{h_{k+1} - h_k} (R_{k+1} - R_k) \quad \text{for } h_k < h \leq h_{k+1}$$

which can be rewritten as

$$R(h) = \frac{R_{k+1} - R_k}{h_{k+1} - h_k} h + \frac{(R_k h_{k+1} - R_{k+1} h_k)}{h_{k+1} - h_k} \quad \text{for } h_k < h \leq h_{k+1}$$

The function HCOFtrm is calculated as

$$HCOFtrm(h_k, h_{k+1}, R_k, R_{k+1}) = \frac{R_{k+1} - R_k}{h_{k+1} - h_k}$$

The function RHStrm is calculated as

$$RHStrm(h_k, h_{k+1}, R_k, R_{k+1}) = \frac{(R_k h_{k+1} - R_{k+1} h_k)}{h_{k+1} - h_k}$$

15.12 Listing for HCOFtrm and RHStrm Functions

```
Function HCOFtrm(HK, HK1, RK, RK1)
!-----
! This function calculates the HCOF term for the riparian ET
! HK = first of two consecutive vertices head values
! HK1 = second vertex head value
! RK = first of two consecutive vertices ET flux rate values
! RK1 = second vertex ET flux rate value
!-----
Double Precision :: HCOFtrm
Double Precision :: HK, HK1, RK, RK1
!-----
HCOFtrm = (RK1 - RK) / (HK1 - HK)
End Function HCOFtrm
!
!.....
!
Function RHStrm(HK, HK1, RK, RK1)
```



```

!-----
! This function calculates the RHS term for the riparian ET
! HK = first of two consecutive vertices head values
! HK1 = second vertex head value
! RK = first of two consecutive vertices ET flux rate values
! RK1 = second vertex ET flux rate value
!-----
Double Precision:: RHStrm
Double Precision::HK, HK1, RK, RK1
!-----
RHStrm= (RK*HK1-RK1*HK) / (HK1-HK)
End Function RHStrm

```

Table 10. List of variables in functions HCOFtrm and RHStrm

Variable	Scope	Definition
HK	Function	first of two consecutive vertices head values
HK1	Function	second vertex head value
RK	Function	first of two consecutive vertices ET flux rate values
RK1	Function	second vertex ET flux rate value

16.0 References

- Baird, K.J. and T. Maddock, III. In preparation. A New Method For Determining Riparian Evapotranspiration.
- Banta, E.R. 2000. MODFLOW-2000, the U.S. Geological Survey modular ground-water model-Documentation of packages for simulating evapotranspiration with a segmented function (ETS1) and drains with return flow (DRT1). U.S. Geological Survey Open-File Report 00-466.
- Busch, D. E., N. L. Ingraham, and S. D. Smith. 1992. Water uptake in woody riparian phreatophytes of the southwestern United States: A stable isotope study. *Ecological Applications* 2:450-459.
- Dragoo, C.A., T. Maddock III and K.J. Baird. In preparation. Riparian GIS Preprocessor (RIP-GIS).
- Glennon, R.J. and T. Maddock III. 1994. In search of subflow: Arizona's futile effort to separate groundwater from surface water. *36 Arizona Law Review* 567.
- Goodrich, D. C., R. Scott, J. Qi, B. Goff, C. L. Unkrich, M. S. Moran, D. G. Williams, S. M. Schaeffer, K. A. Snyder, R. D. MacNish, T. Maddock, D. Pool, A. Chehbouni, D. I. Cooper, W. E. Eichinger, W. J. Shuttleworth, Y. Kerr, R. Marsett, and W. Ni. 2000. Seasonal estimates of riparian evapotranspiration using remote and in situ measurements. *Agricultural and Forest Meteorology* 105:281-309.
- Granier, A., P. Biron, and D. Lemoine. 2000. Water balance, transpiration and canopy conductance in two beech stands. *Agricultural and Forest Meteorology* 100:291-308.
- Grimm, N.B., A. Chacon, C.N. Dahm, S.W. Hostetler, O.T. Lind, P.L. Starkweather, and W.W. Wurtsbaugh. 1997. Sensitivity of aquatic ecosystems to climatic and anthropogenic changes: the Basin and Range, American Southwest and Mexico. *Hydrological Processes* 11:1023-1041.
- Hadley, G. 1964. *Nonlinear and Dynamic Programming*, Addison-Wesley Publishing Co. Inc., Reading Massachusetts.
- Harbaugh, A.W., and M.G. McDonald. 1996a, User's documentation for MODFLOW-96: An update to the U.S. Geological Survey modular finite-difference ground-water flow model: U.S. Geological Survey Open-File Report 96-485.
- 1996b, Programmer's documentation for MODFLOW-96, an update to the U.S. Geological Survey modular finite difference ground-water flow model: U.S. Geological Survey Open-File Report 96-486.
- Lavorel, S., S. McIntyre, J. J. Landsberg, and T.D.A Forbes. 1997. Plant functional classifications: from general groups to specific groups based on response to disturbance. *Tree* 12:474-478.
- Leishman, M. R. and M. Westoby. 1992. Classifying plants into groups on the basis of associations of individual traits – evidence from Australian semi-arid woodlands. *Journal of Ecology* 80:417-424.
- McDonald, M.G., and A.W. Harbaugh. 1988. A Modular Three-Dimensional Finite-Difference Ground-Water Flow Model. U.S. Geological Survey TWI 6-A1
- Meinzer, F. C., J. L. Andrade, G. Goldstein, N. M. Holbrook, J. Cavelier, and P. Jackson. 1997. Control of transpiration from the upper canopy of a tropical forest: the role of stomatal layer and hydraulic architecture components. *Plant, Cell and Environment* 20:1242-1252.
- Oren, R., N. Phillips, B. E. Ewers, Pataki D.E., and Megonigal J.P. 1999. Sap-flux-scaled transpiration responses to light, vapor pressure deficit, and leaf area reduction in a flooded *Taxodium distichum* forest. *Tree Physiology* 19:337-347

- Poff, N. L., J. D. Allan, M. B. Bain, J. R. Karr, K. L. Prestegard, B. D. Richter, and J. C. Stromberg. 1997. The natural flow regime: A paradigm for river conservation and restoration. *BioScience* 47:769-784.
- Shafroth, P.B., J.C. Stromberg, and D.T. Patten. 2000. Woody riparian vegetation response to different alluvial water table regimes. *Western North American Naturalist* 60(1):66-76.
- Snyder, K. A. and D. G. Williams. 2000. Water sources used by riparian trees varies among stream types on the San Pedro River, Arizona. *Agricultural and Forest Meteorology* 105:227-240.
- Stromberg, J.C. 1993. Fremont cottonwood-Goodding willow riparian forests: A review of their ecology, threats, and recovery potential. *Journal of the Arizona-Nevada Academy of Science* 26(3):97-110.
- Stromberg, J.C, R. Tiller, and B. Richter. 1996. Effects of groundwater decline on riparian vegetation of semiarid regions: the San Pedro, Arizona. *Ecological Applications* 6(1): 113-131.
- Williams, D. G., Brunel, J.-P., Schaeffer, S. M., and Snyder, K. A., 1998. Biotic controls over the functioning of desert riparian ecosystems. In; *Proceedings from the Special Symposium on Hydrology*. (Eds) Wood, E. F., Chehbouni, A. G., Goodrich, D. C., Seo, D. J., and Zimmerman J.R. pp. 43-48. Boston MA, American Meteorological Society.

APPENDIX A, PLANT FUNCTIONAL SUBGROUP CURVES

Listed here are the heads, ET flux rates, *fdh* and *fdR* for the plant functional groups developed for RIP-ET. Values are the result of field work, literature review and researcher input (Baird and Maddock, in preparation). The head is defined as zero at the land surface, positive above land surface, and negative below. The units of head are *cm* and the units of ET-Flux are *cm/day* for all curves. In the RIP-ET package, Vertex 1 and segment 1 of the flux curve must start at the PFSG's extinction depth. Therefore, *fdhs* and *fdRs* array indices must start at that point as well.

Table A1. Head, ET flux rates for Obligate wetland PFG

Vertex	Head (cm)	ET flux rate (cm/day)
1	-75	0
2	-33	0.20
3	-15	0.32
4	-10	0.35
5	-7	0.35
6	-4	0.32
7	0	0.23
8	20	0

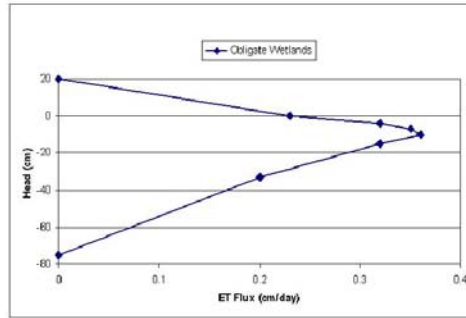


Figure A1: ET flux rates for Obligate wetland PFG

Table A2. *fdh* and *fdR* for Obligate wetland PFG

Segment	<i>fdh</i>	<i>fdR</i>
1	0.4421	0.5556
2	0.1895	0.3333
3	0.0526	0.1111
4	0.0316	-0.0278
5	0.0316	-0.0833
6	0.0421	-0.2500
7	0.2105	-0.6389

Table A3. Head, ET flux rates for Shallow-rooted riparian PFG

Vertex	Head (cm)	ET flux rate (cm/day)
1	-160	0
2	-100	0.10
3	-60	0.31
4	-50	0.33
5	-40	0.31
6	-32	0.17
7	0	0

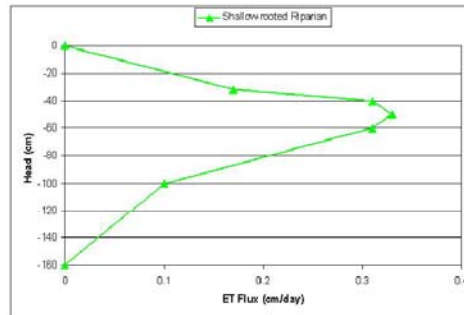


Figure A2: ET flux rates for Shallow-rooted riparian PFG

Table A4. fdh and fdR for Shallow-rooted riparian PFG

Segment	fdh	fdR
1	0.3750	0.3030
2	0.2500	0.6364
3	0.0625	0.0606
4	0.0625	-0.0606
5	0.0500	-0.4242
6	0.2000	-0.5152

Table A5. Head, ET flux rates for average Deep-rooted riparian PFG

Vertex	Head (cm)	ET flux rate (cm/day)
1	-500	0.00
2	-400	0.12
3	-300	0.21
4	-200	0.29
5	-150	0.31
6	-100	0.28
7	-75	0.17
8	0	0.00

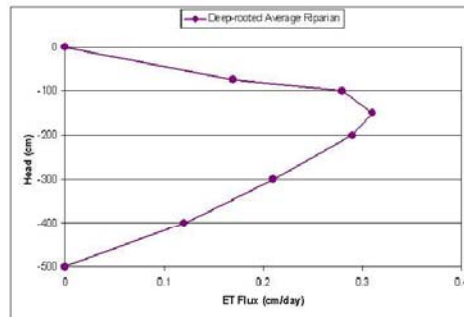


Figure A3: ET flux rates for average Deep-rooted riparian PFG

Table A6. fdh and fdR for average Deep-rooted riparian PFG

Segment	fdh	fdR
1	0.2000	0.3871
2	0.2000	0.2903
3	0.2000	0.2581
4	0.1000	0.0645
5	0.1000	-0.0968
6	0.0500	-0.3548
7	0.1500	-0.5484

Table A7. Head, ET flux rates for Transitional riparian PFG

Vertex	Head (cm)	ET flux rate (cm/day)
1	-600	0
2	-500	0.11
3	-400	0.20
4	-340	0.27
5	-300	0.28
6	-260	0.27
7	-175	0.16
8	-50	0.00

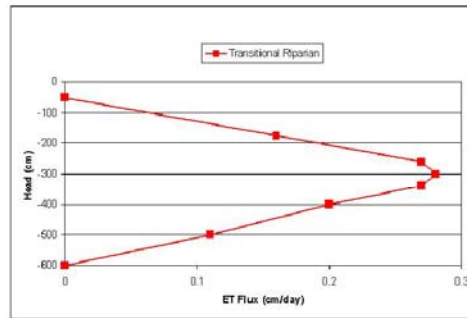


Figure A4: ET flux rates for Transitional riparian PFG

Table A8. fdh and fdR for Transitional riparian PFG

Segment	fdh	fdR
1	0.1818	0.3929
2	0.1818	0.3371
3	0.1091	0.2343
4	0.0727	0.0357
5	0.0727	-0.0357
6	0.1545	-0.3811
7	0.2273	-0.5832

Table A9. Head, ET flux rate for Deep-rooted riparian size classes

Head (cm)	Size class (cm/day)			
	Small	Medium	Large	X-Large
-500		0	0	0
-400	0	0.0838	0.1032	0.1100
-300	0.0501	0.1650	0.2064	0.2199
-200	0.1001	0.2450	0.2759	0.2940
-150	0.1602	0.2615	0.2944	0.3137
100	0.2003	0.2357	0.2653	0.2827
75	0.1742	0.1506	0.1400	0.1492
0	0	0	0	0

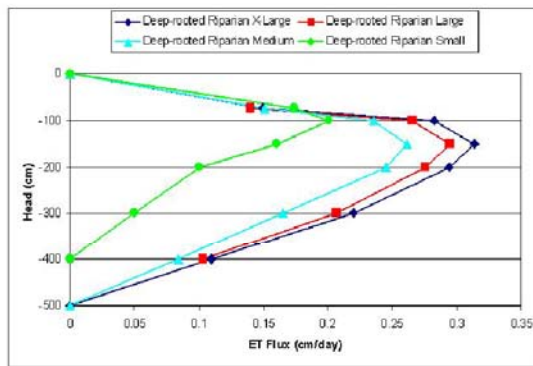


Figure A5: ET flux rates for small, medium, large and X-large Deep-rooted riparian PFG

Table A10. *fdhs* and *fdRs* for Deep-rooted riparian size classes

Segment Number	Small		Medium		Large		X-large	
	<i>fdh</i>	<i>fdR</i>	<i>fdh</i>	<i>fdR</i>	<i>fdh</i>	<i>fdR</i>	<i>fdh</i>	<i>fdR</i>
1	0.2500	0.2501	0.2000	0.3218	0.2000	0.3505	0.2000	0.3503
2	0.2500	0.2496	0.2000	0.3103	0.2000	0.3505	0.2000	0.3503
3	0.1250	0.3001	0.2000	0.3066	0.2000	0.2362	0.2000	0.2382
4	0.1250	0.2002	0.1000	0.0613	0.1000	0.0628	0.1000	0.0612
5	0.0625	-0.1303	0.1000	-0.0958	0.1000	-0.0988	0.1000	-0.0986
6	0.1875	-0.8697	0.0500	-0.3257	0.0500	-0.4256	0.0500	-0.4252
7			0.1500	-0.5785	0.1500	-0.4756	0.1500	-0.4762

Appendix B, Adapting RIP-ET to MODFLOW 2000

Introduction

Minor but non-trivial changes are required to modify the MODFLOW 96 RIP-ET version to MODFLOW 2000. Primarily, these changes have their origins in how memory is managed in MODFLOW 2000. In MODFLOW 96, most of the model data is stored in a single X array. In MODFLOW 2000, 9 separate arrays are used. The use of the additional arrays is necessary for two reasons. First, it prevents compiler warning message when integers and double precision array are stored in the Real X array. Second, MODFLOW 2000 uses dynamically allocated arrays, and needs to use some of the X array type data prior to the point where all the data have been allocated. The X array is broken into nine pieces composed of three different data types, and the three types are allocated at three different places in the code. RIP-ET needs to assign its data into three of the nine data arrays. The real data goes into the RX array, the integer data goes into the IR array, and the double precision data goes into the RZ array.

The only changes in RIP-ET itself are the change in the subroutine names, and array partitioning in the subroutine RIP2AL, renamed GWF1RIP2AL. The rest of the changes occur in the MODFLOW 2000 program MAIN and the subroutines GWF1BAS6AL, and MEMCHKR.

Changes to Subroutine Names

MODFLOW 2000 uses longer subroutine names. The new names have an additional prefix. Thus the names in RIP-ET change as follows,

RIP2AL	->	GWF1RIP2AL
RIP2RP1	->	GWF1RIP2RP1
RIP2RP2	->	GWF1RIP2RP2
RIP2FM	->	GWF1RIP2FM
RIP2BD	->	GWF1RIP2BD

These subroutines are found in the file gwfrqip2.f90

Changes to GWF1RIP2AL

Because arrays are dynamically allocated in MODFLOW 2000, there is no need to check if available memory is exceeded. Therefore, the LENX variable no longer needs to be passed to the allocate subroutines. However, it will be necessary to pass three "ISUM" variables to the RIP-ET allocation subroutine. These are ISUMRX, ISUMIR, and ISUMRZ, which track the locations in the RX, IR and RZ arrays.

```
Subroutine GWF1RIP2AL( ISUMRX, ISUMIR, ISUMRZ, LCSxd, LCArd, LCRmax, LCRsxd, &  
LCNuSEG, LCFdh, LCFGR, LCRip, LCC1, LCC2, LCETR, IN, IOUT, &  
IFREEM, MAXRIP, IRIPCB, IRIPCB1, NRIPCL, NRIPVL, &  
MAXTS, MXSEG, IRIPAL, IHSURF)
```

Because RIP-ET is written in FORTRAN 90 and uses an Implicit None statement, ISUMRX, ISUMIR and ISUMRZ must be declared as integer variables,

```
Integer:: ISUMRX, ISUMIR, ISUMRZ
```

In MODFLOW 96, the X array was partitioned using LC variables, and the same LC variables may be used in MODFLOW 2000. However, the LC variable must be set equal to the appropriate ISUM variable data type, and that ISUM variable must be incrementally increased accordingly. For example, NUSEG is an integer array, so LCNUSEG should be set equal to ISUMIR, and then ISUMIR should be incrementally increased by the size of NUSEG. For double precision data, the "*2" should be removed from the space allocations because the RZ variables are directly declared as double precision unlike the old X array.

```
!5a----Simulation variables, Sxd, Ard, Rmax, Rxd, fdh, fdR, NuSeg
!
  ISPRX=ISUMRX
  LCSxd=ISUMRX
  ISUMRX=ISUMRX+MAXTS
  LCArd=ISUMRX
  ISUMRX=ISUMRX+MAXTS
  LCRmax=ISUMRX
  ISUMRX=ISUMRX+MAXTS
  LCRsxd=ISUMRX
  ISUMRX=ISUMRX+MAXTS
  LCFdh=ISUMRX
  ISUMRX=ISUMRX+MAXTS*MXSEG
  LCFdR=ISUMRX
  ISUMRX=ISUMRX+MAXTS*MXSEG
  LCRIP=ISUMRX
  ISUMRX=ISUMRX+NRIPVL*MAXRIP
!
  ISPIR=ISUMIR
  LCNUSEG=ISUMIR
  ISUMIR=ISUMIR+MAXTS
!
!5b----Stress period variables, C1, C2, ETR
!
  ISPRZ=ISUMRZ
  LCC1=ISUMRZ
  ISUMRZ=ISUMRZ+MAXRIP*MAXTS
  LCC2=ISUMRZ
  ISUMRZ=ISUMRZ+MAXRIP*MAXTS
  LCETR=ISUMRZ
  ISUMRZ=ISUMRZ+MAXRIP*MAXTS
```

The memory-usage write statement need to be modified to reflect data type, and the check for not enough memory needs to be removed.

```
!
!6----Print amount of space used by the Riparian package.
!
  ISPRX=ISUMRX-ISPRX
  ISPIR=ISUMIR-ISPIR
  ISPRZ=ISUMRZ-ISPRZ
  Write(IOUT,160) ISPRX
160 Format(1x,I10,' ELEMENTS OF RX ARRAY ARE USED BY RIP')
  Write(IOUT,170) ISPIR
170 Format(1x,I10,' ELEMENTS OF IR ARRAY ARE USED BY RIP')
  Write(IOUT,180) ISPRZ
180 Format(1x,I10,' ELEMENTS OF RZ ARRAY ARE USED BY RIP')
```

Changes to Calling Arguments in Main

When calling the RIP-ET subroutines from MAIN in file mf2k.f, the "X(...)" arguments that pass the RIP-ET data must be changed to reflect the new data variable. For example, C1 in RIP-ET is double precision, so it will be

stored in the RZ array and passed to a subroutine as RZ(LCC1). Likewise, NUSEG in RIP-ET is integer, so it will be stored in the IR array and passed to a subroutine as IR(LCNUSEG).

When passing global data to the RIP-ET subroutines, change "X(...)" to refer to the correct new data variables, thus

```
X(LCNEW)   ->   GZ(LCHNEW)
X(LCRHS)   ->   GX(LCRHS)
X(LCHCOF)  ->   GX(LCHCOF)
X(LCIBOU)  ->   IG(LCIBOU)
X(LCIBUFF) ->   GX(LCIBUFF)
X(LCDELIR) ->   GX(LCDELIR)
X(LCDELIC) ->   GX(LCDELIC)
```

Changes to Allocation of Double Precision Arrays in Main

Prior to RIP-ET, none of the packages needed to allocate double precision data in the RZ array so the pointer variable ISUMRZ was not actually incorporated into the MODFLOW 2000 code. To include ISUMRZ into the code requires several changes to MAIN. These changes are as follows,

1. In the first double precision statement at the beginning of MAIN, add the variable RZ.

```
DOUBLE PRECISION RZ, GZ, VAR, Z
```

2. In the first ALLOCATABLE statement at the beginning of MAIN, add RZ(:).

```
ALLOCATABLE GX(:), IG(:), X(:), IX(:), RX(:), IR(:), GZ(:), Z(:),
&           RZ(:), XHS(:), NIPRNAM(:), EQNAM(:), NAMES(:),
&           OBSNAM(:)
```

3. Change the comment statement C4 to "allocate space in the RX, IR and RZ arrays."
4. The RZ array needs to be allocated so go to the line with the statement " ALLOCATE (RX(LENRX), IR(LENIR))" and add RZ(LENRZ) to the statement.

```
ALLOCATE (RX(LENRX), IR(LENIR), RZ(LENRZ))
```

5. Add the following two lines before the above ALLOCATE statement,

```
LENRZ=ISUMRZ-1
IF(LENRZ.LE.0) LENRZ=1
```

6. A different IUNIT location is needed. In MODFLOW 96, it was IUNIT(22) but this is now used by the LAK package in MODFLOW 2000. In this version of MODFLOW 2000, IUNIT(42) was available.
7. Add 'RIP ' to the 42nd position (or whatever IUNIT location is used) in the CUNIT data statement.

```
DATA CUNIT/'BCF6', 'WEL ', 'DRN ', 'RIV ', 'EVT ', ' ', ' ', 'GHB ',
&         'RCH ', 'SIP ', 'DE4 ', 'SOR ', 'OC ', 'PCG ', 'LMG ',
&         ' ', 'FHB ', 'RES ', 'STR ', 'IBS ', 'CHD ', 'HFB6',
&         'LAK ', 'LPF ', 'DIS ', 'SEN ', 'PES ', 'OBS ', 'HOB ',
&         'ADV2', 'COB ', 'ZONE', 'MULT', 'DROB', 'RVOB', 'GBOB',
&         'STOB', 'HUF ', 'CHOB', 'ETS ', 'DRT ', 'DFOB', 'RIP ',
&         'HYD ', ' ', 'SFOB', 'GAGE', ' ', ' ', ' ', 'LMT6',
&         ' ', ' ', 50* ' ' /
```

Initialization of ISUMRZ in GWF1BAS6AL

The partition variable ISUMRZ needs to be initialized to 1. This can be done in one of two ways. First, the statement,

```
ISUMRZ = 1
```

Can be placed as an assignment statement in MAIN right after the comment statement labeled C4.

The second way is more complicated but more elegant. The variables ISUMRX and ISUMIR are initialized in the subroutine GWF1BAS6AL found in the file gwf1bas6.f. Add the ISUMRZ to the subroutine argument list,

```
      SUBROUTINE GWF1BAS6AL(HEADNG,NPER,TOTIM,NCOL,NROW,NLAY,NODES,  
1      INBAS,IOUT,IXSEC,ICHFLG,IFREFM,ISUMRX,ISUMIR,ISUMRZ,  
2      LCIOFL,ISTRRT,IAPART)
```

and add ISUMRZ = 1 below the line labeled 20 where ISUMRX and ISUMIR are initialized,

```
      20  ISUMRX=1  
          ISUMIR=1  
          ISUMRZ=1
```

then add ISUMRZ to the argument list of the calling statement in MAIN,

```
      CALL GWF1BAS6AL(HEADNG,NPER,TOTIM,NCOL,NROW,NLAY,NODES,INBAS,  
1      IOUT,IXSEC,ICHFLG,IFREFM,ISUMRX,ISUMIR,ISUMRZ,  
2      LCIOFL,ISTRRT,IAPART)
```

Changes to MEMCHKR

The subroutine MEMCHKR needs to be modified to print the amount of memory used by the RZ array. MEMCHKR is called immediately after the comment C5. ISUMRZ and LENRZ need to be added the argument list and into statements in the main body of the subroutine. This short subroutine is found in the file memchk.f

```
      SUBROUTINE MEMCHKR(ISUMRX,ISUMIR,ISUMRZ,LENRX,LENIR,LENRZ,IOUT,  
&      IERRX,IERRU)  
C  
      IERR = 0  
      WRITE(IOUT,10)  
      WRITE(IOUT,10) ISUMRX-1,LENRX  
10  FORMAT(1X,I10,' ELEMENTS OF RX ARRAY USED OUT OF ',I10)  
      WRITE(IOUT,12) ISUMIR-1,LENIR  
12  FORMAT(1X,I10,' ELEMENTS OF IR ARRAY USED OUT OF ',I10)  
      WRITE(IOUT,14) ISUMRZ-1,LENRZ  
14  FORMAT(1X,I10,' ELEMENTS OF RZ ARRAY USED OUT OF ',I10)  
C  
      IF (ISUMRX-1.GT.LENRX) IERR = IERR + 1  
      IF (ISUMIR-1.GT.LENIR) IERR = IERR + 1  
      IF (ISUMRZ-1.GT.LENRZ) IERR = IERR + 1  
      IF (IERR.NE.0) THEN  
          WRITE(IOUT,13) IERR  
          WRITE(IERRU,13) IERR  
          IERRX = 1  
          RETURN  
      ENDIF  
13  FORMAT(/,1X,I1,' ARRAY(S) NEED(S) TO BE DIMENSIONED LARGER')  
C  
      RETURN  
      END
```

The Five Calling Statement to RIP-ET from MAIN

The follow calling statements are added to MAIN as specified,

1. After the statement,

```

IF(IUNIT(40).GT.0)
& CALL GWFLDRTIAL(ISUMRX, LCDRTE, MXDRT, NDRTCL, IUNIT(40), IOUT,
& IDRTCB, NDRTVL, IDRTAL, IFREFM, NPDRT, IDRTPB,
& NDRTNP, IDRTFL, NOPRDT)

```

add the statement,

```

C--RIPARIAN SYSTEMS
IF(IUNIT(42).GT.0)
& CALL GWFLRIP2AL(ISUMRX, ISUMIR, ISUMRZ, LCSxd, LCARD, LCRmax,
& LCRsxd, LCNUSEG, LCFdh, LCFdR, LCRIP, LCC1, LCC2,
& LCETR, IUNIT(42), IOUT, IFREFM, MAXRIP, IRIPCB,
& IRIPCB1, NRIPCL, NRIPVL, MAXTS, MXSEG, IRIPAL, IHSURF)

```

2. After the statement,

```

IF(IUNIT(40).GT.0)
& CALL GWFLDRTIRQ(IUNIT(40), IOUTG, NDRTVL, IDRTAL, NCOL, NROW,
& NLAY, NPDRT, RX(LCDRTE), IDRTPB, MXDRT, IFREFM,
& ITERPK, IDRTFL, INAMLOC, NOPRDT)

```

add the statement,

```

C--RIPARIAN SYSTEMS
IF(IUNIT(42).GT.0)
& CALL GWFLRIP2RPL(RX(LCSxd), RX(LCARD), RX(LCRmax), RX(LCRsxd),
& IR(LCNUSEG), RX(LCFdh), RX(LCFdR), MAXTS, MXSEG,
& IFREFM, IUNIT(42), IOUT)

```

3. After the statement,

```

IF(IUNIT(40).GT.0)
& CALL GWFLDRTIRP(RX(LCDRTE), NDRTCL, MXDRT, IUNIT(40),
& IOUT, NDRTVL, IDRTAL, IFREFM, NCOL, NROW, NLAY,
& NDRTNP, NPDRT, IDRTPB, IDRTFL, NRELOW, NOPRDT)

```

add the statement,

```

C--RIPARIAN SYSTEMS
IF(IUNIT(42).GT.0)
& Call GWFLRIP2RP2(RX(LCRIP), NRIPCL, NRIPVL, IRIPAL, MAXRIP,
& MAXTS, IHSURF, IUNIT(42), IOUT, IFREFM)

```

4. After the statement,

```

IF(IUNIT(21).GT.0)
& CALL GWFLHFB6FM(GX(LCBOTM), GX(LCCC), GX(LCCR),
& GX(LCDEL), GX(LCDEL), RX(LCHF),
& GX(LCHNEW), MXACTFB, NBOTM, NCOL, NHFB,
& NLAY, NROW, LAYHDT)

```

add the statement,

```

C---RIPARIAN SYSTEMS
IF(IUNIT(42).GT.0)
& CALL GWFLRIP2FM(NRIPCL, NRIPVL, MAXRIP, MAXTS, IHSURF,
& MXSEG, RX(LCRIP), RX(LCSxd), RX(LCARD), RX(LCRmax),
& RX(LCRsxd), IR(LCNUSEG), RX(LCFdh), RX(LCFdR),
& RZ(LCC1), RZ(LCC2), GZ(LCHNEW), GX(LCHCOF), GX(LCRHS),
& IG(LCIBOU), NLAY, NCOL, NROW,
& GX(LCDEL), GX(LCDEL))

```

5. After the statement,

```

IF(IUNIT(40).GT.0)
& CALL GWFLDRT1BD(NDRTCL, MXDRT, VENM, VBVL, MSUM, RX(LCDRTE),
& DELT, GZ(LCHNEW), NCOL, NROW, NLAY,
& IG(LCIBOU), KKSTP, KKPER, IDRTCB, ICBCFL,
& GX(LCBUFF), IOUT, PERTIM, TOTIM, NDRTVL,

```

```

&                                IDRTAL, IDRTEL, NRELOW, IAUXSV)

add the statement,

C--RIPARIAN SYSTEMS
  IF (IUNIT(42).GT.0)
&    CALL GWF1RIP2BD(RZ(LCC1), RZ(LCC2), RX(LCRIP), RZ(LCETR),
&    MAXRIP, MAXTS, NRIPCL, NRIPVL, GZ(LCHNEW), NCOL, NROW, NLAY,
&    DELT, VBVL, VBNM, MSUM, ICBCFL, IRIPCB, IRIPCBL, GX(LCBUFF),
&    IOUT, IRIPAL, KSTP, KPER, IHSURF)

```

RIP-ET Disk

All the changes to MODFLOW 2000 for RIP-ET are included in a CD (or an attachment if you receive this note by email). The disk includes four FORTRAN files, mf2k.f, gwf1bas6.f, memchk.f and gwf1rip2.f90, an executable file MF2K.exe, and this documentation file.

References

- Anderson, T. W., Geoffrey W. Freethey, and Patrick Tucci, Geohydrology and Water Resources of Alluvial Basins in South Central Arizona and Parts of Adjacent States, U.S. Geological Survey Professional Paper 1406-B, United States Government Printing Office, Washington, 1992.
- Baird, K.J. and T. Maddock III. 2005. Simulating Riparian Evapotranspiration: A New Methodology and Application for Groundwater Models. *Journal of Hydrology* 312: 176-190.
- Baird, K.J., J.C. Stromberg and T. Maddock III. 2005. Linking Riparian Dynamics and Groundwater: An eco-hydrologic approach to modeling groundwater and riparian vegetation. *Environmental Management* 36(4): 551-564.
- Goode, Tomas and Thomas Maddock III, 1999, Simulation of Groundwater Conditions in the Upper San Pedro Basin for the Evaluation of Alternative Futures, University of Arizona, Department of Hydrology and Water Resources, HWR No. 00-020, pp-1-113.
- GMS v3.0 Reference Manual, Brigham Young University, Environmental Modeling Research Laboratory, 1999.
- Harbaugh, A.W., and M.G. McDonald. 1996a, User's documentation for MODFLOW-96: An update to the U.S. Geological Survey modular finite-difference ground-water flow model: U.S. Geological Survey Open-File Report 96-485.
- MacNish, R.D., C.L. Unkrich, Evelyn Smythe, D.C. Goodrich, and Thomas Maddock, III "Comparison of Riparian Evapotranspiration Estimates based on a Water Balance Approach and Sap Flow Measurements," Special SALSA Edition of Journal of Agricultural and Forest Meteorology (JAFM), June, 2000
- Maddock III, T. and K.J. Baird. 2003. A riparian evapotranspiration package for MODFLOW-96 and MODFLOW-2000. HWR No. 02-03. Department of Hydrology and Water Resources, University of Arizona Research Laboratory for Riparian Studies, University of Arizona, 60 pp.
- Maddock, T. III, L. B. Vionnet, Groundwater Capture Processes under a Seasonal Variation in Natural Recharge and Discharge, *Hydrogeology Journal*, 6:24-32, 1998
- Steinitz, Carl, H.M.Arias, Scott Bassett, Michael Flaxman, Tomas Goode, Thomas Maddock III, David Mouat, Richard Peiser and Allan Shearer, 2003, Alternative Futures for Changing Landscapes, The Upper San Pedro River Basin in Arizona and Sonora, Island Press, pp 202
- Williams, D. G., Brunel, J.-P., Schaeffer, S. M., and Snyder, K. A., 1998. Biotic controls over the functioning of desert riparian ecosystems. In; Proceedings from the Special Symposium on Hydrology. (Eds) Wood, E. F., Chehbouni, A. G., Goodrich, D. C., Seo, D. J., and Zimmerman J.R. pp. 43-48. Boston MA, American Meteorological Society.

6.4 RIP-ET Preprocessor Users Manual

PRE-RIP-ET

A preprocessor for RIP-ET



by

**Kathryn J. Baird
Carolyn A. Dragoo
Thomas Maddock III**

**Department of Hydrology and Water Resources
University of Arizona
Tucson, Arizona 85721**

March, 2004

i

Table of Contents

Table of Contents	ii
Figures	v
Tables	vii
1 Introduction	1
What is PRE-RIP-ET?	1
What is a Plant Functional Subgroup?	1
What is a PFSG Curve?	2
What are the PFSG Parameters?	2
How Does PRE-RIP-ET Process Parameters?	3
What is a PFSG Curve File	5
How Many PFSG Curve Files in a Simulation?	7
How Are the Curves Applied?	7
What is the Fraction of Active Habitat?	8
What is the Fraction of Plant Functional Subgroup?	8
What is the Fraction of Plant Canopy or Flux Area?	9
What is Fractional Coverage?	9
How does Land Surface Elevation Affect the Coverage?	10
So What Have We Learned?	10
2 Getting Started	12
System Requirements	12
Code Information	12
CD Information	12
Documentation Folder	12
Program Folder	12

PFSG Raw Data Folder.....	12
CRV Data Folder.....	13
Manual Organization.....	13
3 Learning the Basics.....	14
Getting Started.....	14
Getting to Know the PRE-RIP-ET Main Menu.....	14
A Quick Look at the Toolbars.....	15
Basic Operations.....	16
PFSG Data File.....	16
Fractional Coverage File.....	20
Output Control File.....	26
Building the MODFLOW RIP-ET File.....	31
4 PFSG Curve Files.....	32
PFSG Raw-Data Sets.....	32
PFSG Curve File Utility Module.....	34
Name and Dimension Group.....	34
Unit Conversion Group.....	35
PFSG Curve Data Group.....	36
Calculated Parameter Button.....	37
Plot PSFG Curve Button.....	41
Create Curve File Button.....	41
5 GIS Module.....	43
Requirements.....	43
The PFSG Name File.....	44
Starting the GIS Module.....	45
Preprocessor.....	46
Creating/Converting Riparian Theme.....	46



Attributing Riparian Theme.....	47
Importing Grid from MODFLOW.....	49
Rotating grid shapefile.....	50
Creating the textfile that will be imported by MODFLOW.....	51
6 Importing An Existing MODFLOW RIP-ET File.....	52
Importing the RIP-ET File.....	52
7 Quick Summary of PRE-RIP-ET Procedures.....	56
How Do You Start PRE-RIP-ET?.....	56
How Do You Exit PRE-RIP-ET?.....	56
How Do You Construct a PFSG Data File?.....	56
How Do You Load an Existing PFSG Data File?.....	57
How Do You Construct a Fractional Coverage File from Keyboard?.....	57
How Do You Load an Existing Fractional Coverage File?.....	58
How Do You Construct an Output Control File from Keyboard?.....	58
How Do You Load an Existing Output Control File?.....	59
How Do You Create a MODFLOW RIP File?.....	59
How Do You Import an Existing MODFLOW RIP-ET File?.....	59
How Do You Create a PFSG Curve File?.....	60
8 Glossary.....	62
9 References.....	64

Figures

Figure 1-1: Generic PFSG curve.....	2
Figure 1-2. PFSG curves for Wetlands, Shallow-rooted Riparian, Deep-rooted Riparian, Transitional Riparian and Bare ground/Open water Evaporation.....	4
Figure 1-3: Segmented PFSG curve from PFSG raw-data set showing linear interpolation of head (d's) and linear interpolation of ET flux (dR's).....	5
Figure 1-4. PFSG curve file for obligate wetlands.....	7
Figure 1-5: Area of active habitat in a cell.....	8
Figure 1-6. Area associated with plant functional subgroups.....	8
Figure 1-7. Flux area associated with canopy.....	9
Figure 1-8. Average surface elevation and actual habitat surface elevation.....	10
Figure 3-1. PRE-RIP-ET desktop.....	14
Figure 3-2. Toolbar tool tips.....	15
Figure 3-3. Plant Functional Subgroup Dimension Data dialog box.....	17
Figure 3-4. PFSG Data dialog box.....	17
Figure 3-5. File selection dialog box.....	18
Figure 3-6. Name of the PFSG entered into the listbox.....	18
Figure 3-7. Error message for mixed units.....	19
Figure 3-8. Label change when all PFSG curve files have been read.....	19
Figure 3-9: Main window with <i>ETC</i> file and Log file.....	20
Figure 3-10. The fraction coverage, <i>RIPex1_1.csv</i> , for the first season of a two season model using a spreadsheet for display.....	21
Figure 3-11. Coverage Dimension dialog box.....	22
Figure 3-12. Coverages dialog box.....	23
Figure 3-13. Screen after clicking Select Coverage button, placing 25 in Number of Riparian Cells in Coverage spinner box, and clicking Set.....	23
Figure 3-14. CSV dialog box with <i>RIPex1_1.csv</i> highlighted.....	24

Figure 3-15. Screen after loading <i>RIPex1_1.csv</i>	25
Figure 3-16. Main menu with <i>ETC</i> file, <i>ETV</i> file and Log file.	26
Figure 3-17. Output Control Parameter dialog box	28
Figure 3-18. Stress Period dialog box	29
Figure 3-19. Order of Coverages dialog box	29
Figure 3-20: Main window upon completion of Output Control File (ETO).....	30
Figure 3-21. MODFLOW RIP-ET File save dialog box	31
Figure 4-1. PFSG curve for small deep rooted riparian	33
Figure 4-2: Start of PFSG Curve Data dialog box with <i>Name and Dimension</i> group highlighted.	34
Figure 4-3. PFSG Curve Data dialog box with <i>Unit Conversion</i> group enabled.	36
Figure 4-4. PFSG Curve Data dialog box with PFSG Curve Data entered	37
Figure 4-5. PFSG Curve Data dialog box with PFSG parameters and dimensionless segments calculated.....	38
Figure 4-6. PFSG Curve	39
Figure 4-7. PFSG curve plot for small deep rooted riparian in feet and year dimension units .	41
Figure 4-8. Dialog box for saving .crv files	41
Figure 4-9. PFSG ET curve data set for small deep-rooted riparian vegetation.	42
Figure 5-1, File selection dialog box for PFSG Name File (INX).....	44
Figure 5-3, Exit PRE-RIP-ET dialog box.....	45
Figure 5.2, Arcview screen with preprocessing popup window.....	45
Figure 5.3, New riparian polygons are drawn over an aerial photo.....	46
Figure 5.4, Riparian theme with attribute table. Highlighted record is selected both on the map and in the table.	47
Figure 5.5, PFSG window for entering percentage of habitat covers.	48
Figure 5.4, Import MODFLOW Grid dialog box.....	49
Figure 6-1, MODFLOW Riparian File dialog box for file choice.	52
Figure 6-2, Coverage Time and Uniqueness Dimension dialog box on main menu.	53
Figure 6-3, Order of Coverage dialog box on main menu.	54

Figure 6-4. Final window..... 55

Tables

Table 1-1: PFSG data set for Obligate Wetlands in Southwestern United States4

Table 4-1. PFSG raw-data set for small deep rooted riparianin Southwestern United States (** Maximum ET flux). 33

1 Introduction

Use this chapter to familiarize your self with the basic concepts behind PRE-RIP-ET.

What is PRE-RIP-ET?

PRE-RIP-ET is a Windows program designed to help you create a RIP-ET data file for MODFLOW-96 (Harbough and McDonald, 1996) or MODFLOW-2000 (Harbough et al). RIP-ET is an evapotranspiration package for MODFLOW that was developed to simulate water table evapotranspiration from riparian/wetland systems in a manner that reflects their ecology and physiology (Maddock and Baird, 2002). User-defined plant functional subgroups (PFSGs) are used to elucidate the interactive processes of plant ET with groundwater conditions.

What is a Plant Functional Subgroup?

Riparian and wetland ecosystems are composed of a variety of plant types and species. Plant functional groups are groupings of plant species that exhibit similar responses to environmental conditions and have similar effects on the dominant ecosystem processes (Lavorel et al., 1997). The identification and use of plant functional groups can assist in reducing the enormous complexity of individual species into a smaller, more manageable number of categories (Leishman and Westoby, 1992; Williams et al., 1998). In the RIP-ET package for MODFLOW, plant functional groups based on transpiration rates, plant rooting depths, and ranges of water level tolerance are used to elucidate the interactive processes of plants (and plant ET) with groundwater conditions.

Five generalized functional groups: obligate wetland, shallow-rooted riparian, deep-rooted riparian, transitional riparian and bare ground/open water are presented in this manual. The last category, while not a plant group, must be included to accurately model evaporation (the non-transpiration portion of ET) from the cell or active modeling area. The evapotranspiration rates and range of groundwater elevations over which these groups exist differ for each plant functional group.

Within each plant functional group, plant size and density also play roles in determining evapotranspiration rates. Large woody plants have different maximum rooting depths, hydraulic architecture and transpiration rates than smaller trees (Meinzer et al., 1997). Furthermore, areas with dense plant cover are likely to show increased transpiration rates

compared to sparsely covered areas. Taken together, the plant functional group and plant size or density comprise a plant functional subgroup (PFSG). For each of these plant functional subgroups, PRE-RIP-ET allows you to construct PFSG curves from head and ET flux data. You have the choice of using the examples provided or creating a new suite of plant functional groups appropriate for your simulation and geographic region. While the functional groups presented here are relevant for semi-arid environments, the methodology can be applied universally.

What is a PFSG Curve?

Traditional approaches to modeling ET processes assume a piecewise linear relationship between ET flux rate and hydraulic head. RIP- ET replaces the traditional relationship with a segmented, nonlinear dimensionless ET flux rate curve, or PFSG curve, that reflects the eco-physiology of riparian and wetland ecosystems (Figure 1-1). Development of eco-physiologically based ET curves results in more accurate determinations of riparian ET, improved basin scale water budgets, and allows for the quantification of riparian water requirements. The PFSG curves are developed from a common set of descriptive parameters determined for each plant functional subgroup.

What are the PFSG Parameters?

Figure 1-1 illustrates a representative ET flux rate or PFSG curve. For each plant functional subgroup there is a water table elevation or extinction depth elevation (H_{xd} in Figure 1- 1) below which the roots cannot obtain water and ET is nonexistent. When the water table rises and water becomes available to the root system, the ET rates rise until

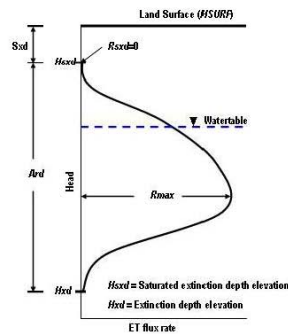


Figure 1-1: Generic PFSG curve

they reach an average maximum ET flux (R_{max}). At higher water table elevations, the root systems in plants other than obligate wetland species, become oxygen deficient and ET rates decline until the plants die of anoxia. In obligate wetland plants, the upper limit of water depth tolerance is determined by additional factors such as light availability. The water table elevation associated with plant death is the saturated extinction depth elevation (H_{sxd} in Figure 1-1). Although Figure 1-1 shows H_{sxd} to be below the land surface elevation, it need not be. It can be at, or even above, the ground surface elevation as some wetland species tolerate as much as a meter of standing water.

For modeling purposes, the PFSG parameters in PRE-RIP-ET are defined as depths or distances [L]. The distance between the two extinction depths is called the active root zone depth (Ard). While saturated extinction depth (Sxd) is measured with respect to the land surface elevation, $HSURF$. If H_{sxd} is below the land surface elevation, Sxd is positive; if it is above, Sxd is negative. R_{sxd} , the ET flux rate at the saturated extinction depth equals zero for all plant groups. In creating the evaporation curve for bare ground or open water, H_{sxd} is set to the traditional MODFLOW maximum ET surface elevation and R_{sxd} is equal to R_{max} .

How Does PRE-RIP-ET Process Parameters?

PRE-RIP-ET provides you with the following nine PFSG raw-data sets in spreadsheet comma-separated variable format (csv): Obligate Wetlands (Wetlands.csv), Shallow-rooted Riparian (SRRiparian.csv), Small Deep-rooted Riparian (DRRipSmall.csv), Medium Deep-rooted Riparian (DRRipMedium.csv), Large Deep-rooted Riparian (DRRipLarge.csv), Extra Large Deep-rooted Riparian (DRRipXLarge.csv), Average Deep-rooted Riparian (RRipAvg.csv), Transitional Riparian (TransRip.csv), and Evaporation (Evaporation.csv). These files are found in the directory named PFSG_Raw_Data on your PRE-RIP-ET disk and were developed by Baird and Maddock (2002) for the Kern River in California.

A typical PFSG raw-data set is show in Table 1-1. Note that the vertices must be labeled from the extinction depth upwards to the saturated extinction depth. This example raw-data set happens to be for Obligate Wetlands in the Southwestern United States. The PRE-RIP-ET program assumes that the head at land surface elevation is zero, above land surface head is positive, and below land surface is negative. Therefore, a positive head indicates standing water.

Table 1-1: PFSG data set for Obligate Wetlands in Southwestern United States

Vertices	ET Flux (cm/day)	Head (cm)
8	0	20
7	0.23	0
6	0.32	-4
5	0.35	-7
4	0.36	-10
3	0.32	-15
2	0.2	-33
1	0	-75

Using a utility module, PRE-RIP-ET inputs the name (*RIPNM*), and determines the values of *Sxd*, *Ard*, maximum ET flux rate (*Rmax*), and ET flux rate at saturated extinction depth (*Rxsd*) for each plant functional subgroup from the PFSG raw-data sets. ET flux rate curves for the major plant functional groups are illustrated in Figure 1-2. PRE-RIP-ET ensures that the distance and ET flux units are consistent with the MODFLOW simulation. All the PFSG raw-data sets included with this manual have distance units of cm and ET flux units of cm/day. However, the utility module can set the unit dimension of *Ard*, *Sxd*, *Rmax* and *Rxsd* consistent with the units of your MODFLOW simulation producing a PFSG Curve file in the appropriate units.

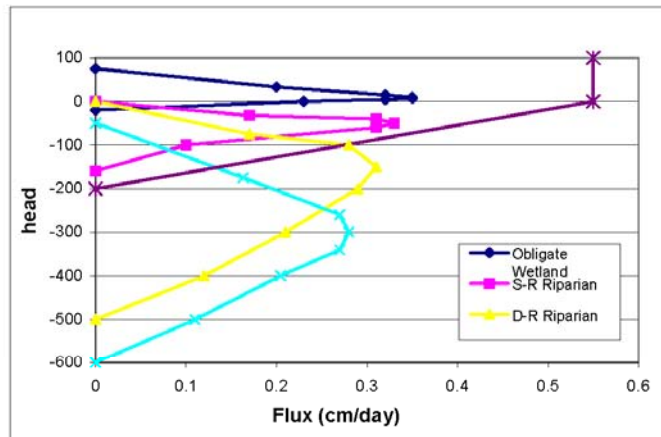


Figure 1-2. PFSG curves for Wetlands, Shallow-rooted Riparian, Deep-rooted Riparian, Transitional Riparian and Bare ground/Open water Evaporation

What is a PFSG Curve File

The MODFLOW RIP-ET Package does not use the continuous curve of Figure 1-1, but instead uses an approximation based on linear segments as illustrated in Figure 1-3. The segments for the approximation to the curve are based on the PFSG raw-data set.

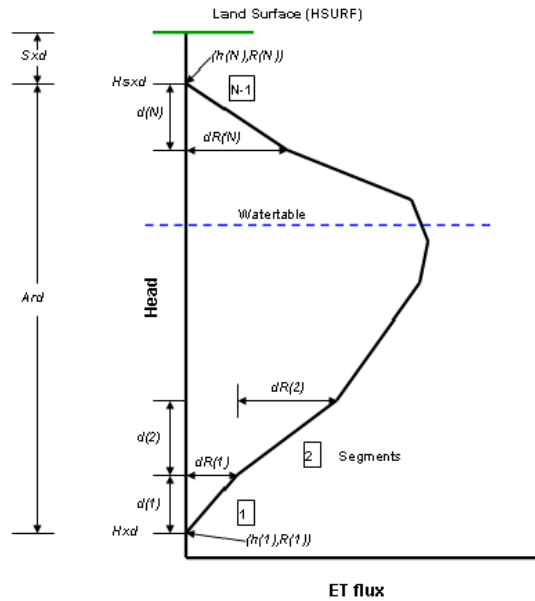


Figure 1-3: Segmented PFSG curve from PFSG raw-data set showing linear interpolation of head (d's) and linear interpolation of ET flux (dR's)

The curve segments are defined by vertices $h^{(k)}$, and $R^{(k)}$. In Figure 1-3, $d^{(1)}$, $d^{(2)}$, ... $d^{(n)}$, are in length units and represent the change in head over a segment, while $dR^{(1)}$, $dR^{(2)}$, ... $dR^{(n)}$ are in flux rate units and represent the change in flux over a segment. In general, for N segments and $1 \leq k \leq N$, where the numbering of k starts at the extinction depth and moves upward toward the saturated extinction depth,

$$d^{(k)} = h^{(k+1)} - h^{(k)}$$

and

$$dR(k) = R(k+1) - R(k)$$

For a functional subgroup the following dimensionless segment variables are defined,

$$fdh(k) = \frac{d(k)}{Ard}$$

and

$$fdR(k) = \frac{dR(k)}{Rmax}$$

You will note that for the N segments,

$$\sum_{i=1}^N fdh(i) = 1$$

and

$$\sum_{i=1}^N fdR(i) = \frac{Rsxd}{Rmax}$$

Within a simulation, $fdh(k)$ and $fdR(k)$ are known constants for each plant functional subgroup, and when multiplied by Ard and $Rmax$ in their appropriate units, the segment variables $d(k)$ and $dR(k)$ are recovered. For the evaporation curve (bare ground/open water), $Rsxd$ equals $Rmax$ and is non-zero.

The PFSG Curve File for the obligate wetlands is shown in Figure 1-4. The first line of the file contains the name of the plant functional subgroup. The names can be up to 24 characters in length but apostrophes must appear as the first character and the 24th character. For the example curve file in Figure 1-6, the name is 'Wetland'. The second line of the file contains the distance and time units for this PFSG curve file. For our example, the distance unit is feet and the time unit is seconds. The third line reports the saturated extinction depth ($Sxd = -0.6562$), the active root depth ($Ard = 3.1168$), the maximum ET flux ($Rmax = 0.1367 \times 10^6$), the ET flux at the saturated extinction depth ($Rsxd = 0$), and the number of segments ($NuSeg = 7$). Lines 5 and 6 contain the dimensionless segment variables, $fdh(k)$'s and $fdR(k)$'s. The $fdh(k)$'s are listed in line 5, and the $fdR(k)$ are listed in line 6. The listing from left to right proceeds from extinction depth to saturated extinction depth. You should note the $fdh(k)$'s and $fdR(k)$'s will be the same regardless of how the units of Sxd , Ard , $Rmax$, and $Rsxd$ are reported.

```

'Wetlands
ft sec
-0.6562      3.1168  0.1367E-06  0.0000E+00      7
0.44211  0.18947  0.05263  0.03158  0.03158  0.04211  0.21053
0.55556  0.33333  0.11111  -0.02778  -0.08333  -0.25000  -0.63889

```

Figure 1-4. PFSG curve file for obligate wetlands

How Many PFSG Curve Files in a Simulation?

You will need a PFSG Curve file for every plant functional subgroup present in the modeled region. The maximum number of plant functional subgroup present over the whole region is contained in the variable MAXTS. It is quite possible that a single modeling cell within a riparian region contains only one or two plant functional subgroups, but over all of the riparian cells many more plant functional subgroup will be present.

How Are the Curves Applied?

Within a groundwater model, volumetric ET [L^3/T] is determined by multiplying the ET flux rate [L/T] derived from the new PFSG curves by the cell area [L^2]. Cell sizes in a groundwater model are generally quite large so only a portion of the cell is likely to contain active habitat (Figure 1-5). Since few riparian or wetland areas are monotypic, a cell is also likely to contain a mixture of plant functional subgroups. Furthermore, the amount of canopy coverage (or coverage of flux area) may change from cell to cell. The ET estimation methodology in RIP-ET allows for fractional coverage or multiple flux rates within a cell. To accomplish this, you need information about the distribution of plant functional subgroups within the active modeling areas is required.

The portion of the cell covered by a plant functional subgroup is the PFSG fractional coverage, which quantifies the distribution of the plant functional subgroups within the riparian cells in the active modeling areas. You need to know the fractional coverage for each of the plant functional subgroups present for a cell to simulate the habitat mixture. For bare areas not supported by shallow water tables, ET rates can be excluded from the cell area or assigned flux rates of zero (e.g. the non-habitat area in Figure 1-5). The fractional cover within a cell has three components: 1) fraction of active habitat, 2) fraction of plant functional subgroup, and 3) fraction of plant canopy or flux area.

What is the Fraction of Active Habitat?

The fraction of active habitat (f_{AH}) refers to the fraction of the cell that contains wetland or riparian habitat (see Figure 1-6) and is defined as

$$f_{AH} = \frac{\text{area of active habitat}}{\text{area of cell}}$$

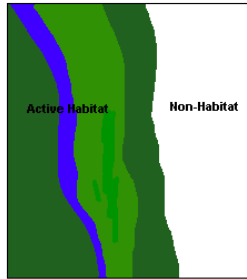


Figure 1-5: Area of active habitat in a cell

What is the Fraction of Plant Functional Subgroup?

The active habitat area in a cell may be composed of a variety of plant functional subgroups (see Figure 1-6). The fraction of i^{th} plant functional subgroup is defined as

$$f_{SG(i)} = \frac{\text{area subgroup } i}{\text{area of active habitat}}$$

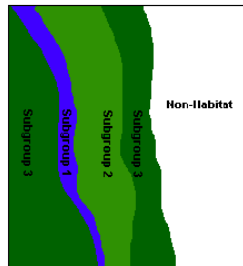


Figure 1-6: Area associated with plant functional subgroups

What is the Fraction of Plant Canopy or Flux Area?

Within any habitat, plant canopy or plant cover rarely equals 100 percent (Figure 1-7). Percent canopy or plant cover may vary, depending on habitat type and resource availability. To accurately determine ET, the area of canopy cover or plant cover is required, as most flux rates are evaluated on canopy or plant cover. Note that for open water areas the fraction of plant coverage is equal to one. The fraction of plant coverage is defined as

$$fPC(i) = \frac{\text{canopy area for subgroup } i}{\text{area subgroup } i}$$

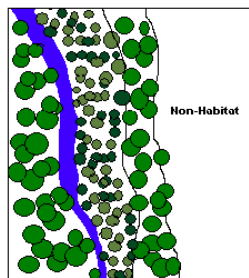


Figure 1-7. Flux area associated with canopy

What is Fractional Coverage?

The fractional coverage of the i^{th} plant functional subgroup in a cell ($fCov(i)$) is given by the equation,

$$fCov(i) = fAH \times fSG(i) \times fPC(i)$$

The components of fractional cover can be determined using a combination of GIS techniques, aerial photography and ground verification. The fractional covers ($fCov$) are determined for each plant functional subgroup for each cell. If a plant functional subgroup is not present in a cell, its fraction is zero. The GIS module of PRE-RIP-ET determines fractional coverage. The fractional coverage can also be determined externally to PRE-RIP-ET, and input via the keyboard using either csv spreadsheet files or directly typing in the values.

How does Land Surface Elevation Affect the Coverage?

Within the model area, the land surface elevation (*HSURF*) will vary from cell to cell. It may also vary within a cell. The magnitude of this change is important. If *HSURF* varies on the same order of magnitude as the extinction depths within the cell, the ET calculations will be affected. You have an option of either assigning a single *HSURF* for the average surface elevation of the cell, or assigning an *HSURF* value for each plant functional group within a cell. If a single value of *HSURF* is used, the average surface elevation of the cell is used to calculate *Hxd* (see Figure 1-8). If *HSURF* is assigned for each plant functional subgroup, the actual surface elevation of the habitat within the cell is used to calculate the extinction depth, *Hxd*. If there is considerable terrain relief within cells, you should consider using a denser grid since the groundwater flow model assumes a constant water table within a cell. You should note that the MODFLOW model assumes that the water table elevation is constant within the cell boundary.

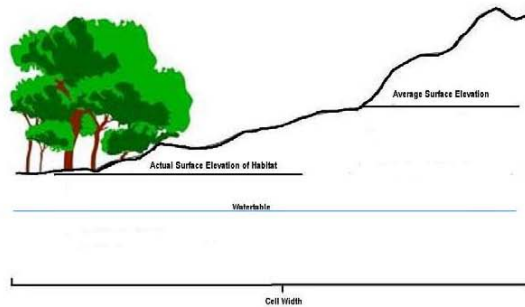


Figure 1-8. Average surface elevation and actual habitat surface elevation

So What Have We Learned?

Traditional approaches to modeling ET processes within a groundwater model assume a monotonically increasing piecewise quazi-linear relationship between the ET flux rate and hydraulic head (McDonald and Harbaugh, 1988; Harbaugh and McDonald, 1996a and 1996b; Banta 2000). These approaches are problematic in several ways. First, ET flux rates in plant species or PFSG vary with groundwater depths due to differences in rooting depths and plant physiology. Second, no allowance is made for a reduction in ET due to prolonged anoxic conditions. Third, a single flux rate is applied to the entire area of the

designated cell making it difficult to deal with fractional habitat coverage. PRE-RIP-ET produces a data set for the RIP-ET Package that replaces the traditional relationship with a set of nonlinear dimensionless curves that reflects the ecophysiology and distribution of riparian and wetland plants.

PRE-RIP-ET produces a data set for a MODFLOW package that simplifies the complex structure of wetland and riparian plant communities into a workable set of plant functional groups. While the groups presented here are for semi-arid environments, the methodology can be applied universally. The five plant functional groups presented in this manual are: obligate wetlands, shallow-rooted riparian, deep-rooted riparian, transitional riparian and bare soil and open water. The groups can be further divided into subgroups based on plant size or density. Each subgroup has an ET flux curve that relates ET flux to water table elevation. A key characteristic of these flux curves is the existence of a saturated extinction depth along with the more traditional MODFLOW extinction depth, with the distance between them referred to as the active root depth. The ET flux curves are represented by a series of dimensionless, linear segments based on measured or approximated ET values.

PRE-RIP-ET produces a fractional coverage for each of the plant functional subgroups present within the groundwater model cell. A MODFLOW cell from the finite difference formulation may contain several plant functional subgroups within its boundaries. Typically, not all of a cell contains habitat and only a portion of the habitat area has canopy or flux coverage. The fraction of habitat area within the cell, the fraction of PFSG area within the habitat, and the canopy or flux area within the PFSG constitute the fractional plant coverage within a cell. The product of PFSG's ET flux rate times the plant coverage times the surface area of the cell gives the PFSG's volumetric ET rate for the cell. Summing over the PFSG in the cell gives the volumetric ET rate for that cell; summing over all the riparian cells gives the global ET rate for the modeled region. The combination of physically based ET curves and plant coverage estimates provides more accurate estimates of riparian evapotranspiration and improves the modeling results.

2 Getting Started

System Requirements

To use PRE-RIP-ET, you need the following.

- Windows® 98/2000/ME/XP
- Pentium® II 400 MHz or greater
- 256 MB Ram
- 4X speed CD-ROM
- 20 MB+ minimum available hard drive space.

If you wish to use the GIS portion of the PRE-RIP-ET you will need ArcView GIS®.

Code Information

PRE-RIP-ET is written in FORTRAN 90 and Winteracter, Version 4.10f, provides the Window's graphic interface code. The program is compiled using Compact Digital FORTRAN, Version 6.6.


CD Information

PRE-RIP-ET arrives on a CD containing two folders. One is entitled *Documentation* and the other is entitled *Program*.

Documentation Folder

The *Documentation* folder contains this manual as a Microsoft Word file and as an Adobe PDF file. Presenting both options allows the user to reproduce the manual in color if they so choose.

Program Folder

The *Program* folder contains the executable program, PRE-RIP-ET.exe (indicated by the  icon), two folder subdirectories entitled *CRV Data* and *PFSG Raw Data*, and three comma separated variable (.csv) files. The three .csv files are used with the tutorial presented in Chapter 3.

PFSG Raw Data Folder

The PFSG Raw Data folder contains the nine data files used in Chapter 4. These data files contain head and ET flux information for eight riparian plant functional subgroups and

evaporation. In Chapter 4, you will be instructed on how to convert these data into PFSG curve files.

CRV Data Folder

The *CRV Data* folder contains ten PFSG curve files required for the tutorial presented in Chapter 3. The units in nine of these curves files are reported in feet and seconds while the tenth is in centimeter and days. These files allow you to complete the tutorial without using the *PFSG Curve Data* utility presented in Chapter 4.

Manual Organization

The manual is composed of eight chapters. Chapter 1 presents the concepts of plant functional subgroups (PFSG) and fractional coverage. Chapter 2 presents the system requirements and chapter organization. Chapter 3 presents a tutorial to construct a RIP-ET input file for MODFLOW. Chapter 4 presents the utility module that constructs the PFSG curve files. Chapter 5 presents the GIS utility module using Arc View® GIS to construct fractional coverages. Chapter 6 presents a utility module that reads an existing MODFLOW RIP-ET file and produces a PFSG Data File, a Fractional Coverage File and an Output Control File. Chapter 7 presents a quick summary of PRE-RIP-ET commands and procedures that are presented in the tutorial and subsequent chapters. Chapter 8 presents a glossary of PRE-RIP-ET terms used in the tutorial and subsequent chapters. Chapter 9 contains references.

3 Learning the Basics

This chapter contains a tutorial that is designed to get you up and running. The tutorial is divided into three parts. The first part will teach you how to develop the PFSG Data File, the second how to develop the Fractional Coverage File, and the third how to use output control and time parameters to develop the Output Control File.

Getting Started

If you haven't already done so, start PRE-RIP-ET (click the .exe file with the tree icon, ) , and take a quick tour around the PRE-RIP-ET environment.

Getting to Know the PRE-RIP-ET Main Menu

The PRE-RIP-ET main menu contains a menu bar, a toolbar, and four file windows.

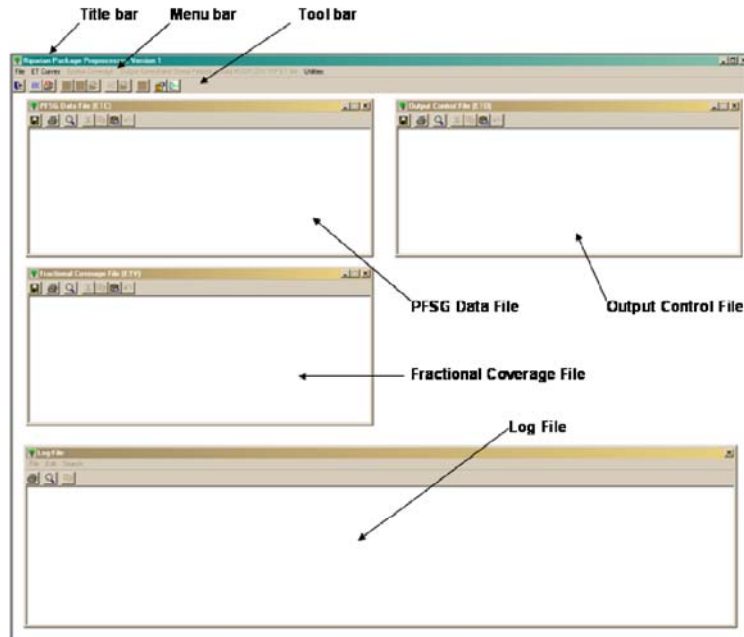


Figure 3-1. PRE-RIP-ET desktop

Here is a brief description of the components you see on the screen:

Title bar	Gives you the title and version of PRE-RIP-ET.
Menu bar	Contains the six major menus: File, ET Curve, Spatial Coverage, Output Control and Stress Periods, Build MODFLOW RIP-ET File, and Utilities.
Toolbar	Contains shortcut buttons to the submenus of the six major menus.
PFSG Data File	Displays PFSG data, and is a file with an .etc extension.
Fractional Coverage File	Displays fractional coverage data, and is a file with an .etv extension.
Output Control File	Displays output control and stress period data, and is a file with an .eto extension.
Log File	Gives you a running history of all activities performed by the Program.

A Quick Look at the Toolbars

PRE-RIP_ET has a toolbar for quick and easy access to the menus and dropdown submenus on the menu bar. When you position your cursor over a toolbar button, text pops up telling you what the button does (i.e. *tool tips*).

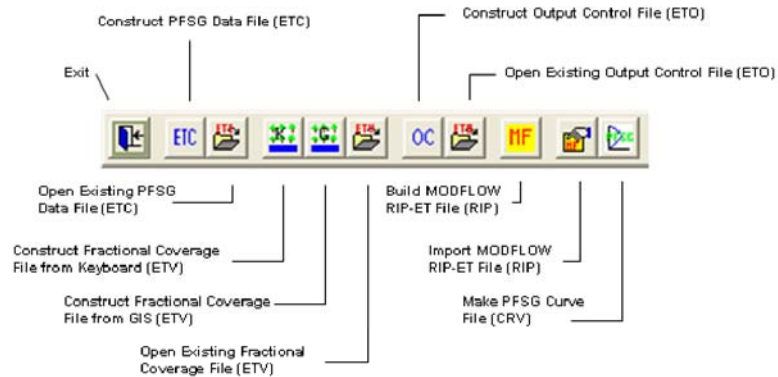


Figure 3-2. Toolbar tool tips.

To exit the program click on either the menu bar item **File** and then the dropdown menu item **Exit**, or click on the toolbar button .

Basic Operations


Using PRE-RIP-ET, you will construct 3 files: the PFSG Data File, the Fractional Coverage File and the Output Control File. Once these all files are completed, you will construct the RIP-ET File.

PFSG Data File

To construct the *PFSG Data File*, you will need to know the total number of plant functional subgroups present in your simulation, and the maximum number of segments that can be in any one PFSG ET flux curves (Figure 1-3). You will also need to have access to the *PFSG Curve Files (.crv)* for all of the subgroups present in your simulated area. The *PFSG Curve Files* are prepared by the Utility module described in Chapter 4 of this manual, and must be completed prior to constructing the data files. The following nine example *PFSG Curve Files* are supplied with this manual. They can be found on the disk in the folder entitled "CRV Data":

Obligate Wetlands	Wetlands.crv
Shallow-rooted Riparian	SRRiparian.crv
Average Deep-rooted Riparian	DRRipAvg.crv
Small Deep-rooted Riparian	DRRipSmall.crv
Medium Deep-rooted Riparian	DRRipMedium.crv
Large Deep-rooted Riparian	DRRipLarge.crv
Extra Large Deep-rooted Riparian	DRRipXLarge.crv
Transitional Riparian	TransRip.crv
Evaporation	Evaporation.crv

For these data sets, the units of distance are in feet and the units of ET flux are feet/sec. These units were chosen because they match the units used in our example. Within these plant functional subgroup curves, the maximum number of segments is seven. The small deep-rooted riparian curve has six segments, evaporation has one segment, and the rest of the plant functional subgroups curves all have seven. With this information and data on hand, there are two ways to start.

If you haven't already started PRE-RIP-ET, go to the directory containing the PreRipET.exe (it has the icon ). Click on the icon to bring up the main menu. Click on either the menu bar item **ET Curves** and then the dropdown submenu item **Construct**

PFSG Data File, or click on the toolbar button **ETC**. Upon performing either of these tasks, a new dialog box appears entitled **Plant Functional Subgroup Dimension Data** (see Figure 3-3). Enter the maximum number of plant functional subgroups and the maximum number of segments. You may use the spinner or simply write over the existing values to enter the data into the dialog box.

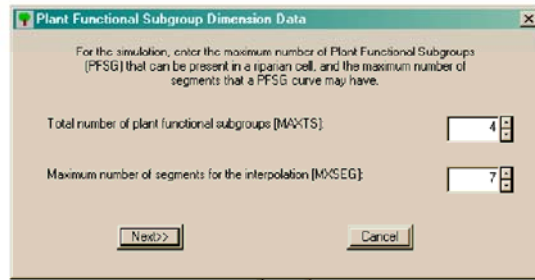


Figure 3-3. Plant Functional Subgroup Dimension Data dialog box.

For the tutorial, you have four plant functional subgroups and a maximum of seven segments. Move the spinners till four and seven appear in the appropriate boxes, or overwrite the initial values and press the **Next>>** button. If you need to stop for some reason, press the **Cancel** button. If you press the **Cancel** button, you will be asked if you wish to return to the main menu or continue. If you return to the main menu at this stage, nothing will be saved and you need to start over.

Pressing the **Next>>** button will bring up the **PFSG Data** dialog box (see Figure 3-4).

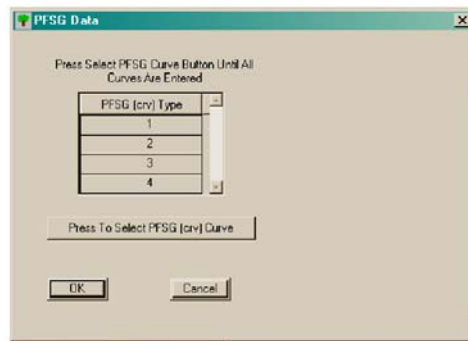


Figure 3-4. PFSG Data dialog box.

Because you entered 4 as the number of plant functional subgroup in the simulation, the listbox contains four numbered curves blanks. Next click on the **Press To Select PFSG Curve** button and a file choice box appears (See Figure 3-5) and prompts you for a file name with an .crv extension. You may need to change directories until you find where the crv files are located. In the example, they are located the *CRV Data* directory.

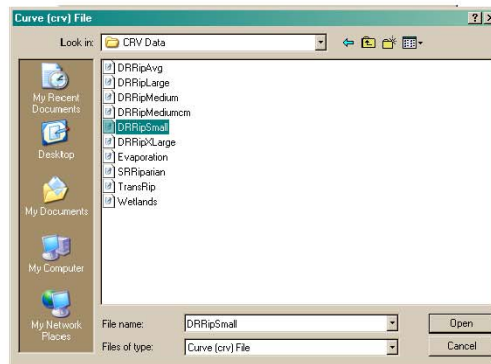


Figure 3-5. File selection dialog box.

Select the file *DRRipSmall.crv* and click on the *Open* button. The .crv file now appears in the PFSG Data dialog box (Figure 3-6).

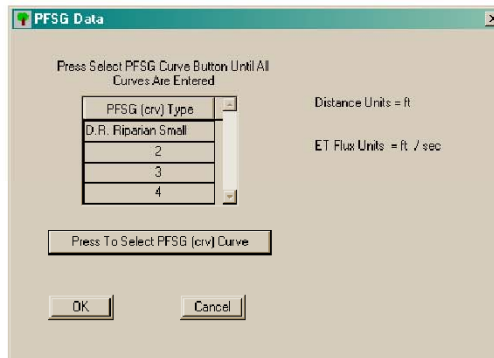


Figure 3-6. Name of the PFSG entered into the listbox.

On the right-hand side of the dialog box, the distance and ET flux units are reported. All remaining curve entries must have the same units as the first data set or an error will result. In Figure 3-7, an ET curve file with units of *cm* for distance and *cm/day* for ET flux has been entered. Because the units of the first curve file were in *ft* and *ft/sec*, an error

message has appeared on the right side of the dialog box. You need to enter the ET Curve file with the proper units and continue.

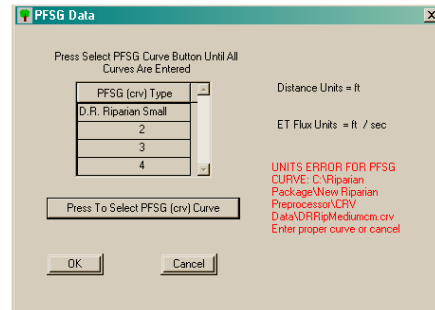


Figure 3-7. Error message for mixed units.

Add the rest of PFSG curves by alternately clicking on the **Press To Select PFSG Curve** button and picking PFSG curve files: DRRipMedium.crv, DRRipLarge.crv, and Evaporation.crv. When all four PFSG curve files appear in the listbox, the label above the listbox reports that all the PFSG curve files have been read and the **Press To Select PFSG Curve** button is disabled so no more curves can be read (see Figure 3-8). After all the PFSG curves have been read, the curve data is automatically written to the Log File and the PFSG Data file (.etc) in the main window.

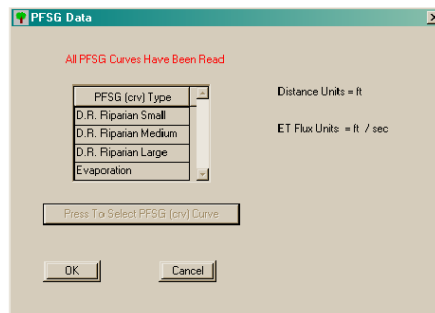




Figure 3-8. Label change when all PFSG curve files have been read.

Click on the **OK** button to return to the main window (Figure 3-9). At this point you can save the (.etc) *ETC* file. Click on the disk icon  in the **PFSG Data File (ETC)** sub menu, and save the (.etc) *ETC* file as Exmpl.etc. Because you were just loading PFSG Curve Files, you will be in the sub-directory *CRV Data*. Go back to the directory where PRE-RIP-ET.exe is located and save there. You may now exit the program without losing any data.

Upon restarting the program, either click on the menu item **ET Curves** and then on the dropdown submenu item **Open Existing PFSG Data File (ETC)** or click on the  button.

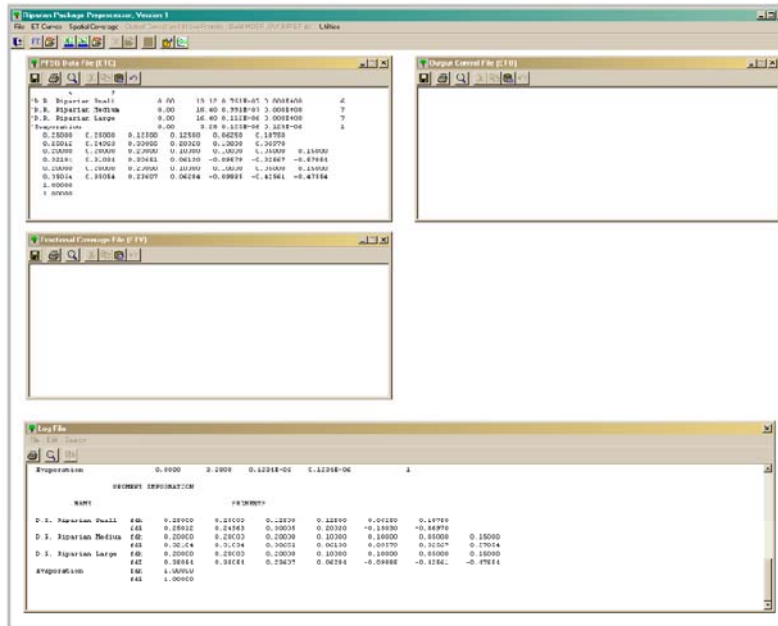


Figure 3-9: Main window with ETC file and Log file.

Fractional Coverage File

A fractional coverage file contains the set of data detailing the physical layout of the riparian and wetland habitat conditions. Each time this condition changes a new coverage needs to be created. To construct the *Coverage File*, you will need to know the maximum number of riparian cells in your simulation, and the percent cover for each plant functional subgroup within a cell. You will also need to know the number of unique fractional coverages. In general, every stress period will not require a unique fractional coverage. In all likelihood, there will be a unique coverage for each season that will be repeated annually. For example, a two-season model would have two unique fractional coverages. Even with two seasons there may be coverage changes in the later stress periods. If for example, development removed riparian areas, the simulation would require more than two unique coverages.

An input for the land surface elevation for each riparian cell is also necessary. You have two choices, either you specify a single land surface elevation for the cell, or you specify a land surface elevation for each plant functional subgroup present in a cell.



The fractional coverage file requires a significant amount of data, so it is unlikely that you will enter the data into PRE-RIP-ET from a keyboard unless there are only a small number of riparian cells. The most likely way to construct the Fractional Coverage File is from a GIS coverage. Instructions on how to use GIS will be covered in Chapter 5 of this manual. For the purposes of the tutorial, we will assume that you have early entered the data from the keyboard, and have stored the each of the fractional coverages in comma separated variable formatted (.csv) file. Figure 3-10 presents *RIPex1_1.csv*, one of two .csv files for fractional coverage (*RIPex1_1.csv* and *RIPex1-2.csv*).

1	2	2	3793	0.03	3793	0.045	3793	0.075	3793	0
1	2	3	3786	0.03	3786	0.045	3786	0.075	3786	0
1	2	4	3782	0.03	3782	0.045	3782	0.075	3782	0
1	3	4	3781	0.03	3781	0.045	3781	0.075	3781	0
1	4	4	3780	0.03	3780	0.045	3780	0.075	3780	0
1	4	5	3778	0.03	3778	0.045	3778	0.075	3778	0
1	4	6	3776	0.03	3776	0.045	3776	0.075	3776	0
1	4	7	3771	0.03	3771	0.045	3771	0.075	3771	0
1	4	8	3767	0.03	3767	0.045	3767	0.075	3767	0
1	4	9	3763	0.03	3763	0.045	3763	0.075	3763	0
1	4	10	3760	0.03	3760	0.045	3760	0.075	3760	0
1	4	11	3756	0.03	3756	0.045	3756	0.075	3756	0
1	3	11	3755	0.03	3755	0.045	3755	0.075	3755	0
1	3	12	3752	0.03	3752	0.045	3752	0.075	3752	0
1	3	13	3749	0.03	3749	0.045	3749	0.075	3749	0
1	3	14	3745	0.03	3745	0.045	3745	0.075	3745	0
1	3	15	3741	0.03	3741	0.045	3741	0.075	3741	0
1	3	16	3740	0.03	3740	0.045	3740	0.075	3740	0
1	4	16	3739	0.03	3739	0.045	3739	0.075	3739	0
1	5	16	3738	0.03	3738	0.045	3738	0.075	3738	0
1	6	16	3737	0.03	3737	0.045	3737	0.075	3737	0
1	6	17	3734	0.03	3734	0.045	3734	0.075	3734	0
1	6	18	3730	0.03	3730	0.045	3730	0.075	3730	0
1	6	19	3727	0.03	3727	0.045	3727	0.075	3727	0
1	6	20	3723	0.03	3723	0.045	3723	0.075	3723	0

Figure 3-10. The fraction coverage, *RIPex1_1.csv*, for the first season of a two season model using a spreadsheet for display

The first three columns in Figure 3-10 are the layer, row and column of the MODFLOW grid. Since these values are required, the MODFLOW grid must be known before you begin to use PRE-RIP-ET. Columns four, six, eight and ten are the land surface elevations for the plant functional subgroups whose fractional coverages are listed in columns five, seven, nine and eleven, respectively. The fractional coverages are for small deep rooted riparian, medium deep rooted riparian, large deep rooted riparian and bare ground evaporation. Note that the land surface elevation for each plant functional subgroups is the

same so that a single land surface elevation for the cell could have been used. Also note that in the example, the fractional coverage for a plant functional subgroup does not vary over the cells. In many riparian systems this will not be the case, and fractional coverage for a plant functional subgroup will vary from cell to cell and may even be absence for a cell.

If you have exited PRE-RIP-ET, start PRE-RIP-ET (click on the  icon) and load the PFSG data file using the  button. You must complete or load the plant functional subgroup data file before beginning to construct the fractional coverage file. Once the plant functional subgroup data file has been loaded, the *coverage* selections on the main menu and the tool bar will be enabled.

If you should click on the **Cancel** button for any of the *Coverage File* dialog boxes, you will be given the option of returning to the main window or continuing. Returning to the main window by this means, will necessitate that you start the *Coverage File* process over again. You will not be able to save the *Coverage File* till the last *Coverage File* dialog box is completed and its **OK** button clicked.

Either click on the menu item **Spatial Coverage** and then on the submenu item **Construct Coverage File from Keyboard**, or click on the  icon.

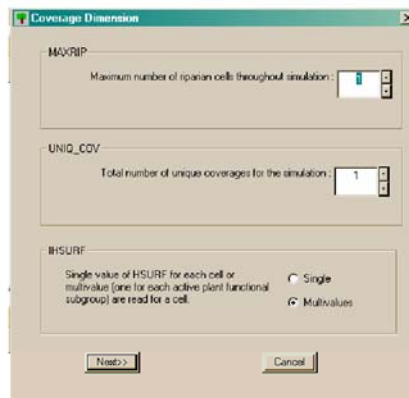


Figure 3-11. Coverage Dimension dialog box.

The **Coverage Dimension** dialog box will appear (see Figure 3-11). For our example, there are 25 riparian cells and 2 unique fractional coverages. Thus place 25 in the MAXRIP spinner box and 2 in UNIQ_COV spinner box. The example assumes that a land surface elevation is read for each plant functional subgroup, so make sure that

IHSURF Multivalued is chosen. Now press the **Next>>** button and the **Coverages** dialog box will appear (see Figure 3-12).

Only the listbox with the title *Press Select Coverage Button to Start Loading Coverage* is active. There are two entries in the listbox, one for each of the two unique fractional coverages you have specified.

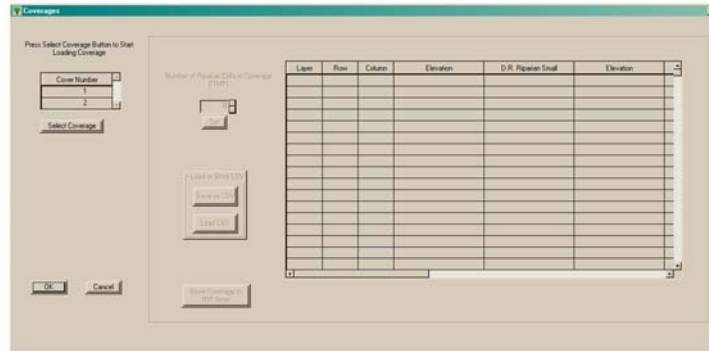


Figure 3-12. Coverages dialog box

Press the **Select Coverage** button. The word **Loading** appears in the first entry of the list box, **Cover 1** appears in labels above and to the left of the grid, and the set button for the number of riparian cells in coverage (ITMP) is activated (see Figure 3-13). There are

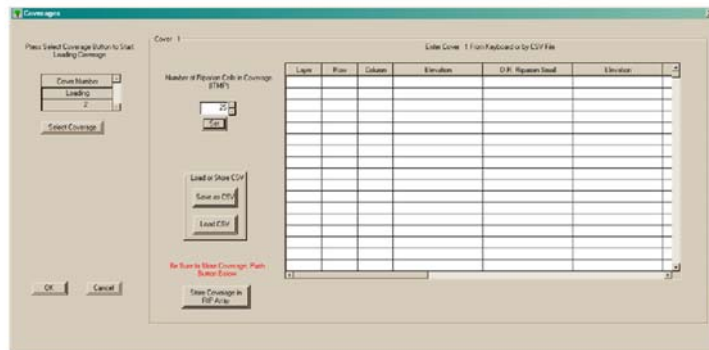


Figure 3-13. Screen after clicking Select Coverage button, placing 25 in Number of Riparian Cells in Coverage spinner box, and clicking Set.

going to be 25 active cells in each of the two coverages, so set the value in the spinner box to 25, and click on the **Set** button. At this point you can either start typing in values in the grid, or read in a spreadsheet .csv file. The ability to load a .csv file was activated when the **Set** button was clicked.

Rather than typing in the fractional coverage data, we will load .csv files. Click on the **Load CSV** button and the **CSV File** dialog box appears (see Figure 3-14). The first file you want to load is *RIPex1_1.csv*. You may use the browsing capability of the dialog box if the file is not in the present directory.

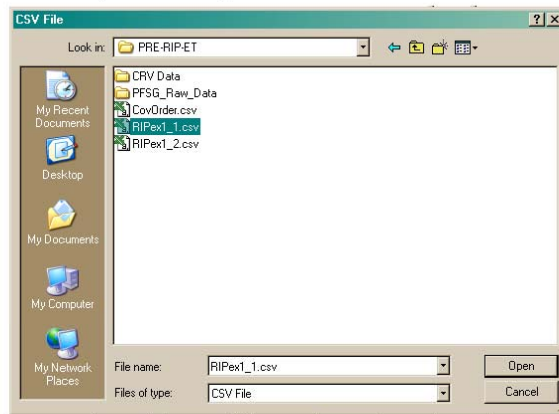


Figure 3-14. CSV dialog box with *RIPex1_1.csv* highlighted

Click open and *RIPex1_1.csv* is loaded into the grid on the screen. Because you set the *IHSURF* to *multivalues* in the **Coverage Dimension** dialog box (see Figure 3-11), there is a land surface elevation recorded for each plant functional subgroup (see Figure 3-15). You may use the horizontal and vertical scroll bars on the grid box to see all of the data.

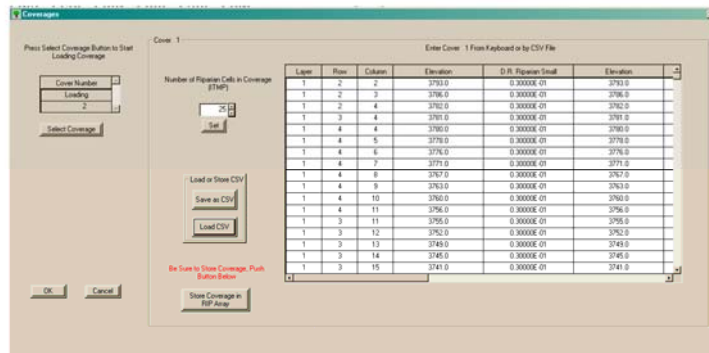


Figure 3-15. Screen after loading *RIPex1_1.csv*

Now click on the **Store Coverage in RIP Array** button and the first set of fractional coverage data is displayed in the **Coverage File (ETV)** and the **Log File** on the main screen.

Repeat the process, this time loading the csv file *RIPex1_2.csv*, and remember to click on the **Store Coverage in RIP Array** button when finished. The number of riparian cells in this coverage (*ITMP*) is also 25. Now both sets of fractional coverages are in the **Coverage File** and the **Log File**. Click the **OK** button in the **Coverages** dialog box and you are back in the main menu (see Figure 3-16).

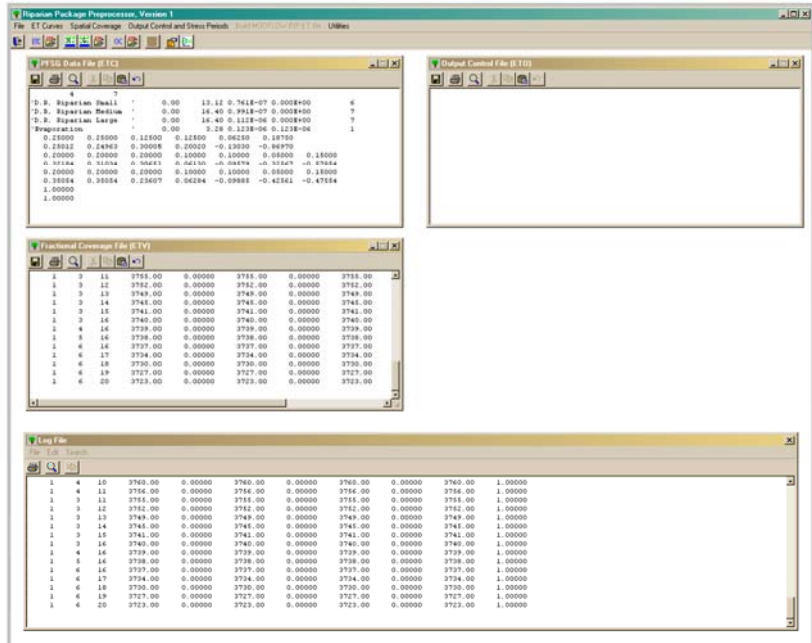


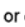


Figure 3-16. Main menu with ETC file, ETV file and Log file.

At this point you can save the ETV file. Click the disk icon  in the **Coverage File** sub menu, and save the ETV file as Exmpl.etv. You now have entered and saved all the fractional coverage data. You may now exit the program without losing data. If you have exited and saved your data, you may restart the coverage section of the program by either clicking both the menu bar item **Spatial Coverage** and the dropdown submenu item **Open Existing Coverage File (ETV)** or clicking on the  button. If you are restarting, you must load the ETC data (click the  button or use the main menu) before you can "reload the ETV data.




Output Control File

The Output Control File is composed of two parts. The first part contains data for the output presentation of RIP-ET within MODFLOW, and the second part contains data pertaining to the stress periods and the fractional coverages present for those stress periods.

The output presentation part allows you to save or list the total volumetric ET rate for each riparian cell (the IRIPCB flag). It also allows you to save for each cell: its location $((j,i,k)$ coordinates), its land surface elevations and its volumetric ET rate by plant functional subgroup (the IRIPCB1 flag). As with other MODFLOW packages, RIP-ET has an option character set, "CBC", that indicates memory should be allocated to store the total volumetric ET rate for each riparian cell (the IRIPAL flag).

The stress period part allows you to specify the type of temporal analysis: steady state, steady oscillatory, or transient. A steady oscillatory solution contains stress periods that vary by seasons but cycle from year to year with the same seasonal values. With steady oscillatory and transient simulations you are required to specify the number of seasons and the number of years or multiple years. For each of the stress periods, you will also be required to specify a unique coverage that pertains to that time.

For the tutorial example you will want to 1) list the total volumetric ET rate for each cell; 2) save location $((J,I,K)$ coordinates), land surface elevations, and volumetric ET rate by plant functional subgroup on Unit 50 for a each cell; and 3) allocate no memory to store the total volumetric ET rate for each riparian cell. Your simulation will be a steady oscillatory with 2 seasons for 5 year for a total of 10 stress periods. Your two fractional coverages will alternate between stress periods.

If you have exited PRE-RIP-ET, start PRE-RIP-ET (click on the  icon) and load the PFSG data file using the  button and the coverage file using the  button. You must complete or load the PFSG data file and the Coverage file before beginning to construct the Output Control file. Once the PFSG data file and the Coverage file have been loaded, the Output Control selections on the main menu and the tool bar will be enabled.

Either click on the menu item **Output Control and Stress Periods** then click on the submenu item **Construct Output Control File**, or simply click on the  icon.

The **Output Control Parameter** dialog box will appear. In the *IRIPCB Flag* group, check *Write total ET rate for each cell to List File*; in the *IRIPCB1 Flag* group, check *Save Values* and place 50 into the spinner box; and in the *IRIPAL Flag* Group, leave the check box blank (see Figure 3-17).

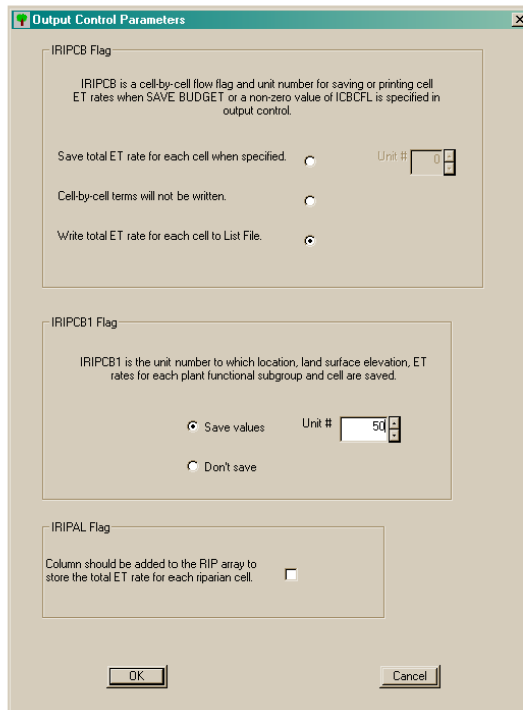


Figure 3-17. Output Control Parameter dialog box

Now click the **OK** button and the **Stress Periods** dialog box will appear.

If you should click on the **Cancel** button for the **Output Control Parameter** dialog boxes, you will be given the option of returning to the main menu or continuing.

Within the **Stress Periods** dialog box, click on **Steady Oscillatory**, place the value 2 in the **Number of Seasons** spinner box, and place a 5 in the **Number of Years or Cycles** spinner box (see Figure 3-18). When you have finished doing this, click on the **OK** button to continue.

If you click on the cancel button, you will be given the option of returning to the main menu or continuing. If you return to the main menu, you will have to reenter the **Stress Periods** data and the previous **Output Control Parameter** dialog.

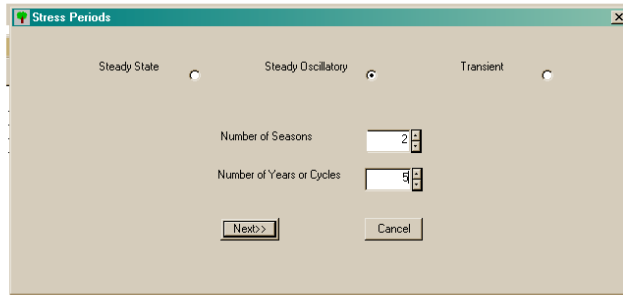


Figure 3-18. Stress Period dialog box

The **Order of Coverage** dialog box will appear (see Figure 3-19). Place the number 1 under the *Coverage* column for stress period 1, a 2 under *Coverage* column for stress period 2, a 1 under *Coverage* column for stress period 3,..., and continue alternating fractional coverages till all 10 *Coverage* columns are filled. It is also possible for you to load or to save the order of the fractional coverages using a *csv* file.

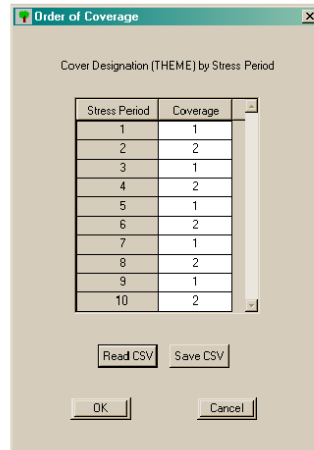


Figure 3-19. Order of Coverages dialog box.

When you have finished entering the order of coverage, click on the **OK** button, and you will return to the main menu.

As before, if you click on the cancel button, you will be given the option of returning to the main menu or continuing. If you return to the main menu you have to reenter the **Stress Periods** data and the previous **Output Control Parameter** dialog.

After clicking the OK button and returning to the main menu, you will see the output control parameters, the stress period data, and the order of coverage data displayed in the **Output Control File (ETO)** sub window and in the **Log File** sub window (Figure 2-20).

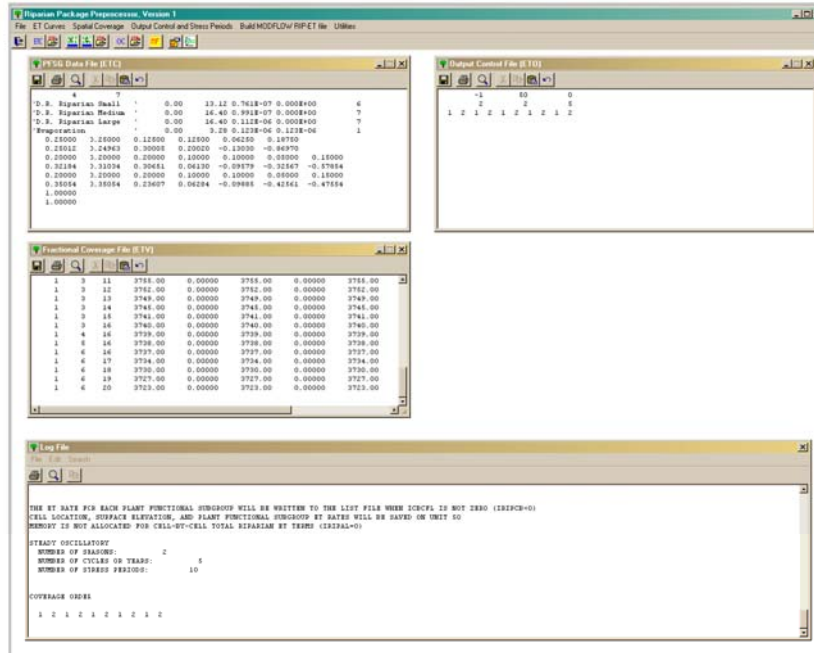








Figure 3-20: Main window upon completion of Output Control File (ETO)

At this point you can save the **ETO** file. Click the disk icon  on the **Output Control File (ETO)** subwindow, and save the **ETO** file as **Exmpl.eto**. You now have entered and saved all the output control and stress period data. You may now exit the program without losing data. To restart the output control section of the program click the menu bar item **Output Control and Stress Periods** and the dropdown submenu item **Open Existing Output Control File (ETO)**, or click on the  button. If you are restarting the program, you must

load the *ETC* data (click the  button or use the main menu) and the *ETV* data (click the  button or use the main menu) before you can reload the *ETO* data.

Building the MODFLOW RIP-ET File

You now the three files, PFSG Data File (.etc), Coverage File (.etv), and the Output Control File (.eto) completed. When all three files are loaded, the **Build MODFLOW RIP-ET file** item on the main menu and the  button on the toolbar are enabled. To generate the MODFLOW RIP-ET file simply click on the main menu item **Build MODFLOW RIP-ET file** or click on the  button on the toolbar.

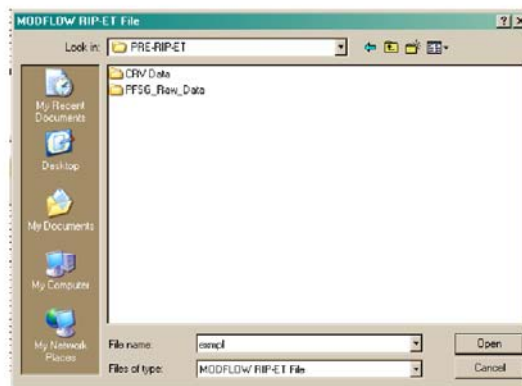


Figure 3-21. MODFLOW RIP-ET File save dialog box.

The **MODFLOW RIP File** dialog will appear. Type in *exmpl* in the *File Name* box, and click on **Open**. Figure 3-21 indicates that the RIP file will be saved to the PRE-RIP-ET directory. This is the directory where *PRE-RIP-ET.exe* is found.

Congratulations. You have just completed the tutorial and have created a MODFLOW-96 RIP-ET file entitled *exmpl.rip*.

4 PFSG Curve Files

This chapter presents the utility module that calculates a PFSG Curve File. You will need a PFSG Curve File for each plant functional subgroup used in your MODFLOW simulation. The data set contains the name of the plant functional subgroup, and its associated active root depth, saturated extinction depth, max ET flux, and ET flux at the saturated extinction depth. The data set also contains the dimensionless curve segment data for reconstructing the actual ET curve. The PFSG Curve Files have a *.crv* extension and are used in the **PFSG Data** dialog box presented in Chapter 3.

PFSG Raw-Data Sets

To construct a PFSG Curve File, you must have the raw-data set for the plant functional subgroup. The raw-data set consists of a set of vertices from the ET flux-head curve, and the ET flux and head values at those vertices. There should be sufficient vertices to characterize the curve. The heads are defined relative to the land surface. Thus the head values are set to zero at land surface, negative if below, and positive if above. On your PRE-RIP-ET disk, in a folder entitled **Raw_ET_Data**, you will find nine data sets. Eight are for actual plant functional subgroups: obligate wetland, shallow-rooted riparian, average deep-rooted riparian, small deep-rooted riparian, medium deep-rooted riparian, large deep-rooted riparian, extra large deep-rooted riparian and transitional riparian. The ninth is a summer evaporation data set. These data sets, based on extensive literature review and field measurements, represent average daily growing season values for Southwestern United States vegetation (Baird and Maddock, 2003). All these data sets have a *.csv* extension, and can be read by a text file reader and most spreadsheets. You are encouraged to develop your own raw-ET data sets for the plant functional subgroups in your study area through a combination of field studies, literature review and input from local plant ecologist or botanists.

Table 4-1 presents the PFSG raw-data set for the small deep rooted riparian PFSG (Note that Table 1-1 in Chapter 1 presents the raw-data set for the obligate wetlands PFSG). The vertices are points on the PFSG curve shown in Figure 4-1. As you can see, seven vertices adequately describe the ET flux-head curve for the small deep-rooted riparian group. The vertices are numbered from the extinction depth elevation (-400 cm) to the saturated extinction elevation (0 cm). In general, all plant functional groups applicable to

groundwater modeling should have a saturated extinction depth. Because the saturated extinction depth for this plant subgroup is at the land surface, the head is taken as 0 cm. The maximum ET flux (0.2003 cm/day) occurs at the elevation -100 cm

The vertices numbering scheme is important. For vegetation, the numbering should start at the extinction depth and should proceed sequentially along the curve to the saturated extinction depth. For traditional MODFLOW evaporation, there are only two vertices. The first is at the extinction depth elevation and the second is at the maximum ET surface elevation. For evaporation, the saturated extinction depth is set equal to the maximum ET surface.

Table 4-1. PFSG raw-data set for small deep rooted riparian in Southwestern United States (** Maximum ET flux).

Vertices	ET Flux (cm/day)	Head (cm)
7	0	0
6	0.1742	-75
**5	0.2003	-100
4	0.1602	-150
3	0.1001	-200
2	0.0501	-300
1	0	-400

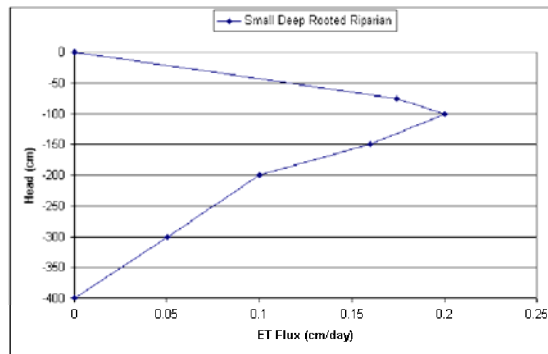



Figure 4-1. PFSG curve for small deep rooted riparian

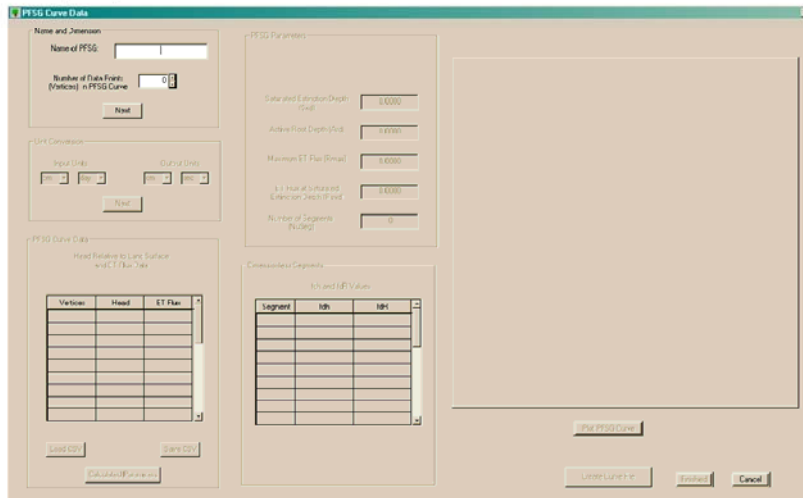
PFSG Curve File Utility Module

The PFSG raw-data sets are transformed into PFSG curve files using the PFSG Curve File utility module. The module processes the raw data for one PFSG curve file at a time. To start the PFSG Curve File utility module, click on **Utilities** and then click on **Construct a PFSG Curve File** in the main menu, or click on the  icon. The dialog box shown in Figure 4-2 appears.

To quit, you may press the **Cancel** button at any time but all data that you entered into the *PFSG Curve Data* dialog box will be lost. Normal termination is to click the **Finished** button after all data has been entered.

Name and Dimension Group

Starting in the upper left hand corner of the dialog box, enter the name of the plant functional subgroup in the text box labeled *Name of PFSG* (under *Name and Dimension*). The names can be up to 22 characters in length, and may contain spaces but no apostrophes.



Vertex	Head	ET Flow

Segment	Infl	MFC

Figure 4-2: Start of PFSG Curve Data dialog box with *Name and Dimension* group highlighted.

Enter the number of vertices into the spinner box labeled *Number of Data Points (Vertices) in PFSG Curve*.

For the example small deep-rooted riparian, you could enter *D.R. Riparian Small* in the text box and enter 7 in the spinner box. When you click on the **Next** button, the name and vertices information is written to the *Log File* and the *Unit Conversion* group is enabled (Figure 4-3).

Unit Conversion Group

The *Unit Conversion* group is divided into two parts, one labeled *Input Units*, the other, *Output Units*. The *Input Units* are the distance and time units associated with the PFSG raw-data sets. For this version of PRE-RIP-ET, the units of distance available are centimeters, meters, and feet. The time units are seconds, days and years. All the nine PFSG raw-data sets available with the PRE-RIP-ET package (found on the disk in the **Raw_ET_Data** directory) have the distance units of centimeters and the time units of days. The *Input Units* list boxes are defaulted to centimeters and days, so if you are supplying your own PFSG raw-data set, set the list boxes to the appropriate units if they are different from the default.

The *Output Units* are the distance and time units that you want for your MODFLOW simulation. For example, if the units for the MODFLOW simulation were in feet and seconds, you would set the list boxes under *Output Units* accordingly.

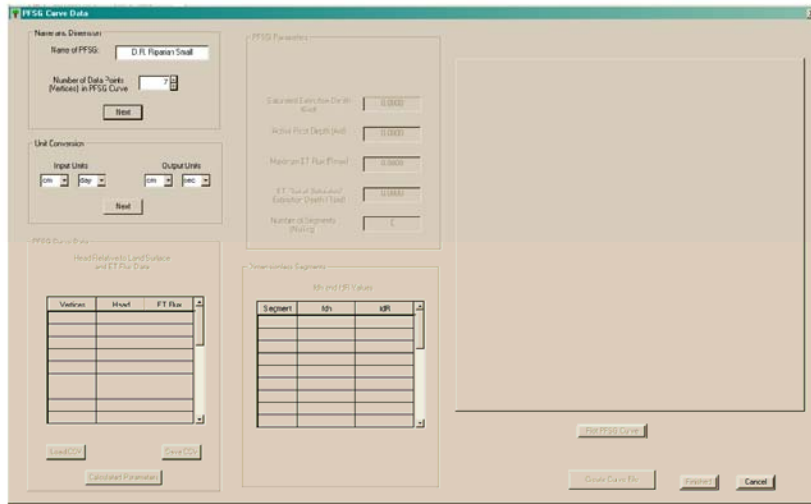


Figure 4-3. PFSG Curve Data dialog box with *Unit Conversion* group enabled.

After the units have been set, click on the **Next** button to write unit conversion information to the *Log File* and enable the *PFSG Curve Data* group.

PFSG Curve Data Group

This is where you enter the PFSG raw-data values: vertices, heads and ET fluxes. You may enter them directly from the keyboard, or since the PFSG raw-data values are stored as *.csv* files, you may load them clicking on the *Load CSV* button. Figure 4-4 illustrates a loaded PFSG raw-data set. If you have entered the numbers by the keyboard, you have the option of saving them as a *.csv* file.

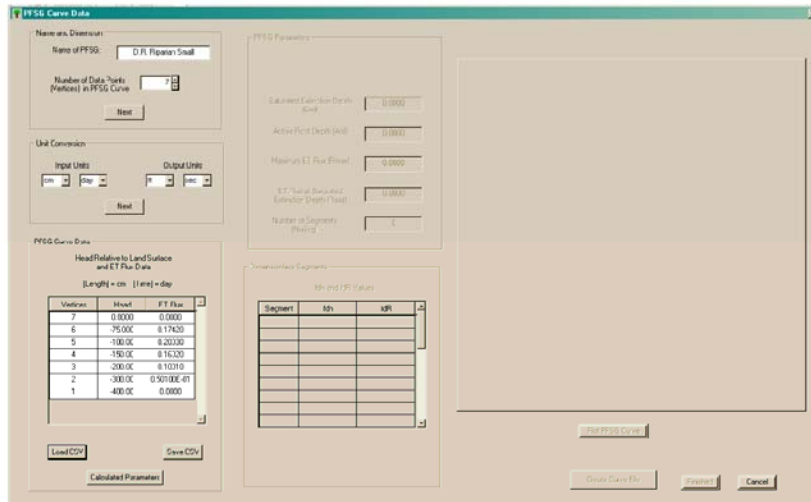


Figure 4-4. PFSG Curve Data dialog box with PFSG Curve Data entered.

Although the vertices numbering scheme is important, you may enter the vertex number and associated ET flux and head in any order. PRE-RIP-ET will sort the rows internally to the proper descending order. Thus vertex 1 (extinction depth) values could be listed first, vertex 2 values second, and so on. After entering the PFSG raw data, you have completed the data entry phase of the utility module. Click on the **Calculated Parameter** button.

Calculated Parameter Button

Upon clicking the **Calculated Parameter** button, PRE-RIP-ET performs the following calculations and actions on the grid value in the *PFSG Curve Data* group. First, the head value (in input dimensions) for Vertex 1 is set equal to H_{xd} , the extinction depth elevation relative to the land surface elevation; and the last vertex (number 7 for small deep rooted riparian) is set equal to H_{sxd} , the saturated extinction depth elevation relative to the land surface elevation. Because it is the referenced elevation, the land surface elevation, $HSURF$, is zero for the PFSG Curve File module. Next, the H_{sxd} and H_{xd} values are translated from the input dimensions to the output dimension (e.g. cm \rightarrow ft). The $HSURF$ remain zero under the transformation. Note, the process of assigning actual land surface elevations is performed in the MODFLOW RIP-ET package. The saturated extinction depth, Sxd , is calculated as,

$$Sxd = HSURF - H_{sxd}$$

and the active root depth, Ard , is calculated as,

$$Ard = Hsxd - Hxd$$

You should note that the saturated extinction depth (Sxd) is positive if $Hsxd$ is below land surface ($Hsxd < HSURF$), zero if $Hsxd$ is at land surface ($Hsxd = HSURF$), and negative if $Hsxd$ is above land surface ($Hsxd > HSURF$). The active root depth (Ard) should always be positive.

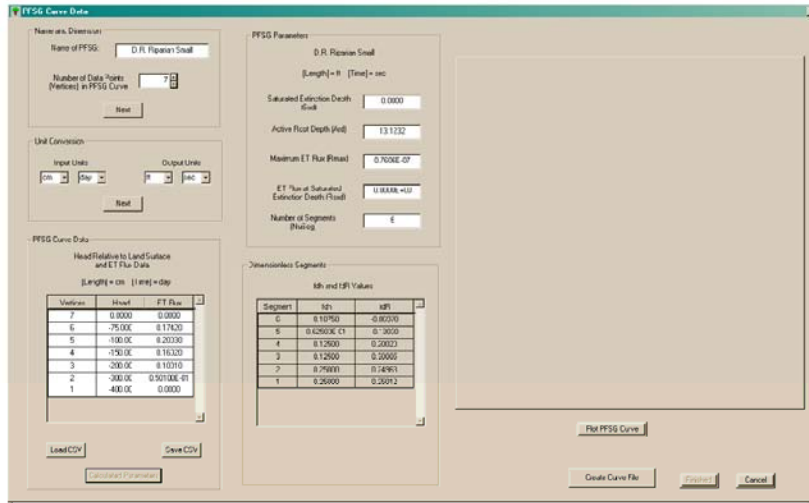


Figure 4-5. PFSG Curve Data dialog box with PFSG parameters and dimensionless segments calculated

PRE-RIP-ET determines the vertex with the largest ET flux and assigns this value to $Rmax$, the maximum ET flux rate. R_{sxd} , the ET flux at the saturated extinction depth, is set to the ET flux value for the last vertex, which is usually zero for vegetation. For evaporation, R_{sxd} is set equal to $Rmax$. Both $Rmax$ and R_{sxd} are transformed into output dimensions (e.g. $cm/day \rightarrow ft/sec$).

The number of segments is then calculated. The number of segment will be one less than the number of vertices. The values of these parameters are reported in the *PFSG Parameter* group (see Figure 4-5).

With a click of the **Calculated Parameter** button, PRE-RIP-ET calculates the set of dimensionless segments used by the MODFLOW RIP-ET package to reconstruct the

PFSG curves in the proper dimensions. Figure 4-6 will aid in developing the concept of dimensionless segments. For a thorough discussion of the development of the dimensionless segments see Maddock and Baird (2002).

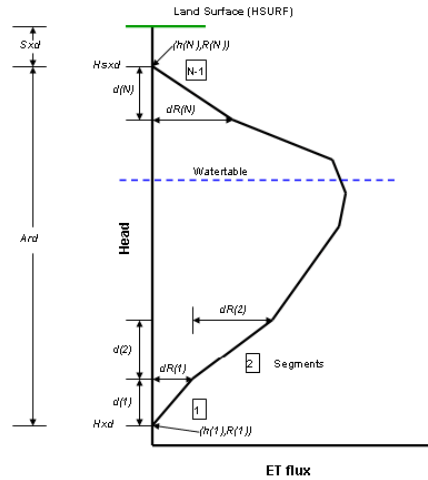


Figure 4-6. PFSG Curve

We define the dimensionless segment variable in the ordinate (X) direction as, $fdh(k) = d(k)/Ard$. Similarly we define the dimensionless segment variable in the abscissa (Y) direction as, $fdR(k) = dR/Rmax$.

You should note that for vegetation, the rising portion of the curve (from the extinction depth vertex to the vertex with $R = Rmax$), the fdR 's are positive, while on the falling portion of the curve (from the vertex with $R = Rmax$ to the saturated extinction depth vertex) the fdR 's are negative. In fact, for vegetation, summing the fdR values over all the segments gives,

$$\sum_{k=1}^N fdR(k) = 0$$

For evaporation, there is only one segment, and $fdR(1)=1$ because at the end of the segment, $R = R_{sxd} = Rmax$ (that is the ET flux value at the maximum ET surface).

The fdh values are always positive and summing the fdh values over all segments gives,

$$\sum_{k=1}^M fdh(k) = 1$$

Once *HSURF*, *Sxd*, *Ard*, and *Rmax*, are determined, the program can reconstruct the head values.

The *h* and the *R* values will have the distance and time units the same as *Sxd*, *Ard*, *Rmax* and *Rxsd*. You will recall from Chapter 3 that the actual land surface elevation *HSURF* (commonly referenced to mean-sea level) is read either as a single value for the cell or a value for each plant functional group in a cell. Using the actual land surface elevation referenced to mean-sea level in MODFLOW, gives heads, *h(k)*'s, referenced to mean-sea level in MODFLOW.

The values of *fdh*'s and *fdR*'s are reported in the *Dimensionless Segment* group (see Figure 4-5). The *fdh*'s and *fdR*' do not change when you change the units of *Sxd*, *Ard*, *Rmax* and *Rxsd*. To see this, return to *Unit Conversion Group* and change the *Output Unit* values, say from feet and seconds to meters and years, click **Next**, and then click on the **Calculated Parameter** button. The values reported in the *PFSG Parameter* group will change, but the values in the *Dimensionless Segment* group remain unchanged.

Clicking on the **Calculated Parameter** button writes the parameter and dimensionless segment data to the *Log File*, and enables the **Plot PFSG Curve** and the **Create Curve File** buttons.

Plot PSFG Curve Button

Clicking the **Plot PSFG Curve** button creates a graph of the PSFG curve in output units. Figure 4-7 show the curves plotted with data transformed into feet and year unit dimensions.

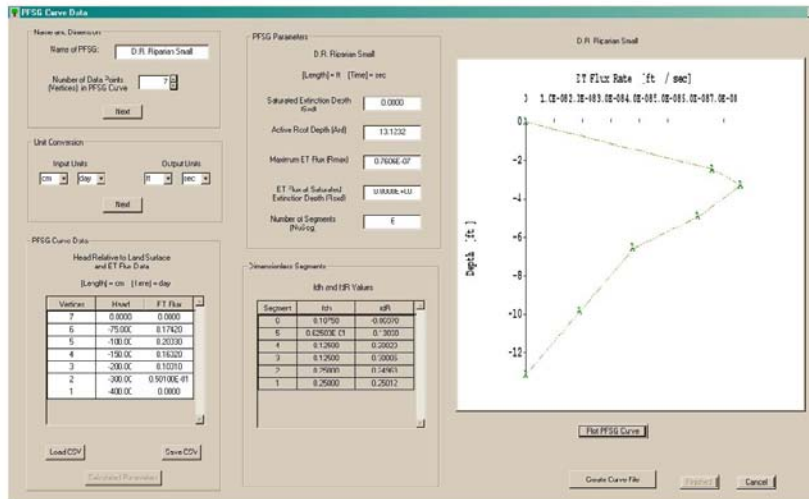


Figure 4-7. PSFG curve plot for small deep rooted riparian in feet and year dimension units

Create Curve File Button

Clicking the **Create Curve File** button brings up the request for a file name to save the PSFG curve file (see Figure 4.8). The file name will be given a .crv extension if you do not specify one.

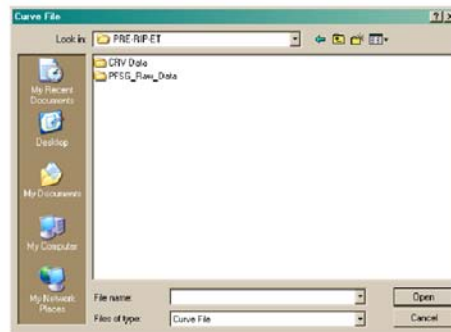


Figure 4-8. Dialog box for saving .crv files.

The PFSG curve file for small deep rooted-riparian is shown in Figure 4.9

```
'D.F. Riparian Small '
ft sec
0.0000 13.1232 0.7606E-07 0.0000E+00 6
0.25000 0.25000 0.12500 0.12500 0.06250 0.18750
0.25012 0.24963 0.30005 0.20020 -0.13030 -0.86970
```

Figure 4-9. PFSG ET curve data set for small deep-rooted riparian vegetation.

The first line contains the name, and the second contains the output units. The third line contains the saturated extinction depth (Sx_0), the active root depth (Arc), the maximum ET flux ($Rmax$), the ET flux at the saturated extinction depth (Rsx_0), and the number of segments. The fourth line presents the dimensionless segment component for the X axis (the head axis). The fifth line presents the dimensionless segment for the Y axis (the ET-flux axis).

Once you've clicked the **Create Curve File** button and saved the PFSG Curve file the **Finished** button is enabled. Clicking the **Finished** button returns you to the main menu. You should repeat this process for every PFSG in your simulation. Once you have completed developing your PFSG curve files, you may begin to construct your RIP-ET data set.

5 GIS Module

This chapter presents a GIS module that is an abbreviated version of RIPGIS (Dragoo, 2003). The GIS module creates the Fractional Coverage File (ETV) and is external to PRE-RIP-ET. The GIS Module is a custom application written in Avenue, the programming language using ArcView GIS. PRE-RIP-ET generates a required data set for the GIS module.

Requirements

To use the GIS module you must have ArcView 3.X and the Spatial Analyst extension, products of ESRI, Inc., installed on your computer, and you must have basic knowledge of how to use these commercially available packages.

The MODFLOW grid must be completed and available. For MODFLOW 96 this means that the .bas and .bcf files are available, and for MODFLOW 2000 this means the .dis and .ba6 files are available.

A digital elevation model (DEM) must be available to add as a theme within an ArcView project. The United States Geological Survey (USGS) DEMs can be downloaded from <http://data.geocomm.com/>. Depending on the location and size of the study area, a 10- to 30-meter DEM can be downloaded. Generally, it is best to get the highest resolution possible.

You must define and spatially locate plant functional groups or sub-groups found in the model. Riparian regions are often digitized using aerial photography, or another appropriate background image. Therefore, we assume that you have either a completed riparian theme or an image on which to digitize a new theme.


The GIS module will guide you through attributing the riparian theme with the appropriate PFSGs, importing grid cells from MODFLOW, attributing the grid cells according to the riparian theme, and assigning a riparian land surface elevation. The module will then calculate the fractional coverage of each sub-group by cell and create a Fractional Coverage File (ETV) that can be imported into PRE-RIP-ET.

Before starting to use the GIS Module, be sure the following files exist within the same (writeable) directory as PreProRip.exe.

rippis.apr – This is the ArcView project file (the GIS MODULE program),

watgrid.avl – This is an ArcView legend file for depth to water grid classification, and

The PFSG Name File.

The PFSG Name File is a file created by PRE-RIP-ET that contains the names of the PFSG to be used in the MODFLOW model. It has the extension .inx. To create PFSG Name File, you must have created or loaded the PSFG Data File (ETC) in PRE-RIP-ET. Click on either the menu bar item **Spatial Coverage** and then the dropdown submenu item **Construct Coverage File from GIS**, or click on the  icon on the main menu tool bar. The **PFSG Name File** dialog box will appear (Figure 5-1). Use the *Look in:* list box to place the file in the same directory as rippis.apr (which is usually in the directory with PRE-RIP-ET.exe), enter the name for the file in the *File name* list box and click on the **Save** button. PRE-RIP-ET writes the *PFSG Name File*

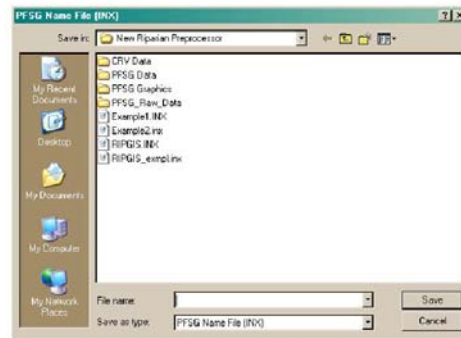


Figure 5-1, File selection dialog box for PFSG Name File (INX)

to the desired directory. An example of the *PFSG Name File* is shown in Figure 5-2.

```
Wetlands
Evaporation
D.R. Riparian Average
TransRip
```

Figure 5-2, Example PFSG Name File created by PRE-RIP-ET

Once the *PFSG Name File* is created, PRE-RIP-ET will ask you if you wish to exit to enter ArcView (Figure 5-3). Click on **Yes** button, and you will exit PRE-RIP-ET, click on the **No** button and you will be returned to the PRE-RIP-ET main menu.



Figure 5-3, Exit PRE-RIP-ET dialog box

Starting the GIS Module

After ArcView starts, a popup menu titled "GIS MODULE" will open along the right side of the View (Figure 5.2). If this menu is not automatically displayed, or to re-open the menu, click "Riparian Menu" → "Open Riparian Menu" at the top of the View.

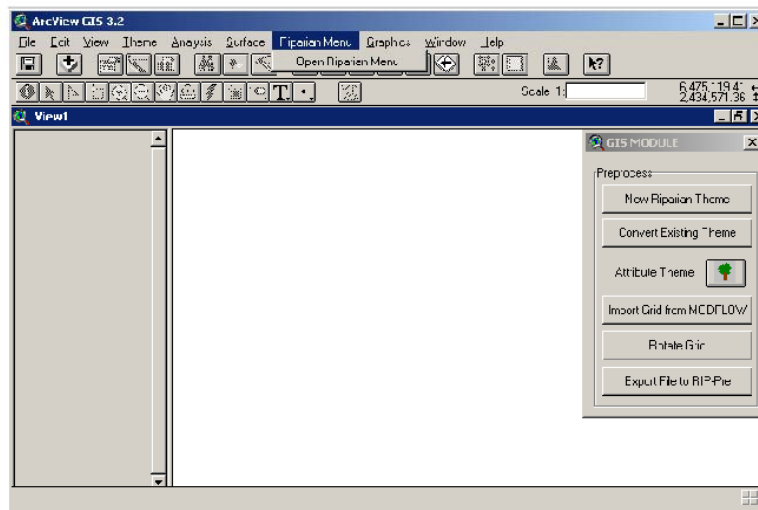



Figure 5.2, Arcview screen with preprocessing popup window

Preprocessor

The GIS MODULE popup menu consists of six buttons entitled, New Riparian Theme, Covert Existing Theme, Attribute Theme , Import Grid from MODFLOW, Rotate Grid, and Export File to PRE-RIP-ET.

Creating/Converting Riparian Theme

The preprocessor requires the use of specific fields within the riparian theme. The user can either create a new theme that will automatically contain the appropriate fields or convert an existing theme. Converting an existing theme will copy the current theme to a new theme and add the required fields.

If you do not have a riparian theme:

 New Riparian Theme

Click "New Riparian Theme" under the Riparian menu. You will be prompted for a location and name of your new theme. The theme will be added to the view and the necessary fields (column names) will be added to the theme's attribute table. The new riparian theme is now ready for digitization. Correct location of the new riparian polygons can be determined from digital USGS maps, aerial photography, or other background image. In Figure 5.3, riparian polygons are shown overlaying aerial photos. For more information on adding new polygons to a theme, see the ArcView GIS manual.

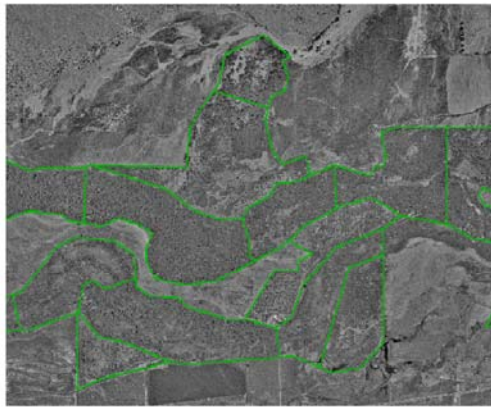


Figure 5.3, New riparian polygons are drawn over an aerial photo

After you are finished digitizing, proceed to the next section on attributing the new riparian theme.

If you already have a riparian theme:

Convert Existing Theme

Add your existing theme to the view. Then click "Convert Existing Theme". You will be prompted to select your existing riparian theme from the list, and to create a new name and location for the converted theme. The converted theme will be added to the view and the necessary fields (column names) will be added to the theme's attribute table. Figure 5.4 shows the attribute table for a newly converted riparian theme. In this figure, all of the values are zero, because the polygons have not yet been attributed with PFSG percentages. Each PFSG field in the table can be assigned a value as described in the next section.

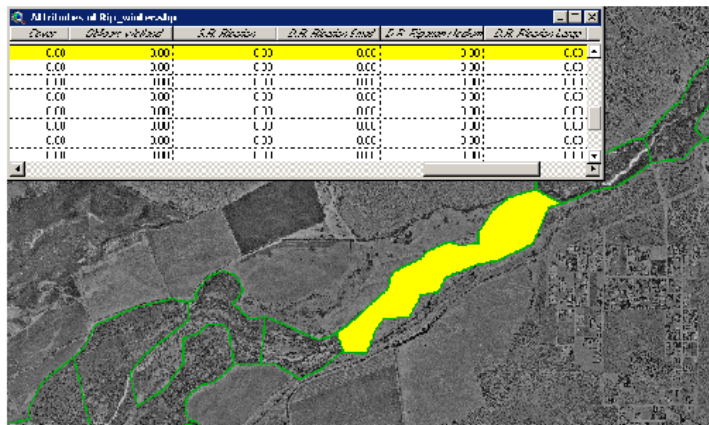



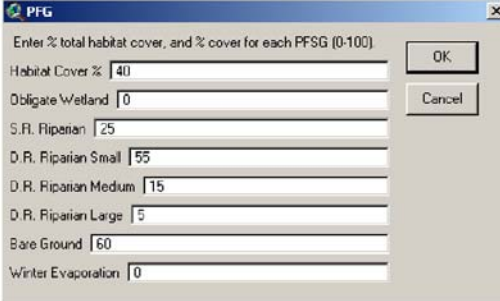
Figure 5.4, Riparian theme with attribute table. Highlighted record is selected both on the map and in the table.

Once the new or converted theme is added to the view, it will be ready for editing and attribution.

Attributing Riparian Theme

The new or converted riparian theme must be attributed with the percent cover, and the percentage of each plant functional group that exists within the polygon.

The Riparian Tool, represented by  icon, will aid in attribution. Each polygon must be attributed separately using the tool, or you can open the theme table and edit manually (see ArcView GIS manual). To use the tool, activate (highlight) the theme you would like to edit, click the tree icon, and then click on the polygon you would like to attribute. A window will open prompting you for the percent cover and each PFSG in the selected polygon (Figure 5.5).



Field	Value
Habitat Cover %	40
Obligate Wetland	0
S.R. Riparian	25
D.R. Riparian Small	55
D.R. Riparian Medium	15
D.R. Riparian Large	5
Bare Ground	60
Winter Evaporation	0

Figure 5.5. PFG window for entering percentage of habitat covers.

Habitat Cover % – This is the percentage within the riparian polygon that is covered by plant canopy or the coverage parameter that matches the users scaling factor (see RIP-ET Package manual). The “Bare Ground” field is calculated automatically from this value. It is the opposite of habitat cover (100 - habitat cover).

The next seven items in Figure 5.5 are the names of the Plant Functional Subgroups (PFSG) or habitat type. A PFSG is the PFG along with the plant size (if applicable). Each subgroup should have a different evapotranspiration curve within the MODFLOW Riparian ET package. These names are imported from PRE-RIP-ET through the textfile called ripgis.inx. In this case, bare ground and winter evaporation are both treated as PFSGs.

% PFSG – This is the percentage of the total cover that contains the specified plant functional subgroup.

For example, if the selected polygon has 40% canopy cover, and contains 25% Shallow Rooted Riparian, 55% Small Deep Rooted Riparian, 15% Medium Deep Rooted Riparian and 5% Large Deep Rooted Riparian, then the attribution window would look like Figure

5.5. Click "OK" to save, or "Cancel" to close the window. Because of ArcView limitations, the window is not refreshed if moved. It will appear to have two of the same windows.

Importing Grid from MODFLOW

The grid constructed here must match the grid in the MODFLOW simulation. Therefore, the grid dimensions must be imported from the MODFLOW files in order to be placed and then geo-rectified correctly in ArcView. If importing from MODFLOW96, the .bas and .bct files are read. If importing from MODFLOW 2000, the .ba6 and .dis files are read. These files contain all the necessary information to construct the grid except the starting location on the map. Therefore, the user must either enter coordinates for the upper left starting point of the grid or point to the upper left location on the map. For any real world application, we strongly recommend that the coordinate system be entered. Proceed as follows:

a) Click 

The following dialog box will open:

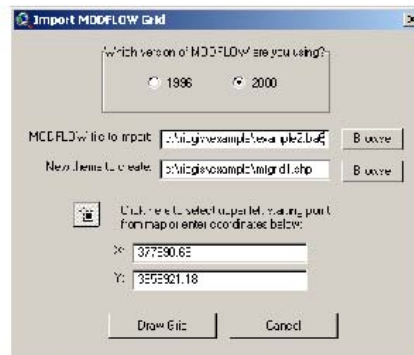


Figure 5.4, Import MODFLOW Grid dialog box

b) Select the version of MODFLOW the grid files are written in. Currently, only MODFLOW 96 and 2000 are supported.

c) Click the browse button next to "MODFLOW file to import".

If you are using MODFLOW96, the browse function will ask for the .bas file. Note that the program automatically accesses the .bcf file. Therefore, these files must be in the same directory with the same base name. For example, if you are using project1.bas, then the accompanying bcf file must be called project1.bcf.


If you are using MODFLOW2000, the browse function will ask for the .ba6 file. The program also accesses the .dis file. Again, these files must be in the same directory with the same base name.

d) Click the browse button next to "New theme to create".

Browse to a new location for your theme, and give it a new name.

e) Define the upper left starting point of the grid location.

This point can be defined by entering coordinates directly into the *X* and the *Y* boxes (recommended) or by using the tool. If entering the coordinates directly, these should be the UPPER LEFT coordinates of the grid.

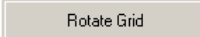
To use the tool, click , and then click the point on the view that corresponds to the UPPER LEFT point of the grid. The *X* and *Y* boxes will be filled in automatically.

e) Click 

A new grid theme will be added to the view. The appropriate layer, row and column will be assigned to each grid cell. The layer will always be shown as "1" because currently, the grid is only shown in 2-dimensions.

Rotating grid shapefile

In some cases, the MODFLOW grid is not oriented directly north-south, and must be rotated.

Click 

You will be prompted to select the grid shapefile from a list of themes, enter the rotation angle, and enter coordinates for a pivot point. THE SHAPEFILE WILL BE CHANGED, SO SAVE A BACKUP IF UNSURE ABOUT ANGLE OR PIVOT POINT.

Creating the textfile that will be imported by MODFLOW

After you have attributed all the riparian polygons and imported the grid cells, the textfile can be written.

Click

Export File to RIP-Pre

You will be prompted for the riparian theme(s), the grid cell theme, and the DEM. This function finds the percentage of PFG by area for each cell, and determines the elevation of each cell. The new textfile will be called "ripgis.otx".

RIPGIS.OTX Format:

For each simulation:

MAXRIP COVNUM

MAXRIP = Max number of grid cells overlain by any riparian theme
COVNUM = Number of unique themes

For each unique theme:

ITMP NUMCELL

TMP = Current theme number
NUMCELL = Number of riparian cells in current theme

For each grid cell:

Layer Row Column [Elevation] [Percent Subgroup]

(An elevation and a percent cover are listed for each subgroup used in the simulation.


If that sub-group is not present in the cell, both values will be written as zero.)

After the textfile ripgis.otx is created successfully, you will be prompted to close ArcView GIS and return to PRE-RIP-ET. Once ArcView closes, PRE-RIP-ET will read*** the textfile for the necessary fractional coverages.

6 Importing An Existing MODFLOW RIP-ET File

This chapter presents a utility module that reads an existing MODFLOW RIP-ET file and produces a PFSG Data File (.etc), a Fractional Coverage File (.etv) and an Output Control File (.eto). Before you import the RIP-ET file, you must know the time status of the data set, that is, is it a steady state, a steady oscillatory or a transient data set. You must also know the number of stress periods, the number of unique fractional coverages and the order of the fractional coverages over the stress periods.

Importing the RIP-ET File

To import an existing RIP-ET file, click on **Utilities** and then click on **Import MODFLOW RIP-ET File** in the main menu, or click on the  icon. A file choice box titled **MODFLOW Riparian File** appears (See Figure 6-1) and prompts you for a file name with a .rip extension. Click on the .rip file name you wish to load (for example **exmpl.rip**), and then click on the Open button. The PFSG data is read from the .rip file and written to the PFSG Date File (ETO) window. This data includes all of the

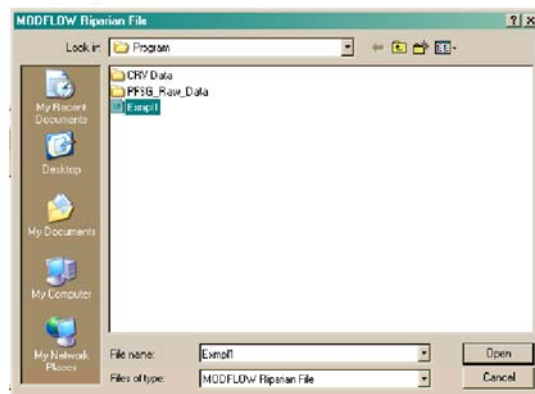


Figure 6-1, MODFLOW Riparian File dialog box for file choice.

PFSG names (RIPNM), their saturated extinction depth (Sxd), their active root depth (Ard), their maximum ET flux rate (Rmax), their ET flux rate at the saturation extinction depth (Rstd), and the number of segments in their curve (NuSeg). The data also includes the

active root depth segment factor and the ET flux rate segment factors for each of their curves.

The first line of the Output Control File (ETO) is also written to its window, and includes the cell-by-cell flag and unit number (IRIPCB), the save flag and unit number (IRIPCB1), and the dimension increment and flag for the optional memory allocation (IRPAL). The Log File window will report all the above data input and the Coverage Time and the Uniqueness Dimensions dialog box will appear.

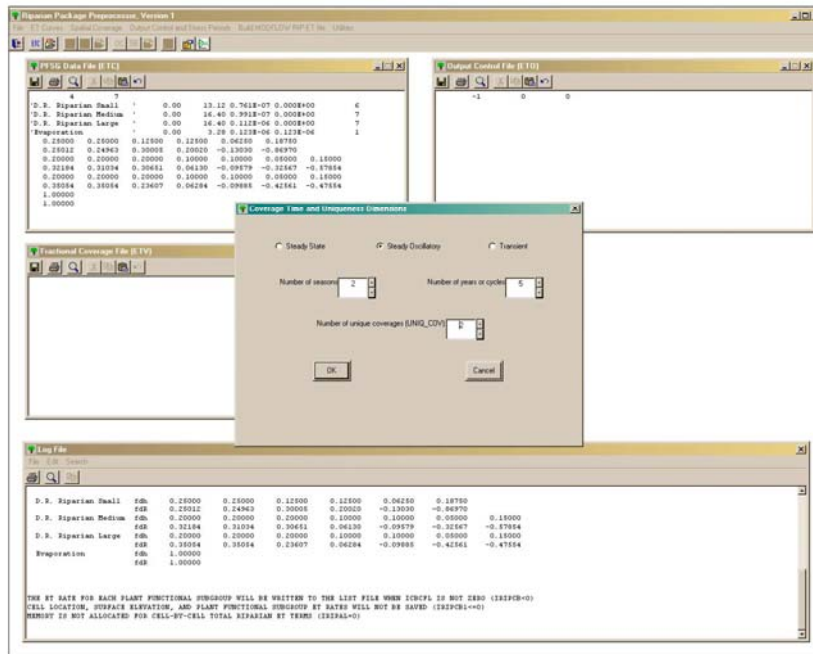


Figure 6-2. Coverage Time and Uniqueness Dimension dialog box on main menu.

This dialog box requests the time status, that is, whether you are reading in a steady state, steady oscillatory or transient data set. It requests the number of seasons per year and the number of years or cycles, and it requests the number of unique coverages.

Let suppose that Exmpl.rip, has a steady oscillatory time status, has two seasons and five cycles, and has two unique fractional coverages. Enter this data into the appropriate spinner boxes (see Figure 6-2), and click the OK button.

These values are reported in the Log File, and entered into the second line of the Output Control File (ETO) window. The maximum number of riparian cells (MAXRIP), the number unique coverages (UNQ_COV), and the flag for surface elevations (IHSURF) are automatically entered into the Fractional Coverage (ETV) window.

The Order of Coverage dialog box appears. This dialog box reads in the order of unique coverages, which you may do from the keyboard or with a .csv file (for the example **exmpl.rip**, there is a .csv file named **CovOrder.csv** in the PRE-RIP-ET directory that can be used for this purpose).

In the example **Exmpl.rip**, the two unique coverages alternate from season to season for a total of ten stress periods.

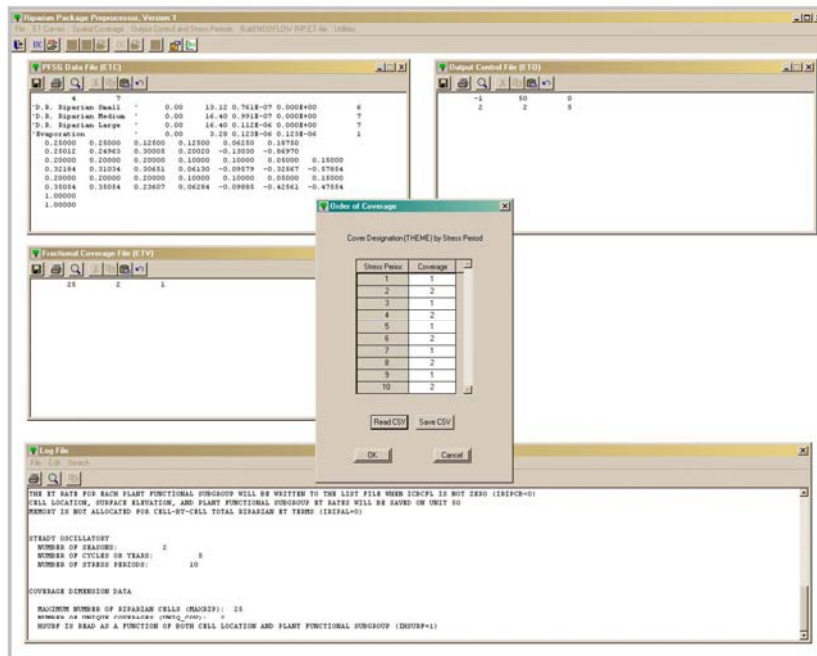


Figure 6-3, Order of Coverage dialog box on main menu.

Clicking the **OK** button on the **Order of Coverage** dialog box enters the rest of the data for the Fractional Coverage File, the Output Control File and the Log Window (see Figure 6-4).

At this point you can save the PFSG Data File, the Fractional Coverage File and the Output Control file by clicking on the disk icon  in the appropriate window.

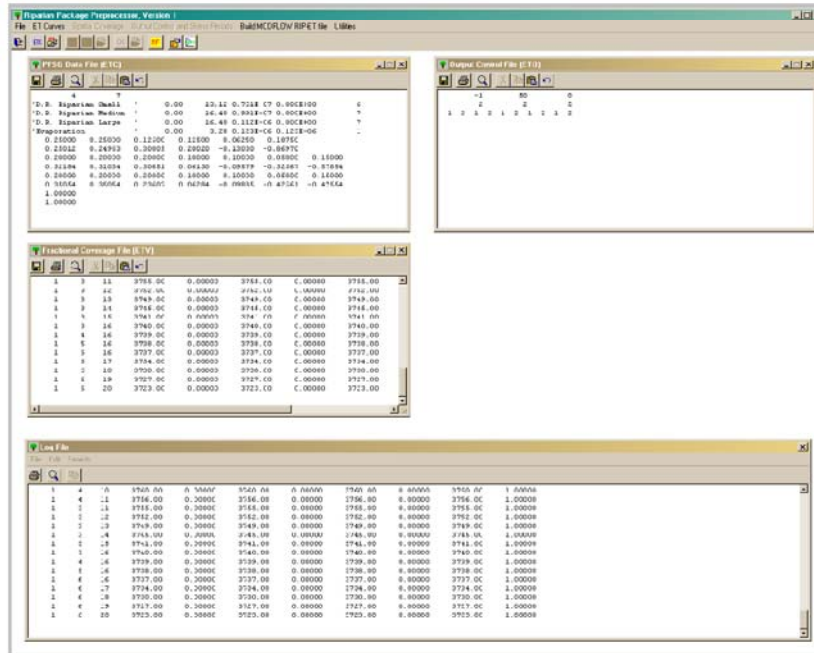



Figure 6-4. Final window

7 Quick Summary of PRE-RIP-ET Procedures


This chapter contains a summary of all operations and data entry used by PRE-RIP-ET. It is presented in a how-to-do-it format.

How Do You Start PRE-RIP-ET?

Go to the directory containing the file PRE-RIP-ET.exe. PRE-RIP-ET.exe has the icon, . Click on the icon and the main menu will appear.



How Do You Exit PRE-RIP-ET?

There are two ways of exiting PRE-RIP-ET.

1. Click on the **File** on the menu bar, then click on **Exit** on the drop down menu, or
2. Click on the icon  on the tool bar.


How Do You Construct a PFSG Data File?

Start by,

1. Click on the menu bar item **ET Curve** and then click on the dropdown submenu item **Construct PFSG Data File**, or click on the icon  on the tool bar.
2. Enter the total number of plant functional subgroups and the maximum number of segments in the spinner boxes in the **Plant Functional Subgroup Dimension Data** dialog box (Figure 3-3), then click on **Next**. The PFSG Data dialog box will appear (Figure 3-4).
3. Click on the **Press To Select PFSG (crv) Curve** button and the **Curve (crv) File** file-choice box will appear. Locate the subdirectory where the crv files are stored and select a desired file (Figure 3-5). Continue to click on the **Press To Select PFSG (crv) Curve** button until all the plant functional subgroups crv files have been selected (Figure 3-8).
4. When all the files have been selected, the **Press To Select PFSG (crv) Curve** button is disabled, and the PFSG Data File is written to the **PFSG Data File** and **Log File** windows.
5. You should save the PFSG Data File by clicking the  icon in the **PFSG Data File (ETC)** submenu. To continue in PreRipET, press the **OK** button.


How Do You Load an Existing PFSG Data File?


There are two ways to load an existing PFSG Data File (ETC),

1. Click on the menu bar item **ET Curves** and then on the dropdown menu item **Open Existing PSFG Data File (ETC)**, or
2. Click on the icon  on the tool bar.

How Do You Construct a Fractional Coverage File from Keyboard?


Start by,

1. Create or load the PFSG Data File, this will enable the menus and tool bar items for the Fractional Coverage File.
2. Click on the menu bar item **Spatial Coverage** and then click on the dropdown submenu item **Construct Coverage File from Keyboard**, or click on the icon  on the tool bar.
3. Enter the maximum number of riparian cells throughout simulation, and the total number of unique coverages for the simulation in the appropriate spinner boxes in the **Coverage Dimension** dialog box (Figure 3-11). Also check the radio box for single or multivalued of land surface elevations. Click on the **Next** button to continue.
4. The **Coverages** dialog box now appears (Figure 3-12) only the listbox titled *Press Select Coverage Button to Start Loading Coverage* is active. Click on the **Select Coverage** button and the word *Loading* in the first entry of the listbox. The *Number of Riparian Cells in Coverage (ITMP)* spinner is now active.
5. Enter the number of active riparian cells for the coverage and click on the **Set** button below the spinner. The grid and **Load or Store CSV** selections are now active. You may then either start typing values into the grid or read in a spreadsheet CSV file. If you type in the values to the grid you may save the resulting grid to a CSV file. When you have finished, click **Store Coverage in RIP Array** button, and ITMP and the coverage data appear in the **Fractional Coverage File (ETV)** window (Figure 3-16).
6. Continue to click of the **Select Coverage** button, entering the ITMP values and entering the grid values or CSV files, remembering each time to click the **Store Coverage in RIP Array** button, until all the coverages have been entered.

7. You should save the ETV file by clicking on the  icon on the **Fractional Coverage File (ETV)** menu window tool bar.
8. Click on the **OK** button when finished, you will be returned to the main menu, and the coverage data will be printed to the **Fractional Coverage File (ETV)** and **Log File** windows.


How Do You Load an Existing Fractional Coverage File?


You need to have loaded the PFSG Data File (ETC) before the Fractional Coverage Menu bar and toolbar items are enabled. There are two ways to load an existing Fractional Coverage File (ETV),

1. Click on the menu bar item **Spatial Coverage** and then on the dropdown menu item **Open Existing Coverage File (ETV)**, or
2. Click on the icon  on the tool bar.

How Do You Construct an Output Control File from Keyboard?


Start by,

1. Create or load the PFSG Data File and the Fractional Coverage File, this will enable the menus and tool bar items for the Output Control File.
2. Click on the menu bar item **Output Control and Stress Periods** and then click on the dropdown submenu item **Construct Output Control File**, or click on the icon  on the tool bar.
3. The **Output Control Parameter** dialog box will appear (Figure 3-17). Check the appropriate radio button for the IRIPCB and IRIPCB2 flags, and enter the unit number in the Unit # spinner box if required. Check or leave unchecked the IRIPAL flag. When finished with these tasks, click the **OK** button and the **Stress Periods** dialog box appears (Figure 3-18).
4. Click on the appropriate radio button for Steady State, Steady Oscillatory or Transient. If transient or Steady Oscillatory radio buttons have been clicked, enter the Number of Seasons and the Number of Years or Cycles in their spinner boxes. These spinner boxes are disabled if the radio button for Steady State is clicked. When finished with this task, click on the **Next** button and the **Order of Coverage** dialog box appears (Figure 3-19).

5. Enter the Coverage numbers into the *Cover Designation (THEME) by Stress Period* grid from the keyboard or from an CSV file. If you have entered the numbers by keyboard, you may save them to a CSV file by clicking on the **Save CSV** button.
6. Click on the **OK** button when all the coverage numbers have been entered and saved. You will be returned to the main window, and the output control, the stress period, and cover order data will be written to the **Output Control File (ETO)** and **Log File** windows.
7. You should save the ETO file by clicking on the  icon on the **Output Control File (ETO)** menu window tool bar.

How Do You Load an Existing Output Control File?

You need to have loaded the PFSG Data File (ETC) and the Fractional Coverage File (ETV) before the Output Control menu bar and toolbar items are enabled. There are two ways to load an existing Output Control File (ETO),

1. Click on the menu bar item **Output Control and Stress Periods** and then on the dropdown menu item **Open Existing Output Control File (ETO)**, or
2. Click on the icon  on the tool bar.

How Do You Create a MODFLOW RIP File?

To create a MODFLOW RIP file, you must have first created and/or loaded the PFSG Data File (ETC), the Fractional Coverage File (ETV), and Output Control File (ETO).

When all three files are loaded the **Build MODFLOW RIP-ET** item on the main menu and the  icon on the tool bar are enabled. To create a MODFLOW RIP-ET file, either,


1. Click on the **Build MODFLOW RIP-ET File** item on the main menu bar, or
2. Click on the  icon on the main menu tool bar.

The MODFLOW RIP-ET File dialog box will appear, you should enter the name you wish to call the MODFLOW RIP-ET file. Click on the **Open** button and the file is created in the directory where PRE-RIP-ET.exe is located.

How Do You Import an Existing MODFLOW RIP-ET File?


Start by,

1. Click on **Utilities** and then click on **Import MODFLOW RIP-ET File** in the main menu bar, or click on the  icon on the main menu tool bar.

2. The **MODFLOW Riparian File** dialog box will appear (Figure 6-1) and prompt you for a file with the .rip extension. Browse until you find your desired file, highlight it, and click on the **Open** button.
3. The **Coverage Time and Uniqueness Dimensions** dialog box will appear (Figure 6-2), click on the radio buttons to choose what time characteristic the RIP file was using: Steady State, Steady Oscillatory or transient. If your RIP file is a steady oscillatory or transient, you need to enter the number of seasons, the number of years or cycles and the number of unique coverages. Click on the **Ok** button when finished and the **Order of Coverage** dialog box appears (Figure 6-3)
4. Enter the Coverage numbers into the *Cover Designation (THEME) by Stress Period* grid from the keyboard or from a CSV file. If you have entered the numbers by keyboard, you may save them to a CSV file by clicking on the **Save CSV** button.
5. Click the **OK** button and you return to the main menu, an ETC, ETV and ETO values will appear in their respective windows, and the Log File will be updated.
6. You may save the ETC, ETV and ETO files by clicking on the  icons on the **PFSG Data File (ETC)**, **Fractional Coverage File (ETV)**, and **Output Control File (ETO)** window tool bar, respectively.

How Do You Create a PFSG Curve File?

Start by,

1. Click on **Utilities** and then click on **Construct a PFSG Curve File** in the main menu, or click on the  icon on the main menu tool bar.
2. The **PFSG Curve Data** dialog box will appear (Figure 4-2) with only the *Name of PFSG* and *Number of Data Point (Vertices) in PFSG Curve* enabled in the *Name and Dimension* group box. Enter the name of the plant functional subgroup in the text box labeled *Name of PFSG*. The names can be up to 22 characters in length, and may contain spaces but no apostrophes. Enter the number of vertices into the spinner box labeled *Number of Data Points (Vertices) in PFSG Curve*. Click on the **Next** button, the name and vertices information is written to the *Log File* and the *Unit Conversion* group is enabled (Figure 4-3).
3. The *Unit Conversion* group is divided into two parts, one labeled *Input Units*, the other, *Output Units*. The *Input Units* are the distance and time units associated with the PFSG raw-data sets. The *Output Units* are the distance and time units that you want for your MODFLOW simulation. For this version of PRE-RIP-ET, the units of distance available are centimeters, meters, and feet. The time units are seconds, days and

- years. Set the units using the list boxes, and click on the **Next** button to write unit conversion information to the *Log File* and enable the *PFSG Curve Data* group.
4. Enter the PFSG raw-data values: vertices, heads and ET fluxes. You may enter them directly from the keyboard, or since the PFSG raw-data values are stored as *.csv* files, you may load them clicking on the *Load CSV* button. You may enter the vertex number and associated ET flux and head in any order. PRE-RIP-ET will sort the rows internally to the proper descending order. After entering the PFSG raw data, you have completed the data entry phase of the utility module. Click on the **Calculated Parameter** button. PRE-RIP-ET will calculate the PFSG parameters and place their values in the appropriate test box, will calculate the set of dimensionless segments, and will enable the **Plot PFSG Curve** and the **Create Curve File** buttons.
 5. Clicking the **Plot PFSG Curve** button creates a graph of the PFSG curve in output units (Figure 4-7).
 6. Clicking the **Create Curve File** button brings up the request for a file name to save the PFSG curve file (see Figure 4.8). The file name will be given a *.crv* extension if you do not specify one.
 7. Once you've clicked the **Create Curve File** button and saved the PFSG Curve file, the **Finished** button is enabled. Clicking the **Finished** button returns you to the main menu.

8 Glossary

1. **Plant Functional Subgroup** is the grouping of plant species that exhibit similar transpiration responses to environmental conditions, and have similar rooting depths and water tolerance ranges. Plant size and density may be incorporated into the definition of a subgroup.
2. **PFSG Curve** is a curve of transpiration rate as a function of watertable depth that reflects the eco-physiology of riparian and wetlands plants.
3. **Extinction Depth** is the depth to groundwater below which the roots can not obtain water and ET is non existent.
4. **Hxd** is the hydraulic head at the extinction depth.
5. **Saturated extinction depth**, Sxd, is the depth where the plant's root zone is largely below groundwater level causing the plants to die of anoxia. Mathematically, it is negative if Hsxd is above the land surface elevation (wetland species) and is positive if Hsxd is below the land surface.
6. **Hxsd** is the hydraulic head at the saturated extinction depth.
7. **Rmax** is the average maximum ET flux and will depend on the season, PFSG and climate.
8. **Rsxd** is the ET flux rate at the saturated extinction depth. For plant transpiration it will be zero by definition. To model evaporation Rsxd is set equal to the average maximum evaporation rate.
9. **Ard** is the active root depth, and is the distance between Hsxd and Hxd.
10. **fdh(k)** is the k^{th} dimensionless head segment of the PFSG curve.
11. **fdR** is the k^{th} dimensionless ET flux segment of the PFSG curve.

12. **PFSG Raw-Data Set** is a comma separate variable (CSV) file that contains the hydraulic head and ET flux values at a series of vertices along a PFSG curve. The hydraulic head values are relative to a land surface elevation of zero.
13. **PFSG Curve File** is a data set for each PFSG that contains the name of the PFSG and its associated active root depth (Ard), saturated extinction depth (Sxd), average maximum ET flux (Rmax), the ET flux rate at the saturated extinction depth (R_{sxd}), the number of segment in the curve (NuSeg), and the dimensionless curve segment data (fdh's and fdR's). The PFSG Curve Files have the .crv extension.
14. **Fractional Coverage** is the fraction of active habitat within a cell that is covered by a PFSG, or the fraction of the cell contributing to ET.
15. **Unique Coverage** is the number of different fractional coverages that may occur over the stress periods of a simulation, and may be seasonal.
16. **HSURF** is the head at the land surface elevation and can be assigned as a single value for a cell, or for each PFSG in a cell.
17. **PFSG Data File** is created by PRE-RIP-ET and contains all the PFSG curve data that are present in a MODFLOW simulation. PFSG Data Files have the .etc extension.
18. **Fractional Coverage File** is created by PRE-RIP-ET and contains the all the unique fractional coverage data that are present in a MODFLOW simulation. Fractional Coverage Files have the .etv extension.
19. **Output Control File** is created by PRE-RIP-ET and contains output control and stress period information for a MODFLOW simulation. Output Control Files have the .eto extension.
20. **MODFLOW RIP-ET File** is the data set file for the RIP-ET module for MODFLOW that is constructed by PRE-RIP-ET. MODFLOW RIP-ET Files have the .rip extension.

9 References

- Banta, E.R. 2000. MODFLOW-2000, the U.S. Geological Survey modular ground-water model—Documentation of packages for simulating evapotranspiration with a segmented function (ETS1) and drains with return flow (DRT1). U.S. Geological Survey Open-File Report 00-466.
- Baird, K.J. and T. Maddock, III, In preparation, 2003, A new method for determining riparian evapotranspiration.
- Dragoo, C.A., T. Maddock III and K.J. Baird, In preparation, 2003, Riparian GIS Preprocessor (RIP-GIS).
- Harbaugh, A.W., and M.G. McDonald. 1996a, User's documentation for MODFLOW-96: An update to the U.S. Geological Survey modular finite-difference ground-water flow model: U.S. Geological Survey Open-File Report 96-485.
- Harbaugh, A.W., Edward R. Banta, Mary C. Hill, and Michael G. McDonald, MODFLOW-2000, The U.S. Geological Survey Modular Ground-water model—User guide to modularization concepts and the Ground-water flow process: U.S. Geological Survey Open-File Report 00-92.
- Lavorel, S., S. McIntyre, J. J. Landsberg, and T.D.A Forbes. 1997. Plant functional classifications: from general groups to specific groups based on response to disturbance. *Tree* 12:474-478.
- Leishman, M. R. and M. Westoby. 1992. Classifying plants into groups on the basis of associations of individual traits - evidence from Australian semi-arid woodlands. *Journal of Ecology* 80:417-424.
- Maddock, Thomas III, and K. J. Baird, 2002, A Riparian Evapotranspiration Package, Department of Hydrology and Water Resources, University of Arizona, HWR No. 02-03
- McDonald, M.G., and A.W. Harbaugh. 1988. A Modular Three-Dimensional Finite-Difference Ground-Water Flow Model. U.S. Geological Survey TWI 6-A1
- Meinzer, F. C., J. L. Andrade, G. Goldstein, N. M. Holbrook, J. Cavelier, and P. Jackson. 1997. Control of transpiration from the upper canopy of a tropical forest: the role of stomatal layer and hydraulic architecture components. *Plant, Cell and Environment* 20:1242-1252.
- Williams, D. G., Brunel, J.-P., Schaeffer, S. M., and Snyder, K. A., 1998. Biotic controls over the functioning of desert riparian ecosystems. In; *Proceedings from the Special Symposium on Hydrology*. (Eds) Wood, E. F., Chehbouni, A. G., Goodrich, D. C., Seo, D. J., and Zimmerman J.R. pp. 43-48. Boston MA, American Meteorological Society.